2011

Identification and characterization of the major outer membrane proteins of *Haemophilus parasuis* for the rational development of a vaccine candidate and diagnostic for Glässer's disease

Mandy Kay Zimmerli
Iowa State University

Identification and characterization of the major outer membrane proteins of *Haemophilus parasuis* for the rational development of a vaccine candidate and diagnostic for Glässer's disease

by

Mandy Kay Zimmerli

A dissertation submitted to the graduate faculty

in partial fulfillment of the requirements for the degree of

DOCTOR OF PHILOSOPHY

Major: Biochemistry

Program of Study Committee:
Louisa Tabatabai, Co-major Professor
Amy Andreotti, Co-major Professor
Alan DiSpirito
Gustavo MacIntosh
Emily Smith

Iowa State University

Ames, Iowa

2011

TABLE OF CONTENTS

LIST OF TABLES

LIST OF FIGURES

ACKNOWLEDGEMENTS

I would like to begin by acknowledging Louisa Tabatabai who has been a fabulous mentor in the aspects of both science and life. Throughout my graduate career, we have encountered difficult events—both separately and together—and it was the example of her grace that allowed me to move through some very difficult situations in stride. She has challenged me and encouraged me. I feel blessed to have known her as a person and for the opportunity to work with her.

In addition to Louisa, I'd like to extend gratitude to the BBMB department. I was fortunate to work with faculty and students alike through various teaching assistantships. Out of those experiences, I discovered a love for teaching. I am especially grateful for Desi Gunning who has been a wonderful companion throughout my teaching career. Overall, I could not have asked for a better graduate career or a better department in which to complete this study. With that being said, I would like to thank my Co-major Professor, Amy Andreotti, and my POS committee members, Gustavo MacIntosh, Alan DiSpirito, and Emily Smith for their assistance during my academic career. I would also like to thank Emilie Zehr for showing me the ropes when I first entered the Tabatabai lab.

I would like to give special recognition to my older brother, Joe, for bringing levity to some of the worst of times. I am fortunate to have a brother who is also one of my closest friends. His encouragement, along with the support of my dad, has made every step of this process possible. I have a great support network of friends and family. To name everyone would take an eternity, so I will keep this short. To everyone who has supported me on this journey in any way and for those who continue to support me: thank you.

ABSTRACT

Haemophilus parasuis is the causative agent of Glässer's disease, a respiratory illness in swine, which causes significant economic loss in the industry. To date, there is no commercially available cross-protective vaccine or diagnostic for this disease. Because of this, identification and characterization of putative virulence factors is crucial. In order to understand the mechanism of infection of *H. parasuis*, it is imperative to not only identify proteins traditionally associated with virulence but to also recognize differences that exist for those proteins at a molecular and/or expression level. Using a combination of bottom-up and isobaric-tagging for relative and absolute quantification (iTRAQ) proteomic strategies, N-terminal sequencing, molecular modeling and antigenic characterization techniques, putative virulence factors have been identified and characterized. In attempt to identify the P2 and P5 colonization factors of *H. parasuis*, tandem mass spectrometry was performed following 2-D SDS-PAGE immunoblots with a monoclonal antibody to OMP P5 of *H. influenzae*. While OMP P2 was identified using this method, OMP P5 was not. Additional proteins identified include: TRAP solute transporter, glucose-specific PTS system enzyme IIA, acetyl-CoA carboxylase biotin carboxylase subunit, purine nucleoside phosphorylase, chelated iron ABC transporter, probable sugar isomerase, Mn-dependent superoxide dismutase, putative iron ABC transporter, D-ribose transporter, alanine aminotransferase, phosphoribosylglycinamide formyltransferase, FbpA, and hypothetical proteins HPS 06844 and HPS 10240. Sequence and structural alignment of identified proteins with *H. influenzae* OMP P5 were used in order to elucidate common epitopes for antibody 4BF8 with no success. Molecular modeling and

antigenic prediction analysis indicates that regardless of virulence, the OMP P5 protein comprises four surface exposed loops and that these loops have comparable antigenic propensity, with the presence of a linear B-cell epitope at the apex of both loops 3 and 4. Based on preliminary ELISA results using synthetic peptides and sera from animals infected with *H. parasuis*, a subunit vaccine strategy derived from the outer membrane loop 3 and loop 4 peptides of P5 was tested in an animal model, demonstrating that while the loop 3 peptide provided protection against heterologous challenge, the loop 4 peptide provided no protection. Molecular modeling analysis of OMP P2 indicates two forms of the protein that differ by approximately 3-5kDa. OMP P2 comprises eight surface exposed loops and the increase in molecular weight observed for OMP P2 in avirulent strains corresponds to extensions in the loop 3 and loop 5 regions. For OMP P2 of virulent serovars, loop 1, loop 4 and loop 8 have the highest antigenic propensity scores, with predicted continuous B-cell epitopes present on loops 1, 3, 4, 5, 6 and 8. In addition to the P2 and P5 colonization factors, non-traditional proteins may serve as colonization factors as epitopes of surface localized proteins may facilitate attachment. Following anti-P5 (4BF8) immunoblot and N-terminal sequencing, a 36kDa outer membrane protein of *H. parasuis* was identified as glyceraldehyde-3-phosphate dehydrogenase (GAPDH). Studies in other bacterial pathogens indicated that surface localized GAPDH is involved with colonization and it is hypothesized that this protein may play the same role in *H. parasuis*. Given that few proteomic profiling studies have been performed on *H. parasuis*, the iTRAQ method was utilized to not only identify proteins, but to also quantify differential protein expression and evaluate how this differential expression may play a role in virulence of the organism. Results of the OMP P2 protein expression indicated a 1.5 to 2-fold increase in the presence of 7.5% CO_2 when

compared to protein expression in an aerobic environment. Additional differentially expressed proteins for the overall analysis include: MglB, hypothetical protein HPS_06844, Fe^{3+} ABC transporter, TRAP solute transporter, D-ribose transporter subunit RbsB, FbpA, ABC transporters, Cu-Zn SOD, iron binding proteins, chelated iron ABC transporter, hypothetical protein HPS_10240, acyl carrier protein, glucose-specific PTS enzyme IIA, heme-binding protein A, phosphoenolpyruvate-protein phosphotransferase, alanine aminotransferase, hypothetical protein HPS_07840, plp0007 from *Legionella pneumophila*, hypothetical protein GCWU000324_02210 from *Kingella oralis*, transaldolase B, UDP-sugar diphosphatase from *M. haemolytica*, tRNA pseudouridine synthetase C, gamma-glutamyl phosphate reductase and nitrate reductase. Overall, the research presented here not only provides one of the few proteomic profiles of *H. parasuis*, it presents a general methodology for the design of a subunit vaccine and corresponding diagnostic for extracellular pathogens.

CHAPTER 1. GENERAL INTRODUCTION

Introduction

Haemophilus parasuis, a respiratory pathogen in swine, is the causative agent of Glässer's disease, which is associated with polyserositis, meningitis, arthritis, and lameness. Interestingly enough, not all serovars are associated with a diseased state. *H. parasuis* serovars have been classified as highly virulent, causing morbidity; virulent without the result of death; and avirulent. There is little understanding about what causes *H. parasuis* to be highly virulent versus part of the avirulent commensal flora. Because of this, conventional vaccine methods, such as the use of heat-killed organisms, prove problematic. Therefore, it is imperative to understand not only what proteins play a role in virulence of the organism, but also what differences these proteins have at a molecular level that could be exploited in the development of a peptide derived vaccine and/or diagnostic. Since bacteria cannot perpetuate infection without colonization, the study of proteins involved in adherence, including P2 and P5, is particularly important. The aim of this study was to identify and characterize the outer membrane proteins of a variety of serovars of *H. parasuis* using protein and molecular based techniques.

Dissertation Organization

The presentation of this dissertation focuses first on the identification of outer membrane proteins of *H. parasuis* which share epitopes with the monoclonal antibody for OMP P5 from the related organism *H. influenzae* (Chapter 2). Two-dimensional SDS-PAGE immunoblots using a mAb (4BF8) to *H. influenzae* P5 protein followed by tandem mass spectrometry identified not only the P2 colonization factor, but also proteins from *H. parasuis* and related organisms which may serve as relevant virulence factors. These

identified proteins include: OMP P2, TRAP solute transporter, glucose-specific PTS system enzyme IIA, acetyl-CoA carboxylase biotin carboxylase subunit, purine nucleoside phosphorylase, chelated iron ABC transporter, probable sugar isomerase, Mn-dependent superoxide dismutase, putative iron ABC transporter, D-ribose transporter, alanine aminotransferase, phosphoribosylglycinamide formyltransferase, FbpA, and hypothetical proteins HPS 06844 and HPS 10240.

The second paper (Chapter 3) focuses on the structural and antigenic predictions for the OMP P2 and OMP P5 of *H. parasuis*. Jerry K. McVicker is a previous graduate student who studied OMP P2 and OMP P5 in *H. parasuis*. The work presented here is a continuation of his studies, and the paper to be submitted will include unpublished data from his dissertation. Since the P2 and P5 colonization factors have been found to be of importance to the related respiratory pathogen, *H. influenzae*, both the P2 and P5 proteins were sequenced and modeled. The P5 protein was found to comprise four outer membrane surface exposed loops, as well as a domain that is homologous to the P6 protein of *H. influenzae*. No major structural differences were noted for the models of P5 protein. However, this was not the case for P2 protein. The P2 proteins were found to comprise eight outer membrane surface exposed loops. Sequencing of the P2 genes followed by molecular modeling analysis indicated that loops 3 and 5 of the structure are extended for avirulent reference strains, and these extensions account for an increase in the molecular weight of the P2 proteins which was noted by immunoblot analysis. Additionally, antigenic profiles of both proteins show that the highly virulent serovars have a P2 protein that comprises highly antigenic epitopes on outer membrane loop 1, loop 4, and loop 8. The antigenic profiles of OMP P5 remained fairly consistent regardless of virulence. A continuous B-cell epitope was predicted at the

apex of loop 3 and loop 4 for OMP P5. The exact roles of the extensions in loop 3 and loop 5 for OMP P2 are unclear. However, all virulent strains comprised a continuous B-cell epitope in non-extended loop region of loop 3. This epitope was also given the highest scoring predicted antigenic propensity for that particular loop. Extensions of the loop 3 appear to shift or elongate the presence of continuous B-cell epitope. The extension of loop 5 appears to play a role in shifting the predicted continuous B-cell epitope closer to the transmembrane domain. Loop 5 was not considered a highly probably continuous B-cell epitope for highly virulent strains, with the exception of SV1.

The third paper (Chapter 4) is modified from a patent application from collaborative work with Novartis Animal Health for the development of a peptide vaccine for Glässer's disease. Given the findings of the P2 and P5 molecular modeling, a P5 peptide vaccine candidate was designed and used in a challenge study against swine infected with serovar SV13. Results of the study showed that sera of animals not only raised antibodies to the loop 3 peptide, but that the loop 3 peptide provided protection for swine against a heterologous challenge. Superior results, with 90–100% protection, were observed for animals vaccinated with both peptide and bacterin. In an animal study using the recombinant loop 4 peptide, the loop 4 epitope did not provide any protection against heterologous challenge. Therefore, the loop 3 peptide of *H. parasuis* OMP P5 is considered protective, while the loop 4 peptide may act as a decoy. These results are consistent with findings for the *H. influenzae* OMP P5 in a chinchilla model. Preliminary ELISA (enzyme-linked immunosorbent assay) results using loop 3, loop 4, and a combinatorial loop 3–4 synthetic peptides are also presented. Results of preliminary ELISA studies indicated that all peptides have statistically significant ($p<0.05$) antibody titers for animals infected with *H. parasuis* in comparison to control animals.

The fourth paper (Chapter 5) discusses the identification of a surface localized glyceraldehyde-3-phostphate dehydrogenase and its implications as a putative virulence factor for *H. parasuis.* The outer membrane proteins of SV2 were first separated by IEF fractionation and then analyzed by SDS-PAGE. An immunoblot using a mAb to the OMP P5 of *H. influenzae* identified an immunoreactive protein with an apparent molecular weight of 36 kDa and pI between 6.2 and 7.0. N-terminal sequencing was used to identify the protein and molecular modeling, and antigenicity prediction methods were used to elucidate epitopes which could serve as subunit vaccine candidates. Since surface localized glyceraldehyde-3-phosphate dehydrogenase has been identified as a virulence factor in *Steptococcus suis, Streptococcus pyogenes*, *Neisseria meningitidis*, and *Mycoplasma pneumonia*, it is hypothesized that glyceraldehyde-3-phosphate dehydrogenase could have a comparable function in *H. parasuis* as a colonization factor.

The final paper (Chapter 6) is focused on the identification of additional virulence factors based on global differential expression of outer membrane proteins. iTRAQ (isobaric-tagging for relative and absolute quantification) analysis was performed on the outer membrane protein preparations of an avirulent reference strain (HP3), a highly virulent reference strain (HP5), a moderately virulent field isolate (HP2170B), and a virulent field isolate from porcine reproductive and respiratory syndrome virus (PRRSV) co-infection (HP409). All isolates were grown in either aerobic or anaerobic (7.5% CO_2) conditions. The functional role of the differentially expressed proteins will be discussed along with relevance to virulence of the organism. A notable finding for all strains is the 1.5 to 2-fold increase in protein expression of OMP P2 in the 7.5% CO_2 environment as this upregulation of protein expression may play a role in adherence to host epithelial cells in the respiratory tract.

Literature Review

Description of Organism

Haemophilus parasuis is a Gram-negative, nonhemolytic bacterium responsible for the swine respiratory illness known as Glässer's disease [1-3]. The organism was first described in 1910 by Glässer after being recovered from the serous exudates of diseased pigs that presented with meningitis, arthritis, and pericarditis [4]. This disease is prevalent worldwide, is associated with significant economic loss in the swine industry, and most commonly affects young pigs between 5-8 weeks in age [5]. Death can occur as soon as two days post-infection [6]. The diseased state presents with severe septicemia, with pus accumulating in the brain, joints, and around the heart and lungs, resulting in severe pericarditis, pleuritis, arthritis, and meningitis.

H. parasuis is a member of the family *Pasteurellaceae*. The bacteria in this family, including genera *Actinobacillus*, *Haemophilus,* and *Pasteurella*, are non-motile, nonspore forming, and facultative anaerobic bacteria. These organisms are found as commensal flora in the oral mucosa and the upper respiratory tract of both animals and humans. While a related organism, *H. suis,* requires both factor V (β-NAD) and factor X (iron porphyrin) for growth, *H. parasuis* only requires factor V [7, 8]. Biochemical characterization of the NAD-dependent family members of the family *Pasteurellacea* can be found in Table 1.1 [9]. As mentioned previously, serovars either exist as highly virulent, causing morbidity; virulent, associated with a diseased state; or avirulent. Table 1.2 describes the virulence for each serovar as described by Rubies et al. in 1999 [5]. The scheme proposed by Kielstein and Rapp-Gabrielson (KRG) in 1991 is the most common method of serotyping *H. parasuis* to date [10]. The KRG system has identified 15 serovars using agar precipitation method and

heat stable antigens. An additional method of serotyping, developed by Tadjine et al., involves the indirect hemagglutination test (IHA) [11]. A study by Kielstein and Rapp-Gabrielson related virulence of organisms to serotype [12]. Serotypes 1, 5, 10, 12, 13, and 14 were found to cause death and morbidity within 4 days and were classified as highly virulent, while serotypes 2, 4, and 15 did not cause death but were associated with polyserositis and, thus,were identified as virulent. Serotypes 3, 6, 7, 8, 9, and 11 were not associated with any disease state and, thus, were identified as avirulent.

Virulence Factors of *H. parasuis* and Related Pathogens

Since very little is known about the virulence factors of *H. parasuis*, research has focused on identifying the virulence factors in related pathogens. A variety of virulence factors have been identified in the model organism, *H. influenzae*. The virulence factors include: capsulation, fimbrae, pili, secreted molecules and proteins, and the outer membrane proteins [13-24]. Major outer membrane proteins that have been identified in *H. influenzae* include the major outer membrane proteins P1, P2, P4, P5, and P6, and the surface exposed high molecular weight proteins (HMW1 and HMW2) [20, 25-35]. In addition to these membrane proteins, accessory proteins implicated in virulence in family *Pasteurellaceae* include: OapA (opacity associated protein), IgA1 protease, and Hap (*Haemophilus* adhesion protein) [25, 36-38]. Both OapA and Hap are members of the major outer membrane protein family for *H. influenzae*.

An experimental finding by Vahle et al. indicated that *H. parasuis* infection is responsible for the swelling of the nasal and tracheal mucosa, the loss of cilia, and suppurative rhinitis lesions [39]. A hypothesized soluble toxin, such as IgA1 protease or Hap, was implicated to be involved with cellular damage that allowed the organism to gain access

to the blood stream. Hap proteins share significant homology with IgA1 protease of *Neisseria gonorrhea* and *H. influenzae* and are also important to the interactions between bacterium and human epithelium [40, 41]. Recently, IgA1 protease activity was noted for *H. parasuis*, but no genes with homology to *H. influenzae* IgA1 protease were found for *H. parasuis* [42]. A crystal structure of the *H. influenzae* Hap proteins described a mechanism for cell to cell adhesion and ultimately biofilm formation [43].

The presence of a bacterial capsule is used to characterize *H. influenzae* isolates, with six antigenically and structurally distinct capsule serotypes a-f. Non-capsulated strains are considered nontypable [25]. The reports of a capsule for *H. parasuis* have been mixed. A study in 1986 found that *H. parasuis* recovered from upper respiratory tract of healthy pigs were capsulated, and isolates from systemic sites of infection were non-encapsulated [44]. However, capsulation was found to be qualitatively reduced after in vitro passages and that in vivo passages could select for capsulated clones [45].

In *H. parasuis*, a fibril-mediation adherence mechanism has been described [46]. However, results indicated that while fimbriae are critical for the persistence of *Haemophilus* related infection, the expression of fibril structures is not required for *H. parasuis* infection [47]. A 2011 study, using scanning electron and transmission electron microscopy methods, suggested that adherence and invasion of porcine kidney epithelial cells (PK-15) could be a virulence mechanism involved in the lesions caused by *H. parasuis* Nagasaki strain (SV5) [48].

In addition to the above findings, microarray analysis in conditions that mimic the stresses of infection—iron limitation, oxygen limitation, low pH, and increased temperature—identified 75 genes homologous to pathogens of the *Pasteurellacea* family

[49]. Under oxygen limiting, low pH, and heat stress, genes expressed included: the phosphotransferase system (PTSI and PTSII) of *Pasteurella multocida*, *P. multocida* spermidine/putrescine transporter PotD which is required for the uptake of polyamines to assist in cell growth and gene expression, transporters including homologs of GlpT of *P. multocida* for the uptake of glycerol-3-phosphate, and MalF of *Salmonella typhimurium* for the uptake of maltose. Genes that were induced during iron-limitation included the homologues of the *hxuCBA* genes of *H. influenzae* and the *yfeA* genes of *P. multocida*. Additionally, genes homologous to hemolysin HhdA of *H. ducreyi* were upregulated under oxygen limiting conditions; the *P. multocida* stress protein ClpB was upregulated under heat, acidic, and iron-limiting growth conditions; and two putative proteases homologous to *H. influenzae* (HI0419) PrtC, and a serine protease of *Fusobacterium nucleatum* subsp. vincentii with an unknown function were found under acidic, temperature, and heat stress conditions. The results of this study indicated that the expression of virulence factors was relatively conserved among the bacteria of the *Pasteurellaceae* family.

In 2008, genes of *H. parasuis* which were transcribed in necrotic porcine lung tissue were identified using SCOTS (selective capture of transcribed sequences) [50]. Genes include: possible large adhesin and ABC-type transport system. Use of the SCOTS method from a study in 2009 identified genes expressed in *H. parasuis* under the restriction of iron [51]. This included a pilus assembly protein, predicted phage tail protein, PTS enzyme IIC, transferrin binding proteins A and B, and a chelated ABC iron transporter. Additionally, comparative genetic studies were performed to elucidate differences in gene expression of a highly virulent serovar, SH0165, and avirulent serovar, 7140, of *H. parasuis* [52]. Results of genetic subtraction determined genes for proteins expressed in the virulent serovar. This

includes: phage-related products, large adhesins, ABC-type transport systems, transferrin binding proteins, proteins involved with restriction modification, and outer membrane proteins including the OMP P5. A comprehensive proteome analysis of *H. parasuis* strain SH1065 (SV5), published in 2009, identified putative virulence factors, including the major outer membrane proteins P2 and P5 [53].

OMP P2 and P5 of *H. influenzae* and *H. parasuis*

Two major outer membrane proteins identified to be of importance in *H. influenzae* are OMP P2 and OMP P5. Both proteins have been found to be important in the establishment of colonization as well as having bactericidal activity in animal models [35, 54]. The *H. influenzae* OMP P5 (Figure 1.1) schematic was published by Webb et al., indicating a 72.2% secondary structural homology to the OMP A in *E. coli* [55]. Due to the increase in variability of this protein during the course of chronic infections, it was concluded that P5 plays an important role as a target for the immune response [56]. This was later supported by studies that showed the involvement of OMP P5 in the binding to epithelial cells as well as the ability of OMP P5 to bind CEACAM-1 [57]. CEACAMs (carcinoembryonic antigen cellular adhesion molecules) are present on the surface of a variety of cells, including epithelial cells. In other gram-negative organisms, OMP P5, OMPA, and Opa proteins as well as fimbrae have been implicated in the binding to CEACAMs (Figure 1.2) [58-64]. OMP P5 homologs in *H. influenzae, Neisseria meningitidis, and N. gonorrhea* have been shown to bind CEACAM-1 on CD-4+ T-lymphocytes [61]. Because of the coinhibitory role of CEACAM-1, this results in suppression of the host's immune response via ITIM (immunoreceptor tyrosine-based inhibitory motif) signaling (Figure 1.3) [65]. Structural characterization of the binding of *Neisseria* spp. Opa to human

CEACAM-1 indicates that this class of proteins binds preferentially to the non-glycosylated N-domain of CEACAM receptors, including CEACAM-1 (Figures 1.4 and 1.5) [66].

Studies further characterized *H. influenzae* OMP P5 in accordance to functional roles of the loop peptides. For example, the loop 3 peptide is the protective epitope but not the immunodominant region for this particular protein [67]. Although *H. influenzae* OMP P5 was found to be involved in CEACAM-1 binding, the *H. parasuis* OMP P5 showed an inability to bind CEACAM-1 [68]. However, this may be due to the use of human CEACAM-1 as swine CEACAM-1 is not commercially available. Recent studies indicate that recognition of CEACAM-1 by *N. gonorrhea* as well as *N. meningitidis* is limited to the human ortholog of this protein and suggest that CEACAM-1 recognition is species-specific, as no association was noted between the pathogens and the N-terminal domains of bovine, murine, or canine CEACAM-1 [69].

The most abundant outer membrane protein in *H. influenzae* is OMP P2 (Figure 1.6). This protein, like OMP P5, is highly variable on its surface exposed regions and is strongly immunogenic. Characterization of the loop peptides has revealed that loop 5 is the immunodominant epitope while loop 6 remains protective [70-73]. Aside from direct immunogenic function, these loops have been implicated in the activation of JNK and p38 via mitogen-activated protein kinase pathway [74]. Loop 7 of OMP P2 was shown to induce MEK1/MEK2 mitogen activating protein kinase phosphorylation and upregulate cellular adhesion molecule production [75]. Although *H. parasuis* OMP P5 was found incapable of binding human CEACAM-1, the *H. parasuis* OMP P2 was found to bind CEACAM-1 [68].

The OMP P5 of *H. parasuis* was purified by anion exchange and size exclusion chromatography and characterized to have an apparent molecular mass of 32kDa and pI of

5.5 [76]. Additionally, both the P5 and P2 proteins of *H. parasuis* were identified using immunoblot and N-terminal sequencing methods [68]. Recently the OMP P2 and OMP P5 genes from *H. parasuis* have been sequenced as well as translated [77]. Two-dimensional sequence analysis has been performed in an attempt to identify regions of variability, including the work done by Mullins et al. (Figure 1.7) which described the OMP P5 of *H. parasuis* to comprise five outer membrane loops and the OMP P2 of *H. parasuis* to comprise eight outer membrane loops. In addition to this work, a model of the OMPA, a P5 homolog, from *H. parasuis* suggests four surface exposed loops (Figure 1.8), with hypervariability for the loop 3 and loop 4 regions [78]. Moreover, recombinant OMPA from both serovars 4 and 5 cross-reacted to anti-sera from all serovars of *H. parasuis*, indicating that the variability in the loop 3 and loop 4 regions does not affect antigenicity of the OMPA in *H. parasuis* [78]. Monoclonal antibodies raised to *H. parasuis* OMPA provided protection against infection in a mouse model [79].

Glyceraldehyde-3-phoshate Dehydrogenase as a Virulence Factor

While cytosolic glyceraldehyde-3-phoshate dehydrogenase (GAPDH) functions as a glycolytic enzyme, the surface localized form of the protein appears to have a role in colonization in a variety of bacterial pathogens [80-85]. GAPDH has been shown to function as an colonization factor in *Mycoplasma pneumonia*, *Streptococcus suis*, *Streptococcus pyogenes*, *Neisseria meningitidis*, and *Staphylococcus aureus*. In *M. pneumonia*, GAPDH is present in both cytosol and surface of bacteria [81]. However, the concentration of GAPDH is higher at the surface of the pathogen and implicated in binding the upper respiratory tract in humans. In *N. meningitidis*, a GAPDH deficient mutant showed reduction in ability to bind host epithelial and endothelial cells [82]. Similar results were noted for the GAPDH

homologs, GapA and GapB, in *S. aureus*. In an infection model, loss of either homolog resulted in a reduction of virulence of the organism [83]. A vaccination study using GAPDH of *Mycoplasma bovis* indicated that cattle infected with the organism had an antibody titer to the antigen [86].

Peptide and Subunit Vaccine Strategies

To date, there is no cross-protective vaccine against Glässer's disease nor is there a diagnostic. Because only particular serovars are associated with the diseased state, conventional vaccine methods, such as the use of heat killed organisms, prove problematic. The use of a subunit vaccine, such as a peptide, is ideal because it focuses solely on an immunogenic epitope. Since the Opa class proteins are implicated in the evasion of the host's immune response as well as colonization, the P2 and P5 proteins are probable targets for the development of a vaccine and diagnostic candidate for Glässer's disease.

The use of a subunit vaccine is not a new concept. Early subunit vaccine studies date back to 1966, with the first publication of an ether and detergent disrupted influenza virus subunit vaccine administered to rabbits [87]. At that time, the use of ether-split influenza antigen vaccines had been in preparation for almost a decade. In 1972, an influenza vaccine consisting of viral subunits produced by tri-(n-butyl)-phosphate (TNBP) indicated that the TNBP subunit vaccine not only produces antibody to the vaccine strains and the induction of antibodies against related heterologous strains, but that the subunit vaccine could also be administered in higher doses than conventional vaccines of the time without an increase in local reactions [88]. An influenza subunit vaccine comprising hemagglutinin and neuraminidase proved superior to commercially available tween-ether split and fluid whole

cell virus vaccines in 1976 [89]. Since the advent of these studies, a variety of subunit vaccination candidates have been identified in both viruses and bacteria.

Peptides, rather than whole cell bacterins and recombinant proteins, are ideal subunit vaccines as they focus the hosts immune system on the antigenic epitopes. A synthetic peptide vaccine was designed from *Brucella abortus* Cu-Zn superoxide dismutase [90]. This study, published in 1994, showed that a peptide not only conferred protection against brucellosis in mice upon challenge but that the host's immune system also gave rise to antibodies which recognized the synthetic peptides.

One of the major issues in the design of a subunit vaccine is that pathogens often present on their antigens a decoy epitope or epitopes that serve to focus the host's immune system away from the protective epitope, a process known as deceptive imprinting [91]. Two models of this phenomenon are noted for the OMP P5 of *H. influenzae* as well as the surface envelope glycoprotein of the HIV-1 virus. Vaccination studies using a chinchilla animal model using synthetic peptides of outer membrane loops of OMP P5 of *H. influenzae* verified that the host's immune system strongly recognized loop 4, but that this peptide did not confer any protection against the pathogen [67]. Rather, the loop 3 peptide served as the protective epitope. Upon infection with HIV-1, the host's immune system recognizes the V1, V2, and/or V3 epitopes of the surface envelope glycoprotein but not the epitopes which serve as protective [92, 93]. The process of immune refocusing serves to focus the host's immune system on the protective epitopes while discarding the "junk" immunodominant epitopes. This can be done by designing an antigen which has been modified by removal or attenuation of the immunodominant epitopes.

Tables

Table 1.1. Biochemical characterization of the family *Pasteurellaceae* isolated from the upper respiratory tract of pigs

Tests	*A. minor*	*A. porcinus*	*A. indolicus*	*H. parasuis*
V factor dependency	+	+	+	+
Hemolysis	-	-	-	-
Camp Test	-	-	-	-
Nitrate reduction	+	+	+	+
Urease	+	-	-	-
Catalase	-	-	+	+
Indole production	-	-	+	-
ONPG	+	+	+	+
Lysin decarboxylase	-	-	-	-
Ornithine Decarboxylase	-	-	-	-
Acid From				
Glucose	+	+	+	+
Galactose	+	+	+	+
Mannose	+	+	+	+
Fructose	+	-	+	+
Rhamnose	-	-	-	-
L-arabinose	-	-	-	-
Xylose	-	+	-	-
Sucrose	+	+	+	+
Lactose	+	+	-	-
Trehalose	d	d	-	-
Maltose	+	+	+	+
Mannitol	-	+	-	-
Sorbitol	-	+	-	-
Dulcitol	-	-	-	-
Inositol	-	+	-	-
Raffinose	+	+	+	-
Salicin	-	-	-	-
Esculin	-	-	-	-

Source: (Reprinted with permission [9])
+: positive reaction: -: negative reaction; d: different reaction

Table 1.2. The virulence of the *Haemophilus parasuis* serotypes

Serotype	Very High Virulence	High Virulence	Low Virulence
1	+		
2		+	
3			+
4		+	
5	+		
6			+
7			+
8			+
9			+
10	+		
11			+
12	+		
13	+		
14	+		
15		+	

Source: (Adapted from Rubies, 1999 [5])

Figures

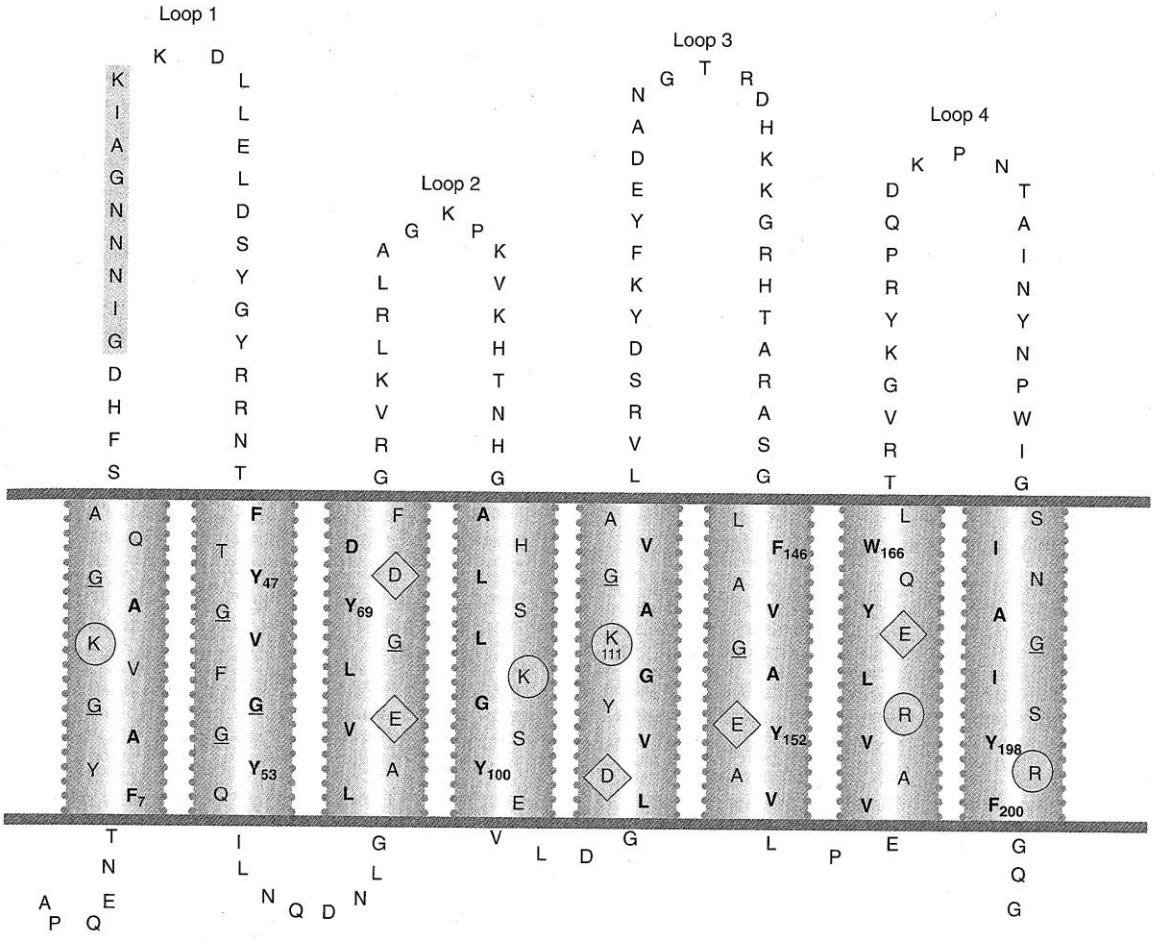

Figure 1.1. The *H. influenzae* OMP P5 secondary structure as predicted by Webb et al. (Reprinted with permission [55])

Bacterial species	Comment	Adhesin type	CEACAM-binding determinants	CEACAM specificity				References
				1	3	5	6	
Neisseria gonorrhoeae	Pathogen: gonorrhoea, pelvic inflammatory disease, conjunctivitis	Opa (integral outer membrane protein)	Protein	+	+	+	+	63,116–118
Neisseria meningitidis	Pathogen: meningitis, septic shock	Opa (integral outer membrane protein)	Protein	+	+	+	+	116,119,120
Neisseria subflava	Commensal: nasopharynx	Opa (integral outer membrane protein)	Protein	+	ND	ND	ND	121
Neisseria lactamica	Commensal: nasopharynx	Opa (integral outer membrane protein)	Protein	+	ND	ND	ND	121
Moraxella catarrhalis	Pathogen: otitis media	UspA1 (fibril-like)	Protein	+	ND	ND	ND	122
Haemophilus influenzae (encapsulated)	Pathogen: meningitis, septic shock	OmpP5 (integral outer membrane protein)	Protein	+	ND	ND	ND	123
Haemophilus influenzae (non-typable)	Pathogen: otitis media, pneumonia	OmpP5 (integral outer membrane protein)	Protein	+	ND	ND	ND	123
Escherichia coli	Pathogen: enteric and urinary-tract infections	Fimbriae	Carbohydrate	ND	ND	+	+	124,125
Diffusely adhering *E. coli* (DAEC)	Commensal: colon	Fimbriae	Carbohydrate	ND	ND	+	+	124,125
E. coli	Pathogen: enteric disease	Afimbrial and fimbrial	ND	+	–	+	+	126
Salmonella typhi	Pathogen: typhoid fever	Fimbriae	Carbohydrate	ND	ND	+	+	125
Salmonella paratyphi	Pathogen: paratyphoid fever	Fimbriae	Carbohydrate	ND	ND	+	ND	125
Salmonella java	Pathogen: enteric fever	Fimbriae	Carbohydrate	ND	ND	+	ND	125

+, strains identified that bind indicated CEACAM receptor; –, strains have been tested for binding to indicated CEACAM receptor, but no binding detected; ND, not determined; Opa, opacity-associated; OmpP5, outer membrane protein P5; Usp, ubiquitous surface protein.

Figure 1.2. CEACAM specificity of adhesin type proteins. (Reprinted with permission [61]).

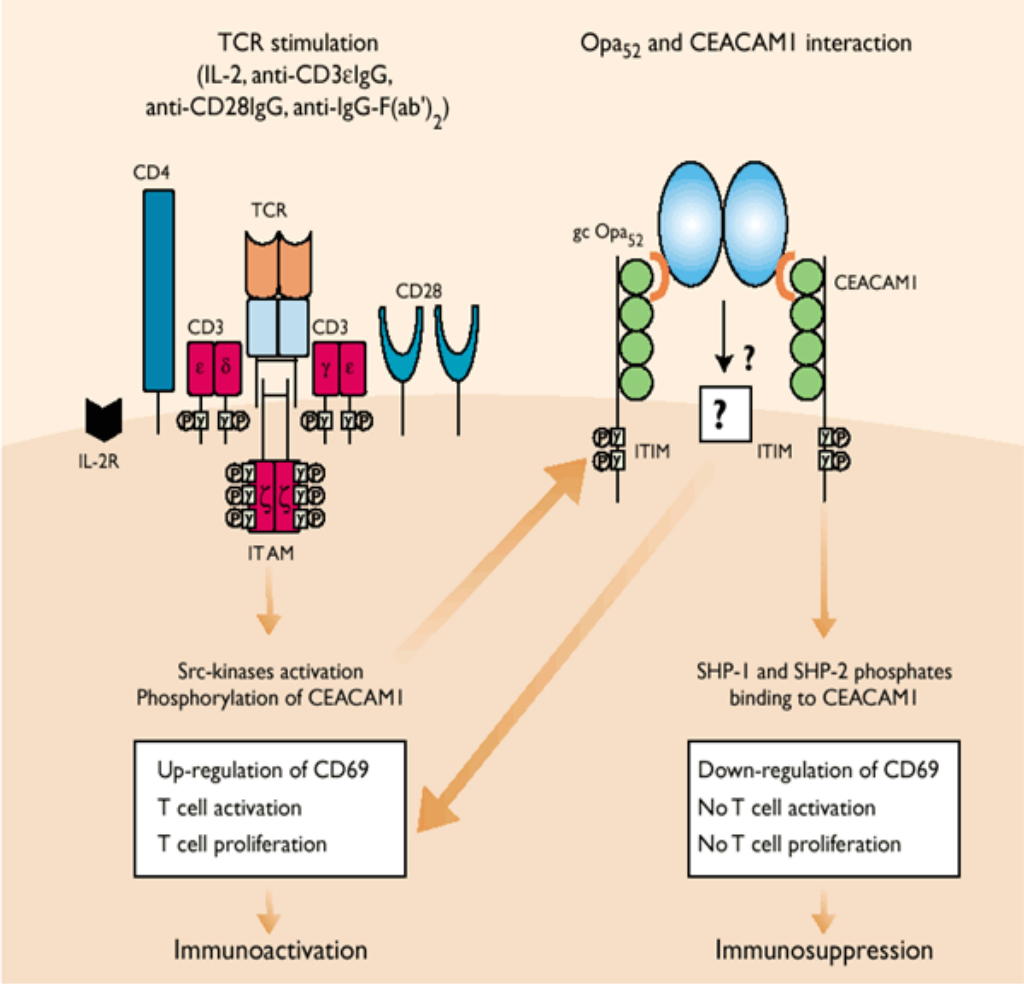

Figure 1.3. Model for the suppression of immune function by Opa from *N. gonorrhea* upon binding to CEACAM-1. (Reprinted with permission [65])

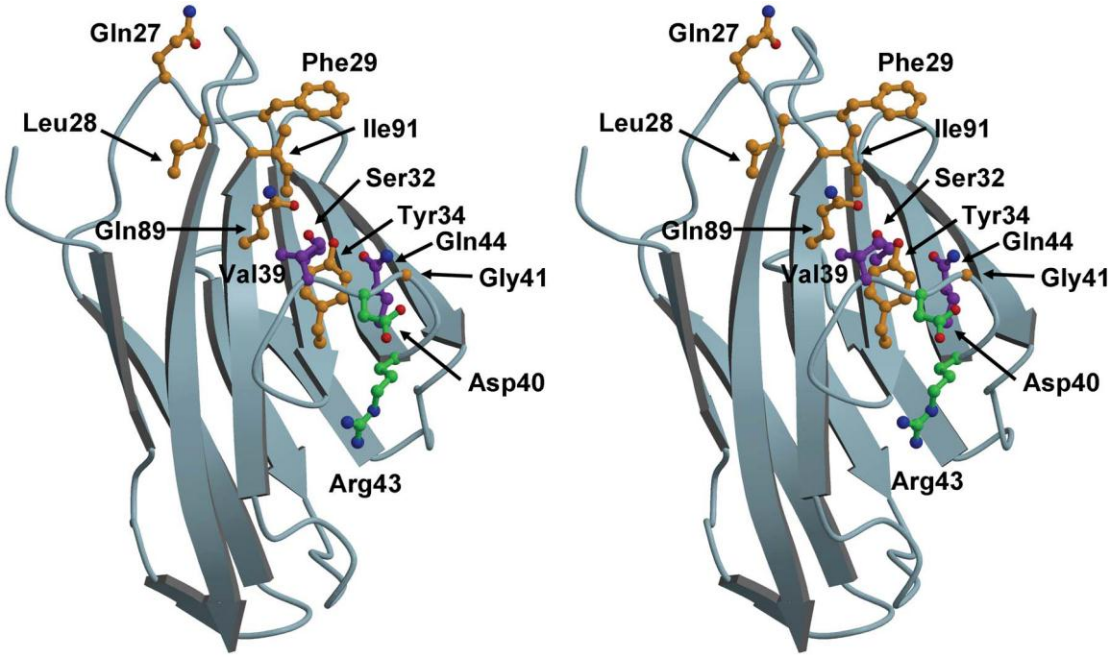

Figure 1.4. Residues implicated in the binding of hCEACAM-1 to Opa protein class. The top stereoview shows the red residues that are required for interactions with all Opa proteins tested; orange residues that are required for interactions with some Opa proteins; purple residues that are involved in interactions with Opa proteins and in homophilic or heterophilic interactions with CEACAMs. (Reprinted with permission [66])

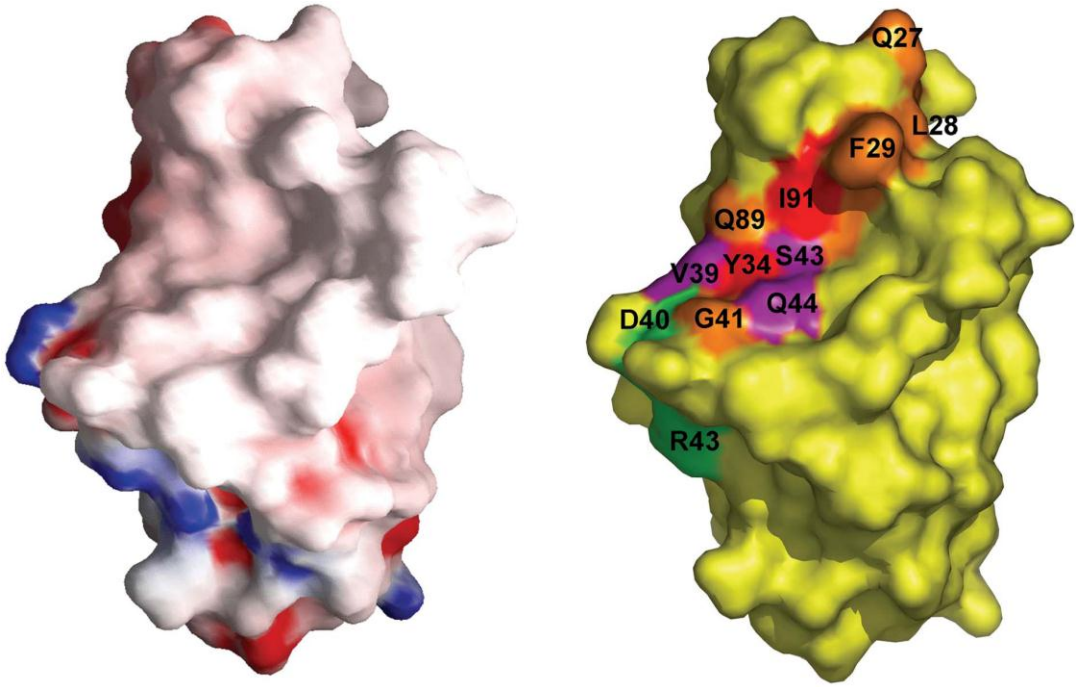

Figure 1.5. An electrostatic plot of hCEACAM-1. Electropositive regions of the molecule are colored blue, electronegative regions are red, and hydrophobic regions are white (left). The regions of hCEACAM-11 that bind Opa proteins and mediate homophilic and heterophilic interactions are shown (right). The surface of the protein is rendered in yellow and the coloring scheme for residues important for binding is the same as in Fig. 1.4. Compared with the view in Fig. 1.4, the molecule has been rotated slightly to the left about the vertical axis. (Reprinted with permission [66])

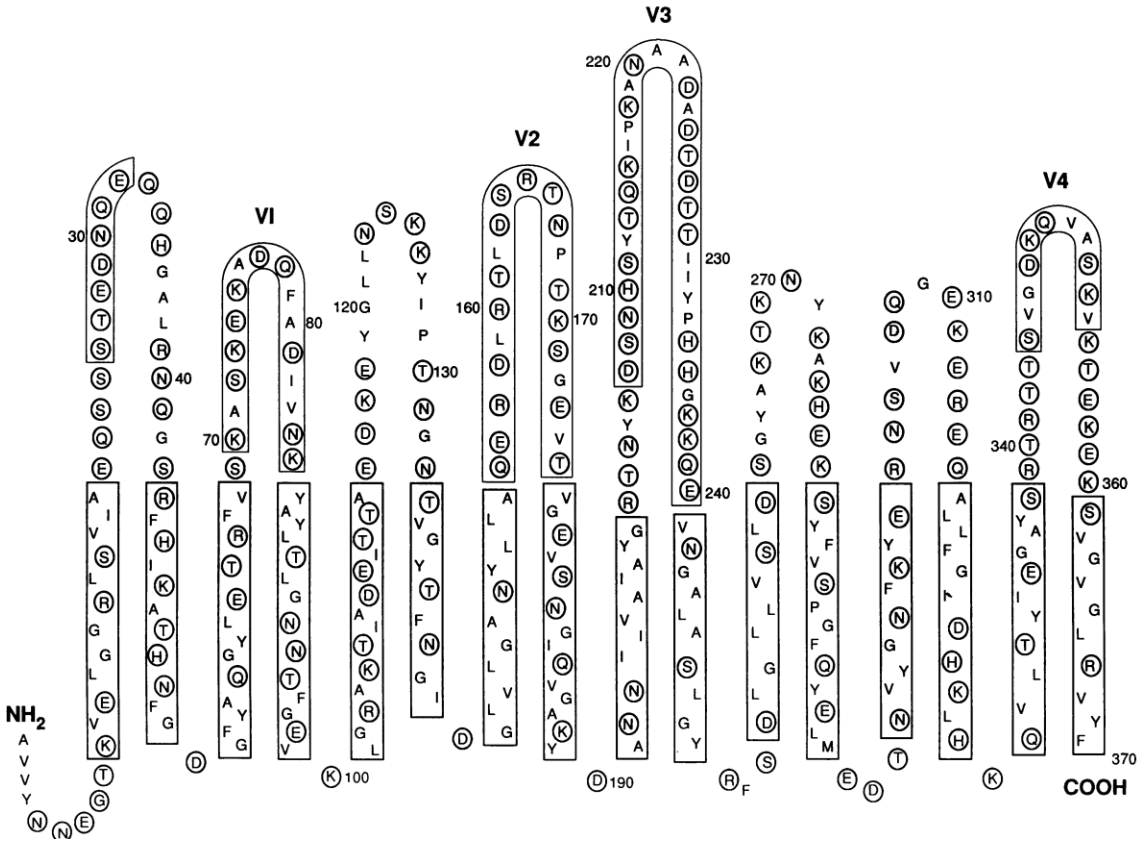

Figure 1.6. Schematic representation of *H. influenzae* OMP P2 secondary structure. (Reprinted with permission [94])

a)

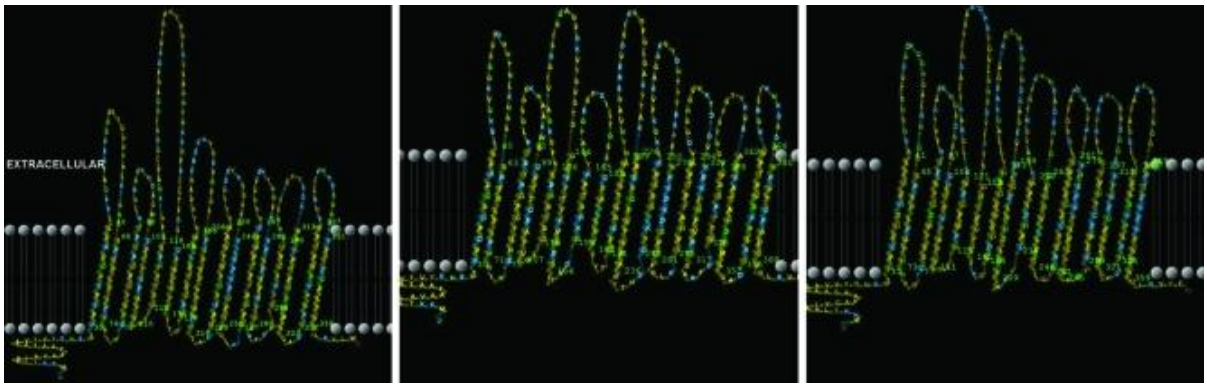

b)

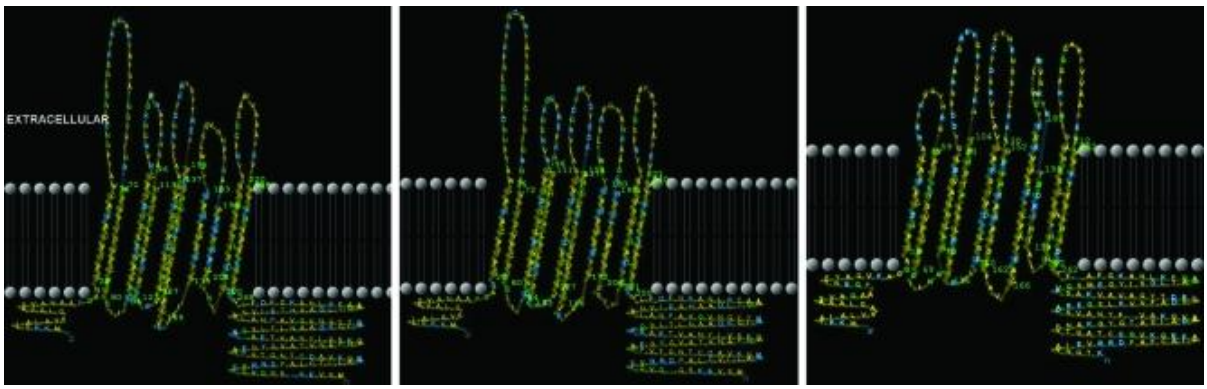

Figure 1.7. Schematic representation of *H. parasuis* OMP P2 (a) and P5 (b). a) *H. parasuis* strain 15677 with eight surface exposed loops (left); *H. parasuis* strain H465 (middle) with nine surface exposed loops; and, for comparison, *H. influenzae* strain Rd KW20 (right). b) P5 protein structural representations for *H. parasuis* strain NADC1 (left); *H. parasuis* strain D74 (middle); and, for comparison, *H. influenzae* strain Rd KW20 (right). All OMP P5 models shown have five surface exposed loops. (Reprinted with permission [77])

Amino acids	Variable sites[a]	amino acids (and nucleotides)[b]
1–20	X	
21–40	XX	
41–60	XXXXXXX	HV1: 41–69 (124–207)
61–80	XXX	
81–100	XX	HV2: 91–104 (274–312)
101–120	XX	
121–140	XX	
141–160	XXXXXXX	HV3: 141–160 (424–480)
161–180	XX	
181–200	XXXXXXXXX	
201–220	XXXXXX	HV4: 188–234 (565–702)
221–240	XX	
241–260	X	
261–280	X	
281–300	X	
301–320		
321–340		
341–360	X	
361–367		

[a] Each X represents a site with a variable amino acid.
[b] These regions encode the 4 putative surface-exposed loops of OmpA. The numbers outside the parentheses are based on the amino acid sequence of OmpA of a serovar 5 reference strain.

Figure 1.8. Variability of two-dimensional analysis of OMPA of *H. parasuis.* Distribution of sequence diversity along outer membrane protein A (OmpA), according to amino acid positions deduced from the *ompA* gene of 15 reference strains and 20 field isolates of *Haemophilus parasuis.* (Reprinted with permission [78])

References

1. K. Nedbalcova, P.S., Z. Jaglic, R. Ondriasova, Z. Kucerova, *Haemophilus parasuis and Glässer's disease in pigs: a review.* Veterinarni Medicina, 2006. **51**(5): p. 168-179.
2. Oliveira, S. and C. Pijoan, *Haemophilus parasuis: new trends on diagnosis, epidemiology and control.* Vet Microbiol, 2004. **99**(1): p. 1-12.
3. Harris, D.L., *Control of common infectious diseases. In: Multi-site pig production.* Iowa State University Press, 2000: p. 98-102.
4. Glasser, K., . Quoted in Krankenheinten des Schweines. 5th ed. , 1910. **1950**(Sharper, Hanover): p. 106.
5. Rubies, X., et al., *Prevalence of Haemophilus parasuis serovars isolated in Spain from 1993 to 1997.* Vet Microbiol, 1999. **66**(3): p. 245-8.
6. Oliveira, S., L. Galina, and C. Pijoan, *Development of a PCR test to diagnose Haemophilus parasuis infections.* J Vet Diagn Invest, 2001. **13**(6): p. 495-501.
7. Lewis, P.A. and R.E. Shope, *Swine Influenza : Ii. A Hemophilic Bacillus from the Respiratory Tract of Infected Swine.* J Exp Med, 1931. **54**(3): p. 361-71.
8. Biberstein, E.L. and D.C. White, *A proposal for the establishment of two new Haemophilus species.* J Med Microbiol, 1969. **2**(1): p. 75-8.
9. Kielstein, P., et al., *Phenotypic and genetic characterization of NAD-dependent Pasteurellaceae from the respiratory tract of pigs and their possible pathogenetic importance.* Vet Microbiol, 2001. **81**(3): p. 243-55.

10. Kielstein, P., H. Rosner, and W. Muller, *Typing of heat-stable soluble Haemophilus parasuis antigen by means of agargel precipitation and the dot-blot procedure.* Zentralbl Veterinarmed B, 1991. **38**(4): p. 315-20.

11. Tadjine, M., et al., *Development of a new serological test for serotyping Haemophilus parasuis isolates and determination of their prevalence in North America.* J Clin Microbiol, 2004. **42**(2): p. 839-40.

12. Rapp-Garielson, P.K.a.V.J., *Designation of 15 serovars of Haemophilus parasuis on the Basis of Immunodiffusion Using Heat-Stable Antigen Extract.* Journal of Clinical Microbiology, 1992. **30**(4): p. 862-865.

13. Weller, P.F., et al., *The role of encapsulation and host age in the clearance of Haemophilus influenzae bacteremia.* Journal of Infectious Diseases, 1977. **135**(1): p. 34-41.

14. Huber, P.S. and I.N. Egwu, *Capsular variation in experimental strains of Haemophilus influenzae.* Med Microbiol Immunol, 1985. **173**(6): p. 345-53.

15. Carlone, G.M., et al., *Potential virulence factors of Haemophilus influenzae biogroup aegyptius in Brazilian purpuric fever. The Brazilian Purpuric Fever Study Group.* Pediatr Infect Dis J, 1989. **8**(4): p. 245-7.

16. Wayoff, M. and R. Jankowski, *Virulence factors of Haemophilus influenzae.* J Chemother, 1989. **1**(4 Suppl): p. 26-8.

17. Wispelwey, B., et al., *Haemophilus influenzae virulence factors in experimental meningitis.* Pediatr Infect Dis J, 1989. **8**(12): p. 903-4.

18. Bishai, W.R., et al., *Characterization and virulence analysis of catalase mutants of Haemophilus influenzae.* Infect Immun, 1994. **62**(11): p. 4855-60.

19. Nizet, V., et al., *A virulent nonencapsulated Haemophilus influenzae.* Journal of Infectious Diseases, 1996. **173**(1): p. 180-6.

20. Rodriguez, C.A., et al., *Prevalence and distribution of adhesins in invasive non-type b encapsulated Haemophilus influenzae.* Infect Immun, 2003. **71**(4): p. 1635-42.

21. Hallstrom, T., et al., *Haemophilus influenzae surface fibrils contribute to serum resistance by interacting with vitronectin.* J Immunol, 2006. **177**(1): p. 430-6.

22. Forsgren, A., K. Riesbeck, and H. Janson, *Protein D of Haemophilus influenzae: a protective nontypeable H. influenzae antigen and a carrier for pneumococcal conjugate vaccines.* Clin Infect Dis, 2008. **46**(5): p. 726-31.

23. Rosadini, C.V., S.M. Wong, and B.J. Akerley, *The periplasmic disulfide oxidoreductase DsbA contributes to Haemophilus influenzae pathogenesis.* Infect Immun, 2008. **76**(4): p. 1498-508.

24. Mason, K.M., et al., *Heme utilization by nontypeable Haemophilus influenzae is essential and dependent on Sap transporter function.* J Bacteriol, 2011. **193**(10): p. 2527-35.

25. Hardy, G.G., S.M. Tudor, and J.W. St Geme, 3rd, *The pathogenesis of disease due to nontypeable Haemophilus influenzae.* Methods Mol Med, 2003. **71**: p. 1-28.

26. Ecevit, I.Z., et al., *Prevalence of the hifBC, hmw1A, hmw2A, hmwC, and hia Genes in Haemophilus influenzae Isolates.* J Clin Microbiol, 2004. **42**(7): p. 3065-72.

27. Hotomi, M., et al., *A recombinant P4 protein of Haemophilus influenzae induces specific immune responses biologically active against nasopharyngeal colonization in mice after intranasal immunization.* Vaccine, 2005. **23**(10): p. 1294-300.

28. Yeo, H.J., et al., *The structure of the Haemophilus influenzae HMW1 pro-piece reveals a structural domain essential for bacterial two-partner secretion.* J Biol Chem, 2007. **282**(42): p. 31076-84.

29. Munson, R., Jr., et al., *Outer membrane proteins P1 and P2 of Haemophilus influenzae type b: structure and identification of surface-exposed epitopes.* J Infect Dis, 1992. **165 Suppl 1**: p. S86-9.

30. Noel, G.J., D.C. Love, and D.M. Mosser, *High-molecular-weight proteins of nontypeable Haemophilus influenzae mediate bacterial adhesion to cellular proteoglycans.* Infect Immun, 1994. **62**(9): p. 4028-33.

31. Reilly, T.J., D.L. Chance, and A.L. Smith, *Outer membrane lipoprotein e (P4) of Haemophilus influenzae is a novel phosphomonoesterase.* J Bacteriol, 1999. **181**(21): p. 6797-805.

32. Reilly, T.J. and A.L. Smith, *Purification and characterization of a recombinant Haemophilus influenzae outer membrane phosphomonoesterase e (P4).* Protein Expr Purif, 1999. **17**(3): p. 401-9.

33. Munson, R.S., Jr. and D.M. Granoff, *Purification and partial characterization of outer membrane proteins P5 and P6 from Haemophilus influenzae type b.* Infect Immun, 1985. **49**(3): p. 544-9.

34. Munson, R.S., Jr., S. Grass, and R. West, *Molecular cloning and sequence of the gene for outer membrane protein P5 of Haemophilus influenzae.* Infect Immun, 1993. **61**(9): p. 4017-20.

35. Reddy, M.S., et al., *Binding between outer membrane proteins of nontypeable Haemophilus influenzae and human nasopharyngeal mucin.* Infect Immun, 1996. **64**(4): p. 1477-9.

36. Farley, M.M., et al., *Pathogenesis of IgA1 protease-producing and -nonproducing Haemophilus influenzae in human nasopharyngeal organ cultures.* J Infect Dis, 1986. **154**(5): p. 752-9.

37. Fink, D.L., et al., *The Haemophilus influenzae Hap autotransporter mediates microcolony formation and adherence to epithelial cells and extracellular matrix via binding regions in the C-terminal end of the passenger domain.* Cell Microbiol, 2003. **5**(3): p. 175-86.

38. Mistry, D.V. and R.A. Stockley, *The cleavage specificity of an IgA1 protease from Haemophilus influenzae.* Virulence, 2011. **2**(2): p. 103-10.

39. Vahle, J.L., J.S. Haynes, and J.J. Andrews, *Interaction of Haemophilus parasuis with nasal and tracheal mucosa following intranasal inoculation of cesarean derived colostrum deprived (CDCD) swine.* Can J Vet Res, 1997. **61**(3): p. 200-6.

40. Qiu, J., et al., *Human milk lactoferrin inactivates two putative colonization factors expressed by Haemophilus influenzae.* Proc Natl Acad Sci U S A, 1998. **95**(21): p. 12641-6.

41. St Geme, J.W., 3rd, M.L. de la Morena, and S. Falkow, *A Haemophilus influenzae IgA protease-like protein promotes intimate interaction with human epithelial cells.* Mol Microbiol, 1994. **14**(2): p. 217-33.

42. Mullins, M.A., et al., *Haemophilus parasuis exhibits IgA protease activity but lacks homologs of the IgA protease genes of Haemophilus influenzae.* Vet Microbiol, 2011.

43. Meng, G., et al., *Crystal structure of the Haemophilus influenzae Hap adhesin reveals an intercellular oligomerization mechanism for bacterial aggregation.* EMBO J, 2011. **30**(18): p. 3864-74.

44. Morozumi, T. and J. Nicolet, *Morphological variations of Haemophilus parasuis strains.* J Clin Microbiol, 1986. **23**(1): p. 138-42.

45. Rapp-Gabrielson, V.J., D.A. Gabrielson, and G.J. Schamber, *Comparative virulence of Haemophilus parasuis serovars 1 to 7 in guinea pigs.* Am J Vet Res, 1992. **53**(6): p. 987-94.

46. Munch, S., S. Grund, and M. Kruger, *Fimbriae and membranes on Haemophilus parasuis.* Zentralbl Veterinarmed B, 1992. **39**(1): p. 59-64.

47. Nicolet, J., *Overview of the virulence attributes of the HAP-group of bacteria.* Can J Vet Res, 1990. **54 Suppl**: p. S12-5.

48. Frandoloso, R., et al., *Haemophilus parasuis serovar 5 Nagasaki strain adheres and invades PK-15 cells.* Vet Microbiol, 2011.

49. Melnikow, E., et al., *Microarray analysis of Haemophilus parasuis gene expression under in vitro growth conditions mimicking the in vivo environment.* Vet Microbiol, 2005. **110**(3-4): p. 255-63.

50. Jin, H., et al., *Identification of genes transcribed by Haemophilus parasuis in necrotic porcine lung through the selective capture of transcribed sequences (SCOTS).* Environ Microbiol, 2008. **10**(12): p. 3326-36.

51. Xie, Q., et al., *Transcriptional responses of Haemophilus parasuis to iron-restriction stress in vitro.* Biometals, 2009. **22**(6): p. 907-16.

52. Wang, X., et al., *Identification and analysis of potential virulence-associated genes in Haemophilus parasuis based on genomic subtraction.* Microb Pathog, 2011. **51**(4): p. 291-6.

53. Zhou, M., et al., *A comprehensive proteome map of the Haemophilus parasuis serovar 5.* Proteomics, 2009. **9**(10): p. 2722-39.

54. Hansen, E.J., et al., *Immune enhancement of pulmonary clearance of nontypable Haemophilus influenzae.* Infect Immun, 1988. **56**(1): p. 182-90.

55. Webb, D.C. and A.W. Cripps, *Secondary structure and molecular analysis of interstrain variability in the P5 outer-membrane protein of non-typable Haemophilus influenzae isolated from diverse anatomical sites.* J Med Microbiol, 1998. **47**(12): p. 1059-67.

56. Duim, B., et al., *Molecular variation in the major outer membrane protein P5 gene of nonencapsulated Haemophilus influenzae during chronic infections.* Infect Immun, 1997. **65**(4): p. 1351-6.

57. Hill, D.J., et al., *The variable P5 proteins of typeable and non-typeable Haemophilus influenzae target human CEACAM1.* Molecular Microbiology, 2001. **39**(4): p. 850-62.

58. Sadarangani, M., A.J. Pollard, and S.D. Gray-Owen, *Opa proteins and CEACAMs: pathways of immune engagement for pathogenic Neisseria.* FEMS Microbiol Rev, 2011. **35**(3): p. 498-514.

59. Bookwalter, J.E., et al., *A carcinoembryonic antigen-related cell adhesion molecule 1 homologue plays a pivotal role in nontypeable Haemophilus influenzae colonization*

of the chinchilla nasopharynx via the outer membrane protein P5-homologous adhesin. Infect Immun, 2008. **76**(1): p. 48-55.

60. Brooks, M.J., et al., *Characterization of the Moraxella catarrhalis opa-like protein, OlpA, reveals a phylogenetically conserved family of outer membrane proteins.* J Bacteriol, 2007. **189**(1): p. 76-82.

61. Gray-Owen, S.D. and R.S. Blumberg, *CEACAM1: contact-dependent control of immunity.* Nat Rev Immunol, 2006. **6**(6): p. 433-46.

62. Gray-Owen, S.D., *Neisserial Opa proteins: impact on colonization, dissemination and immunity.* Scand J Infect Dis, 2003. **35**(9): p. 614-8.

63. Gray-Owen, S.D., et al., *CD66 carcinoembryonic antigens mediate interactions between Opa-expressing Neisseria gonorrhoeae and human polymorphonuclear phagocytes.* EMBO J, 1997. **16**(12): p. 3435-45.

64. Youssef, A.R., et al., *Opa+ and Opa- isolates of Neisseria meningitidis and Neisseria gonorrhoeae induce sustained proliferative responses in human CD4+ T cells.* Infect Immun, 2009. **77**(11): p. 5170-80.

65. Normark, S.e.a., *Gonococci cause immunosuppression by engaging a coinhibitory receptor on T lymphocytes.* Nature Immunology, 2002. **3**(3): p. 210-211.

66. Fedarovich, A., et al., *Structure of the N-terminal domain of human CEACAM1: binding target of the opacity proteins during invasion of Neisseria meningitidis and N. gonorrhoeae.* Acta Crystallogr D Biol Crystallogr, 2006. **62**(Pt 9): p. 971-9.

67. Novotny, L.A. and L.O. Bakaletz, *The fourth surface-exposed region of the outer membrane protein P5-homologous adhesin of nontypable Haemophilus influenzae is*

an immunodominant but nonprotective decoying epitope. J Immunol, 2003. **171**(4): p. 1978-83.

68. McVicker, J.K., *The identification and characterization of P5 and P2 colonization proteins of Haemophilus parasuis and the targeted binding of Carcinoembryonic Antigen (CEA)*, in *PhD Dissertation*2004, Iowa State University: Ames, IA.

69. Maike Voges, V.B., Robert Kammerer, Uri Gophna and Christof R Hauck, *CEACAM1 recognition by bacterial pathogens is species specific.* BMC Microbiology, 2010. **10**: p. 117-128.

70. Yi, K. and T.F. Murphy, *Importance of an immunodominant surface-exposed loop on outer membrane protein P2 of nontypeable Haemophilus influenzae.* Infect Immun, 1997. **65**(1): p. 150-5.

71. Yi, K. and T.F. Murphy, *Mapping of a strain-specific bactericidal epitope to the surface-exposed loop 5 on the P2 porin protein of non-typeable Haemophilus influenzae.* Microb Pathog, 1994. **17**(4): p. 277-82.

72. Neary, J.M. and T.F. Murphy, *Antibodies directed at a conserved motif in loop 6 of outer membrane protein P2 of nontypeable Haemophilus influenzae recognize multiple strains in immunoassays.* FEMS Immunol Med Microbiol, 2006. **46**(2): p. 251-61.

73. Neary, J.M., et al., *Antibodies to loop 6 of the P2 porin protein of nontypeable Haemophilus influenzae are bactericidal against multiple strains.* Infect Immun, 2001. **69**(2): p. 773-8.

74. Galdiero, S., et al., *Role of surface-exposed loops of Haemophilus influenzae protein P2 in the mitogen-activated protein kinase cascade.* Infect Immun, 2003. **71**(5): p. 2798-809.

75. Vitiello, M., et al., *P2 porin and loop L7 from Haemophilus influenzae modulate expression of IL-6 and adhesion molecules in astrocytes.* Microbiol Immunol, 2011. **55**(5): p. 347-56.

76. McVicker, J.K. and L.B. Tabatabai, *Isolation and characterization of the P5 adhesin protein of Haemophilus parasuis serotype 5.* Prep Biochem Biotechnol, 2006. **36**(4): p. 363-74.

77. Mullins, M.A., et al., *Characterization and comparative analysis of the genes encoding Haemophilus parasuis outer membrane proteins P2 and P5.* J Bacteriol, 2009. **191**(19): p. 5988-6002.

78. Tang, C., et al., *Characteristics of the molecular diversity of the outer membrane protein A gene of Haemophilus parasuis.* Can J Vet Res, 2010. **74**(3): p. 233-6.

79. Tian, H., et al., *Identification of the immunogenic outer membrane protein A (OmpA) antigen of Haemophilus parasuis using a proteomics approach and passive immunization of mice with monoclonal antibodies.* Clin Vaccine Immunol, 2011. **18**: p. 1695-1701.

80. Jin, H., S. Agarwal, and V. Pancholi, *Surface export of GAPDH/SDH, a glycolytic enzyme, is essential for Streptococcus pyogenes virulence.* MBio, 2011. **2**(3): p. e00068-11.

81. Dumke, R., M. Hausner, and E. Jacobs, *Role of Mycoplasma pneumoniae glyceraldehyde-3-phosphate dehydrogenase (GAPDH) in mediating interactions with the human extracellular matrix.* Microbiology, 2011. **157**(Pt 8): p. 2328-38.

82. Tunio, S.A., et al., *The role of glyceraldehyde 3-phosphate dehydrogenase (GapA-1) in Neisseria meningitidis adherence to human cells.* BMC Microbiol, 2010. **10**: p. 280.

83. Purves, J., et al., *Comparison of the regulation, metabolic functions, and roles in virulence of the glyceraldehyde-3-phosphate dehydrogenase homologues gapA and gapB in Staphylococcus aureus.* Infect Immun, 2010. **78**(12): p. 5223-32.

84. Brassard, J., M. Gottschalk, and S. Quessy, *Cloning and purification of the Streptococcus suis serotype 2 glyceraldehyde-3-phosphate dehydrogenase and its involvement as an adhesin.* Vet Microbiol, 2004. **102**(1-2): p. 87-94.

85. Alvarez, R.A., M.W. Blaylock, and J.B. Baseman, *Surface localized glyceraldehyde-3-phosphate dehydrogenase of Mycoplasma genitalium binds mucin.* Mol Microbiol, 2003. **48**(5): p. 1417-25.

86. Perez-Casal, J. and T. Prysliak, *Detection of antibodies against the Mycoplasma bovis glyceraldehyde-3-phosphate dehydrogenase protein in beef cattle.* Microb Pathog, 2007. **43**(5-6): p. 189-97.

87. Webster, R.G.a.W.G.L., *Influenza Virus Subunit Vaccines: Immunogenicity and Lack of Toxicity for Rabbits of Ether- and Detergent- Disrupted Virus.* The Journal of Immunology, 1966. **96**: p. 596-605.

88. Jackson, F.L.R.a.G.G., *A New Subunit Influenza Vaccine: Acceptability Compared with Standard Vaccines and Effect of Dose on Antigenicity.* The Journal of Infectious Diseases, 1972. **125**(6): p. 656-664.

89. Kunz, C., et al., *[A new influenza subunit vaccine: reactogenicity and antigenicity in comparison to split and whole virus vaccines (author's transl)]*. Infection, 1976. **4**(2): p. 73-9.

90. Tabatabai, L.B. and G.W. Pugh, Jr., *Modulation of immune responses in Balb/c mice vaccinated with Brucella abortus Cu-Zn superoxide dismutase synthetic peptide vaccine.* Vaccine, 1994. **12**(10): p. 919-24.

91. Nara, P.L., Garrity, R. , *Deceptive imprinting: a cosmopolitan strategy for complicating vaccination.* Vaccine, 1998. **16**(19): p. 1780-1787.

92. Tobin, G.J., et al., *Deceptive imprinting and immune refocusing in vaccine design.* Vaccine, 2008. **26**(49): p. 6189-99.

93. Muller, S., *Avoiding Deceptive Imprinting of the Immune Response to HIV-1 Infection in Vaccine Development.* International Reviews of Immunology, 2004. **23**: p. 423-426.

94. Sikkema, D.J. and T.F. Murphy, *Molecular analysis of the P2 porin protein of nontypeable Haemophilus influenzae.* Infect Immun, 1992. **60**(12): p. 5204-11.

CHAPTER 2. IDENTIFICATION OF IMMUNOREACTIVE OUTER MEMBRANE PROTEINS OF *Haemophilus parasuis* TO THE MONOCLONAL ANTIBODY FOR OMP P5 OF *Haemophilus influenzae*

A paper to be submitted to *Proteomics*

Mandy K. Zimmerli and Louisa B. Tabatabai

Abstract

Haemophilus parasuis, a gram negative organism, is the causative agent of Glässer's disease in swine. Symptoms include polyserositis, meningitis, lameness, and arthritis. Because this organism causes significant economic loss in the swine industry, the need to identify proteins responsible for virulence is crucial. In this study, a monoclonal antibody for the P5 protein of *H. influenzae* was used to identify immunoreactive outer membrane proteins of *H. parasuis* reference serovars 2, 3, 5, 6, 7, 8, and 13, and two field isolates. Following 2-D SDS-PAGE analysis, gel plugs were subjected to trypsin digestion and analyzed by tandem mass spectrometry. Identities were confirmed in Scaffold using both Mascot and X! Tandem databases. Identified proteins include: OMP P2, TRAP solute transporter, glucose-specific PTS system enzyme IIA, acetyl-CoA carboxylase biotin carboxylase subunit, purine nucleoside phosphorylase, chelated iron ABC transporter, probable sugar isomerase, Mn-dependent superoxide dismutase, putative iron ABC transporter, D-ribose transporter, alanine aminotransferase, phosphoribosylglycinamide formyltransferase, FbpA, and hypothetical proteins HPS 06844 and HPS 10240. The functional role of these proteins will be discussed, including notable links to virulence.

Introduction

Haemophilus parasuis is the causative agent of a swine respiratory illness known as Glässer's disease [1-3]. This disease presents with symptoms of arthritis, lameness, pleuritis,

meningitis, and polyserositis and is responsible for significant economic loss in the swine industry. To date, there is no commercially available cross-protective vaccine or diagnostic for Glässer's disease. Because of this, the identification of virulence factors as well as an overall understanding of what gives rise to virulence for *H. parasuis* is crucial. Since *H. parasuis* colonization is not always linked to morbidity, the proteomic comparisons of serovars can provide insight into mechanism of virulence of the individual serovars to determine what distinguishes an avirulent strain from a highly virulent strain.

A variety of genetic profiling methods have been performed on *H. parasuis,* but only one proteomic profile has been published [4-10]. The original intent of this study was to probe for the P2 and P5 colonization factors as they are important virulence factors in *H. influenzae* [11-26]. However, tandem mass spectrometry identified the P2 colonization factor along with other proteins, including putative virulence factors. The results of this study provide the first proteomic profiling of immunoreactive proteins to the anti-P5 (4BF8) monoclonal antibody and provide insight into virulence factors that deserve further characterization to assist in elucidating the role of these proteins in virulence of *H. parasuis*.

Material and Methods

Bacterial strains. Nine *Haemophilus parasuis* strains were studied. Seven of the strains were reference strains obtained from Richard Ross (College of Veterinary Medicine, Iowa State University, Ames, IA). The remaining two strains were field isolates provided by Vicki Rapp-Gabrielson (Schering-Plough, Omaha, NE). The anatomic and geographic origins of these strains are reported in Table 2.1. Strains were grown on Casman agar, supplemented with 5% horse serum (Gibco-BRL, Carlsbad, CA), and overlaid with 0.016% NAD (Sigma Chemical Co., St. Louis, MO) using 5% CO_2 at 37°C. Colonies were selected and grown in a

liquid media consisting of Freys medium (Sigma Chemical Co., St. Louis, MO) supplemented with 20% horse serum (Gibco-BRL, Carlsbad, CA) and 0.016% NAD (Sigma Chemical Co., St. Louis, MO). Tubes were incubated aerobically with shaking (100 rpm) at 37ºC for 24 h. Five mL of inoculum were used to inoculate 100-mL Freys medium. Cultures were incubated with shaking (100 rpm) for 24 h at 37ºC and harvested by centrifugation at 7,500 ×*g* at 4ºC.

Outer membrane protein extraction. Cells were resuspended and washed in 20 mM 4-(2-hydroxyethyl)piperizane-1-ethanesulfonic acid (HEPES) buffer pH 7.4-0.15 M sodium chloride. Cells were resuspended again in 20 mM HEPES buffer pH 7.4-0.45 M sodium chloride and heated at 56ºC for 60 minutes followed by centrifugation at 10,000 × *g* at 4ºC. The protein-containing supernatant was stored at -80ºC until use. Protein concentration was determined using the BCA Assay (Sigma, St. Louis, MO).

2-D SDS PAGE and immunoblotting. 100 micrograms of protein was loaded onto an IPG strip (pH 3-10) according to the Zoom IPGRunner protocol by Invitrogen (Carlsbad, CA). The IPG strip was placed into the well of a Novex 4-12% Bis-Tris Zoom Gel, IPG well (Invitrogen, Carlsbad, CA). Samples were run according to the manufacturer's instructions, stained with Coomassie Blue R250, or transferred electrophoretically to 0.45-µm nitrocellulose (Schleicher and Schuell, Keene, NH) or polyvinyledene diflouride (PVDF) (Millipore, Billerica, MA) for immunoblotting. Immunoblots were blocked with 0.25% fish gelatin in wash buffer consisting of 1.5 mM KH_2PO_4, 20 mM Na_2HPO_4, 125 mM NaCl, 3 mM KCl, 0.05% Tween-20 (PBST, pH=7.2). The blocked membranes were incubated with 1:5,000 dilutions of anti-P5 monoclonal antibody (4BF8), and 1:5,000 dilutions of rabbit anti-mouse IgG horseradish peroxidase-labeled (Jackson ImmunoResearch, West Grove, PA)

sequentially. Blots were developed with 3,3',5,5'-tetramethylbenzidine (TMB) (Kirkegaarde and Perry Labs, Gaithersburg, MD) as the substrate.

Identification and characterization of immunoreactive proteins. Protein spots corresponding to the immunoreactive proteins were removed from the gel with a 16-gauge needle, digested with trypsin, and subjected to MALDI MS/MS and/or ESI MS/MS on a Qstar XL (Applied Biosystems, Foster City, CA) at the Proteomics Facility (Plant Science Institute, Iowa State University, Ames, IA). Tandem mass spectra were extracted, charge state deconvoluted and deisotoped by Analyst QS version 2.0. All MS/MS samples were analyzed using Mascot (Matrix Science, London, UK; version Mascot) and X! Tandem (The GPM, thegpm.org; version 2007.01.01.1). X! Tandem was set up to search NCBInr_20110624 database (selected for Proteobacteria, 3981880 entries). Mascot and X! Tandem were searched with a fragment ion mass tolerance of 0.60 Da and a parent ion tolerance of 1.2 Da. Iodoacetamide derivative of cysteine was specified in Mascot and X! Tandem as a fixed modification. Oxidation of methionine was specified in Mascot and X! Tandem as a variable modification. A reverse database was created in order to rule out false positives for each sample. Moreover, a subset database was used to search unidentified spectra in each sample against previously identified proteins. Scaffold (version Scaffold_3.1.4.1, Proteome Software Inc., Portland, OR) was used to validate MS/MS based peptide and protein identifications. Peptide identifications were accepted if they could be established at greater than 80% probability as specified by the Peptide Prophet algorithm [27]. Protein identifications were accepted if they could be established at greater than 80% probability and contained at least one identified peptide. Protein probabilities were assigned by the Protein Prophet algorithm [28]. Proteins that contained similar peptides and could not

be differentiated based on MS/MS analysis alone were grouped to satisfy the principles of parsimony. The Expasy Compute pI/Mw tool was used to determine the expected molecular weight and pI for identified proteins. Proteins were subjected to sequence/structural-based alignment to OMP P5 of *H. influenzae* Rd KW20 (Accession number: 1171899) using Expresso (TCoffee; [29, 30]).

Results

Identification of immunoreactive proteins of *H. parasuis* to anti-P5 antibody. 2-D SDS-PAGE and corresponding anti-P5 immunoblots are shown in Figures 2.1-2.11. Circled spots on the gel indicate the gel plug removed for tandem mass spectrometry analysis. Tables 2.2-2.10 provide an overview of protein spot identification, Mascot and X! Tandem scores along with identified peptides. Scaffold predicted a 3.2% protein false discovery rate and 0.4% peptide false discovery rate. Detailed information about the identity of the proteins and corresponding peptides is located in Supplementary Figures S2.10-S2.46. In order to identify false positives, fold-change analysis of the forward and reverse database search was performed on the normalized spectral counts for each identified protein. Proteins of significant difference were removed from identification as they were considered false positives. The results of this analysis can be viewed in Supplementary Figures S2.1-S2.9. Additionally, the normalized spectral count of the subset database was compared to both the forward and reverse, with no significant difference noted for the proteins identified here. Since proteins identified by multiple databases are considered highly probable, both Mascot and X! Tandem were used for data analysis in this study.

Table 2.11 shows the comparison of experimentally determined pIs and molecular weights to calculated pI and molecular weights for the identified immunoreactive proteins.

Deviation from calculated molecular weight and pI are noted for: TRAP solute transporter in HP2, OMP P2 in HP2 and HP5, alanine aminotransferase for HP7, phosphoribosylglycinamide formyltransferase for HP3 and HP6 and acetyl-CoA carboxylase biotin carboxylase and hypothetical protein HPS_10240 for HP6.

Identification of a common epitope for anti-P5 antibody 4BF8. Using Expresso, the sequence and structural alignment to the OMP P5 of *H. influenzae* was performed. Results indicated that while there was sequence and structural overlap, that common epitopes could not be elucidated based upon this information. Sequence and structural alignment of OMP P5 with D-ribose transporter RbsB, FbpA, hypothetical protein HPS_10240, and phosphoribosylglycinamide formyltransferase are presented in Supplementary Figures S2.47-S2.50.

Discussion

The exact epitope of monoclonal antibody 4BF8 is unknown. Previous studies have shown that it cross-reacts with proteins other than *H. influenzae* OMP P5 [31]. This could be due to the nature of analysis as denaturing conditions have been shown to affect recognition of epitopes. Since the outer membrane loops of OMP P5 are highly variable, it is hypothesized this monoclonal antibody reacts with conserved transmembrane domains [31-33]. Previous work on the characterization of *H. parasuis* OMP P5 indicated a pI of approximately 5.5 and an apparent molecular weight of 32 kDa [34]. The P2 protein was predicted to have a molecular weight of 48-55kDa [31]. Given this information, gel plugs with these characteristics were analyzed by tandem mass spectrometry following 2-D SDS-PAGE immunoblots. Attempts to elucidate common epitopes for the identified proteins and

OMP P5 were unsuccessful. Nevertheless, while probing for P2 and P5 proteins of *H. parasuis*, other proteins were identified in addition to the colonization factor P2.

One of the limitations of identification of proteins based upon tandem mass spectrometry methods is the availability of information of proteins for an organism in the database. Because the genome of *H. parasuis* was not sequenced until 2008 and limited information is available on the expressed protein profiles of *H. parasuis*, the peptide and protein probability scores were set for 80%, and only one peptide was required for identification in this experiment. However, most proteins presented here were identified with two or more peptides with a Mascot ion score greater than 56 which indicates identity or extensive homology of the peptide.

Another limitation of this method of identification is the database search algorithm. Both Mascot and X! Tandem algorithms were used for identification. Peptide parent ion spectra that were identified more than once in the same sample were compared to ensure the same y and b ion profiles as this verifies the presence of that particular peptide. Additionally, given the nature of the instrumentation, one would expect primarily y ions upon sequencing of the parent ion spectrum.

Comparison of the fold-change of the forward and reverse databases ruled out false positives, and none of the proteins presented here were identified to be false positives. Moreover, a subset database of identified proteins was created for each sample. The unmatched spectra were compared to this database to deepen the search for each protein and identify additional peptides or confirm, based on the y and b ion spectral profiles, the identity of the protein.

As presented in Table 2.11, most of the proteins identified here did not deviate from the calculated molecular weight and pI. Since ion scores of the peptides were consistent with identity or homology, it is likely a homologous protein exists to those identified. A conserved domain may be shared or a shift in either the pI or molecular weight could result from post-translational modification. The method of outer membrane extraction used in this study has been shown to isolate glycosylated proteins [35]. A shift in apparent molecular weight of the P2 protein in denaturing conditions has been observed in previous work, and this shift is correlated with virulence [31].

Virulence factors in organisms related to *H. parasuis* include: capsulation, fimbrae, pili, secreted molecules and proteins, and the outer membrane proteins [36-47]. Major outer membrane proteins that have been identified in *H. influenzae* include the major outer membrane proteins P1, P2, P4, P5, and P6, and the surface exposed high molecular weight proteins (HMW1 and HMW2) [25, 26, 43, 48-56]. In addition to these membrane proteins, accessory proteins implicated in virulence in family *Pasteurellaceae* include: OapA (opacity associated protein), IgA1 protease, and Hap (*Haemophilus* adhesion protein) [48, 57-59]. Iron acquisition proteins and surface-localized proteins involved with colonization are also of consideration as virulence factors.

The OMP P2 of *H. parasuis* was identified in this study for HP2 and HP5, and its role in virulence as a colonization factor has been well documented in *H. influenzae* [12, 13, 18-20, 60-64]. Genetic analysis of *H. parasuis* OMP P2 indicates that variability does exist for surface exposed epitopes [65]. In addition to P2, iron-acquisition proteins were also identified. *H. parasuis*, like other members of the *Pasteurellaceae* family, acquires iron in a siderophore-independent manner [66-71]. Ferric binding protein A (FbpA) was identified in

serovar 5 for both the reference strain, HP5, and serovar 5 field isolate, HPIA84-29755. This protein is involved with transporting iron from the cell exterior to the cytosol and its functional role as well as its role as virulence factor has been studied in a variety of gram-negative pathogens [72-87]. In addition to FbpA, a chelated iron ABC transporter was identified for HP3, HP5, HP6, HP8, HP13, and HP2170B. Genomic subtraction comparing the Nagasaki strain and avirulent *H. parasuis* serovar has identified an ABC transporter, in addition to iron acquisition genes, as a putative virulence factor [4]. The chelated iron ABC transporter presented here is similar to phosphoribosylglycinamide formyltransferase of *H. parasuis*, an enzyme involved in *de novo* purine nucleoside biosynthesis. Based on the data presented here, absolute identification of this protein cannot be made. However, previous proteomic studies using the Nagasaki strain suggests this protein is located in the intracellular or excreted proteome fraction [6]. Additional ABC transporters were identified for HP8, HP13, and HPIA. ABC transporters are involved with the import of solutes, including iron and other essential transition metals, and the export of the O-antigenic polysaccharide portion of lipopolysaccharide (LPS) for gram-negative organisms [88-106]. The ABC transporter identified for HP8 is implicated with the transport of D-ribose. A D-ribose transporter was also identified for HP3, HP5, HP13, and HP2170B, and a TRAP solute receptor was identified for HP2. In addition to colonization, iron acquisition and the uptake of solutes, the secretion of toxins and proper protein folding of surface-localized proteins plays an important role in bacterial pathogenesis. The thiol:disulfide interchange protein, identified in HP5, facilitates the correct folding of secreted or surface-exposed toxins and adherence factors as well as components of the type III secretory pathway. [6, 107-115]. Evasion of the host's immune response is an additional role in bacterial survival. A Mn-SOD was identified in

HP8. This enzyme is involved with bacterial survival in the phagosome by catalyzing the conversion of the highly reactive oxygen species superoxide to hydrogen peroxide [116-119]. The formation of biofilm is another mode of bacterial pathogenesis. The glucose-specific PTS enzyme IIA is a component of a highly conserved phosphotransferase system (PTS) that participates in the phosphorylation of carbohydrates and ultimately mediates the formation of a biofilm in an environment that is suitable for surface association [114].

Aside from traditional putative virulence factors, other proteins presented as immunoreactive to the anti-P5 antibody. Purine nucleoside phosphorylase (PNP), an enzyme associated with the nucleotide-salvage pathways, was identified in HP2, HP3, and HP8. Although not a traditionally associated virulence factor, studies have indicated it is a potential drug target, and it was found to be surface localized in *Streptococcus agalactiae* [120, 121]. A probable sugar isomerase was identified in HP2 and HP3. This protein is similar to L-ribulose-5-phosphate-4-epimerase of *H. parasuis*, an enzyme that catalyzes the isomerization of L-ribulose 5-phosphate to D-xylulose 5-phosphate. Alanine aminotransferase was identified for HP7, and an enzyme associated with lipid biosynthesis, acetyl-coA carboxylase biotin carboxylase was identified for HP6. Hypothetical proteins of unknown function include: HPS_06844 identified for HP5 and HP13, and HPS_10240 identified for HP6. While traditional virulence factors are often explored as a vaccine and diagnostic candidates, the characterization of these proteins should not be overlooked. It is possible that epitopes of these proteins are surface localized and assist in colonization. Surface-localized glyceraldehyde-3-phosphate dehydrogenase is an example of a highly conserved surface-localized protein that functions as a colonization factor [122-128].

Overall, the work presented here provides the first proteomic identification of *H. parasuis* outer membrane proteins that are immunoreactive to the mAb to *H. influenzae* OMP P5. Moreover, this study identified putative virulence factors including the OMP P2, chelated iron ABC transporter, ABC transporters, FbpA, thiol:disulfide interchange protein and Mn-SOD. As more information is made available to the *H. parasuis* proteome, additional identifications can be made particularly for those proteins that deviated from predicted pI and molecular weight. Future work involves the characterization of identified proteins, to resolve whether these proteins are indeed surface localized, to determine if modifications exist that account for the shift in expected pI and calculated molecular weights, and to explore the use of the proteins or subunits of the protein in preparation of a vaccine and diagnostic for Glässer's disease.

Acknowledgements

We would like to thank Muriel van Schilfgaarde for the mAb (4BF8) to OMP P5 of *H. influenzae*; the ISU Protein Facility for assistance with 2-D electrophoresis; Siquan Luo from the Iowa State Proteomics Facility for his assistance with ESI and MALDI MS/MS; and Jana Lee for her assistance with Scaffold.

Tables

Table 2.1. Description of bacterial strains

Serovar	Reference[a] strain	Country of origin	Diagnosis/ isolation site	Virulence[b]
Reference strains				
2	SW140	Japan	Healthy/nose	L
3	SW114	Japan	Healthy/nose	A
5	Nagasaki	Japan	Septicemia/meninges	H
6	131	Switzerland	Healthy/nose	A
7	174	Switzerland	Healthy/nose	A
8	C5	Sweden	Unknown	L
13	84-17975	United States	Unknown/lung	H
Field strains				
5	IA84-29755	United States	Unknown/lung	H
4	2170B	United States	Joint	L

[a] Reference strain information and virulence scores obtained from reference 13.

[b] Virulence designations: H, high virulence; L, moderate/low virulence; A, avirulent.

Table 2.2. Identification of immunoreactive proteins from HP2

Sample ID	Protein name	Accession number	Protein ID[a]	X! Tandem Score[b]	Peptides[c]	Ion Score[d]
HP2-1	purine nucleoside phosphorylase	167855453	95	4.60	(K)YIAETFLENAEQVTNVR(N)	106.6
HP2-2	probable sugar isomerase	167853152[e]	98	1.72	(K)KPSSDTPTHLELYR(Q)	56.5
HP2-3	TRAP solute receptor	167855254	99	N/A	(R)AVFSIHPEPFTVMAR(T)	69.4
HP2-4	OMP P2	167854978[f]	72	N/A	(K)HNINENLYGFGR(Y)	47

[a]Percent probability determined by Scaffold

[b]Scores are reflected –log (e) value

[c]Peptides identified using Scaffold; termini are indicated in parenthesis

[d]Mascot Ion scores >52 indicate identity or extensive homology ($p<0.05$)

[e]Similar protein: L-ribulose-5-phosphate 4-epimerase [*Haemophilus parasuis* SH0165], gi|219692070

[f]Scaffold probability predicated at 72% based on preliminary Mascot search

Table 2.3. Identification of immunoreactive proteins from HP3

Sample ID	Protein name	Accession number	Protein ID[a]	X! Tandem Score[b]	Peptides[c]	Ion Score[d]
HP3-1	Purine nucleoside phosphorylase	167855453	98	N/A	(K)YIAETFLENAEQVTNVR(N)	127.1
HP3-2	Probable sugar isomerase	167855696	99	N/A 1.89	(K)KPSSDTPTHLELYR(Q) (R)QFPEIGGVVHTHSR(H)	75 53.3
HP3-3	Phosphoribosyl-glycinamide formyltransferase	167855535[e]	100	5.41 2.24 N/A	(K)DKPAVVVTEGIEPISIYEGPYK (D) (R)YGGVLYVDSLSTK(D) (K)NALIYIENIR(Q)	102.1 52.6 63.4
HP3-4	D-ribose transporter RbsB	167852756	98	N/A N/A	(K)AVFAQNDEMALGALR(A) (K)VIQLEGIAGTSAAR(E)	58.3 58.3
HP3-5	Phosphoribosyl-glycinamide formyltransferase	167853336[e]	99	N/A	(R)WLVTSEGAFSYLAR(D)	63.5
HP3-6	Phosphoribosyl-glycinamide formyltransferase	167855535[e]	99	N/A N/A	(K)NALIYIENIR(Q) (R)WLVTSEGAFSYLAR(D)	60.4 85.4

[a]Percent probability determined by Scaffold

[b]Scores are reflected –log (e) value

[c]Peptides identified using Scaffold; termini are indicated in parenthesis

[d]Mascot Ion scores >52 indicate identity or extensive homology ($p<0.05$)

[e]Similar protein: chelated iron ABC transporter periplasmic-binding protein [*Haemophilus parasuis* SH0165], gi|219691491

Table 2.4. Identification of immunoreactive proteins from HP5

Sample ID	Protein name	Accession number	Protein ID[a]	X! Tandem Score[b]	Peptides[c]	Ion Score[d]
HP5-1	Thiol:disulfide interchange protein	167852909[e]	63	N/A N/A	(K)QYHVDFLGR(Q) (K)QTQAAEEFKVR(G)	44 29
HP5-2	D-ribose transporter RbsB	167856115	100	N/A 1.70 1.10	(K)AVFAQNDEMALGALR(A) (K)VIQLEGIAGTSAAR(E) (K)NILVVGFDGTDDAVK(A)	101.9 84.2 62.2
HP5-3	FbpA	167853466[f]	98	N/A	(K)LVDEVKFDDFGAK(-)	74.2
HP5-4	OMP P2	299773319	100	1.77 2.57 4.15 N/A	(K)ATAHQFMLGADYK(L) (K)QDVIGDSIGQAGFDK(V) (K)YVNAPFTVAVDGGHGVEK(T) (K)HNINENLYGFGR(Y)	53 69.4 53.8 61.5
HP5-5	D-ribose transporter RbsB	167856115	100	N/A N/A N/A	(K)AVFAQNDEMALGALR(A) (K)VIQLEGIAGTSAAR(E) (K)NIPVITLDR(G)	64 59.1 63.3
HP5-6	Phosphoribosyl-glycinamide formyltransferase	16785553[g]	100	N/A N/A N/A	(R)WLVTSEGAFSYLAR(D) (K)ELYLWAINQDEQGTPK(Q) (K)NALIYIENIR(Q)	85.6 53.9 65.8
HP5-7	Phosphoribosyl-glycinamide formyltransferase	16785553[g]	100	N/A N/A	(K)NALIYIENIR(Q) (R)WLVTSEGAFSYLAR(D)	55.5 80.3
HP5-8	hypothetical protein HPS_06844	16785375[h]	77	N/A N/A N/A N/A N/A	(R)FHQTNLGR(L) (K)LGNPDVTENVVFNDPIK(T) (K)FPFISANVINK(K) (R)FTVLHVNDTHGHFWK(N) (K)ELIDYLNVVALK(E)	36 37 30 31 21

[a]Percent probability determined by Scaffold

[b]Scores are reflected –log (e) value

[c]Peptides identified using Scaffold; termini are indicated in parenthesis

[e]Scaffold probability predicted at 63% based on preliminary Mascot search

[f]Similar protein: periplasmic iron-binding protein [*Haemophilus parasuis* SH0165], gi|219691519

[d]Mascot Ion scores >52 indicate identity or extensive homology ($p<0.05$)

[g]Similar protein: chelated iron ABC transporter periplasmic-binding protein [*Haemophilus parasuis* SH0165], gi|219691491

[h]Scaffold probability predicted at 72% based on preliminary Mascot search; Similar protein: bifunctional UDP-sugar hydrolase/5'-nucleotidase periplasmic [*Haemophilus parasuis* SH0165], gi|219690922

Table 2.5. Identification of immunoreactive proteins from HP6

Sample ID	Protein name	Accession number	Protein ID[a]	X! Tandem Score[b]	Peptides[c]	Ion Score[d]
HP6-1	glucose-specific PTS system enzyme IIA	219871157[e]	100	3.29	(K)LSGEVVAGESTVLVLTK(-)	47.7
				7.12	(K)SVLTPVVISNMDEVTNLQK(L)	71.8
				3.74	(K)IGTDLLVAAGTIEPR(Y)	57
HP6-2	acetyl-CoA carboxylase biotin carboxylase subunit	219871451	95	4.44	(K)AILVNDGEAVEFDQK(L)	122.4
HP6-3	Phosphoribosyl-glycinamide formyltransferase	167855535[f]	100	4.49	(K)AVVESITKPGAEIHDYQPTPQDIVK(A)	54.7
				8.44	(K)DKPAVVVTEGIEPISIYEGPYK(D)	112.2
				3.85	(K)DKPNPHAWMSTK(N)	67.2
				8.57	(K)HQIPVVFSESTISDKPAK(Q)	100.4
				3.23	(R)KHQIPVVFSESTISDKPAK(Q)	24.9
				7.72	(K)VVTTFTVIQDIAQNVAGDK(A)	103.7
				4.23	(K)YDPANAEAYNANAK(A)	74.9
				5.19	(R)YGGVLYVDSLSTK(D)	67.9
HP6-4	Phosphoribosyl-glycinamide formyltransferase	167855535[f]	100	2.24	(K)NALIYIENIR(Q)	63.2
				1.21	(R)YGGVLYVDSLSTK(D)	44.9
HP6-5	hypothetical protein HPS_10240	167855017	100	2.25	(K)DGGYDVIAPSNYFVSK(M)	45.2
				1.28	(K)DLNPDWLNKPYDK(G)	69.7
				3.15	(R)EGMLMELDHSKLPVIK(D)	55.9
				2.15	(K)LTLEIGYPTSNVK(A)	50.3
				3.11	(K)VVVSSLESNETMYAK(L)	55.8
				2.42	(K)LINYLLSAPVAEK(L)	44.2

[a]Percent probability determined by Scaffold

[b]Scores are reflected –log (e) value

[c]Peptides identified using Scaffold; termini are indicated in parenthesis

[d]Mascot Ion scores >52 indicate identity or extensive homology ($p<0.05$)

[e]Similar protein: putative PTS IIA-like nitrogen-regulatory protein PtsN [*Actinobacillus succinogenes* 130Z], gi|150839648

[f] Similar protein: chelated iron ABC transporter periplasmic-binding protein [*Haemophilus parasuis* SH0165], gi|219691491

Table 2.6. Identification of immunoreactive proteins from HP7

Sample ID	Protein name	Accession number	Protein ID[a]	X! Tandem Score[b]	Peptides[c]	Ion Score[d]
HP7-1	alanine aminotransferase	167854835	100	N/A 4.89	(K)ALSDEEKALLDER(K) (K)DGNAADITEEILVAMGGK(M)	59.6 94.3

[a]Percent probability determined by Scaffold

[b]Scores are reflected –log (e) value

[c]Peptides identified using Scaffold; termini are indicated in parenthesis

[d]Mascot Ion scores >52 indicate identity or extensive homology ($p<0.05$)

Table 2.7. Identification of immunoreactive proteins from HP8

Sample ID	Protein name	Accession number	Protein ID[a]	X! Tandem Score[b]	Peptides[c]	Ion Score[d]
HP8-1	Mn-dependent SOD	299773433	95	1.14	(K)LSVVSTANQDSPLMGK(A)	53.8
HP8-2	purine nucleoside phosphorylase	167855453	100	1.47 4.01 3.23	(K)ALTICTVSDHIR(T) (K)LREVIIGVGACTDSK(V) (K)YIAETFLENAEQVTNVR(N)	48.1 55.8 119.5
HP8-3	D-ribose transporter periplasmic-binding compoent RbsB	219871818[e]	100	3.80 3.26 1.22 3.68 2.30 2.68	(R)GVAGIVLAASDPVALVPAVR(K) (K)IVAVGFDGNSDLQNFVR(D) (K)SANSTFWQNVR(K) (K)VAVMSFTQGAASAIER(T) (K)YYQSFLATDNR(A) (K)VTFQGPESETAIDAQVNMVDNAVNR(G)	54.7 112.2 67.2 100.4 24.9 103.7
HP8-4	Phosphoribosyl-glycinamide formyltransferase	167855535[f]	100	2.85 1.38 2.21 1.38	(K)NALIYIENIR(Q) (R)YGGVLYVDSLSTK(D) (K)DKPAVVVTEGIEPISIYEGPYK(D) (K)YDPANAEAYNANAK(A)	58 64 55.7 56.6

[a]Percent probability determined by Scaffold

[b]Scores are reflected –log (e) value

[c]Peptides identified using Scaffold; termini are indicated in parenthesis

[d]Mascot Ion scores >52 indicate identity or extensive homology ($p<0.05$)

[e]Similar protein: periplasmic binding protein/LacI transcriptional regulator [*Haemophilus parasuis* 29755], gi|167852947

[f]Similar protein: chelated iron ABC transporter periplasmic-binding protein [*Haemophilus parasuis* SH0165], gi|219691491

Table 2.8. Identification of immunoreactive proteins from HP13

Sample ID	Protein name	Accession number	Protein ID[a]	X! Tandem Score[b]	Peptides[c]	Ion Score[d]
HP13-1	D-ribose transporter subunit RbsB	167856115	100	2.03 1.36 N/A	(K)NILVVGFDGTDDAVK(A) (K)VIQLEGIAGTSAAR(E) (K)AVFAQNDEMALGALR(A)	37.9 40.0 63.5
HP13-2	D-ribose transporter subunit RbsB	167856115	91	N/A	(K)AVFAQNDEMALGALR(A)	63.5
HP13-3	Phosphoribosyl-glycinamide formyltransferase	167855535[e]	100	1.19 1.47	(K)NALIYIENIR(Q) (R)WLVTSEGAFSYLAR(D)	53.9 77.8
HP13-4	Phosphoribosyl-glycinamide formyltransferase	167855535[e]	100	1.19 1.47	(K)NALIYIENIR(Q) (R)WLVTSEGAFSYLAR(D)	55.2 79.5
HP13-5	Phosphoribosyl-glycinamide formyltransferase	167855535[e]	97	60.6	(R)WLVTSEGAFSYLAR(D)	60.6
HP13-6	ABC transporter, periplasmic binding protein	167855391[f]	100	1.85 2.60	(K)AINIIAEEAALYPIIHR(K) (R)VQAIENVPYLDADR(L)	85.5 50.3
HP13-7	hypothetical protein HPS_06844	167855124[g]	93	N/A	(R)FTVLHVNDTHGHFWK(N)	65.5
HP13-8	hypothetical protein HPS_06844	167855124[g]	55	N/A	(R)FTVLHVNDTHGHFWK(N)	51.5

[a]Percent probability determined by Scaffold

[b]Scores are reflected –log (e) value

[c]Peptides identified using Scaffold; termini are indicated in parenthesis

[d]Mascot Ion scores >52 indicate identity or extensive homology ($p<0.05$)

[e]Similar protein: chelated iron ABC transporter periplasmic-binding protein [*Haemophilus parasuis* SH0165], gi|219691491

[f]Similar protein: oligopeptide ABC transporter periplasmic binding protein [*Haemophilus parasuis* SH0165], gi|219691508

[g]Similar protein: bifunctional UDP-sugar hydrolase/5'-nucleotidase periplasmic [*Haemophilus parasuis* SH0165], gi|219690922

Table 2.9. Identification of immunoreactive proteins from HP2170B

Sample ID	Protein name	Accession number	Protein ID[a]	X! Tandem Score[b]	Peptides[c]	Ion Score[d]
HP21-1	D-ribose transporter subunit RbsB	167856115	98	2.96 1.92	(K)VIQLEGIAGTSAAR(E) (K)AVFAQNDEMALGALR(A)	61.7 52
HP21-2	Phosphoribosyl-glycinamide formyltransferase	167855535[e]	99	1.68 1.51	(K)NALIYIENIR(Q) (R)WLVTSEGAFSYLAR(D)	44.9 72.8
HP21-3	Phosphoribosyl-glycinamide formyltransferase	167855535[e]	100	N/A N/A	(K)NALIYIENIR(Q) (R)WLVTSEGAFSYLAR(D)	70.2 71.5

[a]Percent probability determined by Scaffold

[b]Scores are reflected –log (e) value

[c]Peptides identified using Scaffold; termini are indicated in parenthesis

[d]Mascot Ion scores >52 indicate identity or extensive homology ($p<0.05$)

[e]Similar protein: chelated iron ABC transporter periplasmic-binding protein [*Haemophilus parasuis* SH0165], gi|219691491

Table 2.10. Identification of immunoreactive proteins from HPIA84-29755

Sample ID	Protein name	Accession number	Protein ID[a]	X! Tandem Score[b]	Peptides[c]	Ion Score[d]
HPIA-1	FbpA	167855400[e]	95	1.28	(K)EGELSPADVLLTVDISR(V)	63.6
HPIA-2	ABC transporter, periplasmic binding protein	167855391[f]	98	3.05	(K)AINIIAEEAALYPIIHR(K)	73.4

[a]Percent probability determined by Scaffold

[b]Scores are reflected –log (e) value

[c]Peptides identified using Scaffold; termini are indicated in parenthesis

[d]Mascot Ion scores >52 indicate identity or extensive homology ($p<0.05$)

[e]Similar protein: periplasmic iron-binding protein [*Haemophilus parasuis* SH0165], gi|219691519

[f]Similar protein: oligopeptide ABC transporter periplasmic binding protein [*Haemophilus parasuis* SH0165], gi|219691508

Table 2.11. Comparison of calculated and experimentally determined MW (kDa) and pI

Sample ID	Protein	Accession number[a]	Calculated[b] MW(kDa)/pI	Experimental[c] MW(kDa)/pI
HP2-1	purine nucleoside phosphorylase	167855453	26/5.3	29/5.8
HP2-2	probable sugar isomerase	167853152	26/6.1	32/6.0
HP2-3	TRAP solute transporter[d]	167855254	35/7.1	48/8.2
HP2-4	OMP P2[d]	167854978	36/9.2	52/6.2
HP3-1	purine nucleoside phosphorylase	167855453	26/5.3	28/5.8
HP3-2	probable sugar isomerase	167855696	26/6.1	30/6.2
HP3-3	phosphoribosylglycinamide formyltransferase[d]	167855535	33/7.7	58/9.8
HP3-4	D-ribose transporter RbsB	167856115	30/5.9	27/5.3
HP3-5	phosphoribosylglycinamide formyltransferase	167855535	33/7.8	33/7.0
HP3-6	phosphoribosylglycinamide formyltransferase	167855535	33/7.8	33/7.4
HP5-1	thiol:disulfide interchange protein	167852909	24/5.9	27/5.0
HP5-2	D-ribose transporter RbsB	167856115	30/5.9	36/6.0
HP5-3	FbpA	167853466	38/8.8	42/9.5
HP5-4	OMP P2[d]	299773319	37/9.1	51/9.8
HP5-5	D-ribose transporter RbsB	167856115	30/5.9	30/5.8
HP5-6	phosphoribosylglycinamide formyltransferase	167855535	33/7.8	33/7.0
HP5-7	phosphoribosylglycinamide formyltransferase	167855535	33/7.8	33/7.5
HP5-8	hypothetical protein HPS_06844	167853759	60/6.0	54/6.7
HP6-1	glucose-specific PTS system enzyme IIA	219871157	18/4.6	20/5.0
HP6-2	acetyl-CoA carboxylase biotin carboxylase[d]	219871451	16/4.8	28/5.5
HP6-3	phosphoribosylglycinamide formyltransferase[d]	167855535	33/7.8	58/5.9
HP6-4	Phosphoribosylglycinamide formyltransferase[d]	167855535	33/7.9	45/8.8
HP6-5	hypothetical protein HPS_10240[d]	167855017	38/5.3	48/9.8

[a]NCBI Accession numbers

[b]Determined using Expasy Compute pI/Mw

[c]Determined by 2-D SDS-PAGE

[d]Proteins that deviate from calculated MW and pI

Table 2.11. (continued)

Sample ID	Protein	Accession number[a]	Calculated[b] MW(kDa)/pI	Experimental[c] MW(kDa)/pI
HP7-1	alanine aminotransferase[d]	167854835	30/7.7	44/8.2
HP8-1	Mn-dependent SOD	299773433	24/5.6	30/5.5
HP8-2	purine nucleoside phosphorylase	167855453	26/5.3	32/5.8
HP8-3	ABC D-ribose transporter	219871818	33/6.5	38/6.2
HP8-4	phosphoribosylglycinamide formyltransferase	167855535	33/7.8	37/8.9
HP13-1	D-ribose transporter RbsB	167856115	30/5.9	30/5.8
HP13-2	D-ribose transporter RbsB	167856115	30/5.9	30/6.0
HP13-3	phosphoribosylglycinamide formyltransferase	167855535	33/7.8	31/7.0
HP13-4	phosphoribosylglycinamide formyltransferase	167855535	33/7.8	31/7.3
HP13-5	phosphoribosylglycinamide formyltransferase	167855535	33/7.8	34/8.1
HP13-6	ABC transporter	167855391	58/8.2	51/7.5
HP13-7	hypothetical protein HPS_06844	167853759	60/6.0	57/6.8
HP13-8	hypothetical protein HPS_06844	167853769	60/6.0	57/7.0
HP21-1	D-ribose transporter RbsB	167856115	30/5.9	25/5.5
HP21-2	phosphoribosylglycinamide formyltransferase	167855535	33/7.8	32/7.2
HP21-3	phosphoribosylglycinamide formyltransferase	167855535	33/7.8	32/7.6
HPIA-1	FbpA	167855400	38/8.8	32/6.8
HPIA-2	ABC transporter	167855391	58/8.2	52/7.5

Figures

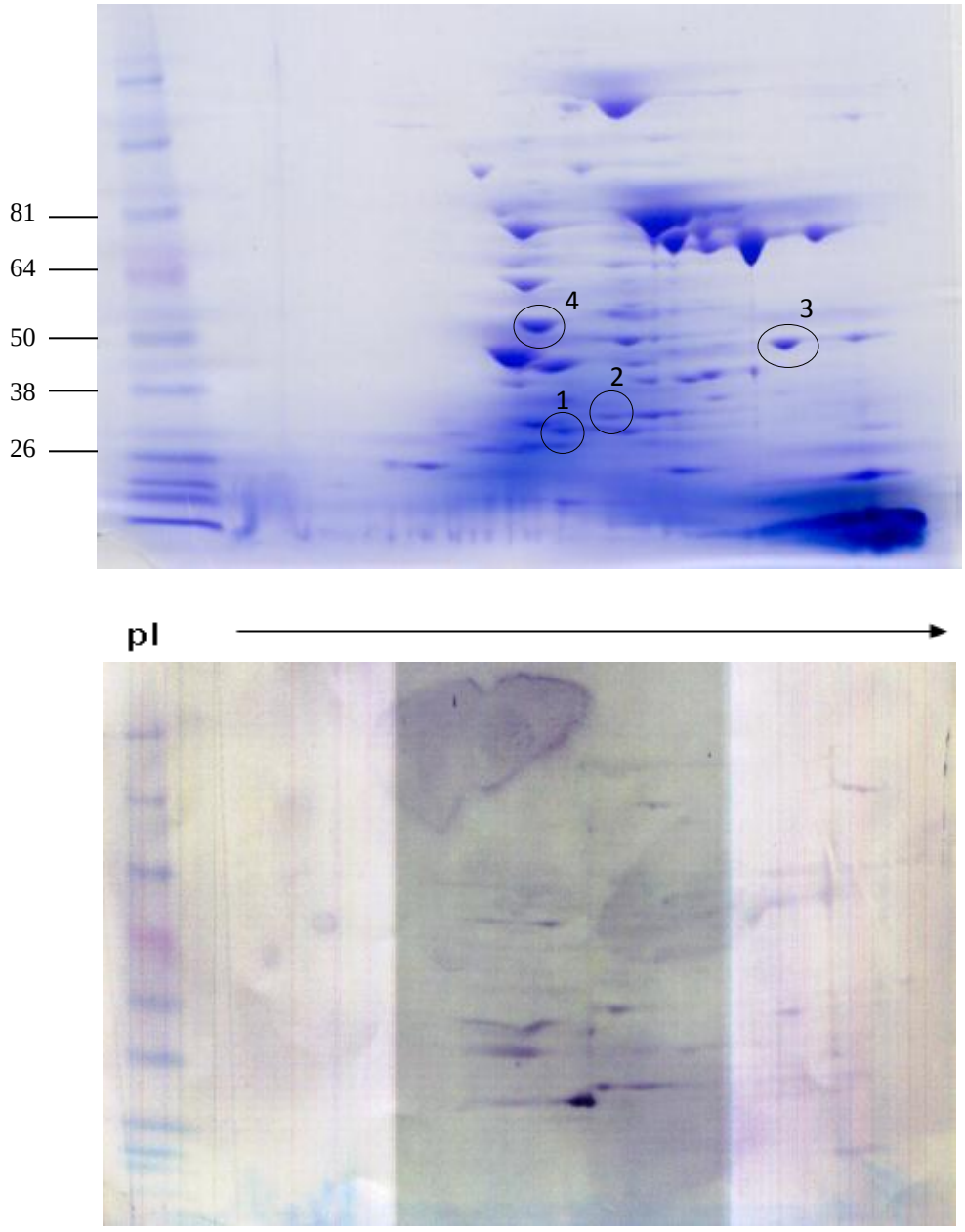

Figure 2.1. 2-D SDS-PAGE and immunoblot analysis of HP2 (SW140). Outer membrane protein preparation from IEF (pI 3-10) separated on 4-12% SDS-PAGE gel. Molecular weight is indicated in kDa. Circled spots correspond to proteins which are immunoreactive to mAb to P5 (4BF8). Proteins were transferred to PVDF and probed with mAb as described in the text.

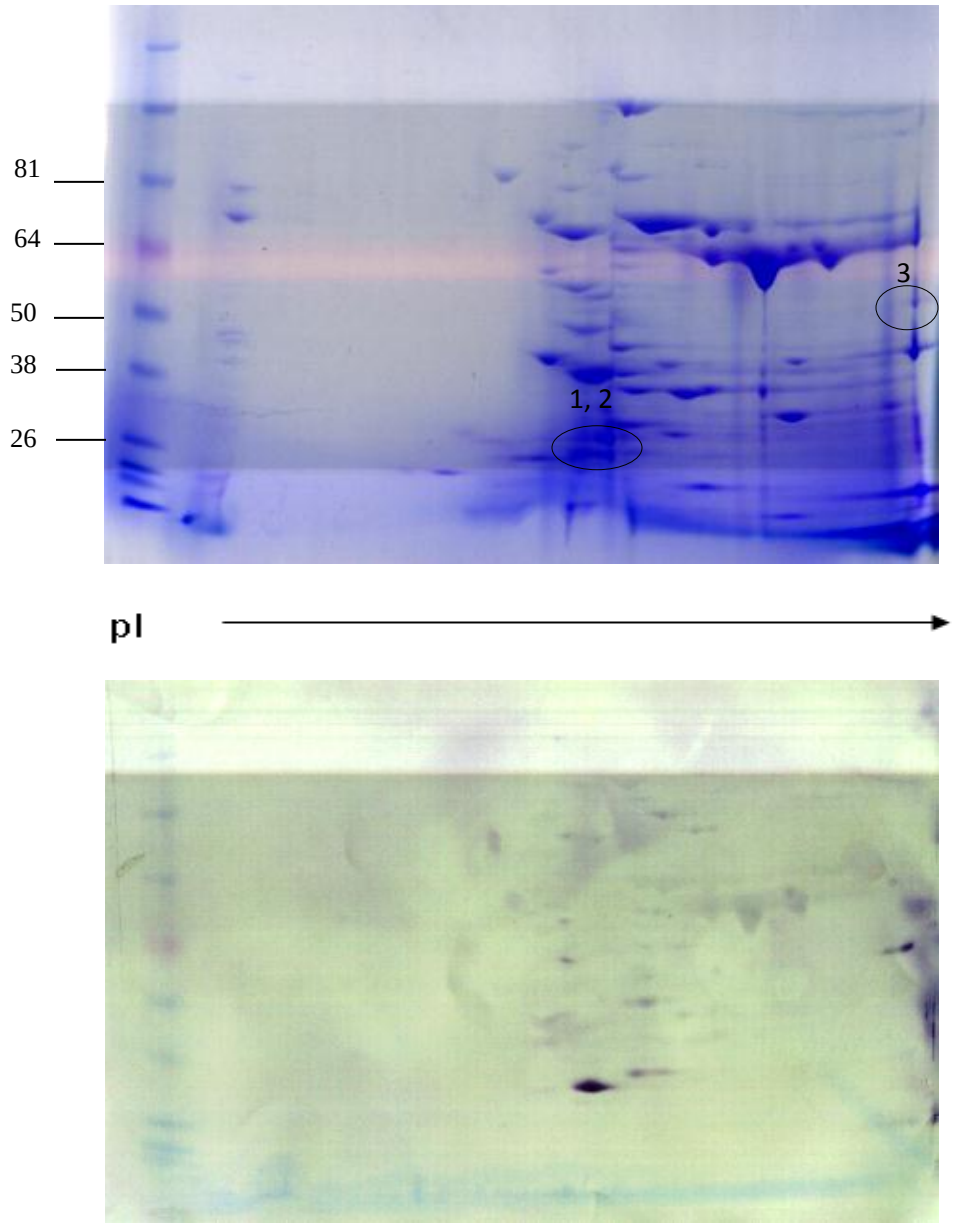

Figure 2.2. 2-D SDS-PAGE and immunoblot analysis of HP3 (SW114). Outer membrane protein preparation from IEF (pI 3-10) separated on 4-12% SDS-PAGE gel. Molecular weight is indicated in kDa. Circled spots correspond to proteins which are immunoreactive to mAb to P5 (4BF8). Proteins were transferred to PVDF and probed with mAb as described in the text.

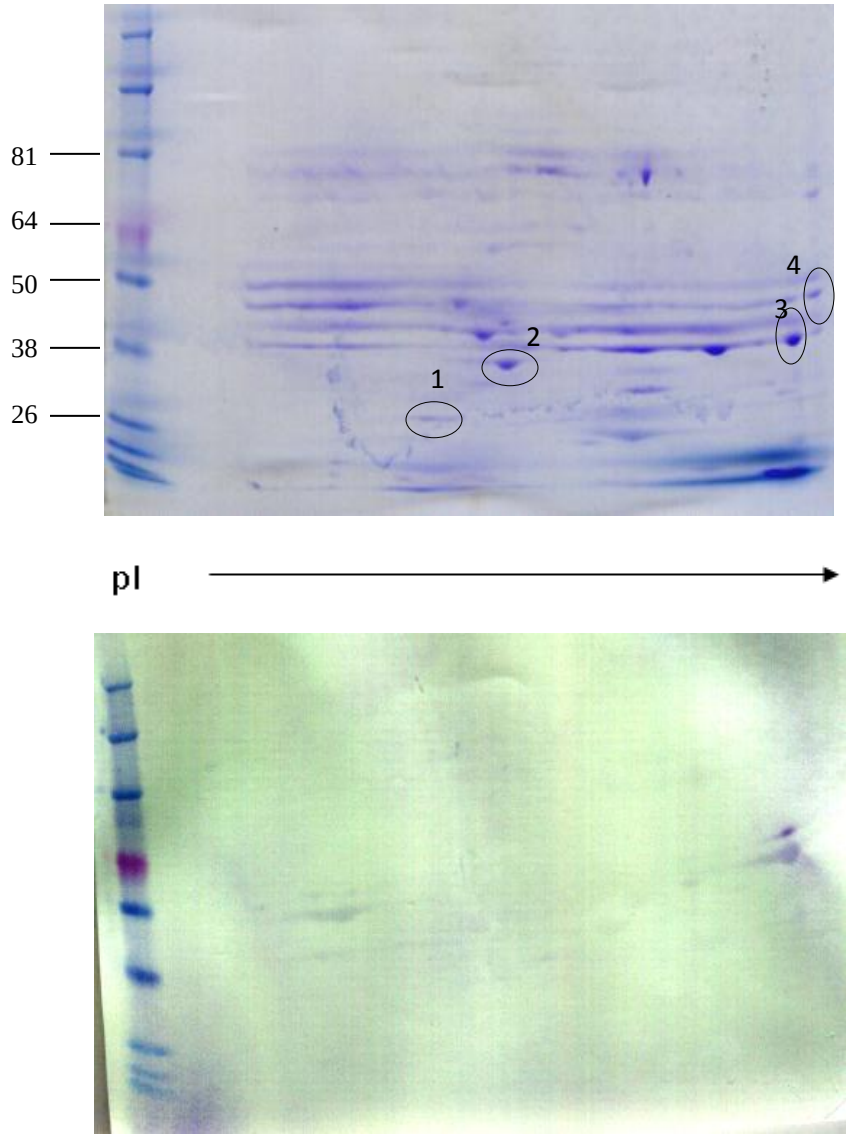

Figure 2.3. 2-D SDS-PAGE and immunoblot analysis of HP5 (Nagasaki). Outer membrane protein preparation from IEF (pI 3-10) separated on 4-12% SDS-PAGE gel. Molecular weight is indicated in kDa. Circled spots correspond to proteins which are immunoreactive to mAb to P5 (4BF8). Proteins were transferred to PVDF and probed with mAb as described in the text.

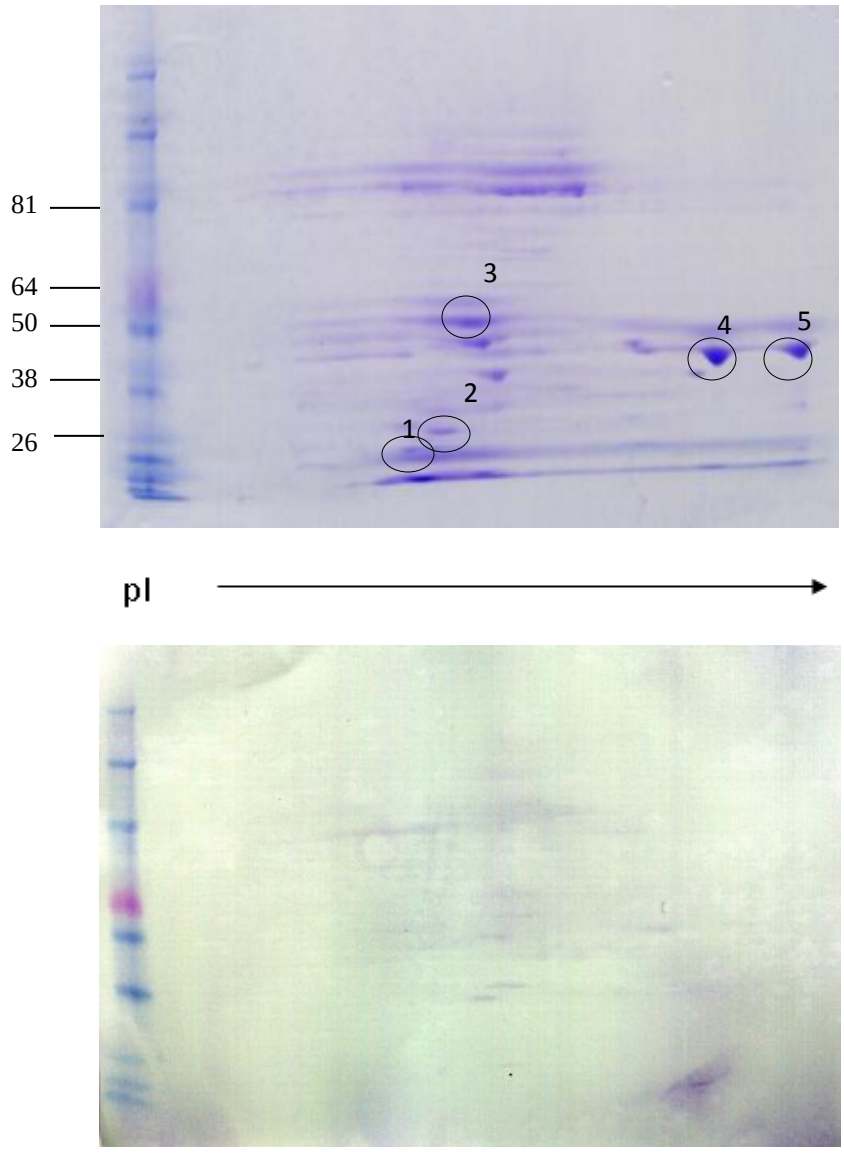

Figure 2.4. 2-D SDS-PAGE and immunoblot analysis of HP6 (131). Outer membrane protein preparation from IEF (pI 3-10) separated on 4-12% SDS-PAGE gel. Molecular weight is indicated in kDa. Circled spots correspond to proteins which are immunoreactive to mAb to P5 (4BF8). Proteins were transferred to PVDF and probed with mAb as described in the text.

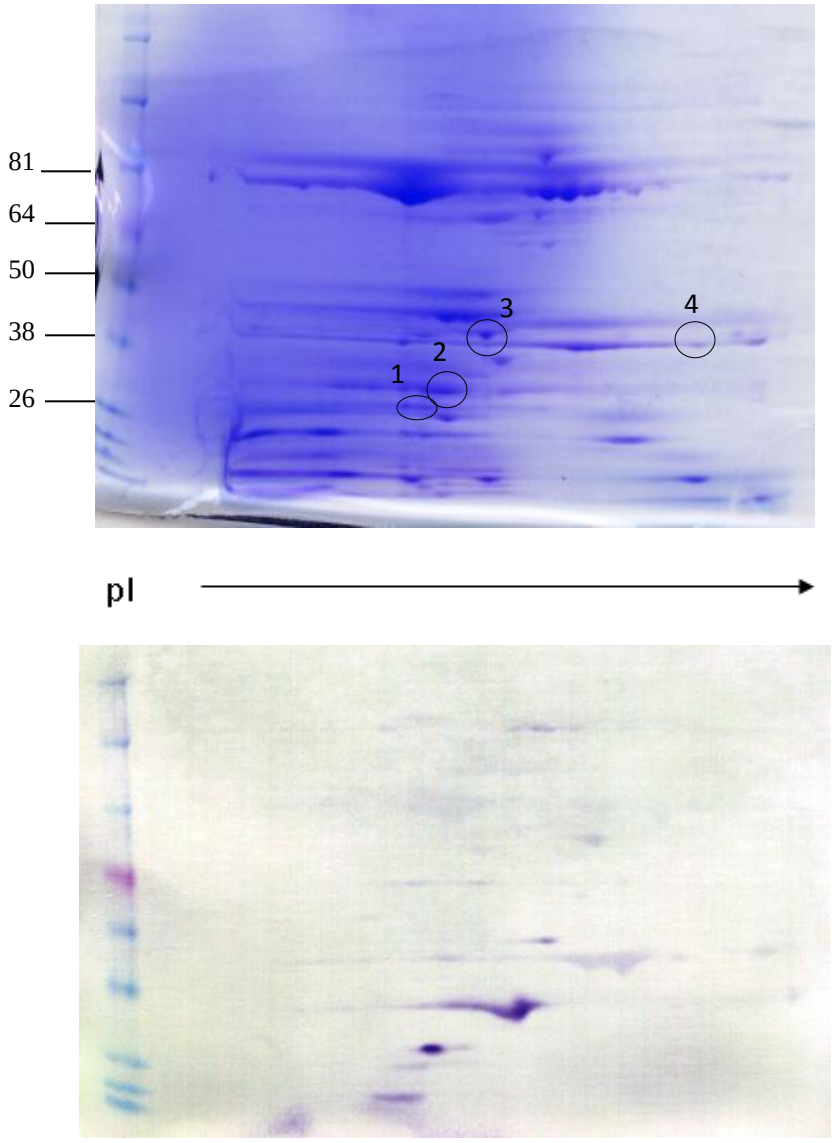

Figure 2.5. 2-D SDS-PAGE and immunoblot analysis of HP8 (C5). Outer membrane protein preparation from IEF (pI 3-10) separated on 4-12% SDS-PAGE gel. Molecular weight is indicated in kDa. Circled spots correspond to proteins which are immunoreactive to mAb to P5 (4BF8). Proteins were transferred to PVDF and probed with mAb as described in the text.

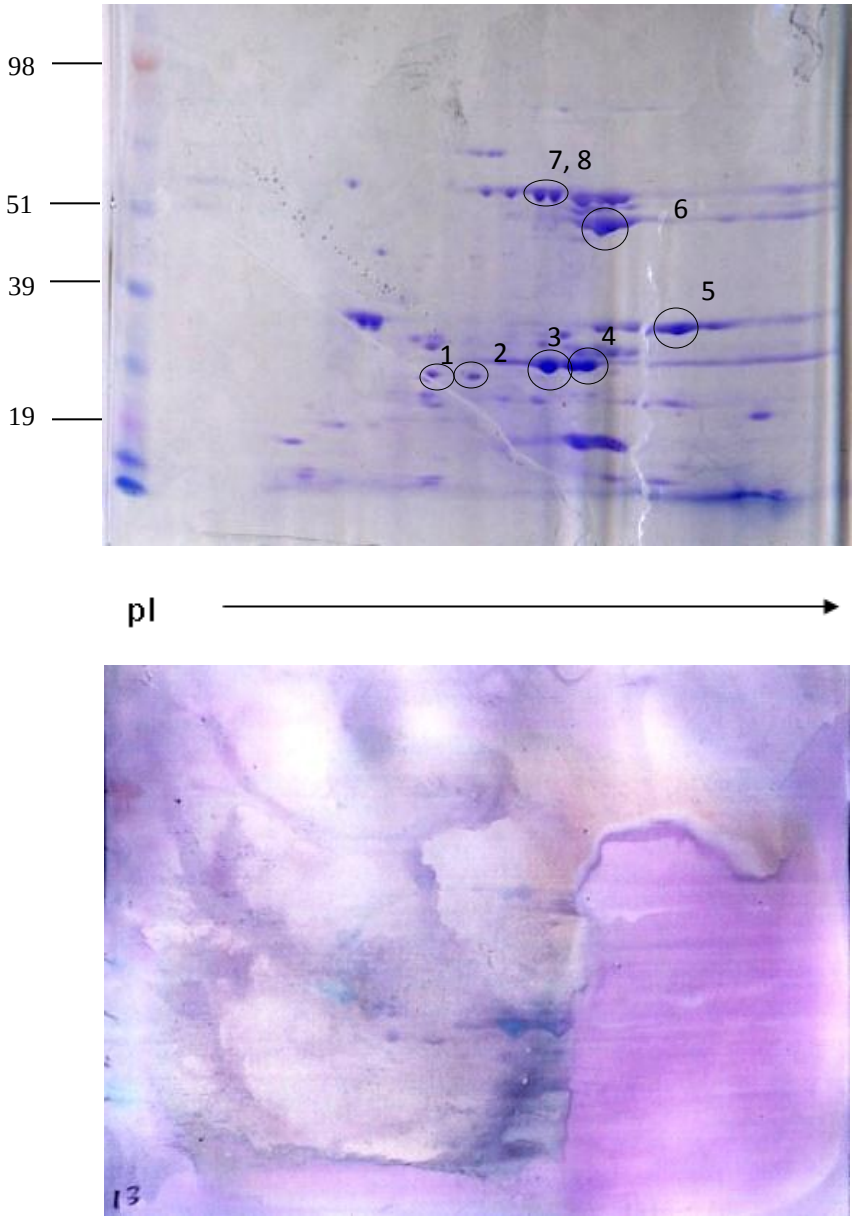

Figure 2.6. 2-D SDS-PAGE and immunoblot analysis of HP13 (84-17975). Outer membrane protein preparation from IEF (pI 3-10) separated on 4-12% SDS-PAGE gel. Molecular weight is indicated in kDa. Circled spots correspond to proteins which are immunoreactive to mAb to P5 (4BF8). Proteins were transferred to PVDF and probed with mAb as described in the text.

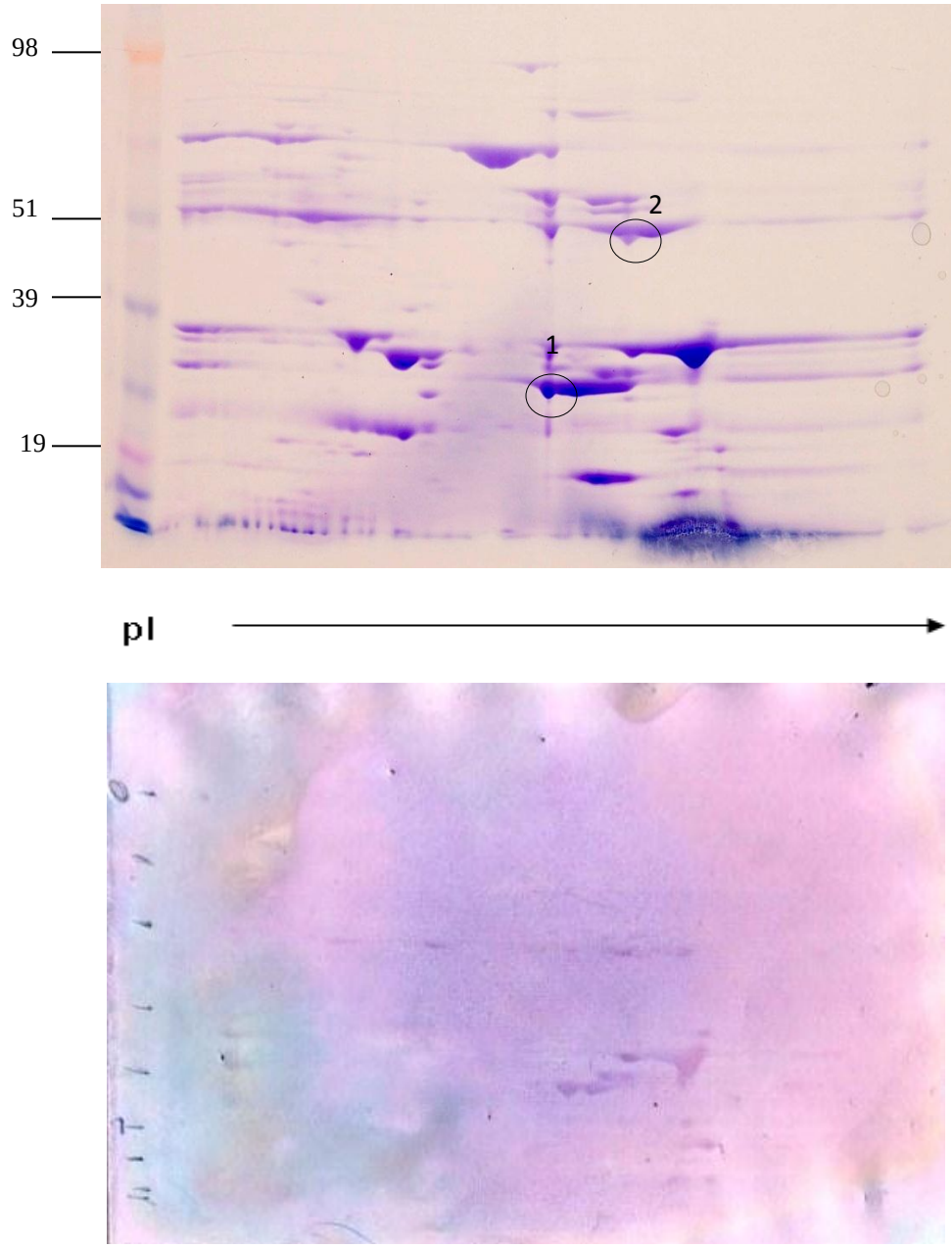

Figure 2.7. 2-D SDS-PAGE and immunoblot analysis of HPIA (84-29755). Outer membrane protein preparation from IEF (pI 3-10) separated on 4-12% SDS-PAGE gel. Molecular weight is indicated in kDa. Circled spots correspond to proteins which are immunoreactive to mAb to P5 (4BF8). Proteins were transferred to PVDF and probed with mAb as described in the text.

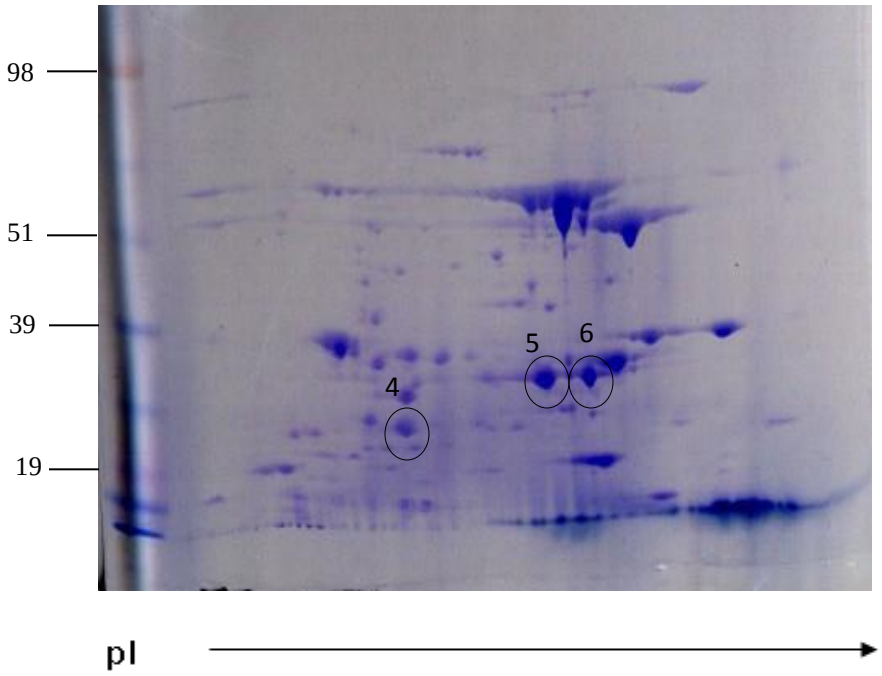

Figure 2.8. 2-D SDS-PAGE analysis of HP3 (SW114). Outer membrane protein preparation from IEF (pI 3-10) separated on 4-12% SDS-PAGE gel. Molecular weight is indicated in kDa. Circled spots correspond to proteins that were analyzed by tandem mass spectrometry. Immunoblot is not shown.

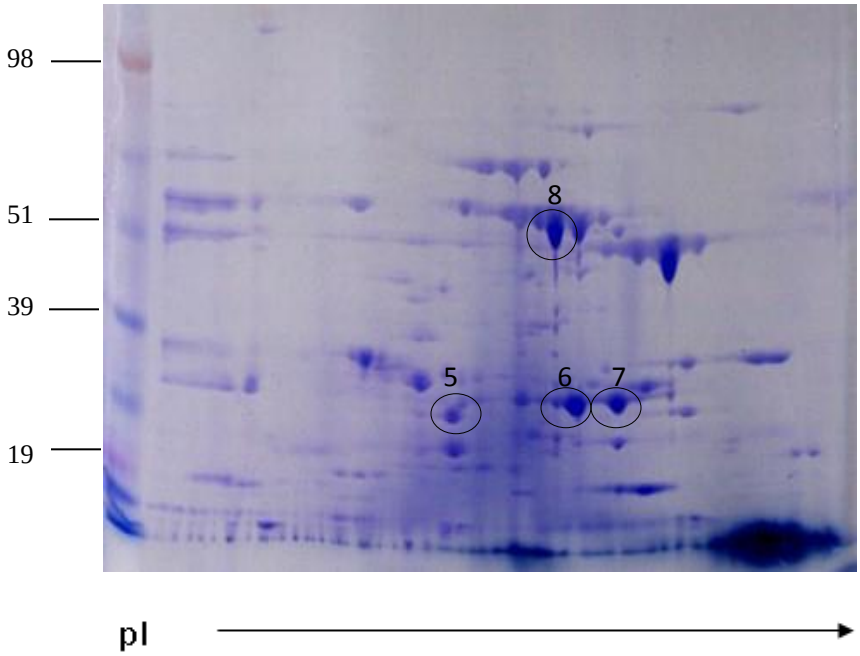

Figure 2.9. 2-D SDS-PAGE analysis of HP5 (Nagasaki). Outer membrane protein preparation from IEF (pI 3-10) separated on 4-12% SDS-PAGE gel. Molecular weight is indicated in kDa. Circled spots correspond to proteins that were analyzed by tandem mass spectrometry. Immunoblot is not shown.

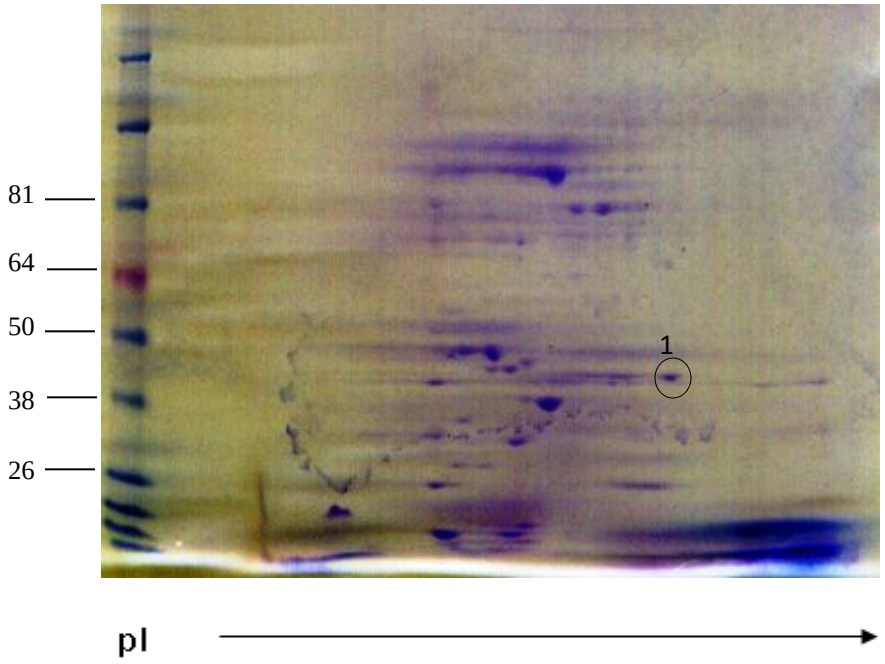

Figure 2.10. 2-D SDS-PAGE analysis of HP7 (174). Outer membrane protein preparation from IEF (pI 3-10) separated on 4-12% SDS-PAGE gel. Molecular weight is indicated in kDa. Circled spots correspond to proteins which were analyzed by tandem mass spectrometry. Immunoblot is not shown.

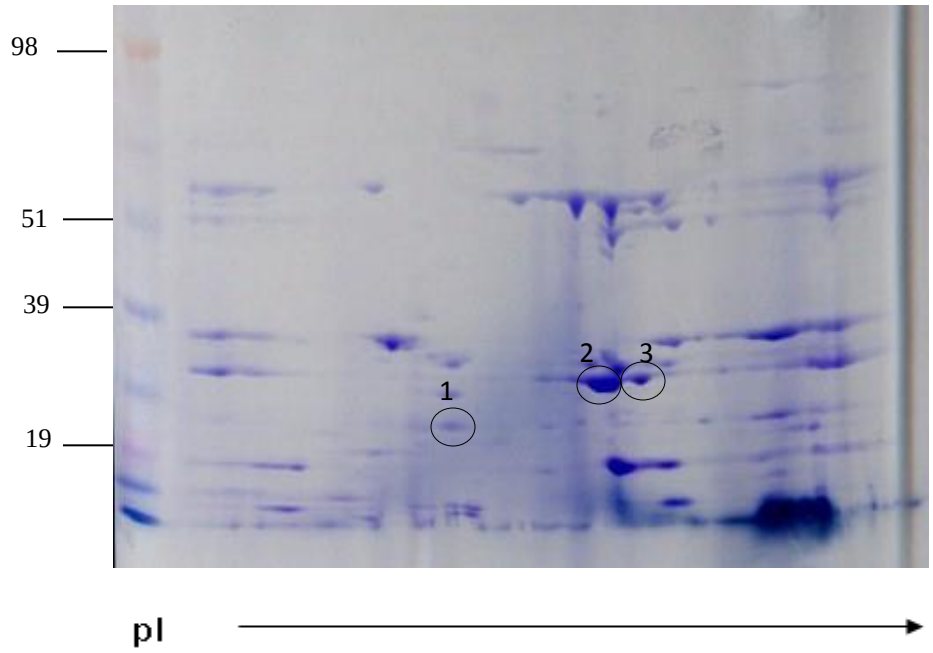

Figure 2.11. 2-D SDS-PAGE analysis of HP2170B. Outer membrane protein preparation from IEF (pI 3-10) separated on 4-12% SDS-PAGE gel. Molecular weight is indicated in kDa. Circled spots correspond to proteins which were analyzed by tandem mass spectrometry. Immunoblot is not shown.

Supplemental Figures

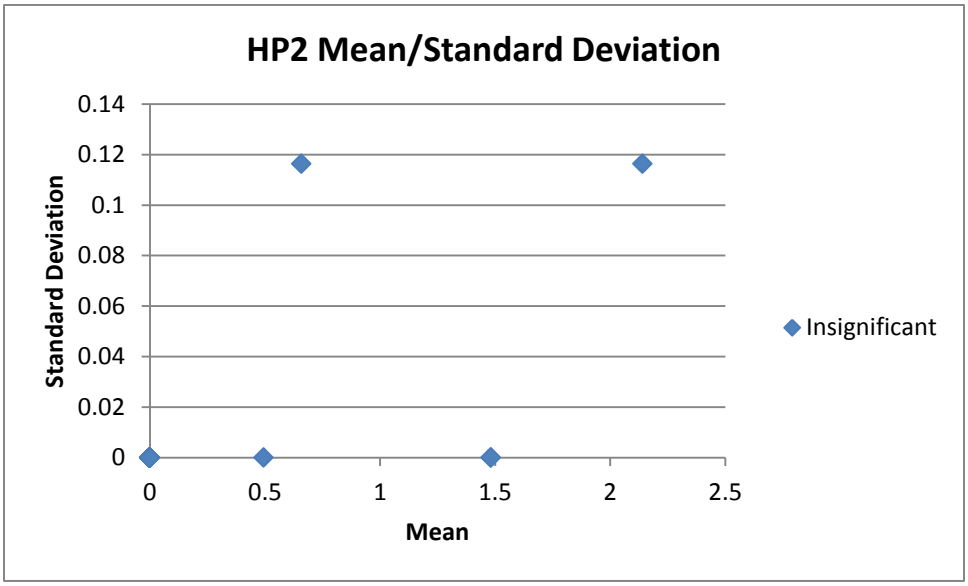

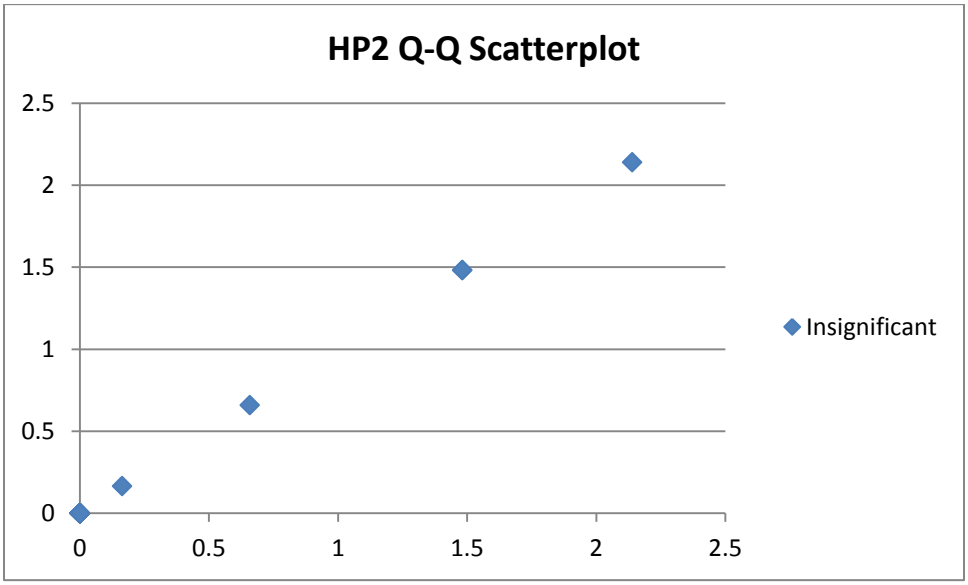

Supplemental Figure S2.1. Quantitative Scatterplots for HP2 based on Fold-change analysis. Normalized spectral counts were compared for the forward and reverse database searches. Proteins that were noted as significantly different were considered false positives.

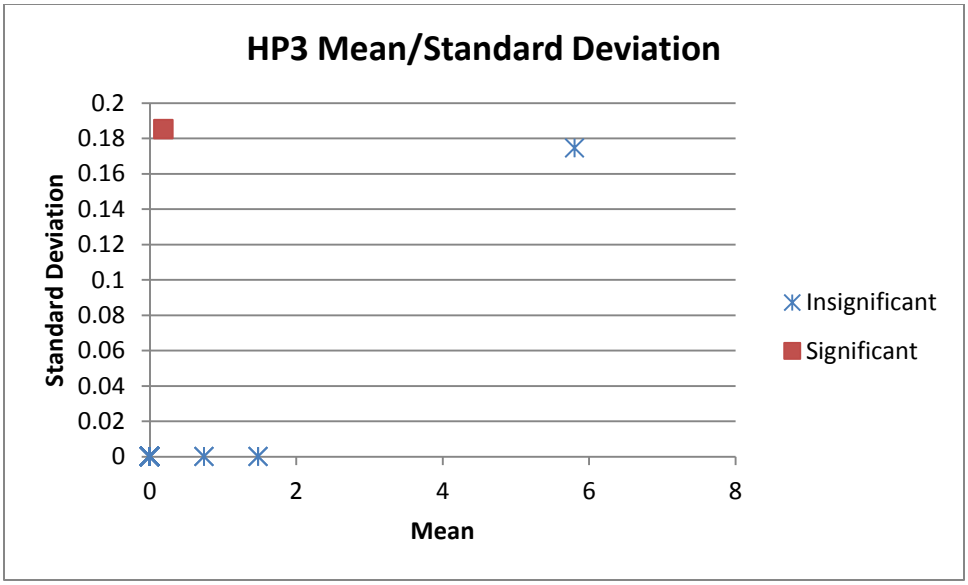

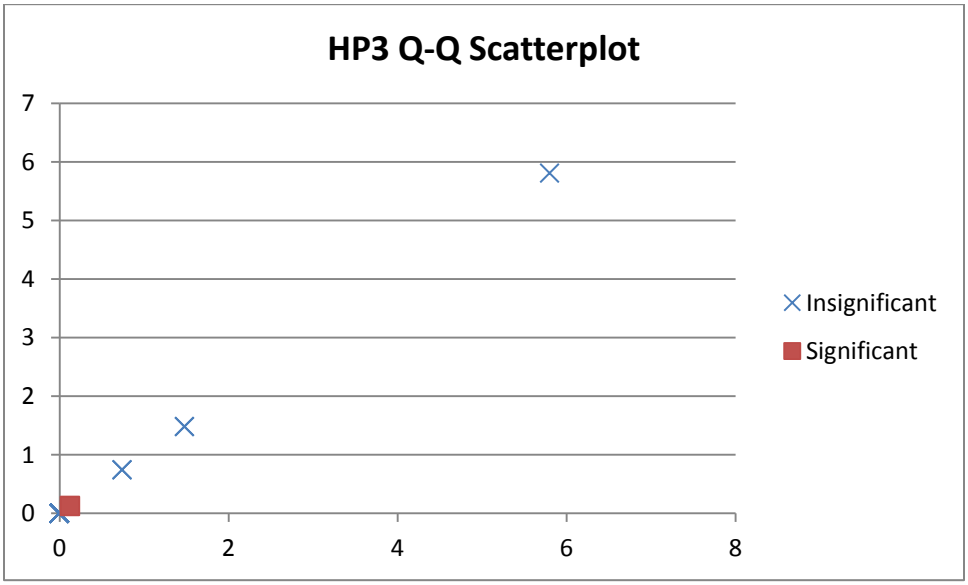

Supplemental Figure S2.2. Quantitative Scatterplots for HP3 based on Fold-change analysis. Normalized spectral counts were compared for the forward and reverse database searches. Proteins that were noted as significantly different were considered false positives.

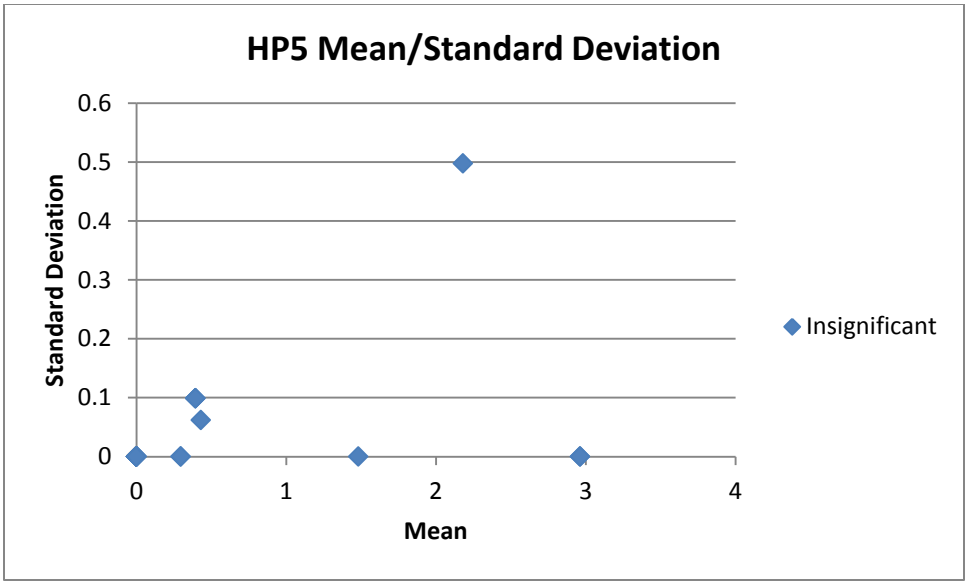

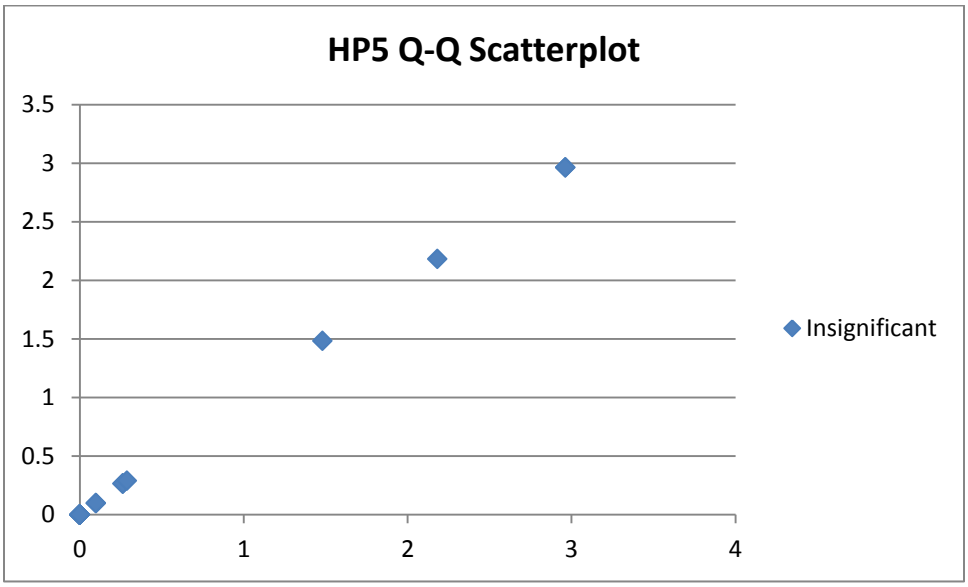

Supplemental Figure S2.3. Quantitative Scatterplots for HP5 based on based on Fold-change analysis. Normalized spectral counts were compared for the forward and reverse database searches. Proteins that were noted as significantly different were considered false positives.

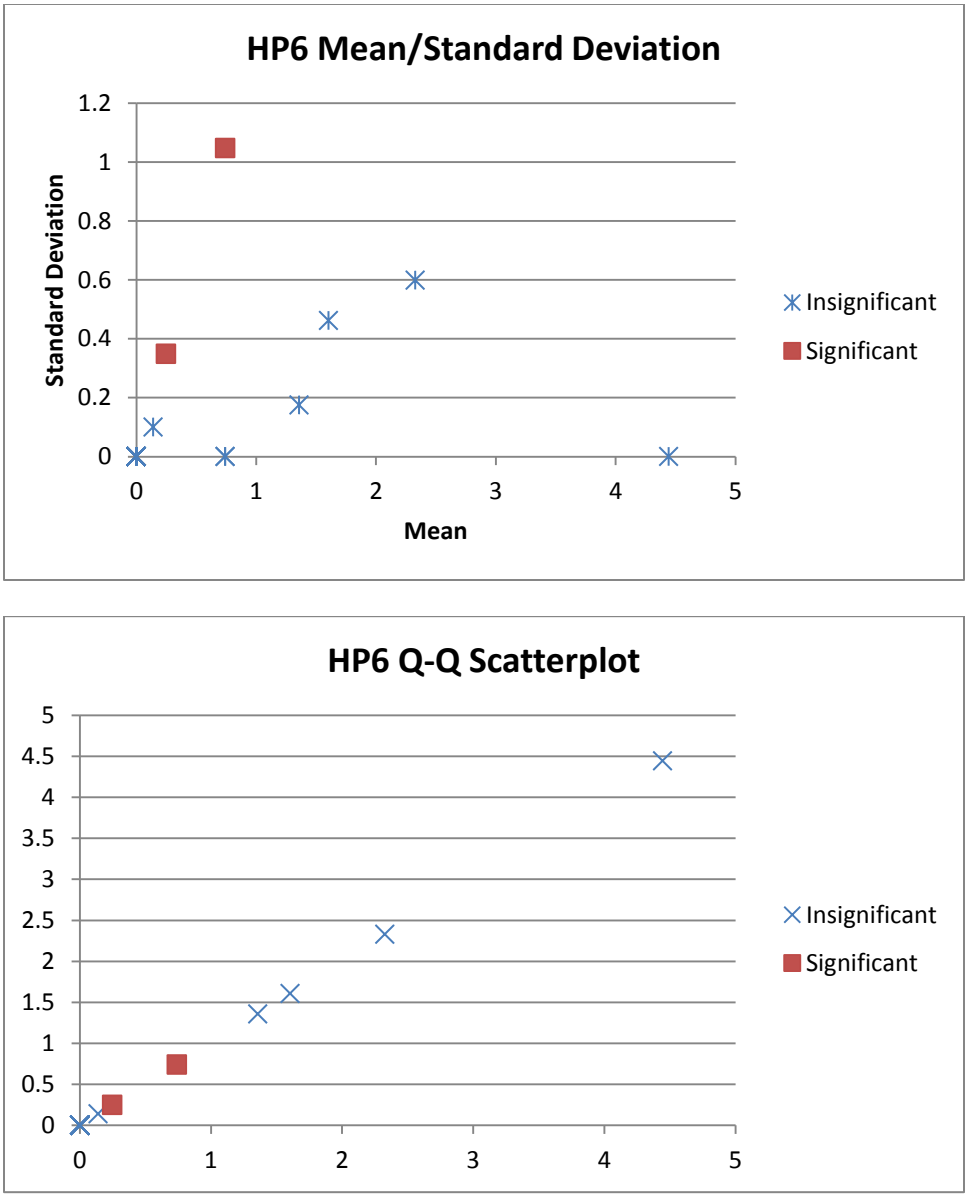

Supplemental Figure S2.4. Quantitative Scatterplots for HP6 based on Fold-change analysis. Normalized spectral counts were compared for the forward and reverse database searches. Proteins that were noted as significantly different were considered false positives.

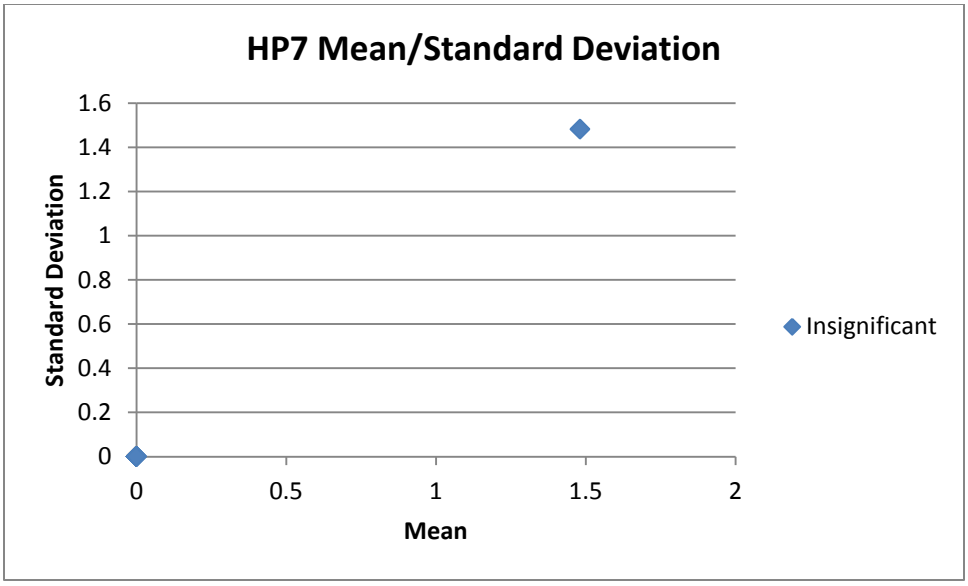

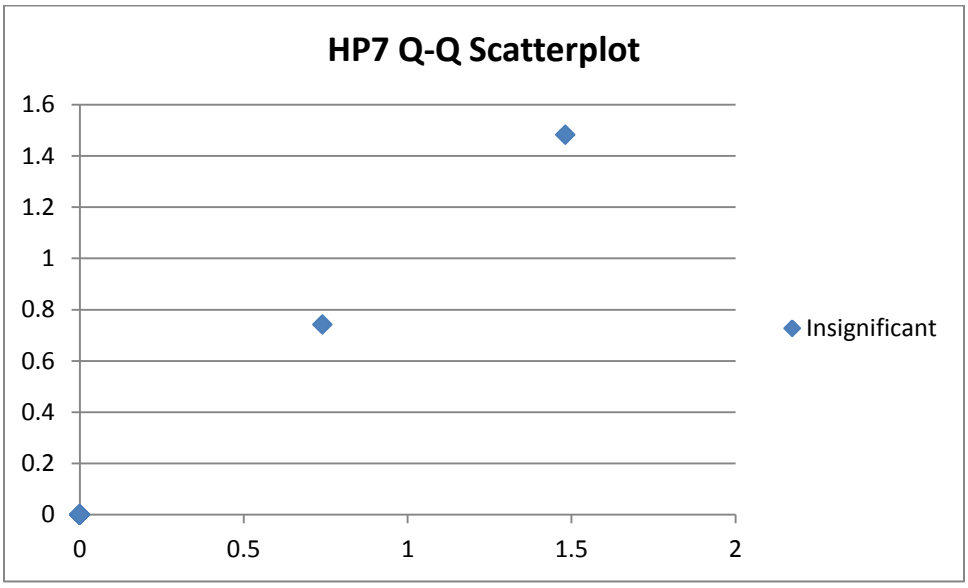

Supplemental Figure S2.5. Quantitative Scatterplots for HP7 based on Fold-change analysis. Normalized spectral counts were compared for the forward and reverse database searches. Proteins that were noted as significantly different were considered false positives.

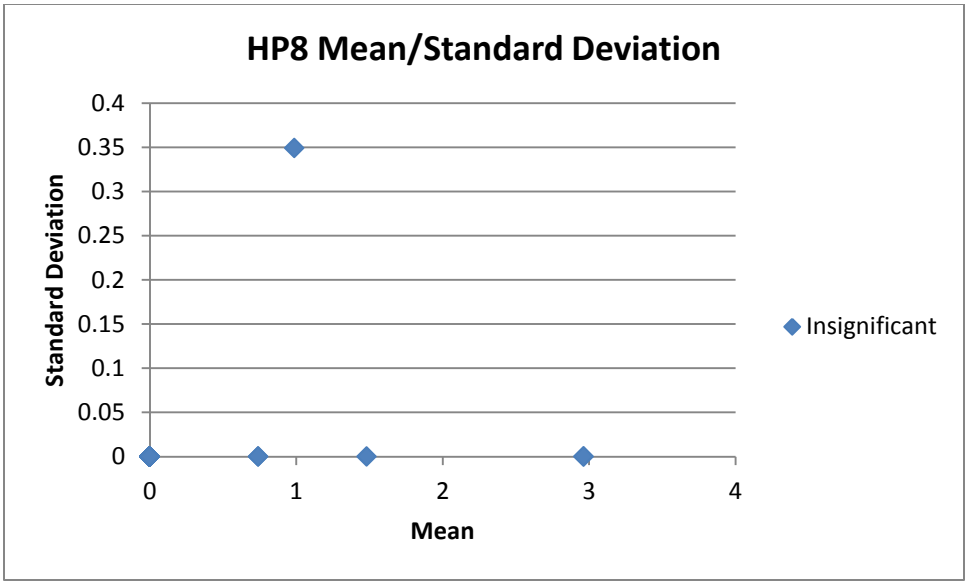

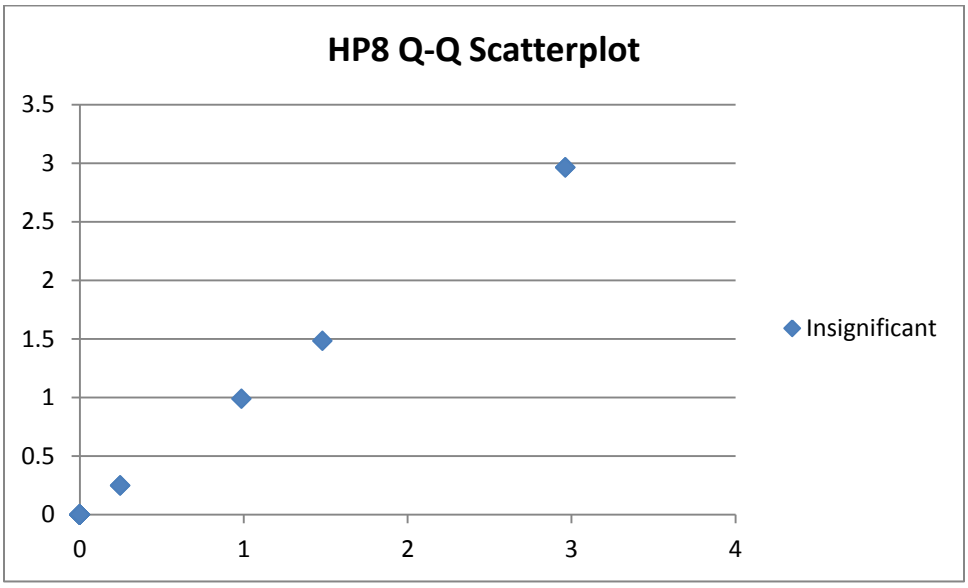

Supplemental Figure S2.6. Quantitative Scatterplots for HP8 based on Fold-change analysis. Normalized spectral counts were compared for the forward and reverse database searches. Proteins that were noted as significantly different were considered false positives.

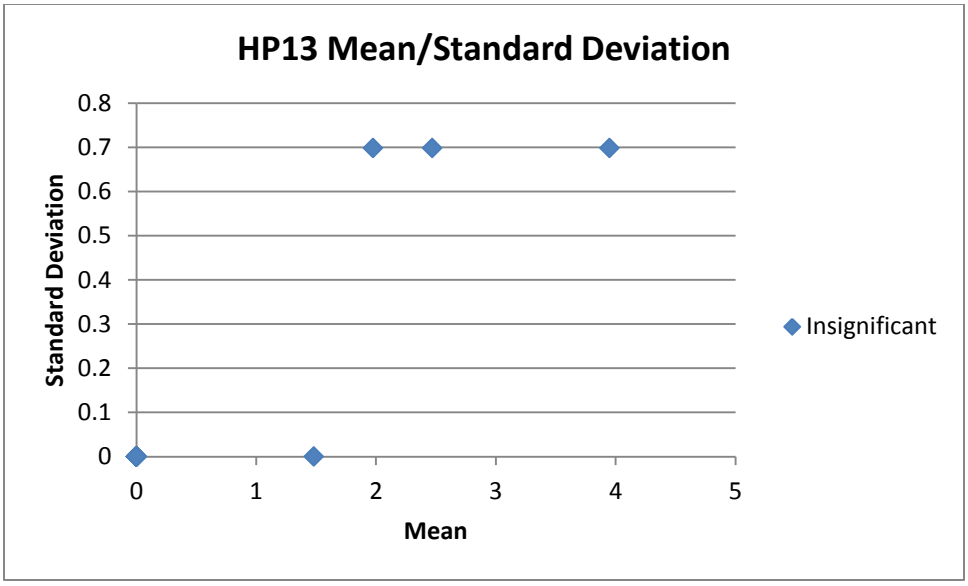

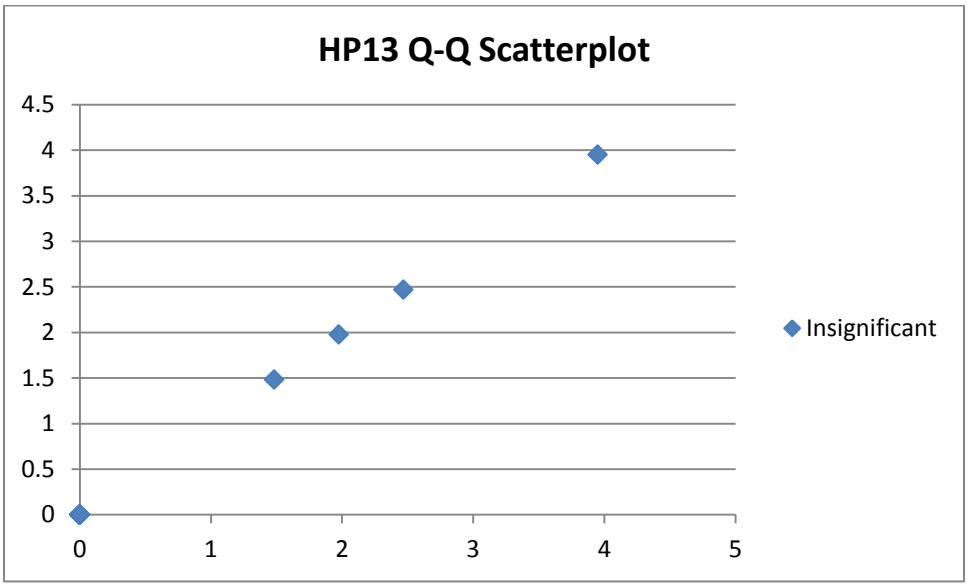

Supplemental Figure S2.7. Quantitative Scatterplots for HP13 based on Fold-change analysis. Normalized spectral counts were compared for the forward and reverse database searches. Proteins that were noted as significantly different were considered false positives.

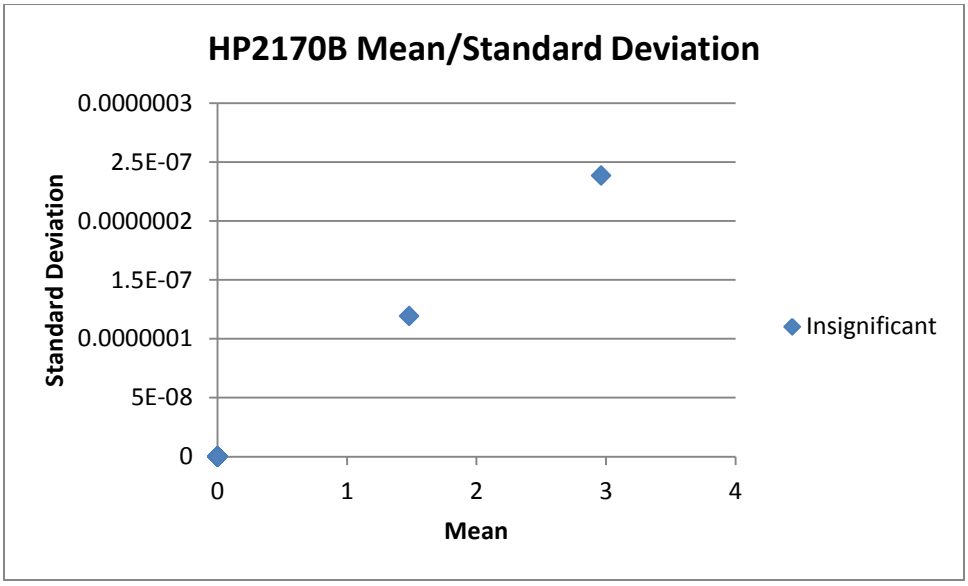

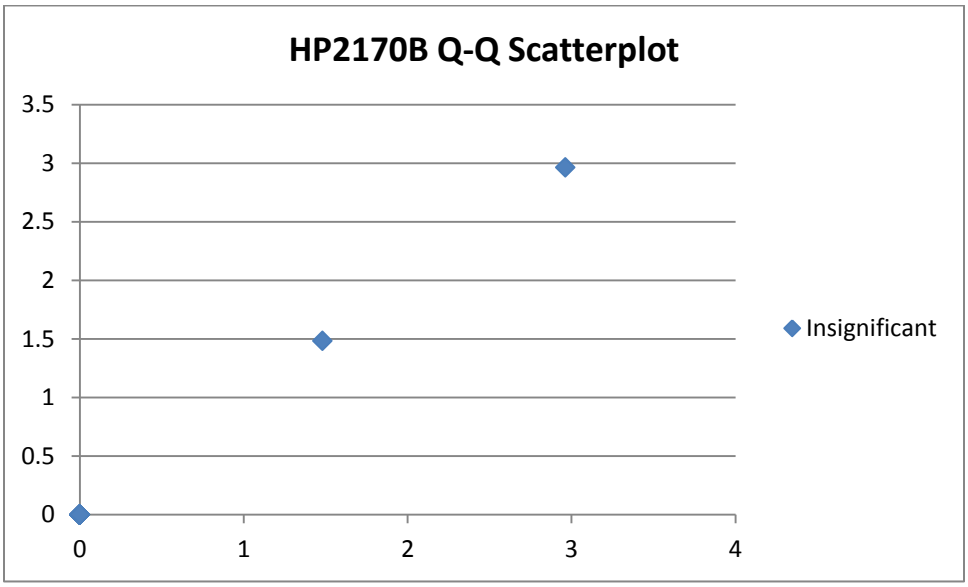

Supplemental Figure S2.8. Quantitative Scatterplots for HP2170B based on Fold-change analysis. Normalized spectral counts were compared for the forward and reverse database searches. Proteins that were noted as significantly different were considered false positives.

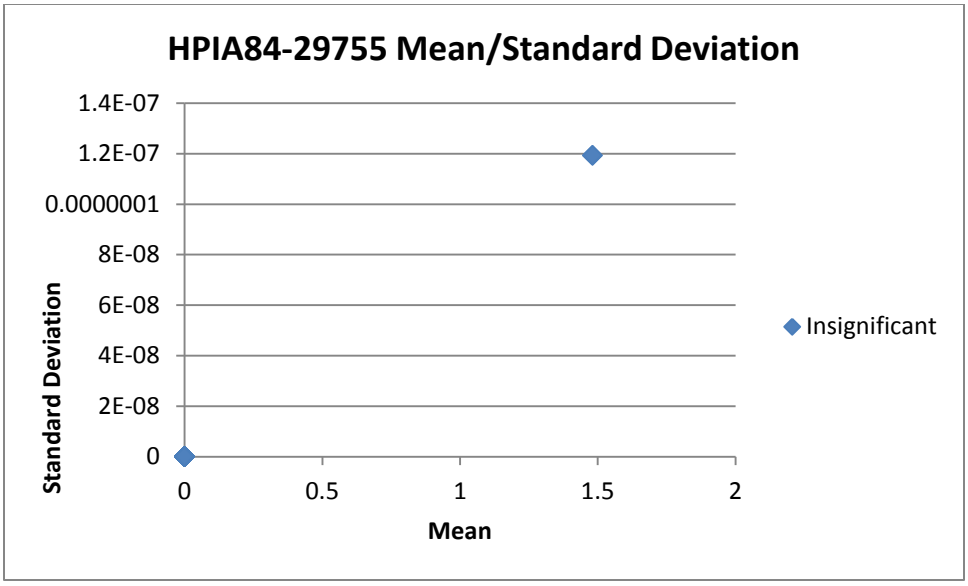

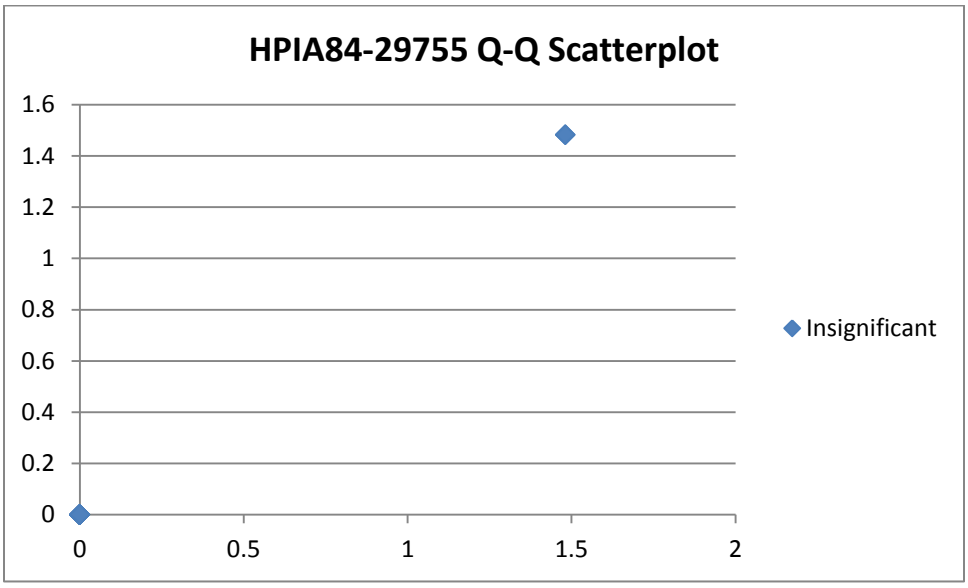

Supplemental Figure S2.9. Quantitative Scatterplots for HPIA based on Fold-change analysis. Normalized spectral counts were compared for the forward and reverse database searches. Proteins that were noted as significantly different were considered false positives.

a)

gi|167855453 (95%), 26,013.2 Da
purine nucleoside phosphorylase [Haemophilus parasuis 29755], gi|219871397|ref|YP_002475772.1| purine nucleoside phosphorylase [Haemophilus parasuis SH0165],
1 unique peptides, 1 unique spectra, 1 total spectra, 17/239 amino acids (7% coverage)

MTPHINAPAG AFADVVLMPG DPLRAKYIAE TFLENAEQVT NVRNMFGYTG TYKGRRISVM
GHGMGIPSCS IYAKELITEY GVKKIIRVGS CGAVRQDVKL REVIIGVGAC TDSKVNRIRF
KDNDFAAIAD FDLTLAAVQA AKAKGINVRV GNLYSADLFY TPDVEMFDVM EKYGILGVEM
EAAGIYGVAA EFGAKALTIC TVSDHIRTHE QTTAEERQLT FNDMIEIALE SVLIGDQQG

b)

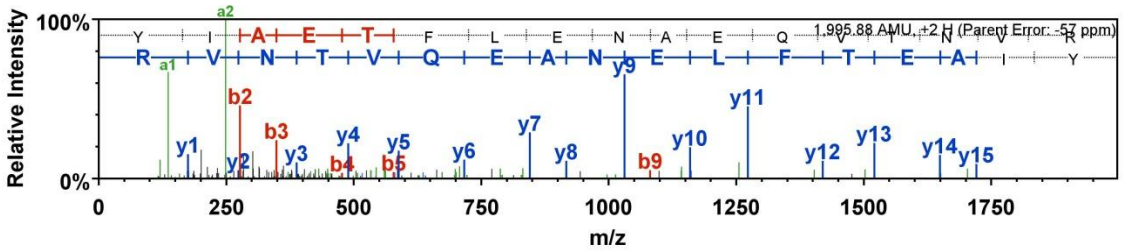

Supplemental Figure S2.10. Protein sequence coverage map for HP2-1 (a) and corresponding peptides (b).

a)

gi|167855696 (98%), 25,913.0 Da
Probable sugar isomerase [Haemophilus parasuis 29755], gi|167853152|gb|EDS24410.1| Probable sugar isomerase [Haemophilus parasuis 29755]
1 unique peptides, 1 unique spectra, 1 total spectra, 14/230 amino acids (6% coverage)

MLKELRERVL KANLELPKYK LVTFTWGNVS EIDRESGLVA VKPSGVDYDV MTADDIVIVD
LQGNRVWGTK KPSSDTPTHL ELYRQFPEIG GVVHTHSRHA TAWAQAGEDI LALGTTQGDY
FYGSVPCTRR MTPEEIAGEY ELETGKVIVE TFRKRAIEPS MVPGVLVHSH GPFTWGKDAF
DAVHNSVVLE EVAYMNFVSH QIRPNIGSMQ QELLDKHYLR KHGKNAYYGQ

b)

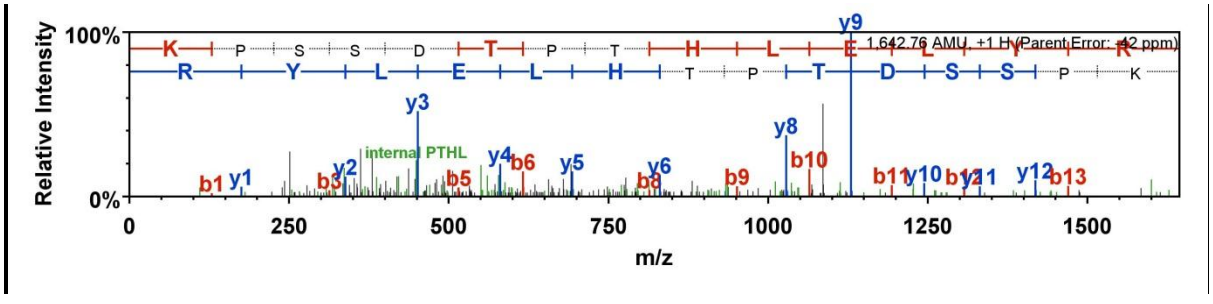

Supplemental Figure S2.11. Protein sequence coverage map for HP2-2 (a) and corresponding peptides (b).

a)

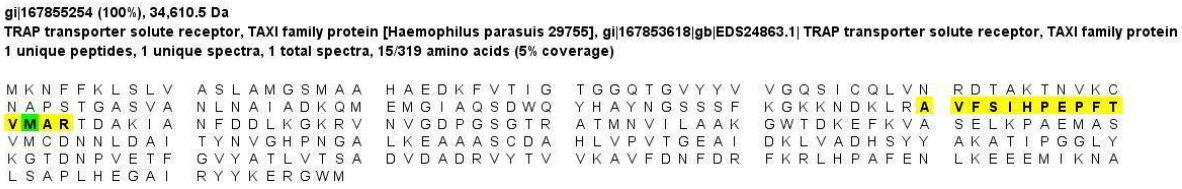

b)

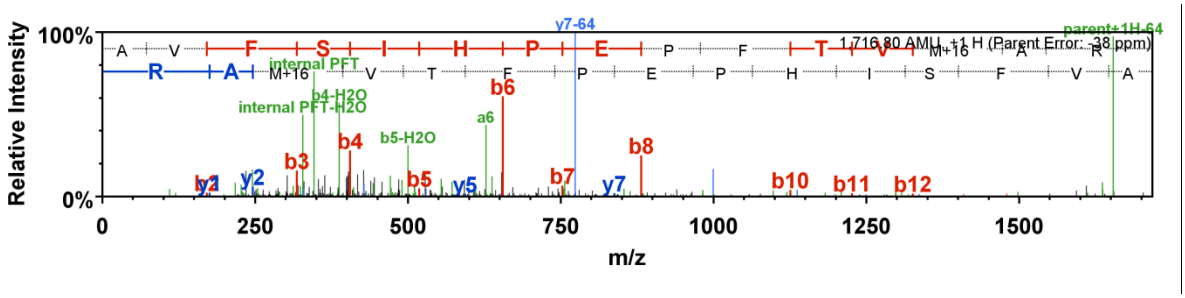

Supplemental Figure S2.12. Protein sequence coverage map for HP2-3 (a) and corresponding peptides (b)

a)

b)

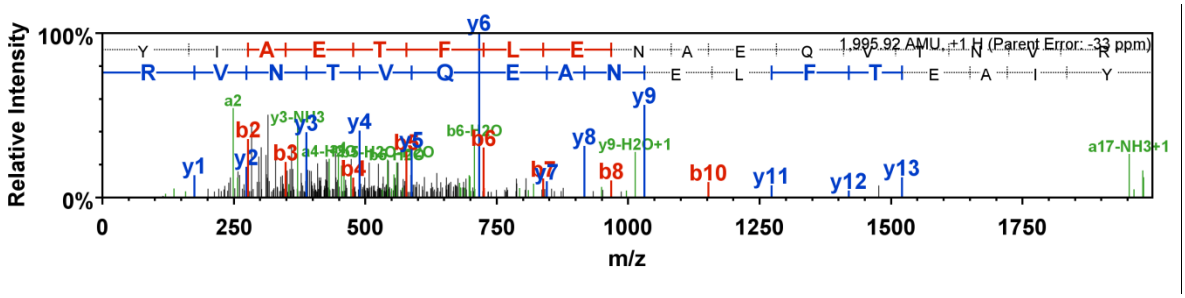

Supplemental Figure S2.13. Protein sequence coverage map for HP3-1 (a) and corresponding peptides (b)

a)

b)

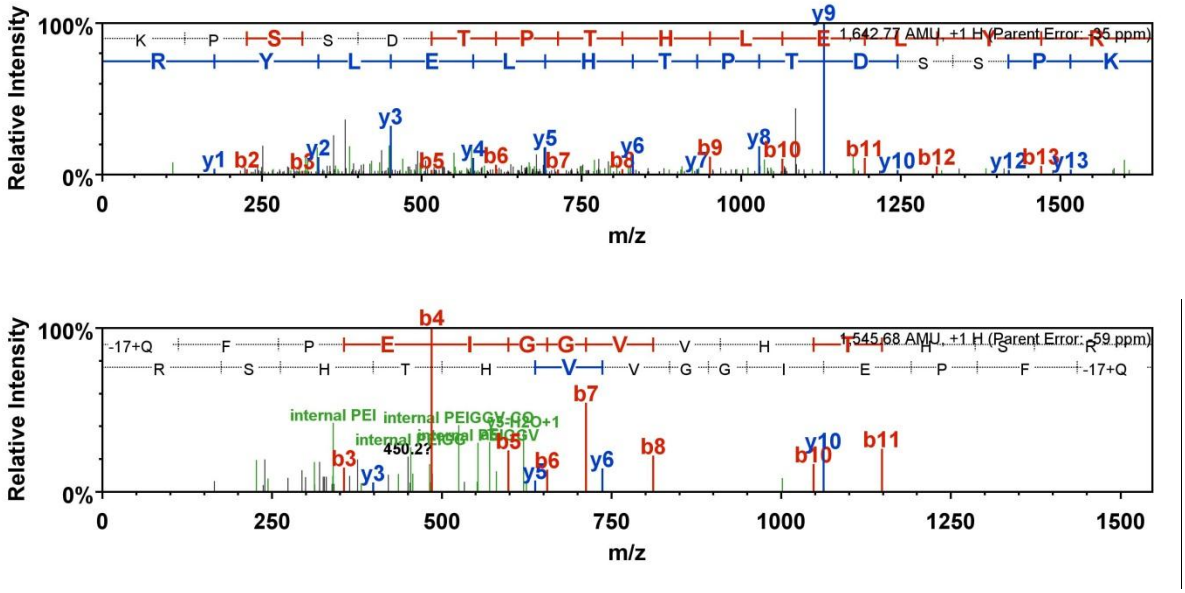

Supplemental Figure S2.14. Protein sequence coverage map for HP3-2 (a) and corresponding peptides (b)

a)

gi|167855535 (100%), 32,638.8 Da
phosphoribosylglycinamide formyltransferase [Haemophilus parasuis 29755], gi|167853336|gb|EDS24588.1| phosphoribosylglycinamide formyltransferase [Haemophilus parasuis 29755]
2 unique peptides, 2 unique spectra, 3 total spectra, 35/292 amino acids (12% coverage)

MKKLAALLSM LFLVSNPLAA QQFKVVTTFT VIQDIAQNVA GDKAVVESIT KPGAEIHDYQ
PTPQDIVKAQ SADLVLWNGM NLESWFERFF AQVKDKPAVV VTEGIEPISI YEGPYKDKPN
PHAWMSTKNA LIYIENIRQA LVKYDPANAE AYNANAKAYA DKIVALDQPL RERLAKVPEA
QRWLVTSEGA FSYLARDYGF KELYLWAINQ DEQGTPKQIR KVIDQVRKHQ IPVVFSESTI
SDKPAKQVAK ESKARYGGVL YVDSLSTKDG KVPTYVDLLN VTVSTIVAGF EK

gi|167855535 (96%), 32,638.8 Da
phosphoribosylglycinamide formyltransferase [Haemophilus parasuis 29755], gi|167853336|gb|EDS24588.1| phosphoribosylglycinamide formyltransferase [Haemophilus parasuis 29755]
1 unique peptides, 1 unique spectra, 1 total spectra, 10/292 amino acids (3% coverage)

MKKLAALLSM LFLVSNPLAA QQFKVVTTFT VIQDIAQNVA GDKAVVESIT KPGAEIHDYQ
PTPQDIVKAQ SADLVLWNGM NLESWFERFF AQVKDKPAVV VTEGIEPISI YEGPYKDKPN
PHAWMSTKNA LIYIENIRQA LVKYDPANAE AYNANAKAYA DKIVALDQPL RERLAKVPEA
QRWLVTSEGA FSYLARDYGF KELYLWAINQ DEQGTPKQIR KVIDQVRKHQ IPVVFSESTI
SDKPAKQVAK ESKARYGGVL YVDSLSTKDG KVPTYVDLLN VTVSTIVAGF EK

b)

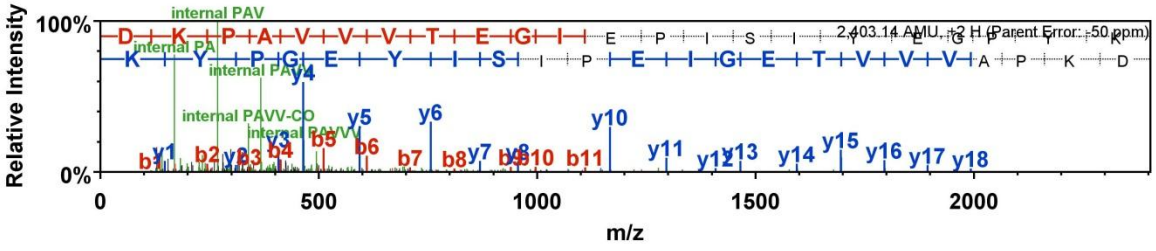

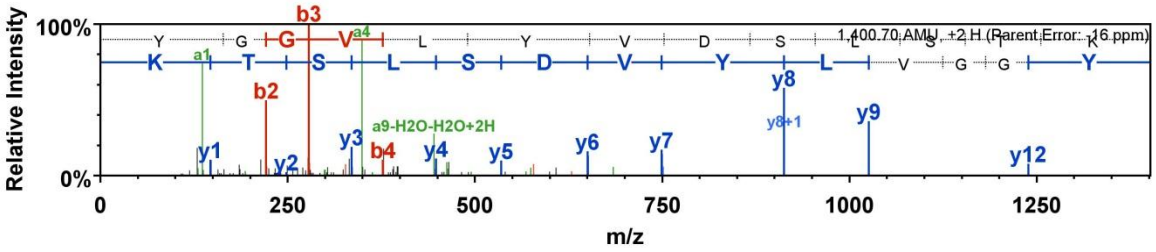

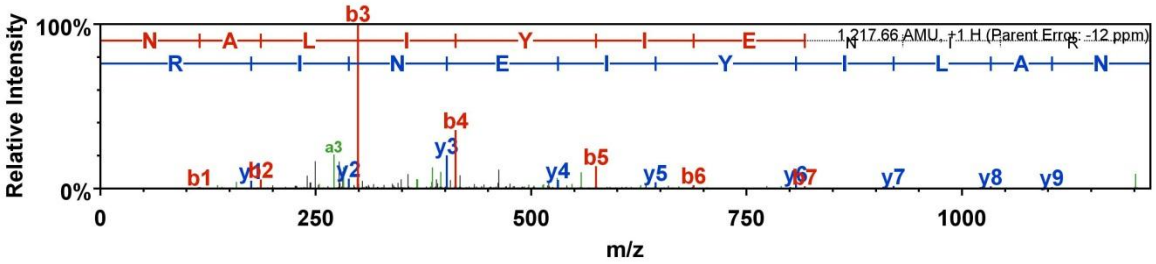

Supplemental Figure S2.15. Protein sequence coverage map for HP3-3 (a) and corresponding peptides (b)

a)

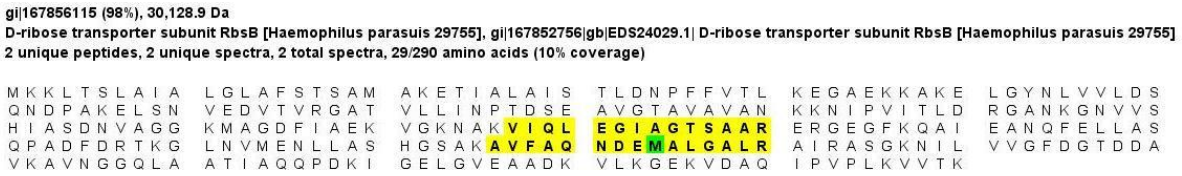

b)

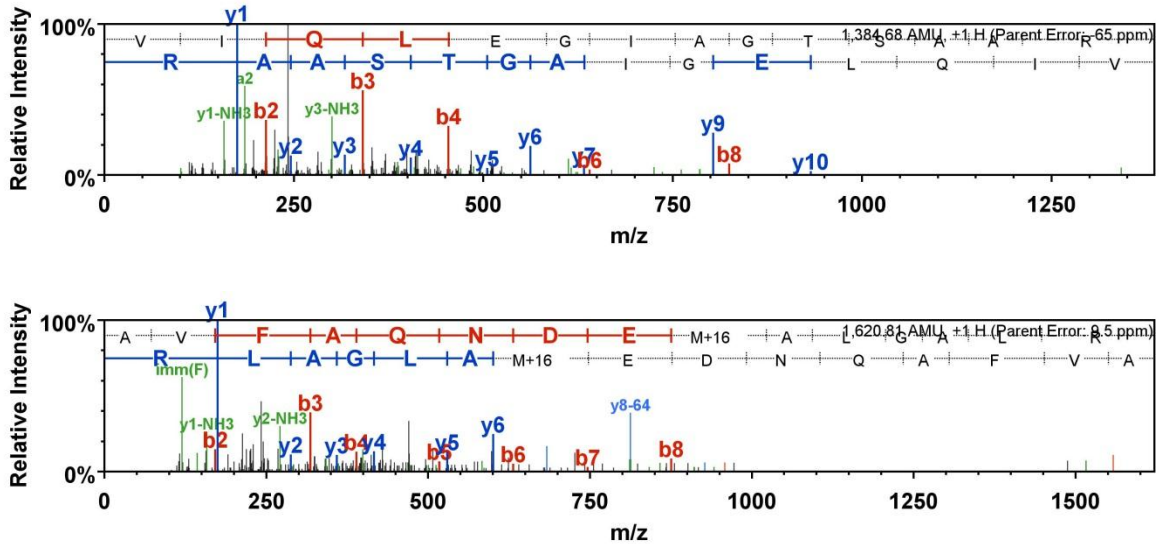

Supplemental Figure S2.16. Protein sequence coverage map for HP3-4 (a) and corresponding peptides (b).

a)

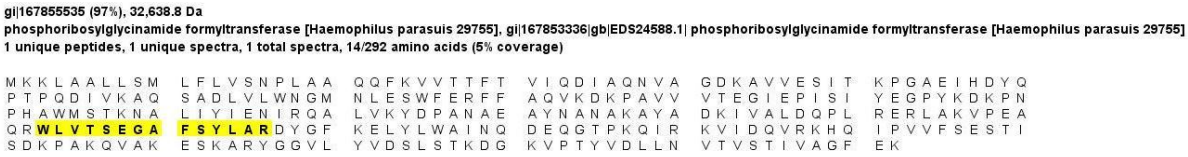

b)

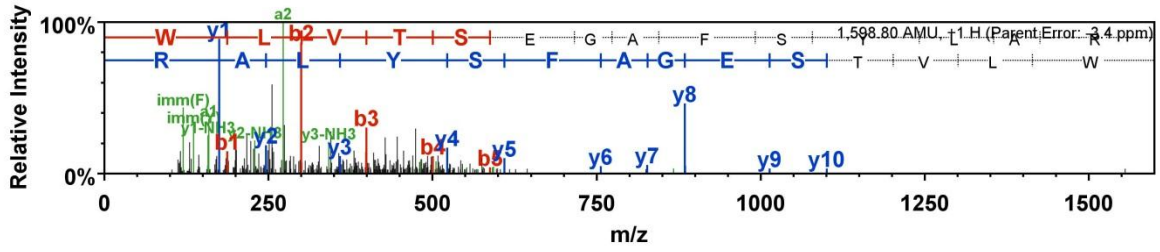

Supplemental Figure S2.17. Protein sequence coverage map for HP3-5 (a) and corresponding peptides (b).

a)

gi|167855535 (99%), 32,638.8 Da
phosphoribosylglycinamide formyltransferase [Haemophilus parasuis 29755], gi|167853336|gb|EDS24588.1| phosphoribosylglycinamide formyltransferase [Haemophilus parasuis 29755]
2 unique peptides, 2 unique spectra, 2 total spectra, 24/292 amino acids (8% coverage)

MKKLAALLSM LFLVSNPLAA QQFKVVTTFT VIQDIAQNVA GDKAVVESIT KPGAEIHDYQ
PTPQDIVKAQ SADLVLWNGM NLESWFERFF AQVKDKPAVV VTEGIEPISI YEGPYKDKPN
PHAWMSTKNA LIYIENIRQA LVKYDPANAE AYNANAKAYA DKIVALDQPL RERLAKVPEA
QRWLVTSEGA FSYLARDYGF KELYLWAINQ DEQGTPKQIR KVIDQVRKHQ IPVVFSESTI
SDKPAKQVAK ESKARYGGVL YVDSLSTKDG KVPTYVDLLN VTVSTIVAGF EK

b)

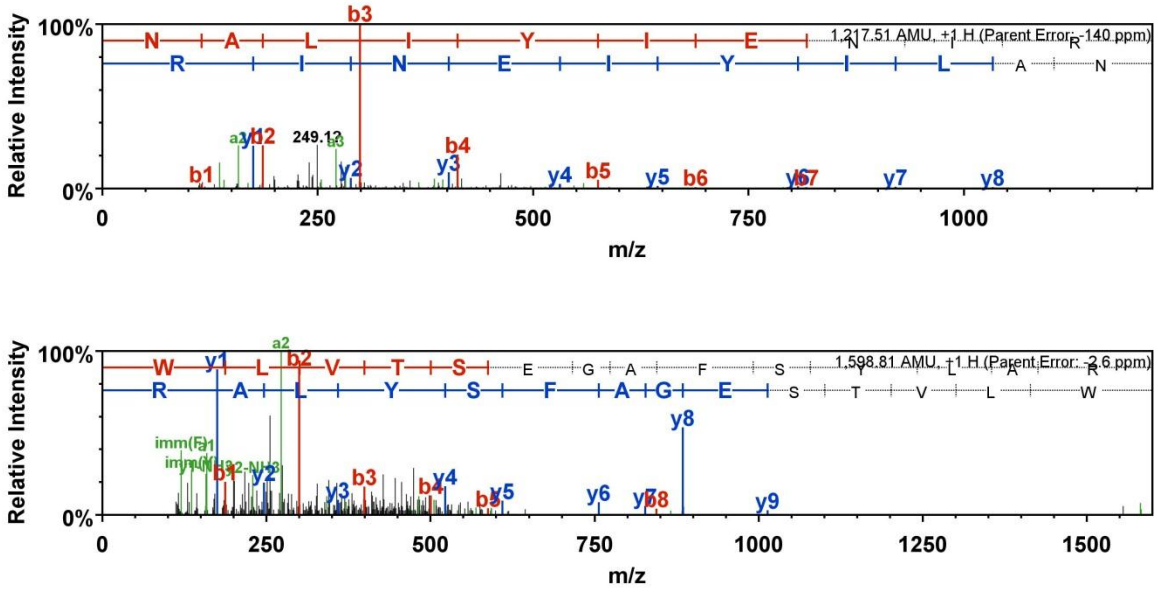

Supplemental Figure S2.18. Protein sequence coverage map for HP3-6 (a) and corresponding peptides (b).

a)

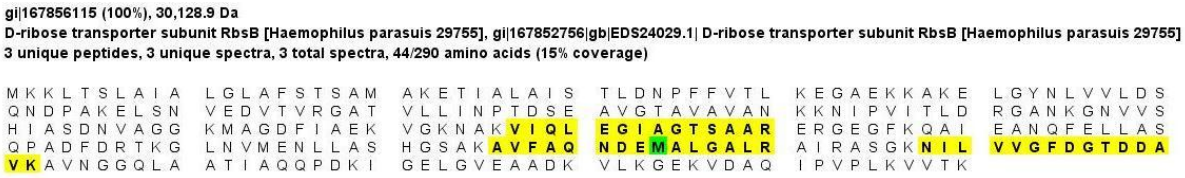

b)

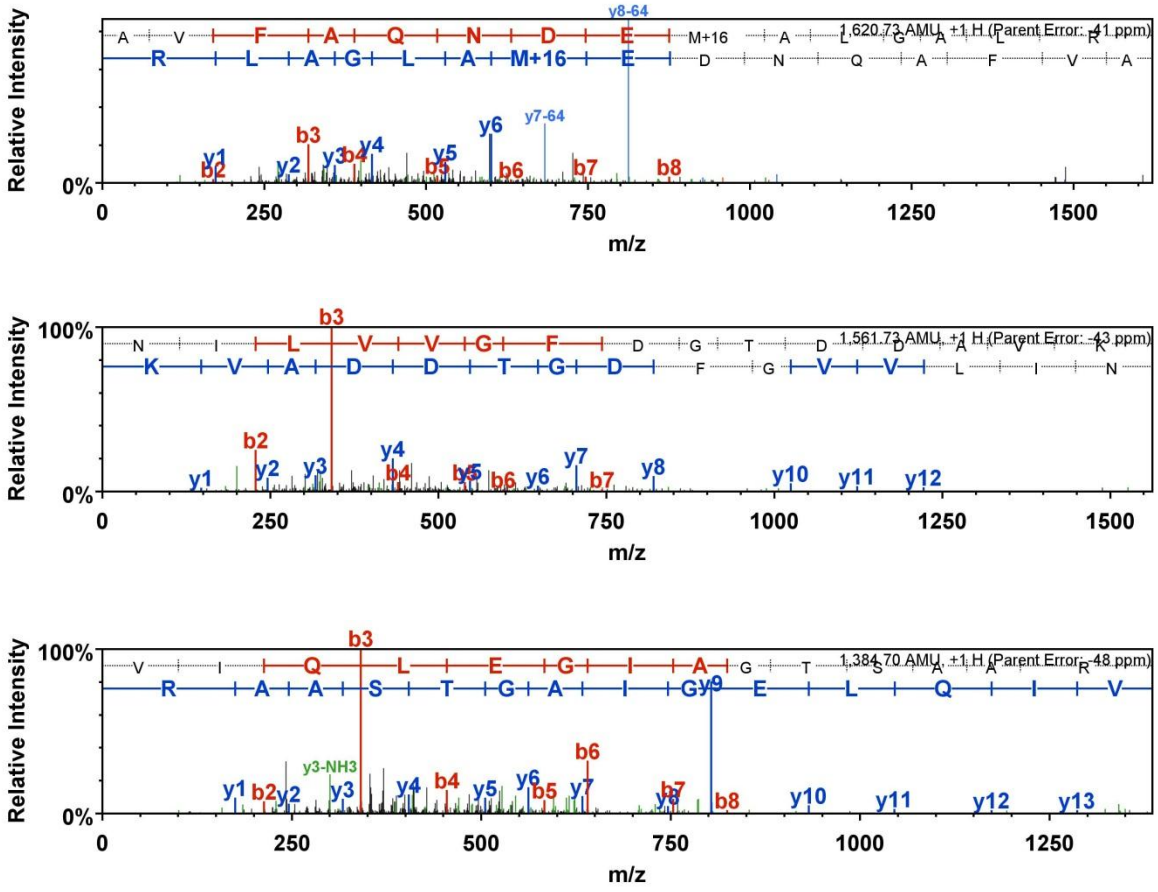

Supplemental Figure S2.19. Protein sequence coverage map for HP5-2 (a) and corresponding peptides (b).

a)

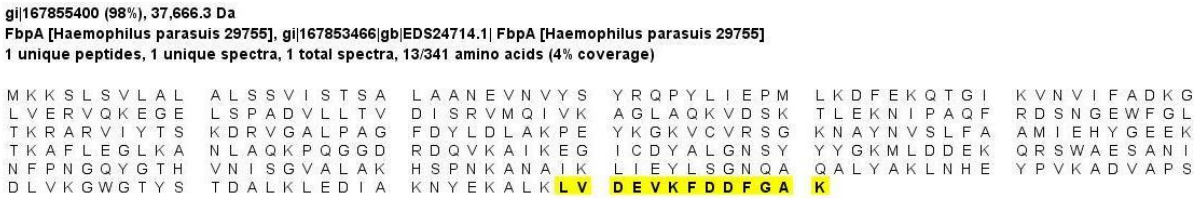

b)

Supplemental Figure S2.20. Protein sequence coverage map for HP5-3 (a) and corresponding peptides (b).

a)

gi|299773319 (100%), 38,748.7 Da
outer membrane protein P2 [Haemophilus parasuis]
3 unique peptides, 3 unique spectra, 3 total spectra, 46/359 amino acids (13% coverage)

M	K	K	T	L	V	A	L	A	V	A	A	F	A	A	S	A	S	A	V	T	V	Y	E	N	E	G	T	K	V	D	F	D	G	Q	L	R	L	L	L	E	E	Q	A	T	K	E	K	G	Q	S	S	T	R	G	H	T	N	L	K
N	N	S	S	R	F	G	I	S	I	K	H	N	I	N	E	N	L	Y	G	F	G	R	Y	E	T	R	L	D	S	N	S	E	N	A	A	G	W	G	D	V	K	T	K	Y	A	Y	V	G	L	G	G	Y	G	H	E	I	S	F	G
K	**Q**	**D**	**V**	**I**	**G**	**D**	**S**	**I**	**G**	**Q**	**A**	**G**	**F**	**D**	**K**	V	Y	G	V	G	T	G	G	I	K	Y	S	A	N	N	T	N	K	K	G	F	D	I	L	T	S	D	S	D	S	A	I	N	Y	T	Y	T	G	I	E	G	L	T	L
G	A	N	Y	N	V	A	N	E	R	D	K	K	T	G	E	V	N	V	G	S	T	K	S	G	F	G	L	G	A	K	Y	T	A	K	I	A	E	S	Q	S	V	T	V	A	A	G	Y	T	H	D	D	Y	K	S	G	S	V	N	K
K	D	K	D	G	V	Y	F	G	L	K	**Y**	**V**	**N**	**A**	**P**	**F**	**T**	**V**	**A**	**V**	**D**	**G**	**G**	**H**	**G**	**V**	**E**	**K**	T	G	N	V	K	E	K	I	D	F	V	R	T	G	A	R	F	D	V	T	P	K	S	G	V	Y	G	N	Y	S	Y
G	T	Y	K	D	K	A	Y	K	**A**	**T**	**A**	**H**	**Q**	**F**	**M**	**L**	**G**	**A**	**D**	**Y**	**K**	L	H	K	Q	V	V	T	F	V	E	G	R	L	I	K	N	K	D	S	N	N	K	K	V	T	D	Q	A	L	G	V	G	L	R	V	L	W

gi|299773319 (90%), 38,748.7 Da
outer membrane protein P2 [Haemophilus parasuis]
1 unique peptides, 1 unique spectra, 1 total spectra, 12/359 amino acids (3% coverage)

M	K	K	T	L	V	A	L	A	V	A	A	F	A	A	S	A	S	A	V	T	V	Y	E	N	E	G	T	K	V	D	F	D	G	Q	L	R	L	L	L	E	E	Q	A	T	K	E	K	G	Q	S	S	T	R	G	H	T	N	L	K
N	N	S	S	R	F	G	I	S	I	K	**H**	**N**	**I**	**N**	**E**	**N**	**L**	**Y**	**G**	**F**	**G**	**R**	Y	E	T	R	L	D	S	N	S	E	N	A	A	G	W	G	D	V	K	T	K	Y	A	Y	V	G	L	G	G	Y	G	H	E	I	S	F	G
K	Q	D	V	I	G	D	S	I	G	Q	A	G	F	D	K	V	Y	G	V	G	T	G	G	I	K	Y	S	A	N	N	T	N	K	K	G	F	D	I	L	T	S	D	S	D	S	A	I	N	Y	T	Y	T	G	I	E	G	L	T	L
G	A	N	Y	N	V	A	N	E	R	D	K	K	T	G	E	V	N	V	G	S	T	K	S	G	F	G	L	G	A	K	Y	T	A	K	I	A	E	S	Q	S	V	T	V	A	A	G	Y	T	H	D	D	Y	K	S	G	S	V	N	K
K	D	K	D	G	V	Y	F	G	L	K	Y	V	N	A	P	F	T	V	A	V	D	G	G	H	G	V	E	K	T	G	N	V	K	E	K	I	D	F	V	R	T	G	A	R	F	D	V	T	P	K	S	G	V	Y	G	N	Y	S	Y
G	T	Y	K	D	K	A	Y	K	A	T	A	H	Q	F	M	L	G	A	D	Y	K	L	H	K	Q	V	V	T	F	V	E	G	R	L	I	K	N	K	D	S	N	N	K	K	V	T	D	Q	A	L	G	V	G	L	R	V	L	W

b)

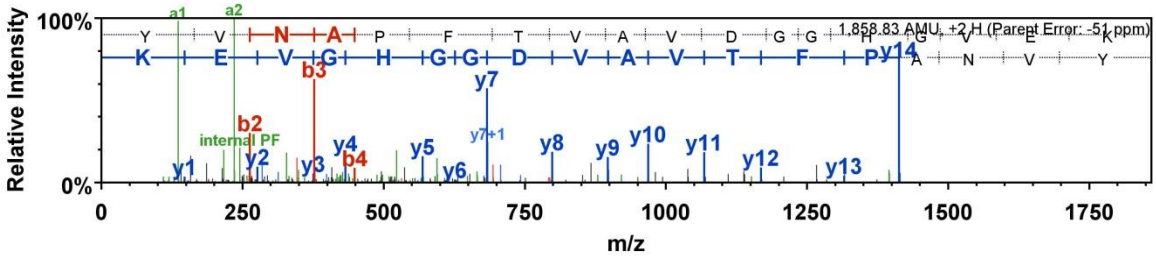

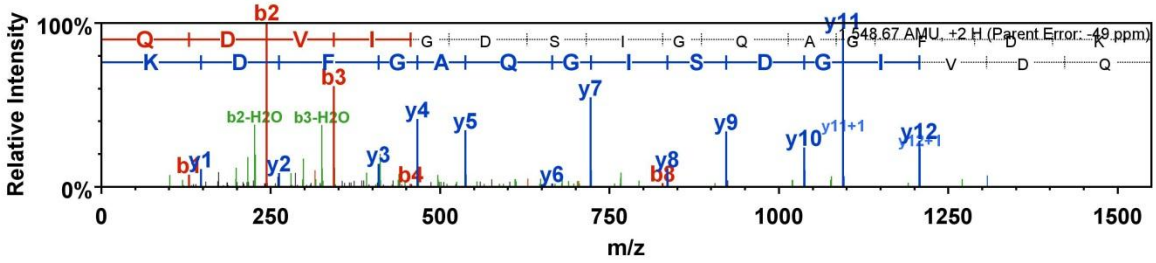

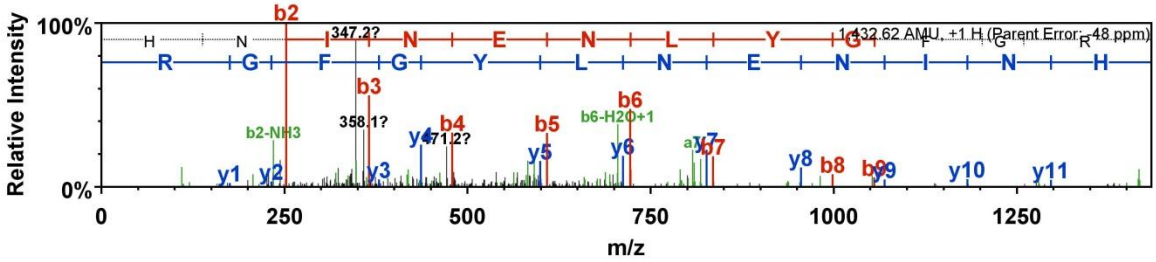

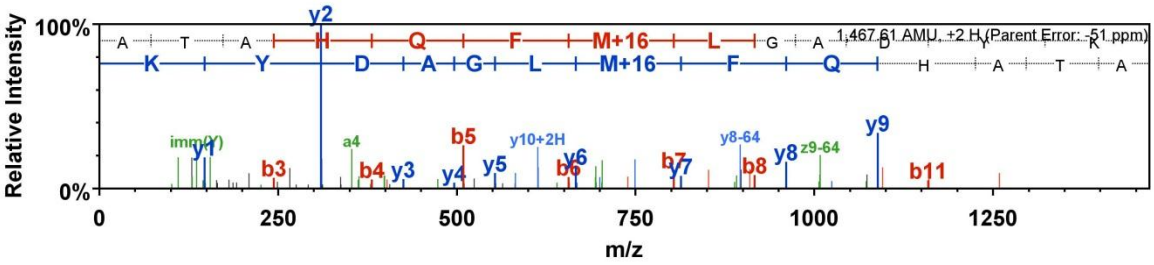

Supplemental Figure S2.21. Protein sequence coverage map for HP5-4 (a) and corresponding peptides (b).

a)

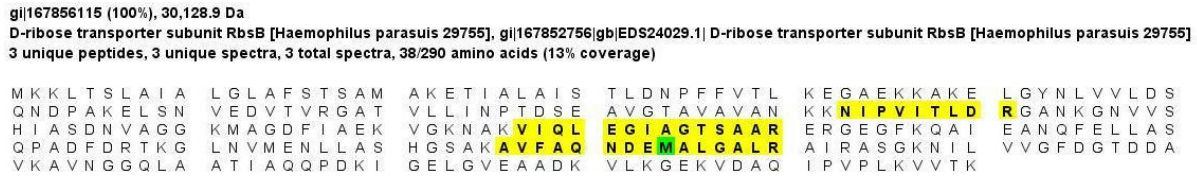

b)

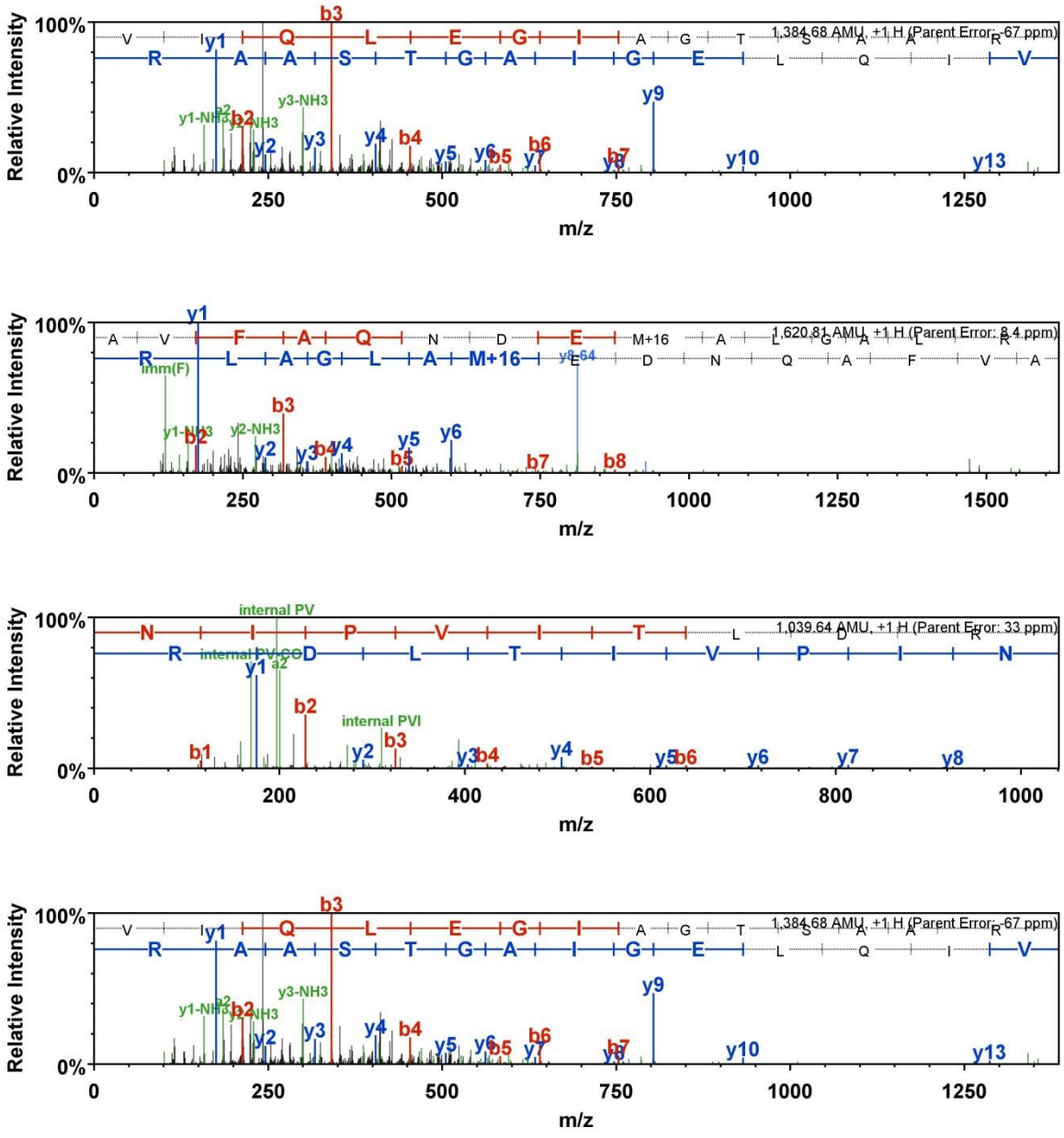

Supplemental Figure S2.22. Protein sequence coverage map for HP5-5 (a) and corresponding peptides (b).

a)

gi|167855535 (100%), 32,638.8 Da
phosphoribosylglycinamide formyltransferase [Haemophilus parasuis 29755], gi|167853336|gb|EDS24588.1| phosphoribosylglycinamide formyltransferase [Haemophilus parasuis 29755]
2 unique peptides, 2 unique spectra, 2 total spectra, 24/292 amino acids (8% coverage)

MKKLAALLSM LFLVSNPLAA QQFKVVTTFT VIQDIAQNVA GDKAVVESIT KPGAEIHDYQ
PTPQDIVKAQ SADLVLWNGM NLESWFERFF AQVKDKPAVV VTEGIEPISI YEGPYKDKPN
PHAWMSTKNA LIYIENIRQA LVKYDPANAE AYNANAKAYA DKIVALDQPL RERLAKVPEA
QRWLVTSEGA FSYLARDYGF KELYLWAINQ DEQGTPKQIR KVIDQVRKHQ IPVVFSESTI
SDKPAKQVAK ESKARYGGVL YVDSLSTKDG KVPTYVDLLN VTVSTIVAGF EK

b)

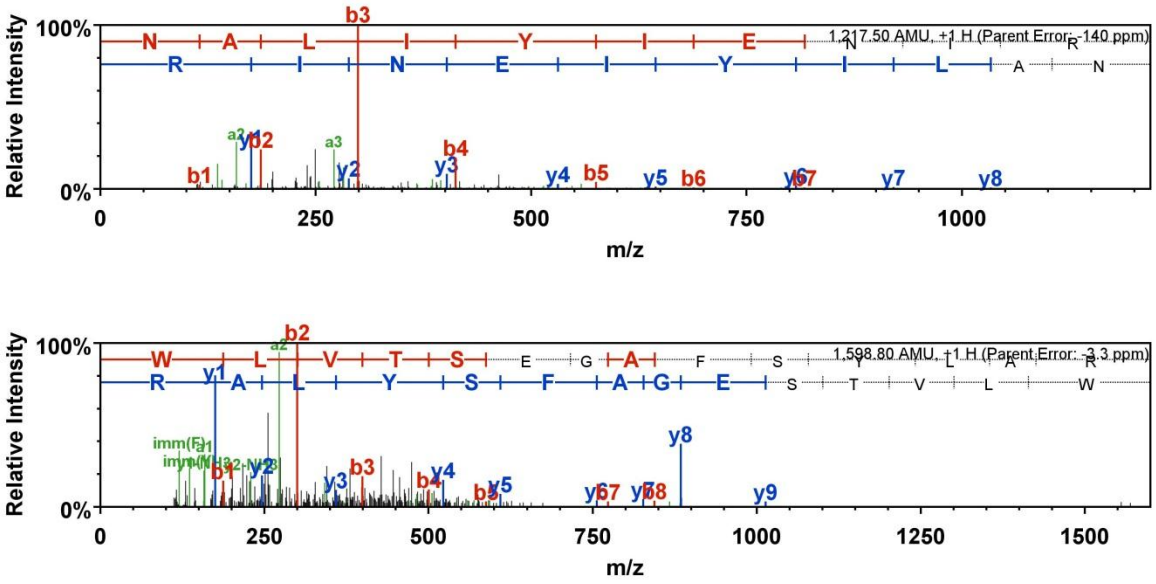

Supplemental Figure S2.23. Protein sequence coverage map for HP5-6 (a) and corresponding peptides (b).

a)

gi|167856489 (100%), 18,036.7 Da
glucose-specific PTS system enzyme IIA component [Haemophilus parasuis 29755], gi|219871157|ref|YP_002475532.1| PTS system glucose-specific transporter subunit
2 unique peptides, 2 unique spectra, 2 total spectra, 36/167 amino acids (22% coverage)

MGFFDKLFGG KKEAVAKEVK IYAPLSGEIV NIEDVPDVVF SEKIVGDGIA IRPTGDMIVA
PVNGTIGKIF ETNHAFSIES EDGVELFVHF GIDTVELKGE GFTRLAEENQ EVKVGDPIIK
FDLELLQSKA KSVLTPVVIS NMDEVTNLQK LSGEVVAGES TVLVLTK

gi|152977925 (95%), 16,894.9 Da
putative PTS IIA-like nitrogen-regulatory protein PtsN [Actinobacillus succinogenes 130Z], gi|150839648|gb|ABR73619.1| putative PTS IIA-like nitrogen-regulatory
1 unique peptides, 1 unique spectra, 1 total spectra, 15/155 amino acids (10% coverage)

MLKESLIENN SIKLNQTAAD WKEAIKIGTD LLVAAGTIEP RYYDHIIDNI EKMGPYIILA
PGLAMPHARP EEGVIKTSFA LVTLKEPVAF QGEDEPVSVF ITLAGSDSDK HMEGLMEITQ
TLDDPDSESG VDLGKILRCQ TNEEVLAVID AALSE

b)

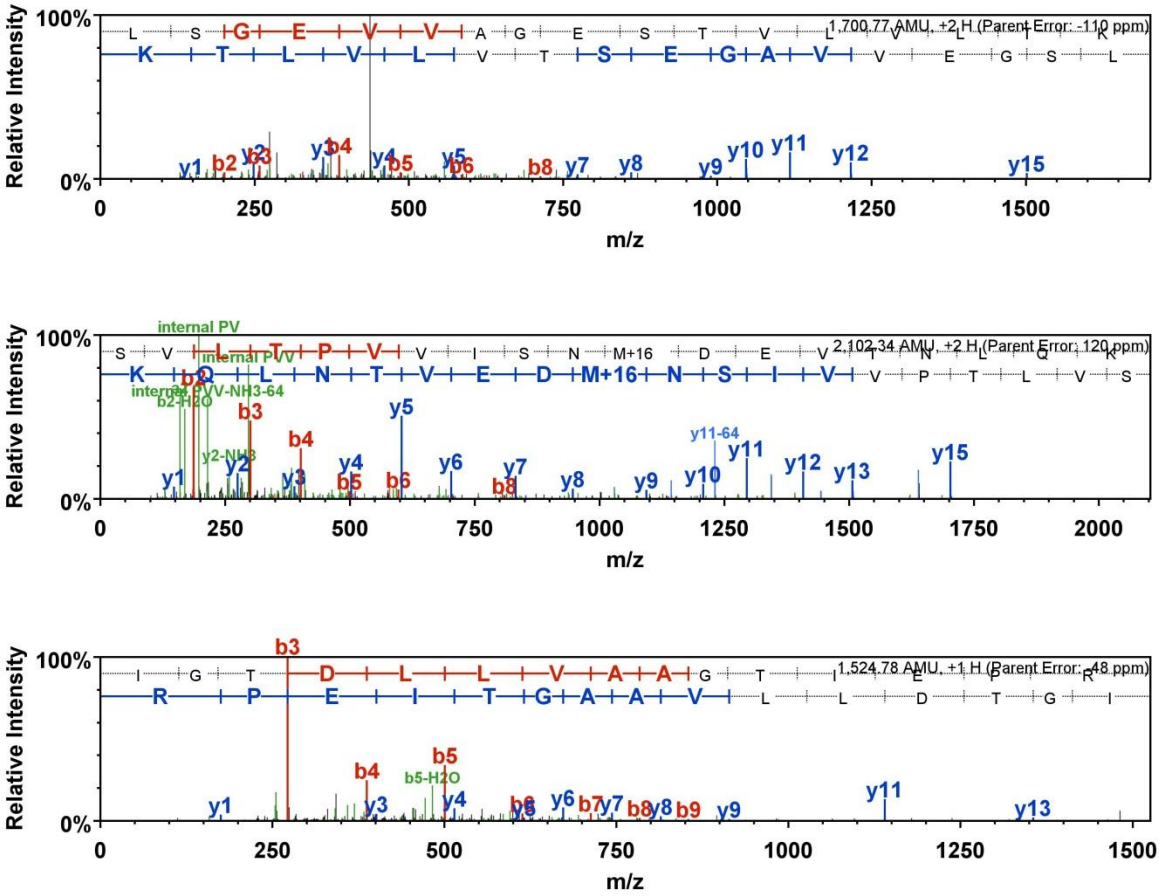

Supplemental Figure S2.24: Protein sequence coverage map for HP6-1 (a) and corresponding peptides (b).

a)

gi|167854855 (95%), 16,264.7 Da
acetyl-CoA carboxylase biotin carboxylase subunit [Haemophilus parasuis 29755], gi|219871451|ref|YP_002475826.1| biotin carboxyl carrier protein of acetyl-CoA
1 unique peptides, 1 unique spectra, 1 total spectra, 15/156 amino acids (10% coverage)

MDIRKIKKLI ELVEESGITE LEVSEEEGTV RISRAAPAVA PAAVQYVAAP QAAPAPAATP
APAAQTAPAA APAPTAEVSG HAILSPMVGT FYRSPSPEAA PFVEVGKTVK VGDTLCIVEA
MKMMNRIESD KAGVIKAILV NDGEAVEFDQ KLFIIE

b)

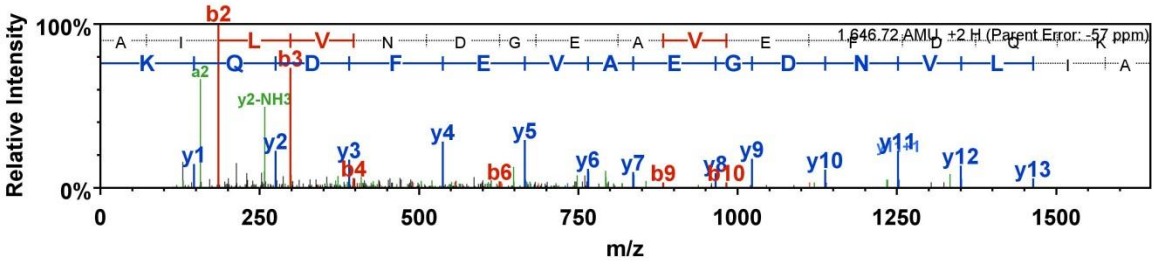

Supplemental Figure S2.25. Protein sequence coverage map for HP6-2 (a) and corresponding peptides (b).

a)

gi|167855535 (100%), 32,638.8 Da
phosphoribosylglycinamide formyltransferase [Haemophilus parasuis 29755], gi|167853336|gb|EDS24588.1| phosphoribosylglycinamide formyltransferase [Haemo
8 unique peptides, 8 unique spectra, 8 total spectra, 124/292 amino acids (42% coverage)

MKKLAALLSM LFLVSNPLAA QQFKVVTTFT VIQDIAQNVA GDKAVVESIT KPGAEIHDYQ
PTPQDIVKAQ SADLVLWNGM NLESWFERFF AQVKDKPAVV VTEGIEPISI YEGPYKDKPN
PHAWMSTKNA LIYIENIRQA LVKYDPANAE AYNANAKAYA DKIVALDQPL RERLAKVPEA
QRWLVTSEGA FSYLARDYGF KELYLWAINQ DEQGTPKQIR KVIDQVRKHQ IPVVFSESTI
SDKPAKQVAK ESKARYGGVL YVDSLSTKDG KVPTYVDLLN VTVSTIVAGF EK

b)

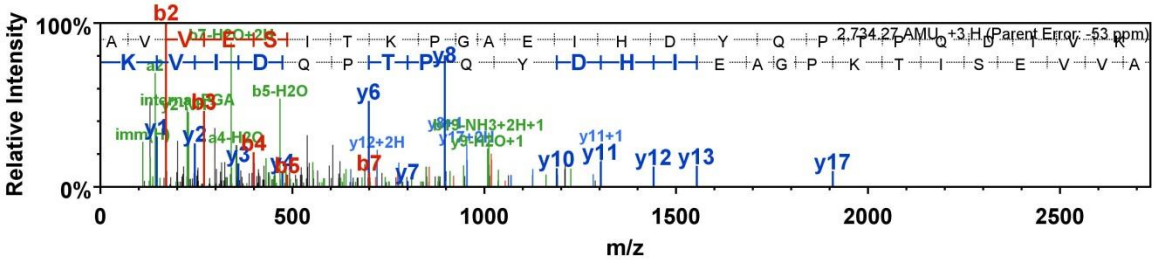

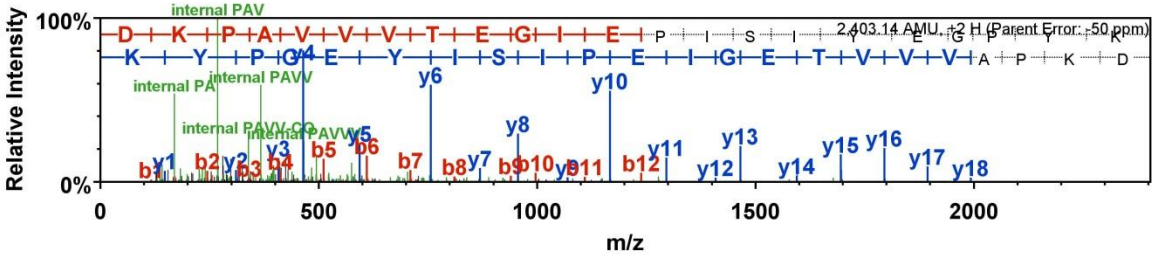

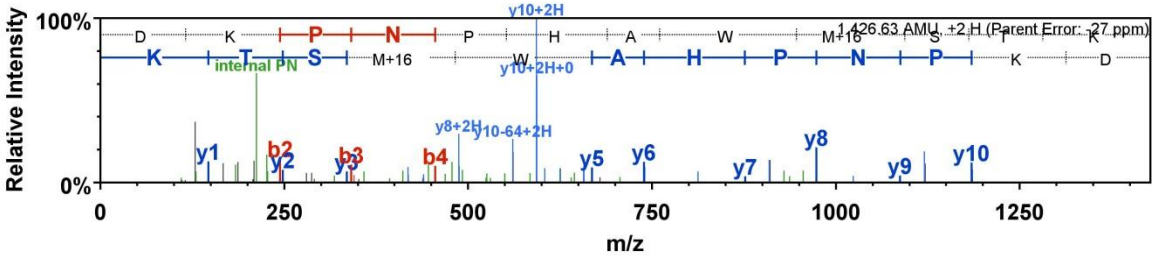

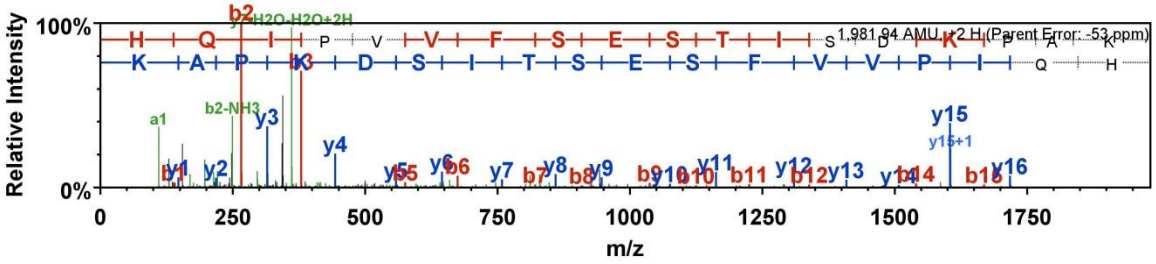

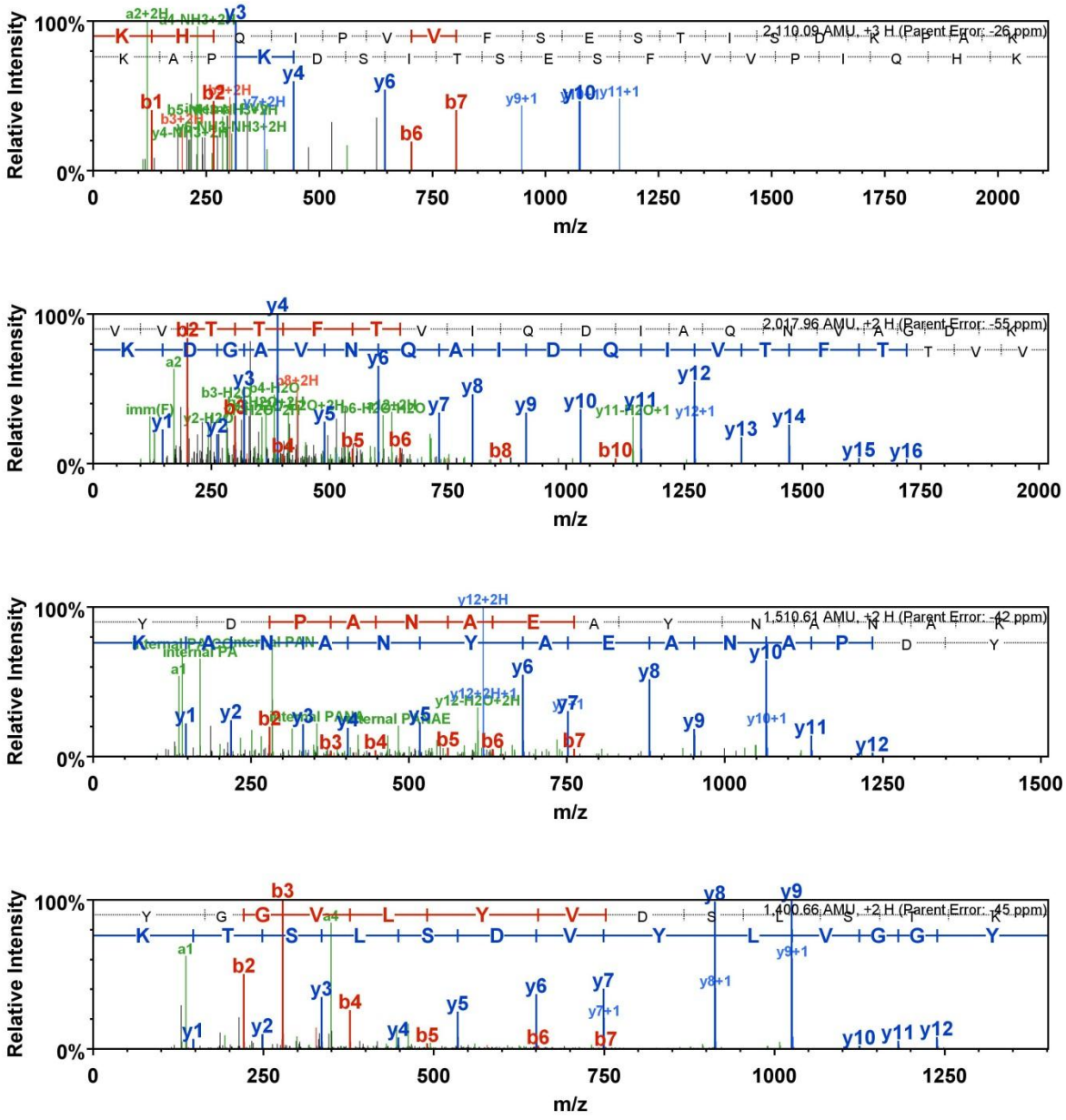

Supplemental Figure S2.26. Protein sequence coverage map for HP6-3 (a) and corresponding peptides (b).

a)

gi|167855535 (100%), 32,638.8 Da
phosphoribosylglycinamide formyltransferase [Haemophilus parasuis 29755], gi|167853336|gb|EDS24588.1| phosphoribosylglycinamide formyltransferase [Haem
2 unique peptides, 2 unique spectra, 2 total spectra, 23/292 amino acids (8% coverage)

MKKLAALLSM LFLVSNPLAA QQFKVVTTFT VIQDIAQNVA GDKAVVESIT KPGAEIHDYQ
PTPQDIVKAQ SADLVLWNGM NLESWFERFF AQVKDKPAVV VTEGIEPISI YEGPYKDKPN
PHAWMSTKNA LIYIENIRQA LVKYDPANAE AYNANAKAYA DKIVALDQPL RERLAKVPEA
QRWLVTSEGA FSYLARDYGF KELYLWAINQ DEQGTPKQIR KVIDQVRKHQ IPVVFSESTI
SDKPAKQVAK ESKARYGGVL YVDSLSTKDG KVPTYVDLLN VTVSTIVAGF EK

b)

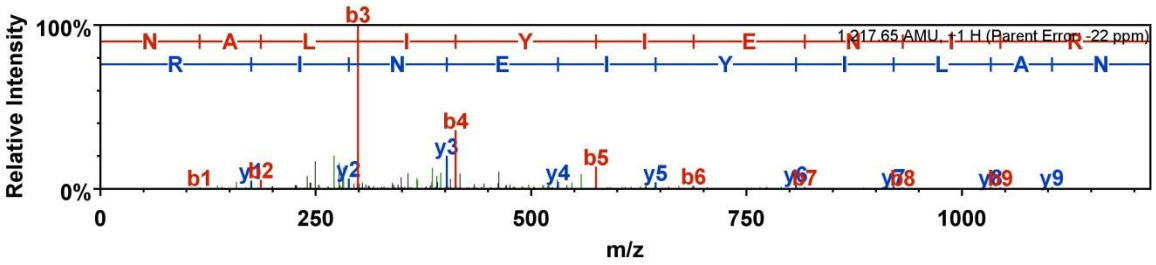

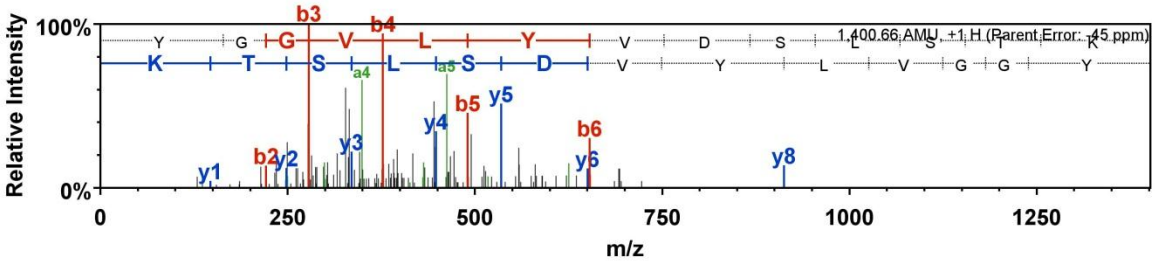

Supplemental Figure S2.27. Protein sequence coverage map for HP6-4 (a) and corresponding peptides (b).

a)

gi|167855017 (100%), 38,465.4 Da
hypothetical protein HPS_10240 [Haemophilus parasuis 29755], gi|167853865|gb|EDS25105.1| hypothetical protein HPS_10240 [Haemophilus parasuis 29755]
5 unique peptides, 5 unique spectra, 6 total spectra, 73/346 amino acids (21% coverage)

MKKWAVAFTS GMVMLGANSA LANDTVHLYT WTEYVPEGLL EEFTKQTGIK VVVSSLESNE
TMYAKLKIQG KDGGYDVIAP SNYFVSKMGR EGMLMELDHS KLPVIKDLNP DWLNKPYDKG
NKYSLPQLLG APGIAFNTNS YKGDNFTAWG DLWKPEFKGK VQLLDDAREV FNIALLKLGQ
DPNTKDPAVI KAAYEELLKL RPNVLAFSSD NPANSFISGE VEVGQLWNGS VRIAKKEQAP
VNMVFPKEGP VLWVDTLAIP SNAKNPDAAH KLINYLLSAP VAEKLTLEIG YPTSNVKALE
KLPKEITEDP AIYPTSEVLQ KSQWQDDVGD AIELYEKYYQ ELKAAK

gi|167855017 (100%), 38,465.4 Da
hypothetical protein HPS_10240 [Haemophilus parasuis 29755], gi|167853865|gb|EDS25105.1| hypothetical protein HPS_10240 [Haemophilus parasuis 29755]
2 unique peptides, 2 unique spectra, 2 total spectra, 29/346 amino acids (8% coverage)

MKKWAVAFTS GMVMLGANSA LANDTVHLYT WTEYVPEGLL EEFTKQTGIK VVVSSLESNE
TMYAKLKIQG KDGGYDVIAP SNYFVSKMGR EGMLMELDHS KLPVIKDLNP DWLNKPYDKG
NKYSLPQLLG APGIAFNTNS YKGDNFTAWG DLWKPEFKGK VQLLDDAREV FNIALLKLGQ
DPNTKDPAVI KAAYEELLKL RPNVLAFSSD NPANSFISGE VEVGQLWNGS VRIAKKEQAP
VNMVFPKEGP VLWVDTLAIP SNAKNPDAAH KLINYLLSAP VAEKLTLEIG YPTSNVKALE
KLPKEITEDP AIYPTSEVLQ KSQWQDDVGD AIELYEKYYQ ELKAAK

b)

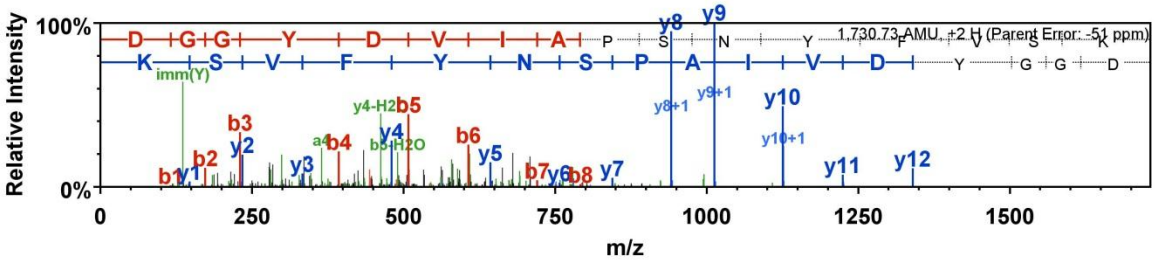

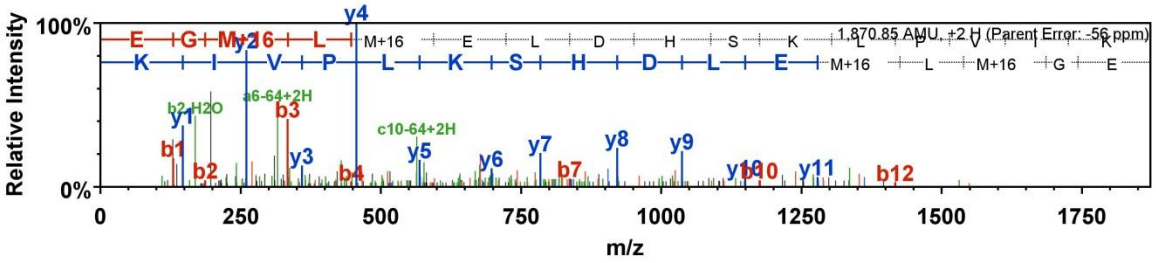

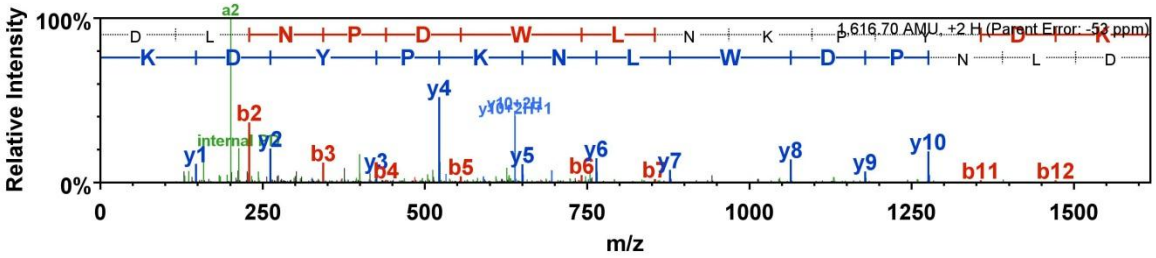

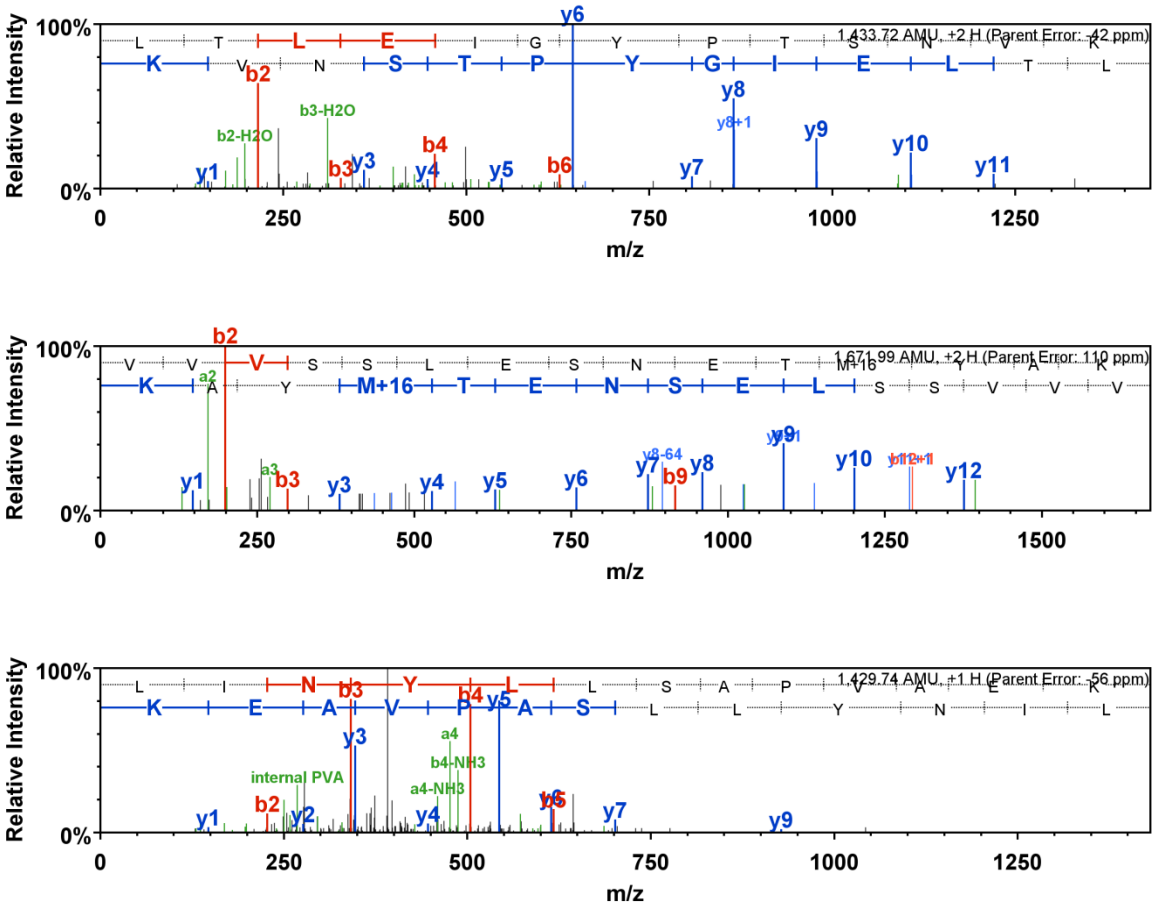

Supplemental Figure S2.28. Protein sequence coverage map for HP6-5 (a) and corresponding peptides (b).

a)

gi|167854835 (100%), 29,764.5 Da
alanine aminotransferase [Haemophilus parasuis 29755], gi|219871433|ref|YP_002475808.1| outer membrane protein 26 [Haemophilus parasuis SH0165], gi|16785
2 unique peptides, 2 unique spectra, 2 total spectra, 31/267 amino acids (12% coverage)

MKNLFKLAAV ASALAFSANT VNANEKIGFV DPNFLIQNHP LTIEANDKFT KFMKDTESKF
APREKQLAAE NKALSDEEKA LLDERKKIEE DAQKLQKEQV TLEAAMKKKV AQLEKDAPRL
KAKEIQARQD KINAEAKPFQ NKVSALQQRE VEFGKKAEEF QKRADEFQKK VAAFQEEIAK
VQKESGVITP EQVQQKVVED INAKIKQVAE SKGYTLVLPP SVALYAKDGN AADITEEILV
AMGGKMPEAP KTEVPAAEVT KPEEVKK

b)

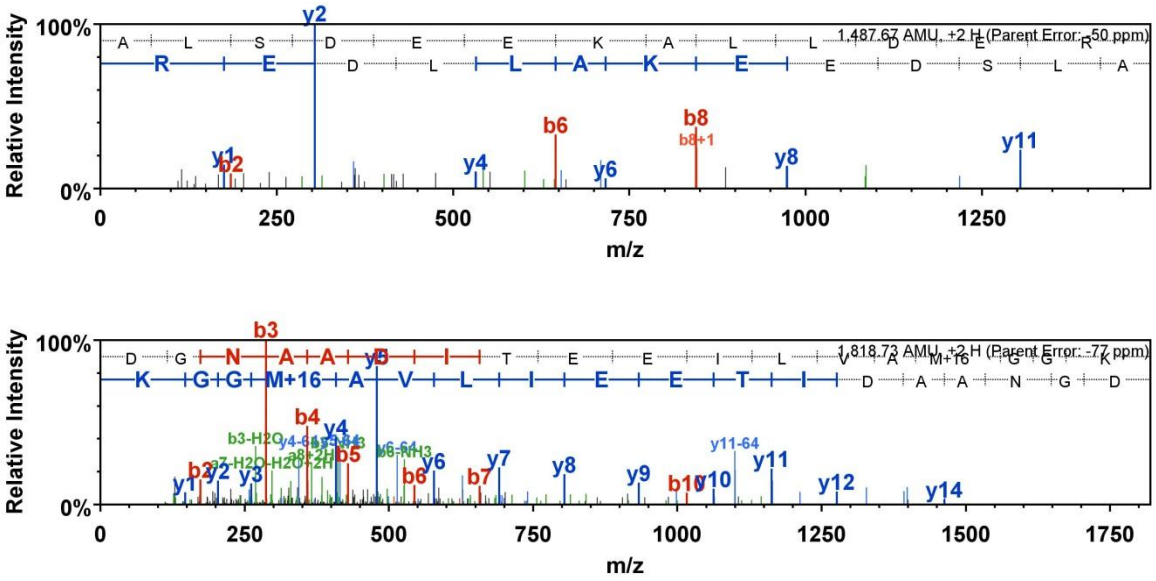

Supplemental Figure S2.29. Protein sequence coverage map for HP7-1 (a) and corresponding peptides (b).

a)

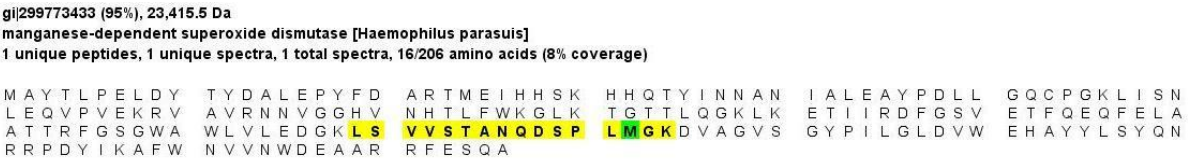

b)

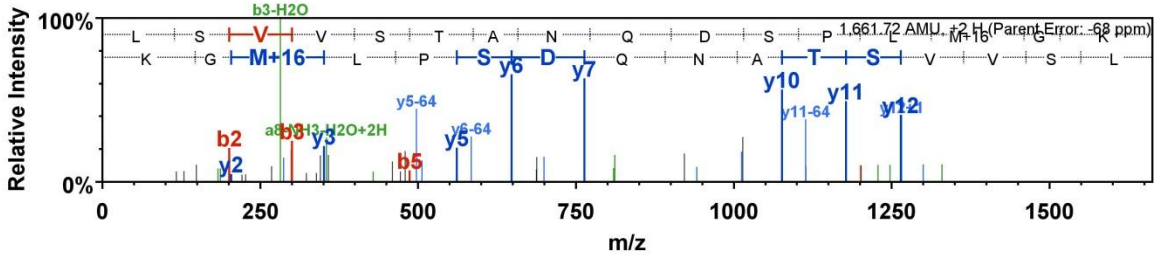

Supplemental Figure S2.30. Protein sequence coverage map for HP8-1 (a) and corresponding peptides (b).

a)

gi|167855453 (100%), 26,013.2 Da
purine nucleoside phosphorylase [Haemophilus parasuis 29755], gi|219871397|ref|YP_002475772.1| purine nucleoside phosphorylase [Haemophilus parasuis SH0165]
3 unique peptides, 3 unique spectra, 3 total spectra, 44/239 amino acids (18% coverage)

```
MTPHINAPAG  AFADVVLMPG  DPLRAKYIAE  TFLENAEQVT  NVRNMFGYTG  TYKGRRISVM
GHGMGIPSCS  IYAKELITEY  GVKKIIRVGS  CGAVRQDVKL  REVIIGVGAC  TDSKVNRIRF
KDNDFAAIAD  FDLTLAAVQA  AKAKGINVRV  GNLYSADLFY  TPDVEMFDVM  EKYGILGVEM
EAAGIYGVAA  EFGAKALTIC  TVSDHIRTHE  QTTAEERQLT  FNDMIEIALE  SVLIGDQQG
```

b)

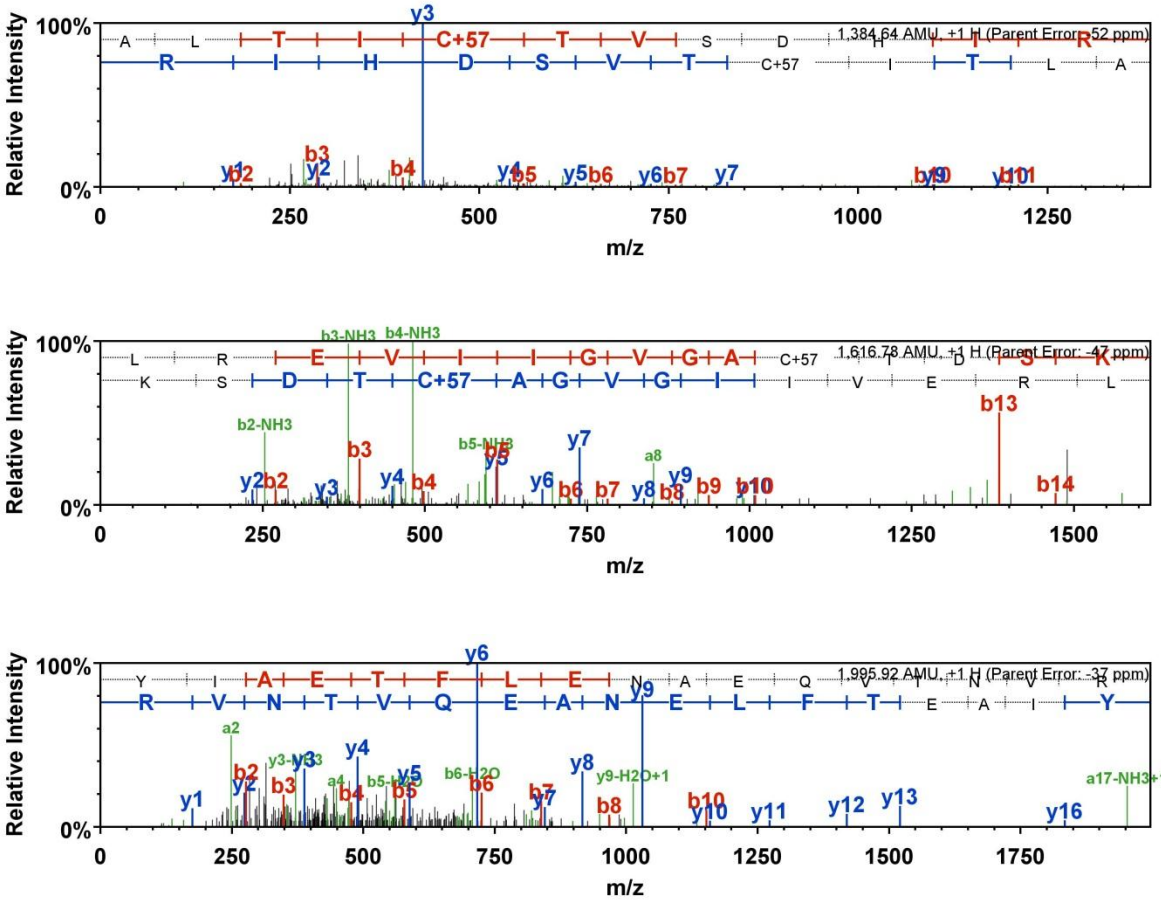

Supplemental Figure S2.31. Protein sequence coverage map for HP8-2 (a) and corresponding peptides (b).

a)

gi|167855953 (100%), 32,976.6 Da
periplasmic binding protein/LacI transcriptional regulator [Haemophilus parasuis 29755], gi|167852947|gb|EDS24213.1| periplasmic binding protein/LacI transcriptional
4 unique peptides, 4 unique spectra, 5 total spectra, 78/315 amino acids (25% coverage)

MKKLAIVTAT VLGLSTLFAG SAWAKSDEIA VIVKSANSTF WQNVRKGAET AGADLGGKYK
VTFQGPESET AIDAQVNMVD NAVNRGVAGI VLAASDPVAL VPAVRKAYES GIPVVLIDSG
LNSDGKYYQS FLATDNRAAG KLAAEKLLAK VKGGKVAVMS FTQGAASAIE RTGGFIDEVK
SKADYKIVGP YYSNSEMVTA LNQTEDVLGS NPDIAAIFGA NEPTAVGMAR AVKQKGFAGK
IVAVGFDGNS DLQNFVRDGT LDGIVVQSSY QMGYKGVDTI GKIIKGEKVE KVIDTGVVYV
TKENIDSPEA KAVLY

gi|219871818 (100%), 33,032.8 Da
ABC D-ribose transporter periplasmic-binding compoent RbsB [Haemophilus parasuis SH0165], gi|219692022|gb|ACL33245.1| ABC D-ribose transporter periplasmic-
5 unique peptides, 5 unique spectra, 5 total spectra, 75/315 amino acids (24% coverage)

MKKLAIVTTT VLGLSTLFAG LAWAKSDEIA VIVKSANSTF WQNVRKGAET AGADLGGKYK
VTFQGPESET AIDAQVNMVD NAVNRGVAGI VLAASDPVAL VPAVRKAYES GIPVVLIDSG
LNSDGKYYQS FLATDNRAAG KLAAEKLLAK VKGGKVAVMS FTQGAASAIE RTGGFIDEVK
SKADYKIVGP YYSNSEMVTA LNQTEDVLGS NPDIAAIFGA NEPTAVGMAR AVKQKGFAGK
IVAVGFDGNS DLQNFVRDGT LDGIVVQSSY QMGYKGVDTI GKIIKGEKVE KVIDTGVVYV
TKENIDSPEA KAVLY

b)

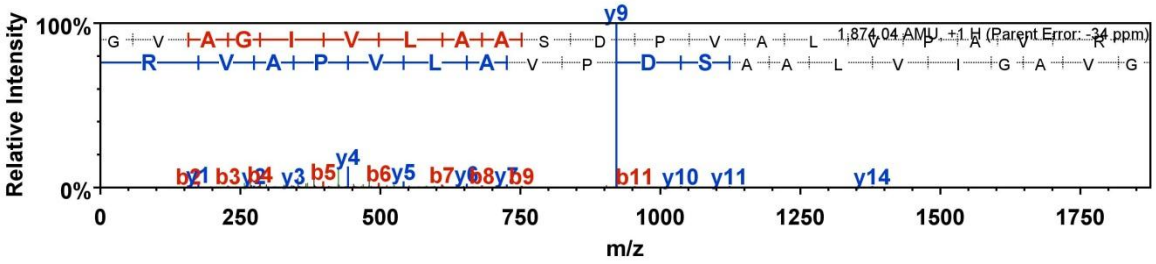

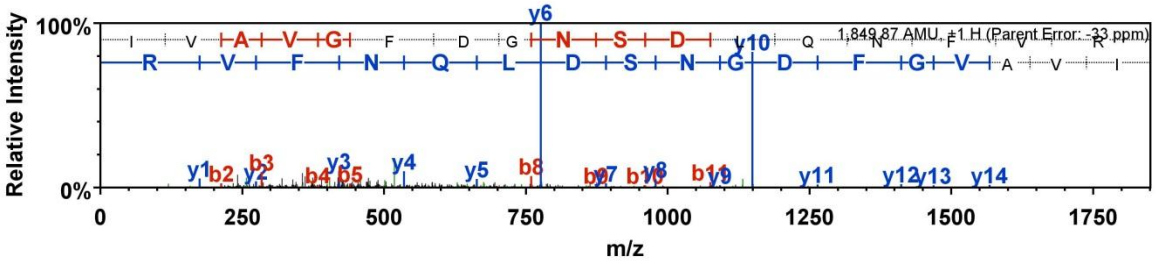

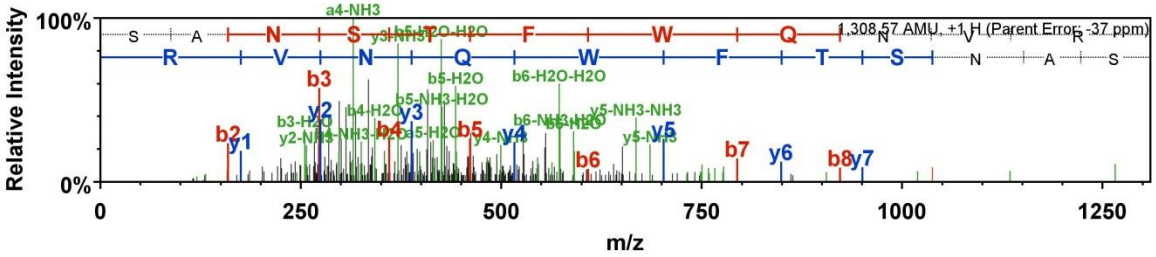

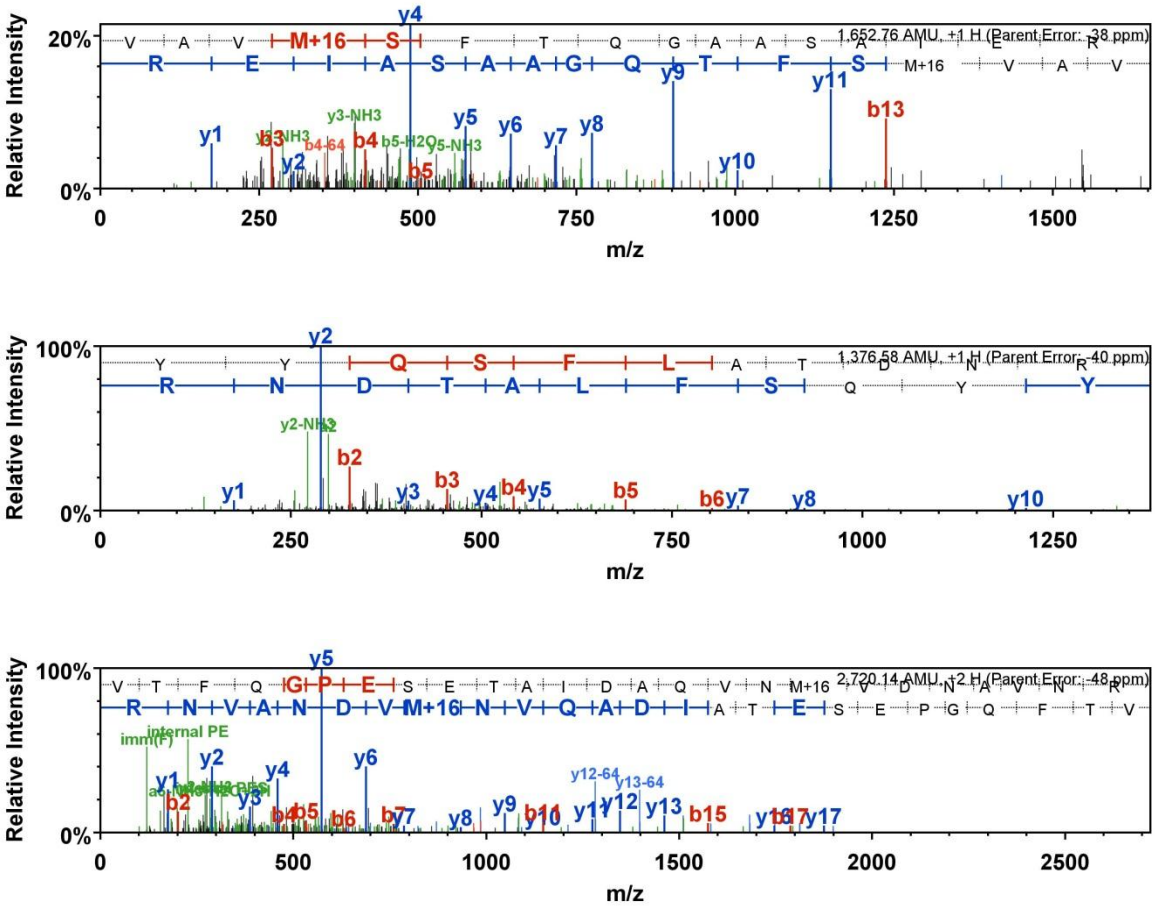

Supplemental Figure S2.32. Protein sequence coverage map for HP8-3 (a) and corresponding peptides (b).

a)

gi|167855535 (95%), 32,638.8 Da
phosphoribosylglycinamide formyltransferase [Haemophilus parasuis 29755], gi|167853336|gb|EDS24588.1| phosphoribosylglycinamide formyltransferase [Haemophilus parasuis 29755]
1 unique peptides, 1 unique spectra, 1 total spectra, 10/292 amino acids (3% coverage)

MKKLAALLSM LFLVSNPLAA QQFKVVTTFT VIQDIAQNVA GDKAVVESIT KPGAEIHDYQ
PTPQDIVKAQ SADLVLWNGM NLESWFERFF AQVKDKPAVV VTEGIEPISI YEGPYKDKPN
PHAWMSTKNA LIYIENIRQA LVKYDPANAE AYNANAKAYA DKIVALDQPL RERLAKVPEA
QRWLVTSEGA FSYLARDYGF KELYLWAINQ DEQGTPKQIR KVIDQVRKHQ IPVVFSESTI
SDKPAKQVAK ESKARYGGVL YVDSLSTKDG KVPTYVDLLN VTVSTIVAGF EK

gi|167855535 (100%), 32,638.8 Da
phosphoribosylglycinamide formyltransferase [Haemophilus parasuis 29755], gi|167853336|gb|EDS24588.1| phosphoribosylglycinamide formyltransferase [Haemophilus parasuis 29755]
3 unique peptides, 3 unique spectra, 3 total spectra, 49/292 amino acids (17% coverage)

MKKLAALLSM LFLVSNPLAA QQFKVVTTFT VIQDIAQNVA GDKAVVESIT KPGAEIHDYQ
PTPQDIVKAQ SADLVLWNGM NLESWFERFF AQVKDKPAVV VTEGIEPISI YEGPYKDKPN
PHAWMSTKNA LIYIENIRQA LVKYDPANAE AYNANAKAYA DKIVALDQPL RERLAKVPEA
QRWLVTSEGA FSYLARDYGF KELYLWAINQ DEQGTPKQIR KVIDQVRKHQ IPVVFSESTI
SDKPAKQVAK ESKARYGGVL YVDSLSTKDG KVPTYVDLLN VTVSTIVAGF EK

b)

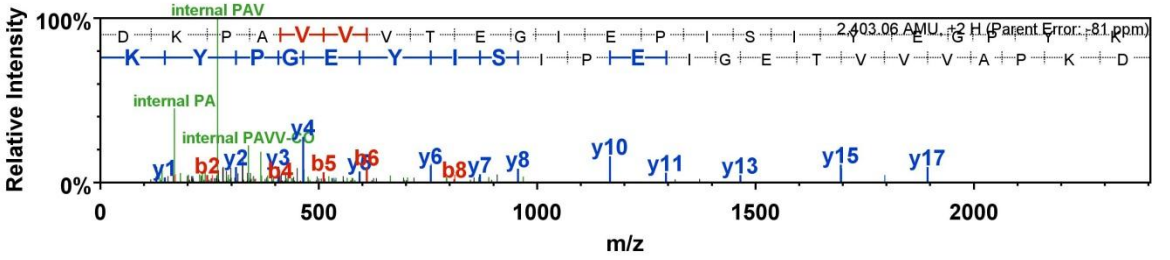

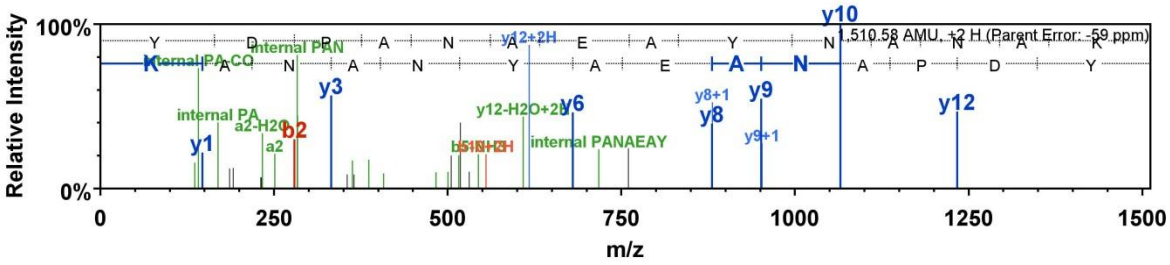

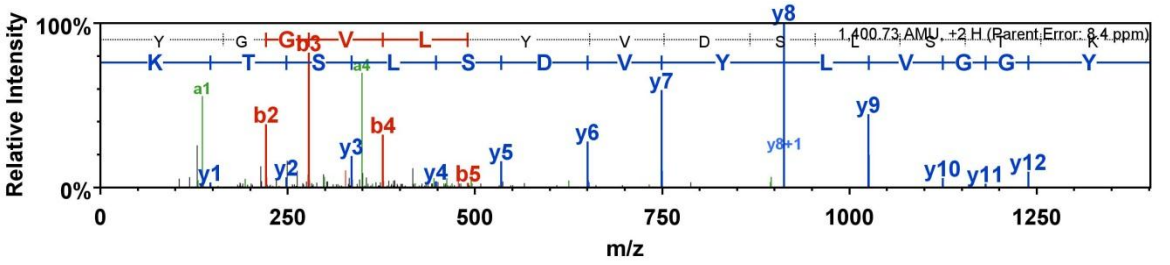

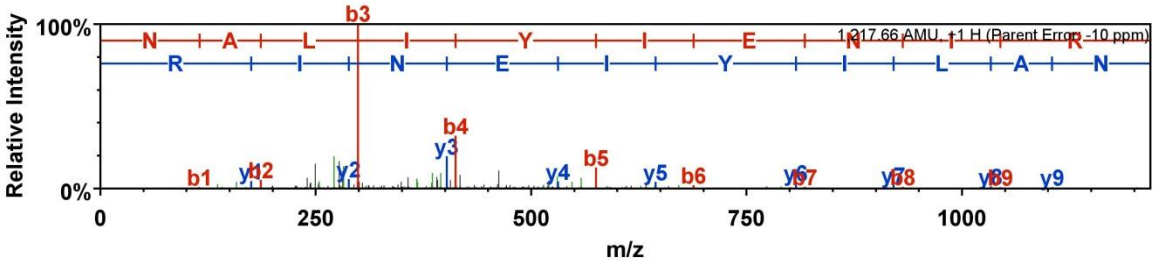

Supplemental Figure S2.33. Protein sequence coverage map for HP8-4 (a) and corresponding peptides (b).

a)

gi|167856115 (100%), 30,128.9 Da
D-ribose transporter subunit RbsB [Haemophilus parasuis 29755], gi|167852756|gb|EDS24029.1| D-ribose transporter subunit RbsB [Haemophilus parasuis 29755]
2 unique peptides, 2 unique spectra, 2 total spectra, 29/290 amino acids (10% coverage)

MKKLTSLAIA LGLAFSTSAM AKETIALAIS TLDNPFFVTL KEGAEKKAKE LGYNLVVLDS
QNDPAKELSN VEDVTVRGAT VLLINPTDSE AVGTAVAVAN KKNIPVITLD RGANKGNVVS
HIASDNVAGG KMAGDFIAEK VGKNAKVIQL EGIAGTSAAR ERGEGFKQAI EANQFELLAS
QPADFDRTKG LNVMENLLAS HGSAKAVFAQ NDEMALGALR AIRASGKNIL VVGFDGTDDA
VKAVNGGQLA ATIAQQPDKI GELGVEAADK VLKGEKVDAQ IPVPLKVVTK

gi|167856115 (91%), 30,128.9 Da
D-ribose transporter subunit RbsB [Haemophilus parasuis 29755], gi|167852756|gb|EDS24029.1| D-ribose transporter subunit RbsB [Haemophilus parasuis 29755]
1 unique peptides, 1 unique spectra, 1 total spectra, 15/290 amino acids (5% coverage)

MKKLTSLAIA LGLAFSTSAM AKETIALAIS TLDNPFFVTL KEGAEKKAKE LGYNLVVLDS
QNDPAKELSN VEDVTVRGAT VLLINPTDSE AVGTAVAVAN KKNIPVITLD RGANKGNVVS
HIASDNVAGG KMAGDFIAEK VGKNAKVIQL EGIAGTSAAR ERGEGFKQAI EANQFELLAS
QPADFDRTKG LNVMENLLAS HGSAKAVFAQ NDEMALGALR AIRASGKNIL VVGFDGTDDA
VKAVNGGQLA ATIAQQPDKI GELGVEAADK VLKGEKVDAQ IPVPLKVVTK

b)

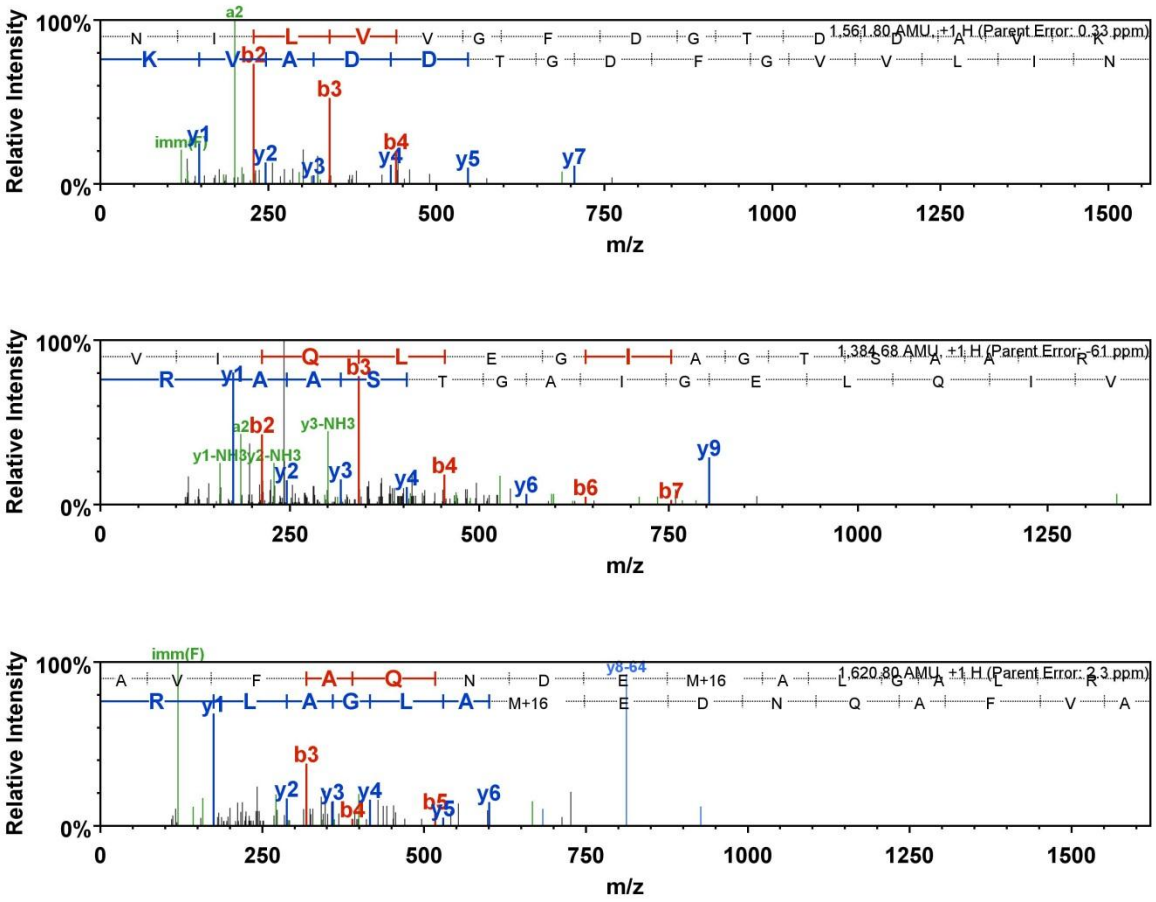

Supplemental Figure S2.34. Protein sequence coverage map for HP13-1 (a) and corresponding peptides (b).

a)

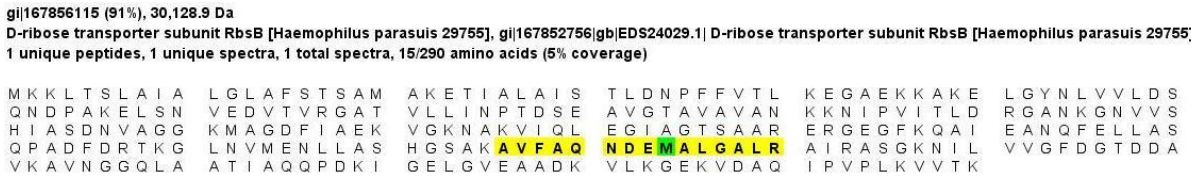

b)

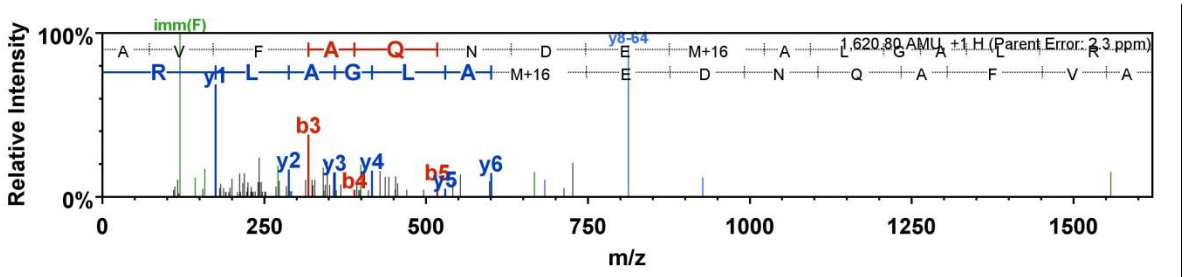

Supplemental Figure S2.35. Protein sequence coverage map for HP13-2 (a) and corresponding peptides (b)

a)

b)

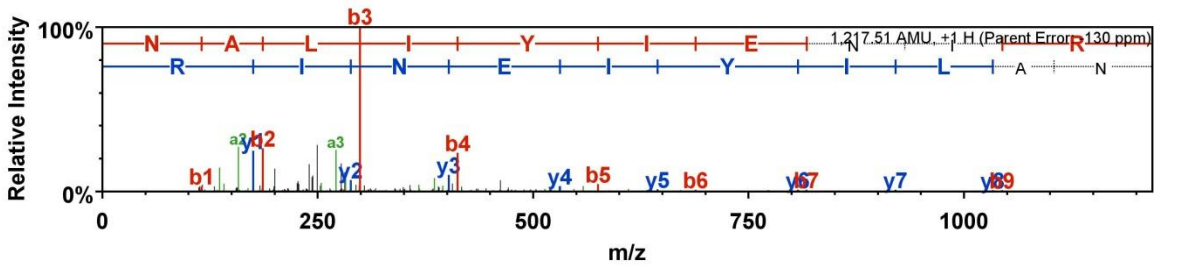

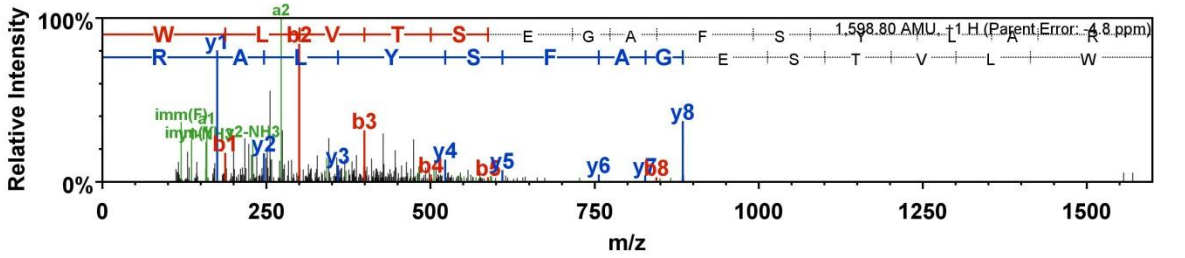

Supplemental Figure S2.36. Protein sequence coverage map for HP13-3 (a) and corresponding peptides (b).

a)

b)

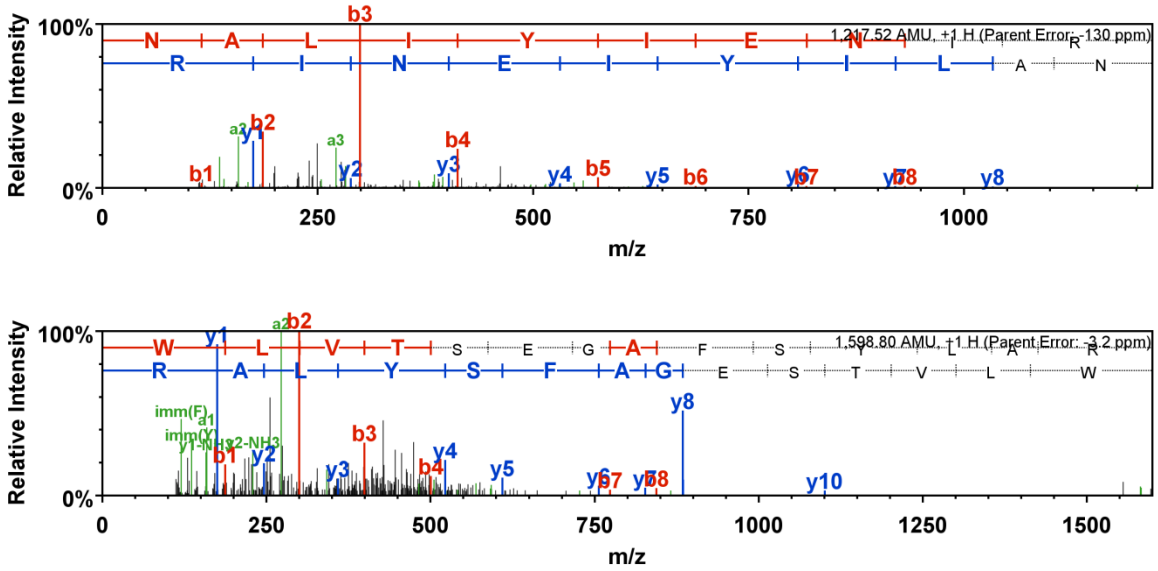

Supplemental Figure S2.37. Protein sequence coverage map for HP13-4 (a) and corresponding peptides (b).

a)

b)

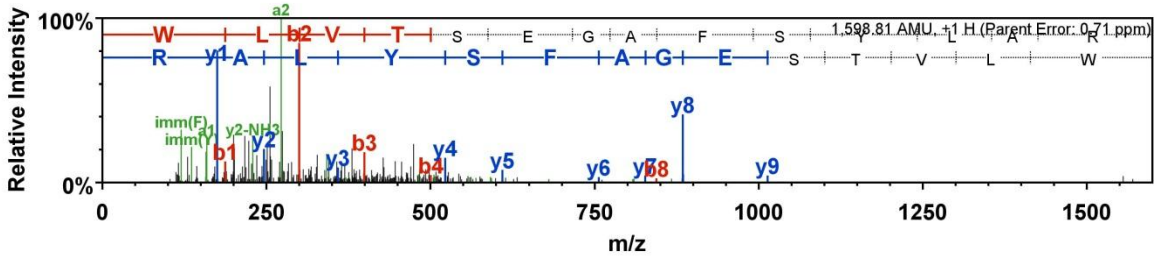

Supplemental Figure S2.38. Protein sequence coverage map for HP13-5 (a) and corresponding peptides (b).

a)

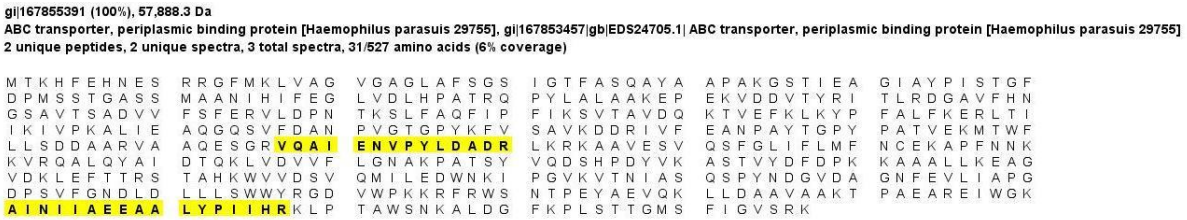

b)

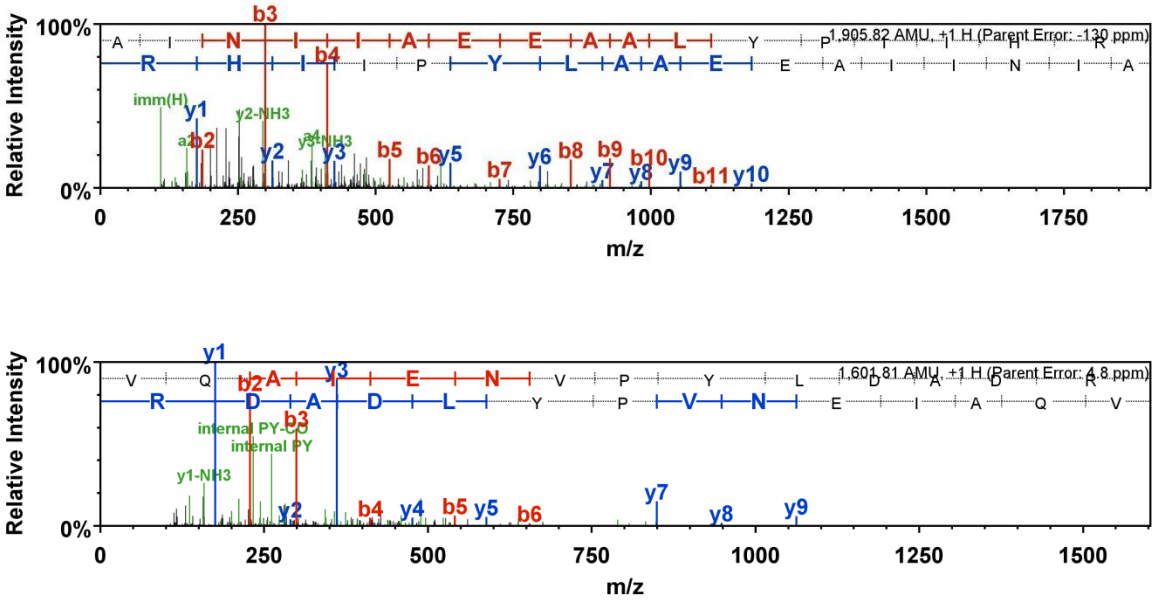

Supplemental Figure S2.39. Protein sequence coverage map for HP13-6 (a) and corresponding peptides (b).

a)

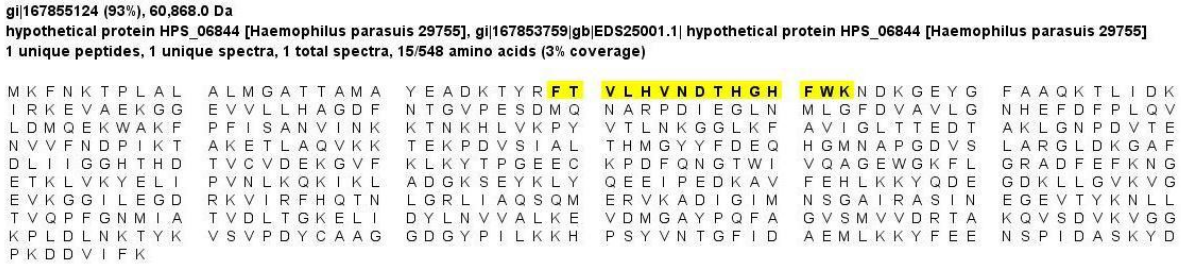

Supplemental Figure S2.40. Protein sequence coverage map for HP13-7 (a) and corresponding peptides (b).

a)

Supplemental Figure S2.41. Protein sequence coverage map for HP13-8 (a) and corresponding peptides (b).

a)

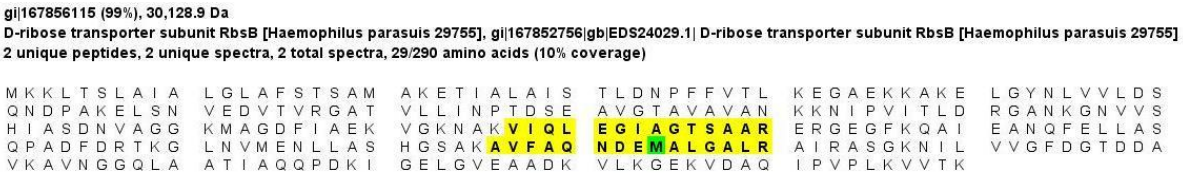

b)

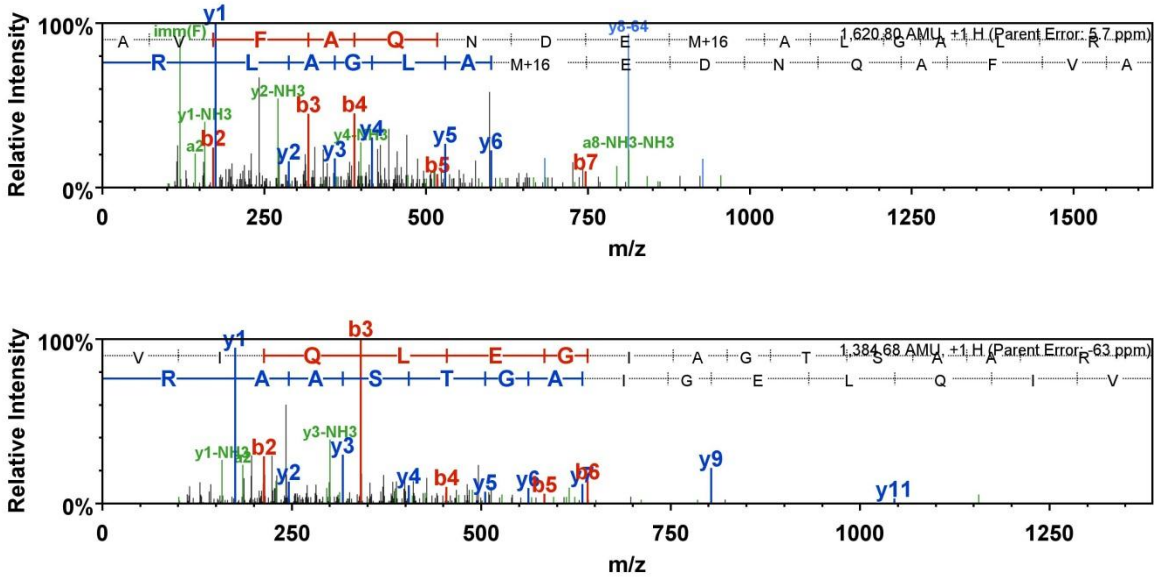

Supplemental Figure S2.42. Protein sequence coverage map for HP21-1 (a) and corresponding peptides (b).

a)

gi|167855535 (100%), 32,638.8 Da
phosphoribosylglycinamide formyltransferase [Haemophilus parasuis 29755], gi|167853336|gb|EDS24588.1| phosphoribosylglycinamide formyltransferase [Haemophilus parasuis 29755]
2 unique peptides, 2 unique spectra, 3 total spectra, 24/292 amino acids (8% coverage)

```
MKKLAALLSM  LFLVSNPLAA  QQFKVVTTFT  VIQDIAQNVA  GDKAVVESIT  KPGAEIHDYQ
PTPQDIVKAQ  SADLVLWNGM  NLESWFERFF  AQVKDKPAVV  VTEGIEPISI  YEGPYKDKPN
PHAWMSTKNA  LIYIENIRQA  LVKYDPANAE  AYNANAKAYA  DKIVALDQPL  RERLAKVPEA
QRWLVTSEGA  FSYLARDYGF  KELYLWAING  DEQGTPKQIR  KVIDQVRKHQ  IPVVFSESTI
SDKPAKQVAK  ESKARYGGVL  YVDSLSTKDG  KVPTYVDLLN  VTVSTIVAGF  EK
```

b)

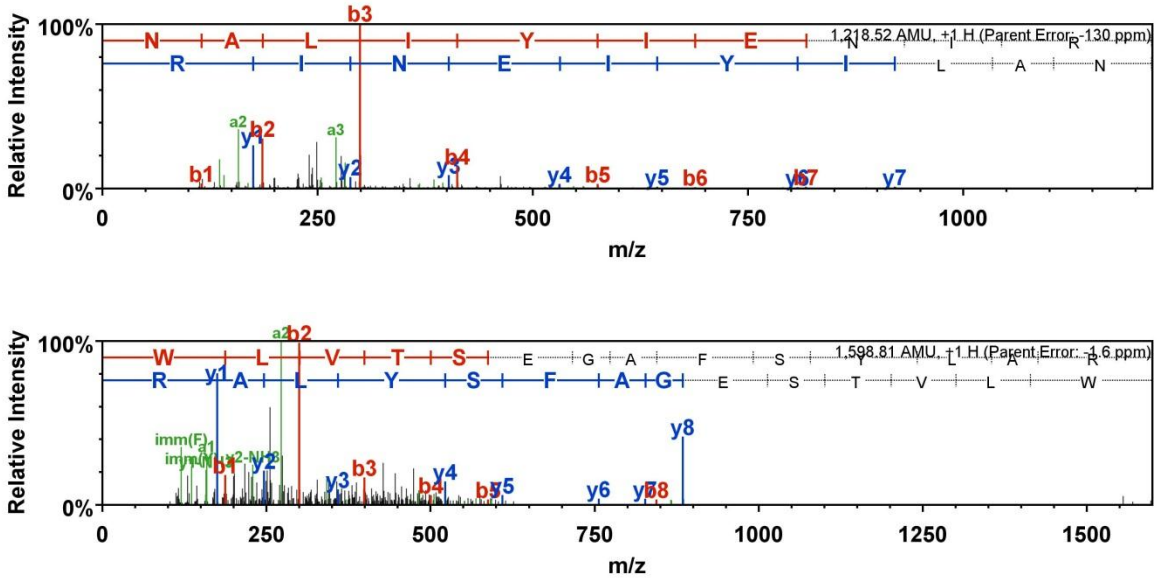

Supplemental Figure S2.43. Protein sequence coverage map for HP21-2 (a) and corresponding peptides (b).

a)

gi|167855535 (100%), 32,638.8 Da
phosphoribosylglycinamide formyltransferase [Haemophilus parasuis 29755], gi|167853336|gb|EDS24588.1| phosphoribosylglycinamide formyltransferase [Haemophilus parasuis 29755]
2 unique peptides, 2 unique spectra, 2 total spectra, 24/292 amino acids (8% coverage)

MKKLAALLSM LFLVSNPLAA QQFKVVTTFT VIQDIAQNVA GDKAVVESIT KPGAEIHDYQ
PTPQDIVKAQ SADLVLWNGM NLESWFERFF AQVKDKPAVV VTEGIEPISI YEGPYKDKPN
PHAWMSTKNA LIYIENIRQA LVKYDPANAE AYNANAKAYA DKIVALDQPL RERLAKVPEA
QRWLVTSEGA FSYLARDYGF KELYLWAINQ DEQGTPKQIR KVIDQVRKHQ IPVVFSESTI
SDKPAKQVAK ESKARYGGVL YVDSLSTKDG KVPTYVDLLN VTVSTIVAGF EK

b)

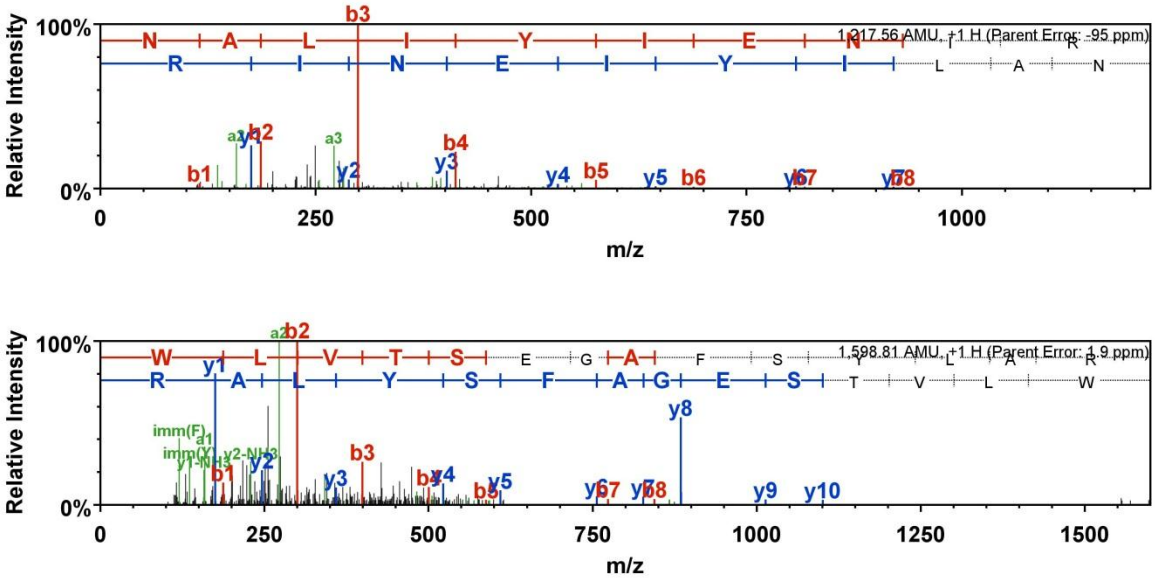

Supplemental Figure S2.44. Protein sequence coverage map for HP21-3 (a) and corresponding peptides (b).

a)

gi|167855400 (95%), 37,666.3 Da
FbpA [Haemophilus parasuis 29755], gi|167853466|gb|EDS24714.1| FbpA [Haemophilus parasuis 29755]
1 unique peptides, 1 unique spectra, 1 total spectra, 17/341 amino acids (5% coverage)

```
MKKSLSVLAL  ALSSVISTSA  LAANEVNVYS  YRQPYLIEPM  LKDFEKQTGI  KVNVIFADKG
LVERVQKEGE  LSPADVLLTV  DISRVMQIVK  AGLAQKVDSK  TLEKNIPAQF  RDSNGEWFGL
TKRARVIYTS  KDRVGALPAG  FDYLDLAKPE  YKGKVCVRSG  KNAYNVSLFA  AMIEHYGEEK
TKAFLEGLKA  NLAQKPQGGD  RDQVKAIKEG  ICDYALGNSY  YYGKMLDDEK  QRSWAESANI
NFPNGQYGTH  VNISGVALAK  HSPNKANAIK  LIEYLSGNQA  QALYAKLNHE  YPVKADVAPS
DLVKGWGTYS  TDALKLEDIA  KNYEKALKLV  DEVKFDDFGA  K
```

b)

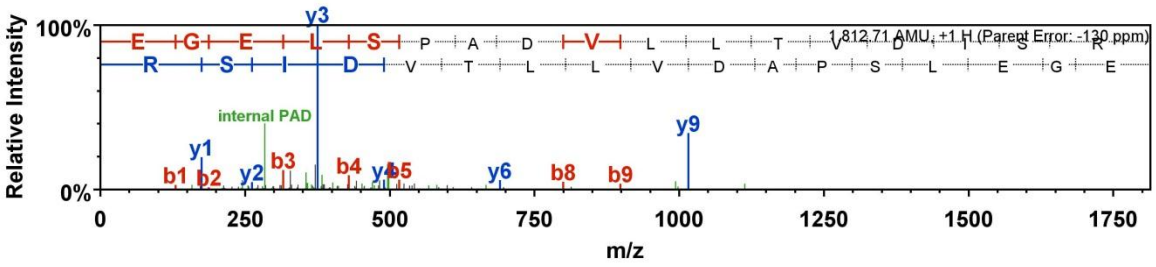

Supplemental Figure S2.45. Protein sequence coverage map for HPIA-1 (a) and corresponding peptides (b).

a)

gi|167855391 (93%), 57,888.3 Da
ABC transporter, periplasmic binding protein [Haemophilus parasuis 29755], gi|167853457|gb|EDS24705.1| ABC transporter, periplasmic binding protein [Haemophilus parasuis 29755]
1 unique peptides, 1 unique spectra, 1 total spectra, 17/527 amino acids (3% coverage)

```
MTKHFEHNES  RRGFMKLVAG  VGAGLAFSGS  IGTFASQAYA  APAKGSTIEA  GIAYPISTGF
DPMSSTGASS  MAANIHIFEG  LVDLHPATRQ  PYLALAAKEP  EKVDDVTYRI  TLRDGAVFHN
GSAVTSADVV  FSFERVLDPN  TKSLFAQFIP  FIKSVTAVDQ  KTVEFKLKYP  FALFKERLTI
IKIVPKALIE  AQGQSVFDAN  PVGTGPYKFV  SAVKDDRIVF  EANPAYTGPY  PATVEKMTWF
LLSDDAARVA  AQESGRVQAI  ENVPYLDADR  LKRKAAVESV  QSFGLIFLMF  NCEKAPFNNK
KVRQALQYAI  DTQKLVDVVF  LGNAKPATSY  VQDSHPDYVK  ASTVYDFDPK  KAAALLKEAG
VDKLEFTTRS  TAHKWVVDSV  QMILEDWNKI  PGVKVTNIAS  QSPYNDGVDA  GNFEVLIAPG
DPSVFGNDLD  LLLSWWYRGD  VWPKKRFRWS  NTPEYAEVQK  LLDAAVAAKT  PAEAREIWGK
AINIIAEEAA  LYPIIHRKLP  TAWSNKALDG  FKPLSTTGMS  FIGVSRK
```

b)

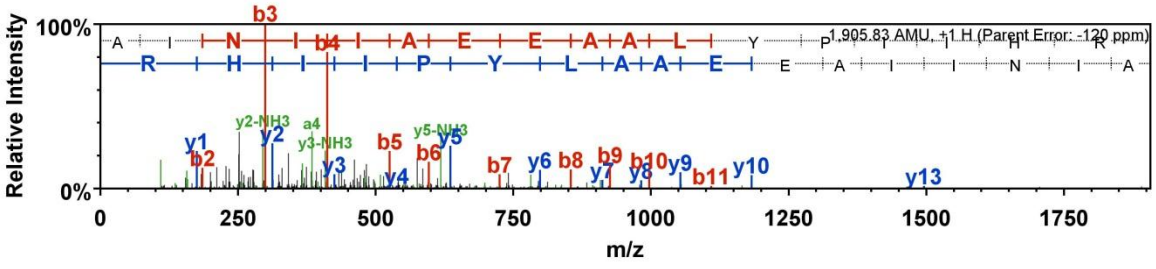

Supplemental Figure S2.46. Protein sequence coverage map for HPIA-2 (a) and corresponding peptides (b).

Supplemental Figure 2.47. Expresso alignment of *H. influenzae* OMP P5 with D-ribose transporter

Supplemental Figure 2.48. Expresso alignment of *H. influenzae* OMP P5 with FbpA.

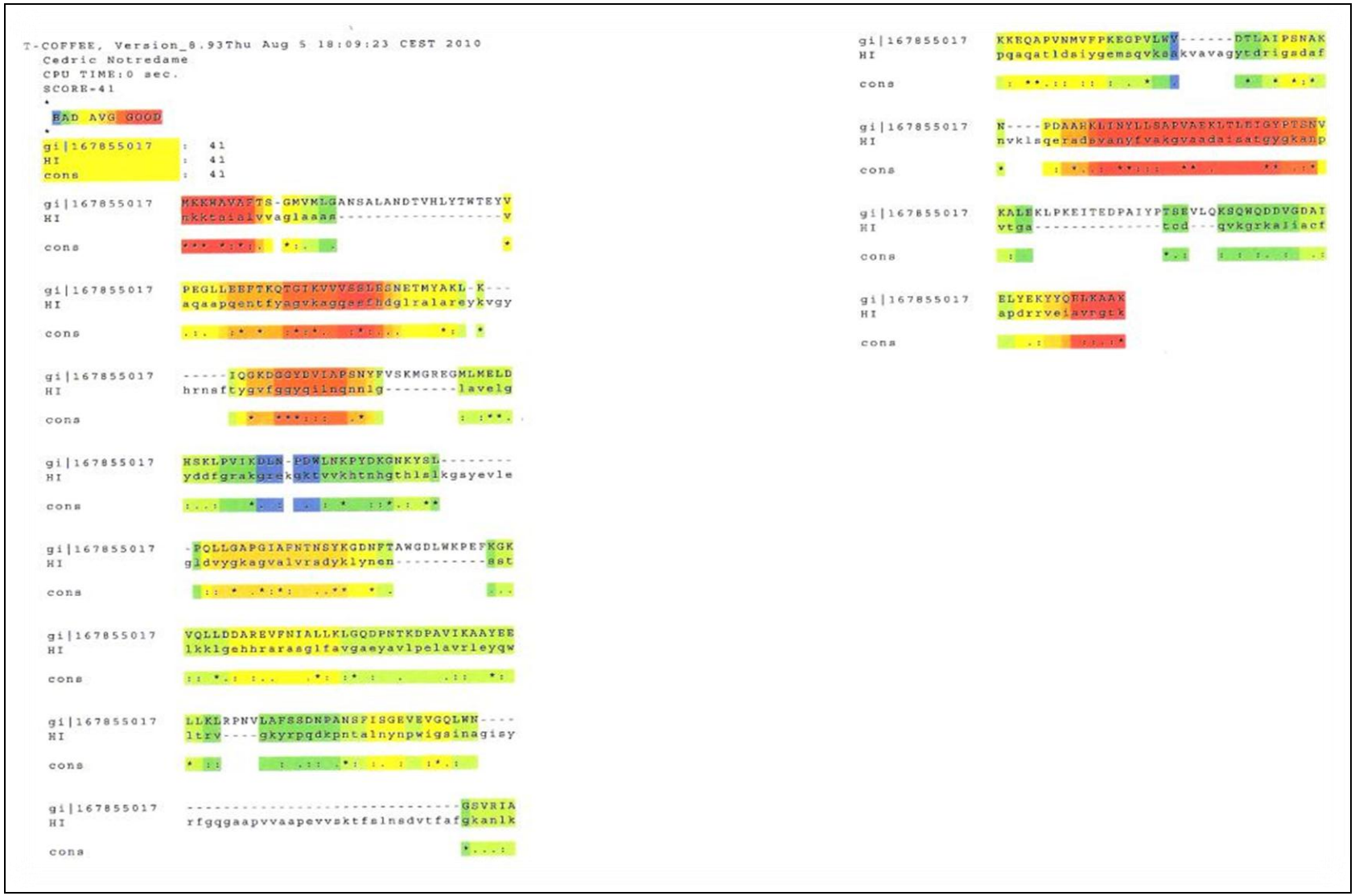

Supplemental Figure 2.49. Expresso alignment of *H. influenzae* OMP P5 with hypothetical protein HPS_10240.

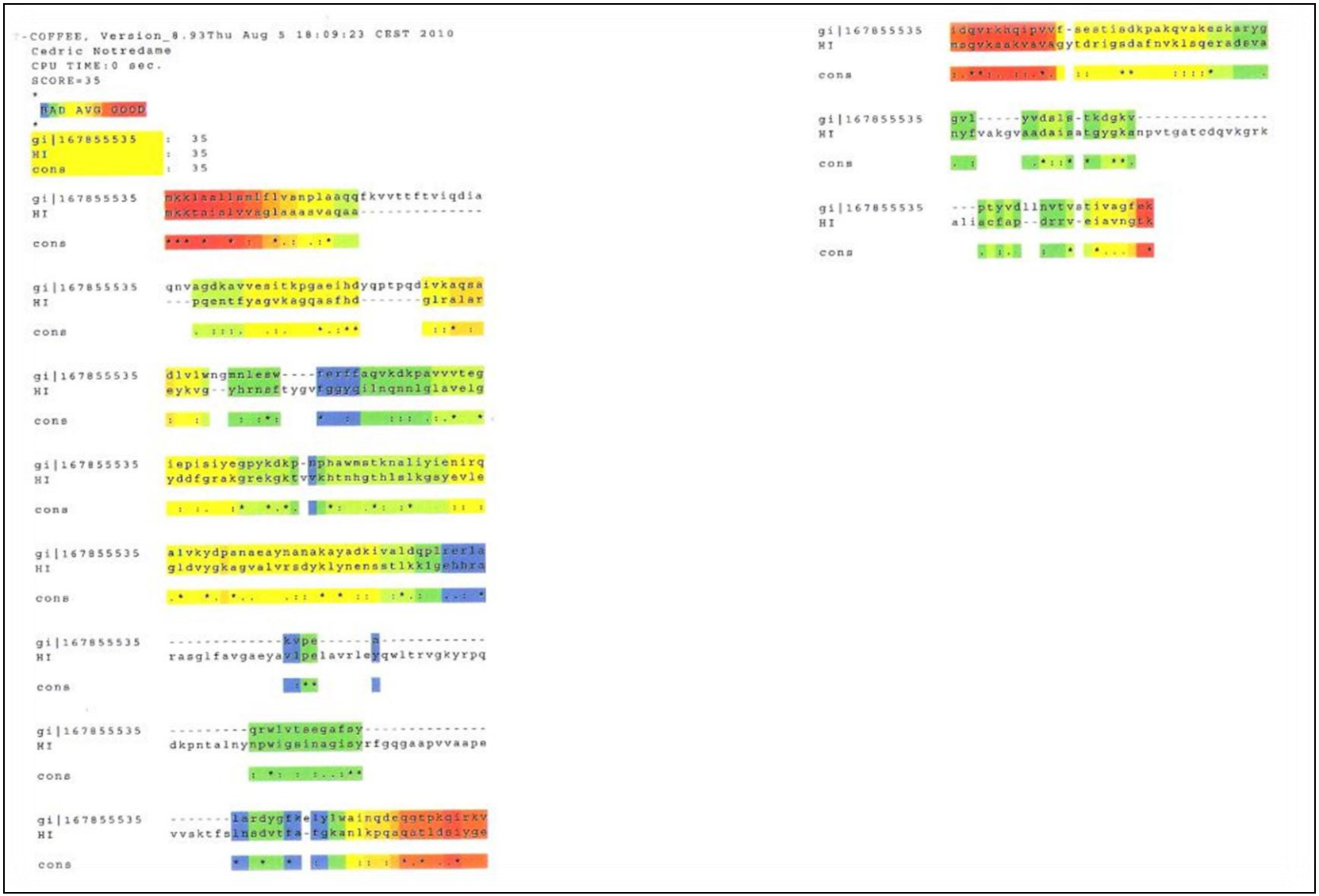

Supplemental Figure 2.50. Expresso alignment of *H. influenzae* OMP P5 with phosphoribosylglycinamide formlytransferase.

References

[1] Glasser, K., . *Quoted in Krankenheinten des Schweines. 5th ed.* 1910, *1950*, 106.

[2] Oliveira, S., Pijoan, C., *Haemophilus parasuis*: new trends on diagnosis, epidemiology and control. *Veterinary microbiology* 2004, *99*, 1-12.

[3] Harris, D. L., Control of common infectious diseases. In: Multi-site pig production. *Iowa State University Press* 2000, 98-102.

[4] Wang, X., Xu, X., Zhang, S., Guo, F., *et al.*, Identification and analysis of potential virulence-associated genes in *Haemophilus parasuis* based on genomic subtraction. *Microbial pathogenesis* 2011, *51*, 291-296.

[5] Zhou, H., Yang, B., Xu, F., Chen, X., *et al.*, Identification of putative virulence-associated genes of *Haemophilus parasuis* through suppression subtractive hybridization. *Veterinary microbiology* 2010, *144*, 377-383.

[6] Zhou, M., Zhang, A., Guo, Y., Liao, Y., *et al.*, A comprehensive proteome map of the *Haemophilus parasuis* serovar 5. *Proteomics* 2009, *9*, 2722-2739.

[7] Xie, Q., Jin, H., Luo, R., Wan, Y., *et al.*, Transcriptional responses of *Haemophilus parasuis* to iron-restriction stress in vitro. *Biometals : an international journal on the role of metal ions in biology, biochemistry, and medicine* 2009, *22*, 907-916.

[8] Jin, H., Wan, Y., Zhou, R., Li, L., *et al.*, Identification of genes transcribed by *Haemophilus parasuis* in necrotic porcine lung through the selective capture of transcribed sequences (SCOTS). *Environmental microbiology* 2008, *10*, 3326-3336.

[9] Metcalf, D. S., MacInnes, J. I., Differential expression of *Haemophilus parasuis* genes in response to iron restriction and cerebrospinal fluid. *Canadian journal of veterinary research = Revue canadienne de recherche veterinaire* 2007, *71*, 181-188.

[10] Melnikow, E., Dornan, S., Sargent, C., Duszenko, M., *et al.*, Microarray analysis of *Haemophilus parasuis* gene expression under in vitro growth conditions mimicking the in vivo environment. *Veterinary microbiology* 2005, *110*, 255-263.

[11] Neary, J. M., Murphy, T. F., Antibodies directed at a conserved motif in loop 6 of outer membrane protein P2 of nontypeable *Haemophilus influenzae* recognize multiple strains in immunoassays. *FEMS immunology and medical microbiology* 2006, *46*, 251-261.

[12] Neary, J. M., Yi, K., Karalus, R. J., Murphy, T. F., Antibodies to loop 6 of the P2 porin protein of nontypeable *Haemophilus influenzae* are bactericidal against multiple strains. *Infection and immunity* 2001, *69*, 773-778.

[13] Yi, K., Murphy, T. F., Importance of an immunodominant surface-exposed loop on outer membrane protein P2 of nontypeable *Haemophilus influenzae*. *Infection and immunity* 1997, *65*, 150-155.

[14] Vogel, L., Duim, B., Geluk, F., Eijk, P., *et al.*, Immune selection for antigenic drift of major outer membrane protein P2 of *Haemophilus influenzae* during persistence in subcutaneous tissue cages in rabbits. *Infection and immunity* 1996, *64*, 980-986.

[15] Duim, B., Vogel, L., Puijk, W., Jansen, H. M., *et al.*, Fine mapping of outer membrane protein P2 antigenic sites which vary during persistent infection by *Haemophilus influenzae*. *Infection and immunity* 1996, *64*, 4673-4679.

[16] Dium, B. e. a., Fine Mapping of Outer Membrane Protein P2 Antigenic Sites Which Vary during Persistent Infection by *Haemophilus influenzae*. *Infection and immunity* 1996, *64*, 4673-4679.

[17] Haase, E. M., Yi, K., Morse, G. D., Murphy, T. F., Mapping of bactericidal epitopes on the P2 porin protein of nontypeable *Haemophilus influenzae*. *Infection and immunity* 1994, *62*, 3712-3722.

[18] Sikkema, D. J., Murphy, T. F., Molecular analysis of the P2 porin protein of nontypeable *Haemophilus influenzae*. *Infection and immunity* 1992, *60*, 5204-5211.

[19] van Alphen, L., Eijk, P., Geelen-van den Broek, L., Dankert, J., Immunochemical characterization of variable epitopes of outer membrane protein P2 of nontypeable *Haemophilus influenzae*. *Infection and immunity* 1991, *59*, 247-252.

[20] Cope, L. D., Pelzel, S. E., Latimer, J. L., Hansen, E. J., Characterization of a mutant of *Haemophilus influenzae* type b lacking the P2 major outer membrane protein. *Infection and immunity* 1990, *58*, 3312-3318.

[21] Novotny, L. A., Bakaletz, L. O., The fourth surface-exposed region of the outer membrane protein P5-homologous adhesin of nontypable *Haemophilus influenzae* is an immunodominant but nonprotective decoying epitope. *J Immunol* 2003, *171*, 1978-1983.

[22] Kyd, J. M., Cripps, A. W., Novotny, L. A., Bakaletz, L. O., Efficacy of the 26-kilodalton outer membrane protein and two P5 fimbrin-derived immunogens to induce clearance of nontypeable *Haemophilus influenzae* from the rat middle ear and lungs as well as from the chinchilla middle ear and nasopharynx. *Infection and immunity* 2003, *71*, 4691-4699.

[23] Hill, D. J., Toleman, M. A., Evans, D. J., Villullas, S., *et al.*, The variable P5 proteins of typeable and non-typeable *Haemophilus influenzae* target human CEACAM1. *Molecular Microbiology* 2001, *39*, 850-862.

[24] Webb, D. C., Cripps, A. W., A P5 peptide that is homologous to peptide 10 of OprF from *Pseudomonas aeruginosa* enhances clearance of nontypeable *Haemophilus influenzae*

from acutely infected rat lung in the absence of detectable peptide-specific antibody. *Infection and immunity* 2000, *68*, 377-381.

[25] Reddy, M. S., Bernstein, J. M., Murphy, T. F., Faden, H. S., Binding between outer membrane proteins of nontypeable *Haemophilus influenzae* and human nasopharyngeal mucin. *Infection and immunity* 1996, *64*, 1477-1479.

[26] Munson, R. S., Jr., Granoff, D. M., Purification and partial characterization of outer membrane proteins P5 and P6 from *Haemophilus influenzae* type b. *Infection and immunity* 1985, *49*, 544-549.

[27] Keller, A., Nesvizhskii, A. I., Kolker, E., Aebersold, R., Empirical statistical model to estimate the accuracy of peptide identifications made by MS/MS and database search. *Analytical chemistry* 2002, *74*, 5383-5392.

[28] Nesvizhskii, A. I., Keller, A., Kolker, E., Aebersold, R., A statistical model for identifying proteins by tandem mass spectrometry. *Analytical chemistry* 2003, *75*, 4646-4658.

[29] Di Tommaso, P., Moretti, S., Xenarios, I., Orobitg, M., *et al.*, T-Coffee: a web server for the multiple sequence alignment of protein and RNA sequences using structural information and homology extension. *Nucleic acids research* 2011, *39*, W13-17.

[30] Taly, J. F., Magis, C., Bussotti, G., Chang, J. M., *et al.*, Using the T-Coffee package to build multiple sequence alignments of protein, RNA, DNA sequences and 3D structures. *Nature protocols* 2011, *6*, 1669-1682.

[31] McVicker, J. K., *PhD Dissertation*, Iowa State University, Ames, IA 2004.

[32] Webb, D. C. a. A. W. C., Secondary Structure and molecular analysis of interstrain variability in the P5 outer-membrane protein of non-typable *Haemophilus influenzae* isolated from diverse anatomical sites. *Journal of Medical Microbiology* 1998, *47*, 1059-1067.

[33] Duim, B., Bowler, L. D., Eijk, P. P., Jansen, H. M., *et al.*, Molecular variation in the major outer membrane protein P5 gene of nonencapsulated *Haemophilus influenzae* during chronic infections. *Infection and immunity* 1997, *65*, 1351-1356.

[34] McVicker, J. K., Tabatabai, L. B., Isolation and characterization of the P5 adhesin protein of *Haemophilus parasuis* serotype 5. *Preparative biochemistry & biotechnology* 2006, *36*, 363-374.

[35] Syuto, B. a. M., M., Purification of a Protective Antigen form a Saline Extract of *Pasteurella multocida*. *Infection and immunity* 1981, *37*, 1218-1226.

[36] Weller, P. F., Smith, A. L., Anderson, P., Smith, D. H., The role of encapsulation and host age in the clearance of *Haemophilus influenzae* bacteremia. *Journal of Infectious Diseases* 1977, *135*, 34-41.

[37] Huber, P. S., Egwu, I. N., Capsular variation in experimental strains of *Haemophilus influenzae*. *Medical microbiology and immunology* 1985, *173*, 345-353.

[38] Carlone, G. M., Gorelkin, L., Gheesling, L. L., Hoiseth, S. K., *et al.*, Potential virulence factors of *Haemophilus influenzae* biogroup aegyptius in Brazilian purpuric fever. The Brazilian Purpuric Fever Study Group. *The Pediatric infectious disease journal* 1989, *8*, 245-247.

[39] Wayoff, M., Jankowski, R., Virulence factors of *Haemophilus influenzae*. *J Chemother* 1989, *1*, 26-28.

[40] Wispelwey, B., Hansen, E. J., Lesse, A., Scheld, W. M., *Haemophilus influenzae* virulence factors in experimental meningitis. *The Pediatric infectious disease journal* 1989, *8*, 903-904.

[41] Bishai, W. R., Howard, N. S., Winkelstein, J. A., Smith, H. O., Characterization and virulence analysis of catalase mutants of *Haemophilus influenzae*. *Infection and immunity* 1994, *62*, 4855-4860.

[42] Nizet, V., Colina, K. F., Almquist, J. R., Rubens, C. E., Smith, A. L., A virulent nonencapsulated *Haemophilus influenzae*. *Journal of Infectious Diseases* 1996, *173*, 180-186.

[43] Rodriguez, C. A., Avadhanula, V., Buscher, A., Smith, A. L., *et al.*, Prevalence and distribution of adhesins in invasive non-type b encapsulated *Haemophilus influenzae*. *Infection and immunity* 2003, *71*, 1635-1642.

[44] Hallstrom, T., Trajkovska, E., Forsgren, A., Riesbeck, K., *Haemophilus influenzae* surface fibrils contribute to serum resistance by interacting with vitronectin. *J Immunol* 2006, *177*, 430-436.

[45] Forsgren, A., Riesbeck, K., Janson, H., Protein D of *Haemophilus influenzae*: a protective nontypeable H. influenzae antigen and a carrier for pneumococcal conjugate vaccines. *Clinical infectious diseases : an official publication of the Infectious Diseases Society of America* 2008, *46*, 726-731.

[46] Rosadini, C. V., Wong, S. M., Akerley, B. J., The periplasmic disulfide oxidoreductase DsbA contributes to *Haemophilus influenzae* pathogenesis. *Infection and immunity* 2008, *76*, 1498-1508.

[47] Mason, K. M., Raffel, F. K., Ray, W. C., Bakaletz, L. O., Heme utilization by nontypeable *Haemophilus influenzae* is essential and dependent on Sap transporter function. *Journal of bacteriology* 2011, *193*, 2527-2535.

[48] Hardy, G. G., Tudor, S. M., St Geme, J. W., 3rd, The pathogenesis of disease due to nontypeable *Haemophilus influenzae*. *Methods in molecular medicine* 2003, *71*, 1-28.

[49] Ecevit, I. Z., McCrea, K. W., Pettigrew, M. M., Sen, A., *et al.*, Prevalence of the hifBC, hmw1A, hmw2A, hmwC, and hia Genes in *Haemophilus influenzae* Isolates. *J Clin Microbiol* 2004, *42*, 3065-3072.

[50] Hotomi, M., Ikeda, Y., Suzumoto, M., Yamauchi, K., *et al.*, A recombinant P4 protein of *Haemophilus influenzae* induces specific immune responses biologically active against nasopharyngeal colonization in mice after intranasal immunization. *Vaccine* 2005, *23*, 1294-1300.

[51] Yeo, H. J., Yokoyama, T., Walkiewicz, K., Kim, Y., *et al.*, The structure of the *Haemophilus influenzae* HMW1 pro-piece reveals a structural domain essential for bacterial two-partner secretion. *The Journal of biological chemistry* 2007, *282*, 31076-31084.

[52] Munson, R., Jr., Brodeur, B., Chong, P., Grass, S., *et al.*, Outer membrane proteins P1 and P2 of *Haemophilus influenzae* type b: structure and identification of surface-exposed epitopes. *J Infect Dis* 1992, *165 Suppl 1*, S86-89.

[53] Noel, G. J., Love, D. C., Mosser, D. M., High-molecular-weight proteins of nontypeable *Haemophilus influenzae* mediate bacterial adhesion to cellular proteoglycans. *Infection and immunity* 1994, *62*, 4028-4033.

[54] Reilly, T. J., Chance, D. L., Smith, A. L., Outer membrane lipoprotein e (P4) of *Haemophilus influenzae* is a novel phosphomonoesterase. *Journal of bacteriology* 1999, *181*, 6797-6805.

[55] Reilly, T. J., Smith, A. L., Purification and characterization of a recombinant *Haemophilus influenzae* outer membrane phosphomonoesterase e (P4). *Protein expression and purification* 1999, *17*, 401-409.

[56] Munson, R. S., Jr., Grass, S., West, R., Molecular cloning and sequence of the gene for outer membrane protein P5 of *Haemophilus influenzae*. *Infection and immunity* 1993, *61*, 4017-4020.

[57] Farley, M. M., Stephens, D. S., Mulks, M. H., Cooper, M. D., *et al.*, Pathogenesis of IgA1 protease-producing and -nonproducing *Haemophilus influenzae* in human nasopharyngeal organ cultures. *J Infect Dis* 1986, *154*, 752-759.

[58] Fink, D. L., Buscher, A. Z., Green, B., Fernsten, P., St Geme, J. W., 3rd, The *Haemophilus influenzae* Hap autotransporter mediates microcolony formation and adherence to epithelial cells and extracellular matrix via binding regions in the C-terminal end of the passenger domain. *Cellular microbiology* 2003, *5*, 175-186.

[59] Mistry, D. V., Stockley, R. A., The cleavage specificity of an IgA1 protease from *Haemophilus influenzae*. *Virulence* 2011, *2*, 103-110.

[60] Hansen, E. J., Pelzel, S. E., Orth, K., Moomaw, C. R., *et al.*, Structural and antigenic conservation of the P2 porin protein among strains of *Haemophilus influenzae* type b. *Infection and immunity* 1989, *57*, 3270-3275.

[61] Munson, R., Jr., Bailey, C., Grass, S., Diversity of the outer membrane protein P2 gene from major clones of *Haemophilus influenzae* type b. *Mol Microbiol* 1989, *3*, 1797-1803.

[62] Duim, B., Dankert, J., Jansen, H. M., van Alphen, L., Genetic analysis of the diversity in outer membrane protein P2 of non-encapsulated *Haemophilus influenzae*. *Microbial pathogenesis* 1993, *14*, 451-462.

[63] Galdiero, S., Capasso, D., Vitiello, M., D'Isanto, M., *et al.*, Role of surface-exposed loops of *Haemophilus influenzae* protein P2 in the mitogen-activated protein kinase cascade. *Infection and immunity* 2003, *71*, 2798-2809.

[64] Vitiello, M., Finamore, E., Cantisani, M., Bevilacqua, P., *et al.*, P2 porin and loop L7 from *Haemophilus influenzae* modulate expression of IL-6 and adhesion molecules in astrocytes. *Microbiology and immunology* 2011, *55*, 347-356.

[65] Mullins, M. A., Register, K. B., Bayles, D. O., Loving, C. L., *et al.*, Characterization and comparative analysis of the genes encoding *Haemophilus parasuis* outer membrane proteins P2 and P5. *Journal of bacteriology* 2009, *191*, 5988-6002.

[66] del Rio, M. L., Gutierrez-Martin, C. B., Rodriguez-Barbosa, J. I., Navas, J., Rodriguez-Ferri, E. F., Identification and characterization of the TonB region and its role in transferrin-mediated iron acquisition in *Haemophilus parasuis*. *FEMS immunology and medical microbiology* 2005, *45*, 75-86.

[67] Ekins, A., Bahrami, F., Sijercic, A., Maret, D., Niven, D. F., *Haemophilus somnus* possesses two systems for acquisition of transferrin-bound iron. *Journal of bacteriology* 2004, *186*, 4407-4411.

[68] Whitby, P. W., Sim, K. E., Morton, D. J., Patel, J. A., Stull, T. L., Transcription of genes encoding iron and heme acquisition proteins of *Haemophilus influenzae* during acute otitis media. *Infection and immunity* 1997, *65*, 4696-4700.

[69] Schryvers, A. B., Gray-Owen, S., Iron acquisition in *Haemophilus influenzae*: receptors for human transferrin. *J Infect Dis* 1992, *165 Suppl 1*, S103-104.

[70] Morton, D. J., Williams, P., Siderophore-independent acquisition of transferrin-bound iron by *Haemophilus influenzae* type b. *Journal of general microbiology* 1990, *136*, 927-933.

[71] Pidcock, K. A., Wooten, J. A., Daley, B. A., Stull, T. L., Iron acquisition by *Haemophilus influenzae*. *Infection and immunity* 1988, *56*, 721-725.

[72] Clarke, T. E., Tari, L. W., Vogel, H. J., Structural biology of bacterial iron uptake systems. *Current topics in medicinal chemistry* 2001, *1*, 7-30.

[73] Khun, H. H., Deved, V., Wong, H., Lee, B. C., fbpABC gene cluster in *Neisseria meningitidis* is transcribed as an operon. *Infection and immunity* 2000, *68*, 7166-7171.

[74] Belzer, C. A., Tabatabai, L. B., Frank, G. H., Purification and characterization of the *Pasteurella haemolytica* 35 kilodalton periplasmic iron-regulated protein. *Preparative biochemistry & biotechnology* 2000, *30*, 343-355.

[75] Smoot, L. M., Bell, E. C., Crosa, J. H., Actis, L. A., Fur and iron transport proteins in the Brazilian purpuric fever clone of *Haemophilus influenzae* biogroup aegyptius. *J Med Microbiol* 1999, *48*, 629-636.

[76] Ferreiros, C., Criado, M. T., Gomez, J. A., The neisserial 37 kDa ferric binding protein (FbpA). *Comparative biochemistry and physiology. Part B, Biochemistry & molecular biology* 1999, *123*, 1-7.

[77] Turner, P. C., Thomas, C. E., Elkins, C., Clary, S., Sparling, P. F., *Neisseria gonorrhoeae* heme biosynthetic mutants utilize heme and hemoglobin as a heme source but fail to grow within epithelial cells. *Infection and immunity* 1998, *66*, 5215-5223.

[78] Willemsen, P. T., Vulto, I., Boxem, M., de Graaff, J., Characterization of a periplasmic protein involved in iron utilization of *Actinobacillus actinomycetemcomitans*. *Journal of bacteriology* 1997, *179*, 4949-4952.

[79] Kirby, S. D., Gray-Owen, S. D., Schryvers, A. B., Characterization of a ferric-binding protein mutant in *Haemophilus influenzae*. *Mol Microbiol* 1997, *25*, 979-987.

[80] Forng, R. Y., Ekechukwu, C. R., Subbarao, S., Morse, S. A., Genco, C. A., Promoter mapping and transcriptional regulation of the iron-regulated *Neisseria gonorrhoeae* fbpA gene. *Journal of bacteriology* 1997, *179*, 3047-3052.

[81] Desai, P. J., Angerer, A., Genco, C. A., Analysis of Fur binding to operator sequences within the *Neisseria gonorrhoeae* fbpA promoter. *Journal of bacteriology* 1996, *178*, 5020-5023.

[82] Parker Siburt, C. J., Mietzner, T. A., Crumbliss, A. L., FbpA - A bacterial transferrin with more to offer. *Biochimica et biophysica acta* 2011.

[83] Weaver, K. D., Gabricevic, M., Anderson, D. S., Adhikari, P., *et al.*, Role of citrate and phosphate anions in the mechanism of iron(III) sequestration by ferric binding protein: kinetic studies of the formation of the holoprotein of wild-type FbpA and its engineered mutants. *Biochemistry* 2010, *49*, 6021-6032.

[84] Siburt, C. J., Roulhac, P. L., Weaver, K. D., Noto, J. M., *et al.*, Hijacking transferrin bound iron: protein-receptor interactions involved in iron transport in *N. gonorrhoeae*. *Metallomics : integrated biometal science* 2009, *1*, 249-255.

[85] Khan, A. G., Shouldice, S. R., Tari, L. W., Schryvers, A. B., The role of the synergistic phosphate anion in iron transport by the periplasmic iron-binding protein from *Haemophilus influenzae*. *The Biochemical journal* 2007, *403*, 43-48.

[86] Dhungana, S., Anderson, D. S., Mietzner, T. A., Crumbliss, A. L., Kinetics of iron release from ferric binding protein (FbpA): mechanistic implications in bacterial periplasm-to-cytosol Fe3+ transport. *Biochemistry* 2005, *44*, 9606-9618.

[87] Dhungana, S., Anderson, D. S., Mietzner, T. A., Crumbliss, A. L., Phosphate ester hydrolysis is catalyzed by a bacterial transferrin: potential implications for in vivo iron transport mechanisms. *Journal of inorganic biochemistry* 2004, *98*, 1975-1977.

[88] Cuthbertson, L., Kimber, M. S., Whitfield, C., Substrate binding by a bacterial ABC transporter involved in polysaccharide export. *Proceedings of the National Academy of Sciences of the United States of America* 2007, *104*, 19529-19534.

[89] Wu, Z., Zhang, W., Shao, J., Wang, Y., *et al.*, Immunoproteomic assay of secreted proteins of *Streptococcus suis* serotype 9 with convalescent sera from pigs. *Folia microbiologica* 2011.

[90] Tefon, B. E., Maass, S., Ozcengiz, E., Becher, D., *et al.*, A comprehensive analysis of *Bordetella pertussis* surface proteome and identification of new immunogenic proteins. *Vaccine* 2011, *29*, 3583-3595.

[91] Klein, J. S., Lewinson, O., Bacterial ATP-driven transporters of transition metals: physiological roles, mechanisms of action, and roles in bacterial virulence. *Metallomics : integrated biometal science* 2011.

[92] Zou, L., Wang, J., Huang, B., Xie, M., Li, A., A solute-binding protein for iron transport in *Streptococcus iniae*. *BMC Microbiol* 2010, *10*, 309.

[93] Toyoda, T., Okano, S., Shibata, Y., Abiko, Y., Oxidative stress induces phosphorylation of the ABC transporter, ATP-binding protein, in *Porphyromonas gingivalis*. *Journal of oral science* 2010, *52*, 561-566.

[94] Kalscheuer, R., Weinrick, B., Veeraraghavan, U., Besra, G. S., Jacobs, W. R., Jr., Trehalose-recycling ABC transporter LpqY-SugA-SugB-SugC is essential for virulence of *Mycobacterium tuberculosis*. *Proceedings of the National Academy of Sciences of the United States of America* 2010, *107*, 21761-21766.

[95] Jonsson, I. M., Juuti, J. T., Francois, P., AlMajidi, R., *et al.*, Inactivation of the Ecs ABC transporter of *Staphylococcus aureus* attenuates virulence by altering composition and function of bacterial wall. *PloS one* 2010, *5*, e14209.

[96] Hiron, A., Posteraro, B., Carriere, M., Remy, L., *et al.*, A nickel ABC-transporter of *Staphylococcus aureus* is involved in urinary tract infection. *Mol Microbiol* 2010, *77*, 1246-1260.

[97] Stauff, D. L., Skaar, E. P., The heme sensor system of *Staphylococcus aureus*. *Contributions to microbiology* 2009, *16*, 120-135.

[98] Tanabe, M., Mirza, O., Bertrand, T., Atkins, H. S., *et al.*, Structures of OppA and PstS from *Yersinia pestis* indicate variability of interactions with transmembrane domains. *Acta crystallographica. Section D, Biological crystallography* 2007, *63*, 1185-1193.

[99] Whalan, R. H., Funnell, S. G., Bowler, L. D., Hudson, M. J., *et al.*, Distribution and genetic diversity of the ABC transporter lipoproteins PiuA and PiaA within *Streptococcus pneumoniae* and related streptococci. *Journal of bacteriology* 2006, *188*, 1031-1038.

[100] Speziali, C. D., Dale, S. E., Henderson, J. A., Vines, E. D., Heinrichs, D. E., Requirement of *Staphylococcus aureus* ATP-binding cassette-ATPase FhuC for iron-restricted growth and evidence that it functions with more than one iron transporter. *Journal of bacteriology* 2006, *188*, 2048-2055.

[101] Rodriguez, G. M., Smith, I., Identification of an ABC transporter required for iron acquisition and virulence in *Mycobacterium tuberculosis*. *Journal of bacteriology* 2006, *188*, 424-430.

[102] Hanks, T. S., Liu, M., McClure, M. J., Lei, B., ABC transporter FtsABCD of *Streptococcus pyogenes* mediates uptake of ferric ferrichrome. *BMC Microbiol* 2005, *5*, 62.

[103] Gat, O., Mendelson, I., Chitlaru, T., Ariel, N., *et al.*, The solute-binding component of a putative Mn(II) ABC transporter (MntA) is a novel *Bacillus anthracis* virulence determinant. *Mol Microbiol* 2005, *58*, 533-551.

[104] Anderson, D. S., Adhikari, P., Nowalk, A. J., Chen, C. Y., Mietzner, T. A., The hFbpABC transporter from *Haemophilus influenzae* functions as a binding-protein-dependent ABC transporter with high specificity and affinity for ferric iron. *Journal of bacteriology* 2004, *186*, 6220-6229.

[105] Martin, P. R., Mulks, M. H., Cloning and characterization of a gene encoding an antigenic membrane protein from *Actinobacillus pleuropneumoniae* with homology to ABC transporters. *FEMS immunology and medical microbiology* 1999, *25*, 245-254.

[106] Smoot, L. M., Bell, E. C., Paz, R. L., Corbin, K. A., *et al.*, Molecular and genetic analysis of iron uptake proteins in the brazilian purpuric fever clone of *Haemophilus influenzae* biogroup aegyptius. *Frontiers in bioscience : a journal and virtual library* 1998, *3*, D989-996.

[107] Thomas, R. M., Twine, S. M., Fulton, K. M., Tessier, L., *et al.*, Glycosylation of DsbA in *Francisella tularensis* subsp. tularensis. *Journal of bacteriology* 2011, *193*, 5498-5509.

[108] Shouldice, S. R., Heras, B., Walden, P. M., Totsika, M., *et al.*, Structure and function of DsbA, a key bacterial oxidative folding catalyst. *Antioxidants & redox signaling* 2011, *14*, 1729-1760.

[109] Shouldice, S. R., Heras, B., Jarrott, R., Sharma, P., *et al.*, Characterization of the DsbA oxidative folding catalyst from *Pseudomonas aeruginosa* reveals a highly oxidizing protein that binds small molecules. *Antioxidants & redox signaling* 2010, *12*, 921-931.

[110] Ruiz, N., Chng, S. S., Hiniker, A., Kahne, D., Silhavy, T. J., Nonconsecutive disulfide bond formation in an essential integral outer membrane protein. *Proceedings of the National Academy of Sciences of the United States of America* 2010, *107*, 12245-12250.

[111] Negoda, A., Negoda, E., Reusch, R. N., Resolving the native conformation of *Escherichia coli* OmpA. *The FEBS journal* 2010, *277*, 4427-4437.

[112] Denoncin, K., Vertommen, D., Paek, E., Collet, J. F., The protein-disulfide isomerase DsbC cooperates with SurA and DsbA in the assembly of the essential beta-barrel protein LptD. *The Journal of biological chemistry* 2010, *285*, 29425-29433.

[113] Yu, J., Kroll, J. S., DsbA: a protein-folding catalyst contributing to bacterial virulence. *Microbes and infection / Institut Pasteur* 1999, *1*, 1221-1228.

[114] Houot, L., Chang, S., Pickering, B. S., Absalon, C., Watnick, P. I., The phosphoenolpyruvate phosphotransferase system regulates *Vibrio cholerae* biofilm formation through multiple independent pathways. *Journal of bacteriology* 2010, *192*, 3055-3067.

[115] Miki, T., Okada, N., Danbara, H., Two periplasmic disulfide oxidoreductases, DsbA and SrgA, target outer membrane protein SpiA, a component of the *Salmonella* pathogenicity island 2 type III secretion system. *The Journal of biological chemistry* 2004, *279*, 34631-34642.

[116] San Mateo, L. R., Toffer, K. L., Kawula, T. H., The sodA gene of *Haemophilus ducreyi* encodes a hydrogen peroxide-inhibitable superoxide dismutase. *Gene* 1998, *207*, 251-257.

[117] D'Mello, R. A., Langford, P. R., Kroll, J. S., Role of bacterial Mn-cofactored superoxide dismutase in oxidative stress responses, nasopharyngeal colonization, and sustained bacteremia caused by *Haemophilus influenzae* type b. *Infection and immunity* 1997, *65*, 2700-2706.

[118] Kroll, J. S., Langford, P. R., Saah, J. R., Loynds, B. M., Molecular and genetic characterization of superoxide dismutase in *Haemophilus influenzae* type b. *Mol Microbiol* 1993, *10*, 839-848.

[119] Korshunov, S. S., Imlay, J. A., A potential role for periplasmic superoxide dismutase in blocking the penetration of external superoxide into the cytosol of Gram-negative bacteria. *Mol Microbiol* 2002, *43*, 95-106.

[120] Hughes, M. J., Moore, J. C., Lane, J. D., Wilson, R., *et al.*, Identification of major outer surface proteins of *Streptococcus agalactiae*. *Infection and immunity* 2002, *70*, 1254-1259.

[121] Zanchi, F. B., Caceres, R. A., Stabeli, R. G., de Azevedo, W. F., Jr., Molecular dynamics studies of a hexameric purine nucleoside phosphorylase. *Journal of molecular modeling* 2010, *16*, 543-550.

[122] Jin, H., Agarwal, S., Pancholi, V., Surface export of GAPDH/SDH, a glycolytic enzyme, is essential for *Streptococcus pyogenes* virulence. *mBio* 2011, *2*, e00068-00011.

[123] Dumke, R., Hausner, M., Jacobs, E., Role of *Mycoplasma pneumoniae* glyceraldehyde-3-phosphate dehydrogenase (GAPDH) in mediating interactions with the human extracellular matrix. *Microbiology* 2011, *157*, 2328-2338.

[124] Tunio, S. A., Oldfield, N. J., Ala'Aldeen, D. A., Wooldridge, K. G., Turner, D. P., The role of glyceraldehyde 3-phosphate dehydrogenase (GapA-1) in *Neisseria meningitidis* adherence to human cells. *BMC Microbiol* 2010, *10*, 280.

[125] Purves, J., Cockayne, A., Moody, P. C., Morrissey, J. A., Comparison of the regulation, metabolic functions, and roles in virulence of the glyceraldehyde-3-phosphate dehydrogenase homologues gapA and gapB in *Staphylococcus aureus*. *Infection and immunity* 2010, *78*, 5223-5232.

[126] Fourrat, L., Iddar, A., Valverde, F., Serrano, A., Soukri, A., Cloning, gene expression and characterization of a novel bacterial NAD-dependent non-phosphorylating glyceraldehyde-3-phosphate dehydrogenase from *Neisseria meningitidis* strain Z2491. *Molecular and cellular biochemistry* 2007, *305*, 209-219.

[127] Brassard, J., Gottschalk, M., Quessy, S., Cloning and purification of the *Streptococcus suis* serotype 2 glyceraldehyde-3-phosphate dehydrogenase and its involvement as an adhesin. *Veterinary microbiology* 2004, *102*, 87-94.

[128] Alvarez, R. A., Blaylock, M. W., Baseman, J. B., Surface localized glyceraldehyde-3-phosphate dehydrogenase of *Mycoplasma genitalium* binds mucin. *Mol Microbiol* 2003, *48*, 1417-1425.

CHAPTER 3. STRUCTURAL AND ANTIGENIC ANALYSIS OF THE OUTER MEMBRANE PROTEINS P2 AND P5 OF *Haemophilus parasuis*

Modified from a paper to be submitted to *Biochemistry*

Mandy K. Zimmerli, Jerry K. McVicker, and Louisa B. Tabatabai

Abstract

Haemophilus parasuis is the causative agent of a swine respiratory infection, Glässer's disease, which results in significant economic loss for the industry. The P2 and P5 proteins of *H. influenzae* have been found to be important in the establishment of colonization. Because of this, the P2 and P5 proteins of *H. parasuis* may also play a role in confirming virulence. Three dimensional molecular modeling analysis, antigenic prediction, and continuous B-cell epitope prediction methods were used to analyze and compare the P2 and P5 of 15 reference strains of *H. parasuis* as well as two field isolates. Results indicate OMPP P5 comprises an N-terminal OMPA domain with four outer membrane loops and a C-terminal domain highly homologous to the OMP P6 protein of *H. influenzae*. OMP P2 is homologous to OMPII of *Neisseria meningitidis* and comprises eight surface exposed loops. Two forms of OMP P2 are expressed with an increase in apparent molecular weight for avirulent serovars due to extensions in the outer membrane loop 3 and loop 5. While two genes for the P2 protein have been sequenced for some strains, only one form of the protein appears to be expressed as determined by immunoblot and N-terminal sequence analysis. This is the first report of a three-dimensional model for both proteins that combines antigenicity and continuous B-cell epitope prediction methodologies in order to identify OMP P2-derived subunit vaccine candidates for Glässer's disease. The approach presented

here can be applied to outer membrane proteins of extracellular pathogens for the identification and design of a subunit vaccine and corresponding diagnostic.

Introduction

The causative agent of Glässer's disease is *Haemophilus parasuis*, a Gram-negative, nonhemolytic bacterium. Infection occurs in the worldwide swine population, with presentation as either an acute or chronic illness, depending on the serotype of strain as well as whether or not viral co-infection exists (*1-4*). To date, there is no commercially available cross protective vaccine or diagnostic for Glässer's disease. Therefore, it is relevant that virulence factors, including the OMP P2 and OMP P5 proteins, are studied to identify potential subunit vaccines and subunit based diagnostics. In doing so, a herd can not only be vaccinated against highly virulent serotypes, but it can also be checked for animals that are carriers of a virulent serotype of the bacterium. OMP P2 and OMP P5 are important virulence factors in the related organism, *H. influenzae*. Both proteins have been found to be important in the establishment of colonization and have been identified as potential vaccine candidates (*5-18*). Using *H. influenzae* as a model organism, it was proposed that these proteins could exhibit similar activities in *H. parasuis*.

Secondary structural analysis of *H. influenzae* OMP P5 shows considerable homology to the OMPA in *E. coli*, comprising four surface exposed loops (*19*). Due to the increase in variability of OMP P5 during the course of chronic infections, it was concluded that P5 plays an important role as a target for the immune response (*20*). Peptide vaccination studies in a chinchilla animal model show that the loop 3 region of *H. influenzae* OMP P5 is a protective epitope while the loop 4 region serves as an immunodominant decoy epitope (*14*). Variability in the nucleotide as well as primary amino acid sequence has also been shown to exist for

OMP P5 of *H. parasuis (21).* Additionally, an OMPA protein, a homologue to OMP P5, was identified in *H. parasuuis*. Two-dimensional modeling demonstrated that OMPA has four surface exposed loops, with hypervariability existing for the predicted loop 3 and loop 4 regions(*22*). Moreover, recombinant OMPA from both serovars 4 and 5 cross reacted to anti-sera from all serovars of *H. parasuis,* indicating that the variability in the loop 3 and loop 4 regions does not affect antigenicity of the OMPA in *H. parasuis (23).* Antibodies raised to OMPA have been found to provide protection against *H. parasuis* in a mouse model (*24*).

The most abundant outer membrane protein in *H. influenzae* is OMP P2. This protein, like OMP P5, is highly variable on its surface exposed regions and is strongly immunogenic. Characterization of the loop peptides of the *H. influenzae* OMP P2 has revealed that loop 5 is the immunodominant epitope while loop 6 remains protective (*6-9*). Aside from direct immunogenic function, these loops have been implicated in the activation of JNK and p38 via mitogen-activated protein kinase pathway (*25*). Previous work has found that the OMP P2 of *H. parasuis* is variable and exists in two forms which differ by approximately 3-5kDa in size (*21*). Moreover, results of a vaccination challenge study in mice revealed that a recombinant form of the P2 protein is protective against challenge and inhibits colonization (*26*). While OMP P5 of *H. influenzae* has been shown to bind human CEACAM-1, an interaction involved with the probable evasion of host's immune response, human CEACAM-1 has been shown to bind OMP P2 of *H. parasuis (27).*

A number of OMP P2 and OMP P5 genes of *H. parasuis* have been sequenced. However, three dimensional structure predictions indicating the number and location of the flexible surface exposed loops have been based on two dimensional models. Previous work hypothesized that OMP P5 comprises five surface exposed regions while OMP P2 comprises

eight surface exposed regions with two forms of loop 3 (*21*). Additionally, previous predictions of antigenic sites for *H. parasuis* OMP P2 and OMP P5 were based on out of date methods *(21*). Because of this, an accurate depiction of propensity of antigenicity as well as location of continuous B-cell epitopes for either OMP P2 or OMP P5 in *H. parasuis* is not available. The results of the previous work cites that OMP P5 only contains one area of high antigenicity in the hypothesized loop 5 region and that the hypothesized loop 3 region of OMP P2 is highly antigenic.

The goal of this study was to sequence as well as model the three-dimensional structure of OMP P2 and OMP P5 sequences of *H. parasuis* based on a homology modeling method. The primary sequences of both proteins were analyzed by ANTIGENpro and COBEpro in order to determine regions of antigenicity as well as continuous B-cell epitopes. The results of this study not only provide a three-dimensional model for OMP P2 and OMP P5 and an up to date prediction of the antigenic sites and continuous B cell epitopes, but also a general method for predicting regions of surface exposed proteins from extracellular bacterial pathogens that could be exploited in the design of peptide based vaccines and diagnostics.

Material and Methods

Bacterial Strains. Seventeen *Haemophilus parasuis* strains were studied. Fifteen of the strains were reference strains obtained from Richard Ross (College of Veterinary Medicine, Iowa State University, Ames, IA). Three field strains were obtained from Vicki Rapp-Gabrielson (Shering-Plough, Omaha, NE) and Kelly Lager (National Animal Disease Center, Ames, IA). Table 3.1 describes the bacterial strains used for this study.

Primary sequence analysis. Template DNA was extracted using the High Pure PCR Template according to the manufacturer instructions (Roche, Indianapolis, IN). Primers corresponding to OMP P2 (NCBI Accession No. 167853935) and OMP P5 (NCBI Accession: 167856404) of *H. parasuis* were designed (Table 3.2). PCR reactions were prepared according to manufacturer's instructions (Invitrogen, Carlsbad, CA) using strains designated in Table 3.1 along with a negative control. Reaction steps performed as follows: denaturation step (2 min at 94ºC); 30 cycles each of 1 minutre of denaturation at 94C, 1.5 minutes of annealing at 55ºC, and 1 min of elongation at 72ºC; and then a 30 min final elongation step at 72^{o}C. Products were analyzed on 1% agarose gel in TAE (pH8.0) containing ethidium bromide at a concentration of 0.05 µg/100 ml (Sigma Chemical Co., St. Louis, MO). The PCR products from each reaction were either inserted into a pBAD TOPO-Thio vector for sequencing as stated by manufacturer (Invitrogen, Carlsbad, CA) or sequenced with corresponding forward and reverse primers (Table 3.2). Sequencing was done by the Iowa State University DNA Facility (Ames, IA). DNA sequences were translated using the Translate tool (Expasy), and sequence homologies were determined by using the BLAST server of the National Center for Biotechnology Information (NCBI). Sequence alignments to the P2 and P5 proteins available in NCBI were performed using T-Coffee *(28, 29*).

Molecular Modeling and antigenic and B-cell epitope prediction of OMP P2 and P5 proteins. The OMP P2 and P5 proteins from primary sequence analysis as well as additional OMP P2 and P5 sequences (Accession numbers in figures and supplementary information) were modeled using the Modeller program *(30*) following tertiary structural analysis by HHPred (*31, 32*) using pdb70_16Jul11 HMM database. Sequences for OMP P2 and P5

proteins were submitted to Scratch protein predictor *(33*). ANTIGENpro *(34*) and COBEpro *(35*) were used to identify antigenic sites and continuous B-cell epitopes.

Results

Identification of P2 and P5 of *H. parasuis*. Analysis of PCR reactants on 1% agarose gel for SV2, SV3, SV4, SV5, SV6, SV13, field isolates 2170B (SV4), 84-29755 (SV5), and 409KL (Unknown) (Figure 3.1) indicate the presence of two amplicons for P2 and P5 with primers used in this study (Tables 3.4 and 3.5). Comparison of our sequencing data to that of previous data indicates that there is only one form of OMP P5 that is expressed. The smaller fragment observed at approximately 592 bp corresponds to the OMPA domain of *H. parasuis* OMP P5. The presence of a band at approximately 590 bp and an additional amplicon at 1100 bp was observed for other primers designed to the *H. parasuis* OMP P5 gene (results not shown). Additional results with primers specific to the OMPA domain of OMP P5, used for protein expression, revealed a single amplification.

Unlike OMP P5, there is evidence that more than one gene exists for *H. parasuis* OMP P2 and that multiple copies of P2 porins are present for other *Haemophilus sp.* (*21*, *36*). The results of sequencing of reference strain Nagasaki (SV5) indicates the presence of two genes of P2 which differ by approximately 4.5 kDa upon translation of the primary amino acid sequence (Figure 3.2; Supplementary Figure S3.39, and Accession number: ACS36765). However, protein analysis techniques presented here have identified only one form of OMP P2 is expressed for all reference strains used in this study (Supplemental Figure S3.2, Supplemental Table S3.1), with an apparent molecular weight varying between 48-55 kDa. Immunoblot followed by N-terminal sequencing (Supplemental information) identified the OMP P2 and OMP P5 proteins for *H. parasuis* SV2 and SV3 (Supplemental Table S3.1). As

shown in Supplementary Figure S3.2, the P2 reactive bands present at a higher apparent molecular weight for the avirulent serovars, except SV7. This difference in molecular weight of P2 protein appears to correlate with virulence of the organism. While the calculated molecular weight of the P2 proteins based on translated genes is 36-42 kDa, the apparent molecular weight for the P2 proteins presented here ranges from 48-55 kDa. This difference in calculated, and apparent molecular weight could be due to a decreased mobility from either a large stokes radius of the protein and/or decreased binding of SDS to the protein prior to SDS-PAGE analysis or modification of the protein with glycosylation. In addition to the predicted 839 bp amplicon, a smaller amplicon was observed at 405 bp, 455 bp and 524 bp (Figure 3.1). Translation of the smaller amplicons reveals it codes for an internal region of OMP P2.

Modeling of OMP P5 and OMP P2. Figure 3.3 shows the three dimensional model of OMP P5 for 84-29755 (SV5). The model shows that OMP P5 is a beta-barrel that comprises four surface exposed regions on the N-terminal domain, which has high homology to OMPA, and a C-terminal domain which is highly homologous to the OMP P6 of *H. influenzae*. The regions of the model which are surface exposed are colored as well as the P6-like domain. The molecular models of the OMP P5 for all reference and field strains (Table 1) take on this same structure, regardless of virulence of organism (Supplemental Figures 3.3-3.18).

Unlike OMP P5, there are two forms of the OMP P2 proteins as indicated by the models of the 85-29755 (SV5) and SW114 (SV3) OMP P2 proteins (Fig 3.5 and 3.7). A beta-barrel porin with eight surface exposed regions is characteristic of both forms, with an extension in loop 3 and loop 5 regions existing in only one form of the P2 protein, notably expressed in the avirulent serovars. Modeling of the OMP P2 protein indicates these loop

extensions exist for all reference avirulent serovars except SV7 and that the highly virulent reference strain SV4 contains the loop extensions (Supplemental Figures S3.35-3.50). Proof of the 3-5kDa difference in apparent molecular weight of the two forms of the P2 protein, which comes primarily from the loop 3 and loop 5 extension, has been verified by protein immunoblot and sequencing analysis (Supplemental Figure S3.1 and S3.2). Additionally, while the reference strain SV4 contains the loop extensions, the field isolate 2170B (SV4, Supplementary Figure S3.50) does not comprise the extension in the loop 3 and loop 5 regions. It is possible that reference strains SV4 and SV7 were interchaged upon transfer of cultures as colleagues have found SV7 reference strain to present as a virulent serotype while reference strain SV4 presents as avirulent *(27, 37, 38).*

Prediction of antigenic sites and B-cell epitopes. Since the goal of this work was to elucidate differences in antigenicity of the OMP P5 and OMP P2 proteins and exploit those differences in the development of a probable subunit vaccine, the protein sequences were analyzed for regions of antigenicity by ANTIGENpro and predicted continuous B-cell epitopes by COBEpro. A summary of these results is presented in Tables 3.5 and 3.6.

The results of antigenic site prediction and continuous B-cell epitope prediction for OMP P5 of 84-29755 is found in Figure 3.4. Information on additional strains can be found in Supplementary Figures S3.19-S3.34. The overall antigenicity of the highly virulent OMP P5, as predicted by ANITGENpro, was 83-86%. All outer membrane loops for the highly virulent strains, including the field isolate 84-29755 (SV5), presented with high as well as comparable antigenicity with prominent B-cell epitopes (>70% probability) present on the OMP P6-like domain as well as the loop 3 and loop 4 regions of the OMPA domain. The moderately virulent serovars also presented with 83-86% overall protein antigenicity. As

seen in the virulent serovars, the moderately virulent serovars outer membrane loops of OMP P5 were also predicted to be antigenic. However, the loop 4 region has a lower propensity of antigenicity than the other loops for SW140 (SV2) and SW124 (SV4). Both SW124 (SV4) and SW140 (SV2) had B-cell epitopes >70% only present for the OMP P6-like domain. The epitope at the loop 3 apex was given a 68% probability of being a continuous B-cell epitope for both strains. For SW124 (SV4) and SW140 (SV2), the loop 4 epitope was given a continuous B-cell epitope probability of 67% and 65%, respectively. As seen with the highly virulent strains, the moderately virulent strains C5 (SV8), 84-15995 (SV15), and field isolate 2170B (SV4) had a continuous B-cell epitope probability greater than 70% for the apex of the loop 3 and loop 4 outer membrane regions. The outer membrane loops of the avirulent serovars, like that of the moderarely and highly virulent serovars, also presented with outer menbrane loops with high antigenic propensity scores. However, the scores of loop 2 were higher for strains D74 (SV9) and H465 (SV11). The overall predicted antigenicity of the OMP P5 for avirulent serovars is approximately 84-85%. The loop 4 region of the OMP P5 of strains 131 (SV6) and D74 (SV9) were found to have a probable B-cell epitope. Moreover, these strains have a 67% probability of having a continuous B-cell epitope on the apex of outer membrane loop 3. Strain SW114 (SV3) also has a highly probably continuous B-cell epitope at the apex of loop 3 and a 68% predicted probability of comprising a continuous B-cell epitope at the apex of loop 4. The strain 174 (SV7), unlike the rest of the avirulent serovars, does not contain a highly probable continuous B-cell epitope for the OMPA-domain of OMP P5. It does, however, have a 65% and 68% predicted probability of comprising continuous B-cell epitopes on outer membrane loops 3 and 4.

The antigenicity and B-cell epitope maps for the OMP P2 of 84-29755 (SV5) and SW114 (SV3) are presented in Figures 3.6 and 3.8. Information on additional strains can be found in Supplementary Figures S3.51-S3.66. The OMP P2 of highly virulent strains, including the field isolate 84-29755 (SV5), were given a predicted probability of antigenicity of 91-93% with all surface exposed outer membrane loops comprising antigenic epitopes. A comparison of the non-extended and extended forms of P2 for strain No. 4 (SV1) are shown in Supplementary Figure S3.51 and S3.52. In both the extended and non-extended forms, a continuous B-cell epitope is present for loop 3, loop 5, loop 6, and the region of the loop closest to the transmembrane domain for loop 1 and loop 8. While both forms are presented here, the non-extended form of OMP P2 for strain No. 4 was considered as it is consistent with the findings of N-terminal sequencing and immunoblot analysis. For P2 of No. 4, loop 4 had the highest antigenic score while loops 8, 1, and 5 followed with the next highest score for antigenic probability. Consistent with the findings for No. 4 (SV1), the highly virulent reference strains Nagasaki (SV5), H367 (SV10), H425 (SV12), 84-17975 (SV13), 84-22113 (SV14), and field isolate 84-29755 (SV5) also scoring antigenic sites located on loops 1, 4, and 8. The highest scoring continuous B-cell epitope was located on loop 8 for strains Nagasaki (SV5), 84-17975 (SV13), 84-22113 (SV14), and field strain 84-29755 (SV5) while the highest scoring continuous B-cell epitope for H367 (SV10) and H425 (SV12) was located on loop 4. No. 4 (SV1), unlike the other strains, had the highest scoring continuous B-cell epitope located on loop 3. All highly virulent serovars had a probable continuous B-cell epitope on loop 3 that is also the highest scoring antigenic epitope for that particular loop. Like the highly virulent serovars, the moderately virulent serovars also comprised antigenic regions on their predicted outer membrane loops, with a predicted probability of antigenicity

ranging from 90-93%. Moreover, loops 4 and 8 had the highest antigenic propensity scores compared to other loops for all moderately virulent reference strains and the field isolate. In addition to these antigenic loops, the strains SW140 (SV2), SW124 (SV4), 85-15995 (SV15), and 2170B (SV4) had high antigenicity score for loop 1. Strain SW124 (SV4) was set apart from the others in that it had a higher antigenic propensity score for outer membrane loop 5, particularly in the noted extension. While the moderately virulent serovars shared the commonality of both loops 4 and 8 having high antigenic propensity score, there was disagreement amongst the analysis of the strains as to the antigenicity of the loop 3 region. Strains SW140 (SV2) and SW124 (SV4) had a lower scoring epitope on loop 3 in comparison to the virulent serovars. However, strains C5 (SV8), 84-15995 (SV15), and 2170B (SV4) had a predicted angtigenic region in loop 3 which coincided with a predicted continuous B-cell epitope. This is an epitope shared with the highly virulent serovars and is the highest scoring continuous B-cell epitope for strain 84-15995 (SV15). In addition to the loop 3 B-cell epitope, the highest scoring predicted continuous B-cell epitope for strains SW140 (SV2), SW124 (SV4), and C5 (SV8) was located on loop 4 while the highest scoring continuous B-cell epitope was predicted to be on loop 8 for the field isolate 2170B (SV4). The results of 2170B was comparable to that observed in highly virulent strains. The predicted probability of antigenicity for the OMP P2 of the avirulent strains was determined to be 90-92%. For strains SW114 (SV3), 131 (SV6), and D74 (SV9), the antigenic propensity of the outer membrane loops was comparable, with both loop 2 and loop 6 scoring lower than the other loops. Strain 465 (SV11) had the highest antigenicity associated with the loop 5 extended region while the loop 3, 4, and loop 6 were lower in comparison to the other outer membrane loops. Probability of continuous B-cell epitope predictions was highest on loop 3

for D74 (SV9) and H465 (SV11). The outer membrane loop 4 was also analyzed to be a highly probable continuous B-cell epitope for strains SW114 (SV3) and 131 (SV6). While loop 5 was a high scoring probable continuous B-cell epitope for all avirulent reference strains, it should be noted that the extension in the loop 5 region moves the predicted continuous B-cell epitope out of the apex region and closer to the transmembrane domain. The reference strain 174 (SV7) presented with characteristics similar to that of the moderate to highly virulent serovars, with antigenicity being the highest for loops 1, 4, and 8. In addition to this, the loop 3 has the lowest antigenic propensity score. The highest ranking predicted continuous B-cell epitope for 174 is loop 8, with loops 4 and 3 ranking closely behind. Overall, the P2 proteins of all serovars comprised epitopes with antigenic propensity for the predicted outer membrane loops. All strains, with the exception of SW124 (SV4), shared a probable continuous B-cell epitope for outer membrane loop 3. However, SW124 has a loop 3 continuous B-cell epitope prediction of approximately 67%. In addition to this loop 3 epitope, a loop 5 continuous B-cell epitope was predicted for the OMP P2 of all avirulent reference strains. Additionally, this epitope was also predicted for the highly virulent No. 4 (SV1), moderately virulent SW124 (SV4), C5 (SV8), and 84-15995 (SV15). It should be noted that the extension of the prediction outer membrane loop 5 appears to move the continuous B-cell epitope from the apex of the loop and closer to the transmembrane domain. All serovars, regardless of virulence comprised a predicted B-cell epitope for the outer membrane loop 4, loop 6, and loop 8.

Discussion

The OMP P2 and OMP P5 genes of *H. parasuis* have been identified in a variety of reference strains as well as field isolates. However, few studies have been done in elucidating

protein expression profiles of *H. parasuis*. An immunoblot using a mAb for *H. influenaze* OMP P5, which was found to cross react with OMP P2, followed by N-terminal sequencing (Supplementary Figures S3.1, S3.2, and Table S3.1) confirms the identity of the P2 and P5 proteins in *H. parasuis*. Additionally, the P2 protein was found to express in one of two different forms, which differ by approximately 3-5kDa in size, and this extension coincides with virulence of the organism (Supplementary Figure S3.2). As shown in Supplementary Figure S3.2, the P2 reactive bands present at a higher molecular weight for the avirulent serovars, except SV7. However, it should be noted that previous work has indicated a possible mislabeling of the laboratory reference strains upon transfer (*27, 37, 38*). Sequencing of a P2 gene from strain 174 by another group (Accession number: ADJ38728) provides evidence of a P2 protein comprising the hypothesized loop 3 and loop 5 extensions. This also explains why the SW124 (SV4) strain was set apart from the moderately virulent and presented similar to the avirulent serovars in having a high antigenic propensity score for the OMP P2 loop 5 extension.

Results presented here for the amplification of P5 genes of *H. parasuis* indicate the presence of two amplicons, with one coding for the OMP P5 and the other amplicon coding for the OMPA domain of *H. parasuis*. While no data exists to suggest multiple copies of the P5 genes to date, there is information that suggests that in addition to the P5 protein, *H. parasuis* also has an OMPA protein (*22*). The 592 bp amplicon corresponded with the OMPA domain of OMP P5. OMPA is a highly conserved protein in gram-negative bacteria and has been found to be important in the establishment of colonization, evasion of the host's immune response, participation in biofilm formation and serving as a receptor for bacteriophages (*39-41*).

Molecular modeling analysis shows that the OMP P5 of *H. parasuis* has four surface exposed loops and that structure is not dependent on the virulence of the organism. The previous two-dimensional model of OMP P5 indicated a fifth loop, which does not coincide with our analysis as this hypothesized fifth loop presents in our model as a linker between the two domains (*21*). The length of this linker is approximately 14.4 nm, which would only allow it to span the outer membrane (~7-10 nm) once, without presentation of any surface exposed residues. In addition to homology to OMPA, the C-terminal domain of P5 is highly homologous to OMP P6 of *H. influenzae* as well as *E.coli* Pal. Previous studies have been done in *H. influenzae* involving P6 as a vaccine candidate that is surface exposed (*6, 42-66*). However, a recent study using protein prediction and structural analysis has indicated that P6 has homology and considerable structural identity to *E. coli* Pal, a protein which is not surface exposed and anchored by a lipid moiety to the inner lipid layer of the outer membrane of *E. coli (44)*. These results and the analysis provided here indicate the C-terminal domain of OMP P5 most likely protrudes into the periplasmic space. This does not preclude the use of the P6 protein and the P6-like domain of OMP P5 as a possible vaccine candidate as there is evidence that periplasmic proteins are effective vaccine candidates (*67-69*). There could be a mechanism that exists to expose the periplasmic proteins to the outer membrane surface or a mechanism in which bacterial fusion with a lysosome causes the outer membrane to become porous, allowing for the protein or domains of proteins located in the periplasmic space to transverse the outer membrane.

Previous results of sequencing the P2 genes of *H. parasuis* did not reveal a correlation between predicted loop extensions and virulence(*21*). However, these results were based on two-dimensional modeling analaysis and gene sequencing alone and did not take

into account protein expression. The current findings suggest that OMP P2 protein, which comprises eight surface exposed loops, is only expressed in one form in each serovar, either in the extended loop or non-extended loop conformation. However, both forms of P2 genes have been sequenced in previous studies following PCR amplification in some strains. For example, nucleotide sequencing of the No.4 highly virulent reference strain indicates both the presence and absence of the loop 3 and loop 5 extenstions upon translation (Supplementary Figure S3.34 and S3.35). This trend is seen in other reference strains presented here including: Nagasaki (Figure 3.2; Supplementary Figure S3.39 and Accession number: ACS717681), 174 (Supplementary Figure S3.41 and Accession number: ACS71770), D74 (Supplementary Figure S3.43 and Accession number: ACS71772), H367 (Supplementary figure S3.44 and Accession number: ADJ38730), and H465 (Supplementary Figure S3.45 and ACS71763). In addition to this information, evidence exists that multiple copies of the P2 gene exists for some strains (*21*). These results indicates that perhaps there exists a mechanism in which one or both forms of the P2 protein is selected to be expressed, either as a native characteristic of the bacterial serovar or in response to co-infection and/or the presence of epithelial cells. Or this may indicate that P2 is present in both forms in these strains, but the detection method used in this study only identifies one form. However, given that other *Haemophilus* species present with multiple gene copies for P2 proteins and select the expression of a particular P2 protein, or multiple forms, it is feasible that this occurs in *H. parasuis* strains with multiple copies of the P2 gene (*36*). Comparable to the results presented here, a recent study using different *H. parasuis* refernce strains and field isolates noted a correlation between the type of P2 protein expressed and virulence of the organism (*26*).

Since modeling of the two forms of P2 indicated an extension in the loop 3 and loop 5 regions, the role of these extensions may have implications in the virulence of the organism.

The outer membrane loops of the OMP P5 and OMP P2 proteins contained regions of antigenicity for all serovars, regardless of virulence of the strain. Previous reseach indicated that the hypothecial loop 5 of OMP P5 and loop 3 of OMP P2 were the only regions of high antigenicity (*21*). Using our method, the OMP P5 was given a propensity of antigenicity ranging from 83-86% while the OMP P2 was given higher propensity of antigenicit ranging from 90-93%. Although both proteins were predicted as antigenic, differences were noted for the antigenicity profiles of each. Focus was placed specifically on the outer membrane loops since these would be the portions of the protein exposed to host upon infection and these epitopes may also have implications in colonization.

For OMP P5, all outer membrane surface exposed loops of all serovars were found to contain the same antigenic profile with the exception of a lower antigenic propensity score for loop 2 for strains D74 (SV9) and H465 (SV11) and loop 4 for SW140 (SV2) and SW124 (SV4). The OMP P6-like domain, which is predicted to be perisplasmic, was also found to have a consistent antigenic profile.

Unlike the OMP P5, marked differences were noted in the antigenicity profiles of the outer membrane loops of OMP P2. Given the results, it appears the outer membrane loops of OMP P2 for highly virulent serovars are most antigenic for the loop 1, loop 4 and loop 8 regions. Moderately virulent serovars share the antigenic profile of OMP P2 at loop 4 and loop 8. Although 2170B (SV4) is classified as moderately virulent, it was predicted to have a highly antigenic epitope for outer membrane loop 1, in addition to loop 4 and loop 8. Differences were noted for SW124 (SV4), a moderately virulent serovar, as it also comprised

a region of high antigenicity in the region of the loop 5 extension. It has been noted that SW124 and 174 may have been swapped upon labeling in the laboratory. Our reference strain 174 (SV7) presents with a virulent antigenic profile in comparison to the avirulent serovars, by comprising regions of high antigenicity on loop 1, loop 4 and loop 8. Since extensions are presents in the loop 3 and loop 5 regions for avirulent serovars, antigenic profiles at these regions were compared. In our model, the loop 3 presents with structural α-helix. Taking into account the approximate location of the helix within the membrane, along with the length of the outer membrane (~7-10nm), the extension in the loop is predicted to be placed outside of the outer membrane space by approximately 8nm. This places the area of highest antigenic propensity as predicted for loop 3 outside of the membrane. For highly virulent serovars, these regions did not have a prominent score in comparison to loop 1, loop 4 and loop 8. It was noted that the loop 3 region for SW140 (SV2) and SW124 (SV4) moderately virulent strains had a lower antigenic propensity score when compared to loops 1, 4 and 8. A drop in antigenicity was also noted for the loop 3 extension for the avirulent strains 131 (SV6) and H465 (SV11). While all loops presented comparable antigenicity for D74 (SV9), antigenicity was only noted for the loop 3 region that is not associated with loop extension. For the avirulent strain SW114 (SV3), loop 3 scored higher for antigenicity than the other loops. The extension in the loop 5 region of SW124 (SV4) had the highest score of antigenicity for its outer membrane loops.

Since *H. parasuis* is an extracellular pathogen, epitopes which elicit a humoral response are most desirable for the design of a subunit vaccine. While most B-cell epitopes are predicted to be discontinuous, in the design of a subunit vaccine from flexible loop peptides, a continuous B-cell epitope is most desireable. The loop 3 and loop 4 of OMP P5

were found to comprise continuous B-cell epitopes for all highly virulent serovars. In addition to the outer membrane loops, regions of the OMP P6-like domain may also serve as probable subunit vaccines as fusion with the lysozome may expose epitopes which were previously hidden in the perisplasmic space. Continuous B-cell epitopes of OMP P2 associated with high virulence were predicted for outer membrane loop 8, loop 4 and loop 3. However, the continuous B-cell epitopes of loop 8 are not predicted to be at the apex of loop 8 for all highly virulent serovars. For No. 4 (SV1), H367 (SV10) and H425 (SV12), this epitope is located closer to the transmembrane domain. This is the same finding for the predicted continuous B-cell epitopes for loop 1 of OMP P2 for all serovars. The loop 4 epitope, however, is a more promising subunit vaccine candidate as it comprises a continuous B-cell epitope which spans a majority of the outer membrane predicted loop 4 in all strains except SW140 (SV2) and H465 (SV11). All highly virulent serovars comprise a continuous B-cell epitope for loop 3 which does not correspond with the loop extension noted for the avirulent serovars. It was predicted to be the highest scoring region of antigenicity in the loop 3 region. Moreover, the extension in outer membrane loop 3 for strains 131 (SV6), C5 (SV8), D74 (9), and H465 (SV11) resulted in either a shift of continuous B-cell epitope or extension of the continuous B-cell epitope noted for the highly virulent strains.

While the methods presented here have provided insight into the structure of the P2 and and P5 proteins and how the structural differences may be implicated in virulence, molecular modeling analysis is not a substitute for obtaining an actual protein structure by NMR or X-ray crystallographic methods. However, three dimensional modeling based on homology and sequence and structural based alignment provides a good platform to design future research in a case where no model exists for a protein. Overall, this paper describes the

identification and molecular and antigenic characterization of the outer membrane proteins P2 and P5. Molecular modeling analysis provides a prediction of three dimensional structure which can be combined with antigenicity predictions and continuous B-cell epitope predictions to identify epitopes that not only give rise to antigenicity and antigenicity profiles that vary among the strains for a particular protein, but also epitopes that can also be exploited in the development of a subunit vaccine. The use of a subunit vaccine could include peptides or engineered proteins which serve to focus the host's immune system on protective epitopes. The method described here could be used to idenitify probable subunit vaccine candidates based upon outer membrane proteins of extracellular pathogens.

Future research is required in order to elucidate whether the predicted outer membrane loops are indeed surface exposed. Additionally, peptides corresponding to outer membrane loops must be screened to determine whether or not animals infected with *H. parasuis* have an antibody titer to these epitopes.

Acknowledgements

We would like to thank Muriel van Schilfgaarde for the mAb and *H. influenzae* outer membrane proteins d1 and d4; the ISU Protein Facility for assistance with N-terminal sequencing; and the ISU DNA Facility for assistance with sequencing of P2 and P5 genes.

Tables

Table 3.1. Description of bacterial strains

Serovar	Reference [a] strain	Country of origin	Diagnosis/ isolation site	Virulence[b]
Reference Strains				
1	No. 4	Japan	Healthy/nose	H
2[d]	SW140	Japan	Healthy/nose	L
3[d]	SW114	Japan	Healthy/nose	A
4[d]	SW124	Japan	Healthy/nose	L
5[d]	Nagasaki	Japan	Septicemia/meninges	H
6[d]	131	Switzerland	Healthy/nose	A
7	174	Switzerland	Healthy/nose	A
8	C5	Sweden	Unknown	L
9	D74	Sweden	Unknown	A
10	H367[c]	Germany	Unknown	H
11	H465	Germany	Pneumonia/trachea	L
12	H425	Germany	Polyserositis/lung	H
13[d]	84-17975	United States	Unknown/lung	H
14	84-22113	United States	Unknown/joint	H
15	84-15995	United States	Pneumonia/lung	L
Field strains				
5[d]	84-29755	United States	Unknown/lung	H
4[d]	2170B	United States	Joint	L
Unknown[d]	HP409KL	United States	Unknown	H

[a] Reference strain information and virulence scores obtained from reference 13.

[b] Virulence designations: H, high virulence; L, moderate/low virulence; A, avirulent.

[c] H367 is a field strain with the same characteristics as the original reference strain H555.

[d]Strains shown in this study for PCR

Table 3.2. Description of primers

Primer	Sequence	Predicted length (bp)	Observed length (bp)[a]
P5-F2	CGACCTTTAACTGCGTCA	949	675
P5-R2	AAGCTGCTCCACAAGCTA		950
P2-F2	CATTTGCAGCATCAGCA	839	650-700
P2-R2	GTTTCCATACACGCCAGA		850-950
P2-F4	GCGGCATTTGCAGCA	1022	1000-1200
P2-R4	CACGTAAACCAACACCA		

[a]Corresponds to products of PCR reactions in Figure 3.1.

Table 3.3. Description of PCR products for OMP P2 using P2 F2,R2 primers

Sample	Product length(bp)	Accession number[a]	Protein [a]	MW (kDa)[b]
HP2-P2	798	FJ402848	OMP P2	29.3
HP3-P2	719	FJ402849	OMP P2	24.0
HP4-P2[c]	455	FJ402850	OMP P2	16.6
HP5-P2	924	FJ402868	OMP P2	33.9
HP6-P2	993	FJ402846	OMP P2	36.4
HP13-P2	695	FJ402851	OMP P2	25.5
HP21-P2	409	FJ402852	OMP P2	15.0
HPIA-P2	899	FJ402854	OMP P2	33.0
HP409[c]	524	FJ402852	OMP P2	19.2

[a] National Center for Biotechnology Information

[b]Fragment MW predicted by Translate (Expasy)

[c]Sequenced smaller amplicon than expected

Table 3.4. Description of PCR products for OMP P5

Sample	Product length(bp)	Accession number[a]	Protein I.D[a]	MW (kDa)[b]
HP3-P5[c]	592	FJ402855	OMP P5	21.7
HP4-P5	866	FJ402856	OMP P5	31.8
HP5-P5	806	FJ402866	OMP P5	29.6
HP6-P5	765	FJ402867	OMP P5	28.1
HP13-P5	910	FJ402858	OMP P5	33.4
HP21-P5	912	FJ402859	OMP P5	33.4
HPIA-P5	728	FJ402847	OMP P5	26.7
HP409KL	875	FJ402860	OMP P5	32.1

[a] National Center for Biotechnology Information

[b]Fragment MW predicted by Translate (Expasy)

[c]Sequenced smaller amplicon than expected

Table 3.5. Consensus antigenicity profiles and continuous B-cell epitopes for OMP P5

	Antigenic sequence[a]	Net votes[b]	B-cell epitope[a]	Score[c]
Highly virulent				
Loop 1	NQLNSKYKNDARYATSANGYVINRN	10-25	None	N/A
Loop 2	RVRGNKQEFR(A/E)FKHS	22-35	KQEFR(A/E)FKH	65-78
Loop 3	YKRY(S/F)(Q/T)TXXXVXXK(A/S)HN	20-25	RY(S/F)(Q/T)XXX	69-71
			DYKRYSTTX	72
Loop 4	GNFTKAEAKENRRAT[d]	22-35	KENRRAT	70-83
			AQKRGDTAM	74
Moderately virulent				
Loop 1	NQLNSKYKNDARYATSANGYVINRN	10-25	None	N/A
Loop 2	RVRGNKQEFR(A/E)FKHS	22-30	GNKQEFR(A/E)	67-69
			FRAFKH	73-76
Loop 3	YK(R/F)Y(D/F/S)XXXK(A/S)HNLK	17-25	RY(S/F)(Q/T)XXX	67-70
			DYKRYSTTX	73
Loop 4	GNFTKAEAKENRRAT[d]	20-25	KENRRAT	65-70
			AQKRGDTAM	74
Avirulent				
Loop 1	NQLNSKYKNDARYATSANGYVINRN	10-25	None	N/A
Loop 2	RVRGNKQEFR(A/E)FKHS	25-35	GNKQEFR(A/E)	67-69
			FRAFKH	72-83
Loop 3	YK(R/F)Y(F/D)XTXE(P/D)XK(A/S)HNLK	15-25	FYDXTXE(P/D)KA	67-69
			Y(F/D)XTXE(P/D)XK	73
Loop 4	GNFTKAEAKENRRAT[d]	15-20	FTKAEMKE	65-66
			AQKRGDTAM	73-74

[a]Consensus sequence: X denotes presence or absence of any amino acid

[b]Determined by ANTIGENpro

[c]Determined by COBEpro: probability in percent

[d] Strain No. 4, C5, 131 and D74 have following concensus: (G/N)NANKAAQKRGDTAM

Table 3.6. Consensus antigenicity profiles and continuous B-cell epitopes for OMP P2

	Antigenic sequence[a]	Net votes[b]	B-cell epitope[a]	Score[c]
Highly virulent				
Loop 1	(L/K)G(K/Q)SSTXGHTXLKNNS	25-35	LKNNG	75-76
Loop 2	(G/D/N)SKN(A/D)XWGDV	10-20	AAGEWGDVK	68-74
			DSNSENAAGWGDV	73
Loop 3	GVGGIKYSANNTN	7-15	GTGGIKYS	74-82
Loop 4	NERD(D/K)KXGXXGS(I/T)K	25-30	ERD(D/K)KXGXXGS(I/T)K	72-85
Loop 5	YKSG(A/S)VNKK	12-20	YKSGAVNKK	69-73
Loop 6	T(D/G)NV	15-20	T(D/G)NV	74
			NVKEK	73-76
Loop 7	KDKAY	10-15	KAYK	68
Loop 8	NK(D/N)S(D/N)NXKVTD(K/Q)A	25-35	KV(T/Y)DQAL	74-83
			(D/N)S(D/N)NXKVT	83-84
Moderately virulent				
Loop 1	(L/K)G(K/Q)SSTXGHTXLKNN(S/G)	20-25	LKNN(S/G)	75-77
Loop 2	DSXS(E/K)NA(A/E)EGWG	14-20	DSXS(E/K)NA(A/E)EGWG[d]	67-74
			AGEWGDVK[d]	74-76
Loop 3	GTGGIKYSYSANNT	13-15	GTGGIKYSYS	77-81
	YTYEVEEP[e]	20	YTYEVEEP[e]	70
	GTGGIKYTYKVD[f]	10	(D/S)SDSA	72-78
	(D/S)SDSA	5-20	AGFDK[g]	73
			STGIRI	76
Loop 4	NERD(D/K)KXGXXGS(I/T)K	25-32	NERD(D/K)KXGXXGS(I/T)K	72-81
Loop 5	DDYKSG(A/S)VNKK	12-20	DYKSG(A/S)	68-71
	FVQ(A/T)NGTS[f]	17	(A/S)VNKK[g]	71
			FVQ(A/T)NGTS[f]	80
			GGKSTD[e]	80
Loop 6	KT(D/G)(D/N)VK	15-17	(D/G)(D/N)VK	71-75
Loop 7	KDKAYKA	15-18	KDKAYKA[h]	65-67
	KVEDFK(A/V)TE[e,f]	15	KVED	74-75
Loop 8	NK(D/N)S(D/N)NXKVTD(K/Q)A	20-35	K(D/N)S(D/N)NXKVTD(K/Q)A	83
			KKVTDQAL	75-80
			K(D/N)S(D/N)N[i]	75

Table 3.6. (continued)

	Antigenic sequence[a]	Net votes[b]	B-cell epitope[a]	Score[c]
Avirulent				
Loop 1	(K/E)G(K/Q)SSTDGHTNLKNNS	24-30	LKNNS	75-76
Loop 2	GSGSKNAAKWGDVT	12-16	AAKWGDVT	69-76
Loop 3	GTGGIKYTYKVEDESITVNNTQGT	10-20	GFDKVYGVGTGGIK	73
	LTQSSDSA	7	YTYKVEDESITVNNTQGT	81-82
	QAGFDVK	7-10	QSSDSA	76
Loop 4	NERE(D/K)ADVKVDS(I/T)KS	10-32	NERE(D/K)ADVKVDS(I/T)KS	71-81
Loop 5	DYKSGSV(Q/K)	10-22	DYKSG(S/A)VQ	71-85
	DYKSG(A/S)VNKKDK[k]	15		
	LKGKFVQANGTS[l]	5-25[j]		
	SFN	5		
Loop 6	(Y/V)KTDDVKEK	6-12	TDDVKEK	73-75
Loop 7	KV(E/K)(D/A)(Y/F)KA	12-20	KV(E/K)(D/A)(Y/F)	74-75
	KDKAY[k]	12	DKAY[k]	67
Loop 8	NKDSDNNKVTD	17-30[m]	KDSDNNKVT	74-83

[a]Consensus sequence: X denotes presence or absence of any amino acid

[b]Determined by ANTIGENpro

[c]Determined by COBEpro (in percent)

[d]N/A for strain SW140

[e]Strain C5

[f]Strain SW124

[g]Strain 84-15995

[h]N/A for 84-15995

[i]Strain SW140

[j]Strain H465 has high scoring antigenic propensity: 25 net votes

[k]Strain 174

[l]Absent in strain 174

[m]Strain 174 has high scoring antigenic propensity: 30 net votes

Figures

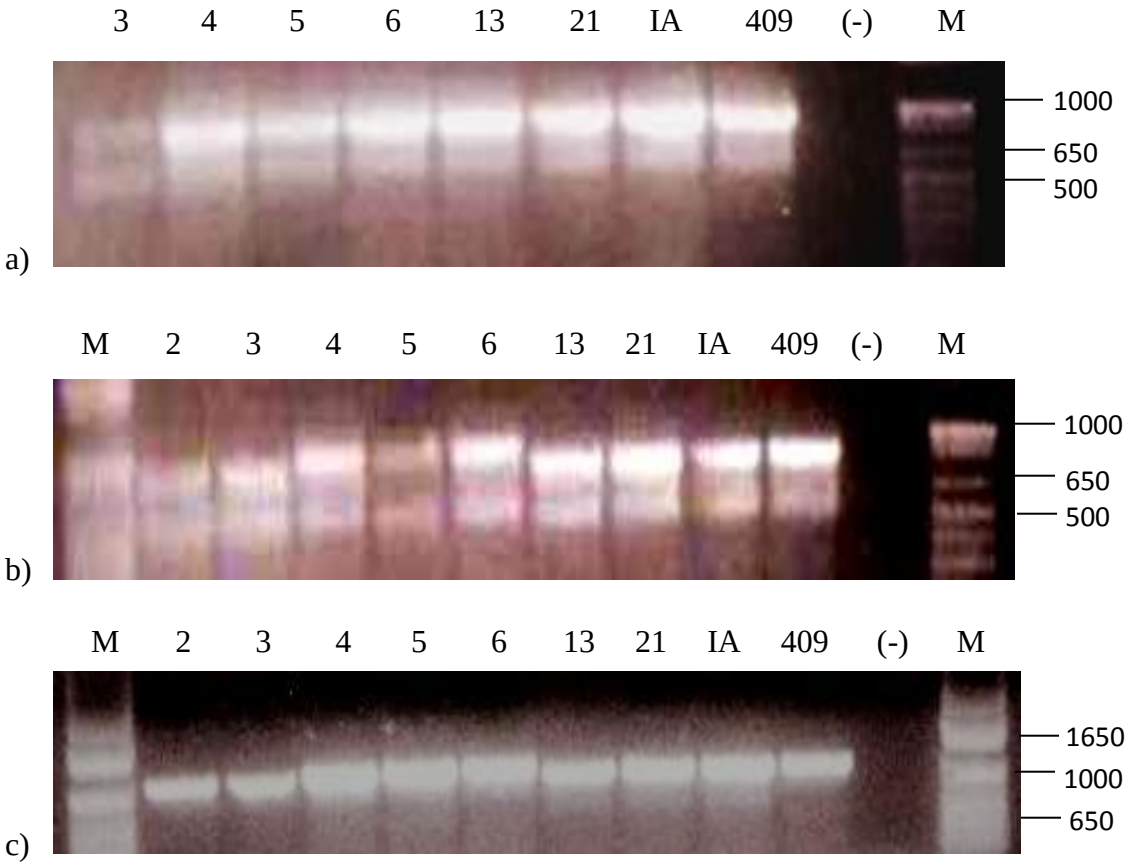

Figure 3.1. PCR analysis of reference and field strains. Analysis of PCR amplification on 1% agarose gel indicates two amplicons using P5 F2, R2 primers for OMP P5 (a) and P2 F2, R2 primers (b) and P2 F4, R4 (c) for OMP P2. Primers are described in Table 3.1. HP2 (2), HP3 (3), HP4 (4), HP5 (5) HP6 (6), HP13 (13), HPIA84-29755 (IA), HP2170B (21), HP409KL (40), negative control (-) and nucleotide marker (M) are shown. Standard markers are in base pairs.

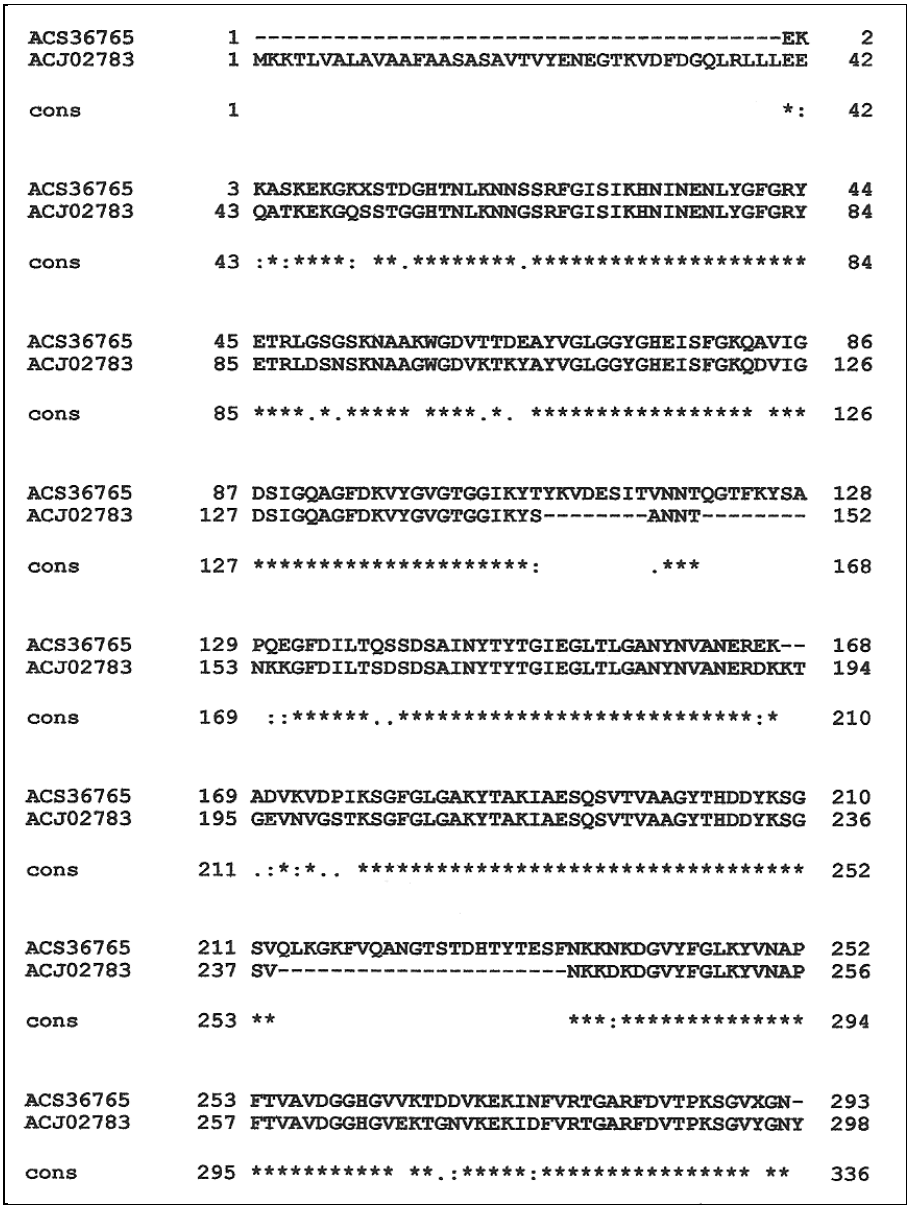

Figure 3.2. Sequence alignment of OMP P2 of Nagasaki (SV5). Both the extended and non-extended forms of P2 protein have been sequenced. ACS36765 corresponds to the extended form and ACJ0278 corresponds to the non-extended form of P2. Extensions exist for the predicted loop 3 and loop 5 regions. Conserved regions are noted underneath the sequence alignment (*).

aapqantfyv gakagwatfh ndinqlnsky kndaryatsa ngyvinrnsv tygvfggyqi
idnlavelgy dyfgrvrgnk qefrafkhsa hgthlslkps yevlngldvy gkvgaalvrn
dykrysqtag vqtqkahnlk tslvlgagve yailpelafr veyqwlsnvg nftkaeaken
rratynyspd shsvtagisy rfgqgaapva aapevvtknf afssdvlfdf gkanlkpaaa
qtldavhtei vnlglanpav qvngytdrig kdaanltlsq kraetvanyi vskgvnpanv
tavgygeanp vtgntcdavk grkalitcla pdrrveiqvq gskevsm

Region	Sequence
OMP P5 Loop 1	tfhndinqlnskykndaryatsangyvinrns
OMP P5 Loop 2	fgrvrgnkqefrafkhs
OMP P5 Loop 3	lvrndykrysqtagvqtqkahnlktsl
OMP P5 Loop 4	lsnvgnftkaeakenrratynyspdsh

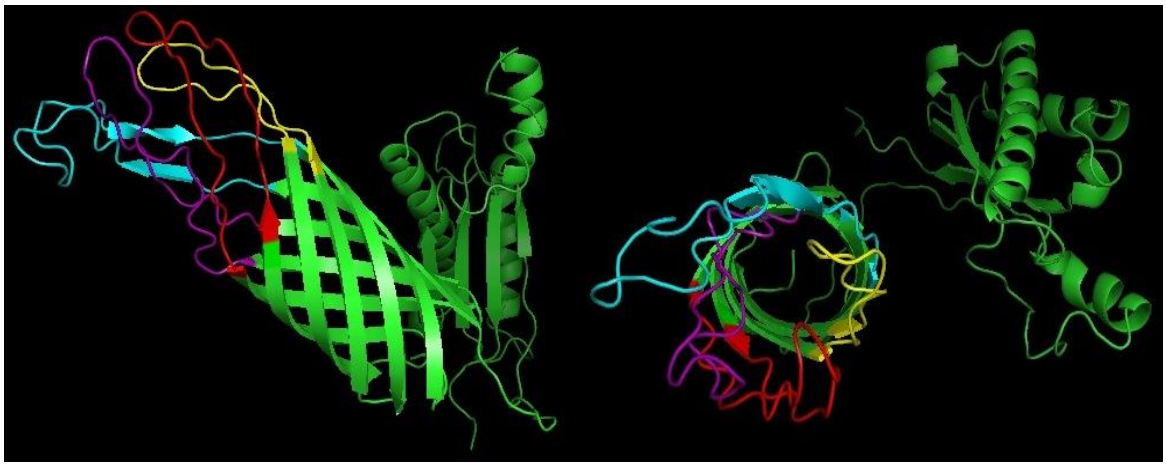

Figure 3.3. Model of 84-29755 OMP P5. The protein sequence (Accession: EDS23759) is shown with predicted surface exposed regions shown in color. A side view (left) and down the β-barrel view (right) are shown.

aapqantfyv gakagwatfh ndinqlnsky kndaryatsa ngyvinrnsv tygvfggyqi
idnlavelgy dyfgrvrgnk qefrafkhsa hgthlslkps yevlngldvy gkvgaalvrn
dykrysqtag vqtqkahnlk tslvlgagve yailpelafr veyqwlsnvg nftkaeaken
rratynyspd shsvtagisy rfgqqgaapva aapevvtknf afssdvlfdf gkanlkpaaa
qtldavhtei vnlglanpav qvngytdrig kdaanltlsq kraetvanyi vskgvnpanv
tavgygeanp vtgntcdavk grkalitcla pdrrveiqvq gskevsm

Region	Sequence
OMP P5 Loop 1	tfhndinqlnskykndaryatsangyvinrns
OMP P5 Loop 2	fgrvrgnkqefrafkhs
OMP P5 Loop 3	lvrndykrysqtagvqtqkahnlktsl
OMP P5 Loop 4	lsnvgnftkaeakenrratynyspdsh

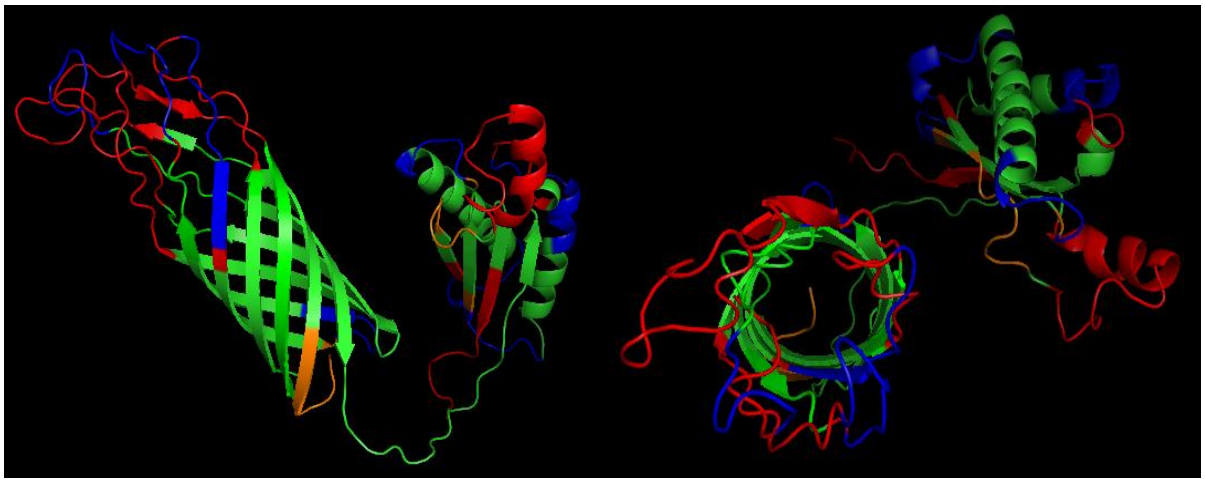

Figure 3.4. Predicted antigenic sites and continuous B-cell epitopes of 84-29755 OMP P5. Antigenic sites are highlighted in orange (moderate < 5 net votes) and red (high >5 net votes). Predicted continuous B-cell epitopes (>70% probability) are shown in blue. A side view (left) and down the β-barrel view (right) are shown.

mkktlvalav aafaasasav tvyenegtkv dfdgqlrlll eeqatkekgq sstgghtnlk
nngsrfgisi khninenlyg fgryetrlds nsknaagwgd vktkyayvgl ggygheisfg
kqavigdsig qagfdkvygv gtggikysan ntnkkgfdil tsdsdsainy tytgiegltl
ganynvaner dkktgevnvg stksgfglga kytakiaesq svtvaagyth ddyksgsvnk
kdkdgvyfgl kyvnapftva vdgghgvekt gnvkekidfv rtgarfdvtp ksgvygnysy
gtykdkayka tahqfmlgad yklhkqvvtf vegrliknkd snnkkvtdqa lgvglrvlw

Region	Sequence
OMP P2 Loop 1	atkekgqsstgghtnlknn
OMP P2 Loop 2	dsnsknaagwgdvk
OMP P2 Loop 3	fgkqavigdsigqagfdkvygvgtggikysanntnkkgfdiltsdsdsa
OMP P2 Loop 4	nvanerdkktgevnvgstksg
OMP P2 Loop 5	ddyksgsvnkkdk
OMP P2 Loop 6	tgnvkek
OMP P2 Loop 7	kdkayka
OMP P2 Loop 8	knkdsnnkkvtd

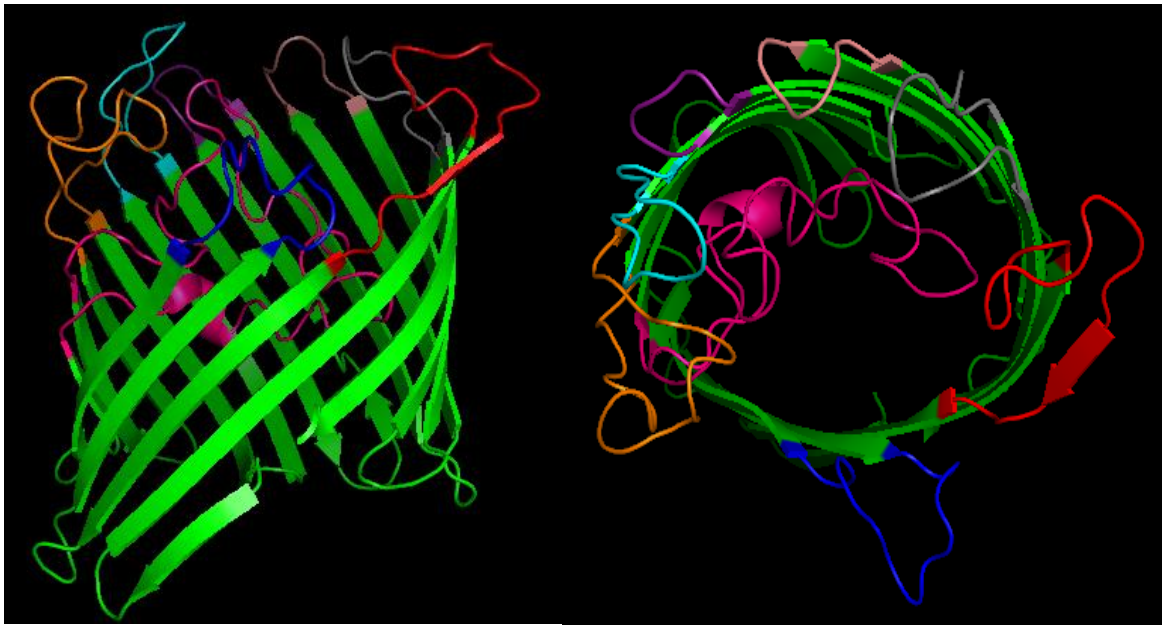

Figure 3.5. Model of 84-29755 (SV5) OMP P2. The protein sequence (Accession: ACJ02809) is shown with predicted surface exposed regions shown in color. A side view (left) and down the β-barrel view (right) are shown.

mkktlvalav aafaasasav tvyenegtkv dfdgqlrlll eeqatkekgq sstgghtnlk
nngsrfgisi khninenlyg fgryetrlds nsknaagwgd vktkyayvgl ggygheisfg
kqavigdsig qagfdkvygv gtggikysan ntnkkgfdil tsdsdsainy tytgieqltl
ganynvaner dkktgevnvg stksgfglga kytakiaesq svtvaagyth ddyksgsvnk
kdkdgvyfgl kyvnapftva vdgghgvekt gnvkekidfv rtgarfdvtp ksgvygnysy
gtykdkayka tahqfmlgad yklhkqvvtf vegrliknkd snnkkvtdqa lgvglrvlw

Region	Sequence
OMP P2 Loop 1	atkekgqsstgghtnlknn
OMP P2 Loop 2	dsnsknaagwgdvk
OMP P2 Loop 3	fgkqavigdsigqagfdkvygvgtggikysanntnkkgfdiltsdsdsa
OMP P2 Loop 4	nvanerdkktgevnvgstksg
OMP P2 Loop 5	ddyksgsvnkkdk
OMP P2 Loop 6	tgnvkek
OMP P2 Loop 7	kdkayka
OMP P2 Loop 8	knkdsnnkkvtd

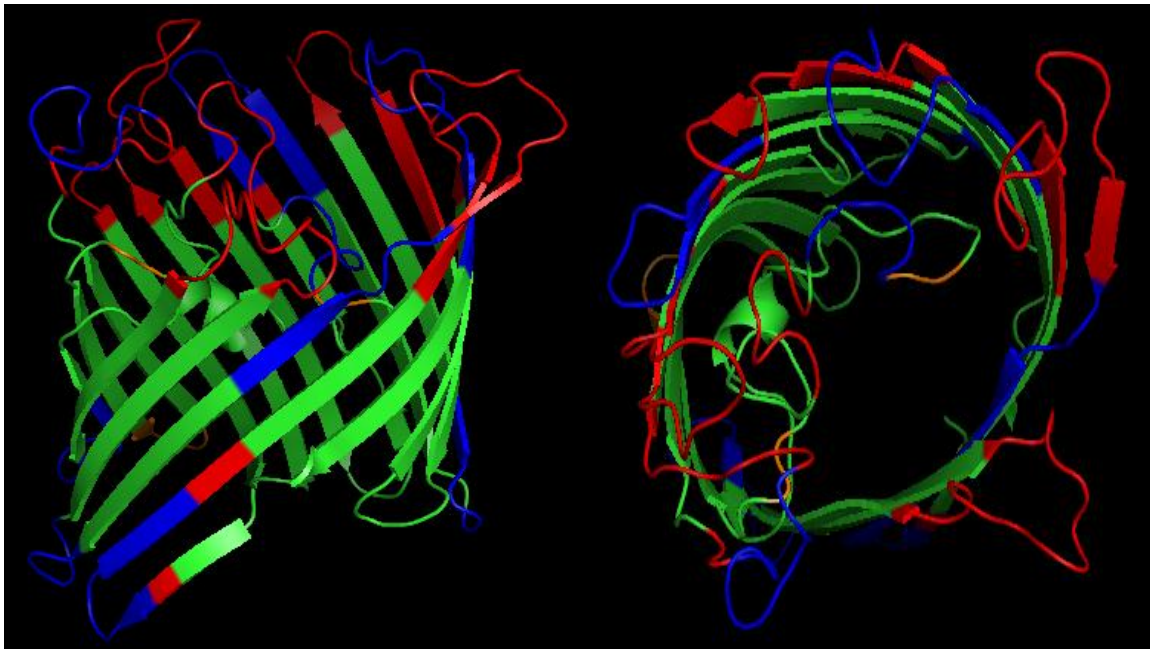

Figure 3.6. Predicted antigenic sites and continuous B-cell epitopes of 84-29755 (SV5) OMP P2. Antigenic sites are highlighted in orange (moderate < 5 net votes) and red (high >5 net votes). Predicted continuous B-cell epitopes (>70% probability) are shown in blue. A side view (left) and down the β-barrel view (right) are shown.

mkktlvalav atfaasasav tvyenegtkv dfdgqlrlll ekqaskekgk sstdghtnlk
nnssrfgisi khninenlyg fgryetrlgs gsknaakwgd vttdeayvgl ggygheisfg
kqavigdsig qagfdkvygv gtggikytye veesitvdnk qgtfkysaaq egfdiltqss
dsainytytg iegltlgany nvanerekad vkvdsiksgf glgakytaki aesqsvtvaa
gythddyksg svklkgkfve aggkstdhty tkkpfnkkdk dgvyfglkyv napftvavdg
ghgvvktddv kekinfvrtg arfdvtpksg vygnysygty kvedfkvtah qfmlgadykl
hkqvvtfveg rliknkdsdn nkvtdkalgv glrvlw

Region	Sequence
OMP P2 Loop 1	kqaskekgksstdghtnlknns
OMP P2 Loop 2	gsgsknaakwgdv
OMP P2 Loop 3	kqavigdsigqagfdkvygvgtggikytyeveesitvdnkqgtfkysaaqegfdiltqsssa
OMP P2 Loop 4	nvanerekadvkvdsik
OMP P2 Loop 5	ddyksgsvklkgkfveaggkstdhtytkkpfnk
OMP P2 Loop 6	ktddvkek
OMP P2 Loop 7	kvedfkvta
OMP P2 Loop 8	knkdsdnnkvtdkal

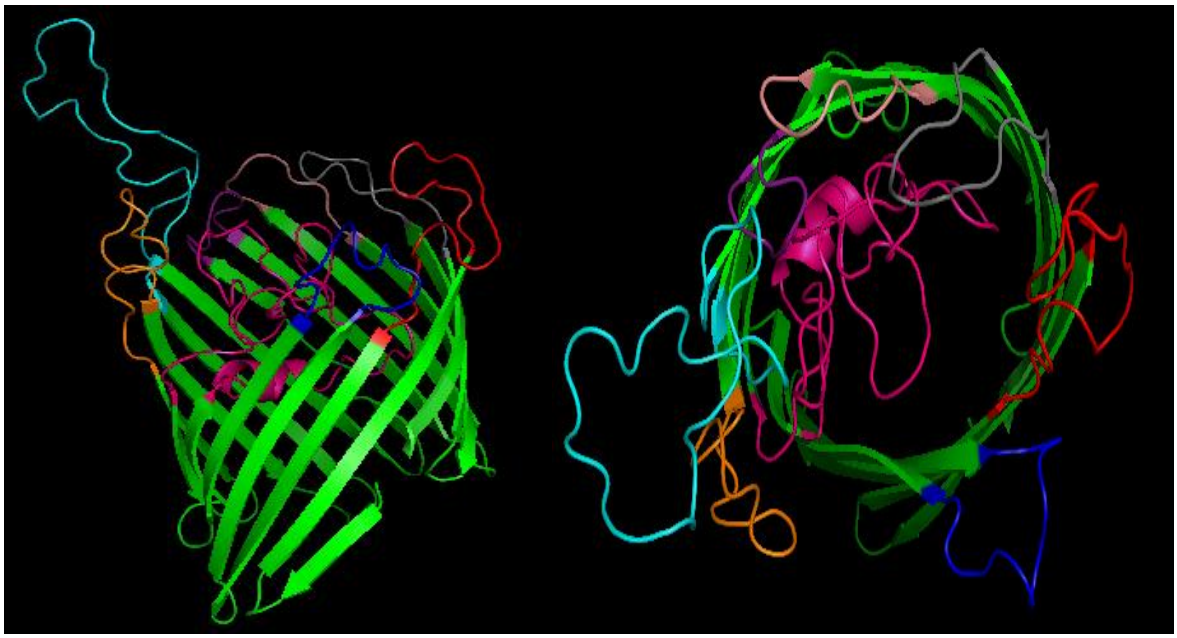

Figure 3.7. Model of SW114 (SV3) OMP P2. The protein sequence (Accession: ACJ02782) is shown with predicted surface exposed regions shown in color. A side view (left) and down the β-barrel view (right) are shown.

mkktlvalav atfaasasav tvyenegtkv dfdgqlrlll ekqaskekgk sstdghtnlk
nnssrfgisi khninenlyg fgryetrlgs gsknaakwgd vttdeayvgl ggygheisfg
kqavigdsig qagfdkvygv gtggikytye veesitvdnk qgtfkysaaq egfdiltqss
dsainytytg iegltlgany nvanerekad vkvdsiksgf glgakytaki aesqsvtvaa
gythddyksg svklkgkfve aggkstdhty tkkpfnkkdk dgvyfglkyv napftvavdg
ghgvvktddv kekinfvrtg arfdvtpksg vygnysygty kvedfkvtah qfmlgadykl
hkqvvtfveg rliknkdsdn nkvtdkalgv glrvlw

Region	Sequence
OMP P2 Loop 1	kqaskekgksstdghtnlknns
OMP P2 Loop 2	gsgsknaakwgdv
OMP P2 Loop 3	kqavigdsigqagfdkvygvgtggikytyeveesitvdnkqgtfkysaaqegfdiltqsssa
OMP P2 Loop 4	nvanerekadvkvdsik
OMP P2 Loop 5	ddyksgsvklkgkfveaggkstdhtytkkpfnk
OMP P2 Loop 6	ktddvkek
OMP P2 Loop 7	kvedfkvta
OMP P2 Loop 8	knkdsdnnkvtdkal

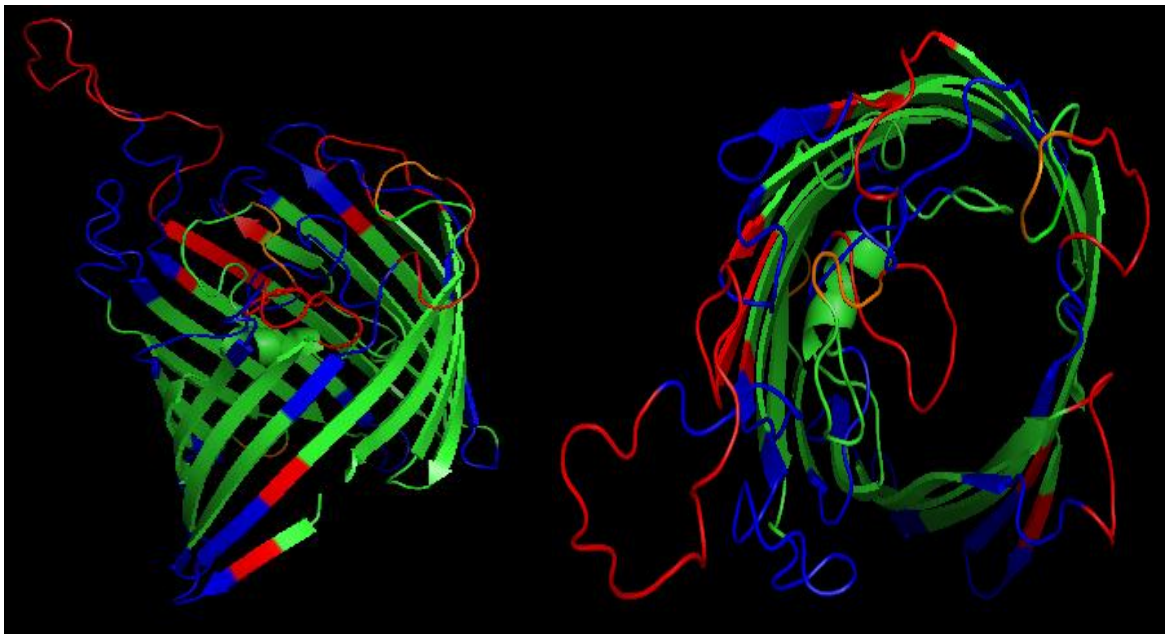

Figure 3.8. Predicted antigenic sites and continuous B-cell epitopes of SW114 (SV3) OMP P2. Antigenic sites are highlighted in orange (moderate < 5 net votes) and red (high >5 net votes). Predicted continuous B-cell epitopes (>70% probability) are shown in blue. A side view (left) and down the β-barrel view (right) are shown.

Supplemental Information

SDS-PAGE and immunoblotting. Samples were boiled for 5 minutes in a SDS treatment buffer consisting of 62.5 mM Tris, 10% glycerol, 5% 2-mercaptoethanol, 1 % SDS, and 0.001% bromophenol blue prior to electrophoresis through 4-12% gradient SDS-polyacrylamide gels (InVitrogen, Carlsbad, CA). Gels were stained with Coomassie Brilliant Blue R250 or transferred electophoretically to 0.45-µm nitrocellulose (Schleicher and Schuell, Keene, NH) or polyvinyledene diflouride (PVDF) (Millipore, Billerica, MA) for immunoblotting. Immunoblots were blocked with 0.25% fish gelatin in wash buffer consisting of 1.5 mM KH_2PO_4, 20 mM Na_2HPO_4, 125 mM NaCl, 3 mM KCl, 0.05% Tween-20 (pH 7.2). For the blots aimed at detecting P5, the blocked membranes were incubated with 1:5,000 dilutions of anti-P5 monoclonal antibody (4BF8), and 1:5,000 dilutions of rabbit anti-mouse IgG horseradish peroxidase-labeled (Jackson ImmunoResearch, West Grove, PA) sequentially. For the blots aimed at detecting recombinant protein expression, the blocked membranes were incubated with 1:5,000 dilutions of horseradish peroxidase labeled anti-V5 monoclonal antibody (InVitrogen, Carlsbad, CA). Blots were developed with 3,3',5, 5'-tetramethylbenzidine (TMB) (Kirkegaarde and Perry Labs, Gaithersburg, MD) as the substrate. The cross reactive monoclonal antibody (4BF8) used here has been described earlier. It has been shown to react with several variants of P5 suggesting that it does not react with the variable surface exposed loops.

Protein sequencing. Following SDS-PAGE, gels were blotted electrophoretically to PVDF (Millipore, Billerica, MA) and stained with Coomassie Brilliant Blue R250. Bands were excised from the PVDF and sequenced with a model 494 Procise protein/peptide sequencer (Applied Biosystems, Foster City, CA) at the Iowa State University Protein Facility.

Sequence identities were determined by using the BLAST server of the National Center for Biotechnology Information.

Supplemental Table and Figures

Supplemental Table S3.1. N-terminal sequences and identity of bands from Figure S3.1

Band (Figure S3.1)	MW (kDa)	Source	Sequence	Identity[a]
a	32	*H. influenzae* d1	APQENTFYAGV	*H. influenzae* P5[b]
b	48	*H. influenzae* d1	APQENTFYA	*H. influenzae* P5[b]
c	55	*H. influenzae* d1	AVVYNNEGTKV	*H. influenzae* P2[c]
d	32	*H.parasuis* SV2 (virulent)	APQANSFYVGAKAG	*H. parasuis* P5[d]
e	48	*H.parasuis* SV2 (virulent)	ATVYENEGTKV	*H. parasuis* P2[e]
f	32	*H.parasuis* SV3 (avirulent)	APQANSFYVGAKAGD	*H. parasuis* P5[d]
g	55	*H.parasuis* SV3 (avirulent)	ATVYENEGTKV	*H. parasuis* P2[e]

[a]BLAST server of the National Center for Biotechnology Information (Altshul et al., 1997)

[b] Accession number AAC22819

[c] Accession number AAA24995

[d]Accession number ADJ38698

[e]Accession number ADJ38729

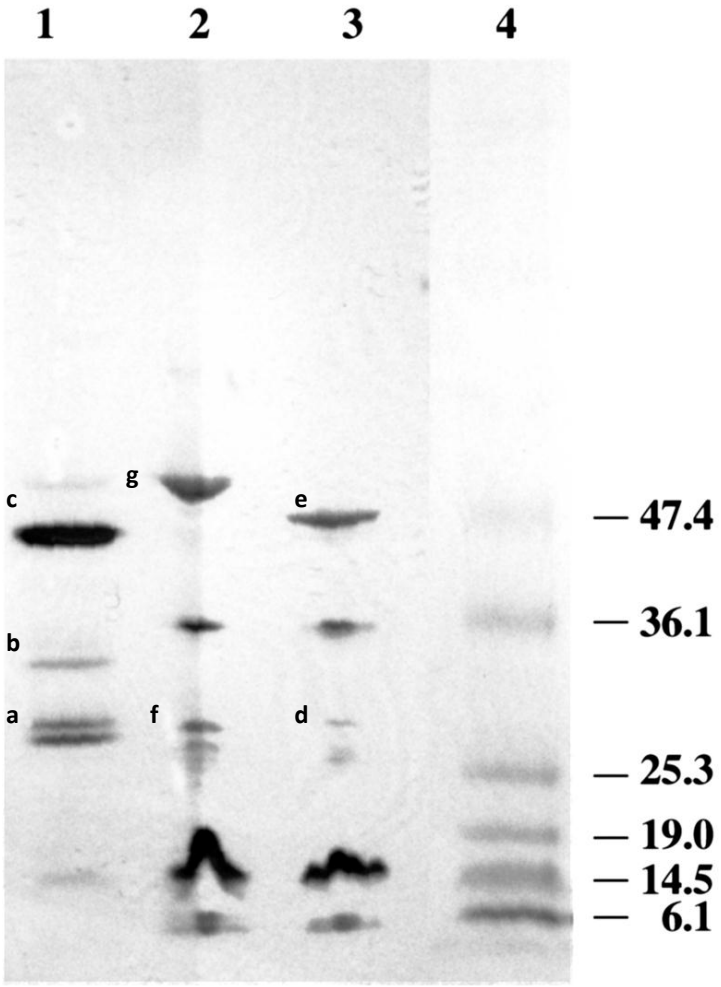

Supplemental Figure S3.1. Anti-P5 (4BF8) immunoblot of *H. influenzae* and two *H. parasuis* reference strains. Lanes: 1, *H. influenzae* d1 (P5 positive strain); 2, *H. parasuis* serotype 3, strain SW114 (avirulent); 3, *H. parasuis* serotype 2, strain SW140 (virulent). Whole cell proteins were separated with a 4-12% SDS-PAGE gel, blotted to nitrocellulose, and probed with anti-P5 monoclonal antibody (4BF8) as described in the text. Molecular weights of the standards are indicated in kilodaltons.

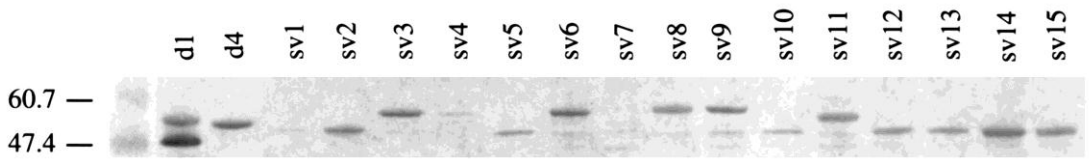

Supplemental Figure S3.2. Anti-P5 (4BF8) immunoblot of *H. influenzae* strains d1 and d4 and all 15 *H. parasuis* reference strains (SV1-SV15) focusing on the 47.4 to 60.7 kDa molecular weight range. Whole cell proteins were separated with a 4-12% SDS-PAGE gel, blotted to PVDF, and probed with anti-P5 monoclonal antibody (4BF8) as described in the text.

aapqansfyv gakagwatfh ndinqlnsky endaryatsa ngyginrnsv tygvfggyqi
idnlavelgy dyfgrvrgke qefrafkhsa hgthlslkps yevlngldvy gkvgaalvrn
dykryfqtre pvkshnlkts livgagveya ilpelafrve yqwlsrvgna nkaaqkrgdt
amfgpgstys pdahsvsagi syrfgqgaap apaapevvtk nfafssdvlf dfgkanlkpa
aaqtldaaha eivnlglanp avqvngytdr igkdaanltl sqkraetvan yivskgvnpa
nvtavgygea npvtgntcda vkgrkalivc lapdrrveiq vqgskevsm

Region	Sequence
OMP P5 Loop 1	tfhndinqlnskykndaryatsangyvinrns
OMP P5 Loop 2	grvrgnkqefrafkhs
OMP P5 Loop 3	dykryfqtrepvkshnlk
OMP P5 Loop 4	wlsrvgnankaaqkrgdtamfgpgstyspdah

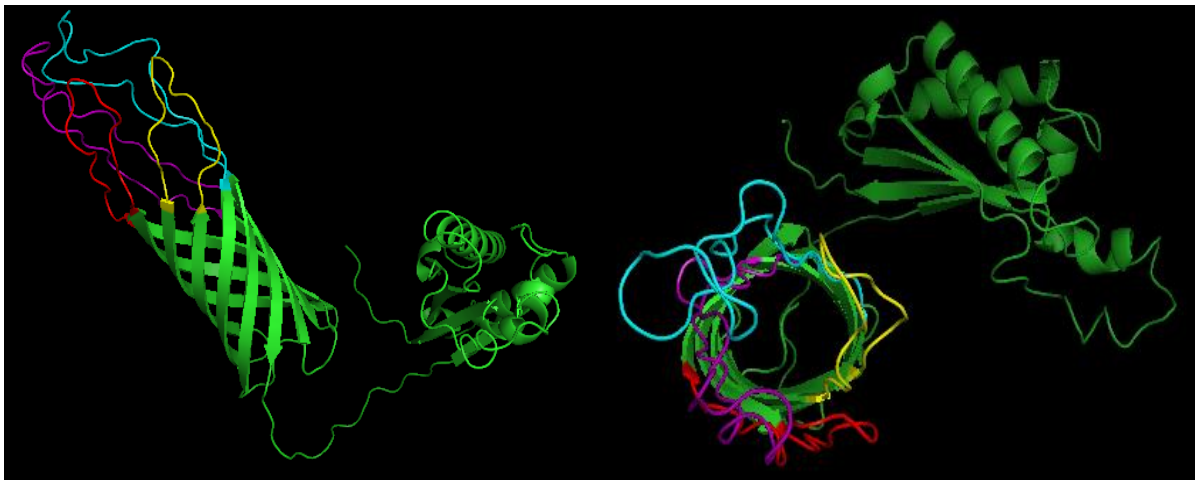

Supplemental Figure S3.3. Model of No.4 (SV1) OMP P5. The protein sequence (Accession: ACJ02815) is shown with predicted surface exposed regions shown in color. A side view (left) and down the β-barrel view (right) are shown.

aapqadsfyv gakagwatfh ndinqlnfky kndaryatsa ngyginrnsv tygvfggyqi
idnlavelgy dyfgrvrgnk qefrefkhsa hgthlslkps yevlsgldvy gkvgaalvrn
dykryfqtre pvkshnlkts livgagveya ilpelafrve yqwlsnvgnf tkaemkenrr
atynyspdsh svtagisyrf gqgaapvaaa pevvtknfaf ssdvlfdfgk anlkpaaaqt
ldaahteivn lglanpavqv ngytdrigkd aanltlsqkr aetvanyivs kgvnpanvta
vgygeanpvt gntcdavkgr kalivclapd rrveiqvqgs kevsm

Region	Sequence
OMP P5 Loop 1	tfhndinqlnskykndaryatsangyvinrns
OMP P5 Loop 2	rvrgnkqefrefkhsa
OMP P5 Loop 3	vrndykryfqtrepvkshnlk
OMP P5 Loop 4	lsnvgnftkaemkenrratynyspds

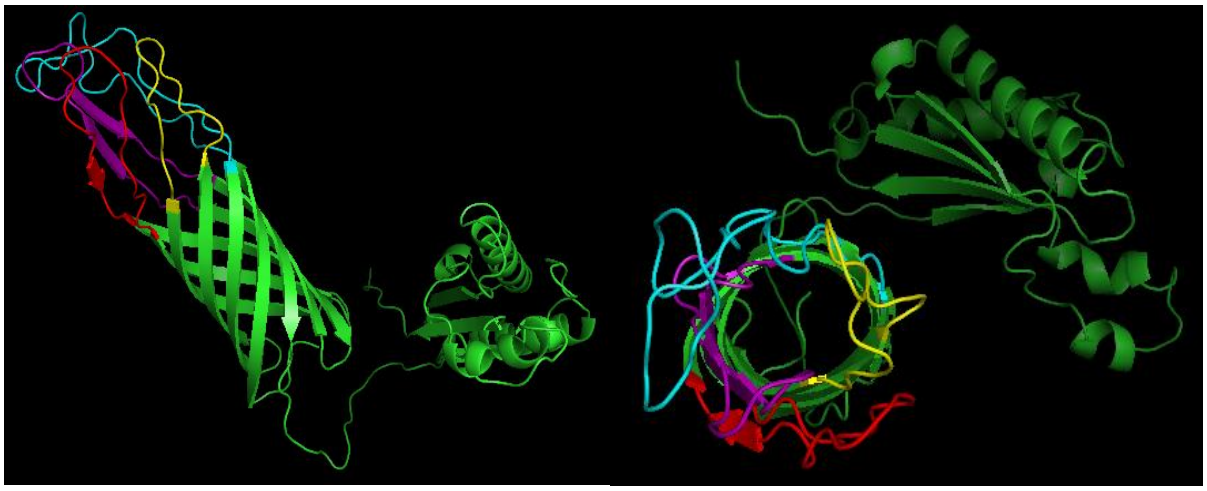

Supplemental Figure S3.4. Model of SW140 (SV2) OMP P5. The protein sequence (Accession: ACJ02816) is shown with predicted surface exposed regions shown in color. A side view (left) and down the β-barrel view (right) are shown.

aapqansfyv gakagwatfh ndinqlnsky endaryatsa ngyginrnsv tygvfggyqi
idnlavelgy dyfgrvrgnk qefrafkhsa hgthlslkps yevlngldvy gkvgaalvrn
dykryfqtre pvkshnlkts livgagveya ilpelafrve yqwlsnvgnf tkaevkenrr
atynyspdsh svtagisyrf gqgaapvaaa pevvtknfaf ssdvlfdfgk anlkpasaqt
ldaahteivn lglanpavqv ngytdrigkd aanltlsqkr aetvanyivs kgvnpanvta
vgygeanpvt gntcdavkgr kalivclapd rrveiqvqgs kevsm

Region	Sequence
OMP P5 Loop 1	tfhndinqlnskyendaryatsangyginrn
OMP P5 Loop 2	grvrgnkqefrafkhs
OMP P5 Loop 3	dykryfqtrepvkshnlk
OMP P5 Loop 4	wlsnvgnftkaevkenrratynyspdsh

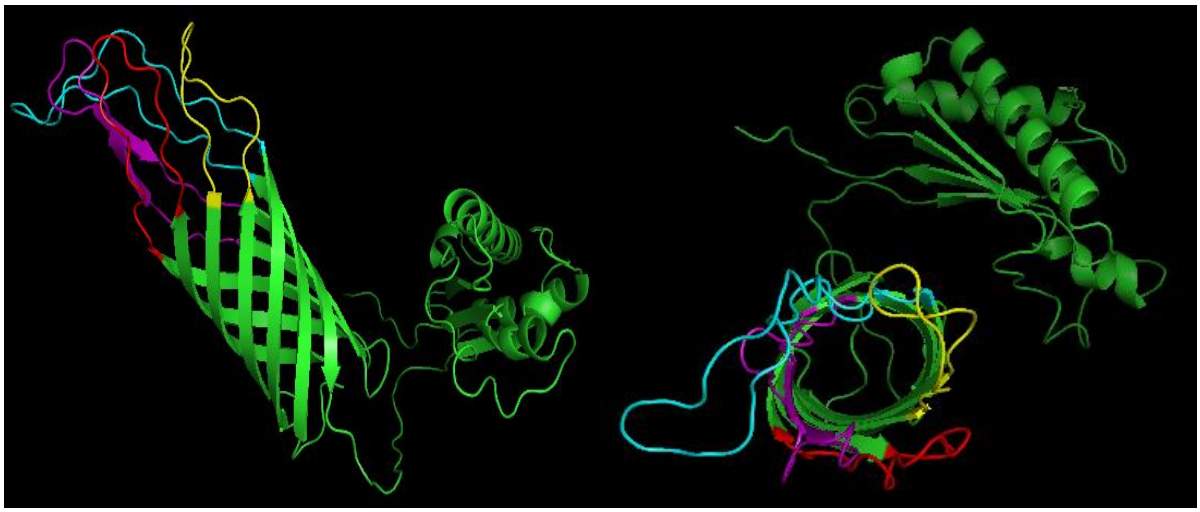

Supplemental Figure S3.5. Model of SW114 (SV3) OMP P5. The protein sequence (Accession: ACJ02817) is shown with predicted surface exposed regions shown in color. A side view (left) and down the β-barrel view (right) are shown.

aapqansfyv gakagwatfh ndinqlnsky kndaryatsa nryginrnsv tygvfggyqi
idnlavelgy dyfgrvrgnk qefrefkhsa hgthlslkps yevlsgldvy gkvgaalvrn
dykryfqtre pvkshnlkts livgagveya ilpelafrve yqwlsnvgnf tkaevkenrr
atynyspdsh svtagisyrf gqgaapvaaa pevvtknfaf ssdvlfdfgk anlkpaaaqt
ldaahteivn lglenpavqv ngytdrigkd aanltlsqkr aetvanyivs kgvnpanvta
vgygeanpvt gntcdavkgr kalivclapd rrveiqvqgs kevsm

Region	Sequence
OMP P5 Loop 1	tfhndinqlnskykndaryatsanryginrns
OMP P5 Loop 2	grvrgnkqefrefkhsa
OMP P5 Loop 3	rndykryfqtrepvkshnlk
OMP P5 Loop 4	wlsnvgnftkaevkenrratynyspdsh

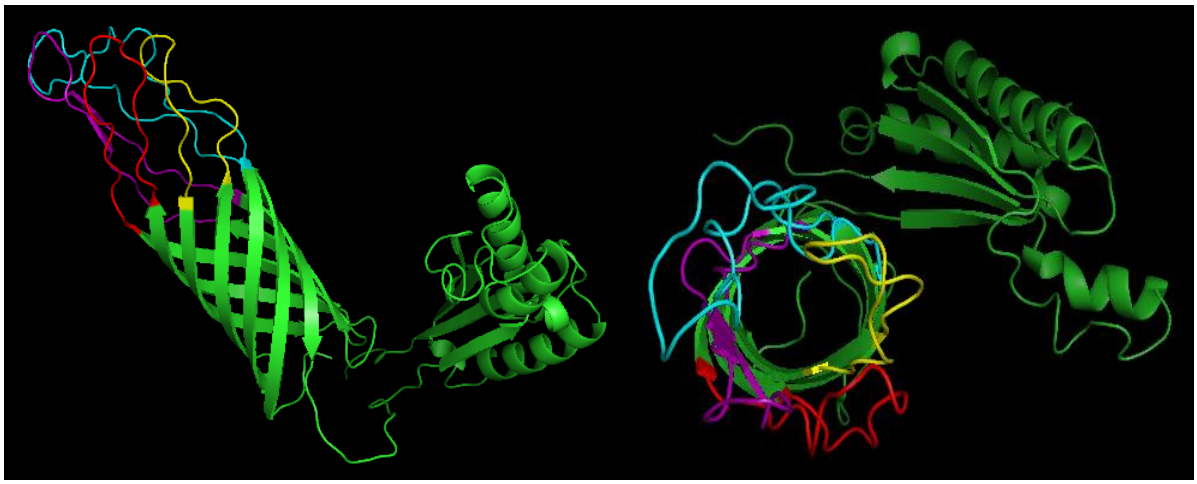

Supplemental Figure S3.6. Model of SW124 (SV4) OMP P5. The protein sequence (Accession: ACJ02818) is shown with predicted surface exposed regions shown in color. A side view (left) and down the β-barrel view (right) are shown.

aapqantfyv gakagwatfh ndinqlnsky kndaryatsa ngyvinrnsv tygvfggyqi
idnlavelgy dyfgrvrgnk qefrafkhsa hgthlslkps yevlngldvy gkvgaalvrn
dykrysqtag vqtqkahnlk tslvlgagve yailpelafr veyqwlsnvg nftkaeaken
rratynyspd shsvtagisy rfgqqgaapva aapevvtknf afssdvlfdf gkanlkpaaa
qtldavhtei vnlglanpav qvngytdrig kdaanltlsq kraetvanyi vskgvnpanv
tavgygeanp vtgntcdavk grkalitcla pdrrveiqvq gskevsm

Region	Sequence
OMP P5 Loop 1	tfhndinqlnskykndaryatsangyvinr
OMP P5 Loop 2	rvrgnkqefrafkh
OMP P5 Loop 3	ndykrysqtagvqtqkahnlk
OMP P5 Loop 4	lsnvgnftkaeakenrratynyspds

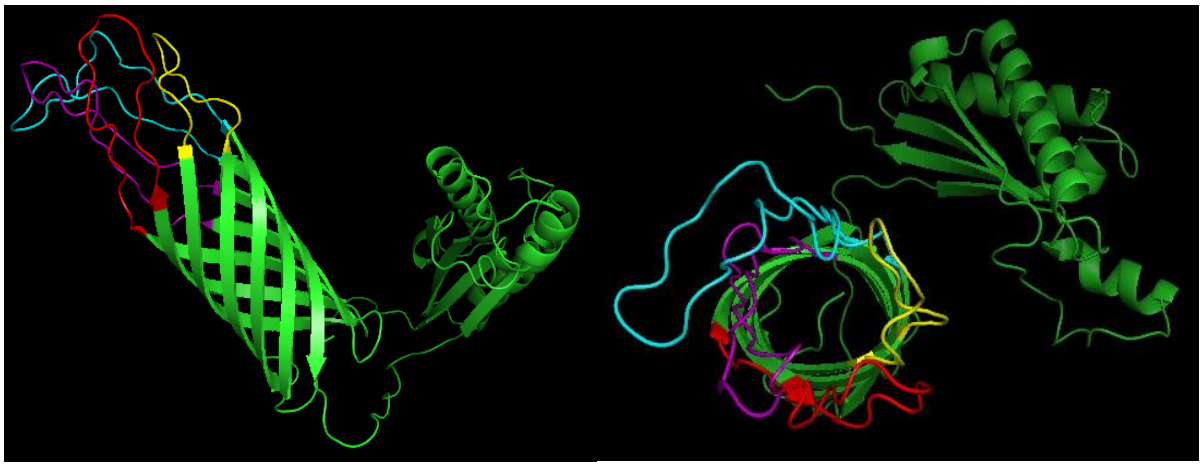

Supplemental Figure S3.7. Model of Nagasaki (SV5) OMP P5. The protein sequence (Accession: ACJ02819) is shown with predicted surface exposed regions shown in color. A side view (left) and down the β-barrel view (right) are shown.

aapqansfyv gakagwatfh ndinqlnsky endaryatsa ngyginrnsv tygvfggyqi
idnlavelgy dyfgrvrgke qefrafkhsa hgthlslkps yevlngldvy gkvgaalvrn
dykfydtedk ahnlktslll gagveyailp elafrveyqw lsrvgnanka aqkrgdtamf
gpgstyspda hsvsagisyr fgqgaapapa aapevvtknf afssdvlfdf gkanlkpaaa
qtldaahaei vnlglanpav qvngytdrig kdaanltlsq kraetvanyi vskgvnpanv
tavgygeanp vtgntcdavk grkalivcla pdrrveiqvq gskevsm

Region	Sequence
OMP P5 Loop 1	atfhndinqlnskyendaryatsangyginrns
OMP P5 Loop 2	rvrgkeqefrafkh
OMP P5 Loop 3	dykfydtedkahnlk
OMP P5 Loop 4	lsrvgnankaaqkrgdtamfgpgstyspda

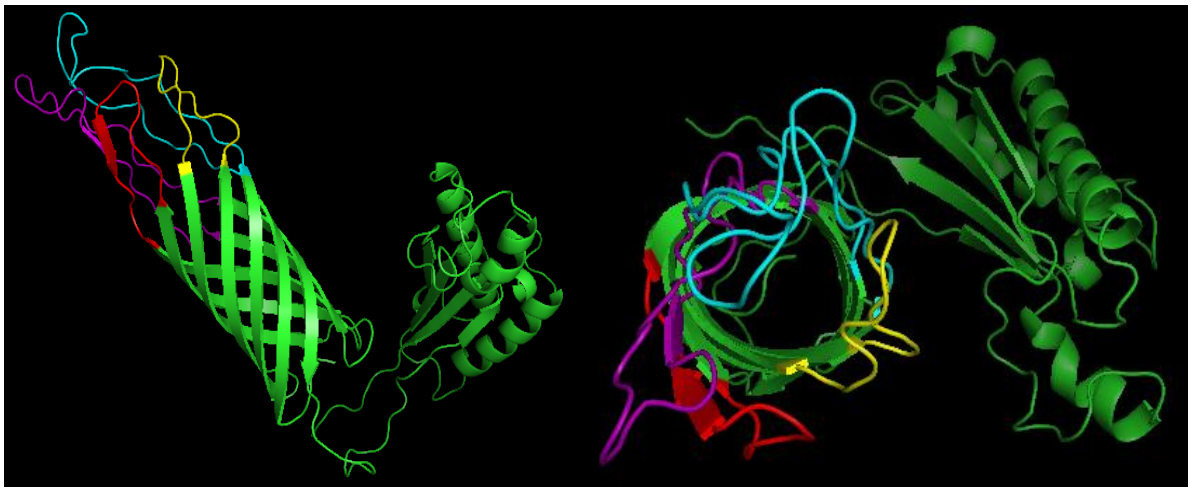

Supplemental Figure S3.8. Model of 131 (SV6) OMP P5. The protein sequence (Accession: ACJ02820) is shown with predicted surface exposed regions shown in color. A side view (left) and down the β-barrel view (right) are shown.

aapqansfyv gakagwatfh ndinqlnsky kndaryatsa ngyginrnsv tygvfggyqi
idnlavelgy dyfgrvrgnk qefrefkhsa hgthlslkps yevlsgldvy gkvgaalvrn
dykryfqtre pvkshnlkts livgagveya ilpelafrve yqwlsnvgnf tkaemkenrr
atynyspdsh svtagisyrf gqgaapvaaa pevvtknfaf ssdvlfdfgk anlkpasaqt
ldaahteivn lglanpavqv ngytdrigkd aanltlsqkr aetvanyivs kgvnpanvta
vgygeanpvt gntcdavkgr kalivclapd rrveiqvqgs kevsm

Region	Sequence
OMP P5 Loop 1	fhndinqlnskykndaryatsangyginrns
OMP P5 Loop 2	grvrgnkqefrefkhs
OMP P5 Loop 3	dykryfqtrepvkshnlk
OMP P5 Loop 4	lsnvgnftkaemkenrratynyspd

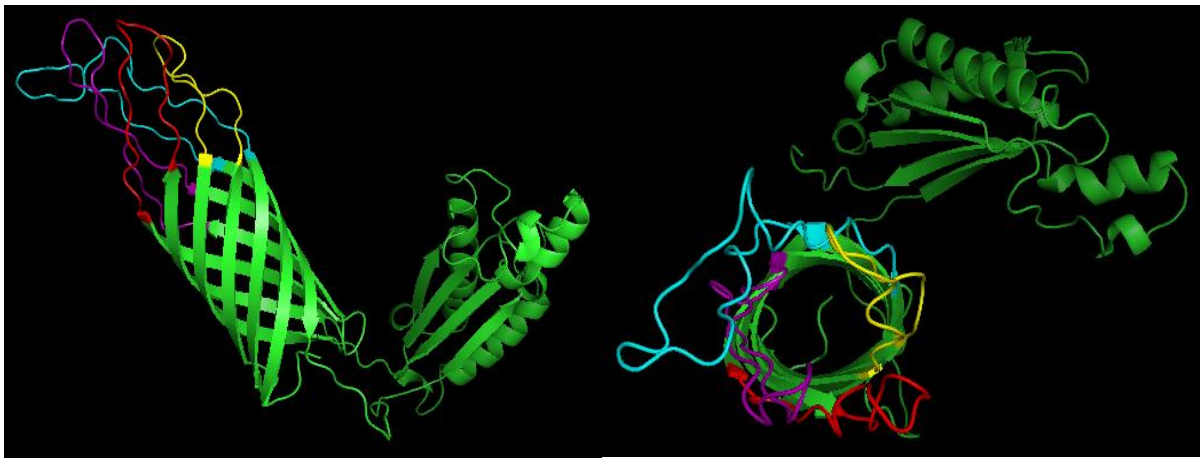

Supplemental Figure S3.9. Model of 174 (SV7) OMP P5. The protein sequence (Accession: ACJ02821) is shown with predicted surface exposed regions shown in color. A side view (left) and down the β-barrel view (right) are shown.

aapqansfyv gakagwatfh ndinqlnsky endaryatsa ngyginrnsv tygvfggyqi
idnlavelgy dyfgrvrgke qefrafkhsa hgthlslkps yevlngldvy gkvgaalvrn
dykfydtedk ahnlktslll gagveyailp elafrveyqw lsrvgnanka aqkrgdtamf
gpgstyspda hsvsagisyr fgqgaapapa aapevvtknf afssdvlfdf gkanlkpaaa
qtldaahaei vnlglanpav qvngytdrig kdaanltlsq kraetvanyi vskgvnpanv
tavgygeanp vtgntcdavk grkalivcla pdrrveiqvq gskevsm

Region	Sequence
OMP P5 Loop 1	atfhndinqlnskyendaryatsangyginrns
OMP P5 Loop 2	rvrgkeqefrafkh
OMP P5 Loop 3	dykfydtedkahnlk
OMP P5 Loop 4	lsrvgnankaaqkrgdtamfgpgstyspda

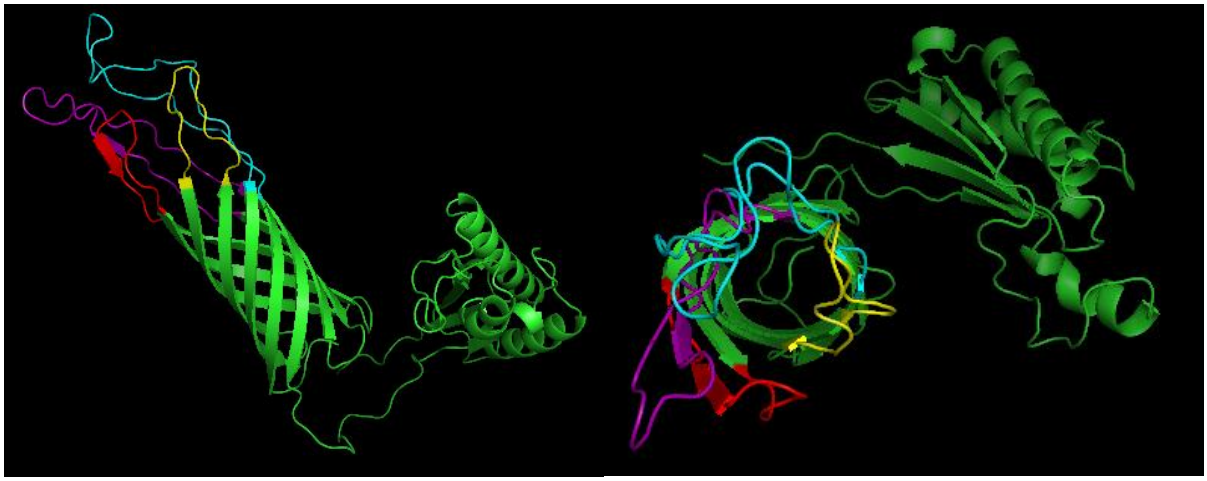

Supplemental Figure S3.10. Model of C5 (SV8) OMP P5. The protein sequence (Accession: ACJ02822) is shown with predicted surface exposed regions shown in color. A side view (left) and down the β-barrel view (right) are shown.

aapqadsfyv gakagwatfh ndinqlnfky kndaryatsa ngyginrnsv tygvfggyqi
idnlavelgy dyfgrvrgnk qefrefkhsa hgthlslkps yevlngldvy gkvgaalvrn
dykfydtedk ahnlktslll gagveyailp elafrveyqw lsrvgnanka aqkrgdtamf
gpgstyspda hsvsagisyr fgqgaapapa aapevvtknf afssdvlfdf gkanlkpaaa
qtldaahaei vnlglanpav qvngytdrig kdaanltlsq kraetvanyi vskgvnpanv
tavgygeanp vtgntcdavk grkalivcla pdrrveiqvq gskevsm

Region	Sequence
OMP P5 Loop 1	tfhndinqlnfkykndaryatsangyginrns
OMP P5 Loop 2	rvrgnkqefrefkh
OMP P5 Loop 3	dykfydtedkahnlk
OMP P5 Loop 4	wlsrvgnankaaqkrgdtamfgpgstyspdah

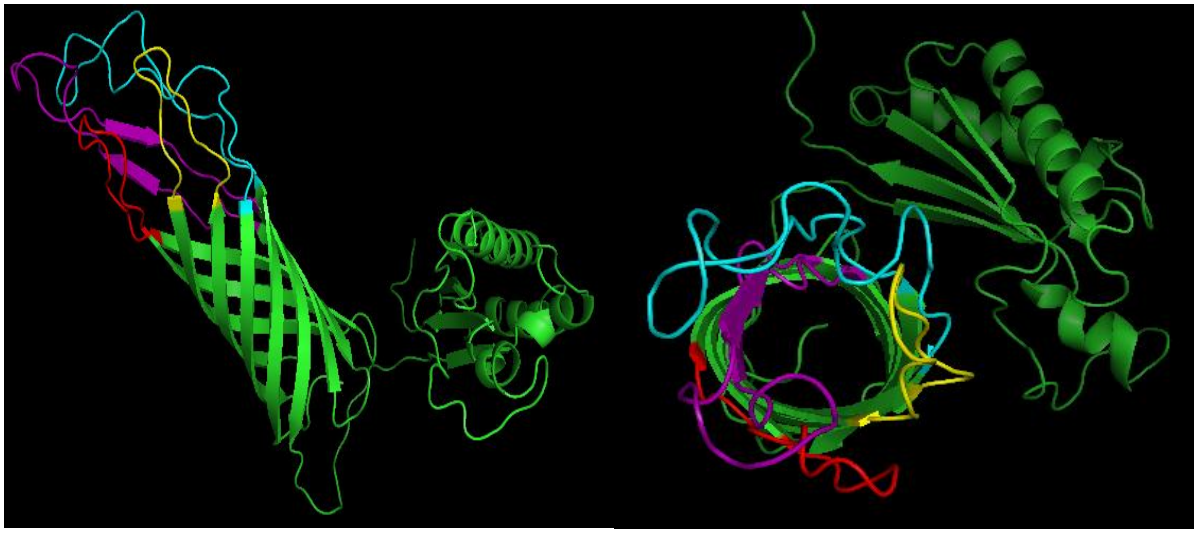

Supplemental Figure S3.11. Model of D74 (SV9) OMP P5. The protein sequence (Accession: ACJ02823) is shown with predicted surface exposed regions shown in color. A side view (left) and down the β-barrel view (right) are shown.

aapqantfyv gakagwatfh ndinqidsky andarydatn lkygisrnsv tygvfggyqi
idnlavelgy dyfgrvrgnk qefrefkhsa hgthlslkps yevlngldvy gkvgaalvrn
dykrysttie pvkshnlkts livgagveya ilpelafrve yqwlsnvgnf tkaeakenrr
atynyspdsh svtagisyrf gqgaapvaaa pevvtknfaf ssdvlfdfgk anlkpaaaqt
ldavhteivn lglanpavqv ngytdrigkd aanltlsqkr aetvanyivs kgvnpanvta
vgygeanpvt gntcdavkgr kalitclapd rrveiqvqgs kevsm

Region	Sequence
OMP P5 Loop 1	fhndinqidskyandarydatnlkygisrn
OMP P5 Loop 2	rvrgnkqefrefkh
OMP P5 Loop 3	dykrysttiepvkshnl
OMP P5 Loop 4	lsnvgnftkaeakenrratynyspds

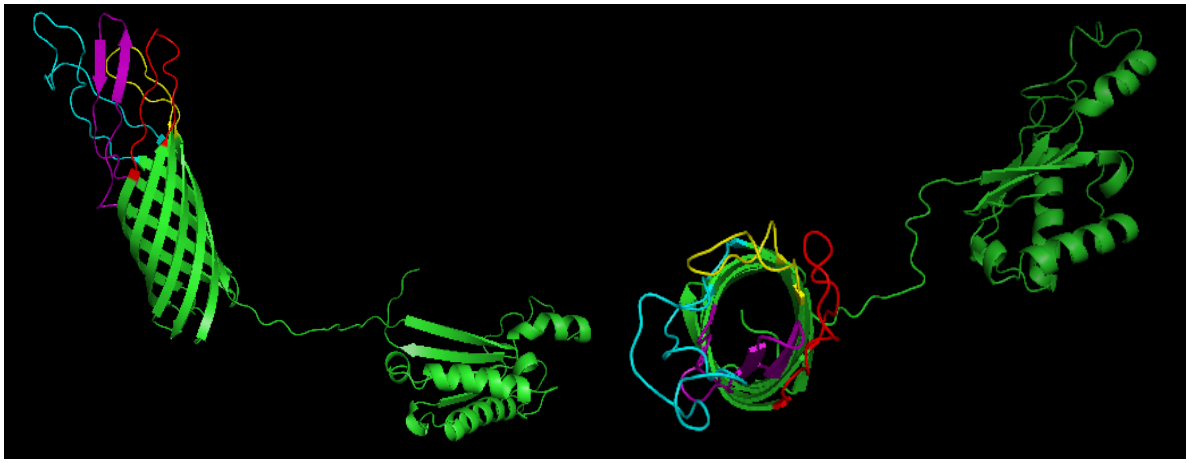

Supplemental Figure S3.12. Model of H367 (SV10) OMP P5. The protein sequence (Accession: ACJ02824) is shown with predicted surface exposed regions shown in color. A side view (left) and down the β-barrel view (right) are shown.

aapqansfyv gakagwatfh ndinqlnsky andaryatsa ngyginrnsv tygvfggyqi
idnlavelgy dyfgrvrgnk qefrafkhsa hgthlslkps yevlngldvy gkvgaalvrn
dykryfqtre pvkshnlkts livgagveya ilpelafrve yqwlsnvgnf tkaemkenrr
atynyspdsh svtagisyrf gqgaapvaaa pevvtknfaf ssdvlfdfgk anlkpasaqt
ldaahaeivn lglanpavqv ngytdrigkd aanltlsqkr aetvanyivs kgvnpanvta
vgygeanpvt gntcdavkgr kalivclapd rrveiqvqgs kevsm

Region	Sequence
OMP P5 Loop 1	tfhndinqlnskyandaryatsangyginrns
OMP P5 Loop 2	fgrvrgnkqefrafkhs
OMP P5 Loop 3	dykryfqtrepvkshnlk
OMP P5 Loop 4	wlsnvgnftkaemkenrratynyspdsh

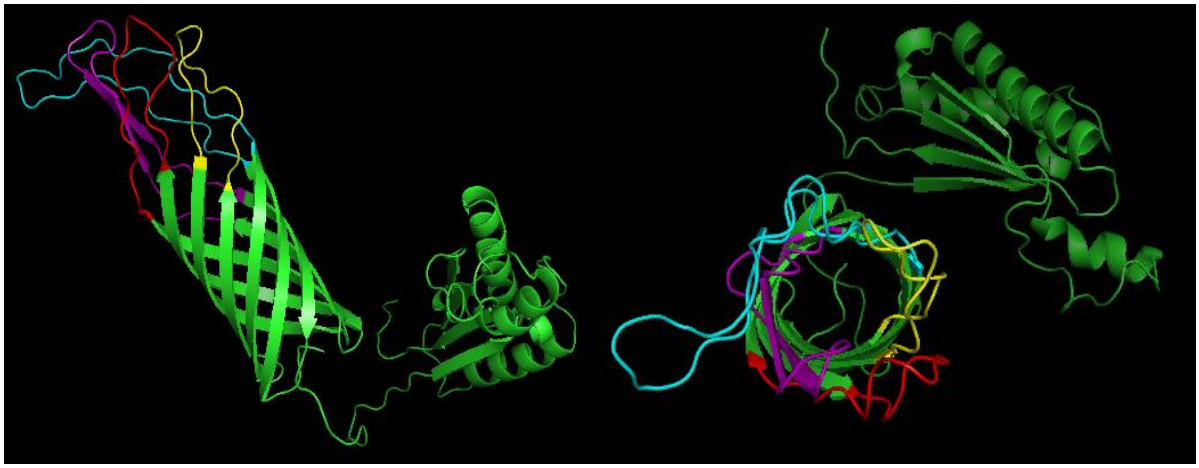

Supplemental Figure S3.13. Model of H465 (SV11) OMP P5. The protein sequence (Accession: ACJ02825) is shown with predicted surface exposed regions shown in color. A side view (left) and down the β-barrel view (right) are shown.

aapqansfyv gakagwatfh ndinqlnsky kndaryatsa ngyvinrnsv tygvfggyqi
idnlavelgy dyfgrvrgnk qefrafkhsa hgthlslkps yevlngldvy gkvgaalvrn
dykrysttre pvkshnlkts livgagveya ilpelafrve yqwlsnvgnf tkaeakenrr
atynyspdsh svtagisyrf gqgaapvaaa pevvtknfaf ssdvlfdfgk anlkpaaaqt
ldavhteivn lglanpavqv ngytdrigkd aanltlsqkr aetvanyivs kgvnpanvta
vgygeanpvt gntcdavkgr kalitclapd rrveiqvqgs kevsm

Region	Sequence
OMP P5 Loop 1	atfhndinqlnskykndaryatsangyvinrnsv
OMP P5 Loop 2	grvrgnkqefrafkhs
OMP P5 Loop 3	rndykrysttrepvkshnlk
OMP P5 Loop 4	lsnvgnftkaeakenrratynyspds

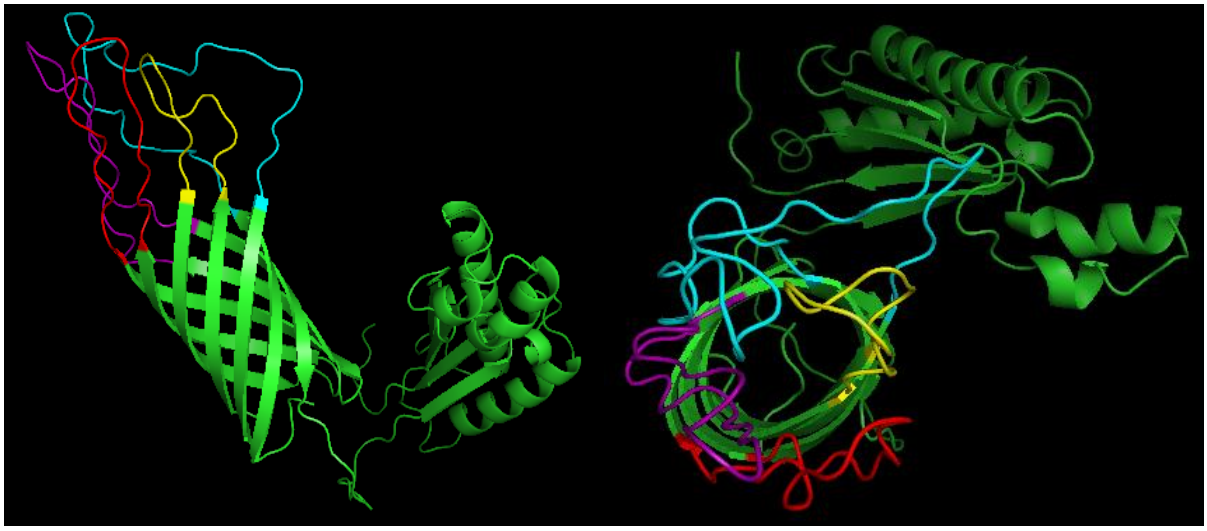

Supplemental Figure S3.14. Model of H425 (SV12) OMP P5. The protein sequence (Accession: ACJ02826) is shown with predicted surface exposed regions shown in color. A side view (left) and down the β-barrel view (right) are shown.

aapqantfyv gakagwatfh ndinqlnsky kndaryatsa ngyvinrnsv tygvfggyqi
idnlavelgy dyfgrvrgnk qefrafkhsa hgthlslkps yevlngldvy gkvgaalvrn
dykrysqtag vqtqkahnlk tslvlgagve yailpelafr veyqwlsnvg nftkaeaken
rratynyspd shsvtagisy rfgqqgaapva aapevvtknf afssdvlfdf gkanlkpaaa
qtldavhtei vnlglanpav qvngytdrig kdaanltlsq kraetvanyi vskgvnpanv
tavgygeanp vtgntcdavk grkalitcla pdrrveiqvq gskevsm

Region	Sequence
OMP P5 Loop 1	tfhndinqlnskykndaryatsangyvinr
OMP P5 Loop 2	rvrgnkqefrafkh
OMP P5 Loop 3	dykrysqtagvqtqkahnlk
OMP P5 Loop 4	lsnvgnftkaeakenrratynyspds

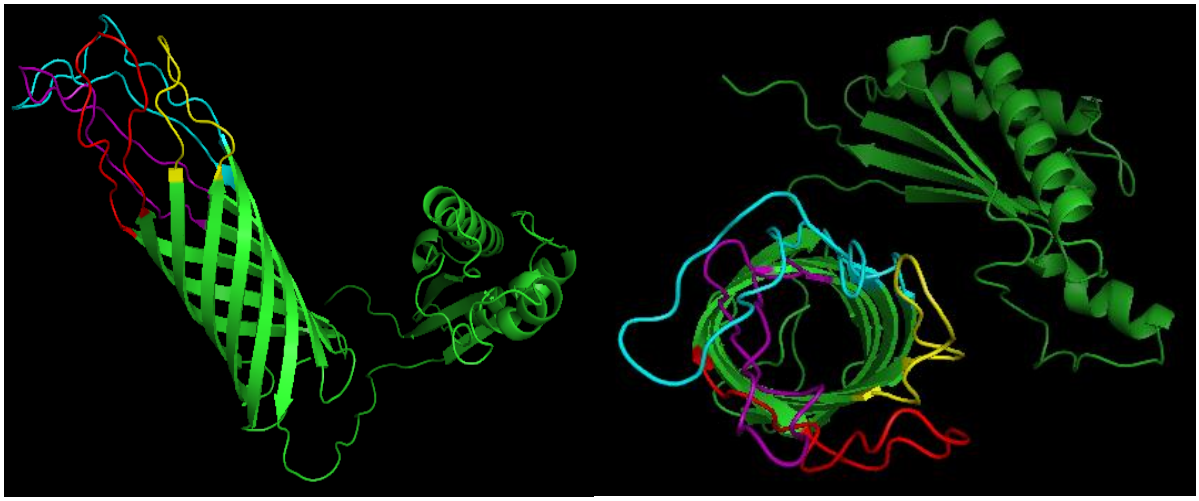

Supplemental Figure S3.15. Model of 84-17975 (SV13) OMP P5. The protein sequence (Accession: ACJ02827) is shown with predicted surface exposed regions shown in color. A side view (left) and down the β-barrel view (right) are shown.

aapqantfyv gakagwatfh ndinqidsky andarydatn lkygisrnsv tygvfggyqi
idnlavelgy dyfgrvrgnk qefrafkhsa hgthlslkps yevlngldvy gkvgaalvrn
dykrysqtag vqtqkahnlk tslvlgagve yailpelafr veyqwlsnvg nftkaeaken
rratynyspd shsvtagisy rfgqqgaapva aapevvtknf afssdvlfdf gkanlkpaaa
qtldavhtei vnlglanpav qvngytdrig kdaanltlsq kraetvanyi vskgvnpanv
tavgygeanp vtgntcdavk grkalitcla pdrrveiqvq gskevsm

Region	Sequence
OMP P5 Loop 1	atfhndinqidskyandarydatnlkygisrns
OMP P5 Loop 2	rvrgnkqefrafkh
OMP P5 Loop 3	dykrysqtagvqtqkahn
OMP P5 Loop 4	lsnvgnftkaeakenrratynyspds

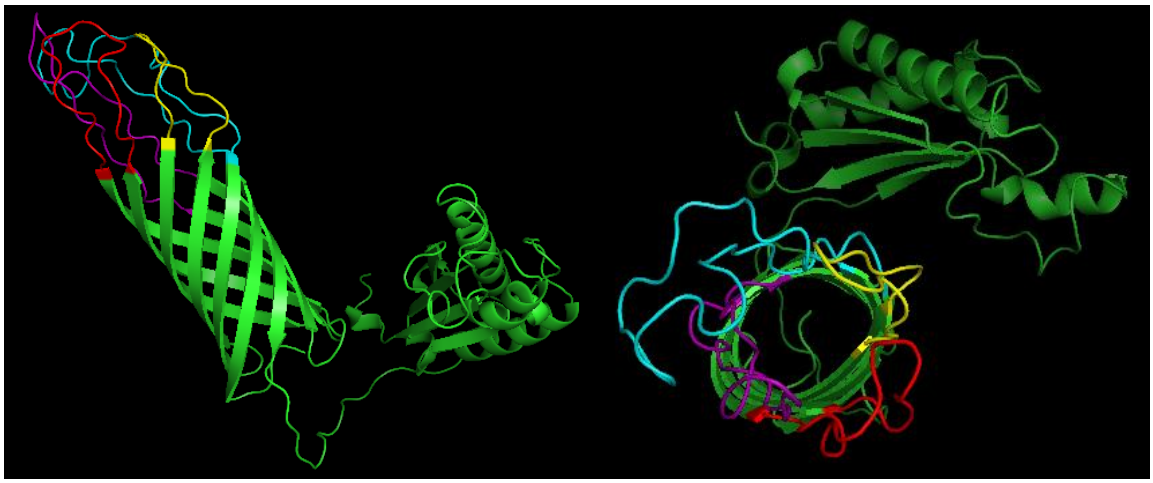

Supplemental Figure S3.16. Model of 84-22113 (SV14) OMP P5. The protein sequence (Accession: ACJ02828) is shown with predicted surface exposed regions shown in color. A side view (left) and down the β-barrel view (right) are shown.

aapqantfyv gakagwatfh ndinqidsky andarydatn lkygisrnsv tygvfggyqi
idnlavelgy dyfgrvrgnk qefrafkhsa hgthlslkps yevlngldvy gkvgaalvrn
dykrysttre pvkshnlkts livgagveya ilpelafrve yqwlsnvgnf tkaeakenrr
atynyspdsh svtagisyrf gqgaapvaaa pevvtknfaf ssdvlfdfgk anlkpaaaqt
ldavhteivn lglanpavqv ngytdrigkd aanltlsqkr aetvanyivs kgvnpanvta
vgygeanpvt gntcdavkgr kalitclapd rrveiqvqgs kevsm

Region	Sequence
OMP P5 Loop 1	atfhndinqidskyandarydatnlkygisrnsv
OMP P5 Loop 2	grvrgnkqefrafkhs
OMP P5 Loop 3	ndykrysttrepvkshnlk
OMP P5 Loop 4	wlsnvgnftkaeakenrratynyspdsh

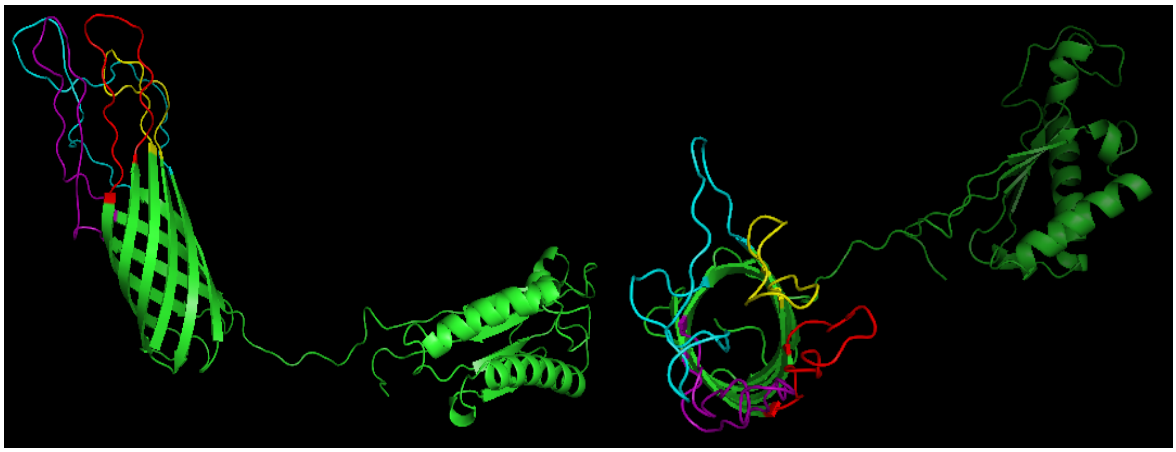

Supplemental Figure S3.17. Model of 84-15995 (SV15) OMP P5. The protein sequence (Accession: ACJ02829) is shown with predicted surface exposed regions shown in color. A side view (left) and down the β-barrel view (right) are shown.

aapqantfyv gakagwatfh ndinqlnsky kndaryatsa ngyvinrnsv tygvfggyqi
idnlavelgy dyfgrvrgnk qefrafkhsa hgthlslkps yevlngldvy gkvgaalvrn
dykrysqtag vqtqkahnlk tslvlgagve yailpelafr veyqwlsnvg nftkaeaken
rratynyspd shsvtagisy rfgqqgaapva aapevvtknf afssdvlfdf gkanlkpaaa
qtldavhtei vnlglanpav qvngytdrig kdaanltlsq kraetvanyi vskgvnpanv
tavgygeanp vtgntcdavk grkalitcla pdrrveiqvq gskevsm

Region	Sequence
OMP P5 Loop 1	tfhndinqlnskykndaryatsangyvinrn
OMP P5 Loop 2	grvrgnkqefrafkh
OMP P5 Loop 3	dykrysqtagvqtqkahnlk
OMP P5 Loop 4	lsnvgnftkaeakenrratynyspds

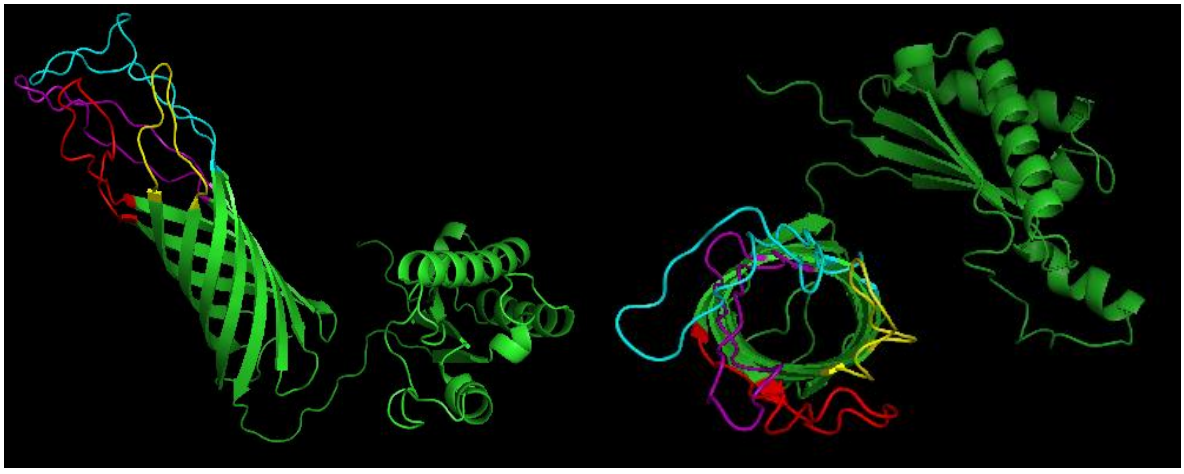

Supplemental Figure S3.18. Model of 2170B (SV4) OMP P5. The protein sequence (Accession: ACJ02811) is shown with predicted surface exposed regions shown in color. A side view (left) and down the β-barrel view (right) are shown.

aapqansfyv gakagwatfh ndinqlnsky endaryatsa ngyginrnsv tygvfggyqi
idnlavelgy dyfgrvrgke qefrafkhsa hgthlslkps yevlngldvy gkvgaalvrn
dykryfqtre pvkshnlkts livgagveya ilpelafrve yqwlsrvgna nkaaqkrgdt
amfgpgstys pdahsvsagi syrfgqgaap apaapevvtk nfafssdvlf dfgkanlkpa
aaqtldaaha eivnlglanp avqvngytdr igkdaanltl sqkraetvan yivskgvnpa
nvtavgygea npvtgntcda vkgrkalivc lapdrrveiq vqgskevsm

Region	Sequence
OMP P5 Loop 1	tfhndinqlnskykndaryatsangyvinrns
OMP P5 Loop 2	grvrgnkqefrafkhs
OMP P5 Loop 3	dykryfqtrepvkshnlk
OMP P5 Loop 4	wlsrvgnankaaqkrgdtamfgpgstyspdah
OMP P6-like domain	knfafssdvlfdfgkanlkpaaaqtldaahaeivnlglanp avqvngytdrigkdaanltlsqkraetvanyivskgvnpa nvtavgygeanpvtgntcdavkgrkalivclapdrrveiq vqgskevsm

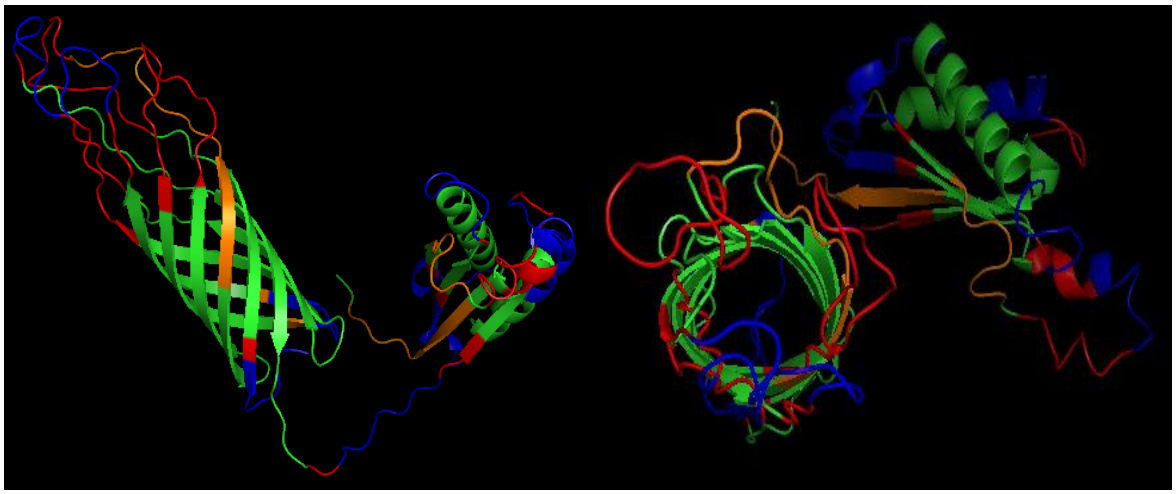

Supplemental Figure S3.19. Predicted antigenic sites and continuous B-cell epitopes of No.4 (SV1) OMP P5. Antigenic sites are highlighted in orange (moderate < 5 net votes) and red (high >5 net votes). Predicted continuous B-cell epitopes (>70% probability) are shown in blue. A side view (left) and down the β-barrel view (right) are shown.

aapqadsfyv gakagwatfh ndinqlnfky kndaryatsa ngyginrnsv tygvfggyqi
idnlavelgy dyfgrvrgnk qefrefkhsa hgthlslkps yevlsgldvy gkvgaalvrn
dykryfqtre pvkshnlkts livgagveya ilpelafrve yqwlsnvgnf tkaemkenrr
atynyspdsh svtagisyrf gqgaapvaaa pevvtknfaf ssdvlfdfgk anlkpaaaqt
ldaahteivn lglanpavqv ngytdrigkd aanltlsqkr aetvanyivs kgvnpanvta
vgygeanpvt gntcdavkgr kalivclapd rrveiqvqgs kevsm

Region	Sequence
OMP P5 Loop 1	tfhndinqlnskykndaryatsangyvinrns
OMP P5 Loop 2	rvrgnkqefrefkhsa
OMP P5 Loop 3	vrndykryfqtrepvkshnlk
OMP P5 Loop 4	lsnvgnftkaemkenrratynyspds
OMP P6-like domain	knfafssdvlfdfgkanlkpaaaqtldaahteivn lglanpavqvngytdrigkdaanltlsqkraetva nyivskgvnpanvtavgygeanpvtgntcdavkgrk alivclapdrrveiqvqgskevsm

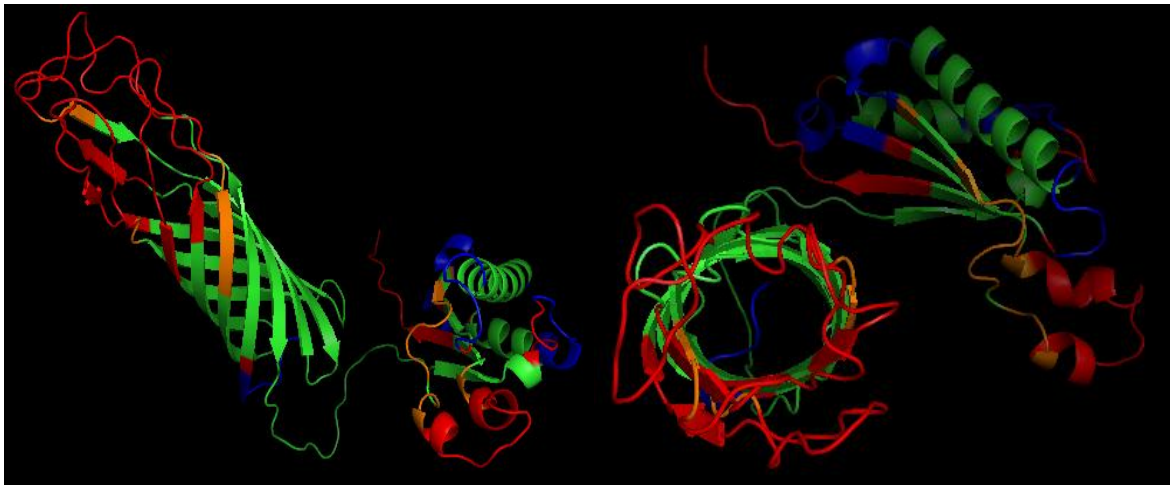

Supplemental Figure S3.20. Predicted antigenic sites and continuous B-cell epitopes of SW140 (SV2) OMP P5. Antigenic sites are highlighted in orange (moderate < 5 net votes) and red (high >5 net votes). Predicted continuous B-cell epitopes (>70% probability) are shown in blue. A side view (left) and down the β-barrel view (right) are shown.

aapqansfyv gakagwatfh ndinqlnsky endaryatsa ngyginrnsv tygvfggyqi
idnlavelgy dyfgrvrgnk qefrafkhsa hgthlslkps yevlngldvy gkvgaalvrn
dykryfqtre pvkshnlkts livgagveya ilpelafrve yqwlsnvgnf tkaevkenrr
atynyspdsh svtagisyrf gqgaapvaaa pevvtknfaf ssdvlfdfgk anlkpasaqt
ldaahteivn lglanpavqv ngytdrigkd aanltlsqkr aetvanyivs kgvnpanvta
vgygeanpvt gntcdavkgr kalivclapd rrveiqvqgs kevsm

Region	Sequence
OMP P5 Loop 1	tfhndinqlnskyendaryatsangyginrn
OMP P5 Loop 2	grvrgnkqefrafkhs
OMP P5 Loop 3	dykryfqtrepvkshnlk
OMP P5 Loop 4	wlsnvgnftkaevkenrratynyspdsh
OMP P6-like domain	knfafssdvlfdfgkanlkpasaqtldaahteivn
	lglanpavqvngytdrigkdaanltlsqkraetvanyivs
	kgvnpanvtavgygeanpvtgntcdavkgrkalivclapd
	rrveiqvqgskevsm

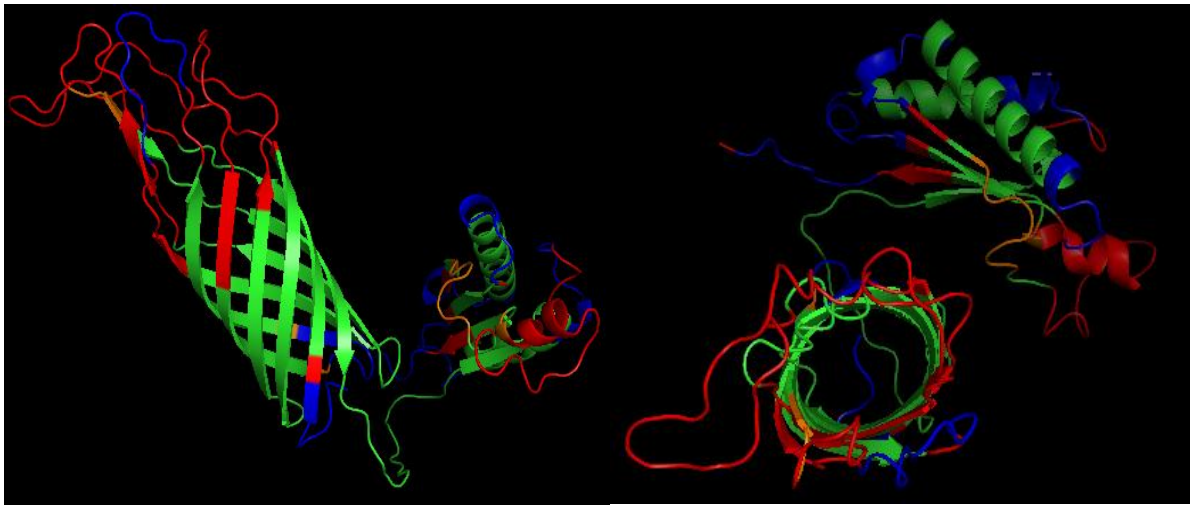

Supplemental Figure S3.21. Predicted antigenic sites and continuous B-cell epitopes of SW114 (SV3) OMP P5. Antigenic sites are highlighted in orange (moderate < 5 net votes) and red (high >5 net votes). Predicted continuous B-cell epitopes (>70% probability) are shown in blue. A side view (left) and down the β-barrel view (right) are shown.

aapqansfyv gakagwatfh ndinqlnsky kndaryatsa nryginrnsv tygvfggyqi
idnlavelgy dyfgrvrgnk qefrefkhsa hgthlslkps yevlsgldvy gkvgaalvrn
dykryfqtre pvkshnlkts livgagveya ilpelafrve yqwlsnvgnf tkaevkenrr
atynyspdsh svtagisyrf gqgaapvaaa pevvtknfaf ssdvlfdfgk anlkpaaaqt
ldaahteivn lglenpavqv ngytdrigkd aanltlsqkr aetvanyivs kgvnpanvta
vgygeanpvt gntcdavkgr kalivclapd rrveiqvqgs kevsm

Region	Sequence
OMP P5 Loop 1	tfhndinqlnskykndaryatsanryginrns
OMP P5 Loop 2	grvrgnkqefrefkhsa
OMP P5 Loop 3	rndykryfqtrepvkshnlk
OMP P5 Loop 4	wlsnvgnftkaevkenrratynyspdsh
OMP P6-like domain	knfafssdvlfdfgkanlkpaaaqtldaahteivn lglenpa vqvngytdrigkdaanltlsqkraetvanyivskgvnpanv tavgygeanpvtgntcdavkgrkalivclapdrrveiqv qgskevsm

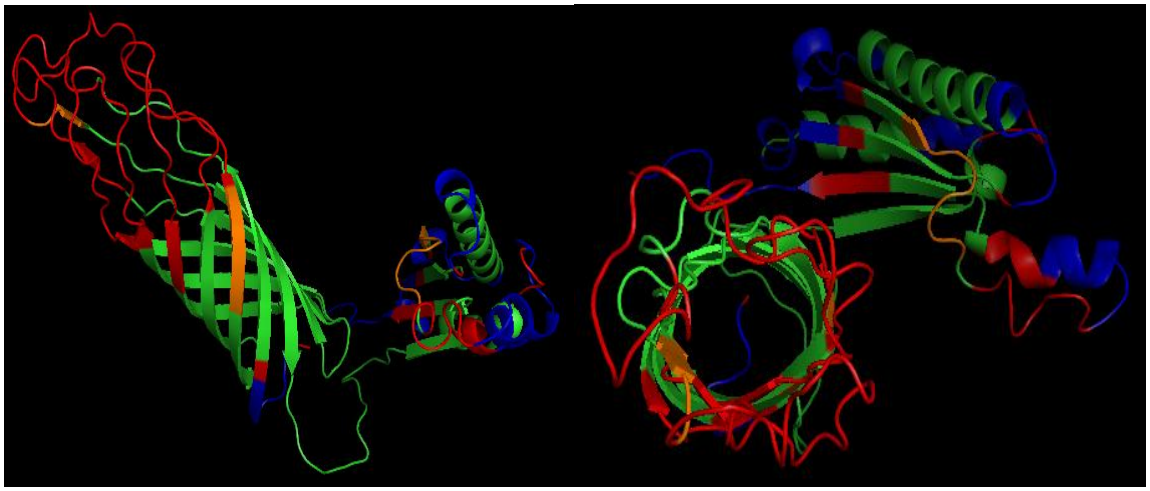

Supplemental Figure S3.22. Predicted antigenic sites and continuous B-cell epitopes of SW124 (SV4) OMP P5. Antigenic sites are highlighted in orange (moderate < 5 net votes) and red (high >5 net votes). Predicted continuous B-cell epitopes (>70% probability) are shown in blue. A side view (left) and down the β-barrel view (right) are shown.

aapqantfyv gakagwatfh ndinqlnsky kndaryatsa ngyvinrnsv tygvfggyqi
idnlavelgy dyfgrvrgnk qefrafkhsa hgthlslkps yevlngldvy gkvgaalvrn
dykrysqtag vqtqkahnlk tslvlgagve yailpelafr veyqwlsnvg nftkaeaken
rratynyspd shsvtagisy rfgqqgaapva aapevvtknf afssdvlfdf gkanlkpaaa
qtldavhtei vnlglanpav qvngytdrig kdaanltlsq kraetvanyi vskgvnpanv
tavgygeanp vtgntcdavk grkalitcla pdrrveiqvq gskevsm

Region	Sequence
OMP P5 Loop 1	tfhndinqlnskykndaryatsangyvinr
OMP P5 Loop 2	rvrgnkqefrafkh
OMP P5 Loop 3	ndykrysqtagvqtqkahnlk
OMP P5 Loop 4	lsnvgnftkaeakenrratynyspds
OMP P6-like domain	knfafssdvlfdfgkanlkpaaaqtldavhteivnlglanpa vqvngytdrigkdaanltlsqkraetvanyivskgvn panvtavgygeanpvtgntcdavkgrkalitclapdrr veiqvqgskevsm

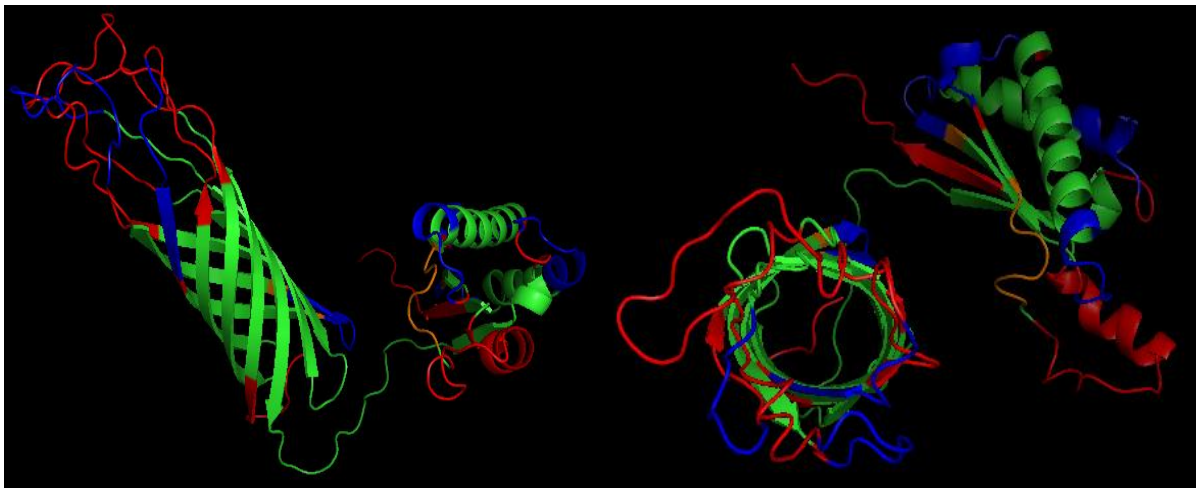

Supplemental Figure S3.23. Predicted antigenic sites and continuous B-cell epitopes of Nagasaki (SV5) OMP P5. Antigenic sites are highlighted in orange (moderate < 5 net votes) and red (high >5 net votes). Predicted continuous B-cell epitopes (>70% probability) are shown in blue. A side view (left) and down the β-barrel view (right) are shown.

aapqansfyv gakagwatfh ndinqlnsky endaryatsa ngyginrnsv tygvfggyqi
idnlavelgy dyfgrvrgke qefrafkhsa hgthlslkps yevlngldvy gkvgaalvrn
dykfydtedk ahnlktslll gagveyailp elafrveyqw lsrvgnanka aqkrgdtamf
gpgstyspda hsvsagisyr fgqgaapapa aapevvtknf afssdvlfdf gkanlkpaaa
qtldaahaei vnlglanpav qvngytdrig kdaanltlsq kraetvanyi vskgvnpanv
tavgygeanp vtgntcdavk grkalivcla pdrrveiqvq gskevsm

Region	Sequence
OMP P5 Loop 1	atfhndinqlnskyendaryatsangyginrns
OMP P5 Loop 2	rvrgkeqefrafkh
OMP P5 Loop 3	dykfydtedkahnlk
OMP P5 Loop 4	lsrvgnankaaqkrgdtamfgpgstyspda
OMP P6-like domain	knfafssdvlfdfgkanlkpaaaqtldaahaeivnlglanpav qvngytdrigkdaanltlsqkraetvanyivskgvnpanv tavgygeanpvtgntcdavkgrkalivclapdrrveiqvq gskevsm

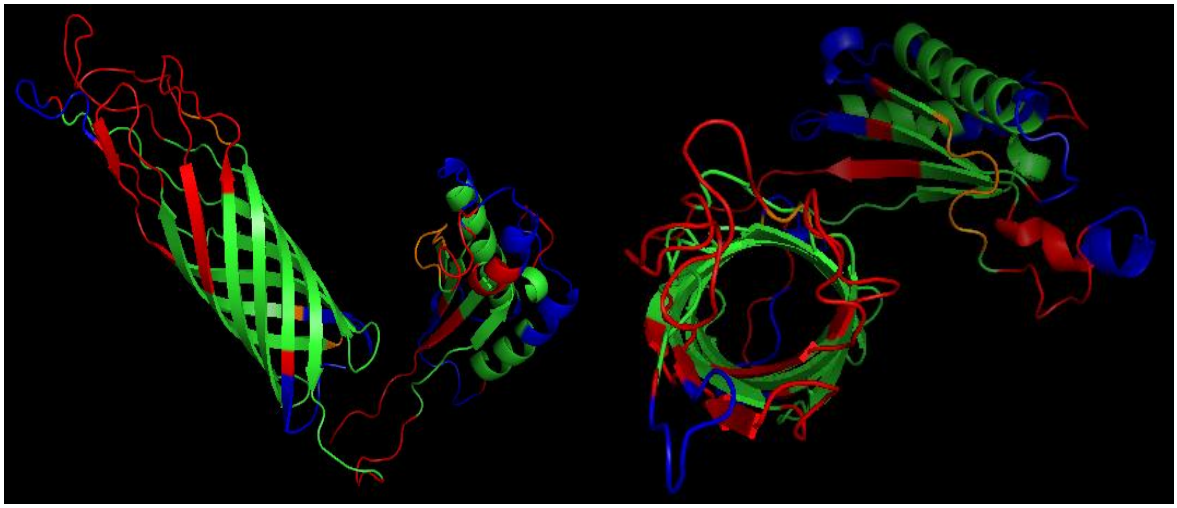

Supplemental Figure S3.24. Predicted antigenic sites and continuous B-cell epitopes of 131 (SV6) OMP P5. Antigenic sites are highlighted in orange (moderate < 5 net votes) and red (high >5 net votes). Predicted continuous B-cell epitopes (>70% probability) are shown in blue. A side view (left) and down the β-barrel view (right) are shown.

aapqansfyv gakagwatfh ndinqlnsky kndaryatsa ngyginrnsv tygvfggyqi
idnlavelgy dyfgrvrgnk qefrefkhsa hgthlslkps yevlsgldvy gkvgaalvrn
dykryfqtre pvkshnlkts livgagveya ilpelafrve yqwlsnvgnf tkaemkenrr
atynyspdsh svtagisyrf gqgaapvaaa pevvtknfaf ssdvlfdfgk anlkpasaqt
ldaahteivn lglanpavqv ngytdrigkd aanltlsqkr aetvanyivs kgvnpanvta
vgygeanpvt gntcdavkgr kalivclapd rrveiqvqgs kevsm

Region	Sequence
OMP P5 Loop 1	fhndinqlnskykndaryatsangyginrns
OMP P5 Loop 2	grvrgnkqefrefkhs
OMP P5 Loop 3	dykryfqtrepvkshnlk
OMP P5 Loop 4	lsnvgnftkaemkenrratynyspd
OMP P6-like domain	knfafssdvlfdfgkanlkpasaqtldaahteivn
	lglanpavqvngytdrigkdaanltlsqkraetvanyivs
	kgvnpanvtavgygeanpvtgntcdavkgrkalivclapd
	rrveiqvqgskevsm

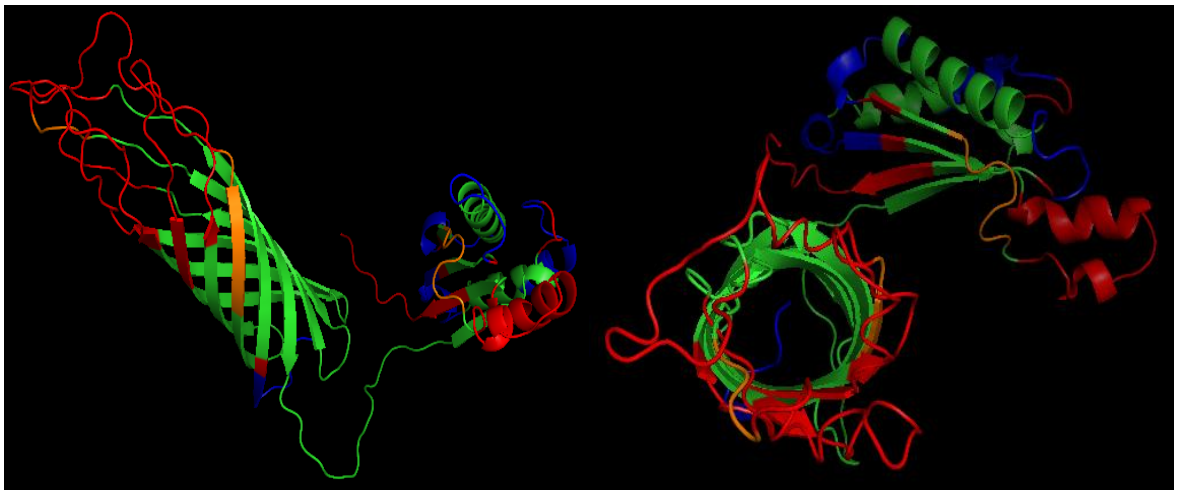

Supplemental Figure S3.25. Predicted antigenic sites and continuous B-cell epitopes of 174 (SV7) OMP P5. Antigenic sites are highlighted in orange (moderate < 5 net votes) and red (high >5 net votes). Predicted continuous B-cell epitopes (>70% probability) are shown in blue. A side view (left) and down the β-barrel view (right) are shown.

aapqansfyv gakagwatfh ndinqlnsky endaryatsa ngyginrnsv tygvfggyqi
idnlavelgy dyfgrvrgke qefrafkhsa hgthlslkps yevlngldvy gkvgaalvrn
dykfydtedk ahnlktslll gagveyailp elafrveyqw lsrvgnanka aqkrgdtamf
gpgstyspda hsvsagisyr fgqgaapapa aapevvtknf afssdvlfdf gkanlkpaaa
qtldaahaei vnlglanpav qvngytdrig kdaanltlsq kraetvanyi vskgvnpanv
tavgygeanp vtgntcdavk grkalivcla pdrrveiqvq gskevsm

Region	Sequence
OMP P5 Loop 1	atfhndinqlnskyendaryatsangyginrns
OMP P5 Loop 2	rvrgkeqefrafkh
OMP P5 Loop 3	dykfydtedkahnlk
OMP P5 Loop 4	lsrvgnankaaqkrgdtamfgpgstyspda
OMP P6-like domain	knfafssdvlfdfgkanlkpaaaqtldaahaeivnlglanpav qvngytdrigkdaanltlsqkraetvanyivskgvnpanv tavgygeanpvtgntcdavkgrkalivclapdrrveiqvq gskevsm

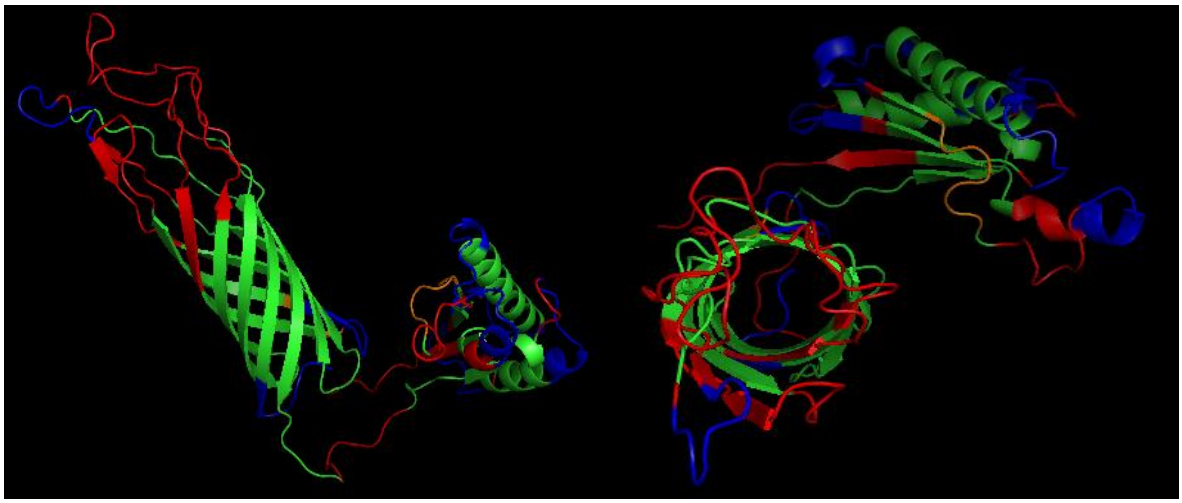

Supplemental Figure S3.26. Predicted antigenic sites and continuous B-cell epitopes of C5 (SV8) OMP P5. Antigenic sites are highlighted in orange (moderate < 5 net votes) and red (high >5 net votes). Predicted continuous B-cell epitopes (>70% probability) are shown in blue. A side view (left) and down the β-barrel view (right) are shown.

aapqadsfyv gakagwatfh ndinqlnfky kndaryatsa ngyginrnsv tygvfggyqi
idnlavelgy dyfgrvrgnk qefrefkhsa hgthlslkps yevlngldvy gkvgaalvrn
dykfydtedk ahnlktslll gagveyailp elafrveyqw lsrvgnanka aqkrgdtamf
gpgstyspda hsvsagisyr fgqgaapapa aapevvtknf afssdvlfdf gkanlkpaaa
qtldaahaei vnlglanpav qvngytdrig kdaanltlsq kraetvanyi vskgvnpanv
tavgygeanp vtgntcdavk grkalivcla pdrrveiqvq gskevsm

Region	Sequence
OMP P5 Loop 1	tfhndinqlnfkykndaryatsangyginrns
OMP P5 Loop 2	rvrgnkqefrefkh
OMP P5 Loop 3	dykfydtedkahnlk
OMP P5 Loop 4	wlsrvgnankaaqkrgdtamfgpgstyspdah
OMP P6-like domain	knfafssdvlfdfgkanlkpaaaqtldaahaeivnlglanpav qvngytdrigkdaanltlsqkraetvanyivskgvnpanv tavgygeanpvtgntcdavkgrkalivclapdrrveiqvq gskevsm

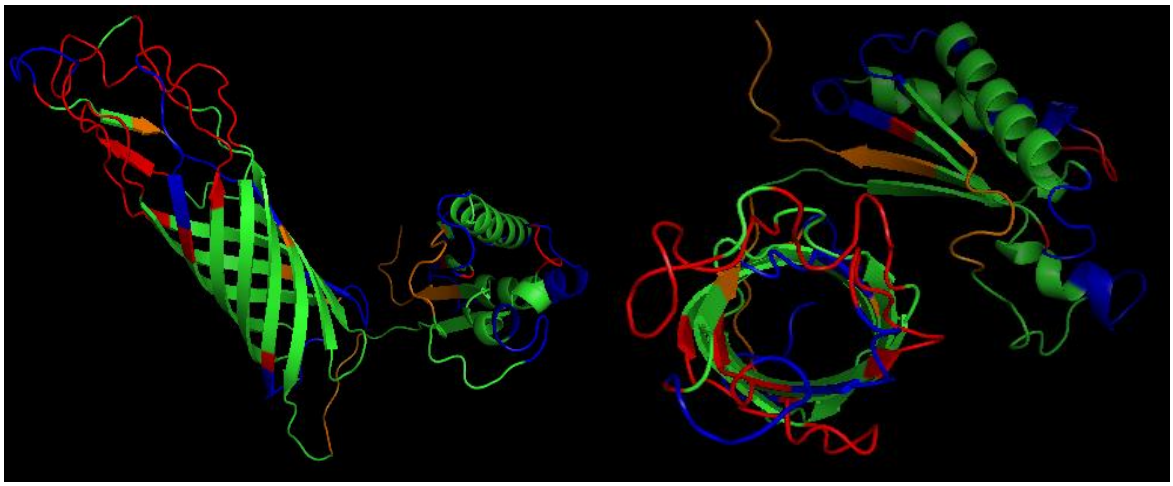

Supplemental Figure S3.27. Predicted antigenic sites and continuous B-cell epitopes of D74 (SV9) OMP P5. Antigenic sites are highlighted in orange (moderate < 5 net votes) and red (high >5 net votes). Predicted continuous B-cell epitopes (>70% probability) are shown in blue. A side view (left) and down the β-barrel view (right) are shown.

aapqantfyv gakagwatfh ndinqidsky andarydatn lkygisrnsv tygvfggyqi
idnlavelgy dyfgrvrgnk qefrefkhsa hgthlslkps yevlngldvy gkvgaalvrn
dykrysttie pvkshnlkts livgagveya ilpelafrve yqwlsnvgnf tkaeakenrr
atynyspdsh svtagisyrf gqgaapvaaa pevvtknfaf ssdvlfdfgk anlkpaaaqt
ldavhteivn lglanpavqv ngytdrigkd aanltlsqkr aetvanyivs kgvnpanvta
vgygeanpvt gntcdavkgr kalitclapd rrveiqvqgs kevsm

Region	Sequence
OMP P5 Loop 1	fhndinqidskyandarydatnlkygisrn
OMP P5 Loop 2	rvrgnkqefrefkh
OMP P5 Loop 3	dykrysttiepvkshnl
OMP P5 Loop 4	lsnvgnftkaeakenrratynyspds
OMP P6-like domain	knfafssdvlfdfgkanlkpaaaqtldavhteivnlglanpav qvngytdrigkd aanltlsqkr aetvanyivskgvnpanvta vgygeanpvtgntcdavkgrkalitclapdrrveiqvqgs kevsm

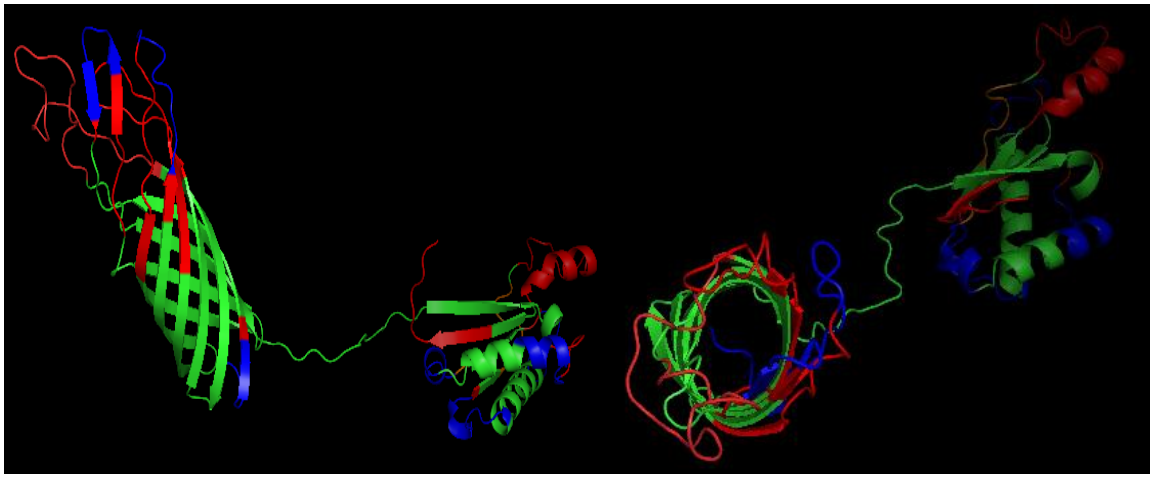

Supplemental Figure S3.28. Predicted antigenic sites and continuous B-cell epitopes of H367 (SV10) OMP P5. Antigenic sites are highlighted in orange (moderate < 5 net votes) and red (high >5 net votes). Predicted continuous B-cell epitopes (>70% probability) are shown in blue. A side view (left) and down the β-barrel view (right) are shown.

aapqansfyv gakagwatfh ndinqlnsky andaryatsa ngyginrnsv tygvfggyqi
idnlavelgy dyfgrvrgnk qefrafkhsa hgthlslkps yevlngldvy gkvgaalvrn
dykryfqtre pvkshnlkts livgagveya ilpelafrve yqwlsnvgnf tkaemkenrr
atynyspdsh svtagisyrf gqgaapvaaa pevvtknfaf ssdvlfdfgk anlkpasaqt
ldaahaeivn lglanpavqv ngytdrigkd aanltlsqkr aetvanyivs kgvnpanvta
vgygeanpvt gntcdavkgr kalivclapd rrveiqvqgs kevsm

Region	Sequence
OMP P5 Loop 1	tfhndinqlnskyandaryatsangyginrns
OMP P5 Loop 2	fgrvrgnkqefrafkhs
OMP P5 Loop 3	dykryfqtrepvkshnlk
OMP P5 Loop 4	wlsnvgnftkaemkenrratynyspdsh
OMP P6-like domain	knfafssdvlfdfgkanlkpasaqtldaahaeivnlglanpav qvngytdrigkdaanltlsqkraetvanyivskgvnpanvta vgygeanpvtgntcdavkgrkalivclapdrrveiqvqgs kevsm

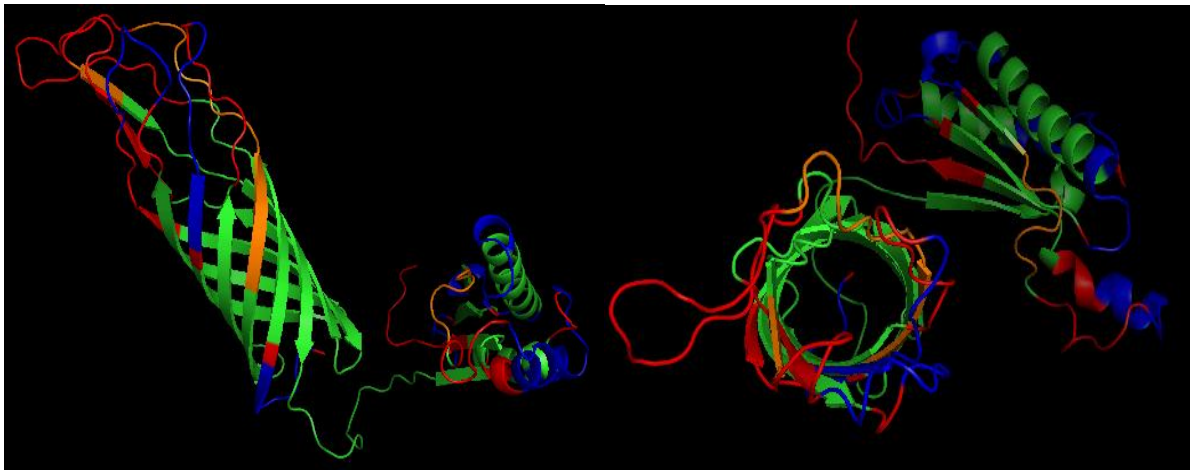

Supplemental Figure S3.29. Predicted antigenic sites and continuous B-cell epitopes of H465 (SV11) OMP P5. Antigenic sites are highlighted in orange (moderate < 5 net votes) and red (high >5 net votes). Predicted continuous B-cell epitopes (>70% probability) are shown in blue. A side view (left) and down the β-barrel view (right) are shown.

aapqansfyv gakagwatfh ndinqlnsky kndaryatsa ngyvinrnsv tygvfggyqi
idnlavelgy dyfgrvrgnk qefrafkhsa hgthlslkps yevlngldvy gkvgaalvrn
dykrysttre pvkshnlkts livgagveya ilpelafrve yqwlsnvgnf tkaeakenrr
atynyspdsh svtagisyrf gqgaapvaaa pevvtknfaf ssdvlfdfgk anlkpaaaqt
ldavhteivn lglanpavqv ngytdrigkd aanltlsqkr aetvanyivs kgvnpanvta
vgygeanpvt gntcdavkgr kalitclapd rrveiqvqgs kevsm

Region	Sequence
OMP P5 Loop 1	atfhndinqlnskykndaryatsangyvinrnsv
OMP P5 Loop 2	grvrgnkqefrafkhs
OMP P5 Loop 3	rndykrysttrepvkshnlk
OMP P5 Loop 4	lsnvgnftkaeakenrratynyspds
OMP P6-like domain	knfafssdvlfdfgkanlkpaaaqtldavhteivn
	lglanpavqvngytdrigkdaanltlsqkraetvanyivs
	kgvnpanvtavgygeanpvtgntcdavkgrkalitclapd
	rrveiqvqgskevsm

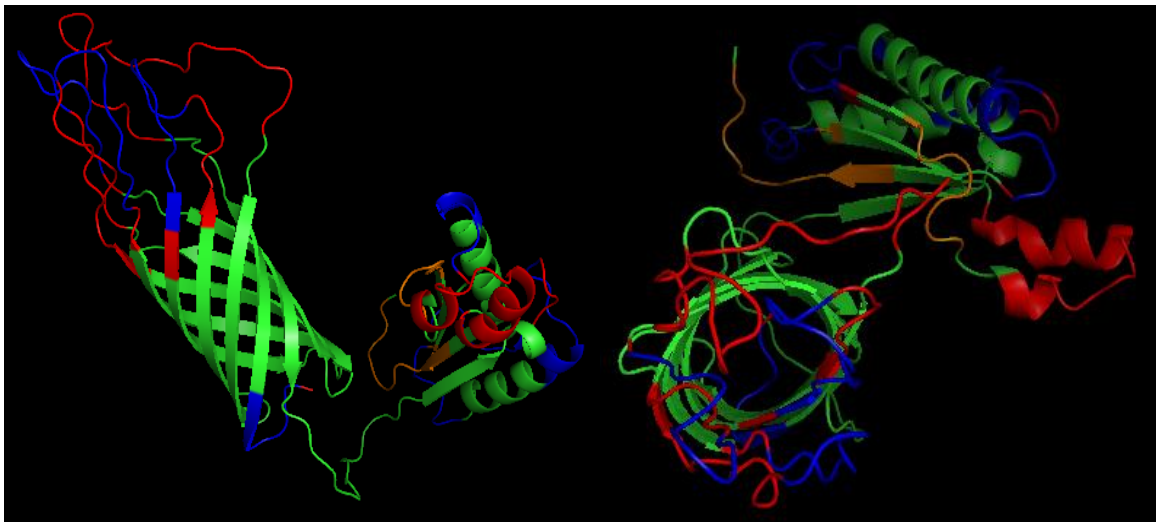

Supplemental Figure S3.30. Predicted antigenic sites and continuous B-cell epitopes of H425 (SV12) OMP P5. Antigenic sites are highlighted in orange (moderate < 5 net votes) and red (high >5 net votes). Predicted continuous B-cell epitopes (>70% probability) are shown in blue. A side view (left) and down the β-barrel view (right) are shown.

aapqantfyv gakagwatfh ndinqlnsky kndaryatsa ngyvinrnsv tygvfggyqi
idnlavelgy dyfgrvrgnk qefrafkhsa hgthlslkps yevlngldvy gkvgaalvrn
dykrysqtag vqtqkahnlk tslvlgagve yailpelafr veyqwlsnvg nftkaeaken
rratynyspd shsvtagisy rfgqqgaapva aapevvtknf afssdvlfdf gkanlkpaaa
qtldavhtei vnlglanpav qvngytdrig kdaanltlsq kraetvanyi vskgvnpanv
tavgygeanp vtgntcdavk grkalitcla pdrrveiqvq gskevsm

Region	Sequence
OMP P5 Loop 1	atfhndinqidskyandarydatnlkygisrns
OMP P5 Loop 2	rvrgnkqefrafkh
OMP P5 Loop 3	dykrysqtagvqtqkahn
OMP P5 Loop 4	lsnvgnftkaeakenrratynyspds
OMP P6-like domain	knfafssdvlfdfgkanlkpaaaqtldavhteivnlglanpav qvngytdrigkdaanltlsqkraetvanyivskgvnpanv tavgygeanpvtgntcdavkgrkalitclapdrrveiqvq gskevsm

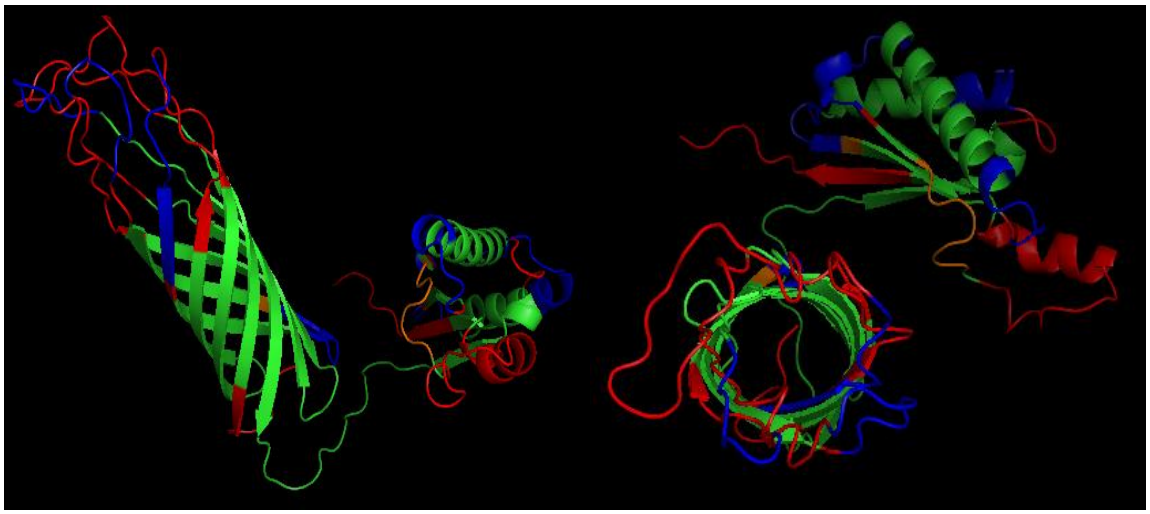

Supplemental Figure S3.31. Predicted antigenic sites and continuous B-cell epitopes of 84-17975 (SV13) OMP P5. Antigenic sites are highlighted in orange (moderate < 5 net votes) and red (high >5 net votes). Predicted continuous B-cell epitopes (>70% probability) are shown in blue. A side view (left) and down the β-barrel view (right) are shown.

aapqantfyv gakagwatfh ndinqidsky andarydatn lkygisrnsv tygvfggyqi
idnlavelgy dyfgrvrgnk qefrafkhsa hgthlslkps yevlngldvy gkvgaalvrn
dykrysqtag vqtqkahnlk tslvlgagve yailpelafr veyqwlsnvg nftkaeaken
rratynyspd shsvtagisy rfgqqgaapva aapevvtknf afssdvlfdf gkanlkpaaa
qtldavhtei vnlglanpav qvngytdrig kdaanltlsq kraetvanyi vskgvnpanv
tavgygeanp vtgntcdavk grkalitcla pdrrveiqvq gskevsm

Region	Sequence
OMP P5 Loop 1	atfhndinqidskyandarydatnlkygisrns
OMP P5 Loop 2	rvrgnkqefrafkh
OMP P5 Loop 3	dykrysqtagvqtqkahn
OMP P5 Loop 4	lsnvgnftkaeakenrratynyspds
OMP P6-like domain	knfafssdvlfdfgkanlkpaaaqtldavhteivnlglanpav qvngytdrigkdaanltlsqkraetvanyivskgvnpanv tavgygeanpvtgntcdavkgrkalitclapdrrveiqvq gskevsm

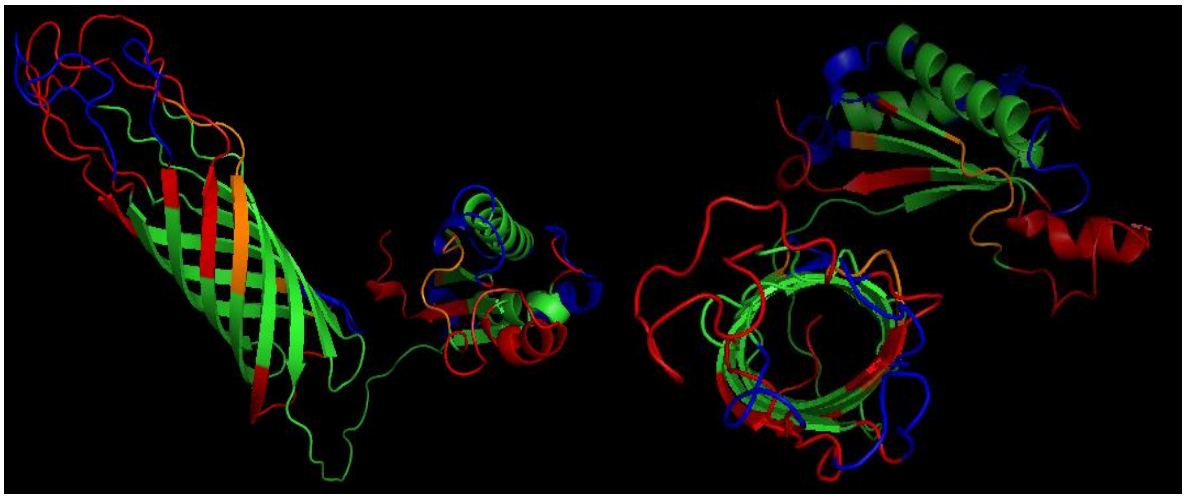

Supplemental Figure S3.32. Predicted antigenic sites and continuous B-cell epitopes of 84-22113 (SV14) OMP P5. Antigenic sites are highlighted in orange (moderate < 5 net votes) and red (high >5 net votes). Predicted continuous B-cell epitopes (>70% probability) are shown in blue. A side view (left) and down the β-barrel view (right) are shown.

aapqantfyv gakagwatfh ndinqidsky andarydatn lkygisrnsv tygvfggyqi
idnlavelgy dyfgrvrgnk qefrafkhsa hgthlslkps yevlngldvy gkvgaalvrn
dykrysttre pvkshnlkts livgagveya ilpelafrve yqwlsnvgnf tkaeakenrr
atynyspdsh svtagisyrf gqgaapvaaa pevvtknfaf ssdvlfdfgk anlkpaaaqt
ldavhteivn lglanpavqv ngytdrigkd aanltlsqkr aetvanyivs kgvnpanvta
vgygeanpvt gntcdavkgr kalitclapd rrveiqvqgs kevsm

Region	Sequence
OMP P5 Loop 1	atfhndinqidskyandarydatnlkygisrnsv
OMP P5 Loop 2	grvrgnkqefrafkhs
OMP P5 Loop 3	ndykrysttrepvkshnlk
OMP P5 Loop 4	wlsnvgnftkaeakenrratynyspdsh
OMP P6-like domain	knfafssdvlfdfgkanlkpaaaqtldavhteivnlglanpavqv ngytdrigkdaanltlsqkraetvanyivskgvnpanvta vgygeanpvtgntcdavkgrkalitclapdrrveiqvqgs kevsm

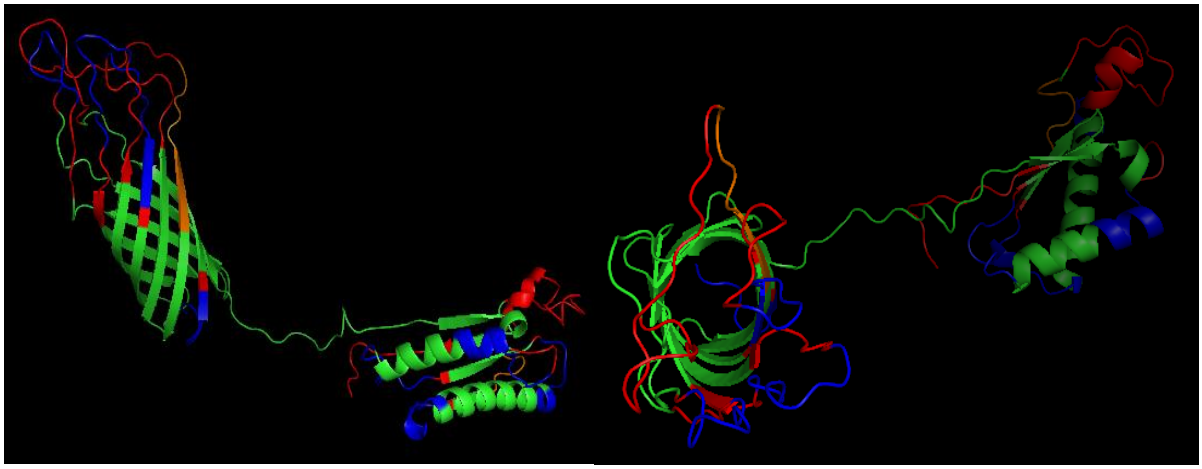

Supplemental Figure S3.33. Predicted antigenic sites and continuous B-cell epitopes of 84-15995 (SV15) OMP P5. Antigenic sites are highlighted in orange (moderate < 5 net votes) and red (high >5 net votes). Predicted continuous B-cell epitopes (>70% probability) are shown in blue. A side view (left) and down the β-barrel view (right) are are shown.

aapqantfyv gakagwatfh ndinqlnsky kndaryatsa ngyvinrnsv tygvfggyqi
idnlavelgy dyfgrvrgnk qefrafkhsa hgthlslkps yevlngldvy gkvgaalvrn
dykrysqtag vqtqkahnlk tslvlgagve yailpelafr veyqwlsnvg nftkaeaken
rratynyspd shsvtagisy rfgqqgaapva aapevvtknf afssdvlfdf gkanlkpaaa
qtldavhtei vnlglanpav qvngytdrig kdaanltlsq kraetvanyi vskgvnpanv
tavgygeanp vtgntcdavk grkalitcla pdrrveiqvq gskevsm

Region	Sequence
OMP P5 Loop 1	tfhndinqlnskykndaryatsangyvinrn
OMP P5 Loop 2	grvrgnkqefrafkh
OMP P5 Loop 3	dykrysqtagvqtqkahnlk
OMP P5 Loop 4	lsnvgnftkaeakenrratynyspds
OMP P6-like domain	knfafssdvlfdfgkanlkpaaaqtldavhteivnlglanpav qvngytdrigkdaanltlsqkraetvanyivskgvnpanv tavgygeanpvtgntcdavkgrkalitclapdrrveiqvq gskevsm

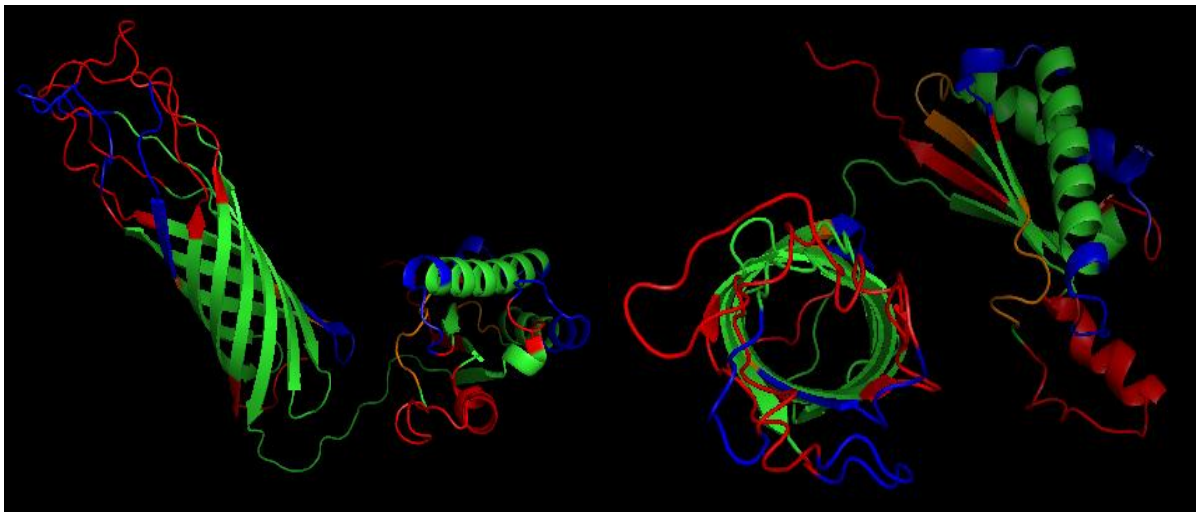

Supplemental Figure S3.34. Predicted antigenic sites and continuous B-cell epitopes of 2170B (SV4) OMP P5. Antigenic sites are highlighted in orange (moderate < 5 net votes) and red (high >5 net votes). Predicted continuous B-cell epitopes (>70% probability) are shown in blue. A side view (left) and down the β-barrel view (right) are shown.

mkktlvalav atfaasasav tvyenegtkv dfdgqlrlll ekqaskekgk sstdghtnlk
nnssrfgisi khninenlyg fgryetrlgs gsknaakwgd vttdeayvgl ggygheisfg
kqavigdsig qagfdkvygv gtggikytye veesitvdnk qgtfkysapq egfdiltqss
dsainytytg iegltlgany nvanereead vkvdsiksgf glgakytaki aesqsvtvaa
gythddyksg svklkgkfvq angtstdhih tekpfnkkdk dgvyfglkyv napftvavdg
ghgvvkkddv kekinfvrtg arfdvtpksg vygnysygty kkvedfkvta hqfmlgadyk
lhkqvvtfve grliknkdsd nnkvtdkalg vglrvlw

Region	Sequence
OMP P2 Loop 1	qaskekgksstdghtnlknns
OMP P2 Loop 2	lgsgsknaakwgdvt
OMP P2 Loop 3	fgkqavigdsigqagfdkvygvgtggikytyeveesitvdnkqgtfkysapqegfdiltqssdsa
OMP P2 Loop 4	nvanereeadvkvdsik
OMP P2 Loop 5	dyksgsvklkgkfvqangtstdhihtekpfnk
OMP P2 Loop 6	vkkddvkek
OMP P2 Loop 7	kkvedfkv
OMP P2 Loop 8	knkdsdnnkvtdkal

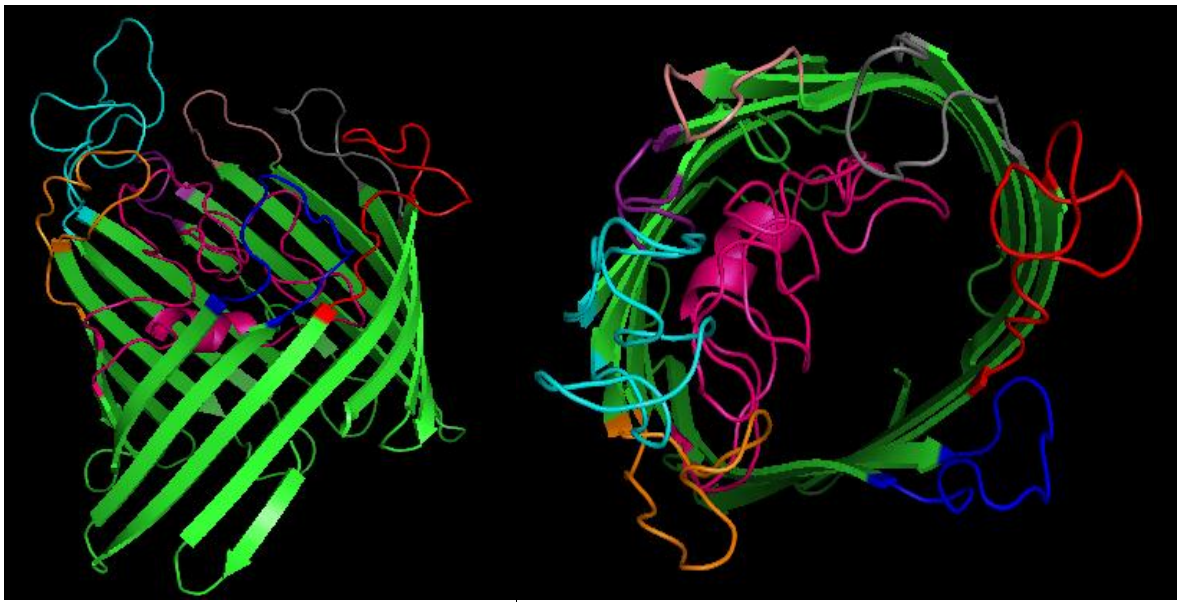

Supplemental Figure S3.35. Model of No.4 (SV1) OMP P2 extended form. The protein sequence (Accession ACJ02780) is shown with predicted surface exposed regions shown in color. A side view (left) and down the β-barrel view (right) are shown.

mkktlvalav aafaasasav tvyenegtkv dfdgqlrlll eeqatkekgq sstgghtnlk
nngsrfgisi khninenlyg fgryetrlgs gsknaaewgd vtteeayvgl ggygheisfg
kqavigdsig qagfdkvygv gtggikysan ntnkkgfdil tassdsainy tytgiegltl
ganynvaner ddkggvkvgs iksgfglgak ytakiaesqs vtvaagythd dyksgavnkk
dkdgvyfglk yvnapftvav dgghgvvktd nvkekidfvr tgarfdvtpk sgvygnysyg
tykdkaykat ahqfmlgady klhkqvvtfv egrliknkds nnnkvtdqal gvglrvlw

Region	Sequence
OMP P2 Loop 1	lleeqatkekgqsstgghtnlknng
OMP P2 Loop 2	gsgsknaaewgdv
OMP P2 Loop 3	kqavigdsigqagfdkvygvgtggikysanntnkkgfdiltassdsa
OMP P2 Loop 4	nvanerddkggvkvgsik
OMP P2 Loop 5	dyksgavnkk
OMP P2 Loop 6	ktdnvkek
OMP P2 Loop 7	kdkayk
OMP P2 Loop 8	knkdsdnnkvtdqa

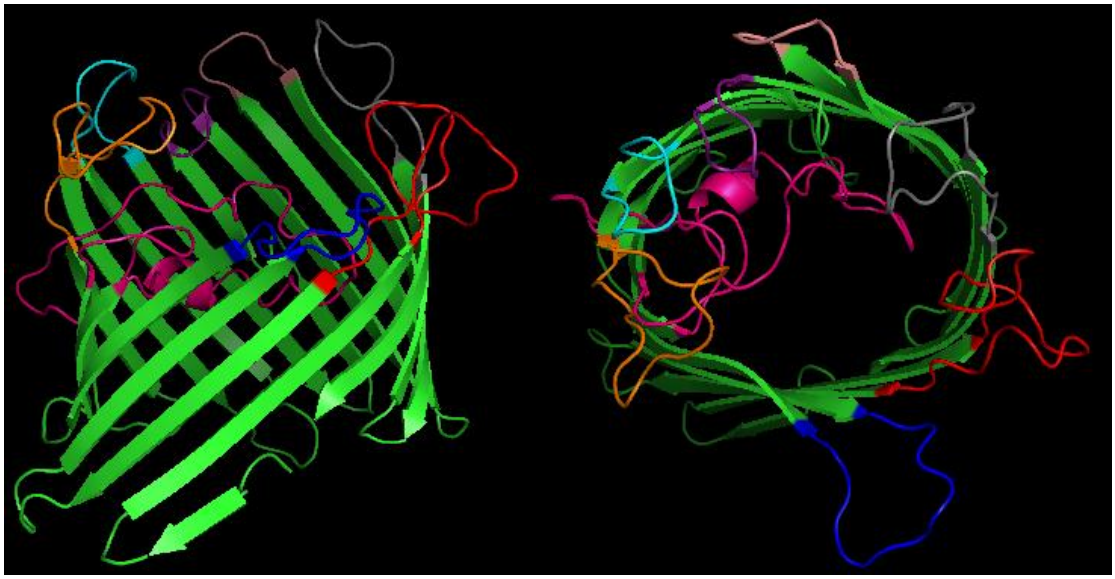

Supplemental Figure S3.36. Model of No.4 (SV1) OMP P2. The protein sequence (Accession ACS717641) is shown with predicted surface exposed regions shown in color. A side view (left) and down the β-barrel view (right) are shown.

mkktlvalav aafaasasav tvyenegtkv dfdgqlrlll ekqaskvkgq sstsghtdlk
nngsrfgisi khninenlyg fgryetrlds nsknaagwgd vktkyayvgl ggygheisfg
kqvvigdsig qagfdkvydv gstgirikyp ansadkkgfd iltsdsdsai nytytgiegl
tlganynvan erdkktgevk vdsaksgfgl gakytakiae sqsvtvaagy thddyksgav
nkkdkdgvyf glkyvnapft vavdgghgvv ktdnvkekid fvrtgarfdv tpksgvygny
sygtykdkay katahqfmlg adyklhkqvv tfvegrlikn kdsnnkkvtd kalgvglrvlw

Region	Sequence
OMP P2 Loop 1	kqaskvkgqsstsghtdlknng
OMP P2 Loop 2	dsnsknaagwgdv
OMP P2 Loop 3	kqvvigdsigqagfdkvydvgstgirikypansadkkgfdiltsdsdsa
OMP P2 Loop 4	nvanerdkktgevkvdsak
OMP P2 Loop 5	dyksgavnkkdk
OMP P2 Loop 6	ktdnvkek
OMP P2 Loop 7	kdkayk
OMP P2 Loop 8	iknkdsnnkkvtdka

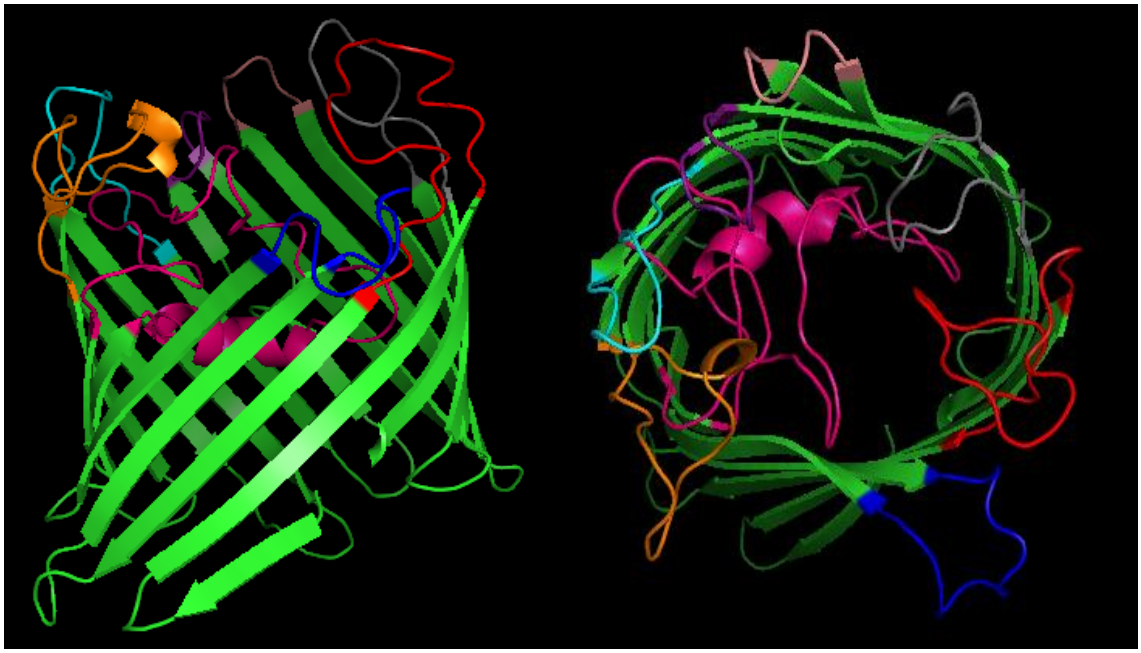

Supplemental Figure S3.37. Model of SW140 (SV2) OMP P2. The protein sequence (Accession ACJ02781) is shown with predicted surface exposed regions shown in color. A side view (left) and down the β-barrel view (right) are shown.

mkktlvalav aafaasasav tvyenegtkv dfdgqlrlll ekqaskvkgq sstdghtnlk
nnssrfgisi khninenlyg fgryetrlds gsknaakwgd vttdeayvgl ggygheisfg
kqavigdsig qagfdkvygv gtggikytyk vdkpitgnnr qgtlysapqk gfdiltqssd
sainytytgi egltlganyn vanerekadv kvdsiksgfg lgakytakia esqsvtvaag
ythddyksgs velkgkfvqt ngtstnhtyt esfnkkdkdg vyfglkyvna pftvavdggh
gvvktddvke kinfvrtgar fdvtpksgvy gnysygtykv edfkatahqf mlgadyklhk
qvvtfvegrl iknknsdnnk vtdkalgvgl rvlw

Region	Sequence
OMP P2 Loop 1	qaskvkgqsstdghtnlknns
OMP P2 Loop 2	dsgsknaakwgdv
OMP P2 Loop 3	kqavigdsigqagfdkvygvgtggikytykvdkpitgnnrqgtlysapqkgfdiltqssdsa
OMP P2 Loop 4	nvanerekadvkvdsik
OMP P2 Loop 5	dyksgsvelkgkfvqt ngtstnhtytesfnkk
OMP P2 Loop 6	gvvktddvkeki
OMP P2 Loop 7	ykvedfkat
OMP P2 Loop 8	nknsdnnkvtdkal

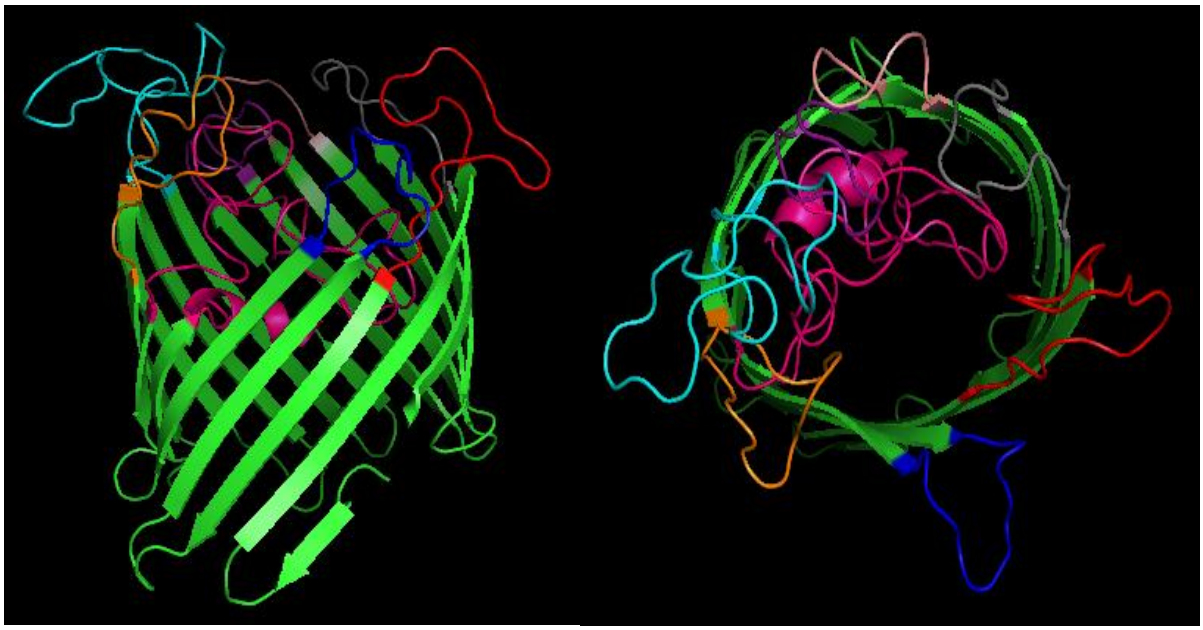

Supplemental Figure S3.38. Model of SW124 (SV4) OMP P2. The protein sequence (Accession ACJ02807) is shown with predicted surface exposed regions shown in color. A side view (left) and down the β-barrel view (right) are shown.

mkktlvalav aafaasasav tvyenegtkv dfdgqlrlll eeqatkekgq sstgghtnlk
nngsrfgisi khninenlyg fgryetrlds nsknaagwgd vktkyayvgl ggygheisfg
kqdvigdsig qagfdkvygv gtggikysan ntnkkgfdil tsdsdsainy tytgiegltl
ganynvaner dkktgevnvg stksgfglga kytakiaesq svtvaagyth ddyksgsvnk
kdkdgvyfgl kyvnapftva vdgghgvekt gnvkekidfv rtgarfdvtp ksgvygnysy
gtykdkayka tahqfmlgad yklhkqvvtf vegrliknkd snnkkvtdqa lgvglrvlw

Region	Sequence
OMP P2 Loop 1	qatkekgqsstgghtnlknngsr
OMP P2 Loop 2	trldsnsknaagwgdvktk
OMP P2 Loop 3	kqdvigdsigqagfdkvygvtggikysanntnkkgfdiltsdsdsa
OMP P2 Loop 4	nvanerdkktgevnvgstk
OMP P2 Loop 5	yksgsvnkk
OMP P2 Loop 6	tgnv
OMP P2 Loop 7	ykdkayka
OMP P2 Loop 8	nkdsnnkkvt

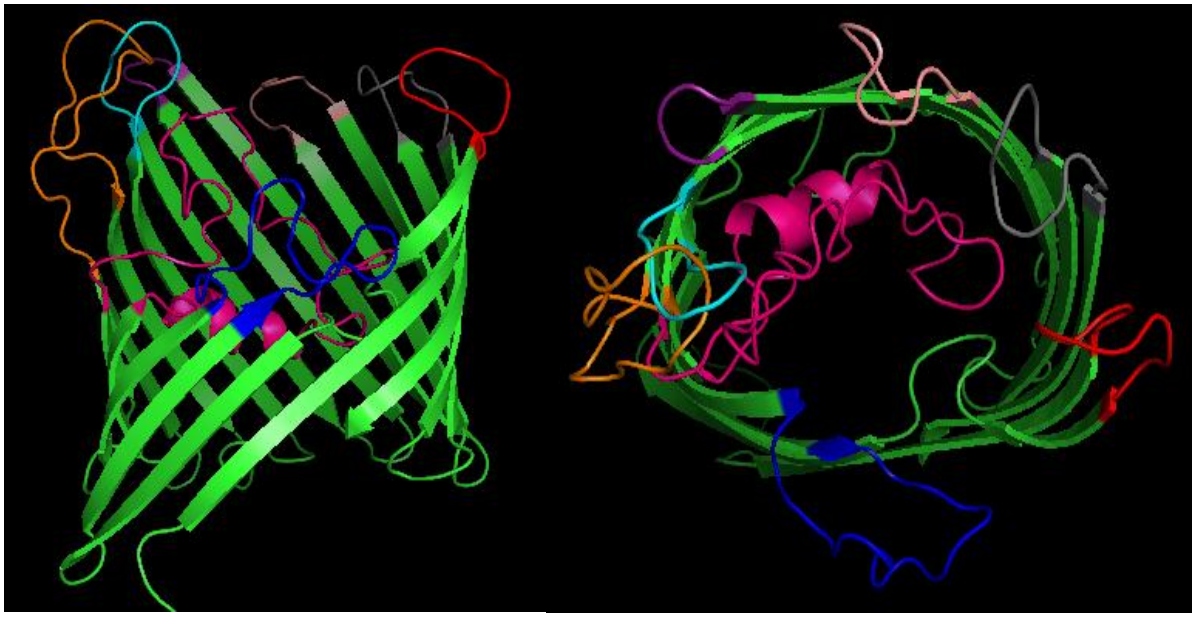

Supplemental Figure S3.39. Model of Nagasaki (SV5) OMP P2. The protein sequence (Accession ACJ02783) is shown with predicted surface exposed regions shown in color. A side view (left) and down the β-barrel view (right) are shown.

mkktlvalav atfaasasav tvyenegtkv dfdgqlrlll ekkaskekgk sstdghtnlk
nnssrfgisi khninenlyg fgryetrlgs gsknaakwgd vttdeayvgl ggygheisfg
kqavigdsig qagfdkvygv gtggikytyk vdesitvnnt qgtfkysapq egfdiltqss
dsainytytg iegltlgany nvanerekad vkvdsiksgf glgakytaki aesqsvtvaa
gythddyksg svqlkgkfvq angtstdhty tesfnkknkd gvyfglkyvn apftvavdgg
hgvvktddvk ekinfvrtga rfdvtpksgv ygnysygtyk vedykatahq fmlgadyklh
kqvvtfvegr liknkdsdnn kvtdkalgvg lrvlw

Region	Sequence
OMP P2 Loop 1	kaskekgksstdghtnlknns
OMP P2 Loop 2	lgsgsknaakwgdvt
OMP P2 Loop 3	kqavigdsigqagfdkvygvgtggikytykvdesitvnntqgtfkysapqegfdiltqssdsa
OMP P2 Loop 4	nvanerekadvkvdsiks
OMP P2 Loop 5	dyksgsvqlkgkfvqangtstdhtytesfnkk
OMP P2 Loop 6	gvvktddvkek
OMP P2 Loop 7	kvedykata
OMP P2 Loop 8	nkdsdnnkvtdkal

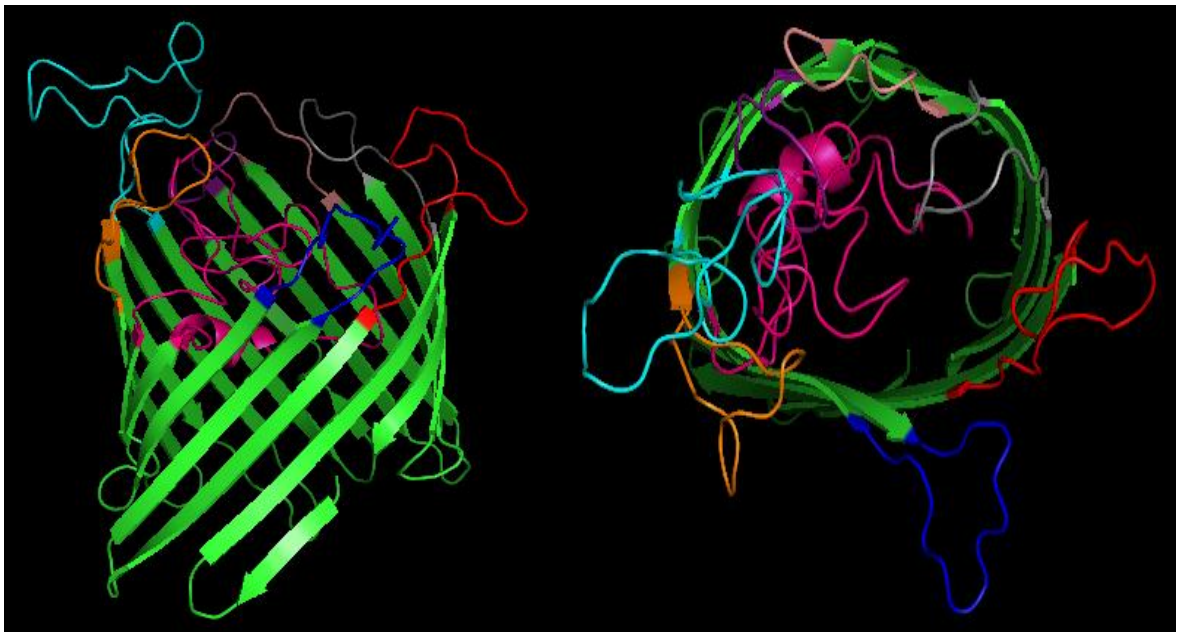

Supplemental Figure S3.40. Model of 131 (SV6) OMP P2. The protein sequence (Accession ACJ02807) is shown with predicted surface exposed regions shown in color. A side view (left) and down the β-barrel view (right) are shown.

mkktlvalav aafaasasav tvyenegtkv dfdgqlrlll eeqatkeegq sstgghtnlk
nngsrfgisi khninenlyg fgryetrlgr nskndagwgd vttdeayvgl ggygheisfg
kqavigdsig qagfdkvydv gtggikysan ntnkkgfdil tassdsainy tytgiegltl
ganynvaner dnkggvkvds tksgfglgak ytakiaesqs vtvaagythd dyksgavnkk
dkdgvyfglk yvnapftvav dgghgvvktd nvkekidfvr tgarfdvtpk sgvygnysyg
tykdkaykat ahqfmlgady klhkqvvtfv egrliknkds nnkkvtdqal gvglrvlw

Region	Sequence
OMP P2 Loop 1	eqatkeegqsstgghtnlknng
OMP P2 Loop 2	grnskndagwgdv
OMP P2 Loop 3	kqavigdsigqagfdkvydvgtggikysanntnkkgfdiltassdsai
OMP P2 Loop 4	nvanerdnkggvkvdstk
OMP P2 Loop 5	dyksgavnkkdkd
OMP P2 Loop 6	ktdnvkek
OMP P2 Loop 7	kdkayk
OMP P2 Loop 8	iknkdsnnkkvtdqal

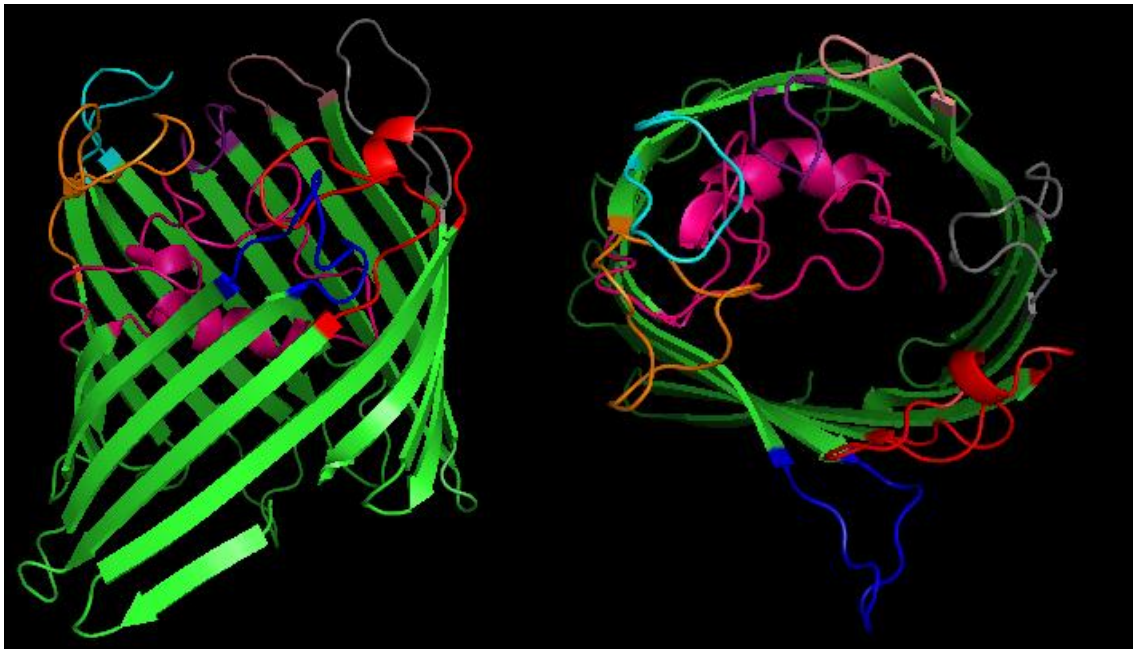

Supplemental Figure S3.41. Model of 174 (SV7) OMP P2. The protein sequence (Accession ACJ02784) is shown with predicted surface exposed regions shown in color. A side view (left) and down the β-barrel view (right) are shown.

mkktlvalav atfaasasav tvyenegtkv dfdgqlrlll ekqaskekgk sstdghtnlk
nnssrfgisi khninenlyg fgryetrlgs gsknaakwgd vttdeayvgl ggygheisfg
kqavigdsig qagfdkvygv gtggikytye veepitvnnt qgtsqgtfky sapqegfdil
tqssdsainy tytgiegltl ganynvaner ekadvkvdsi ksgfglgaky takiaesqsv
tvaagythdd yksgsvklkg kfveaggkst dhihtgkpfn kkdkdgvyfg lkyvnapftv
avdgghgvvk tddvkekinf vrtgarfdvt pksgvygnys ygtykvedfk vtahqfmlga
dyklhkqvvt fvegrliknk dsdnnkvtdk algvglrvlw

Region	Sequence
OMP P2 Loop 1	qaskekgksstdghtnlknnss
OMP P2 Loop 2	gsgsknaakwgdv
OMP P2 Loop 3	fgkqavigdsigqagfdkvygvgtggikytyeveepitvnntqgtsqgtfkysapqegfdiltqssdsa
OMP P2 Loop 4	nvanerekadvkvdsik
OMP P2 Loop 5	dyksgsvklkgkfveaggkstdhihtgkpfnk
OMP P2 Loop 6	vvktddvkek
OMP P2 Loop 7	kvedfkvta
OMP P2 Loop 8	nkdsdnnkvtdka

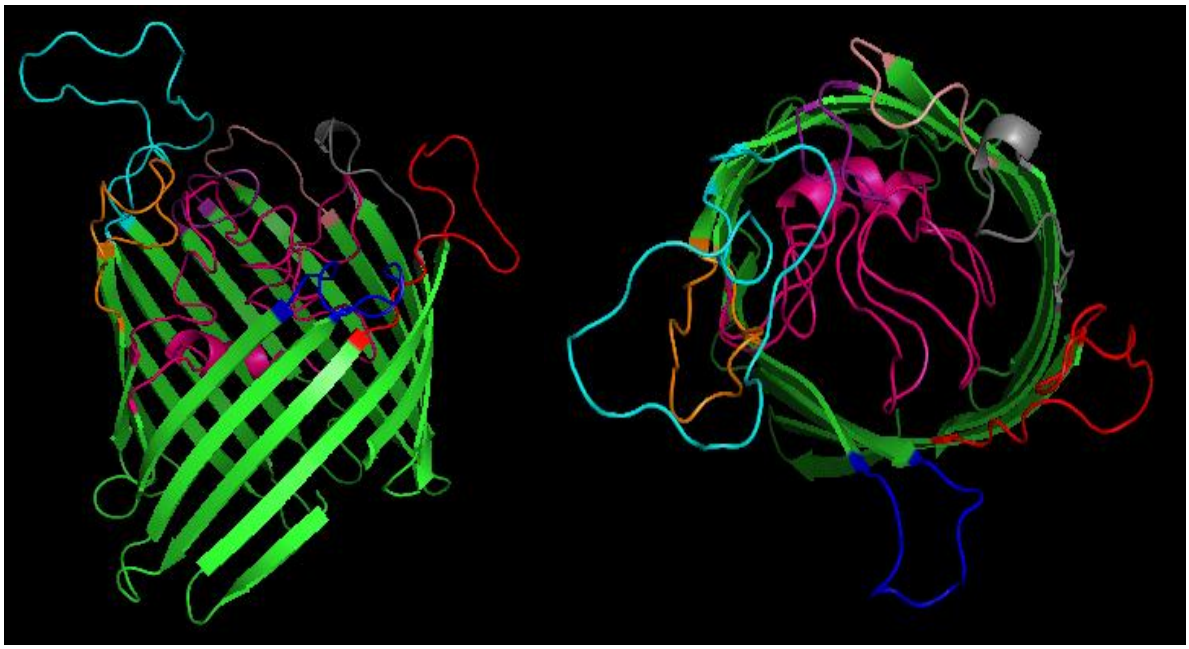

Supplemental Figure S3.42. Model of C5 (SV8) OMP P2. The protein sequence (Accession: ACJ02808) is shown with predicted surface exposed regions shown in color. A side view (left) and down the β-barrel view (right) are shown.

mkktlvalav atfaasasav tvyenegtkv dfdgqlrlll ekqaskekgk sstdghtnlk
nnssrfgisi khninenlyg fgryetrlgs gsknaakwgd vttdeayvgl ggygheisfg
kqavigdsig qagfdkvygv gtggikytyk vdesitvnnt qgtfkysaaq egfdiltqss
dsainytytg iegltlgany nvanerekad vkvdsiksgf glgakytaki aesqsvtvaa
gythddyksg svqlkgkfvq angtstdhty tesfnknknd gvyfglkyvn apftvavdgg
hgvvktddvk ekinfvrtga rfdvtpksgv ygnysygtyk vkdykatahq fmlgadyklh
kqvvtfvegr liknkdsdnn kvtdkalgvg lrvlw

Region	Sequence
OMP P2 Loop 1	qaskekgksstdghtnlknnssr
OMP P2 Loop 2	rlgsgsknaakwgdvttd
OMP P2 Loop 3	kqavigdsigqagfdkvygvgtggikytykvdesitvnntqgtfkysaaqegfdiltqssdsa
OMP P2 Loop 4	nvanerekadvkvdsiksg
OMP P2 Loop 5	dyksgsvqlkgkfvqangtstdhtytesfnk
OMP P2 Loop 6	vktddvkeki
OMP P2 Loop 7	ykvkdykata
OMP P2 Loop 8	nkdsdnnkvt

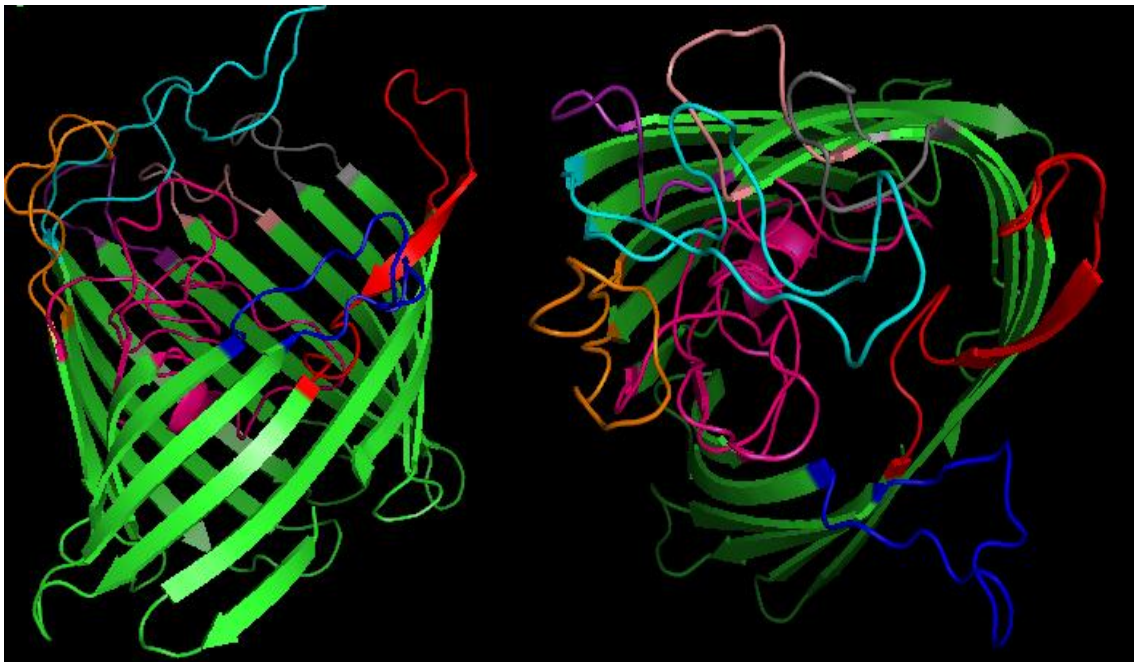

Supplemental Figure S3.43. Model of D74 (SV9) OMP P2. The protein sequence (Accession ACS71772) is shown with predicted surface exposed regions shown in color. A side view (left) and down the β-barrel view (right) are shown.

mkktlvalav aafaasasav tvyenegtkv dfdgqlrlll eeqatkekgq sstgghtnlk
nngsrfgisi khninenlyg fgryetrlgr nskndagwgd vttekayvgl ggygheisfg
kqavigdsig qagfdkvygv gtggikysan ntnkkgfdil tassdsainy tytgiegltl
ganynvaner dnkgevkvds tksgfglgak ytakiaesqs vtvaagythd dyksgavnkk
dkdgvyfglk yvnapftvav dgghgvvktd nvkekidfvr tgarfdvtpk sgvygnysyg
tykdkaykat ahqfmlgady klhkqvvtfv egrliknkds nnkkvtdqal gvglrvlw

Region	Sequence
OMP P2 Loop 1	qatkekgqsstgghtnlknng
OMP P2 Loop 2	grnskndagwgdv
OMP P2 Loop 3	kqavigdsigqagfdkvygvgtggikysanntnkkgfdiltassdsa
OMP P2 Loop 4	ynvanerdnkgevkvdstk
OMP P2 Loop 5	dyksgavnkkdkdg
OMP P2 Loop 6	vvktdnvkek
OMP P2 Loop 7	kdkayk
OMP P2 Loop 8	iknkdsnnkkvtdqa

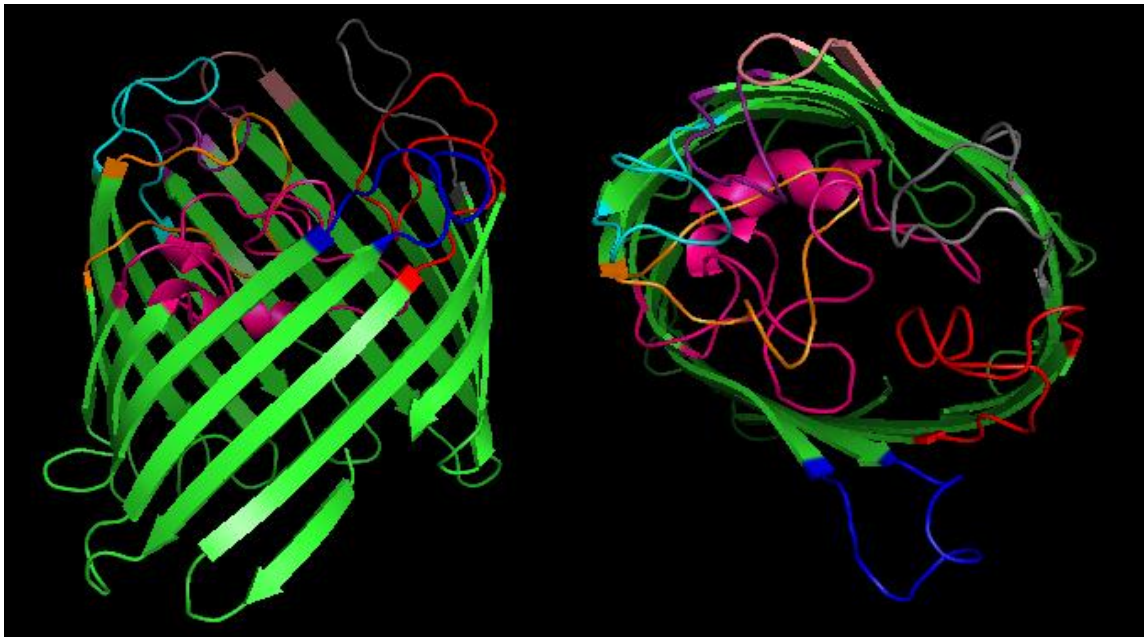

Supplemental Figure S3.44. Model of H367 (SV10) OMP P2. The protein sequence (Accession ACJ028786) is shown with predicted surface exposed regions shown in color. A side view (left) and down the β-barrel view (right) are shown.

mkktlvalav aafaasasav tvyenegtkv dfdgqlrlll ekqvkgqsst dghtnlknns
srfgisikhn inenlygfgr yetrlgsgsk naakwgdvtt deayvglggy gheisfgkqa
vigdsigqag fdkvygvgtg gikytykvne sitvdnkrgt fkysapqegf diltqssdsa
inytytgieg ltlganynva nerevdsiks gfglgakyta kiaesqsvtv aagythddyk
sgsvklkgkf veaggkstdh tytekpfnkk dkdgvyfglk yvnapftvav dgghgvvktd
dvkekinfvr tgarfdvtpk sgvygnysyg tykveafkat ahqfmlgady klhkqvvtfv
egrliknkds dnnkvtdkal gvglrvlw

Region	Sequence
OMP P2 Loop 1	vkgqsstdghtnlknns
OMP P2 Loop 2	lgsgsknaakwgdvt
OMP P2 Loop 3	kqavigdsigqagfdkvygvgtggikytykvnesitvdnkrgtfkysapqegfdiltqssdsa
OMP P2 Loop 4	nvanerevdsik
OMP P2 Loop 5	dyksgsvklkgkfveaggkstdhtytekpfnk
OMP P2 Loop 6	ktddvkek
OMP P2 Loop 7	ykveafka
OMP P2 Loop 8	nkdsdnnkvtd

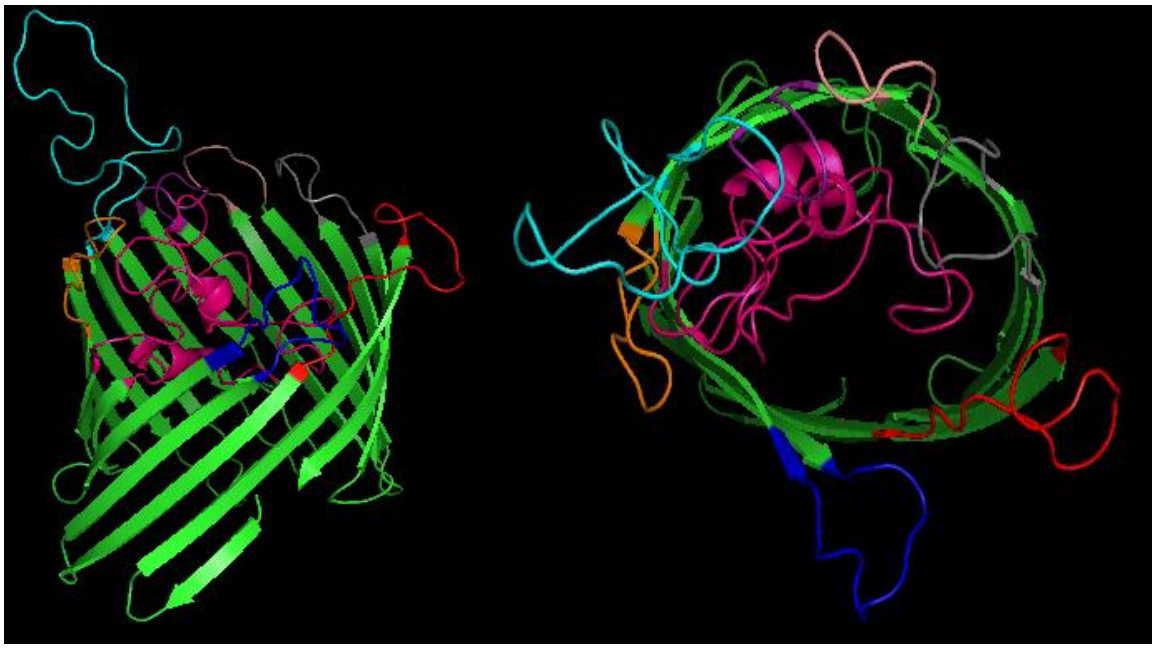

Supplemental Figure S3.45. Model of H465 (SV11) OMP P2. The protein sequence (Accession ACJ02787) is shown with predicted surface exposed regions shown in color A side view (left) and down the β-barrel view (right) are shown.

mkktlvalav aafaasasav tvyenegtkv dfdgqlrlll eeqatkekgq sstgghtnlk
nngsrfgisi khninenlyg fgryetrlgr nskndagwgd vttekayvgl ggygheisfg
kqavigdsig qagfdkvygv gtggikysan ntnkkgfdil tassdsainy tytgiegltl
ganynvaner dnkgevkvds tksgfglgak ytakiaesqs vtvaagythd dyksgavnkk
dkdgvyfglk yvnapftvav dgghgvvktd nvkekidfvr tgarfdvtpk sgvygnysyg
tykdkaykat ahqfmlgady klhkqvvtfv egrliknkds nnkkvtdqal gvglrvlw

Region	Sequence
OMP P2 Loop 1	eqatkekgqsstgghtnlknng
OMP P2 Loop 2	grnskndagwgdv
OMP P2 Loop 3	kqavigdsigqagfdkvygvgtggikysanntnkkgfdiltassdsa
OMP P2 Loop 4	ynvanerdnkgevkvdstk
OMP P2 Loop 5	dyksgavnkkdkdg
OMP P2 Loop 6	vvktdnvkek
OMP P2 Loop 7	kdkay
OMP P2 Loop 8	iknkdsnnkkvtdqa

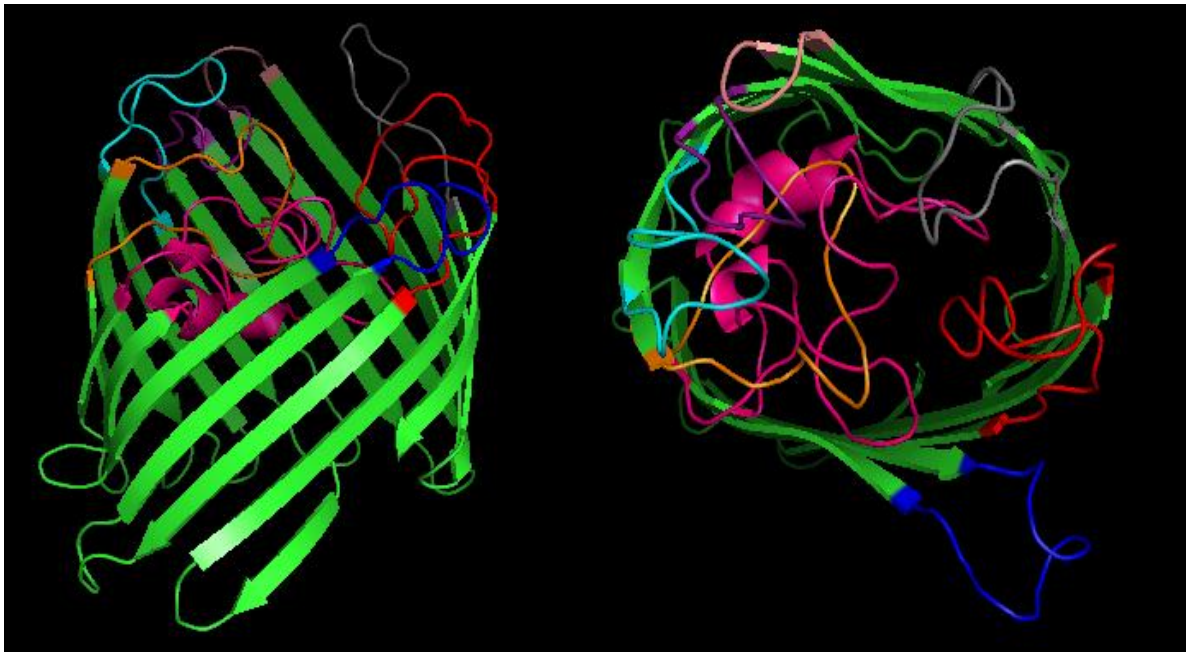

Supplemental Figure S3.46. Model of H425 (SV12) OMP P2. The protein sequence (Accession ACJ02788) is shown with predicted surface exposed regions shown in color. A side view (left) and down the β-barrel view (right) are shown.

mkktlvalav aafaasasav tvyenegtkv dfdgqlrlll eeqatkekgq sstrghtnlk
nnssrfgisi khninenlyg fgryetrlds nsenaagwgd vktkyayvgl ggygheisfg
kqavigdsig qagfdkvygv gtggikysan ntnkkgfdil tsdsdsainy tytgiegltl
ganynvaner dkktgevnvg stksgfglga kytakiaesq svtvaagyth ddyksgsvnk
kdkdgvyfgl kyvnapftva vdgghgvekt gnvkekidfv rtgarfdvtp ksgvygnysy
gtykdkayka tahqfmlgad yklhkqvvtf vegrliknkd snnkkvtdqa lgvglrvlw

Region	Sequence
OMP P2 Loop 1	qatkekgqsstrghtnlk
OMP P2 Loop 2	ldsnsenaagwgdv
OMP P2 Loop 3	kqavigdsigqagfdkvygvgtggikysanntnkkgfdiltsdsdsa
OMP P2 Loop 4	nvanerdkktgevnvgstk
OMP P2 Loop 5	dyksgsvnkkd
OMP P2 Loop 6	ktgnvkek
OMP P2 Loop 7	ykdkayk
OMP P2 Loop 8	iknkdsnnkkvtdqal

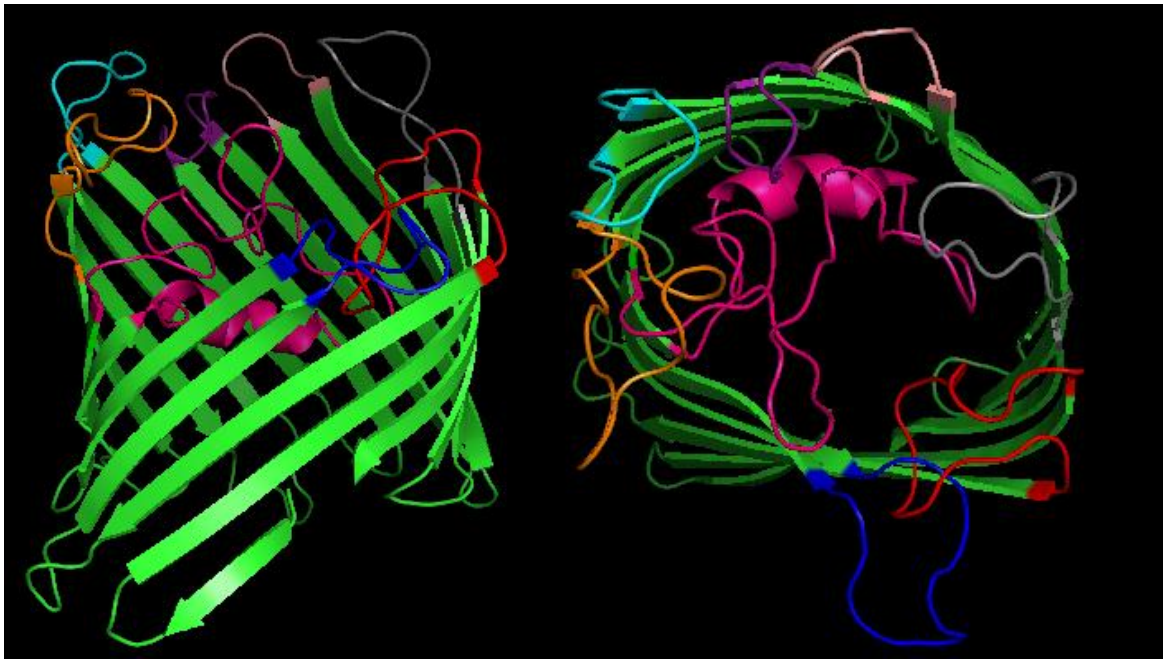

Supplemental Figure S3.47. Model of 84-17975 (SV13) OMP P2. The protein sequence (Accession ACJ02789) is shown with predicted surface exposed regions shown in color. A side view (left) and down the β-barrel view (right) are shown.

mkktlvalav aafaasasav tvyenegtkv dfdgqlrlll eeqatkekgq sstgghtnlk
nngsrfgisi khninenlyg fgryetrlds nsknaagwgd vktkyayvgl ggygheisfg
kqavigdsig qagfdkvygv gtggikysan ntnkkgfdil tsdsdsainy tytgiegltl
ganynvaner dkktgevnvg stksgfglga kytakiaesq svtvaagyth ddyksgsvnk
kdkdgvyfgl kyvnapftva vdgghgvekt gnvkekidfv rtgarfdvtp ksgvygnysy
gtykdkayka tahqfmlgad yklhkqvvtf vegrliknkd snnkkvtdqa lgvglrvlw

Region	Sequence
OMP P2 Loop 1	qatkekgqsstgghtnl
OMP P2 Loop 2	dsnsknaagwgdv
OMP P2 Loop 3	fgkqavigdsigqagfdkvygvgtggikysanntnkkgfdiltsdsdsainy
OMP P2 Loop 4	nvanerdkktgevnvgstksg
OMP P2 Loop 5	ddyksgsvnkkdk
OMP P2 Loop 6	ktgnvkeki
OMP P2 Loop 7	ykdkaykata
OMP P2 Loop 8	nkdsnnkkvtd

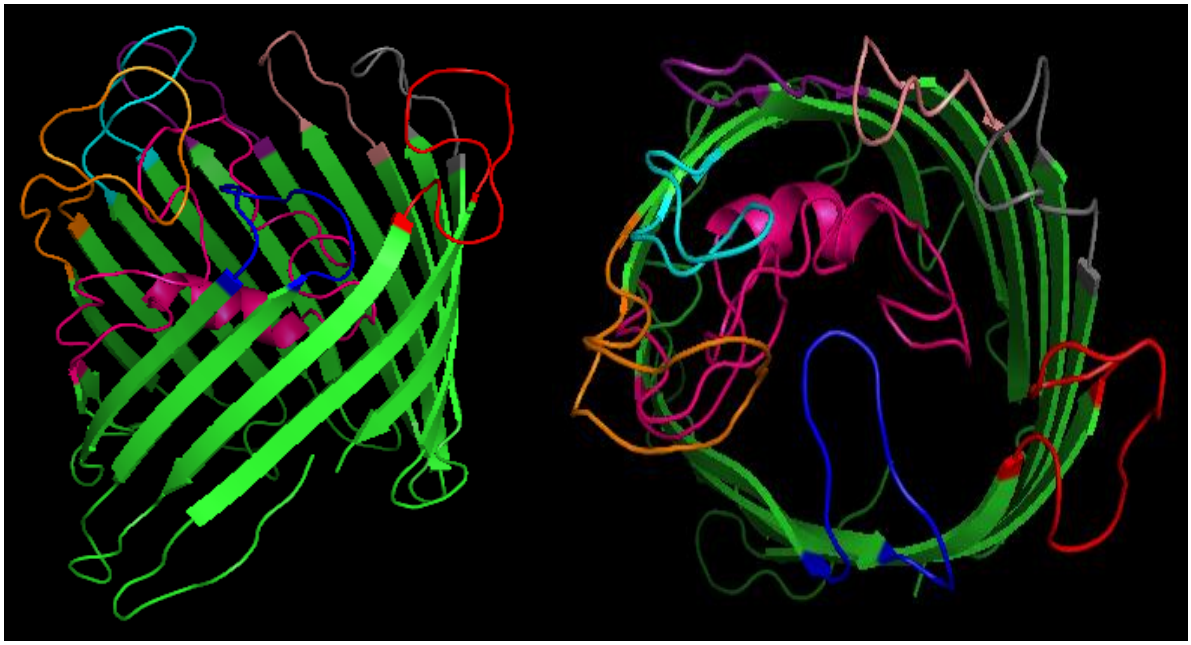

Supplemental Figure S3.48. Model of 84-22113 (SV14) OMP P2. The protein sequence (Accession ACJ02790) is shown with predicted surface exposed regions shown in color. A side view (left) and down the β-barrel view (right) are shown.

mkktlvalav aafaasasav tvyenegtkv dfdgqlrlll eeqatkekgq sstrghtnlk
nnssrfgisi khninenlyg fgryetrlds nsenaagwgd vktkyayvgl ggygheisfg
kqavigdsig qagfdkvygv gtggikysan ntnkkgfdil tdssdsainy tytgiegltl
ganynvaner dkktgevnvg stksgfglga kytakiaesq svtvaagyth ddyksgavnk
kdkdgvyfgl kyvnapftva vdgghgvvkt dnvkekidfv rtgarfdvtp ksgvygnysy
gtykdkayka tahqfmlgad yklhkqvvtf vegrliknkd snnkkvtdqa lgvglrvlw

Region	Sequence
OMP P2 Loop 1	eqatkekgqsstrghtnlknns
OMP P2 Loop 2	dsnsenaagwgdv
OMP P2 Loop 3	kqavigdsigqagfdkvygvgtggikysanntnkkgfdiltdssdsa
OMP P2 Loop 4	nvanerdkktgevnvgstk
OMP P2 Loop 5	ddyksgavnkk
OMP P2 Loop 6	ktdnvkek
OMP P2 Loop 7	kdkaykat
OMP P2 Loop 8	iknkdsnnkkvtdqal

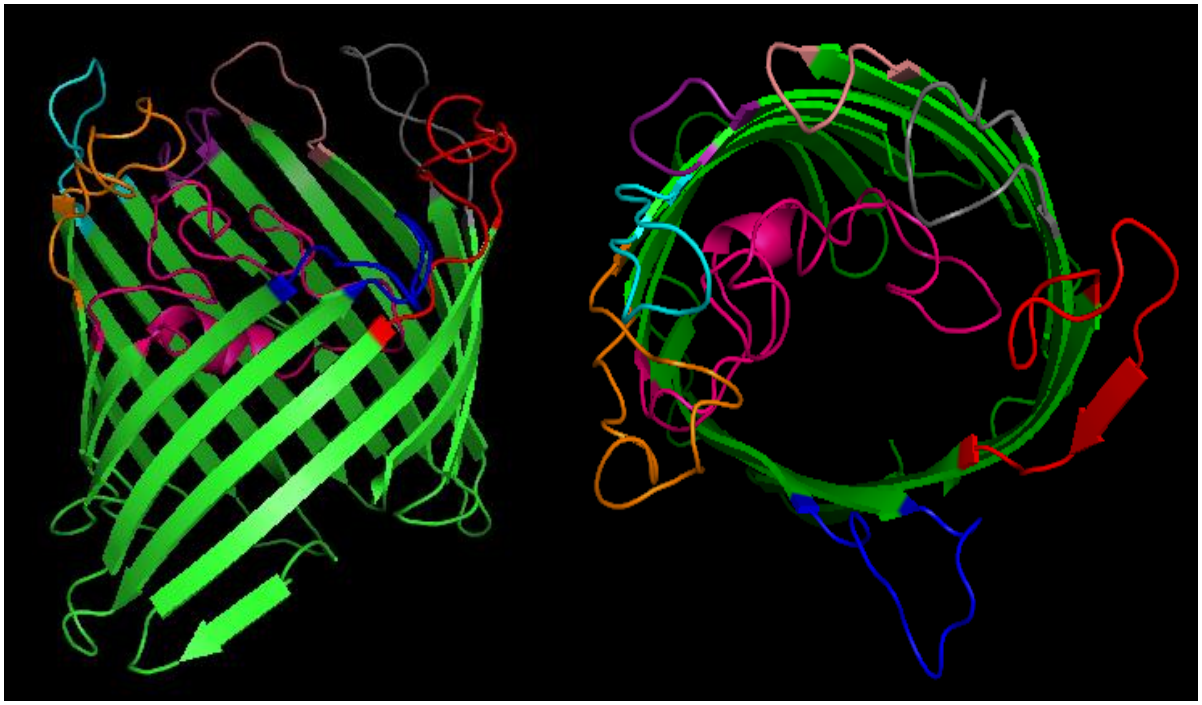

Supplemental Figure S3.49. Model of 84-15995 (SV15) OMP P2. The protein sequence (Accession: ACJ02791) is shown with predicted surface exposed regions shown in color. A side view (left) and down the β-barrel view (right) are shown.

mkktlvalav aafaasasav tvyenegtkv dfdgqlrlll eeqatkekgq sstrghtnlk
nnssrfgisi khninenlyg fgryetrlds nsenaagwgd vktkyayvgl ggygheisfg
kqavigdsig qagfdkvygv gtggikysan ntnkkgfdil tsdsdsainy tytgiegltl
ganynvaner dkktgevnvg stksgfglga kytakiaesq svtvaagyth ddyksgsvnk
kdkdgvyfgl kyvnapftva vdgghgvekt gnvkekidfv rtgarfdvtp ksgvygnysy
gtykdkayka tahqfmlgad yklhkqvvtf vegrliknkd snnkkvtdqa lgvglrvlw

Region	Sequence
OMP P2 Loop 1	eqatkekgqsstrghtnlknns
OMP P2 Loop 2	dsnsenaagwg
OMP P2 Loop 3	kqavigdsigqagfdkvygvgtggikysanntnkkgfdiltsdsdsa
OMP P2 Loop 4	nvanerdkktgevnvg stk
OMP P2 Loop 5	ddyksgsvnkkd
OMP P2 Loop 6	ktgnvk
OMP P2 Loop 7	kdkayka
OMP P2 Loop 8	iknkdsnnkkvtdqa

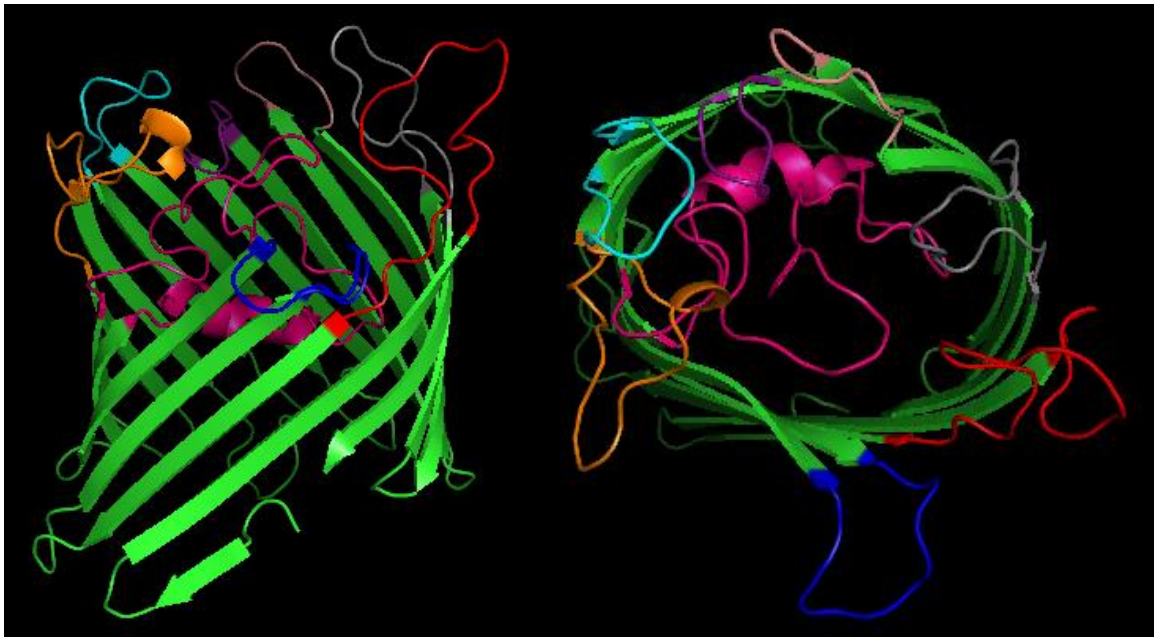

Supplemental Figure S3.50. Model of 2170B (SV4) OMP P2. The protein sequence (Accession ACJ02776) is shown with predicted surface exposed regions shown in color. A side view (left) and down the β-barrel view (right) are shown.

mkktlvalav atfaasasav tvyenegtkv dfdgqlrlll ekqaskekgk sstdghtnlk
nnssrfgisi khninenlyg fgryetrlgs gsknaakwgd vttdeayvgl ggygheisfg
kqavigdsig qagfdkvygv gtggikytye veesitvdnk qgtfkysapq egfdiltqss
dsainytytg iegltlgany nvanereead vkvdsiksgf glgakytaki aesqsvtvaa
gythddyksg svklkgkfvq angtstdhih tekpfnkkdk dgvyfglkyv napftvavdg
ghgvvkddv kekinfvrtg arfdvtpksg vygnysygty kkvedfkvta hqfmlgadyk
lhkqvvtfve grliknkdsd nnkvtdkalg vglrvlw

Region	Sequence
OMP P2 Loop 1	ekqaskekgksstdghtnlknnss
OMP P2 Loop 2	lgsgsknaakwgdvt
OMP P2 Loop 3	fgkqavigdsigqagfdkvygvgtggikytyeveesitvdnkqgtfkysapqegfdiltqssdsa
OMP P2 Loop 4	nvanereeadvkvdsik
OMP P2 Loop 5	dyksgsvklkgkfvqangtstdhihtekpfnk
OMP P2 Loop 6	vkkddvkek
OMP P2 Loop 7	kkvedfkv
OMP P2 Loop 8	knkdsdnnkvtdkal

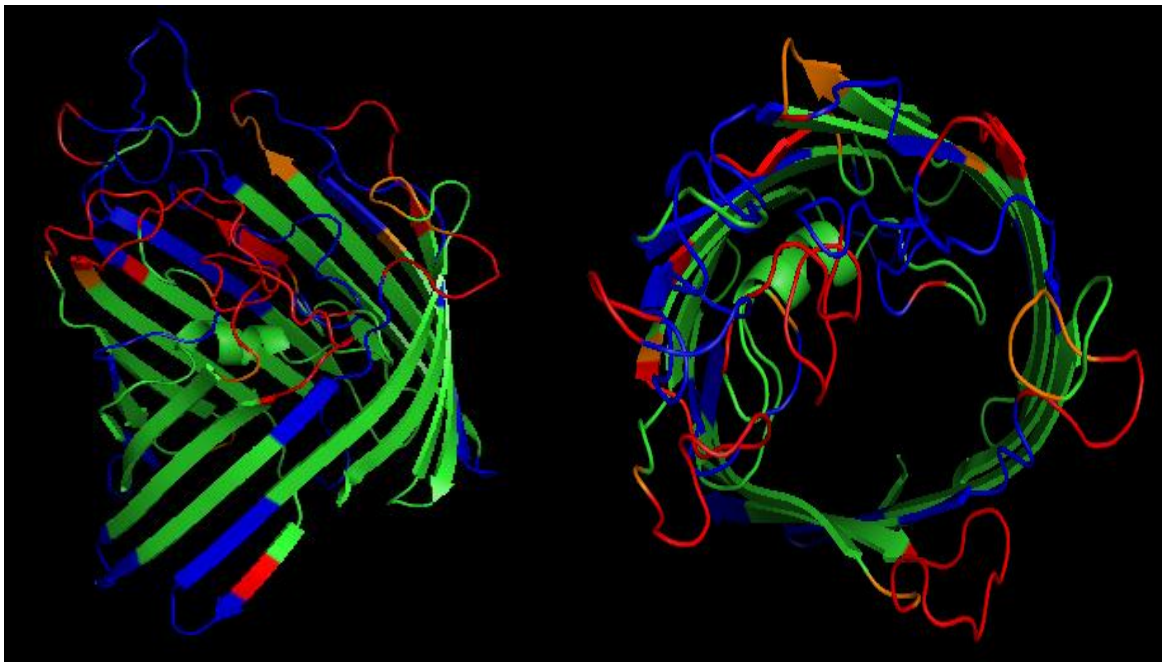

Supplemental Figure S3.51. Predicted antigenic sites and continuous B-cell epitopes of No. 4 (SV1) OMP P2 extended form. Antigenic sites are highlighted in orange (moderate < 5 net votes) and red (high >5 net votes). Predicted continuous B-cell epitopes (>70% probability) are shown in blue. A side view (left) and down the β-barrel view (right) are shown..

mkktlvalav aafaasasav tvyenegtkv dfdgqlrlll eeqatkekgq sstgghtnlk
nngsrfgisi khninenlyg fgryetrlgs gsknaaewgd vtteeayvgl ggygheisfg
kqavigdsig qagfdkvygv gtggikysan ntnkkgfdil tassdsainy tytgieqltl
ganynvaner ddkggvkvgs iksgfglgak ytakiaesqs vtvaagythd dyksgavnkk
dkdgvyfglk yvnapftvav dgghgvvktd nvkekidfvr tgarfdvtpk sgvygnysyg
tykdkaykat ahqfmlgady klhkqvvtfv egrliknkds nnnkvtdqal gvglrvlw

Region	Sequence
OMP P2 Loop 1	lleeqatkekgqsstgghtnlknng
OMP P2 Loop 2	gsgsknaaewgdv
OMP P2 Loop 3	kqavigdsigqagfdkvygvgtggikysanntnkkgfdiltassdsa
OMP P2 Loop 4	nvanerddkggvkvgsik
OMP P2 Loop 5	dyksgavnkk
OMP P2 Loop 6	ktdnvkek
OMP P2 Loop 7	kdkayk
OMP P2 Loop 8	knkdsdnnkvtdqal

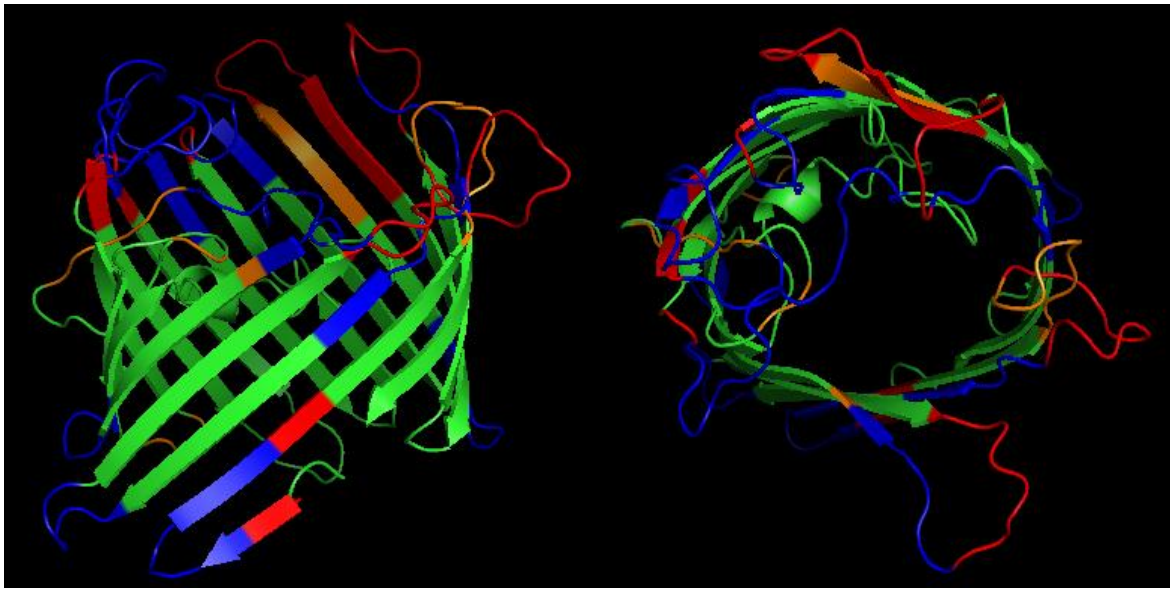

Supplemental Figure S3.52. Predicted antigenic sites and continuous B-cell epitopes of No. 4 (SV1) OMP P2. Antigenic sites are highlighted in orange (moderate < 5 net votes) and red (high >5 net votes). Predicted continuous B-cell epitopes (>70% probability) are shown in blue. A side view (left) and down the β-barrel view (right) are shown.

mkktlvalav aafaasasav tvyenegtkv dfdgqlrlll ekqaskvkgq sstsghtdlk
nngsrfgisi khninenlyg fgryetrlds nsknaagwgd vktkyayvgl ggygheisfg
kqvvigdsig qagfdkvydv gstgirikyp ansadkkgfd iltsdsdsai nytytgiegl
tlganynvan erdkktgevk vdsaksgfgl gakytakiae sqsvtvaagy thddyksgav
nkkdkdgvyf glkyvnapft vavdgghgvv ktdnvkekid fvrtgarfdv tpksgvygny
sygtykdkay katahqfmlg adyklhkqvv tfvegrlikn kdsnnkkvtd kalgvglrvlw

Region	Sequence
OMP P2 Loop 1	kqaskvkgqsstsghtdlknng
OMP P2 Loop 2	dsnsknaagwgdv
OMP P2 Loop 3	kqvvigdsigqagfdkvydvgstgirikypansadkkgfdiltsdsdsa
OMP P2 Loop 4	nvanerdkktgevkvdsak
OMP P2 Loop 5	dyksgavnkkdk
OMP P2 Loop 6	ktdnvkek
OMP P2 Loop 7	kdkayk
OMP P2 Loop 8	iknkdsnnkkvtdka

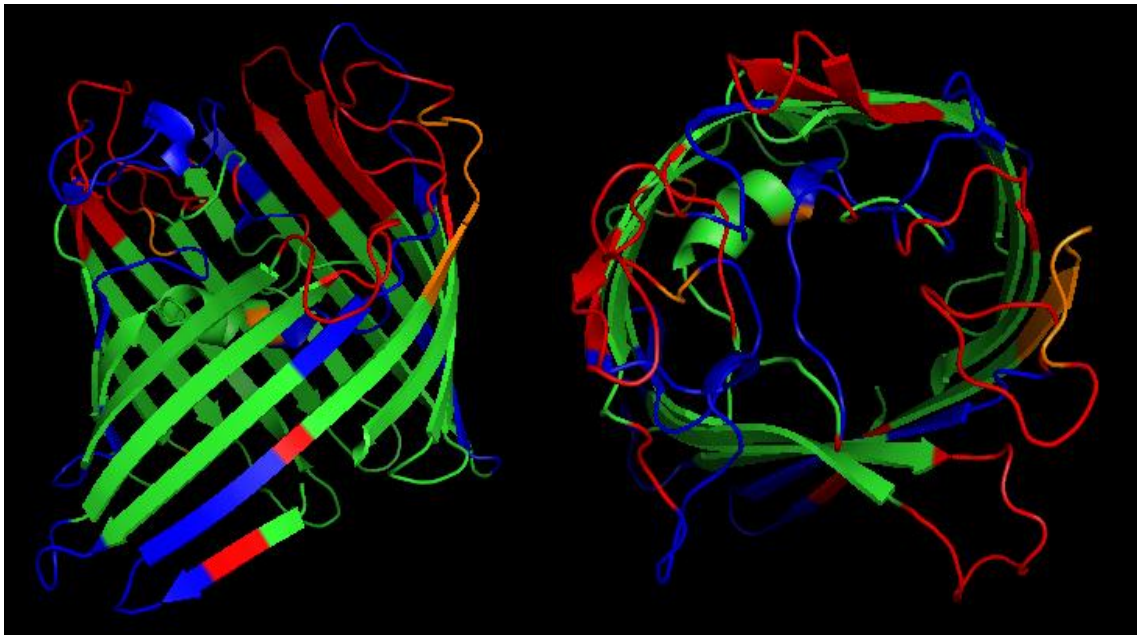

Supplemental Figure S3.53. Predicted antigenic sites and continuous B-cell epitopes of SW140 (SV2) OMP P2. Antigenic sites are highlighted in orange (moderate < 5 net votes) and red (high >5 net votes). Predicted continuous B-cell epitopes (>70% probability) are shown in blue. A side view (left) and down the β-barrel view (right) are shown.

mkktlvalav aafaasasav tvyenegtkv dfdgqlrlll ekqaskvkgq sstdghtnlk
nnssrfgisi khninenlyg fgryetrlds gsknaakwgd vttdeayvgl ggygheisfg
kqavigdsig qagfdkvygv gtggikytyk vdkpitgnnr qgtlysapqk gfdiltqssd
sainytytgi egltlganyn vanerekadv kvdsiksgfg lgakytakia esqsvtvaag
ythddyksgs velkgkfvqt ngtstnhtyt esfnkkdkdg vyfglkyvna pftvavdggh
gvvktddvke kinfvrtgar fdvtpksgvy gnysygtykv edfkatahqf mlgadyklhk
qvvtfvegrl iknknsdnnk vtdkalgvgl rvlw

Region	Sequence
OMP P2 Loop 1	qaskvkgqsstdghtnlknns
OMP P2 Loop 2	dsgsknaakwgdv
OMP P2 Loop 3	kqavigdsigqagfdkvygvgtggikytykvdkpitgnnrqgtlysapqkgfdiltqssdsa
OMP P2 Loop 4	nvanerekadvkvdsik
OMP P2 Loop 5	dyksgsvelkgkfvqt ngtstnhtytesfnkk
OMP P2 Loop 6	gvvktddvkeki
OMP P2 Loop 7	ykvedfkat
OMP P2 Loop 8	nknsdnnkvtdkal

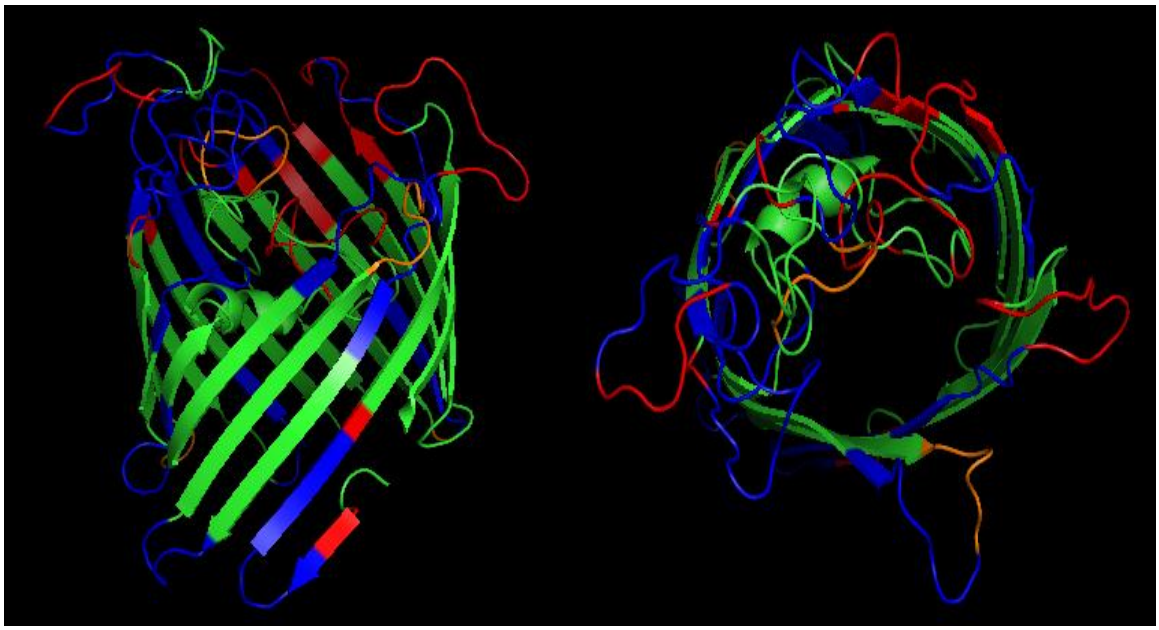

Supplemental Figure S3.54. Predicted antigenic sites and continuous B-cell epitopes of SW124 (SV4) OMP P2. Antigenic sites are highlighted in orange (moderate < 5 net votes) and red (high >5 net votes). Predicted continuous B-cell epitopes (>70% probability) are shown in blue. A side view (left) and down the β-barrel view (right) are shown.

mkktlvalav aafaasasav tvyenegtkv dfdgqlrlll eeqatkekgq sstgghtnlk
nngsrfgisi khninenlyg fgryetrlds nsknaagwgd vktkyayvgl ggygheisfg
kqdvigdsig qagfdkvygv gtggikysan ntnkkgfdil tsdsdsainy tytgiegltl
ganynvaner dkktgevnvg stksgfglga kytakiaesq svtvaagyth ddyksgsvnk
kdkdgvyfgl kyvnapftva vdgghgvekt gnvkekidfv rtgarfdvtp ksgvygnysy
gtykdkayka tahqfmlgad yklhkqvvtf vegrliknkd snnkkvtdqa lgvglrvlw

Region	Sequence
OMP P2 Loop 1	qatkekgqsstgghtnlknngsr
OMP P2 Loop 2	trldsnsknaagwgdvktk
OMP P2 Loop 3	kqdvigdsigqagfdkvygvtggikysanntnkkgfdiltsdsdsa
OMP P2 Loop 4	nvanerdkktgevnvgstk
OMP P2 Loop 5	yksgsvnkk
OMP P2 Loop 6	tgnv
OMP P2 Loop 7	ykdkayka
OMP P2 Loop 8	nkdsnnkkvt

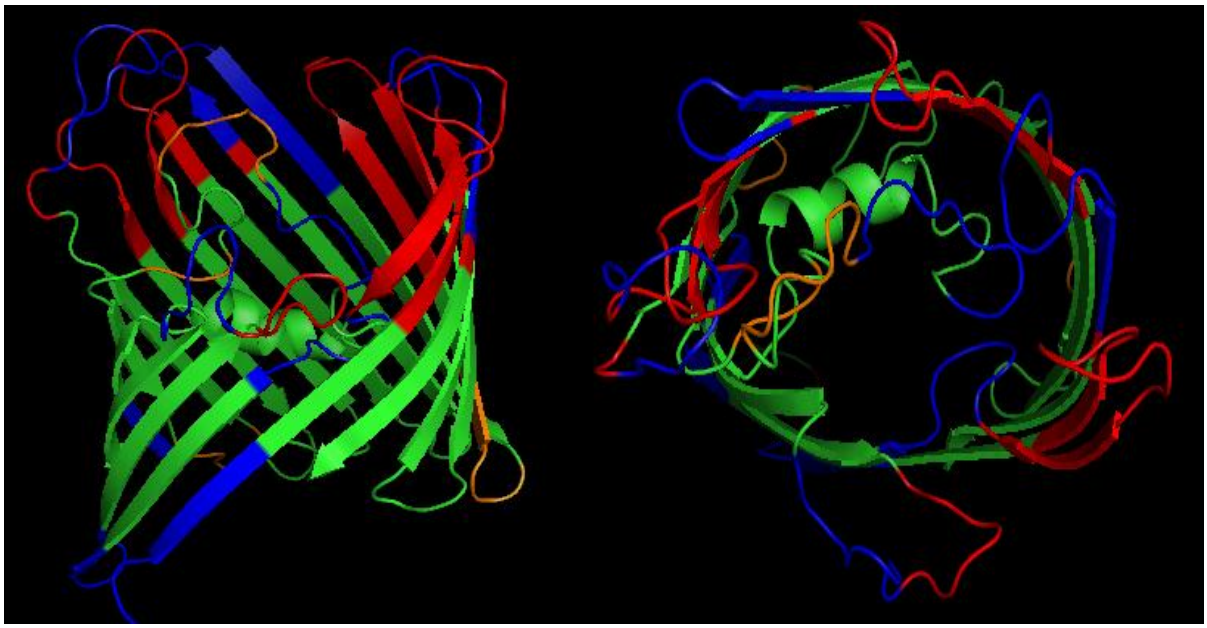

Supplemental Figure S3.55. Predicted antigenic sites and continuous B-cell epitopes of Nagasaki (SV5) OMP P2. Antigenic sites are highlighted in orange (moderate < 5 net votes) and red (high >5 net votes). Predicted continuous B-cell epitopes (>70% probability) are shown in blue. A side view (left) and down the β-barrel view (right) are shown.

mkktlvalav atfaasasav tvyenegtkv dfdgqlrlll ekkaskekgk sstdghtnlk
nnssrfgisi khninenlyg fgryetrlgs gsknaakwgd vttdeayvgl ggygheisfg
kqavigdsig qagfdkvygv gtggikytyk vdesitvnnt qgtfkysapq egfdiltqss
dsainytytg iegltlgany nvanerekad vkvdsiksgf glgakytaki aesqsvtvaa
gythddyksg svqlkgkfvq angtstdhty tesfnkknkd gvyfglkyvn apftvavdgg
hgvvktddvk ekinfvrtga rfdvtpksgv ygnysygtyk vedykatahq fmlgadyklh
kqvvtfvegr liknkdsdnn kvtdkalgvg lrvlw

Region	Sequence
OMP P2 Loop 1	kaskekgksstdghtnlknns
OMP P2 Loop 2	lgsgsknaakwgdvt
OMP P2 Loop 3	kqavigdsigqagfdkvygvgtggikytykvdesitvnntqgtfkysapqegfdiltqssdsa
OMP P2 Loop 4	nvanerekadvkvdsiks
OMP P2 Loop 5	dyksgsvqlkgkfvqangtstdhtytesfnkk
OMP P2 Loop 6	gvvktddvkek
OMP P2 Loop 7	kvedykata
OMP P2 Loop 8	nkdsdnnkvtdkal

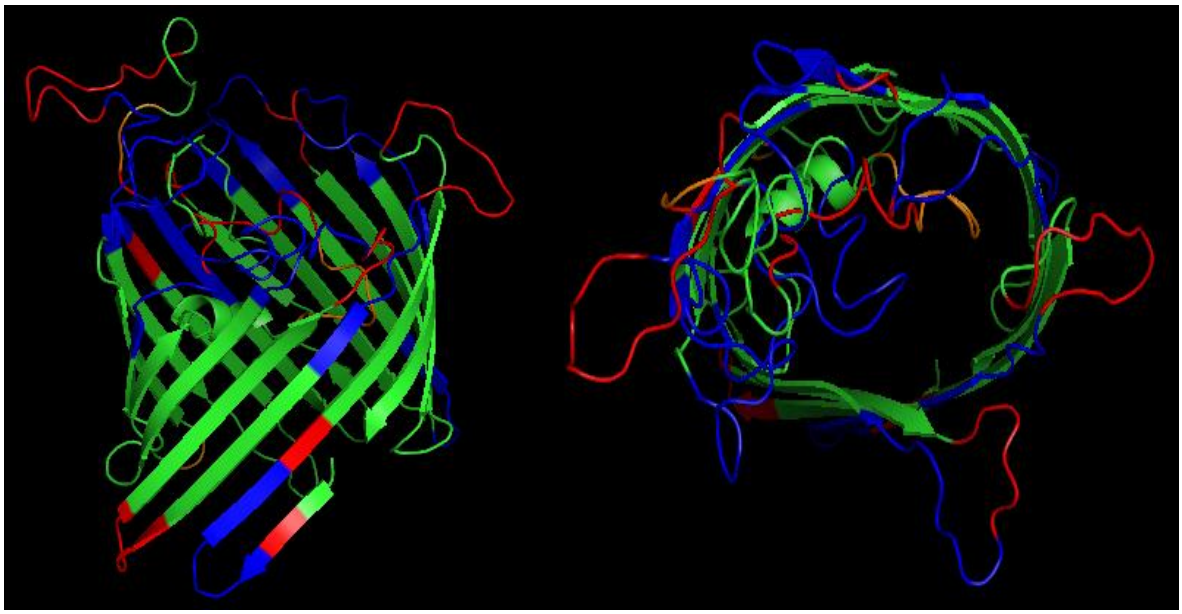

Supplemental Figure S3.56. Predicted antigenic sites and continuous B-cell epitopes of 131 (SV6) OMP P2. Antigenic sites are highlighted in orange (moderate < 5 net votes) and red (high >5 net votes). Predicted continuous B-cell epitopes (>70% probability) are shown in blue. A side view (left) and down the β-barrel view (right) are shown.

mkktlvalav aafaasasav tvyenegtkv dfdgqlrlll eeqatkeegq sstgghtnlk
nngsrfgisi khninenlyg fgryetrlgr nskndagwgd vttdeayvgl ggygheisfg
kqavigdsig qagfdkvydv gtggikysan ntnkkgfdil tassdsainy tytgieglt l
ganynvaner dnkggvkvds tksgfglgak ytakiaesqs vtvaagythd dyksgavnkk
dkdgvyfglk yvnapftvav dgghgvvktd nvkekidfvr tgarfdvtpk sgvygnysyg
tykdkaykat ahqfmlgady klhkqvvtfv egrliknkds nnkkvtdqal gvglrvlw

Region	Sequence
OMP P2 Loop 1	eqatkeegqsstgghtnlknng
OMP P2 Loop 2	grnskndagwgdv
OMP P2 Loop 3	kqavigdsigqagfdkvydvgtggikysanntnkkgfdiltassdsai
OMP P2 Loop 4	nvanerdnkggvkvdstk
OMP P2 Loop 5	dyksgavnkkdkd
OMP P2 Loop 6	ktdnvkek
OMP P2 Loop 7	kdkayk
OMP P2 Loop 8	iknkdsnnkkvtdqal

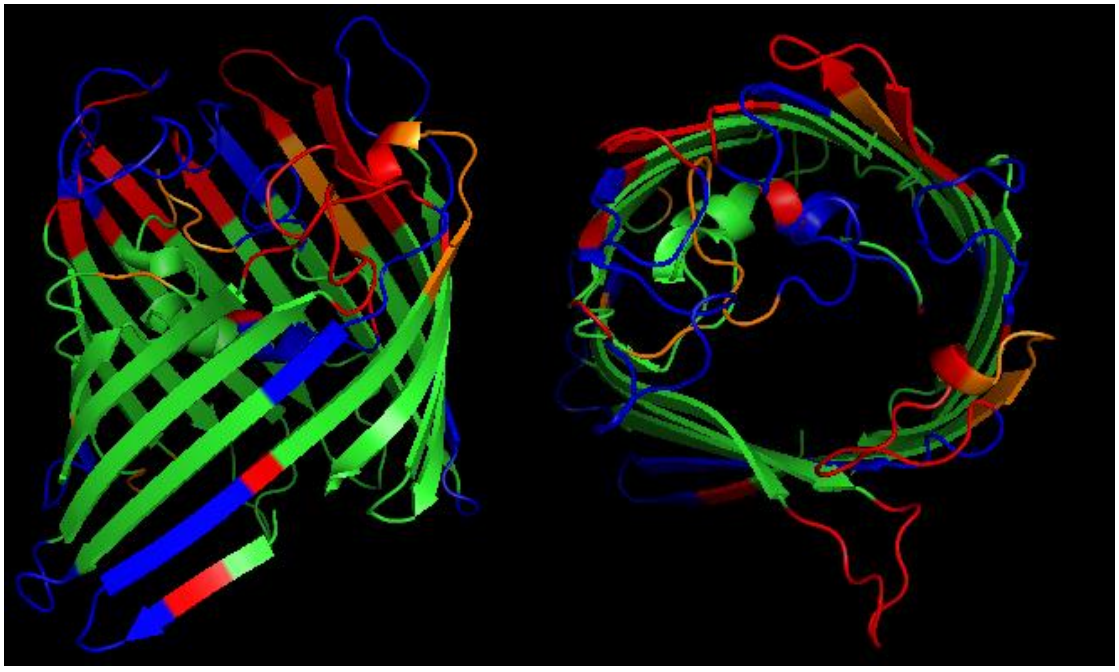

Supplemental Figure S3.57. Predicted antigenic sites and continuous B-cell epitopes of 174 (SV7) OMP P2. Antigenic sites are highlighted in orange (moderate < 5 net votes) and red (high >5 net votes). Predicted continuous B-cell epitopes (>70% probability) are shown in blue. A side view (left) and down the β-barrel view (right) are shown.

mkktlvalav atfaasasav tvyenegtkv dfdgqlrlll ekqaskekgk sstdghtnlk
nnssrfgisi khninenlyg fgryetrlgs gsknaakwgd vttdeayvgl ggygheisfg
kqavigdsig qagfdkvygv gtggikytye veepitvnnt qgtsqgtfky sapqegfdil
tqssdsainy tytgiegltl ganynvaner ekadvkvdsi ksgfglgaky takiaesqsv
tvaagythdd yksgsvklkg kfveaggkst dhihtgkpfn kkdkdgvyfg lkyvnapftv
avdgghgvvk tddvkekinf vrtgarfdvt pksgvygnys ygtykvedfk vtahqfmlga
dyklhkqvvt fvegrliknk dsdnnkvtdk algvglrvlw

Region	Sequence
OMP P2 Loop 1	qaskekgksstdghtnlknnss
OMP P2 Loop 2	gsgsknaakwgdv
OMP P2 Loop 3	fgkqavigdsigqagfdkvygvgtggikytyeveepitvnntqgtsqgtfkysapqegfdiltqssdsa
OMP P2 Loop 4	nvanerekadvkvdsik
OMP P2 Loop 5	dyksgsvklkgkfveaggkstdhihtgkpfnk
OMP P2 Loop 6	vvktddvkek
OMP P2 Loop 7	kvedfkvta
OMP P2 Loop 8	nkdsdnnkvtdka

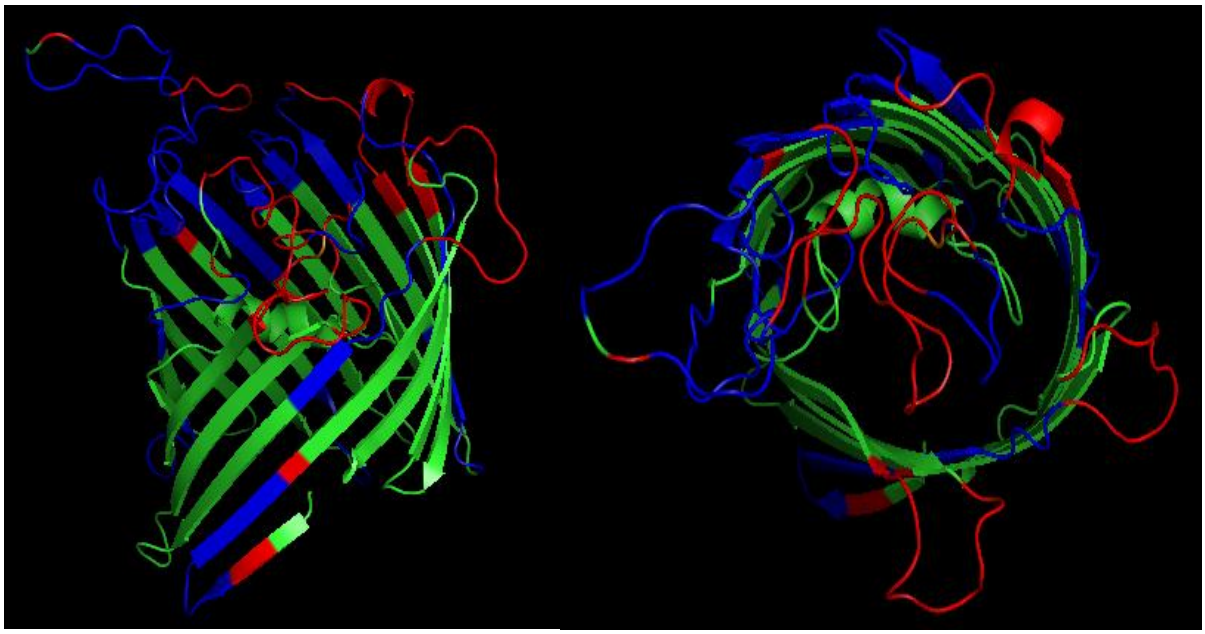

Supplemental Figure S3.58. Predicted antigenic sites and continuous B-cell epitopes of C5 (SV8) OMP P2. Antigenic sites are highlighted in orange (moderate < 5 net votes) and red (high >5 net votes). Predicted continuous B-cell epitopes (>70% probability) are shown in blue. A side view (left) and down the β-barrel view (right) are shown.

mkktlvalav atfaasasav tvyenegtkv dfdgqlrlll ekqaskekgk sstdghtnlk
nnssrfgisi khninenlyg fgryetrlgs gsknaakwgd vttdeayvgl ggygheisfg
kqavigdsig qagfdkvygv gtggikytyk vdesitvnnt qgtfkysaaq egfdiltqss
dsainytytg iegltlgany nvanerekad vkvdsiksgf glgakytaki aesqsvtvaa
gythddyksg svqlkgkfvq angtstdhty tesfnkknkd gvyfglkyvn apftvavdgg
hgvvktddvk ekinfvrtga rfdvtpksgv ygnysygtyk vkdykatahq fmlgadyklh
kqvvtfvegr liknkdsdnn kvtdkalgvg lrvlw

Region	Sequence
OMP P2 Loop 1	qaskekgksstdghtnlknnssr
OMP P2 Loop 2	rlgsgsknaakwgdvttd
OMP P2 Loop 3	kqavigdsigqagfdkvygvgtggikytykvdesitvnntqgtfkysaaqegfdiltqssdsa
OMP P2 Loop 4	nvanerekadvkvdsiksg
OMP P2 Loop 5	dyksgsvqlkgkfvqangtstdhtytesfnk
OMP P2 Loop 6	vktddvkeki
OMP P2 Loop 7	ykvkdykata
OMP P2 Loop 8	nkdsdnnkvt

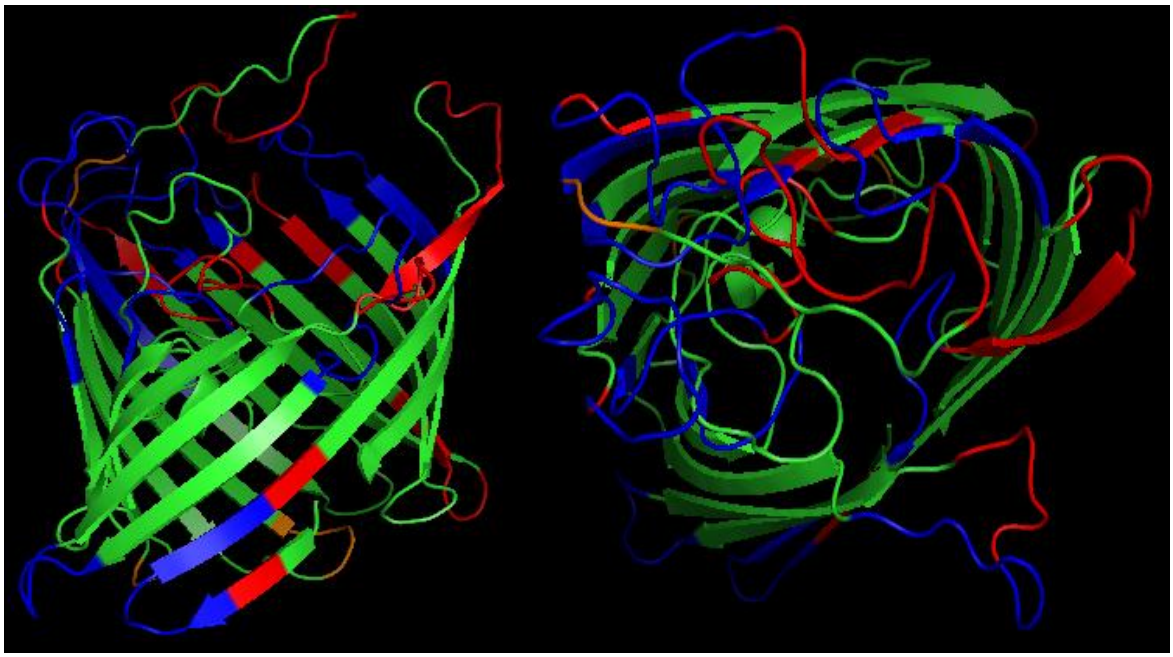

Supplemental Figure S3.59. Predicted antigenic sites and continuous B-cell epitopes of D74 (SV9) OMP P2. Antigenic sites are highlighted in orange (moderate < 5 net votes) and red (high >5 net votes). Predicted continuous B-cell epitopes (>70% probability) are shown in blue. A side view (left) and down the β-barrel view (right) are shown.

mkktlvalav aafaasasav tvyenegtkv dfdgqlrlll eeqatkekgq sstgghtnlk
nngsrfgisi khninenlyg fgryetrlgr nskndagwgd vttekayvgl ggygheisfg
kqavigdsig qagfdkvygv gtggikysan ntnkkgfdil tassdsainy tytgieqltl
ganynvaner dnkgevkvds tksgfglgak ytakiaesqs vtvaagythd dyksgavnkk
dkdgvyfglk yvnapftvav dgghgvvktd nvkekidfvr tgarfdvtpk sgvygnysyg
tykdkaykat ahqfmlgady klhkqvvtfv egrliknkds nnkkvtdqal gvglrvlw

Region	Sequence
OMP P2 Loop 1	qatkekgqsstgghtnlknng
OMP P2 Loop 2	grnskndagwgdv
OMP P2 Loop 3	kqavigdsigqagfdkvygvgtggikysanntnkkgfdiltassdsa
OMP P2 Loop 4	ynvanerdnkgevkvdstk
OMP P2 Loop 5	dyksgavnkkdkdg
OMP P2 Loop 6	vvktdnvkek
OMP P2 Loop 7	kdkayk
OMP P2 Loop 8	iknkdsnnkkvtdqa

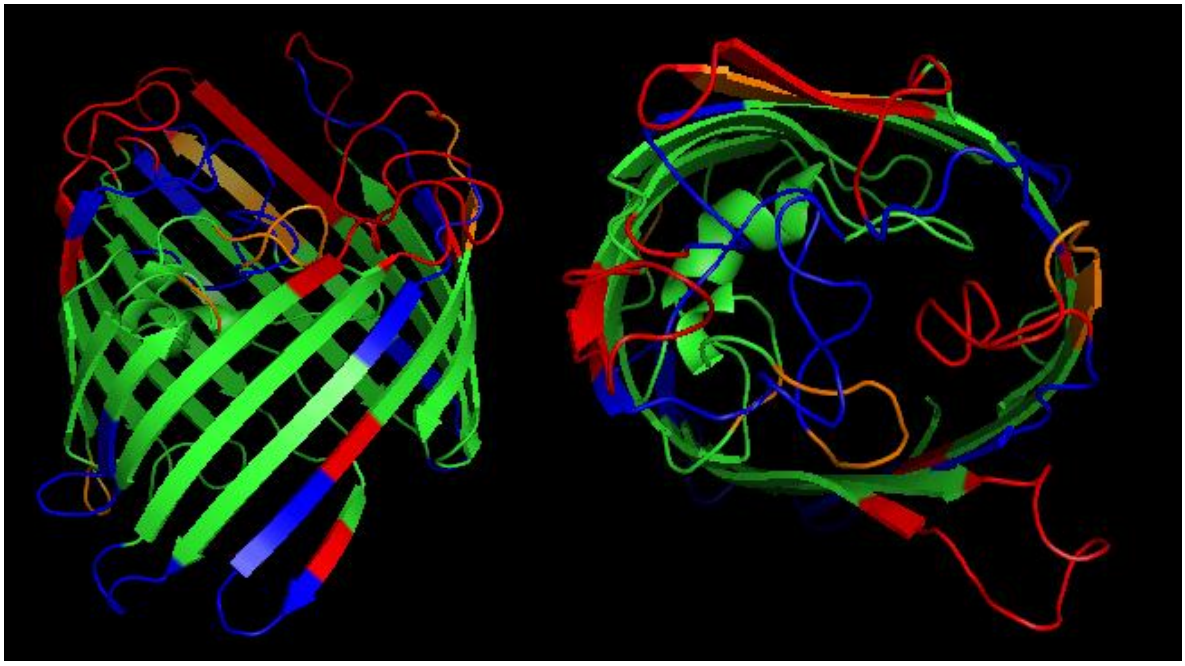

Supplemental Figure S3.60. Predicted antigenic sites and continuous B-cell epitopes of H367 (SV10) OMP P2. Antigenic sites are highlighted in orange (moderate < 5 net votes) and red (high >5 net votes). Predicted continuous B-cell epitopes (>70% probability) are shown in blue. A side view (left) and down the β-barrel view (right) are shown.

mkktlvalav aafaasasav tvyenegtkv dfdgqlrlll ekqvkgqsst dghtnlknns
srfgisikhn inenlygfgr yetrlgsgsk naakwgdvtt deayvglggy gheisfgkqa
vigdsigqag fdkvygvgtg gikytykvne sitvdnkrgt fkysapqegf diltqssdsa
inytytgieg ltlganynva nerevdsiks gfglgakyta kiaesqsvtv aagythddyk
sgsvklkgkf veaggkstdh tytekpfnkk dkdgvyfglk yvnapftvav dgghgvvktd
dvkekinfvr tgarfdvtpk sgvygnysyg tykveafkat ahqfmlgady klhkqvvtfv
egrliknkds dnnkvtdkal gvglrvlw

Region	Sequence
OMP P2 Loop 1	vkgqsstdghtnlknns
OMP P2 Loop 2	lgsgsknaakwgdvt
OMP P2 Loop 3	kqavigdsigqagfdkvygvgtggikytykvnesitvdnkrgtfkysapqegfdiltqssdsa
OMP P2 Loop 4	nvanerevdsik
OMP P2 Loop 5	dyksgsvklkgkfveaggkstdhtytekpfnk
OMP P2 Loop 6	ktddvkek
OMP P2 Loop 7	ykveafka
OMP P2 Loop 8	nkdsdnnkvtd

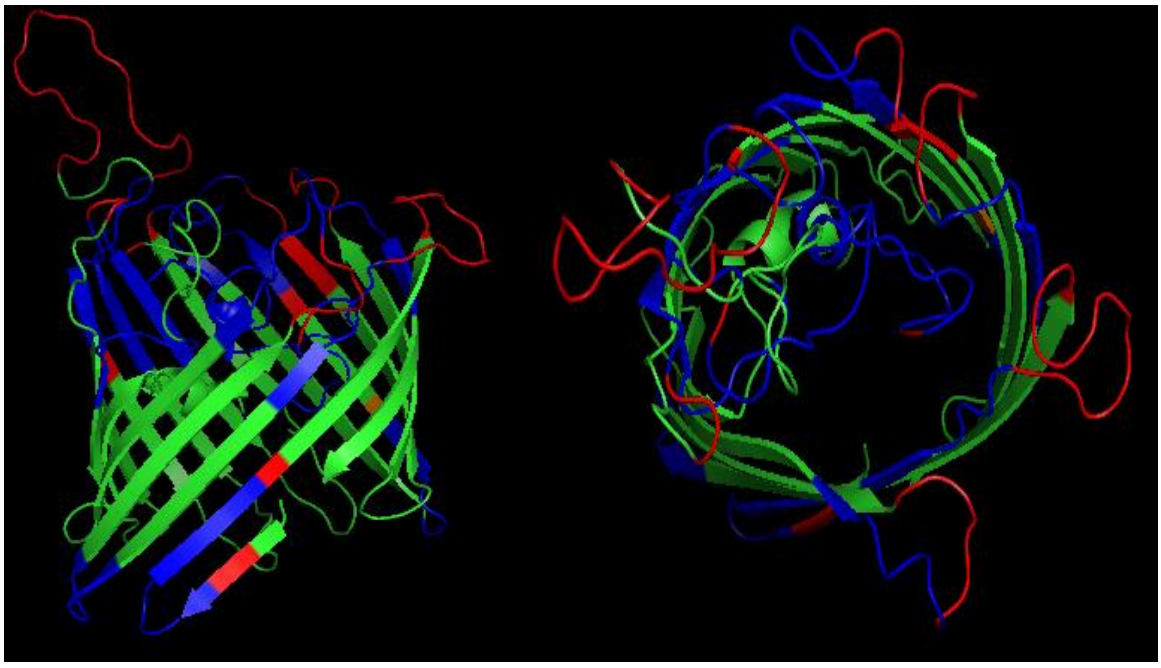

Supplemental Figure S3.61. Predicted antigenic sites and continuous B-cell epitopes of H465 (SV11) OMP P2. Antigenic sites are highlighted in orange (moderate < 5 net votes) and red (high >5 net votes). Predicted continuous B-cell epitopes (>70% probability) are shown in blue. A side view (left) and down the β-barrel view (right) are shown.

mkktlvalav aafaasasav tvyenegtkv dfdgqlrlll eeqatkekgq sstgghtnlk
nngsrfgisi khninenlyg fgryetrlgr nskndagwgd vttekayvgl ggygheisfg
kqavigdsig qagfdkvygv gtggikysan ntnkkgfdil tassdsainy tytgieqltl
ganynvaner dnkgevkvds tksgfglgak ytakiaesqs vtvaagythd dyksgavnkk
dkdgvyfglk yvnapftvav dgghgvvktd nvkekidfvr tgarfdvtpk sgvygnysyg
tykdkaykat ahqfmlgady klhkqvvtfv egrliknkds nnkkvtdqal gvglrvlw

Region	Sequence
OMP P2 Loop 1	eqatkekgqsstgghtnlknng
OMP P2 Loop 2	grnskndagwgdv
OMP P2 Loop 3	kqavigdsigqagfdkvygvgtggikysanntnkkgfdiltassdsa
OMP P2 Loop 4	ynvanerdnkgevkvdstk
OMP P2 Loop 5	dyksgavnkkdkdg
OMP P2 Loop 6	vvktdnvkek
OMP P2 Loop 7	kdkay
OMP P2 Loop 8	iknkdsnnkkvtdqa

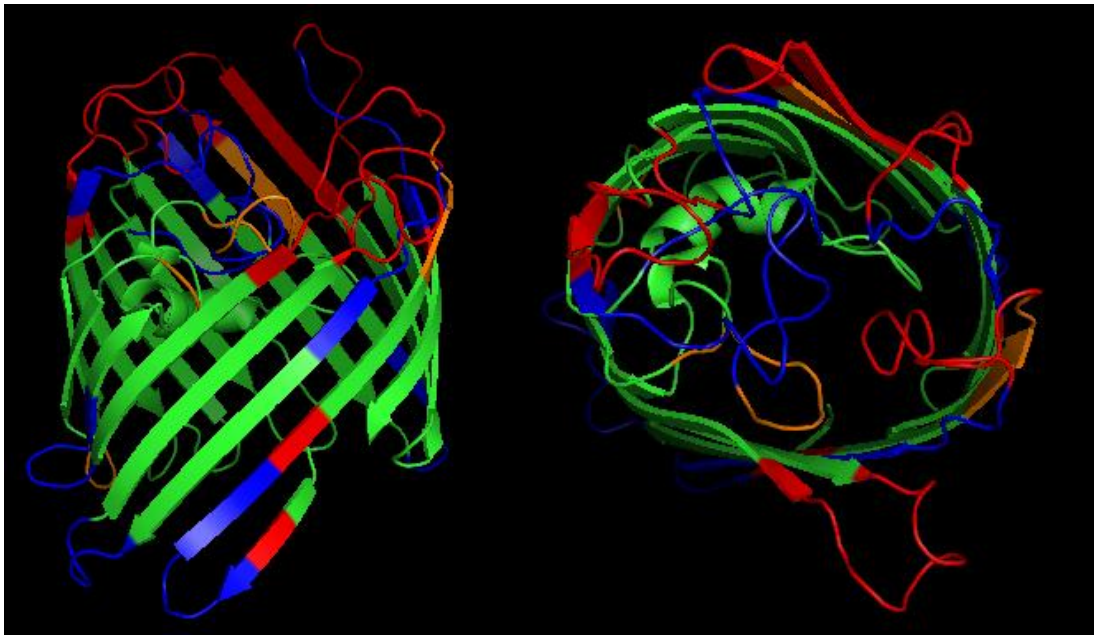

Supplemental Figure S3.62. Predicted antigenic sites and continuous B-cell epitopes of H425 (SV12) OMP P2. Antigenic sites are highlighted in orange (moderate < 5 net votes) and red (high >5 net votes). Predicted continuous B-cell epitopes (>70% probability) are shown in blue. A side view (left) and down the β-barrel view (right) are shown.

mkktlvalav aafaasasav tvyenegtkv dfdgqlrlll eeqatkekgq sstrghtnlk
nnssrfgisi khninenlyg fgryetrlds nsenaagwgd vktkyayvgl ggygheisfg
kqavigdsig qagfdkvygv gtggikysan ntnkkgfdil tsdsdsainy tytgieglt l
ganynvaner dkktgevnvg stksgfglga kytakiaesq svtvaagyth ddyksgsvnk
kdkdgvyfgl kyvnapftva vdgghgvekt gnvkekidfv rtgarfdvtp ksgvygnysy
gtykdkayka tahqfmlgad yklhkqvvtf vegrliknkd snnkkvtdqa lgvglrvlw

Region	Sequence
OMP P2 Loop 1	qatkekgqsstrghtnlk
OMP P2 Loop 2	ldsnsenaagwgdv
OMP P2 Loop 3	kqavigdsigqagfdkvygvgtggikysanntnkkgfdiltsdsdsa
OMP P2 Loop 4	nvanerdkktgevnvgstk
OMP P2 Loop 5	dyksgsvnkkd
OMP P2 Loop 6	ktgnvkek
OMP P2 Loop 7	ykdkayk
OMP P2 Loop 8	iknkdsnnkkvtdqal

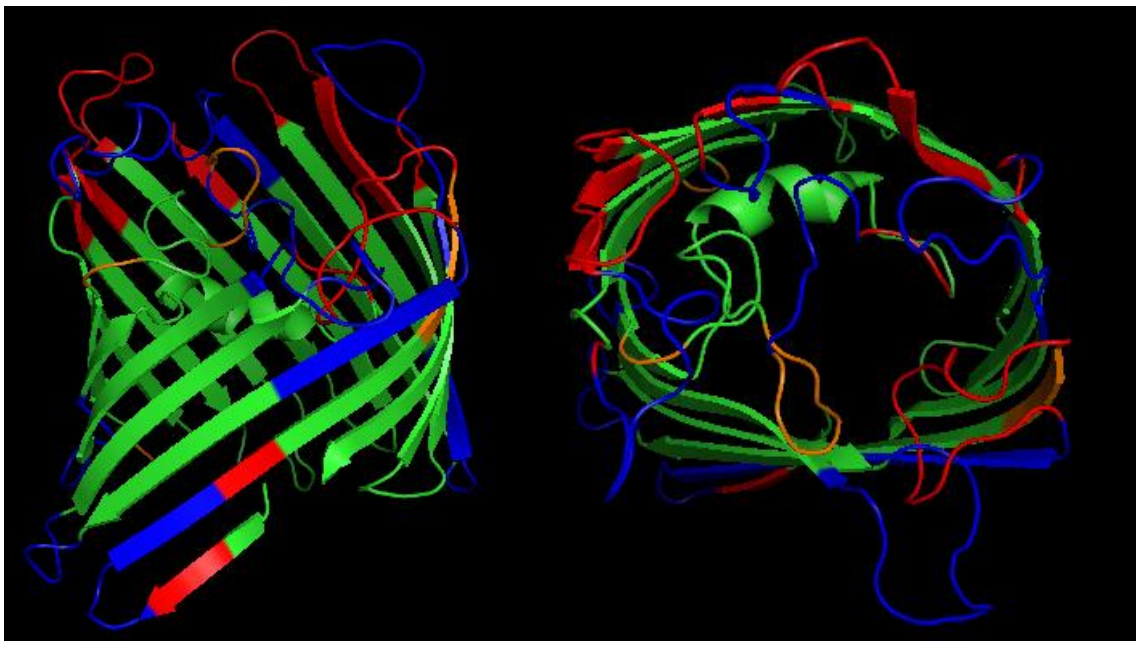

Supplemental Figure S3.63. Predicted antigenic sites and continuous B-cell epitopes of 84-17975 (SV13) OMP P2. Antigenic sites are highlighted in orange (moderate < 5 net votes) and red (high >5 net votes). Predicted continuous B-cell epitopes (>70% probability) are shown in blue. A side view (left) and down the β-barrel view (right) are shown.

mkktlvalav aafaasasav tvyenegtkv dfdgqlrlll eeqatkekgq sstgghtnlk
nngsrfgisi khninenlyg fgryetrlds nsknaagwgd vktkyayvgl ggygheisfg
kqavigdsig qagfdkvygv gtggikysan ntnkkgfdil tsdsdsainy tytgieglt1
ganynvaner dkktgevnvg stksgfglga kytakiaesq svtvaagyth ddyksgsvnk
kdkdgvyfgl kyvnapftva vdgghgvekt gnvkekidfv rtgarfdvtp ksgvygnysy
gtykdkayka tahqfmlgad yklhkqvvtf vegrliknkd snnkkvtdqa lgvglrvlw

Region	Sequence
OMP P2 Loop 1	qatkekgqsstgghtnl
OMP P2 Loop 2	dsnsknaagwgdv
OMP P2 Loop 3	fgkqavigdsigqagfdkvygvgtggikysanntnkkgfdiltsdsdsainy
OMP P2 Loop 4	nvanerdkktgevnvgstksg
OMP P2 Loop 5	ddyksgsvnkkdk
OMP P2 Loop 6	ktgnvkeki
OMP P2 Loop 7	ykdkaykata
OMP P2 Loop 8	nkdsnnkkvtd

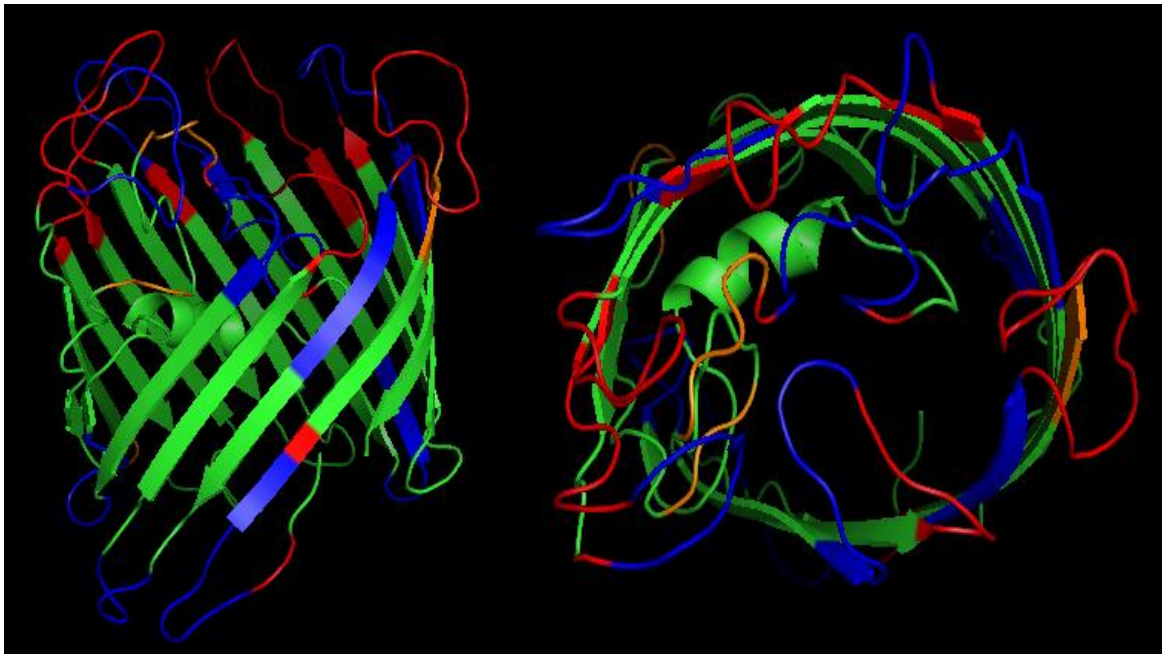

Supplemental Figure S3.64. Predicted antigenic sites and continuous B-cell epitopes of 84-22113 (SV14) OMP P2. Antigenic sites are highlighted in orange (moderate < 5 net votes) and red (high >5 net votes). Predicted continuous B-cell epitopes (>70% probability) are shown in blue. A side view (left) and down the β-barrel view (right) are shown.

mkktlvalav aafaasasav tvyenegtkv dfdgqlrlll eeqatkekgq sstrghtnlk
nnssrfgisi khninenlyg fgryetrlds nsenaagwgd vktkyayvgl ggygheisfg
kqavigdsig qagfdkvygv gtggikysan ntnkkgfdil tdssdsainy tytgiegltl
ganynvaner dkktgevnvg stksgfglga kytakiaesq svtvaagyth ddyksgavnk
kdkdgvyfgl kyvnapftva vdgghgvvkt dnvkekidfv rtgarfdvtp ksgvygnysy
gtykdkayka tahqfmlgad yklhkqvvtf vegrliknkd snnkkvtdqa lgvglrvlw

Region	Sequence
OMP P2 Loop 1	eqatkekgqsstrghtnlknns
OMP P2 Loop 2	dsnsenaagwgdv
OMP P2 Loop 3	kqavigdsigqagfdkvygvgtggikysanntnkkgfdiltdssdsa
OMP P2 Loop 4	nvanerdkktgevnvgstk
OMP P2 Loop 5	ddyksgavnkk
OMP P2 Loop 6	ktdnvkek
OMP P2 Loop 7	kdkaykat
OMP P2 Loop 8	iknkdsnnkkvtdqal

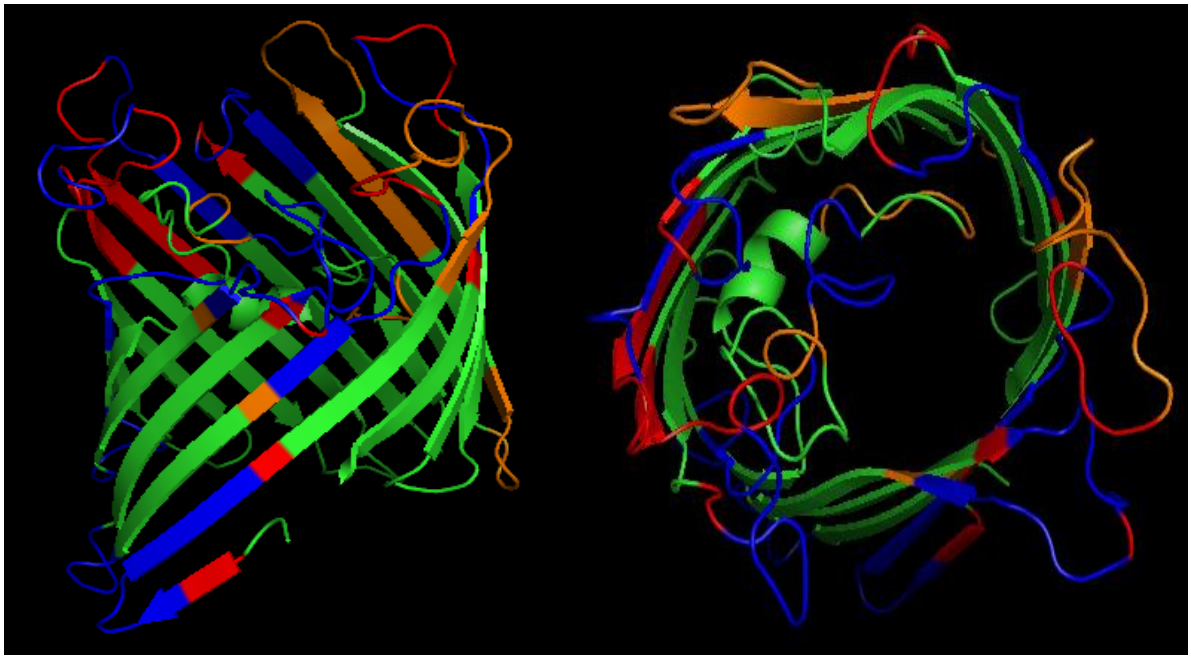

Supplemental Figure S3.65. Predicted antigenic sites and continuous B-cell epitopes of 84-15995 (SV15) OMP P2. Antigenic sites are highlighted in orange (moderate < 5 net votes) and red (high >5 net votes). Predicted continuous B-cell epitopes (>70% probability) are shown in blue. A side view (left) and down the β-barrel view (right) are shown.

mkktlvalav aafaasasav tvyenegtkv dfdgqlrlll eeqatkekgq sstrghtnlk
nnssrfgisi khninenlyg fgryetrlds nsenaagwgd vktkyayvgl ggygheisfg
kqavigdsig qagfdkvygv gtggikysan ntnkkgfdil tsdsdsainy tytgieglt l
ganynvaner dkktgevnvg stksgfglga kytakiaesq svtvaagyth ddyksgsvnk
kdkdgvyfgl kyvnapftva vdgghgvekt gnvkekidfv rtgarfdvtp ksgvygnysy
gtykdkayka tahqfmlgad yklhkqvvtf vegrliknkd snnkkvtdqa lgvglrvlw

Region	Sequence
OMP P2 Loop 1	eqatkekgqsstrghtnlknns
OMP P2 Loop 2	dsnsenaagwg
OMP P2 Loop 3	kqavigdsigqagfdkvygvgtggikysanntnkkgfdiltsdsdsa
OMP P2 Loop 4	nvanerdkktgevnvgstk
OMP P2 Loop 5	ddyksgsvnkkd
OMP P2 Loop 6	ktgnvk
OMP P2 Loop 7	kdkayka
OMP P2 Loop 8	iknkdsnnkkvtdqa

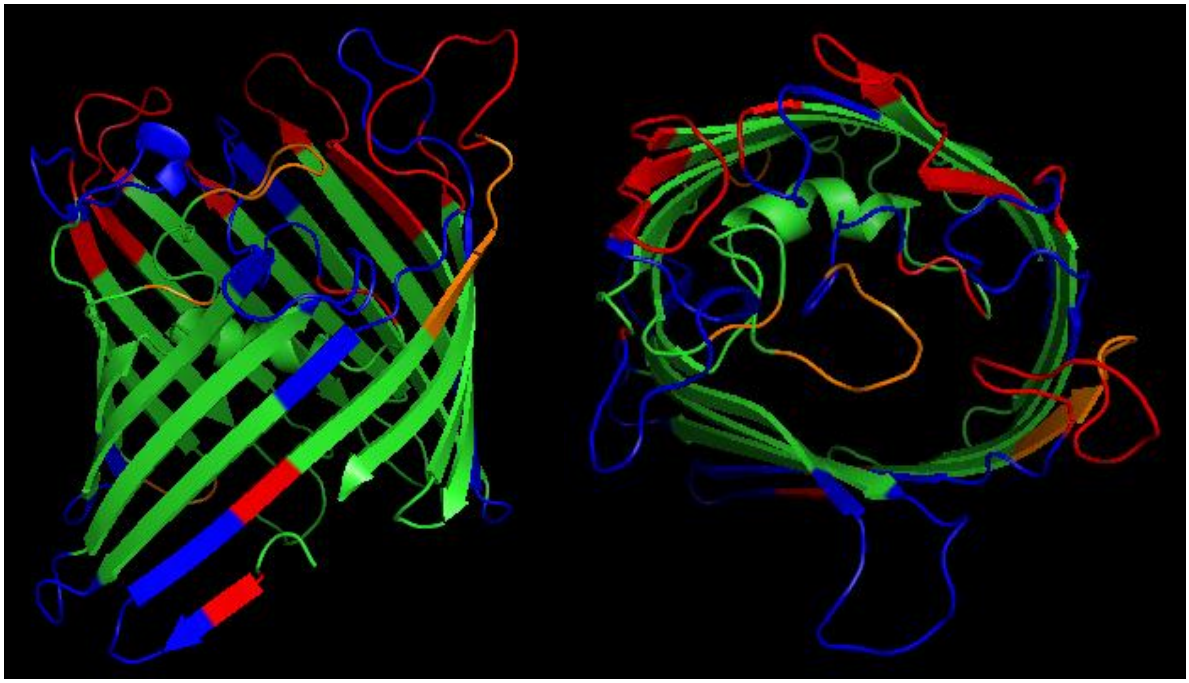

Supplemental Figure S3.66. Predicted antigenic sites and continuous B-cell epitopes of 2170B (SV4) OMP P2. Antigenic sites are highlighted in orange (moderate < 5 net votes) and red (high >5 net votes). Predicted continuous B-cell epitopes (>70% probability) are shown in blue. A side view (left) and down the β-barrel view (right) are shown.

References

1. Harris, D. L. (2000) Control of common infectious diseases. In: Multi-site pig production, *Iowa State University Press*, 98-102.
2. Glasser, K. (1910) *Quoted in Krankenheinten des Schweines. 5th ed. 1950*, 106.
3. Oliveira, S., and Pijoan, C. (2004) *Haemophilus parasuis*: new trends on diagnosis, epidemiology and control, *Veterinary microbiology 99*, 1-12.
4. K. Nedbalcova, P. S., Z. Jaglic, R. Ondriasova, Z. Kucerova. (2006) *Haemophilus parasuis* and Glässer's disease in pigs: a review, *Veterinarni Medicina 51*, 168-179.
5. Ostberg, K. L., Russell, M. W., and Murphy, T. F. (2009) Mucosal immunization of mice with recombinant OMP P2 induces antibodies that bind to surface epitopes of multiple strains of nontypeable *Haemophilus influenzae*, *Mucosal immunology 2*, 63-73.
6. Neary, J. M., and Murphy, T. F. (2006) Antibodies directed at a conserved motif in loop 6 of outer membrane protein P2 of nontypeable *Haemophilus influenzae* recognize multiple strains in immunoassays, *FEMS immunology and medical microbiology 46*, 251-261.
7. Neary, J. M., Yi, K., Karalus, R. J., and Murphy, T. F. (2001) Antibodies to loop 6 of the P2 porin protein of nontypeable *Haemophilus influenzae* are bactericidal against multiple strains, *Infection and immunity 69*, 773-778.
8. Yi, K., and Murphy, T. F. (1997) Importance of an immunodominant surface-exposed loop on outer membrane protein P2 of nontypeable *Haemophilus influenzae*, *Infection and immunity 65*, 150-155.

9. Yi, K., and Murphy, T. F. (1994) Mapping of a strain-specific bactericidal epitope to the surface-exposed loop 5 on the P2 porin protein of non-typeable *Haemophilus influenzae*, *Microbial pathogenesis 17*, 277-282.

10. Haase, E. M., Yi, K., Morse, G. D., and Murphy, T. F. (1994) Mapping of bactericidal epitopes on the P2 porin protein of nontypeable *Haemophilus influenzae*, *Infection and immunity 62*, 3712-3722.

11. Sikkema, D. J., and Murphy, T. F. (1992) Molecular analysis of the P2 porin protein of nontypeable *Haemophilus influenzae*, *Infection and immunity 60*, 5204-5211.

12. Hansen, E. J., Pelzel, S. E., Orth, K., Moomaw, C. R., Radolf, J. D., and Slaughter, C. A. (1989) Structural and antigenic conservation of the P2 porin protein among strains of *Haemophilus influenzae* type b, *Infection and immunity 57*, 3270-3275.

13. Murphy, T. F., and Bartos, L. C. (1988) Purification and analysis with monoclonal antibodies of P2, the major outer membrane protein of nontypable *Haemophilus influenzae*, *Infection and immunity 56*, 1084-1089.

14. Novotny, L. A., and Bakaletz, L. O. (2003) The fourth surface-exposed region of the outer membrane protein P5-homologous adhesin of nontypable *Haemophilus influenzae* is an immunodominant but nonprotective decoying epitope, *J Immunol 171*, 1978-1983.

15. Novotny, L. A., Pichichero, M. E., Denoel, P. A., Neyt, C., Vanderschrick, S., Dequesne, G., and Bakaletz, L. O. (2002) Detection and characterization of pediatric serum antibody to the OMP P5-homologous adhesin of nontypeable *Haemophilus influenzae* during acute otitis media, *Vaccine 20*, 3590-3597.

16. Webb, D. C., and Cripps, A. W. (2000) A P5 peptide that is homologous to peptide 10 of OprF from *Pseudomonas aeruginosa* enhances clearance of nontypeable *Haemophilus influenzae* from acutely infected rat lung in the absence of detectable peptide-specific antibody, *Infection and immunity 68*, 377-381.

17. Novotny, L. A., Jurcisek, J. A., Pichichero, M. E., and Bakaletz, L. O. (2000) Epitope mapping of the outer membrane protein P5-homologous fimbrin adhesin of nontypeable *Haemophilus influenzae*, *Infection and immunity 68*, 2119-2128.

18. Reddy, M. S., Bernstein, J. M., Murphy, T. F., and Faden, H. S. (1996) Binding between outer membrane proteins of nontypeable *Haemophilus influenzae* and human nasopharyngeal mucin, *Infection and immunity 64*, 1477-1479.

19. Webb, D. C. a. A. W. C. (1998) Secondary Structure and molecular analysis of interstrain variability in the P5 outer-membrane protein of non-typable *Haemophilus influenzae* isolated from diverse anatomical sites, *Journal of Medical Microbiology 47*, 1059-1067.

20. Duim, B., Bowler, L. D., Eijk, P. P., Jansen, H. M., Dankert, J., and van Alphen, L. (1997) Molecular variation in the major outer membrane protein P5 gene of nonencapsulated *Haemophilus influenzae* during chronic infections, *Infection and immunity 65*, 1351-1356.

21. Mullins, M. A., Register, K. B., Bayles, D. O., Loving, C. L., Nicholson, T. L., Brockmeier, S. L., Dyer, D. W., and Phillips, G. J. (2009) Characterization and comparative analysis of the genes encoding *Haemophilus parasuis* outer membrane proteins P2 and P5, *Journal of bacteriology 191*, 5988-6002.

22. Cheng Tang, B. Z., Hua Yue, Falong Yang, Guoqing Shao, Quan Hai,, and Xiaofei Chen, D. G. (2010) Characteristics of the molecular diversity of the outer membrane protein A gene of *Haemophilus parasuis*, *The Canadian Journal of Veterinary Research 74*, 233-236.

23. Tang, C., Zhang, B., Yue, H., Yang, F., Shao, G., Hai, Q., Chen, X., and Guo, D. (2010) Characteristics of the molecular diversity of the outer membrane protein A gene of *Haemophilus parasuis*, *Canadian journal of veterinary research = Revue canadienne de recherche veterinaire 74*, 233-236.

24. Tian, H., Fu, F., Li, X., Chen, X., Wang, W., Lang, Y., Cong, F., Liu, C., and Tong, G. (2011) Identification of the immunogenic outer membrane protein A (OmpA) antigen of *Haemophilus parasuis* using a proteomics approach and passive immunization of mice with monoclonal antibodies, *Clinical and vaccine immunology : CVI 18*, 1695-1701.

25. Galdiero, S., Capasso, D., Vitiello, M., D'Isanto, M., Pedone, C., and Galdiero, M. (2003) Role of surface-exposed loops of *Haemophilus influenzae* protein P2 in the mitogen-activated protein kinase cascade, *Infection and immunity 71*, 2798-2809.

26. Li, P., Bai, J., Li, J. X., Zhang, G. L., Song, Y. H., Li, Y. F., Wang, X. W., and Jiang, P. (2011) Molecular cloning, sequencing, and expression of the outer membrane protein P2 gene of Haemophilus parasuis, *Research in veterinary science*.

27. McVicker, J. K. (2004) The identification and characterization of P5 and P2 colonization proteins of *Haemophilus parasuis* and the targeted binding of Carcinoembryonic Antigen (CEA), In *PhD Dissertation*, Iowa State University, Ames, IA.

28. Notredame, C., Higgins, D. G., and Heringa, J. (2000) T-Coffee: A novel method for fast and accurate multiple sequence alignment, *Journal of molecular biology 302*, 205-217.

29. Notredame, C., and Suhre, K. (2004) Computing multiple sequence/structure alignments with the T-coffee package, *Current protocols in bioinformatics / editoral board, Andreas D. Baxevanis ... [et al.] Chapter 3*, Unit3 8.

30. Sali, A. a. B., T.L. (1993) Comparative protein modelling by satisfaction of spatial restraints, *Journal of molecular biology 234*, 779-815.

31. Hildebrand, A., Remmert, M., Biegert, A., and Soding, J. (2009) Fast and accurate automatic structure prediction with HHpred, *Proteins 77 Suppl 9*, 128-132.

32. Soding, J., Biegert, A., and Lupas, A. N. (2005) The HHpred interactive server for protein homology detection and structure prediction, *Nucleic acids research 33*, W244-248.

33. Cheng, J., Randall, A. Z., Sweredoski, M. J., and Baldi, P. (2005) SCRATCH: a protein structure and structural feature prediction server, *Nucleic acids research 33*, W72-76.

34. Magnan, C. N., Zeller, M., Kayala, M. A., Vigil, A., Randall, A., Felgner, P. L., and Baldi, P. (2010) High-throughput prediction of protein antigenicity using protein microarray data, *Bioinformatics 26*, 2936-2943.

35. Sweredoski, M. J., and Baldi, P. (2009) COBEpro: a novel system for predicting continuous B-cell epitopes, *Protein engineering, design & selection : PEDS 22*, 113-120.

36. Prather, D. T., Bains, M., Hancock, R. E., Filiatrault, M. J., and Campagnari, A. A. (2004) Differential expression of porins OmpP2A and OmpP2B of *Haemophilus ducreyi*, *Infection and immunity 72*, 6271-6278.

37. Zehr, E. S. (2008) Relatedness of *Haemophilus parasuis* strains and their proteins' possible roles as virulence factors, In *PhD Dissertation*, Iowa State University, Ames, IA.

38. Zehr, E. S., and Tabatabai, L. B. (2011) Detection of a bacteriophage gene encoding a Mu-like portal protein in *Haemophilus parasuis* reference strains and field isolates by nested polymerase chain reaction, *Journal of veterinary diagnostic investigation : official publication of the American Association of Veterinary Laboratory Diagnosticians, Inc 23*, 538-542.

39. Avadhanula, V., Rodriguez, C. A., Ulett, G. C., Bakaletz, L. O., and Adderson, E. E. (2006) Nontypeable *Haemophilus influenzae* adheres to intercellular adhesion molecule 1 (ICAM-1) on respiratory epithelial cells and upregulates ICAM-1 expression, *Infection and immunity 74*, 830-838.

40. Torres, A. G., and Kaper, J. B. (2003) Multiple elements controlling adherence of enterohemorrhagic *Escherichia coli* O157:H7 to HeLa cells, *Infection and immunity 71*, 4985-4995.

41. Dabo, S. M., Confer, A. W., and Quijano-Blas, R. A. (2003) Molecular and immunological characterization of *Pasteurella multocida* serotype A:3 OmpA: evidence of its role in P. multocida interaction with extracellular matrix molecules, *Microbial pathogenesis 35*, 147-157.

42. Murphy, T. F., Nelson, M. B., and Apicella, M. A. (1992) The P6 outer membrane protein of nontypeable *Haemophilus influenzae* as a vaccine antigen, *J Infect Dis 165 Suppl 1*, S203-205.

43. Murphy, T. F., Bartos, L. C., Campagnari, A. A., Nelson, M. B., and Apicella, M. A. (1986) Antigenic characterization of the P6 protein of nontypable *Haemophilus influenzae*, *Infection and immunity 54*, 774-779.

44. Michel, L. V., Kalmeta, B., McCreary, M., Snyder, J., Craig, P., and Pichichero, M. E. (2011) Vaccine candidate P6 of nontypable *Haemophilus influenzae* is not a transmembrane protein based on protein structural analysis, *Vaccine 29*, 1624-1627.

45. Kodama, S., Hirano, T., Noda, K., Umemoto, S., and Suzuki, M. (2011) Nasal immunization with plasmid DNA encoding P6 protein and immunostimulatory complexes elicits nontypeable *Haemophilus influenzae*-specific long-term mucosal immune responses in the nasopharynx, *Vaccine 29*, 1881-1890.

46. Pichichero, M. E., Kaur, R., Casey, J. R., Sabirov, A., Khan, M. N., and Almudevar, A. (2010) Antibody response to *Haemophilus influenzae* outer membrane protein D, P6, and OMP26 after nasopharyngeal colonization and acute otitis media in children, *Vaccine 28*, 7184-7192.

47. Noda, K., Kodama, S., Umemoto, S., Abe, N., Hirano, T., and Suzuki, M. (2010) Nasal vaccination with P6 outer membrane protein and alpha-galactosylceramide induces nontypeable *Haemophilus influenzae*-specific protective immunity associated with NKT cell activation and dendritic cell expansion in nasopharynx, *Vaccine 28*, 5068-5074.

48. Murphy, T. F., Kirkham, C., and Lesse, A. J. (2006) Construction of a mutant and characterization of the role of the vaccine antigen P6 in outer membrane integrity of nontypeable *Haemophilus influenzae*, *Infection and immunity 74*, 5169-5176.

49. Kodama, S., Hirano, T., Suenaga, S., Abe, N., and Suzuki, M. (2006) Eustachian tube possesses immunological characteristics as a mucosal effector site and responds to P6 outer membrane protein of nontypeable *Haemophilus influenzae*, *Vaccine 24*, 1016-1027.

50. Ishida, Y., Abe, Y., Yanai, M., Kobayashi, H., and Harabuchi, Y. (2006) Identification of human T-cell epitopes and highly immunogenic analog peptides on the non-typeable *Haemophilus influenzae* P6 outer membrane protein, *Clin Immunol 121*, 90-99.

51. McMahon, M., Murphy, T. F., Kyd, J., and Thanavala, Y. (2005) Role of an immunodominant T cell epitope of the P6 protein of nontypeable *Haemophilus influenzae* in murine protective immunity, *Vaccine 23*, 3590-3596.

52. Berenson, C. S., Murphy, T. F., Wrona, C. T., and Sethi, S. (2005) Outer membrane protein P6 of nontypeable *Haemophilus influenzae* is a potent and selective inducer of human macrophage proinflammatory cytokines, *Infection and immunity 73*, 2728-2735.

53. Bertot, G. M., Becker, P. D., Guzman, C. A., and Grinstein, S. (2004) Intranasal vaccination with recombinant P6 protein and adamantylamide dipeptide as mucosal adjuvant confers efficient protection against otitis media and lung infection by nontypeable *Haemophilus influenzae*, *J Infect Dis 189*, 1304-1312.

54. Hotomi, M., Yamanaka, N., Shimada, J., Suzumoto, M., Ikeda, Y., Sakai, A., Arai, J., and Green, B. (2002) Intranasal immunization with recombinant outer membrane protein P6 induces specific immune responses against nontypeable *Haemophilus influenzae*, *International journal of pediatric otorhinolaryngology 65*, 109-116.

55. Karalus, R. J., and Murphy, T. F. (1999) Purification and characterization of outer membrane protein P6, a vaccine antigen of non-typeable *Haemophilus influenzae*, *FEMS immunology and medical microbiology 26*, 159-166.

56. Hotomi, M., Yamanaka, N., Saito, T., Shimada, J., Suzumoto, M., Suetake, M., and Faden, H. (1999) Antibody responses to the outer membrane protein P6 of non-typeable *Haemophilus influenzae* and pneumococcal capsular polysaccharides in otitis-prone children, *Acta oto-laryngologica 119*, 703-707.

57. Badr, W. H., Loghmanee, D., Karalus, R. J., Murphy, T. F., and Thanavala, Y. (1999) Immunization of mice with P6 of nontypeable *Haemophilus influenzae*: kinetics of the antibody response and IgG subclasses, *Vaccine 18*, 29-37.

58. Hotomi, M., Saito, T., and Yamanaka, N. (1998) Specific mucosal immunity and enhanced nasopharyngeal clearance of nontypeable *Haemophilus influenzae* after intranasal immunization with outer membrane protein P6 and cholera toxin, *Vaccine 16*, 1950-1956.

59. Hotomi, M., Yokoyama, M., Kuki, K., Togawa, A., and Yamanaka, N. (1996) Study on specific mucosal immunity by intranasal immunization of outer membrane protein P6 of *Haemophilus influenzae* with cholera toxin B subunit, *Acta oto-laryngologica. Supplementum 523*, 150-152.

60. DeMaria, T. F., Murwin, D. M., and Leake, E. R. (1996) Immunization with outer membrane protein P6 from nontypeable *Haemophilus influenzae* induces bactericidal antibody and affords protection in the chinchilla model of otitis media, *Infection and immunity 64,* 5187-5192.

61. Kyd, J. M., Dunkley, M. L., and Cripps, A. W. (1995) Enhanced respiratory clearance of nontypeable *Haemophilus influenzae* following mucosal immunization with P6 in a rat model, *Infection and immunity 63*, 2931-2940.

62. Kodama, H., and Faden, H. (1995) Cellular immunity to the P6 outer membrane protein of nontypeable *Haemophilus influenzae*, *Infection and immunity 63,* 2467-2472.

63. Kasten, R. W., Hansen, L. M., Hinojoza, J., Bieber, D., Ruehl, W. W., and Hirsh, D. C. (1995) Pasteurella multocida produces a protein with homology to the P6 outer membrane protein of *Haemophilus influenzae*, *Infection and immunity 63*, 989-993.

64. Beck-Sickinger, A. G., Rotering, H., Wiesmuller, K. H., Dorner, F., and Jung, G. (1994) Mapping of antigenic and immunogenic sites of *Haemophilus influenzae* outer membrane protein P6 using synthetic lipopeptides, *Biological chemistry Hoppe-Seyler 375*, 173-182.

65. Yamanaka, N., and Faden, H. (1993) Local antibody response to P6 of nontypable *Haemophilus influenzae* in otitis-prone and normal children, *Acta oto-laryngologica 113,* 524-529.

66. Nelson, M. B., Munson, R. S., Jr., Apicella, M. A., Sikkema, D. J., Molleston, J. P., and Murphy, T. F. (1991) Molecular conservation of the P6 outer membrane protein among strains of *Haemophilus influenzae*: analysis of antigenic determinants, gene

sequences, and restriction fragment length polymorphisms, *Infection and immunity 59*, 2658-2663.

67. Tefon, B. E., Maass, S., Ozcengiz, E., Becher, D., Hecker, M., and Ozcengiz, G. (2011) A comprehensive analysis of *Bordetella pertussis* surface proteome and identification of new immunogenic proteins, *Vaccine 29*, 3583-3595.

68. Cloeckaert, A., Jacques, I., Grillo, M. J., Marin, C. M., Grayon, M., Blasco, J. M., and Verger, J. M. (2004) Development and evaluation as vaccines in mice of *Brucella melitensis* Rev.1 single and double deletion mutants of the bp26 and omp31 genes coding for antigens of diagnostic significance in ovine brucellosis, *Vaccine 22*, 2827-2835.

69. Wu, Z., Zhang, W., Shao, J., Wang, Y., Lu, Y., and Lu, C. (2011) Immunoproteomic assay of secreted proteins of *Streptococcus suis* serotype 9 with convalescent sera from pigs, *Folia microbiologica*.

CHAPTER 4. OMP P5 PEPTIDE VACCINE PROVIDES PROTECTION AGAINST *Haemophilus parasuis* HETEROLOGOUS CHALLENGE

Revised from U.S non-provisional patent application
titled "Swine Vaccine and Methods"

Mandy K. Zimmerli, Sambasivarao Tadepalli, Jerry K. McVicker,
and Louisa B. Tabatabai

Abstract

To date, there is no commercially available cross-protective vaccine for Glässer's disease. Using the results of molecular modeling analysis of the OMP P5 protein of *H. parasuis*, it was hypothesized that the surface exposed loops could serve as a vaccine candidate against Glässer's disease. The peptides were designed in accordance to strain IA84-29755 (SV5) OMP P5. An Fmoc-based synthetic peptide to loop 3 was used in the first vaccination study and provided protection for 50% of the herd upon heterologous challenges with SV13. When the animals were dosed with a second vaccination with bacterin, this provided 90% protection against challenge. When animals were first dosed with bacterin and given a second vaccination with peptide, this provided 100% protection against challenge. In the second study, recombinant peptides were designed corresponding to the loop 4 region and the loop 4 including the transmembrane region. Results of the first vaccination study indicate that antibody titers to the peptide increases following administration of challenge. Overall, the results indicate that loop 3 has a superior protective epitope in comparison to loop 4.

Introduction

Haemophilus parasuis, a respiratory pathogen in swine, is the causative agent of Glässer's disease which is associated with polyserositis, meningitis, pneumonia, lameness and arthritis [1-3]. Interestingly enough, not all serovars are associated with a diseased state.

Serovars have been classified as follows: 1, 5, 10, 12, 13, and 14 are most virulent and cause morbidity; 2, 4, 8, and 15 are virulent but do not result in death; and 3, 6, 7, 9, and 11 are classified as avirulent [4]. Because of this characteristic, conventional vaccine methods, such as the use of heat-killed organisms, have proven problematic. Therefore, it is imperative to identify virulence factors and new vaccine approaches that can be exploited to perpetuate cross-protective immunity. Since colonization is the first line of defense for bacterial pathogens, the study of proteins involved in adherence is particularly important. By elucidating the molecular differences in outer membrane proteins, particularly the outer membrane protein P5 adhesin (OMP P5), a cross-protective vaccine and complimentary diagnostic can be developed.

In *H. influenzae*, a model organism for *H. parasuis*, OMP P5 has been found to be important in colonizing the respiratory tract [5, 6]. The OMP P5 secondary structure was determined by Webb et al., indicating a 72.2% secondary structural homology to the OMP A in *E. coli* [7]. Due to the increase in variability of this protein during the course of chronic infections, it was concluded that P5 plays an important role as a target for the immune response [8]. This was later supported by studies that showed the involvement of OMP P5 in the binding to epithelial cells as well as the ability of OMP P5 to bind CEACAM-1. In a chinchilla model, the loop 3 epitope of OMP P5 was found to be protective while the loop 4 peptide served as an immunodominant but non-protective epitope [9].

Overall, the goal of this study is to develop a vaccine and diagnostic based upon the peptides of the OMP P5 of *H. parasuis* and to test the hypothesis that the loop 3 peptide is protective while the loop 4 peptide serves as a decoy epitope. Since conventional vaccine methods for Glässer's disease have not proven cross-protective, it was hypothesized that

differences in the OMP P5 could be exploited on a molecular level to develop a peptide vaccine approach. Results of primary and molecular modeling analysis, combined with information about *H. influenzae* OMP P5, indicate that the loop 3 peptide could serve as a cross-protective vaccine candidate. Preliminary serology data, prior to the vaccination studies, indicated that animals infected with *H. parasuis* had antibody titers to the synthetic peptides of loop 3 and loop 4 of OMP P5. Moreover, animal studies indicate that loop 4 is not a protective epitope.

Material and Methods

Determination of P5 surface exposed loops. The OMP P5 from HPIA84-29755 (SV5) was modeled using the Modeller program [10] following tertiary structural analysis by HHPred [11, 12]. The model was updated prior to patent application submission, using pdb70_16Jul11 HMM database.

Synthesis and preparation of peptides. Peptides (Table 4.1) were synthesized by Fmoc solid-phase methodology at the Iowa State University Protein Facility (Ames, IA) [13, 14]. In preparation for ELISA, these peptides were conjugated to maleimide-derivative of bovine serum albumin. Protein concentration was determined using A280 method.

ELISA using synthetic peptides. Plates (Corning #3651 black 96-well microtiter plates with clear bottom, Corning Inc., Corning, NJ) were sensitized overnight with 10 nanograms of BSA-conjugated peptides per well in 100 µL of 50 mM sodium carbonate buffer, pH 9.6. After washing the plates three times (Tecan 96PW plate washer, San Jose, CA), with 0.1 M phosphate-buffered saline pH 7.2, containing 0.05% Tween-20, 100 µL of sera (1:100) from swine was added, and plates were incubated at 37^{o}C for 1 hour. Plates were washed three times as previously described and 100 µL per well of goat anti-pig IgG-HRP (Southern

Biotech) diluted 1:1000 was added. Plates were incubated at 37^{o}C for 1 hour and washed three times as previously described. Color was developed for 10 min at room temperature using ABTS peroxidase system (KPL, Gaithersburg, MD). The reaction was stopped by addition of 100 µL 1% SDS, and absorbance was determined at 405 nm using a plate reader. Absorbance values were corrected using maleimide-BSA for preliminary ELISA trials. Additionally, cesarian derived colostrum deprived serum (CDCD) was used as a true negative control. The sera for preliminary ELISAs were obtained from animals either one or two week post-infection. Normal pig and infected pig sera were used as positive and negative controls for ELISAs following challenge studies. Assays were performed in triplicate.

Statistics. Statistical analysis was performed using GraphPad InStat v. 3.0 and GraphPad Prism v. 5.0. Following ANOVA analysis, the samples were subjected to the Dunnett's multiple comparison test using the placebo group, cesarian derived colostrum deprived (CDCD) or non-infected sera as controls.

Results

Modeling of OMP P5 protein and design of synthetic peptide. The OMP P5 of *H. parasuis* was modeled following sequencing of the P5 gene for HP IA84-29755 (SV5). Results for the OMP P5 protein (Figure 4.1) show a β-barrel with four surface exposed loops. The N-terminal domain of OMP P5 is homologous to OMPA while the C-terminal domain is homologous to Pal of *E. coli* and OMP P6 *of H. influenzae.*

The peptides used in the vaccination studies are described in Table 4.1. A consensus sequence was described for the loop 3 peptide (Table 4.2), as the loop 3 epitope of OMP P5 in *H. influenzae* was found to be the protective epitope, and it was hypothesized that this epitope will provide the same protection in *H. parasuis* as the Opa-class of proteins,

including P5, are highly conserved among gram-negative bacteria. Recombinant peptides were designed for the second challenge study, and these sequences are shown in Table 4.1. Additionally, a peptide for loop 4 and a combinatorial peptide, loop3-4, were designed.

Preliminary ELISA with synthetic peptides of OMP P5. Results of the preliminary ELISA studies (Figures 4.2 and 4.3) indicate that in comparison to control animals, animals infected with *H. parasuis* have antibody titers to the loop 3, loop 4, and loop 3-4 peptides. However, an antibody titer to the loop peptides is present for non-infected animals as well. It should be noted that a test for a true *H. parasuis* negative is not available, and animals can carry the bacteria without clinical symptoms of Glässer's disease. In Figure 4.2, the absorbance for serum sample 12 (one week post-infection) was greater than the other samples, and the absorbance for serum sample 18 (two weeks post-infection) was low, which gives rise to variation observed. The results of the combinatorial loop3-4 peptide ELISA is shown in Figure 4.3. In comparison to the CDCD and negative sera, animals one week and two weeks post-infection have a higher antibody titer to the loop 3-4 peptide.

Protection of OMP P5 derived peptides against challenge in animal model. Design and overall results of the first animal study are included in the Supplemental Information and Supplemental Tables S4.1 and S4.2. Figure 4.4 and Supplemental Figure S4.1 present antibody (IgG) titer per group and comparison of titer for each group. In Figure 4.4, it is noted that all groups mount a similar response, with antibody titers to loop 3 peptide decreasing following the 2nd bleed post 2nd vaccination and titers increasing prior to challenge. Groups 1, 2, and 3 received peptide in the first, second, or both vaccination doses. Group 4 had a similar antibody titer even thought it was the placebo group. However, animals given the peptide alone or in combination with bacterin had higher protection against

challenge. Superior protective results were noted for Groups 2 and 3 where the bacterin was given in combination with peptide.

Results of the second challenge study using the recombinant loop 4 peptide are shown in Supplemental Table S4.2. Vaccination with loop 4 peptide only increased survival by 7%. When loop 4 was used in combination with P5, a decrease in survival was noted. Overall, the recombinant loop 4 peptide does not provide protection against heterologous challenge.

Discussion

Molecular modeling analysis of OMP P5 of *H. parasuis* indicates four surface exposed outer membrane regions. This is contrary to a previous published model of P5, based on two-dimensional analysis, which comprises five surface loops [15]. However, a model of the OMPA of *H. parasuis*, which is highly homologous to the N-terminal domain of OMP P5, identified four outer membrane loops [16]. Previous studies using peptides derived from Cu-Zn SOD of *Brucella abortus* provided evidence that the peptides elicited antibody titers and that one of the peptides was protective against infection in a mouse model [17]. Because of the success of this subunit vaccine, peptides corresponding to the outer membrane loops of OMP P5 were synthesized and subjected to preliminary ELISA studies.

Preliminary results of the ELISA study indicated that animals infected with *H. parasuis* had antibody titers to the loop peptides presented here. A true negative control was difficult to identify given that *H. parasuis* can be carried commensally, and no test for *H. parasuis* is commercially available. Because of this, CDCD sera was used as negative control until true negative control sera could be obtained. Given the results that animals infected with *H. parasuis* had antibody titers to the loop peptides, studies were taken to an animal model (Supplemental Information) in collaboration with Novartis Animal Health (Larchwood, IA).

The results of the first experiment (Supplemental Table S4.1) indicate that the peptide was protective in comparison to the control group. However, an additional group was to be included that showed the results of peptide vaccine with an additional adjuvant. Instead, the peptide group was accidentally dosed with bacterin for its second vaccination, while the bacterin group was given a second dose with peptide. The combination of bacterin and peptide proved to be 90-100% protective against heterologous challenge, with the highest protection (100%) when the animal was vaccinated first with bacterin and given a peptide for the second dose.

Because recombinant proteins and peptides are less expensive than synthetic peptides, recombinant peptides were designed and expressed as stated in the Supplemental Information. The second vaccination study used recombinant loop 4. This did not provide any protection against infection (Supplemental Table S4.2). In an animal model, the OMP P5 loop 3 peptide appears to be protective while the loop 4 region presents as a possible decoy epitope. This trend is also seen for *H. influenzae* OMP P5 [9].

Future work includes the screening of the recombinant loop 3, with and without transmembrane domain, in a heterologous challenge model. Additionally, a complimentary diagnostic will be designed.

Acknowledgements

We would like to acknowledge the ISU Protein Facility for peptide synthesis, Susan Brockmeier for donating sera used in preliminary ELISA trials, and Novartis Animal Health for performing the animal studies.

Tables

Table 4.1. Description of Peptides

SEQ. ID. NO.	Designation	Sequence
1	P5 Loop 3[a]	LVRNDYKRYSQTAGVQTQKAHNLKTSL
2	TMU of P5 Loop 3[b]	SYEVLNGLDVYGKVGAA
3	TMD of P5 Loop 3[b]	VLGAGVEYAILPEL
4	TMU + P5 Loop 3 + TMD[b]	SYEVLNGLDVYGKVGAALVRNDYKRYSQTAG VQTQKAHNLKTSLVLGAGVEYAILPEL
5	Cys + P5 Loop 3[a]	CLVRNDYKRYSQTAGVQTQKAHNLKTSL
6	P5 Loop 4[a]	SNVGNFTKAEAKENRRATYNYSPDSHS
7	TMD of P5 Loop 4[b]	VTAGISYRFGQGAAPVA
8	P5 Loop 4 + TMD[b]	SNVGNFTKAEAKENRRATYNYSPDSHSVTAGIS YRFGQGAAPVA
9	Plasmid Upstream of P5 Loop 4 + TMD[b]	MHHHHHHSSGLVPRGSGMKETAAAKFERQHM DSPDLGTDDDDK
10	Plasmid Upstream + P5 Loop 4 + TMD[b]	MHHHHHHSSGLVPRGSGMKETAAAKFERQHM DSPDLGTDDDDKSNVGNFTKAEAKENRRATYN YSPDSHSVTAGISYRFGQGAAPVA
11	P5 Loop 3-4[a]	CVLRBDYKRYSQTAGVQTQKAHNLKTSLSNVG NFTKAEAKENRRATYN

TMU: transmembrane upstream

TMD: transmembrane downstream

[a]Peptides designed by M. Zimmerli; synthesized at ISU Protein Facility

[b]Peptides designed by Novartis Animal Health based on information from M. Zimmerli

Table 4.2. Identification of *H. parasuis* OMP P5 Loop 3 Consensus Sequences

Accession Number	**Reference**
[1]ADJ38689, ADJ38692, ADJ38696, ADJ38699, ADJ38690, ADJ38691, ADJ38699, ADJ38698, [2]ADJ38703, ADJ38701, ADJ38700, ADJ38720 [3]ADJ38719, ADJ38717, ADJ38715, ADJ38705, ADJ38706, ADJ38708, ADJ38702, ADJ38716, ADJ38713, ADJ38695, ADJ38697	Yue,M., Jin,Q. and Chen,H., Genetic relatedness of *Haemophilus parasuis* among reference strains and Chinese epidemic isolates (Unpublished)
[1]ADQ55756, ADQ55758, ADQ55759, ADQ55760, ADQ55761, ADQ55763, ADQ55764, ADQ55765, ADJ38691, ADJ3869, [2]ADQ55772, ADQ55763, ADQ55771 [3]ADQ55776, ADQ55773, ADQ55766, ADQ55767, ADQ55789, ADQ55790, ADQ55787, ADQ55788	Zhang,B. and Liao,M., Molecular typing of *Hameophilus parasuis* using outer membrane protein P5 gene sequence (Unpublished)
[1]ACN62140, ACN62142 [2]ACN62142, ACN62139, ACN62137 [3]ACN62150, ACN62132, ACN62141, ACN62133, ACN62135	Zhang,B., Tang,C. and Yue,H., Characteristics of molecular diversity in the outer membrane protein a gene from *Haemophilus parasuis* (Unpublished)
[3]ACN62141	Yue,M.,et al. Complete genome sequence of *Haemophilus parasuis* SH0165. J. Bacteriol. 191 (4), 1359-1360 (2009)

[1]LVRNDYKRYXQTRXXXEPVKSHNLKTSL (Mullins et al., 2009 [15])

[2]LVRNDYKRYX(Q/T)TRXXXEPVKSHNLKTSL

[3]Does not follow above consensus

Figures

aapqantfyv gakagwatfh ndinqlnsky kndaryatsa ngyvinrnsv tygvfggyqi
idnlavelgy dyfgrvrgnk qefrafkhsa hgthlslkps yevlngldvy gkvgaalvrn
dykrysqtag vqtqkahnlk tslvlgagve yailpelafr veyqwlsnvg nftkaeaken
rratynyspd shsvtagisy rfgqgaapva aapevvtknf afssdvlfdf gkanlkpaaa
qtldavhtei vnlglanpav qvngytdrig kdaanltlsq kraetvanyi vskgvnpanv
tavgygeanp vtgntcdavk grkalitcla pdrrveiqvq gskevsm

Region	Sequence
OMP P5 Loop 1	tfhndinqlnskykndaryatsangyvinrns
OMP P5 Loop 2	fgrvrgnkqefrafkhs
OMP P5 Loop 3	lvrndykrysqtagvqtqkahnlktsl
OMP P5 Loop 4	lsnvgnftkaeakenrratynyspdsh

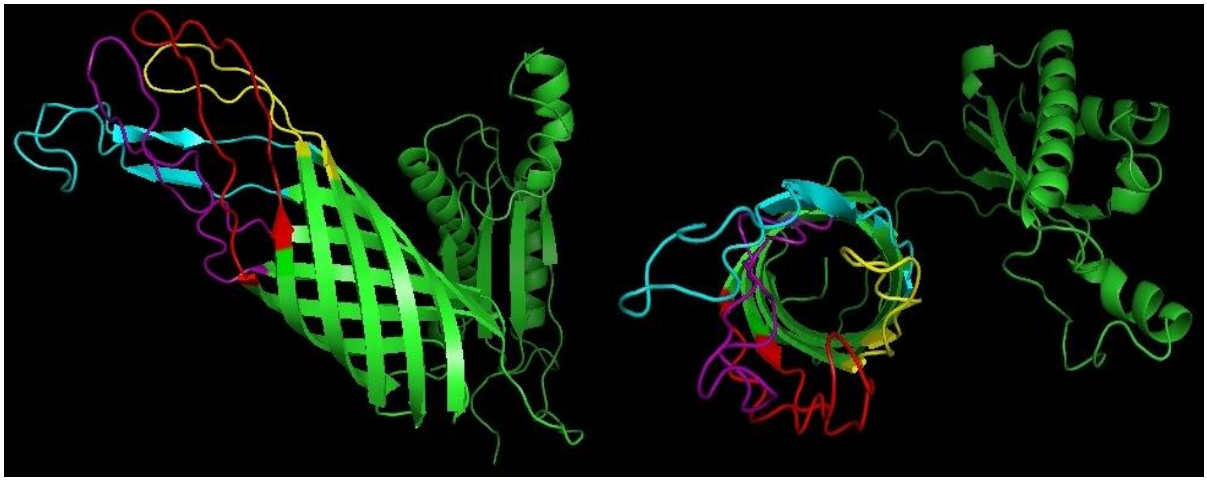

Figure 4.1. Model of HPIA84-29755 OMP P5. The protein sequence (Accession: 167856404) is shown with predicted surface exposed regions shown in color. Side (left) and down the β-barrel (right) views are shown.

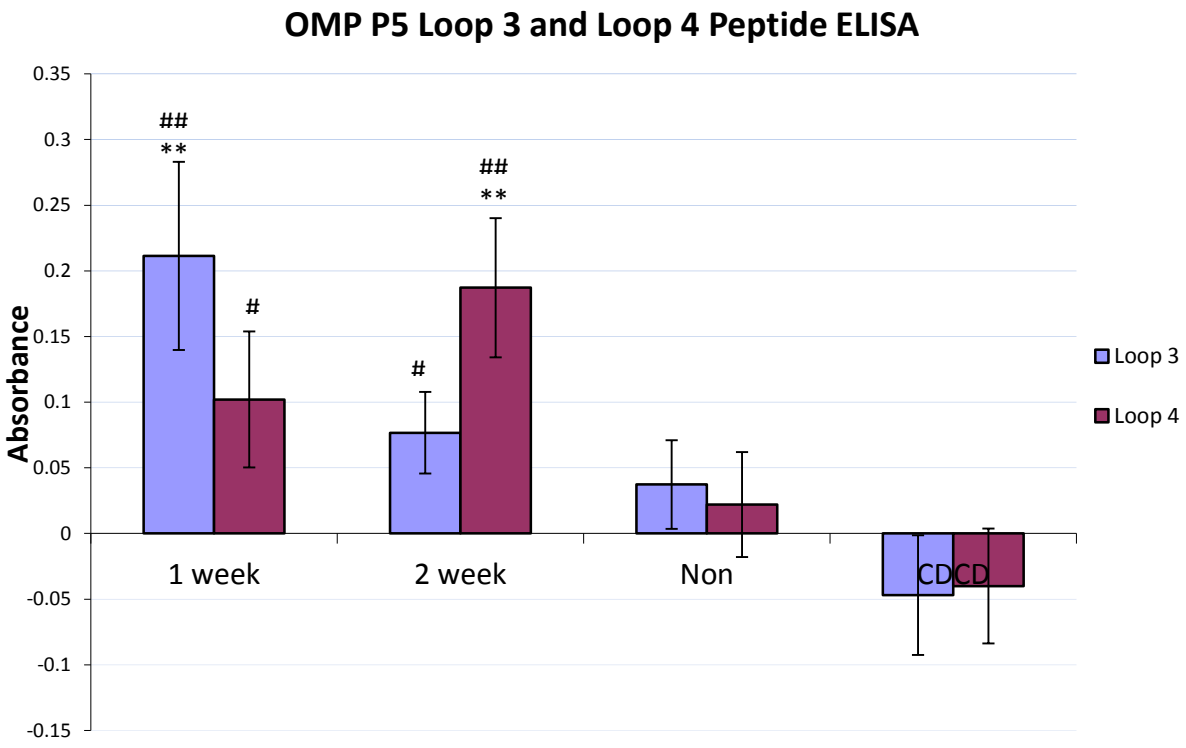

Figure 4.2. Preliminary ELISA data using synthetic peptides Loop 3 and Loop 4 from OMP P5. The average absorbance is indicated for each group along with standard error. Sample number (n)=3; * $p<0.05$ and ** $p<0.01$ for Dunnett's multiple comparison to non-infected sera; # $p<0.05$ and ## $p<0.01$ for Dunnett's multiple comparison to CDCD sera.

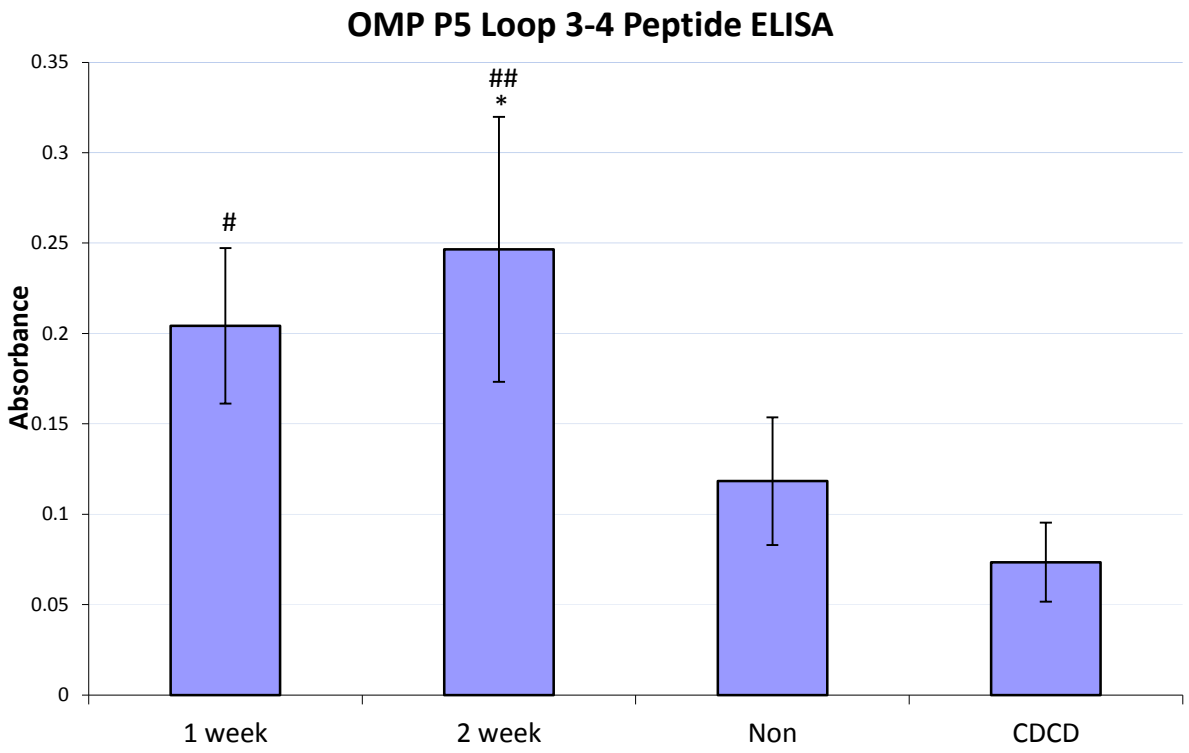

Figure 4.3. Preliminary ELISA data using synthetic peptides Loop 3-4 from OMP P5. The average absorbance is indicated for each group along with standard error. The number in each group is indicated in the chart. Sample number(n)=3; * $p<0.05$ and ** $p<0.01$ for Dunnett's multiple comparison to non-infected sera; # $p<0.05$ and ## $p<0.01$ for Dunnett's multiple comparison to CDCD sera.

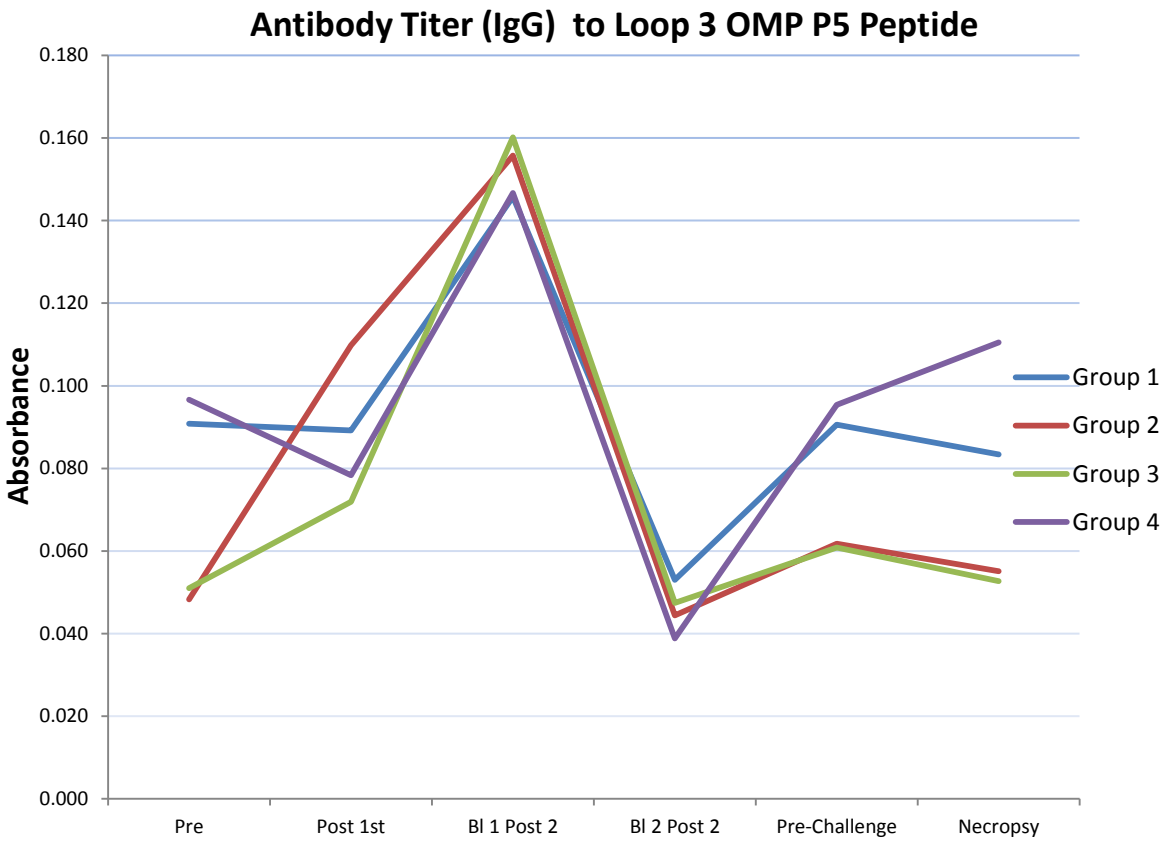

Figure 4.4. Antibody Titer (IgG) ELISA for Animal Study 1. Groups are described in Supplemental Table S4.1. Another presentation of these data, with standard error, is in Supplemental Figure S4.1.

Supplemental Information

Formulation of synthetic peptide for vaccination studies. The synthetic peptide was formulated as 1 and 2 ml doses containing 50 μg of the peptide. The final formulation contained an oil-and-water adjuvant (Sigma Adjuvant Oil System®; #S6322; St. Louis, MO), according to manufacturer's instructions, with a final emulsion containing a 2% oil. Recombinant peptides were formulated into 2 ml doses containing 10 μg of the recombinant peptides, and to contain about 30% water/oil/water (WOW) adjuvant.

Clinical study using bacterin and synthetic peptide. Cesarean-derived, colostrum-deprived (CDCD) piglets, from 5 to 6 weeks of age, were purchased from Struve Laboratories, Manning, IA. On day 1 of birth, the piglets were administered clostridium antiserum, an antibiotic, a bovine colostrum replacement, oral autogenous *E. coli* and *C. perfringens vaccine,* and vitamin E. Vitamin E was again administered on day 11, and iron was administered on day 12. All the CDCD piglets enrolled in the study were randomized into four groups, as indicated in Table 2. At age 5-6 weeks, the animals were given a first intramuscular administration as follows: Group 1, 1 ml peptide formulation; Group 2, 2 ml peptide formulation; Group 3, 2 ml bacterin formulation; and Group 4, none (negative control). Three weeks later, the animals were given a second intramuscular administration as follows: Group 1, 1 ml peptide formulation; Group 2, 2 ml bacterin formulation; Group 3, 2 ml peptide formulation; and Group 4, none (negative control). Three weeks after the second administration, all groups were administered 1.85×10^{11} CFU/ml of live *H. parasuis* isolate GL93. The animals were subsequently observed for 2 weeks to determine survival.

Clinical study using recombinant peptides. CDCD piglets, as described in the previous clinical study, were used. The piglets were randomized into four groups, as indicated in

Table 3. At age 5-6 weeks, and again 3 weeks later, the animals were given intramuscular administrations as follows: Group 1, 2 ml of no antigen control solution; Group 2, 2 ml of the Plasmid Upstream + P5 Loop4+TMD recombinant peptide formulation; Group 3, 2 ml of the Plasmid Upstream + P5 No SS peptide formulation; Group 4, 2 ml containing both the Plasmid Upstream + P5 Loop4+TMD (10 μg peptide) and Plasmid Upstream + P5 No SS (10 μg peptide) formulations. Three weeks after the second administration, all groups were administered 1.85 x 10^{11} CFU/ml of live *H. parasuis* isolate GL93. The animals were subsequently observed for 2 weeks to determine survival. Serum samples were obtained from the piglets at the times of the first and second administrations of the peptides; at 1, 2, and 3 weeks after the second administration (3 weeks after the second administration is also when the *H. parasuis* challenge was administered); and at 2 weeks after administration of the challenge.

Supplemental Tables and Figures

Supplemental Table S4.1. Results of Peptide and Bacterin Challenge Study

Group	No. animals	First dose	Second dose	Animals dead	Animals alive	% survival
1	10	1 ml peptide	1 ml peptide	5	5	50
2	10	2 ml peptide	2 ml bacterin	1	9	90
3	8	2 ml bacterin	2 ml peptide	0	8	100
4	8	None	None	6	2	25

Supplemental Table S4.2. Results of Recombinant Peptide Vaccination and Recombinant P5 Challenge Study

Group	No. animals	First and second doses	Animals dead	Animals alive	% survival
1	8	None	5	3	37
2	9	Plasmid Upstream + P5 Loop4+TMD	5	4	44
3	6	Plasmid Upstream + [a]P5 No SS	3	3	50
4	5	Plasmid Upstream + P5 Loop4+TMD + Plasmid Upstream + [a]P5 No SS	3	2	20

[a] Recombinant OMP P5 without signal sequence

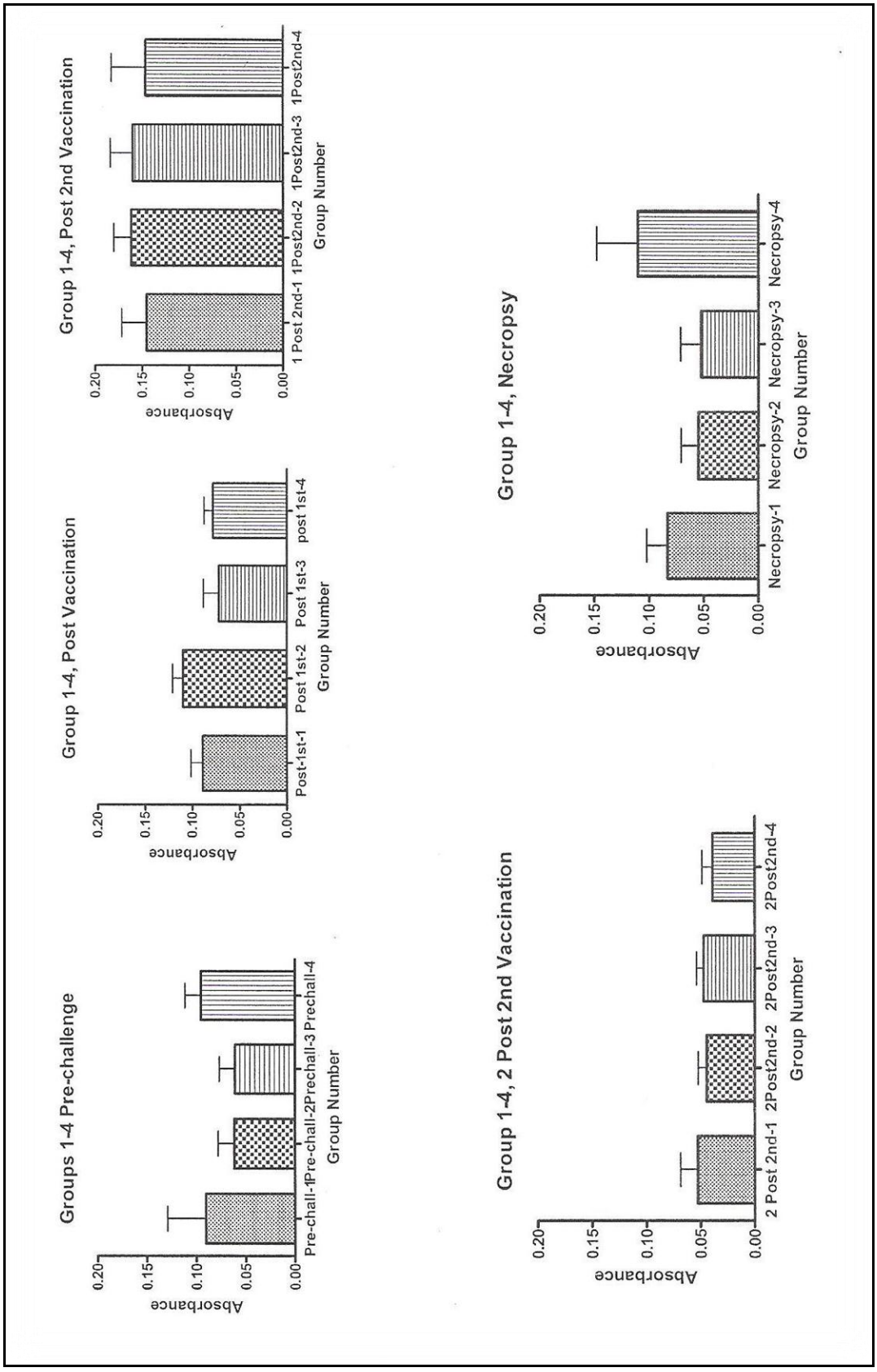

Supplemental Figure S4.1. Results of the first challenge experiment using loop 3 peptide

References

1. K. Nedbalcova, P.S., Z. Jaglic, R. Ondriasova, Z. Kucerova, *Haemophilus parasuis and Glässer's disease in pigs: a review.* Veterinarni Medicina, 2006. **51**(5): p. 168-179.
2. Harris, D.L., *Control of common infectious diseases. In: Multi-site pig production.* Iowa State University Press, 2000: p. 98-102.
3. Glasser, K., . Quoted in Krankenheinten des Schweines. 5th ed. , 1910. **1950**(Sharper, Hanover): p. 106.
4. Rapp-Garielson, P.K.a.V.J., *Designation of 15 serovars of Haemophilus parasuis on the Basis of Immunodiffusion Using Heat-Stable Antigen Extract.* Journal of Clinical Microbiology, 1992. **30**(4): p. 862-865.
5. Hansen, E.J., et al., *Immune enhancement of pulmonary clearance of nontypable Haemophilus influenzae.* Infect Immun, 1988. **56**(1): p. 182-90.
6. Reddy, M.S., et al., *Binding between outer membrane proteins of nontypeable Haemophilus influenzae and human nasopharyngeal mucin.* Infect Immun, 1996. **64**(4): p. 1477-9.
7. Webb, D.C.a.A.W.C., *Secondary Structure and molecular analysis of interstrain variability in the P5 outer-membrane protein of non-typable Haemophilus influenzae isolated from diverse anatomical sites.* Journal of Medical Microbiology, 1998. **47**: p. 1059-1067.
8. Dium, B.e.a., *Fine Mapping of Outer Membrane Protein P2 Antigenic Sites Which Vary during Persistent Infection by Haemophilus influenzae.* Infection and Immunity, 1996. **64**(11): p. 4673-4679.

9. Novotny, L.A. and L.O. Bakaletz, *The fourth surface-exposed region of the outer membrane protein P5-homologous adhesin of nontypable Haemophilus influenzae is an immunodominant but nonprotective decoying epitope.* J Immunol, 2003. **171**(4): p. 1978-83.

10. Sali, A.a.B., T.L, *Comparative protein modelling by satisfaction of spatial restraints.* Journal of Molecular Biology, 1993. **234**: p. 779-815.

11. Hildebrand, A., et al., *Fast and accurate automatic structure prediction with HHpred.* Proteins, 2009. **77 Suppl 9**: p. 128-32.

12. Soding, J., A. Biegert, and A.N. Lupas, *The HHpred interactive server for protein homology detection and structure prediction.* Nucleic Acids Res, 2005. **33**(Web Server issue): p. W244-8.

13. Merrifield, R.B., *Automated Peptide Synthesis.* Nature, 1965. **207**: p. 522-523.

14. Merrifield, R.B., *Solid-Phase Peptide Synthesis, III. An Improved Synthesis of Bradykinin* Biochemistry, 1964. **3**(9): p. 1385-1390.

15. Mullins, M.A., et al., *Characterization and comparative analysis of the genes encoding Haemophilus parasuis outer membrane proteins P2 and P5.* J Bacteriol, 2009. **191**(19): p. 5988-6002.

16. Tang, C., et al., *Characteristics of the molecular diversity of the outer membrane protein A gene of Haemophilus parasuis.* Can J Vet Res, 2010. **74**(3): p. 233-6.

17. Tabatabai, L.B. and G.W. Pugh, Jr., *Modulation of immune responses in Balb/c mice vaccinated with Brucella abortus Cu-Zn superoxide dismutase synthetic peptide vaccine.* Vaccine, 1994. **12**(10): p. 919-24.

CHAPTER 5. IDENTIFICATION AND ANTIGENIC CHARACTERIZATION OF A PUTATIVE SURFACE LOCALIZED GLYCERALDEHYDE-3-PHOSPHATE DEHYDROGENASE OF *Haemophilus parasuis*

A paper to be submitted to *Biochemical and Biophysical Research Communications*

Mandy K. Zimmerli and Louisa B. Tabatabai

Abstract

Haemophilus parasuis is a gram negative organism associated with the manifestation of the swine respiratory illness known as Glässer's disease. Because a commercially available cross-protective vaccine and complimentary diagnostic is unavailable, it is important to identify and characterize putative virulence factors which could serve as a cross-protective vaccine and/or diagnostic. Additionally, it is important to identify and characterize colonization factors as colonization is one of the first steps in establishment of infection. In this study, a surface localized glyceraldehyde-3-phostphate dehydrogenase (GAPDH) was identified in *H. parasuis* by immunoblot and N-terminal sequencing. Close to the calculated molecular weight, the GAPDH presented here has an apparent molecular weight of 35kDa. However, the pI was predicted to be approximately 6.2-7.0, which is higher than the calculated pI of 5.9. Because surface localized GAPDH has been shown to be involved with colonization in other bacterial pathogens, it is hypothesized that this protein could have the same function in *H. parasuis*. This is the first paper to report the identification of a surface localized GAPDH in *H. parasuis* and discuss the protein as a putative virulence factor.

Introduction

Haemophilus parasuis is a non-motile, gram negative, pleomorphic bacterium responsible for a respiratory illness in swine known as Glässer's disease [1,2,3]. Symptoms

of this disease include lameness, arthritis, meningitis, pleuritis, and polyserositis. To date, there is no commercially available cross-protective vaccine to prevent the economic loss in industry due to this pathogen. Additionally, few reports have been done on the protein profile of *H. parasuis*. Research has primarily been focused on the identification of genes.

Since colonization is the first step in establishment of infection, proteins involved in colonizing the respiratory tract make for good vaccine candidates in preventing adherence of the bacteria. Most commonly, adhesins and outer membrane proteins have been discussed given their ability to adhere to the host epithelial cells. In organisms related to *H. parasuis*, these colonization factors include: OMP P2, OMP P5, and Opacity associated protein (Oap) of *H. influenza*, and the Opa protein of *Neisseria sp*. Recent experimental studies are beginning to identify proteins of bacterial pathogens with multiple functions, including glyceraldehyde-3-phosphate dehydrogenase.

Glyceraldehyde-3-phoshate dehydrogenase (GAPDH) is primarily considered a cytosolic-localized glycolytic enzyme. This protein, however, has been experimentally determined to be multifuntional. Studies on this protein in *Mycoplasma pneumonia, Streptococcus pyogenes, Staphyloccucs aureus, Neisseria meningitidis,* and *Streptococcus suis* have identified a surface-localized GAPDH which plays a role in adherence to host cells [4,5,6,7,8]. Additionally, the use of GAPDH as a vaccine candidate has been studied in cattle infected with *Mycoplasma bovis* [9].

To date, the GAPDH of *H. parasuis* has only been identified by proteomic techniques in the cytosolic fraction of strain SH0165 (SV5) and through sequencing of the *H. parasuis* genome [10,11,12]. Here we report the identification of a surface-localized GAPDH for *H. parasuis*. Because this protein has been implicated as being important in the establishment of

colonization, particularly in the related organism *Neisseria meningitidis*, molecular modeling analysis followed by prediction of antigenic propensity was performed in order to identify antigenic epitopes which may serve as protective in the design of a subunit vaccine. These regions may play a role in adherence of GAPDH to the host epithelial cells. Future work on this protein must be done to determine whether or not surface-localized GAPDH of *H. parasuis* actually plays a role in adherence to host epithelial cells.

Material and Methods

Bacterial strains. Table 5.1 describes the reference strain used in this study, HP2. This strain was obtained from Richard Ross (College of Veterinary Medicine, Iowa State University, Ames, IA). The strain was grown on Casman agar, supplemented with 5% horse serum (Gibco-BRL, Carlsbad, CA), and overlaid with 0.016% NAD (Sigma Chemical Co., St. Louis, MO) using 5% CO_2 at 37°C. Colonies were selected and grown in liquid media consisting of Freys medium (Sigma Chemical Co., St. Louis, MO) supplemented with 20% horse serum (Gibco-BRL, Carlsbad, CA) and 0.016% NAD (Sigma Chemical Co., St. Louis, MO). Tubes were incubated aerobically with shaking (100 rpm) at 37ºC for 24 h. 5 mL of inoculum were used to inoculate 100-mL Freys medium. Cultures were incubated with shaking (100 rpm) for 24 h at 37ºC and harvested by centrifugation at 7,500 ×*g* at 4ºC.

Outer membrane protein extraction. Cells were resuspended and washed in 20 mM 4-(2-hydroxyethyl)piperizane-1-ethanesulfonic acid (HEPES) buffer pH 7.4-0.15 M sodium chloride. Cells were resuspended again in 20 mM HEPES buffer pH 7.4-0.45 M sodium chloride and heated at 56^{o}C for 60 minutes followed by centrifugation at 10,000 × *g* at 4ºC. The protein-containing supernatant was stored at -80ºC until use. Protein concentration was

determined using the BCA Assay (Sigma, St. Louis, MO) and dialyzed overnight in 20mM Tris-HCl pH8.0.

2-D SDS PAGE and immunoblotting. Protein samples were reduced with DTT and alkylated with iodoacetamide and prepared and separated according to Zoom IEF Fractionator protocol (Invitrogen, Carlsbad, CA). Samples were loaded into chambers of the Zoom IEF Fractionator, and IEF was performed in accordance with manufacturer's instructions except for the following changes: 100V for 1.5 hours; 200V for 2.5 hours; and 600V for 6 hours. After removal of the samples, approximately 50 microliters from each chamber was concentrated using cold acetone (-20^{o}C) to a final concentration of 80% volume/volume. Following centrifugation, the pellet was dried and resuspended in 20 micoliters of NUPAGE sample buffer. Samples were loaded onto a Novex 4-12% Bis-Tris Zoom Gel, IPG well (Invitrogen). Samples were run according to the manufacturer's instructions, stained with Coomassie Blue R250 or transferred electrophoretically to 0.45-µm nitrocellulose (Schleicher and Schuell, Keene, NH) for immunoblotting. Immunoblots were blocked with 0.25% fish gelatin in wash buffer consisting of 1.5 mM KH_2PO_4, 20 mM Na_2HPO_4, 125 mM NaCl, 3 mM KCl, 0.05% Tween-20 (PBST, pH7.2). The blocked membranes were incubated with 1:5,000 dilutions of anti-P5 monoclonal antibody (4BF8), and 1:5,000 dilutions of rabbit anti-mouse IgG horseradish peroxidase-labeled (Jackson ImmunoResearch, West Grove, PA) sequentially. Blots were developed with 3,3',5,5'-tetramethylbenzidine (TMB) (Kirkegaarde and Perry Labs, Gaithersburg, MD) as the substrate. Calculated pI and molecular weights were determined using ExPasy Calculate pI/Mw tool.

Protein sequencing. Following SDS-PAGE, gels were blotted electrophoretically to PVDF (Millipore, Billerica, MA) and stained with Ponceua S. Bands were excised from the PVDF and sequenced with a model 494 Procise protein/peptide sequencer (Applied Biosystems, Foster City, CA) at the Iowa State University Protein Facility. The identity of the sequence was determined by using the BLAST server of the National Center for Biotechnology.

Molecular modeling and prediction of antigenic propensity. Glyceraldehyde-3-phoshate dehydrogenase (GAPDH) was modeled using the Modeller program [13] following tertiary structural analysis by HHPred [14,15] using pdb70_1Oct11 HMM database. The quality of the model was verified using QMEAN [16,17,18]. The sequence was submitted to Scratch protein predictor [19] in order to identify antigenic epitopes via ANTIGENpro [20].

Results

Identification of *H. parasuis* GAPDH. Figures 5.1 and 5.2 show the 2-D SDS-PAGE and immunoblot analysis using mAb for OMP P5 of *H. influenzae*. The results of N-terminal sequence analysis are presented in Table 5.2. A BLAST search of N-terminal sequence revealed the immunoreactive protein to be GAPDH. The calculated molecular weight of the protein was determined to be approximately 36kDa, while the apparent molecular weight of GAPDH, as determined by SDS-PAGE, is approximately 35kDa. The experimentally observed pI for GAPDH is higher than the calculated pI of 5.8. An additional strain, SW114 (SV3), was also subjected to this analysis with the same results.

Molecular modeling and antigenic propensity analysis of *H. parasuis* GAPDH. Molecular modeling analysis indicates that GAPDH of *H. parasuis* shares sequence and structural homology with a variety of GAPDHs, including GAPDH of *E. coli.* QMEAN predicted the model reliability to be 0.739, with a mean Z-score of -0.43. Results from

QMEAN analysis are shown in Supplemental Figures S5.1-S5.4. The score for QMEAN is based on a combination of six terms (Figure S5.2) and is obtained by comparing the model with the Z-scores of high-resolution structures as solved by X-ray crystallography. Overall, the model for *H. parasuis* GAPDH is reliable, with a few areas which have greater than 3.5Å deviation from expected location (Supplemental Figure S5.1). The Z-scores for individual pseudo-energies are shown in Supplemental Figures S5.2 and S5.3. As shown in both figures, particularly in S5.3, the predicted model has little deviation for the individual energetic terms when compared to that of the high resolution structures. The predicted error associated with each residue (Supplemental Figure S5.4) indicates less than 5% error associated with all residues prior to the last five residues of the structure. However, these residues comprise the C-terminus of the protein and do not form a structure, so deviation is expected. Figures 5.3 and 5.4 show the predicted antigenic propensity of the surface localized GAPDH of *H. parasuis*. Regions of both moderate to high antigenicity had a solvent accessibility score of greater than 40% as predicted by Scratch [19]. The overall antigenic propensity score of the protein is 0.71.

Discussion

Surface localized GAPDH has been shown to be an important colonization factor in other bacteria [5,6,7,8,21,22,23,24]. A study by Jin et. al in 2011 reports global gene expression profiles of virulence factors of *S. pyogenes* are down-regulated when surface localized GAPDH is prevented from exporting to the surface of the bacterium by introduction of a mutation [4]. In a different study, this mutation demonstrated decreased expression of surface localized GAPDH and while the wild type and mutant strains had similar growth profiles, the mutant bacteria bound significantly less human plasminogen,

adhered poorly to human pharyngeal cells, and lost innate antiphagocytic activity[25]. Moreover, the surface-localized GAPDH of *N. meningitidis* has been characterized as non-phosphorylating [26]. While the role of the cytosolic protein is enzymatic oxidative phosphorylation, the role of the surface-localized GAPDH is comparable to an adhesin. Identification and characterization of this protein are important due to its role in the colonization, which is the first step in establishment of infection.

Here we present the identification of a surface-localized GAPDH in *H. parasuis* by immunoblot followed by N-terminal sequencing. Previous proteomic studies on *H. parasuis* have only identified GAPDH in the cytosolic fraction. This could be due to the nature of the outer membrane protein preparation. In accordance with the calculated molecular weight of 36kDa, the *H. parasuis* GAPDH has an apparent molecular weight of 35kDa. The pI, however, was higher than calculated, ranging from 6.2-7.0. It should be noted that the mAb (4BF8) binds to a variety of epitopes and while it was used to probe for the P5 protein, a colonization factor, the antibody cross reacted with other proteins. This has been shown in other work using this particular antibody [27]. The target epitope of 4BF8 is unknown.

Molecular modeling based on sequence homology methods predicted that the structure of GAPDH, not surprisingly, is highly conserved and homologous to the GAPDH of *E. coli*. QMEAN was used to determine the quality of the model, and the model was given a 0.739 reliability score. The area of the protein with greatest error per residue is the last five residues, corresponding to the unstructured C-terminus. Additionally, calculated error exists for a few loop regions and structured regions of the protein. Overall, the model is considered reliable in comparison to known high resolution structures.

Antigenic prediction methods provide a platform for the design of vaccines for existing and emerging pathogens. Methods of the past have relied heavily on homology of known pathogens. However, the advent of ANTIGENpro brought the first homology-free microarray based prediction platform. Accuracy of this platform is approximately 76% as determined by cross-validation experiments [20]. In this case, the predicted antigenic epitopes can be used in the design of a subunit vaccine and/or to understand what antigenic epitopes could be involved with colonization of the host epithelial cells.

This is the first record of identification and antigenic characterization of a surface localized *H. parasuis* GAPDH. While prediction methods are useful in research, they are not a substitute for actual structural determination and experimental methods. Future studies using surface localized *H. parasuis* GAPDH are necessary to elucidate if GAPDH is indeed involved in colonization, what epitopes of GAPDH are important to adhering to epithelial cells, and which predicted antigenic epitopes may serve useful in the design of a subunit vaccine against *H. parasuis* infection.

Acknowledgements

We would like to thank Muriel van Schilfgaarde for the mAb to P5 (4BF8) of *H. influenzae* and the ISU Protein Facility for assistance with N-terminal sequencing.

Tables

Table 5.1. Description of Bacterial Strain

Serovar	Reference[a] strain	Country of origin	Diagnosis/ isolation site	Virulence[b]
2	SW124	Japan	Healthy/nose	L

[a] Reference strain information and virulence scores obtained from reference 13.

[b]Virulence designations: H, high virulence; L, low/moderate virulence; A, avirulent.

Table 5.2. N-terminal Sequence and Identification of Bands from Figure 5.3

Calculated MW(kDa)/pI	Observed MW(kDa)/pI	Source	Sequence	Identity[a]
35/5.8	36/6.2-7.0	*H. parasuis* SV2	AIKIGINGF	*H. parasuis* GAPDH [b]

[a]BLAST server of the National Center for Biotechnology Information (Altshul et al., 1997)

[b]Accession number: ACL31707

Figures

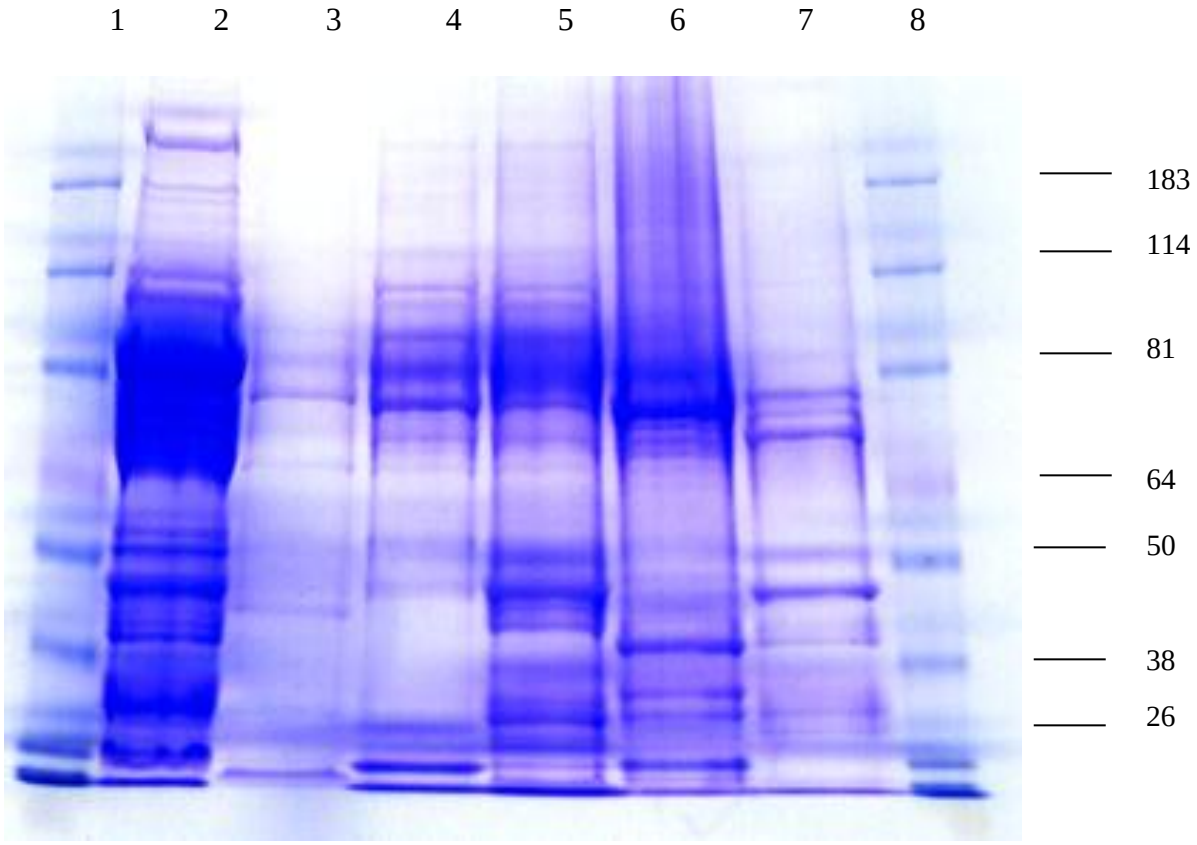

Figure 5.1. 4-12% SDS-PAGE of HP2 outer membrane proteins following IEF Fractionation. Lanes 1 and 8 are molecular weight standards; Lane 2 is prior to fractionation; Lanes 3-7 correspond to fractions with pI of 3.0-4.6, 4.6-5.4, 5.4-6.2, 6.2-7.0, and 7.0-10.0, respectively. Molecular weights of the standards are indicated in kilodaltons.

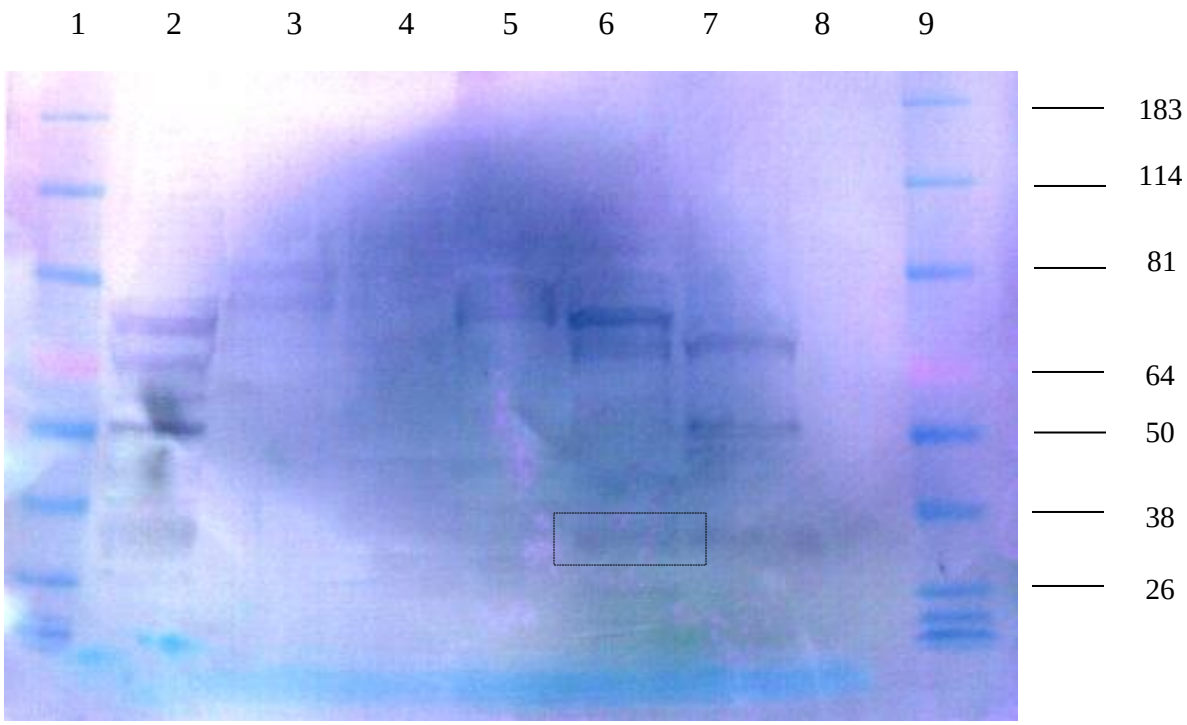

Figure 5.2. Immunoblot of HP2 using anti-P5 mAb. Lanes (from left to right) 1 and 9 are molecular weight standards; Lane 2 is prior to fractionation; Lanes 3-7 correspond to fractions with pI of 3.0-4.6, 4.6-5.4, 5.4-6.2, 6.2-7.0, and 7.0-10.0 respectively; Lane 8 is blank. Molecular weights of the standards are indicated in kilodaltons. The band which was excised for N-terminal sequencing from PVDF is boxed.

maikigingf grigrivfra aqkrddievv gindlidvey maymlkydst hgrfdgtvev
kdgklvvngk eirvtserdp anlkwneigv diaveatglf lddttarkhi eagakkvvlt
gpskdstpmf vngvnfnaya gqdivsnasc ttnclaplar vihetfgike glmttvhatt
atqktvdgps akdwrggrga aqniipsstg aakavgkvlp alngkltgma frvptanvsv
vdltvnlekp asyeeikkai kdaaegktfn gelkgvlgyt edavvstdfn gavetsvfda
dagialtdtf vklvswydne tgysnkvldl vahvynykg

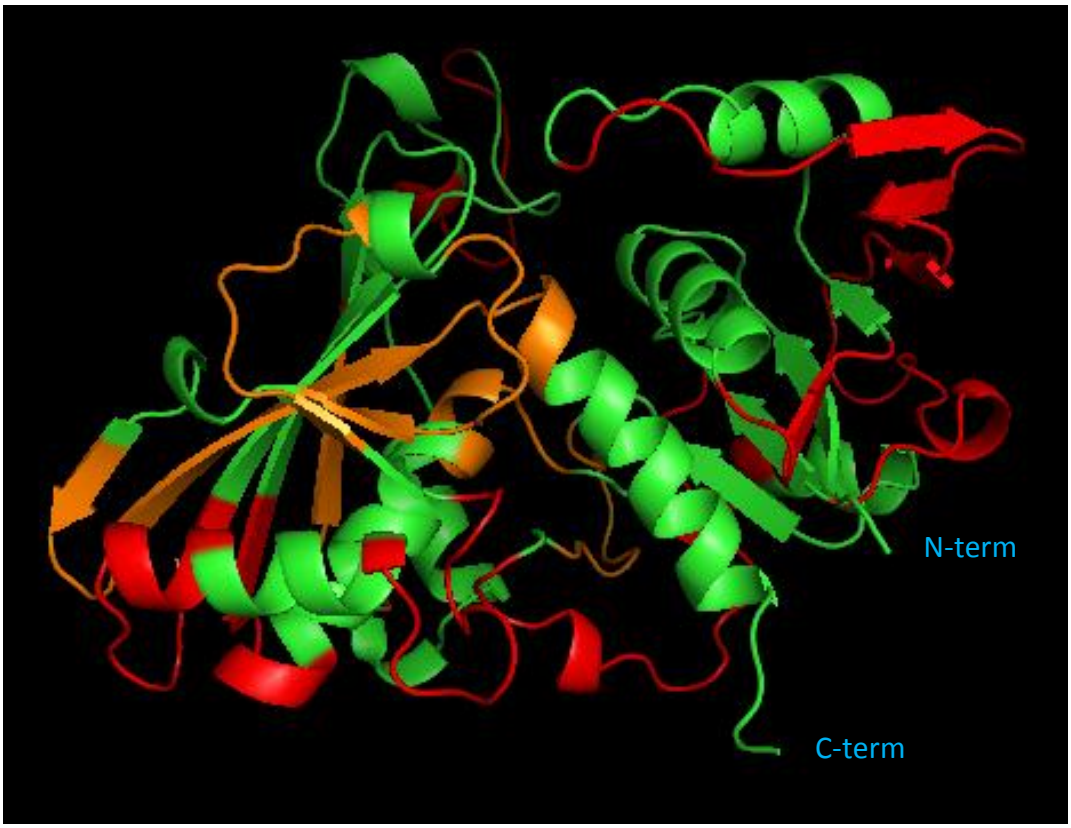

Figure 5.3. Predicted sites of antigenic propensity for *H. parasuis* GAPDH. High scores (>5 net votes) and moderate scores (< 5 net votes) are shown as predicted by ANTIGENpro. The N-terminus (N-term) and C-terminus (C-term) of the protein are designated. ANTIGENpro scores are shown in Figure 5.5 per residue.

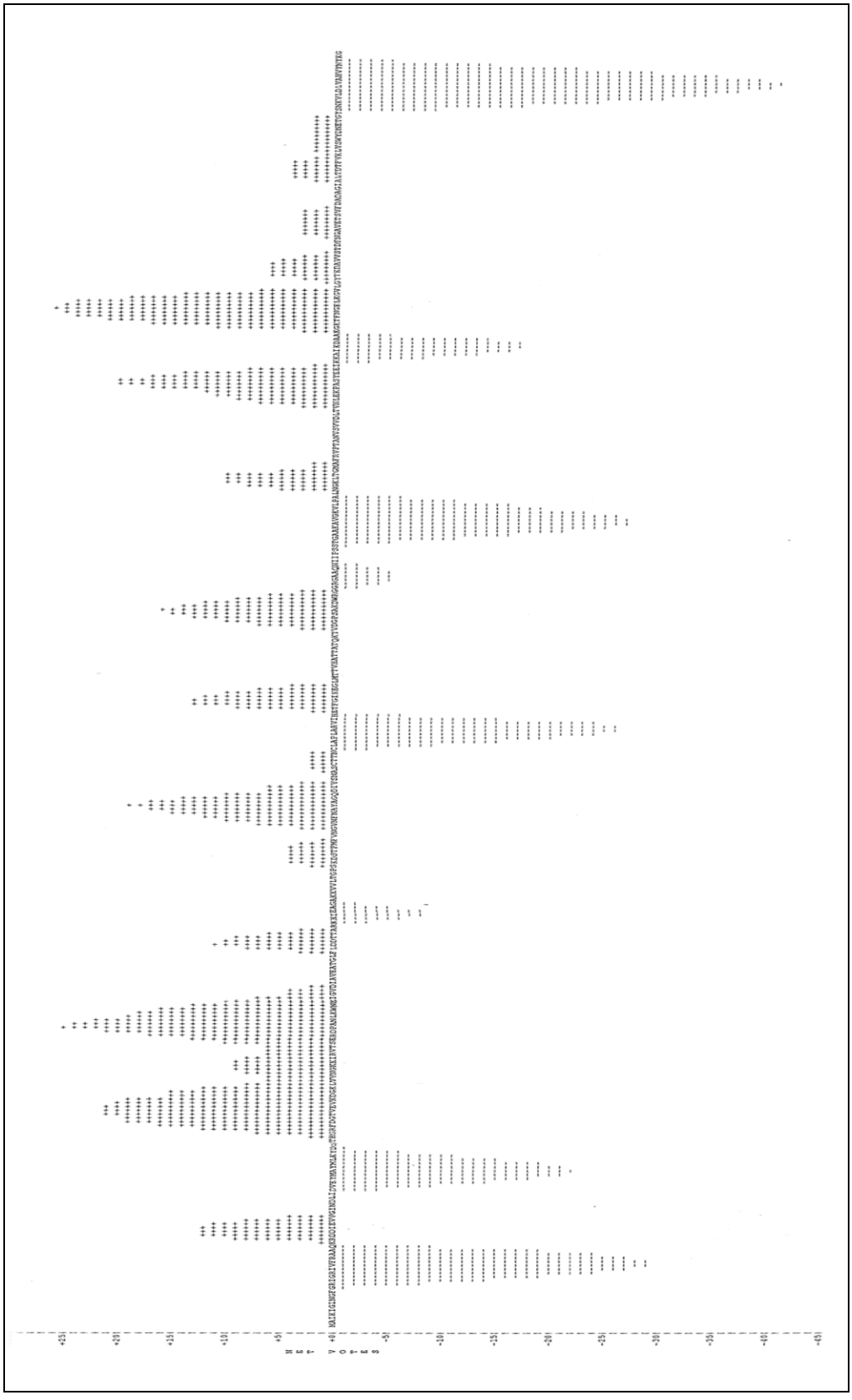

Figure 5.4. Predicted antigenic propensity scores for GAPDH based on ANTIGENPro

Supplemental Figures

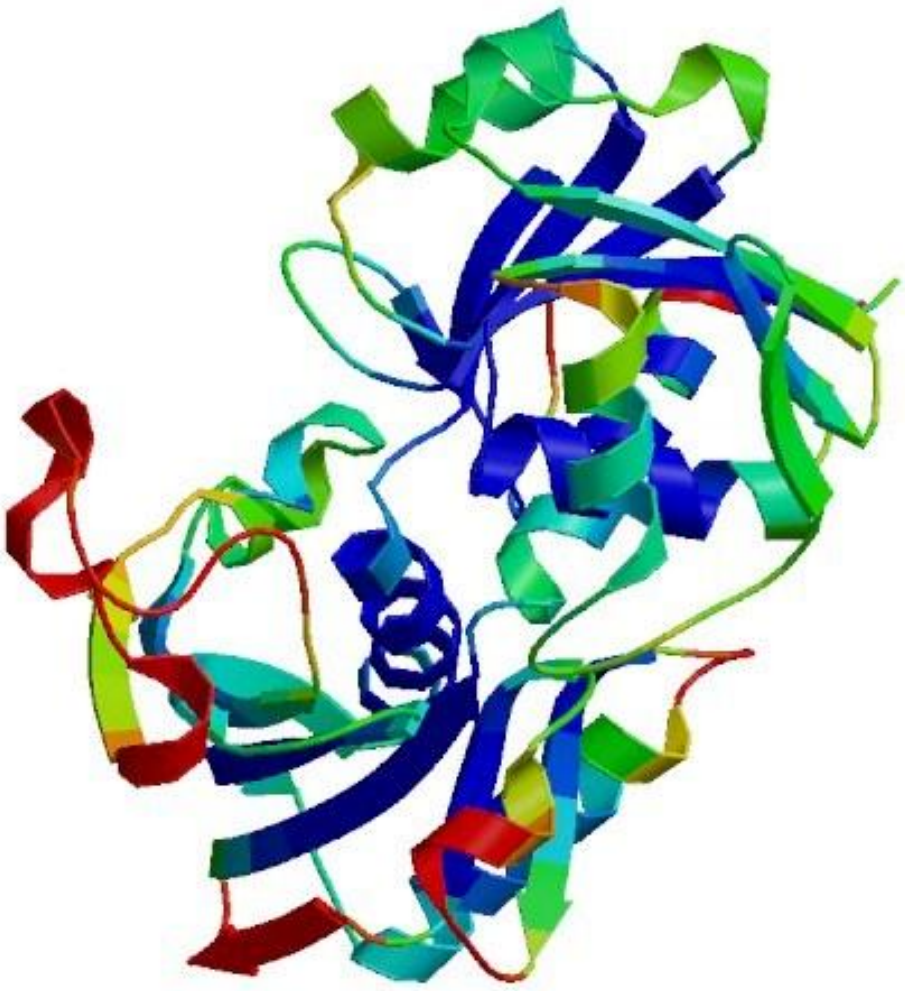

Supplemental Figure 5.1. Estimation of per residue error with blue (reliable regions; < 1 Å) to red (unreliable regions; > 3.5 Å). Overall, the model for *H. parasuis* GAPDH is reliable with few areas of per residue error.

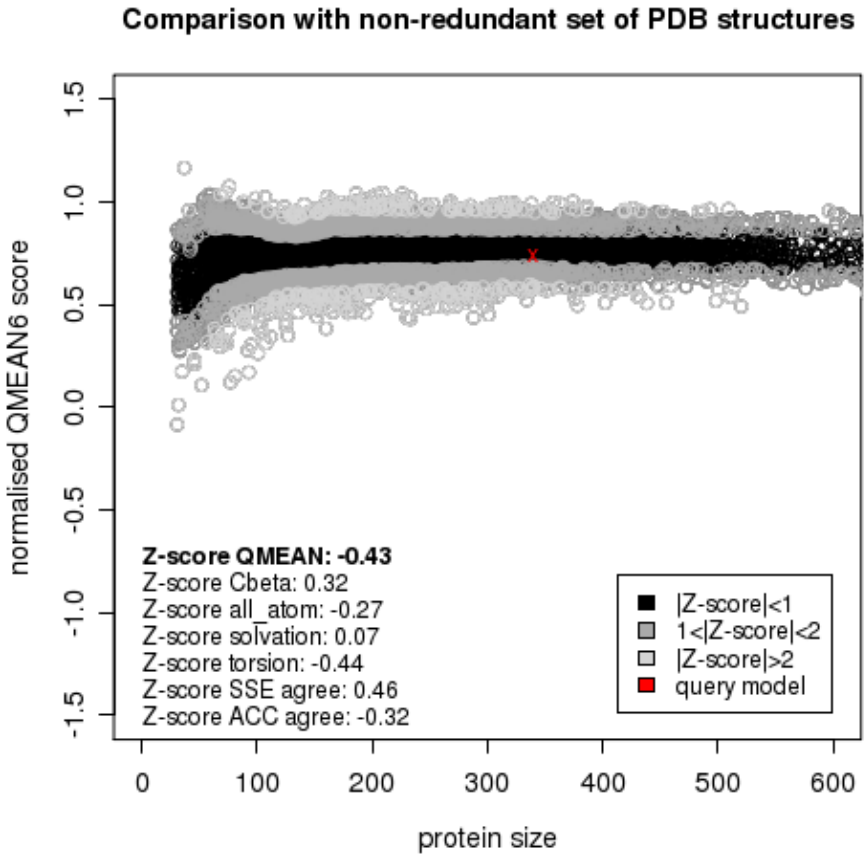

Supplemental Figure 5.2. Estimated absolute quality of model. The GAPDH model is compared to non-redundant set of structures of similar size. The quality of the model is based upon the following parameters: Cβ interaction energy; all-atom pairwise energy; solvation energy; torsion angle energy; secondary structure agreement; and solvent accessibility agreement.

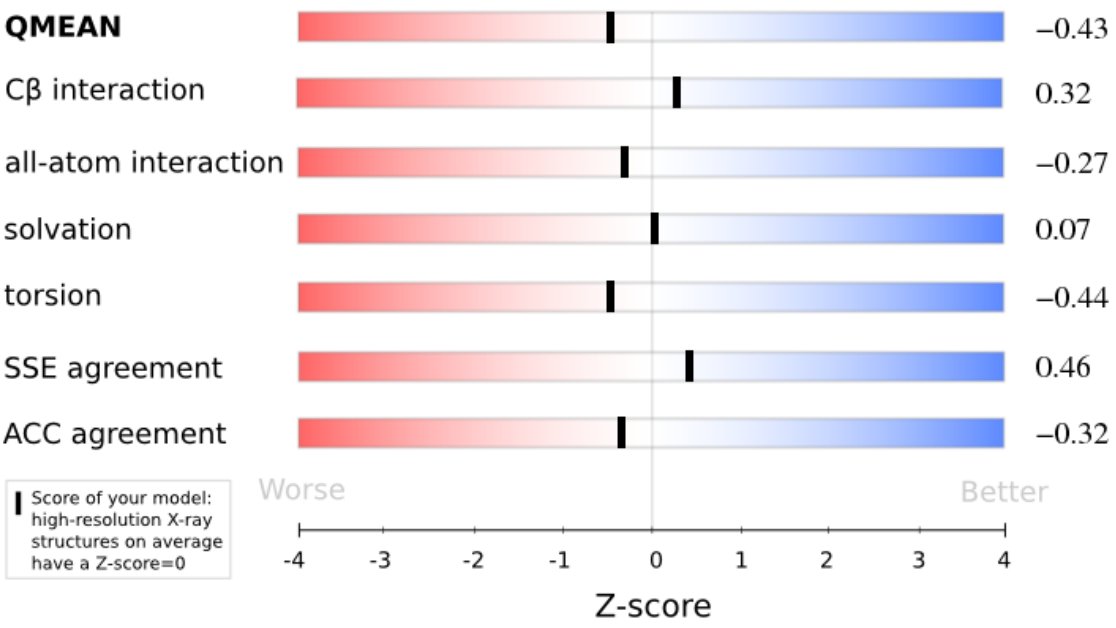

Supplemental Figure 5.3. Z-score of QMEAN terms. Terms are explained in Supplemental Figure S5.2.

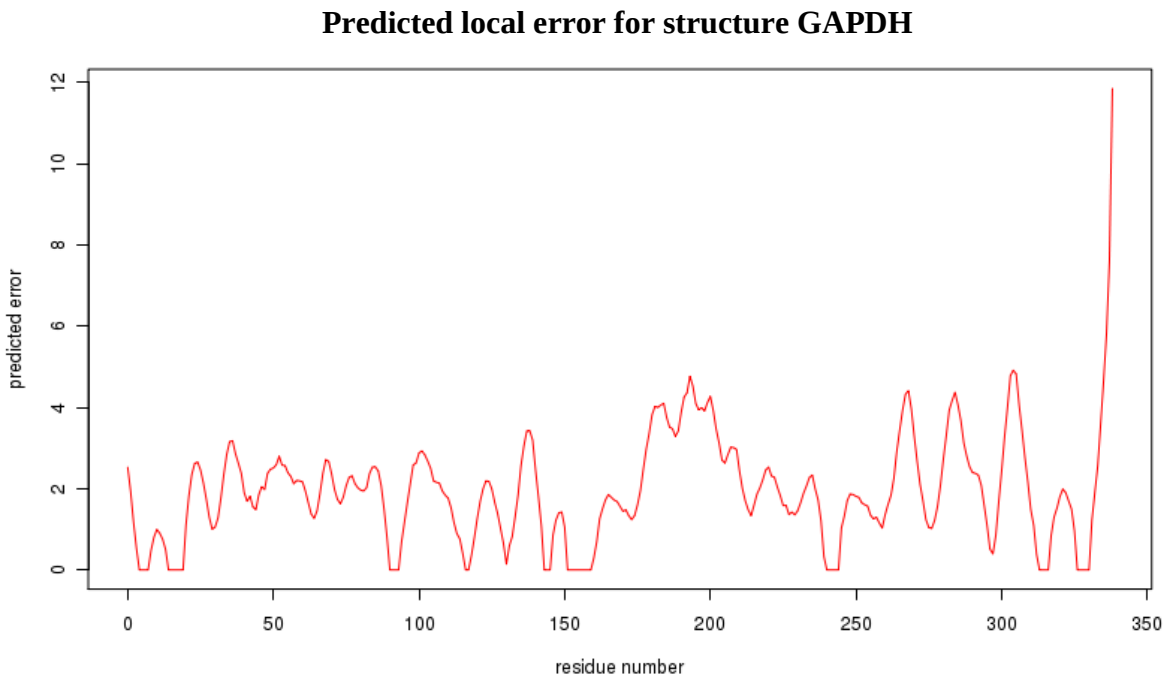

Supplementary Figure 5.4. Energy profile of model with estimated residue errors. Model has less than 5% error associated with each residue, aside from the last five residues.

References

[1] P.S. K. Nedbalcova, Z. Jaglic, R. Ondriasova, Z. Kucerova, *Haemophilus parasuis* and Glässer's disease in pigs: a review, Veterinarni Medicina 51 (2006) 168-179.

[2] D.L. Harris, Control of common infectious diseases. In: Multi-site pig production, Iowa State University Press (2000) 98-102.

[3] K. Glasser, , Quoted in Krankenheinten des Schweines. 5th ed. 1950 (1910) 106.

[4] H. Jin, S. Agarwal, V. Pancholi, Surface export of GAPDH/SDH, a glycolytic enzyme, is essential for *Streptococcus pyogenes* virulence, MBio 2 (2011) e00068-00011.

[5] R. Dumke, M. Hausner, E. Jacobs, Role of *Mycoplasma pneumoniae* glyceraldehyde-3-phosphate dehydrogenase (GAPDH) in mediating interactions with the human extracellular matrix, Microbiology 157 (2011) 2328-2338.

[6] S.A. Tunio, N.J. Oldfield, D.A. Ala'Aldeen, K.G. Wooldridge, D.P. Turner, The role of glyceraldehyde 3-phosphate dehydrogenase (GapA-1) in *Neisseria meningitidis* adherence to human cells, BMC Microbiol 10 (2010) 280.

[7] J. Purves, A. Cockayne, P.C. Moody, J.A. Morrissey, Comparison of the regulation, metabolic functions, and roles in virulence of the glyceraldehyde-3-phosphate dehydrogenase homologues gapA and gapB in *Staphylococcus aureus*, Infect Immun 78 (2010) 5223-5232.

[8] J. Brassard, M. Gottschalk, S. Quessy, Cloning and purification of the *Streptococcus suis* serotype 2 glyceraldehyde-3-phosphate dehydrogenase and its involvement as an adhesin, Vet Microbiol 102 (2004) 87-94.

[9] J. Perez-Casal, T. Prysliak, Detection of antibodies against the *Mycoplasma bovis* glyceraldehyde-3-phosphate dehydrogenase protein in beef cattle, Microb Pathog 43 (2007) 189-197.

[10] X. Wang, X. Xu, S. Zhang, F. Guo, X. Cai, H. Chen, Identification and analysis of potential virulence-associated genes in *Haemophilus parasuis* based on genomic subtraction, Microb Pathog 51 (2011) 291-296.

[11] M. Zhou, A. Zhang, Y. Guo, Y. Liao, H. Chen, M. Jin, A comprehensive proteome map of the *Haemophilus parasuis* serovar 5, Proteomics 9 (2009) 2722-2739.

[12] M. Yue, F. Yang, J. Yang, W. Bei, X. Cai, L. Chen, J. Dong, R. Zhou, M. Jin, Q. Jin, H. Chen, Complete genome sequence of *Haemophilus parasuis* SH0165, J Bacteriol 191 (2009) 1359-1360.

[13] A.a.B. Sali, T.L, Comparative protein modelling by satisfaction of spatial restraints, Journal of Molecular Biology 234 (1993) 779-815.

[14] A. Hildebrand, M. Remmert, A. Biegert, J. Soding, Fast and accurate automatic structure prediction with HHpred, Proteins 77 Suppl 9 (2009) 128-132.

[15] J. Soding, A. Biegert, A.N. Lupas, The HHpred interactive server for protein homology detection and structure prediction, Nucleic Acids Res 33 (2005) W244-248.

[16] P. Benkert, S.C. Tosatto, T. Schwede, Global and local model quality estimation at CASP8 using the scoring functions QMEAN and QMEANclust, Proteins 77 Suppl 9 (2009) 173-180.

[17] P. Benkert, M. Kunzli, T. Schwede, QMEAN server for protein model quality estimation, Nucleic Acids Res 37 (2009) W510-514.

[18] P. Benkert, S.C. Tosatto, D. Schomburg, QMEAN: A comprehensive scoring function for model quality assessment, Proteins 71 (2008) 261-277.

[19] J. Cheng, A.Z. Randall, M.J. Sweredoski, P. Baldi, SCRATCH: a protein structure and structural feature prediction server, Nucleic Acids Res 33 (2005) W72-76.

[20] C.N. Magnan, M. Zeller, M.A. Kayala, A. Vigil, A. Randall, P.L. Felgner, P. Baldi, High-throughput prediction of protein antigenicity using protein microarray data, Bioinformatics 26 (2010) 2936-2943.

[21] G.T. Lu, J.R. Xie, L. Chen, J.R. Hu, S.Q. An, H.Z. Su, J.X. Feng, Y.Q. He, B.L. Jiang, D.J. Tang, J.L. Tang, Glyceraldehyde-3-phosphate dehydrogenase of *Xanthomonas campestris* pv. campestris is required for extracellular polysaccharide production and full virulence, Microbiology 155 (2009) 1602-1612.

[22] H.T. Sojar, R.J. Genco, Identification of glyceraldehyde-3-phosphate dehydrogenase of epithelial cells as a second molecule that binds to *Porphyromonas gingivalis* fimbriae, FEMS Immunol Med Microbiol 45 (2005) 25-30.

[23] K. Maeda, H. Nagata, Y. Yamamoto, M. Tanaka, J. Tanaka, N. Minamino, S. Shizukuishi, Glyceraldehyde-3-phosphate dehydrogenase of *Streptococcus oralis* functions as a coadhesin for Porphyromonas gingivalis major fimbriae, Infect Immun 72 (2004) 1341-1348.

[24] R.A. Alvarez, M.W. Blaylock, J.B. Baseman, Surface localized glyceraldehyde-3-phosphate dehydrogenase of *Mycoplasma genitalium* binds mucin, Mol Microbiol 48 (2003) 1417-1425.

[25] G. Boel, H. Jin, V. Pancholi, Inhibition of cell surface export of group A streptococcal anchorless surface dehydrogenase affects bacterial adherence and antiphagocytic properties, Infect Immun 73 (2005) 6237-6248.

[26] L. Fourrat, A. Iddar, F. Valverde, A. Serrano, A. Soukri, Cloning, gene expression and characterization of a novel bacterial NAD-dependent non-phosphorylating glyceraldehyde-3-phosphate dehydrogenase from *Neisseria meningitidis* strain Z2491, Mol Cell Biochem 305 (2007) 209-219.

[27] J.K. McVicker, The identification and characterization of P5 and P2 colonization proteins of *Haemophilus parasuis* and the targeted binding of Carcinoembryonic Antigen (CEA), PhD Dissertation, Iowa State University, Ames, IA, 2004.

CHAPTER 6. COMPARATIVE ITRAQ AND FUNCTIONAL ANALYSIS OF THE MAJOR OUTER MEMBRANE PROTEINS OF *Haemophilus parasuis*

A paper to be submitted to *Journal of Proteome Research*

Mandy K. Zimmerli and Louisa B. Tabatabai

Abstract

Few studies have attempted to elucidate the mechanism of virulence of *Haemophilus parasuis* at the protein level. This gram-negative pathogen is the causative agent of the swine respiratory illness known as Glässer's disease that results in significant economic loss each year for the industry. Since outer membrane proteins play an important role in virulence, the goal of this study was to identify outer membrane proteins in *H. parasuis* that are differentially expressed in both an aerobic environment and an environment that mimics the oxygen-limiting conditions of infection. The major outer membrane protein preparations of an avirulent reference strain (HP3), a highly virulent reference strain (HP5), a moderately virulent field isolate (HP2170B), and a highly virulent field isolate from PRRSV co-infection (HP409KL) were subjected to 4-plex iTRAQ analysis under aerobic and anaerobic conditions. Identification of proteins was performed using both MASCOT and X! Tandem databases. Quantification of differential protein expression was determined using Scaffold Q+ in order to identify major outer membrane proteins which may serve as vaccine and diagnostic candidates. This study provides the first global proteomic profiling of the major outer membrane proteins of *H. parasuis* and is the first report of quantitative differential outer membrane protein expression as it relates to virulence of the organism and oxygen-limiting conditions.

Introduction

Haemophilus parasuis is the causative agent of Glässer's disease, a respiratory illness in swine, which presents with the symptoms of polyserositis, arthritis, pleuritis, meningitis, and lameness.[1-5] Because this disease causes significant loss in the swine industry, there is not only a necessity to understand the mechanism of virulence, but to also design a cross-protective vaccine and diagnostic. This has proven problematic as not all strains of *H. parasuis* result in morbidity.[6, 7]

Previous studies on *H. parasuis* have identified differences in the genetic profiling of genes from *H. parasuis* as well as related organisms, comparing avirulent to virulent serovars as well as observing differential gene expression under stress conditions relevant to infection. Microarray analysis in conditions that mimic the stresses of infection—iron limitation, oxygen limitation, low pH, and increased temperature—identified 75 genes homologous to pathogens of the *Pasteurellacea* family.[8] Under oxygen-limiting, low pH, and heat stress, genes that were expressed included the phosphotransferase system (PTSI and PTSII) of *Pasteurella multocida*, *P. multocida* spermidine/putrescine transporter PotD, transporters including homologs of GlpT of *P. multocida* for the uptake of glycerol-3-phosphate and MalF of *Salmonella typhimurium* for the uptake of maltose. Genes that were induced during iron-limitation included the homologues of the *hxuCBA* genes of *H. influenzae* and the *yfeA* genes of *P. multocida*. Additionally, a gene homologous to the hemolysin HhdA of *H. ducreyi* was upregulated under oxygen-limiting conditions; the *P. multocida* stress protein ClpB was upregulated under heat, acidic, and iron-limiting growth conditions; and two putative proteases homologous to *H. influenzae* (HI0419) PrtC, and a serine protease of *Fusobacterium nucleatum* subsp. vincentii with an unknown function were found under

acidic, temperature, and heat stress conditions. The results of this study indicated that the expression of virulence factors is relatively conserved among the bacteria of the *Pasteurellaceae* family.

In 2008, genes of *H. parasuis* that were transcribed in necrotic porcine lung tissue were identified using SCOTS (selective capture of transcribed sequences).[9] Genes include possible large adhesin and ABC-type transport system. Use of the SCOTS method from a study in 2009 identified genes expressed in *H. parasuis* under the restriction of iron.[10] This included a pilus assembly protein, predicted phage tail protein, PTS enzyme IIC, transferrin binding proteins A and B, and a chelated ABC iron transporter. Additionally comparative genetic studies were performed to elucidate differences in gene expression of a highly virulent *H. parasuis* serovar, strain SH0165, and an avirulent serovar, 7140.[11] Results of genetic subtraction determined genes for proteins expressed in the virulent serovar. This included phage-related products, large adhesins, ABC-type transport systems, transferrin binding proteins, proteins involved with restriction modification, and outer membrane proteins including the OMP P5. There have been few proteomic profiling studies on *H. parasuis*. A comprehensive proteome analysis of *H. parasuis* strain SH1065 (SV5), published in 2009, identified putative virulence factors, including the major outer membrane proteins P2 and P5.[12]

The goal of this study was to identify major outer membrane proteins and elucidate how differential protein expression may play a role in virulence in both oxygen-rich and oxygen-limiting conditions. The functional role of the identified proteins as well as implications with virulence will be discussed. This study provides the first global proteomic profiling of the major outer membrane proteins of *H. parasuis*. Moreover, this is the first

report of quantitative differential outer membrane protein expression of *H. parasuis* as it relates to virulence and oxygen-limiting conditions.

Material and Methods

Bacterial strains. Four *Haemophilus parasuis* strains were studied. Two of the strains were reference strains obtained from Richard Ross (College of Veterinary Medicine, Iowa State University, Ames, IA). The remaining two strains were field isolates provided by Vicki Rapp-Gabrielson (Schering-Plough, Omaha, NE) and Kelly Lager (National Animal Disease Center, Ames, IA). The geographic and anatomical origins of these strains are reported in Table 6.1. Strains were grown on Casman agar, supplemented with 5% horse serum (Gibco-BRL, Carlsbad, CA), and overlaid with 0.016% NAD (Sigma Chemical Co., St. Louis, MO) using 5% CO_2 at 37°C. Colonies were selected and grown in a liquid media consisting of Freys medium (Sigma Chemical Co., St. Louis, MO) supplemented with 20% horse serum (Gibco-BRL, Carlsbad, CA) and 0.016% NAD (Sigma Chemical Co., St. Louis, MO). Tubes were incubated aerobically or in 7.5% CO_2 with shaking (100 rpm) at 37ºC for 24 h. Five mL of inoculum was used to inoculate 100-mL Freys medium. Cultures were incubated with shaking (100 rpm) for 24 h at 37ºC either aerobically or in 7.5% CO_2 and harvested by centrifugation at 7,500 ×*g* at 4ºC.

Outer membrane protein extraction and labeling for iTRAQ analysis. Cells were resuspended and washed in 20 mM 4-(2-hydroxyethyl)piperizane-1-ethanesulfonic acid (HEPES) buffer pH 7.4-0.15 M sodium chloride. Cells were resuspended again in 20 mM HEPES buffer pH 7.4-0.45 M sodium chloride and heated at 56^{o}C for 60 minutes followed by centrifugation at 10,000 × *g* at 4ºC. The protein-containing supernatant was stored at

-80ºC until use. Protein concentration was determined using the BCA Assay (Sigma, St. Louis, MO). Outer membrane proteins preparations were labeled with 4-plex iTRAQ kit according to manufacturer's instructions (Applied Biosystems, Foster City, CA).

Identification and quantification of proteins. The combined labeled peptides were analyzed by ESI MS/MS on a QStar XL (Applied Biosystems, Foster City, CA) at the Proteomics Facility at Iowa State University (Ames, IA). Identification and quantification were performed using Scaffold Q+ (v. 3.0) using triplicate samples for each experiment (Table 6.2). Tandem mass spectra were extracted, charge state deconvoluted, and deisotoped by Analyst QS version 2.0. All MS/MS samples were analyzed using Mascot (Matrix Science, London, UK) and X! Tandem (The GPM, thegpm.org; version 2007.01.01.1). X! Tandem was set up to search NCBInr_20110808 database (selected for Proteobacteria, 3981880 entries). Mascot and X! Tandem were searched with a fragment ion mass tolerance of 0.60 Da and a parent ion tolerance of 1.2 Da. Methyl methanethiosulfonate of cysteine and Applied Biosystems iTRAQ(TM) multiplexed quantitation chemistry of lysine and the n-terminus were specified in Mascot and X! Tandem as fixed modifications. Oxidation of methionine was specified in Mascot and X! Tandem as a variable modification. A reverse database was created in order to rule out false positives for each sample. Moreover, a subset database was used to search unidentified spectra in each sample against previously identified proteins. Scaffold (version Scaffold_3.1.4.1, Proteome Software Inc., Portland, OR) was used to validate MS/MS based peptide and protein identifications. Peptide identifications were accepted if they could be established at greater than 80.0% probability as specified by the Peptide Prophet algorithm.[13] Protein identifications were accepted if they could be established at greater than 80.0% probability and contained at least one identified peptide.

Protein probabilities were assigned by the Protein Prophet algorithm.[14] Proteins that contained similar peptides and could not be differentiated based on MS/MS analysis alone were grouped to satisfy the principles of parsimony. Quantitative scatterplots of the identifications from the forward, reverse, and subset database to rule out false positives for each iTRAQ experiment are presented in Supplemental Figures S6.1-S6.4.

Quantitative data analysis. Scaffold Q+ (version Scaffold_3.1.4.1, Proteome Software Inc., Portland, OR) was used to quantitate Isobaric Tag (iTRAQ, TMT) peptide and protein identifications. Peptide identifications were accepted if they could be established at greater than 80.0% probability as specified by the Peptide Prophet algorithm.[13] Protein identifications were accepted if they could be established at greater than 80.0% probability and contained at least one identified peptide. Protein probabilities were assigned by the Protein Prophet algorithm.[14] Proteins that contained similar peptides and could not be differentiated based on MS/MS analysis alone were grouped to satisfy the principles of parsimony. Peptides were quantified using the centroided reporter ion peak intensity. Intra-sample channels were normalized based on the median ratio for each channel across all proteins. Multiple isobaric tag samples were normalized by comparing the median protein ratios for the reference channel. Protein quantitative values were derived from uniquely assigned peptides. The minimum quantitative value for each spectrum was calculated as the 5.0% percent of the highest peak. Protein quantitative ratios were calculated as the median of all peptide ratios. Standard deviations were calculated as the interquartile range around the median. Quantitative ratios were Log_2 normalized for final quantitative testing.

Results

Overall identification of proteins for iTRAQ analysis. The overall experimental design is presented in Table 6.2. Proteins identified by the iTRAQ method prior to quantification are listed in Tables 6.3-6.6. Seventeen proteins were identified for HP iTRAQ-1 with a 0% protein and peptide false discovery rate. This experiment comprised outer membrane protein preparations of all strains following growth in aerobic conditions. Identified proteins include: chelated iron ABC transporter, ABC transporter, hypothetical proteins HPS_06844, HPS_07840 and HPS_10240, FbpA, superoxide dismutase (Cu-Zn), D-ribose transporter subunit RbsB, MglB, 50S ribosomal protein L7/L12, acyl carrier protein, transaldolase B, TRAP solute transporter, iron (Fe^{3+}) ABC transporter binding protein, glucose-specific PTS system enzyme IIA, HktE, and nitrate reductase. Twenty-four proteins were identified for HP iTRAQ-2 with a 0% protein and peptide false discovery rate. The samples in this data set were from the outer membrane protein preparations of all strains following growth in 7.5% CO_2. Proteins identified include: ABC transporter, chelated iron ABC transporter, FbpA, 50S ribosomal protein L7/L12, acyl carrier protein, hypothetical proteins HPS_06844, HPS_10240 and plpp0007, DNA binding protein HU, superoxide dismutase (Cu-Zn), multi-sensor signal transduction histidine kinase, glucose-specific PTS system enzyme IIA, elongation factor Ts, 50S ribosomal protein L10, D-ribose transporter subunit RbsB, arginine ABC transporter, transaldolase B, gamma-glutamyl phosphate reductase, acetaldehyde dehydrogenase, urease subunit beta, putative ATP binding ABC transport protein, hydrolase, OMP P2, and TRAP-type C4-dicarboxylate transport system permease. HP iTRAQ-3 is a comparison of outer membrane protein expression in aerobic and 7.5% CO_2 for strains HP2170B and HP409. Overall, twenty proteins were identified with a 0% protein and peptide

false discovery rate. Proteins identified for this sample set include: ABC transporter, chelated iron ABC transporter, FbpA, hypothetical proteins HPS_10240, HPS_06844, HPS_07840 and GCWU000324_02210, superoxide dismutase (Cu-Zn), acyl carrier protein, D-ribose transporter subunit RbsB, DNA-binding protein HU, 50S ribosomal protein L7/L12, glucose-specific PTS system enzyme IIA, heme-binding protein A, OMP P2, alanine aminotransferase/OMP 26, phosphoenolpyruvate-protein phosphotransferase, tRNA pseudouridine synthetase C, transaldolase B, and an iron (Fe^{3+}) ABC transporter binding protein. The final data set, HP iTRAQ-4, consists of outer membrane protein preparations from strains HP3 and HP5 grown in both aerobic and 7.5% CO_2. Sixteen proteins were identified with a protein and peptide false discovery rate of 0%. Proteins identified for this data set include: ABC transporter, chelated iron ABC transporter, FbpA, hypothetical proteins HPS_0684 and HPS_10240, superoxide dismutase (Cu-Zn), UDP-sugar diphosphatase, GGDEF family protein, acyl carrier protein, 50S ribosomal protein L7/L12, D-ribose transporter subunit RbsB, transaldolase B, DNA-binding protein HU, phosphoenolpyruvate-protein phosphotransferase, OMP P2, and glucose-specific PTS system enzyme IIA.

Comparison of outer membrane protein expression in aerobic conditions. Results of outer membrane protein expression are shown in Table 6.7 and Supplemental Figures S6.5-S6.18. The avirulent reference strain, HP3, was compared to the virulent strains. A $\log_2$fold change of at least 0.6 (1.5-fold) was considered significant for protein differential expression. In aerobic conditions, expression of MglB, a galactose binding protein, in HP409 is 2-fold greater than the other strains while the hypothetical protein HPS_06844 has a 2-fold decreased expression in all virulent strains when compared to the avirulent reference strain

HP3. Moreover, expression of a Fe^{3+} ABC transporter, nitrate reductase, HPS_10240 and the TRAP solute transporter is down-regulated 1.5-fold in virulent strains when compared to the avirulent strain in aerobic conditions. A 1.5-fold decrease in protein expression is noted for D-ribose transporter subunit RbsB for the highly virulent reference strain HP5 when compared to the avirulent reference strain. Proteins that are over-expressed 1.5 to 2-fold for virulent strains in aerobic conditions include: FbpA, chelated iron ABC transporter and SOD (Cu-Zn) for HP2170B; ABC transporter and HPS_07840 for HP409; 50S ribosomal protein L7/L12 for HP5 and HP409. A 1.5 to 2-fold decrease in protein expression is observed in HP409 for an iron binding protein.

Comparison of outer membrane protein expression in 7.5% CO_2. Results of outer membrane protein expression for each strain in an anaerobic environment are shown in Table 6.8 and Supplementary Figures S6.19-S6.33. In oxygen-limiting conditions, strains HP2170B and HP409 have a 1.5-fold increase in expression of FbpA and an ABC transporter when compared to the avirulent reference strain HP3. Expression of a chelated iron ABC transporter is 1.5-fold or greater for strains HP2170B and HP5 when compared to the avirulent strain. A 1.5 to 2-fold decrease in protein expression is observed for HP2170B for elongation factor Ts, gamma-glutamyl phosphate reductase, 50S ribosomal protein L10, glucose-specific PTS enzyme IIA, hypothetical protein plp0007 from *Legionella pneumophila*, and acetaldehyde dehydrogenase. While a decrease in protein expression is observed for acetaldehyde dehydrogenase in HP2170B, this protein is over-expressed 1.5-fold for the highly virulent strain HP5. Hypothetical protein plp007 also demonstrates a 1.5-fold decrease in protein expression for HP409, and the glucose-specific PTS enzyme IIA expression is decreased 1.5 to 2-fold for HP5. For strain HP2170B, one peptide from 50S

ribosomal protein L7/L12 was determined to be associated with a 1.5-fold decrease in protein expression. The DNA-binding protein HU demonstrated a 1.5 to 2-fold decrease in protein expression for strains HP409 and HP5. Protein expression that is downregulated 1.5-fold or greater for any virulent serovar in 7.5% CO_2 includes: hypothetical protein HPS_06844, hypothetical protein HPS_10240, and acyl carrier proteins from both *M. haemolytica* and *H. parasuis* species.

Comparison of each strain in aerobic and 7.5% CO_2 conditions. Results are shown in Tables 6.9-6.12 and Supplemental Figures S6.34-S6.69. Proteins that are over-expressed 1.5-fold or greater for HP409 in 7.5% CO_2 include: FbpA, heme-binding protein A, Fe^{3+} ABC transporter, OMP P2, phosphoenolpyruvate-protein phosphotransferase, and 50S ribosomal protein L7/L12. Phosphoenolpyruvate-protein phosphotransferase has the greatest differential protein expression pattern, with a 4-fold increase in protein expression for HP409 in anaerobic conditions. While variations do exist for the peptide profile of FbpA (Supplemental Figure S6.34) and heme-binding protein A (Supplemental Figure S6.36), the highest scoring peptides are indicative of a 1.5 to 2-fold increase in protein expression in anaerobic conditions for HP409. HPS_0784 and tRNA pseudouridine synthetase C demonstrate a 1.5-fold decrease in protein expression levels for HP409 in oxygen-limiting conditions.

In addition to being over-expressed in HP409 under oxygen-limiting conditions, OMP P2, phosphoenolpyruvate-protein phosphotransferase, and heme-binding protein A are also over-expressed in 7.5% CO_2 for HP2170B. Additionally, an ABC transporter protein, DNA binding protein HU, tRNA pseudouridine synthetase C, hypothetical protein GCWU000324_02210 from *Kingella oralis*, and alanine aminotransferase showed increased

expression for this strain in oxygen-limiting conditions. A 1.5 to 2-fold reduction in protein expression in oxygen-limiting conditions for strain HP2170B was noted for: transaldolase B, Fe^{3+} ABC transporter, hypothetical proteins HPS_06844, HPS_ 10240, and HPS_07840, and SOD (Cu-Zn). Variations existed for quantification of peptides for the proteins: ABC transporter, HPS_06844, and SOD (Cu-Zn). In these cases, the highest scoring peptide identities were used to confirm expression profile of the proteins.

For HP3 in 7.5% CO_2, protein expression levels increased at least 1.5-fold for OMP P2, glucose-specific PTS enzyme IIA, DNA binding protein HU, 50S ribosomal protein L7/L12, and acyl carrier protein. A 1.5 to 2-fold decrease in expression for HP3 in oxygen-limiting conditions was noted for a chelated iron ABC transporter and a UDP-sugar diphosphatase from *M. haemolytica.*

Protein expression levels that increased 1.5 to 2-fold in 7.5% CO_2 for the highly virulent strain HP5 include: OMP P2, Cu-Zn SOD, 50S ribosomal protein L7/L12, and D-ribose subunit RbsB. While a decrease in expression was observed for UDP-sugar diphosphatase from *M. haemolytica* in HP3 under oxygen-limiting conditions, in HP5, the expression of this protein increased 1.5 to 2-fold in the same anaerobic environment. HP5 also differed from the virulent field isolates, HP409 and HP2170B, in that the expression of phosphoenolpyruvate phosphatase was decreased at least 1.5-fold in oxygen-limiting conditions. In addition to this protein, a GGDEF family protein has a decreased protein expression profile in 7.5% CO_2 for the highly virulent strain HP5.

Discussion

One of the limitations of identification of proteins based on tandem mass spectrometry methods is the availability of information of proteins for an organism in the

database. Because the genome of *H. parasuis* was not available until 2008 and limited information is available on the protein profiles of *H. parasuis*, the peptide and protein probability scores for this experiment were set for 80.0%, and only one peptide was required for identification in this experiment. An additional limitation of this method of identification is the database search algorithm. Both Mascot and X! Tandem algorithms were used for identification of the proteins in each data set. Comparison of the normalized spectral counts for each peptide identified for the forward, reverse, and subset databases ruled out false positives, and these proteins were removed from the data sets prior to quantification. Moreover, when peptide expression profiles did not give rise to a definitive protein expression profile, peptides scores were taken into account. As more information becomes available for the *H. parasuis* proteome, this will increase the number of identifications as well as the identifications of differentially expressed outer membrane proteins.

Overall, the goal of this experiment was to identify outer membrane proteins from HP3, HP5, HP2170B, and HP409KL grown in both aerobic and oxygen-limited conditions and to determine how differential protein expression may play a role in virulence. Not every protein identified for each experiment was determined to be differentially expressed. However, since few studies have been done on the *H. parasuis* proteome, it is important to take into account the identification of putative virulence factors for future studies.

Virulence factors in organisms related to *H. parasuis* include: capsulation, fimbrae, pili, secreted molecules and proteins, and the outer membrane proteins.[15-26] Accessory proteins implicated in virulence in family *Pasteurellaceae* include: IgA1 protease, OapA (opacity associated protein), and Hap (*Haemophilus* adhesion protein).[27-30] Iron acquisition proteins and surface-localized proteins involved with colonization are also of consideration

as virulence factors. The function of the putative virulence factors presented here include proteins involved with colonization, iron acquisition, protection from reactive oxygen species, acquisition of metabolites, and hypothetical proteins of unknown function.

A variety of ABC transporters were identified in this study and determined to be differentially expressed. ABC transporters are involved with the import of solutes, including iron and other essential transition metals, and the export of the O-antigenic polysaccharide portion of lipopolysaccharide (LPS) for gram-negative organisms.[31-49] Protein expression of a Fe^{3+} ABC transporter decreased 1.5 to 2-fold for virulent strains in aerobic conditions when compared to the avirulent reference strain. However, virulent strains demonstrated increased protein expression of a chelated iron ABC transporter under the same conditions. A chelated iron ABC transporter presented with a 1.5-fold or greater decrease in protein expression levels in HP3 in anaerobic conditions. Both HP409 and HP2170B express an ABC transporter at a significantly greater level than of the protein expression observed for the avirulent strain in oxygen-limiting conditions. Expression of a chelated iron ABC transporter in anaerobic conditions is also observed for the virulent strains HP2170B and HP5. In oxygen-limiting conditions, increased protein expression was noted for the Fe^{3+} ABC transporter of HP409, an ABC transporter of HP2170B, and D-ribose subunit RsbB of HP5. Additionally, a hypothetical protein identified in this study in both aerobic and anaerobic conditions, HPS_10240, is similar to the PotD spermidine/putrescine transporter of *P. multocida*. PotD is involved with polyamine transport and is implicated in the pathogenesis of *Streptococcus pneumonia,*[50-52] *M. haemolytica,*[53] and *E. coli*.[54-57] When compared to the avirulent reference strain in aerobic conditions, all virulent strains demonstrated at least a 1.5-fold decrease in expression of HPS_10240. The same trend was observed when

comparing the avirulent reference strain to virulent reference strains in oxygen-limiting conditions. In addition to the ABC transporters mentioned here, additional transporters were identified. Increased expression of a galactose binding protein, MglB, was observed for strain HP409, and decreased expression of a TRAP solute transporter was observed in virulent strains when compared to the avirulent reference strain in aerobic conditions.

A previous study on microarray profiling of the Nagasaki stain (SV5) of *H. parasuis* under oxygen-limiting conditions[8] demonstrated the role of the phosphotransferase (PTS) system in adaptation of *Pasteurellaceae* family to stressful conditions. The glucose-specific PTS enzyme IIA was identified in this study in oxygen-limiting conditions. This enzyme is a component of a highly conserved phosphotransferase system (PTS) that participates in the phosphorylation of carbohydrates and ultimately mediates the formation of a biofilm in an environment that is suitable for surface association.[58] While previous microarray analysis demonstrated an increase in genes associated with the PTS system[8] under oxygen-limiting conditions, the results here demonstrated protein expression profiling is strain dependent. Decreased expression of the glucose-specific PTS enzyme IIA was observed for the virulent strains HP2170B and HP5. An increase in protein expression levels was observed for this protein in HP3 under oxygen-limiting conditions.

One of the most notable findings of this study was the increase in expression of OMP P2 under oxygen-limiting conditions for all strains. The functional role of OMP P2 as a colonization factor and its role in virulence have been well documented in *H. influenzae.*[59-68] Genetic analysis of *H. parasuis* OMP P2 indicates that variability does exist for surface exposed epitopes[69] and that OMP P2 is a vaccine candidate for protection against Glässer's disease.[70] It is feasible that oxygen-limiting conditions induce increased colonization of the

organism in the respiratory tract by increasing the expression of colonization factors such as OMP P2.

In addition to OMP P2, iron-acquisition proteins were also identified in this study and demonstrated a variety of expression profiles. *H. parasuis*, like other members of the *Pasteurellaceae* family, acquires iron in a siderophore-independent manner.[71-76] Ferric binding protein A (FbpA) was identified in both aerobic and oxygen-limiting conditions. FbpA presented with decreased protein expression in virulent strains in aerobic conditions. In oxygen-limiting conditions, an increase in expression of this protein was observed for HP2170B and HP409. When compared to aerobic conditions, an increase in protein expression of FbpA was observed in oxygen-limiting conditions for HP409. Heme-binding protein A was an additional iron acquisition protein identified in this study. Results demonstrated that HP409 and HP2170B increase protein expression of heme-binding protein A in oxygen-limiting conditions.

Aside from ABC transporters, colonization factors, and iron acquisition proteins, additional virulence factors were identified and determined to be differentially expressed. Evasion of the host's immune response plays a role in bacterial survival. A SOD (Cu-Zn) was identified under aerobic and anaerobic conditions. This enzyme facilitates bacterial survival in the phagosome by catalyzing the conversion of the highly reactive oxygen species superoxide to hydrogen peroxide.[77-80] In virulent strains in aerobic conditions, SOD (Cu-Zn) demonstrated decreased protein expression levels when compared to the avirulent reference strain HP3. Moreover, in oxygen-limiting conditions, the expression of this protein was decreased in HP2170B. However, the expression pattern of this protein increased in oxygen-limiting conditions for the highly virulent reference strain HP5.

The results presented here provide the first differential proteomic profiling of the outer membrane proteins of *H. parasuis* under aerobic and oxygen-limiting conditions. Future work includes the characterization of the putative virulence factors identified in this study along with further identification of proteins of *H. parasuis* using a proteomic profiling approach as it relates to serotype as well as conditions of stress, including iron-limitation, low temperature, and low pH. While there is no commercially available cross-protective vaccine or diagnostic for Glässer's disease, continued work to understand the mechanism of virulence of *H. parasuis* at a protein level will assist in the identification of vaccine and diagnostic candidates.

Acknowledgements

We would like to thank Siquan Luo from the Iowa State Proteomics Facility for his assistance with ESI MS/MS and Jana Lee for her assistance with Scaffold.

Tables

Table 6.1. Description of bacterial strains

Serovar	Reference[a] strain	Country of origin	Diagnosis/ isolation site	Virulence[b]
Reference Strains				
3	SW114	Japan	Healthy/nose	A
5	Nagasaki	Japan	Septicemia/meninges	H
Field strains				
4	2170B	United States	Joint	L
Unknown[c]	409KL	United States	Unknown	H

[a]Reference strain information and virulence scores obtained from reference 13.

[b]Virulence designations: H, high virulence; L, moderate/low virulence; A, avirulent.

[c]PRSSV co-isolate

Table 6.2. Description of experimental design

Experiment	Samples	Growth conditions
HP iTRAQ-1	HP3, HP5, HP2170B and HP409KL	Aerobic
HP iTRAQ-2	HP3, HP5, HP2170B and HP409KL	7.5% CO_2
HP iTRAQ-3	HP2170B and HP409KL	Aerobic vs 7.5% CO_2
HP iTRAQ-4	HP3 and HP5	Aerobic vs 7.5% CO_2

Table 6.3. Outer membrane proteins identified in HP iTRAQ-1

Accession number	Protein	Peptides[a]	Mascot ion[b]	Mascot ID[c]	X! Tandem[d]
219871287	chelated iron ABC transporter	(K)AVVESITKPGAEIHDYQPTPQDIVA)	44.1	54.5	1.08
		(K)DKPAVVVTEGIEPISIYEGPYK(D)	62.6	55.6	3.80
		(K)DKPNPHAWMSTK(N)	37.3	56.0	2.57
		(K)ELYLWAINQDEQGTPK(Q)	58.2	56.1	3.37
		(K)IVALDQPLR(E)	41.3	55.3	4.51
		(R)KHQIPVVFSESTISDKPAK(Q)	38.8	55.9	1.30
		(R)KVIDQVR(K)	28.4	56.3	2.15
		(K)NALIYIENIR(Q)	44.5	56.4	2.66
		(K)VPTYIDLLNVTVSTIVAGFEK(-)	90.3	55.4	4.23
		(K)VVTTFTVIQDIAQNVAGDK(A)	80.4	56.0	6.80
		(R)WLVTSEGAFSYLAR(D)	62.4	56.0	7.62
		(K)YDPANAEAYNANAK(A)	60.4	55.9	1.31
		(R)YGGVLYVDSLSTK(D)	66.0	56.3	13.96
167855391	ABC transporter	(K)AAALLK(E)	30.4	56.6	1.46
		(K)AINIIAEEAALYPIIHR(K)	61.4	55.9	9.89
		(K)ALIEAQGQSVFDANPVGTGPYK(F)	62.2	56.0	4.36
		(K)LLDAAVAAK(T)	63.2	56.2	1.74
		(R)LTIIK(I)	25.3	57.2	2.42
		(K)LVDVVFLGNAK(P)	N/A	N/A	6.89
		(K)MTWFLLSDDAAR(V)	43.7	55.7	7.57
		(R)QPYLALAAK(E)	50.0	56.5	1.28
		(R)VAAQESGR(V)	34.7	57.0	1.20
		(R)WSNTPEYAEVQK(L)	29.2	55.8	1.46
		(K)WVVDSVQMILEDWNK(I)	60.5	56.1	2.72

Table 6.3. (continued)

Accession number	Protein	Peptides[a]	Mascot ion[b]	Mascot ID[c]	X! Tandem[d]
167855124	HPS_06844	(K)ELIDYLNVVALK(E)	62.1	56.1	6.82
		(K)FAVIGLTTEDTAK(L)	79.4	55.9	8.21
		(K)FPFISANVINK(K)	66.3	56.0	3.04
		(R)FTVLHVNDTHGHFWK(N)	40.8	50.9	1.42
		(K)LGNPDVTENVVFNDPLK(T)	35.1	56.0	2.77
		(K)NDKGEYGFAAQK(T)	N/A	N/A	3.46
		(K)VSVPDYCAAGGDGYPILK(K)	64.4	56.0	5.44
		(K)YELIPVNLK(Q)	45.2	56.4	2.89
167855017	HPS_10240[e]	(K)DGGYDVIAPSNYFVSK(M)	39.7	56.1	14.92
		(K)EGPVLWVDTLAIPSNAK(N)	24.3	56.0	3.72
		(R)EVFNIALLK(L)	48.2	56.5	5.96
		(K)GDNFTAWGDLWKPEFK(G)	24.1	55.9	2.70
		(K)LINYLLSAPVAEK(L)	81.9	56.2	5.89
		(K)LTLEIGYPTSNVK(A)	80.4	56.0	15.0
		(K)VQLLDDAR(E)	31.3	56.1	3.17
167855400	FbpA[f]	(K)ADVAPSDLVK(G)	62.1	56.2	4.62
		(K)AFLEGLK(A)	37.5	56.2	1.89
		(K)EGELSPADVLLTVDISR(V)	61.1	56.0	11.89
		(K)LNHEYPVK(A)	45.8	56.1	5.68
		(K)NAYNVSLFAAMIEHYGEEK(T)	77.2	55.8	3.92
		(R)VGALPAGFDYLDLAKPEYK(G)	34.7	56.0	5.92
		(R)VIYTSK(D)	24.0	54.0	3.77
		(K)VNVIFADK(G)	42.3	56.3	3.09
167854701	superoxide dismutase (Cu-Zn)	(K)DVGTVTITESPYGLVFTPNLK(G)	66.3	56.0	8.06
		(K)LVAGLGAGGHWDPK(E)	38.1	56.0	3.00
		(R)SLMIHAGGDNHSDHPAPLGGGGAR(M)	54.5	55.9	4.12
219870435	Fe^{3+} ABC binding protein	(R)SPLQAEVLPQFK(A)	39.9	56.1	11.21
		(K)YNVETQFIHGGTGTILGK(L)	55.0	56.1	6.64
167856115	D-ribose transporter	(K)GLNVMENLLASHGSAK(A)	63.6	56.0	1.59
		(K)VIQLEGIAGTSAAR(E)	29.8	56.0	5.46
167855764	MglB	(K)AKPEGIPVVFFNK(D)	25.0	56.1	3.38
		(K)KLPIFGVDALPEVLQLIQK(G)	50.0	54.6	3.92
		(K)LGIQTEELFVDTGMWDAALAK(D)	81.9	55.9	58.4

Table 6.3 (continued)

Accession number	Protein	Peptides[a]	Mascot ion[b]	Mascot ID[c]	X! Tandem[d]
167856064	acyl carrier protein	(K)IIVDQLGAK(A) (K)IATVQSAIDYVQNNQ(-)	61.5 28.9	55.9 56.1	2.18 3.82
152979644	TRAP transporter	(R)ATMNVILAAK(G)	73.5	56.5	3.80
167856581	50S ribosomal protein L7/L12	(K)SVSEIVELITAMEEK(F)	73.7	56.1	6.57
167855984	nitrate reductase catalytic subunit	(R)GVWANHLIYNIHLLTGK(I)	43.2	56.0	2.85
167856489	glucose-specific PTS system enzyme IIA	(K)FDLELLQSK(A)	55.1	56.0	4.22
167854609	HktE	(K)VWPHADYPVIEVGVLELNR(N)	48.5	56.1	6.51
16273050	transaldolase B	(R)LTIAPALLK(E) (-)LAVNIGLEILK(-)	52.8 40.8	55.1 55.7	N/A N/A
167852903	HPS_07840	(R)AVDAQEHPIGIFWSAK(L)	44.0	56.0	3.46

[a]Peptides identified using Scaffold; termini are indicated in parenthesis

[b]Mascot Ion scores >52 indicate identity or extensive homology ($p<0.05$)

[c]Protein scores >65 are significant ($p<0.05$)

[d]Scores are reflected –log (e) value

[e]Similar to: PotD [*Pasteurella multocida* subsp. multocida str. Pm70], gi|12720490

[f]Similar to: periplasmic iron-binding protein [*Haemophilus parasuis* SH0165], gi|219691519

Table 6.4. Outer membrane proteins identified for HP iTRAQ-2

Accession number	Protein	Peptides[a]	Mascot ion[b]	Mascot ID[c]	X! Tandem[d]
219871287	chelated iron ABC transporter	(K)IVALDQPLR(E)	34.5	55.4	3.64
		(K)NALIYIENIR(Q)	53.5	56.4	2.77
		(K)VPTYIDLLNVTVSTIVAGFEK(-)	57.7	56.0	6.01
		(K)VVTTFTVIQDIAQNVAGDK(A)	42.5	56.0	3.74
		(R)WLVTSEGAFSYLAR(D)	37.9	56.0	4.07
		(R)YGGVLYVDSLSTK(D)	64.4	56.3	12.7
167855391	ABC transporter	(K)AINIIAEEAALYPIIHR(K)	66.8	56.0	6.39
		(K)ALDGFKPLSTTGMSFIGVSR(-)	32.5	56.0	3.10
		(K)ALIEAQGQSVFDANPVGTGPYK(F)	73.5	56.0	3.82
		(K)LLDAAVAAK(T)	63.0	56.2	1.54
		(K)LVDVVFLGNAK(P)	N/A	N/A	4.32
		(K)MTWFLLSDDAAR(V)	49.0	55.6	5.96
		(K)WVVDSVQMILEDWNK(I)	49.5	56.1	3.51
167855124	HPS_06844	(K)EVDMGAYPQFAGVSMVVDR(T)	27.7	56.0	2.72
		(K)FAVIGLTTEDTAK(L)	92.4	55.9	8.16
		(K)GAFDLIIGGHTHDTVCVDEK(G)	49.9	56.0	N/A
		(K)YELIPVNLK(Q)	38.3	56.4	4.92
167855017	HPS_10240[e]	(K)EGPVLWVDTLAIPSNAK(N)	70.9	55.9	5.06
		(R)EVFNIALLK(L)	41.6	56.4	5.62
		(K)LTLEIGYPTSNVK(A)	72.7	56.0	11.72
167855400	FbpA[f]	(K)AFLEGLK(A)	40.6	56.2	1.62
		(K)EGELSPADVLLTVDISR(V)	67.2	56.0	9.28
		(K)FDDFGAK(-)	32.3	56.0	1.59
		(R)QPYLIEPMLK(D)	46.5	56.3	2.44
		(R)VGALPAGFDYLDLAKPEYK(G)	76.7	56.7	5.21
		(R)VIYTSK(D)	30.8	54.4	1.52
		(K)VNVIFADK(G)	42.1	56.3	4.39
		(A)LPAGFDYLDLAKPEYK(G)	N/A	N/A	4.17
167854701	superoxide dismutase (Cu-Zn)	(K)LVAGLGAGGHWDPK(E)	52.3	56.1	2.49
		(R)SLMIHAGGDNHSDHPAPLGGGGAR(M)	43.9	55.9	2.30
167856115	D-ribose transporter	(K)AVFAQNDEMALGALR(A)	61.3	56.2	3.51
167856064	acyl carrier protein	(K)IIVDQLGAK(A)	61.5	55.9	3.92

Table 6.4. (continued)

Accession number	Protein	Peptides[a]	Mascot ion[b]	Mascot ID[c]	X! Tandem[d]
167856581	50S ribosomal protein L7/L12	(K)SVSEIVELITAMEEK(F)	56.9	56.0	4.08
		(K)FGVSAAAAAVAVAAGPAEAAEEK(T)	77.6	56.0	6.32
167856489	glucose-specific PTS system enzyme IIA	(K)FDLELLQSK(A)	58.1	56.0	4.48
		(K)SVLTPVVISNMDEVTNLQK(L)	59.7	56.0	4.43
16273050	transaldolase B	(R)LTIAPALLK(E)	44.3	55.2	N/A
167855819	DNA binding protein HU	(K)AALEATLNAISESLK(K)	85.3	56.0	5.11
		(K)TELVDAIAAGADLSK(K)	67.7	56.2	8.29
		(K)TNEAIEIPAANVPAFVAGK(A)	47.6	56.0	3.18
167855469	elongation factor Ts	(K)SVNTSVANFVR(L)	43.7	56.0	2.77
		(R)VAAEGVILAR(I)	36.3	55.2	1.43
54308748	hydrolase	(K)VVGSHSGQGFNELTGY(-)	37.4	54.5	1.00
113969297	gamma-glutamyl phosphate reductase	(R)ALEVIANAK(V)	36.6	55.9	2.16
157377458	50S ribosomal protein L10	(K)GALSAVVADSR(G)	49.0	56.6	9.89
145639805	OMP P2	(R)LVTDITK(N)	50.6	56.6	2.03
54295850	hypothetical protein plp0007	(K)ILAQEETK(L)	38.4	56.6	1.66
163759990	putative ATP-binding ABC transporter	(K)SSGTSKPQAGAR(E)	37.9	55.4	1.64
111116467	acetaldehyde dehydrogenase	(K)AIEVIGGAAK(G)	43.5	55.8	3.06

Table 6.4. (continued)

Accession number	Protein	Peptides[a]	Mascot ion[b]	Mascot ID[c]	X! Tandem[d]
167855353	arginine ABC transporter	(R)GGFDAAISAIDITEAR(A)	49.8	56.1	5.04
254459404	multi-sensor histidine kinase	(R)ILISSAK(D)	52.9	57.5	N/A
163858136	TRAP C4-dicarboxylate transporter	(K)VLGGP(-)	18.0	47.8	N/A
109947049	urease subunit beta	(-)ADIGIKNGK(-)	37.7	56.8	N/A

[a]Peptides identified using Scaffold; termini are indicated in parenthesis

[b]Mascot Ion scores >52 indicate identity or extensive homology ($p<0.05$)

[c]Protein scores >65 are significant ($p<0.05$)

[d]Scores are reflected –log (e) value

[e]Similar to: PotD [*Pasteurella multocida* subsp. multocida str. Pm70], gi|12720490

[f]Similar to: periplasmic iron-binding protein [*Haemophilus parasuis* SH0165], gi|219691519

Table 6.5. Outer membrane proteins identified for HP iTRAQ-3

Accession number	Protein	Peptides[a]	Mascot ion[b]	Mascot ID[c]	X! Tandem[d]
219871287	chelated iron ABC transporter	(K)AQSADLVLWNGMNLESWFER(F)	43.6	52.8	4.57
		(K)AVVESITKPGAEIHDYQPTPQDIVK(A)	42.0	51.2	1.07
		(K)DGKVPTYIDLLNVTVSTIVAGFEK(-)	82.9	55.3	1.42
		(K)IVALDQPLR(E)	41.3	55.0	9.92
		(K)NALIYIENIR(Q)	45.1	56.4	3.04
		(K)VPTYIDLLNVTVSTIVAGFEK(-)	100.6	52.3	13.22
		(K)VVTTFTVIQDIAQNVAGDK(A)	95.5	54.4	8.70
		(R)WLVTSEGAFSYLAR(D)	65.6	56.0	4.82
		(R)YGGVLYVDSLSTK(D)	72.1	54.6	16.34
167855391	ABC transporter	(K)AINIIAEEAALYPIIHR(K)	61.2	55.9	8.74
		(K)ALDGFKPLSTTGMSFIGVSR(-)	69.7	55.7	6.44
		(K)ALIEAQGQSVFDANPVGTGPYK(F)	61.1	56.0	2.12
		(K)LKYPFALFK(E)	25.0	55.7	4.15
		(K)LLDAAVAAK(T)	58.1	55.5	2.82
		(K)LVDVVFLGNAK(P)	N/A	N/A	4.85
		(K)MTWFLLSDDAAR(V)	53.6	55.8	4.16
		(R)QPYLALAAK(E)	59.2	55.6	3.23
		(K)SLFAQFIPFIK(S)	46.6	54.4	5.24
		(R)VQAIENVPYLDADR(L)	41.5	56.3	4.02
		(R)WSNTPEYAEVQK(L)	42.5	55.9	4.96
		(K)WVVDSVQMILEDWNK(I)	100.5	53.5	7.77
		(K)WVVDSVQMILEDWNLIPGVL(V)	36.0	54.7	2.07
167855124	HPS_06844	(K)ELIDYLNVVALK(E)	67.4	54.5	7.72
		(K)FAVIGLTTEDTAK(L)	63.0	55.9	8.66
		(R)FTVLHVNDTHGHFWK(N)	32.7	53.1	1.89
		(K)YELIPVNLK(Q)	35.3	56.3	2.77
167855017	HPS_10240[e]	(K)AAYEELLK(L)	37.8	55.2	5.74
		(K)EGPVLWVDTLAIPSNAK(N)	55.8	55.6	4.70
		(R)EVFNIALLK(L)	60.0	55.3	5.22
		(K)GDNFTAWGDLWKPEFK(G)	31.9	56.0	2.19
		(K)LINYLLSAPVAEK(L)	79.8	55.9	5.05
		(K)LTLEIGYPTSNVK(A)	84.2	56.0	9.82
		(K)VQLLDDAR(E)	38.3	56.1	4.54

Table 6.5. (continued)

Accession number	Protein	Peptides[a]	Mascot ion[b]	Mascot ID[c]	X! Tandem[d]
167855400	FbpA[f]	(K)ADVAPSDLVK(G)	61.1	55.3	3.52
		(K)AFLEGLK(A)	43.5	55.9	3.47
		(R)DSNGEWFGLTK(R)	28.3	55.7	3.17
		(K)EGELSPADVLLTVDISR(V)	75.9	56.0	5.49
		(K)FDDFGAK(-)	48.1	55.9	1.40
		(K)GWGTYSTDALK(L)	53.5	54.8	11.22
		(K)LIEYLSGNQAQALYAK(L)	101.1	53.6	13.12
		(K)LNHEYPVK(A)	35.3	56.1	3.89
		(A)LPAGFDYLDLALPEYK(G)	49.8	55.9	6.00
		(K)NAYNVSLFAAMIEHYGEEK(T)	81.8	52.9	7.12
		(R)QPYLIEPMLK(D)	46.2	56.3	2.09
		(R)VGALPAGFDYLDLAKPEYK(G)	61.2	56.8	5.22
		(R)VIYTSK(D)	39.6	54.4	1.47
		(K)VNVIFADK(G)	43.0	56.3	2.31
167854701	superoxide dismutase (Cu-Zn)	(K)DVGTVTITESPYGLVFTPNLK(G)	75.1	55.5	7.62
		(K)GLSHGLHGFHIHEkPSCEPK(E)	34.0	52.3	2.00
		(K)LVAGLGAGGHWDPK(E)	65.0	56.1	3.64
		(R)SLMIHAGGDNHSDHPAPLGGGGAR(M)	45.4	52.8	4.14
167856115	DNA binding protein HU	(K)AALEATLNAISESLK(K)	100.1	53.8	10.27
		(K)TELVDAIAAGADLSK(K)	82.8	54.3	11.12
167856115	D-ribose transporter	(K)GLNVMENLLASHGSAK(A)	71.3	55.9	5.59
		(K)VIQLEGIAGTSAAR(E)	82.3	54.8	7.85
219871378	heme-binding protein A	(R)LIFEIVPDATAR(Y)	55.1	56.1	7.74
		(K)LQAGACDLIDFPNAADLEK(M)	40.0	56.0	7.26
		(K)NAIIDAVYR(G)	26.5	56.5	3.82
167856064	acyl carrier protein	(K)IIVDQLGAK(A)	67.5	55.9	4.28
		(K)IATVQSAIDYVQNNQ(-)	51.0	54.2	6.37
145639805	OMP P2	(R)LVTDITK(N)	49.6	56.2	2.96
167856581	50S ribosomal protein L7/L12	(K)SVSEIVELITAMEEK(F)	61.2	56.0	1.96
		(K)TELVDAIAAGADLSK(K)	70.4	54.3	4.22

Table 6.5. (continued)

Accession number	Protein	Peptides[a]	Mascot ion[b]	Mascot ID[c]	X! Tandem[d]
167854655	tRNA pseudouridine synthetase C[g]	(K)FDNTDPIGDYTLDLQINDTIFPTQK(F)	56.1	55.4	2.80
167856489	glucose-specific PTS system enzyme IIA	(K)SVLTPVVISNMDEVTNLQK(L)	54.8	52.9	5.20
167854835	alanine amino-transferase	(K)DGNAADITEEILVAMGGK(M)	50.4	56.1	3.00
167855966	HPS_07840	(K)FDSFSPELQQAILDAAK(E)	47.8	56.0	1.92
167856491	PEP protein phospho-transferase	(K)LQTLGLAQGTIITLSAEGEDEQK(A)	96.1	54.5	6.47
238022303	hypothetical protein GCW	(K)ALNIPSLR(F)	33.7	54.8	N/A
16273050	transaldolase B	(R)LTIAPALLK(E)	50.0	54.4	N/A
		(K)LAVNIGLEILK(L)	54.2	55.2	1.01
254360752	Fe^{3+} ABC transporter	(K)LPAGFDYLDLAKPEYK(G)	49.8	55.9	2.24

[a]Peptides identified using Scaffold; termini are indicated in parenthesis

[b]Mascot Ion scores >52 indicate identity or extensive homology ($p<0.05$)

[c]Protein scores >65 are significant ($p<0.05$)

[d]Scores are reflected –log (e) value

[e]Similar to: PotD [*Pasteurella multocida* subsp. multocida str. Pm70], gi|12720490

[f]Similar to: periplasmic iron-binding protein [*Haemophilus parasuis* SH0165], gi|219691519

[g]Similar to: hypothetical protein HAPS_0711 [*Haemophilus parasuis* SH0165], gi|219691134

Table 6.6: Outer membrane proteins identified for HP iTRAQ-4

Accession number	Protein	Peptides[a]	Mascot ion[b]	Mascot ID[c]	X! Tandem[d]
219871287	chelated iron ABC transporter	(R)FFAQVK(D)	28.4	54.7	1.40
		(K)IVALDQPLR(E)	39.0	61.9	3.70
		(K)NALIYIENIR(Q)	28.0	56.4	1.43
		(K)VPTYIDLLNVTVSTIVAGFEK(-)	72.7	62.2	6.00
		(K)VVTTFTVIQDIAQNVAGDK(A)	65.4	55.6	4.35
		(R)WLVTSEGAFSYLAR(D)	38.4	56.0	4.77
		(R)YGGVLYVDSLSTK(D)	58.5	56.3	12.92
167855391	ABC transporter	(K)AINIIAEEAALYPIIHR(K)	57.4	55.6	1.85
		(K)ALIEAQGQSVFDANPVGTGPYK(F)	42.7	55.5	2.68
		(K)FVSAVK(D)	40.6	62.1	2.05
		(K)LLDAAVAAK(T)	62.5	56.2	1.64
		(K)LVDVVFLGNAK(P)	N/A	N/A	4.68
		(K)MTWFLLSDDAAR(V)	55.7	55.8	4.96
		(R)VLDPNTKK(S)	24.0	56.5	3.43
		(K)WVVDSVQMILEDWNK(I)	70.0	62.4	1.26
		(K)YPFALFK(E)	26.1	56.2	1.47
167855124	HPS_06844	(R)ADFEFK(N)	25.9	55.8	3.36
		(K)ELIDYLNVVALK(E)	57.0	62.6	11.42
		(K)FAVIGLTTEDTAK(L)	61.1	59.9	9.27
		(R)FTVLHVNDTHGHFWK(N)	26.4	61.9	4.23
		(K)LGNPDVTENVVFNDPLK(T)	33.1	56.1	1.92
		(R)LIAQSQMER(V)	N/A	N/A	3.68
		(K)YELIPVNLK(Q)	37.8	56.4	4.04
167855017	HPS_10240[e]	(K)AAYEELLK(L)	27.5	55.9	3.31
		(R)EVFNIALLK(L)	57.8	56.4	1.36
		(K)VQLLDDAR(E)	46.5	56.1	1.15
167855400	FbpA[f]	(K)AFLEGLK(A)	43.2	56.3	1.92
		(K)EGELSPADVLLTVDISR(V)	54.2	55.9	3.24
		(R)VIYTSK(D)	31.9	54.3	1.43
		(K)VNVIFADK(G)	43.1	56.3	2.74
167854701	superoxide dismutase (Cu-Zn)	(K)LVAGLGAGGHWDPK(E)	44.5	62.3	4.29
		(R)SLMIHAGGDNHSDHPAPLGGGGAR(M)	37.1	56.0	4.48
254361285	UDP-sugar diphosphatase	(K)ADIGIMNSGGIR(T)	44.5	62.8	4.82

Table 6.6. (continued)

Accession number	Protein	Peptides[a]	Mascot ion[b]	Mascot ID[c]	X! Tandem[d]
167856064	acyl carrier protein	(K)IIVDQLGAK(A)	65.2	55.9	3.74
167856115	DNA binding protein HU	(K)AALEATLNAISESLK(K)	91.2	55.4	10.60
167856581	50S ribosomal protein L7/L12	(K)SVSEIVELITAMEEK(F)	66.7	56.1	4.68
218676105	GGDEF family protein	(-)MVSAVK(T)	41.5	62.1	2.05
167856489	glucose-specific PTS system enzyme IIA	(K)SVLTPVVISNMDEVTNLQK(L)	39.3	56.0	3.36
167856115	D-ribose transporter	(K)VIQLEGIAGTSAAR(E)	50.0	56.0	4.85
16273050	transaldolase B	(R)LTIAPALLK(E) (-)LAVNIGLEILK(-)	52.8 40.8	55.1 55.7	N/A N/A
167856491	PEP protein phospho-transferase	(K)LQTLGLAQGTIITLSAEGEDEQK(A)	56.7	54.7	4.89
145639805	OMP P2	(R)LVTDITK(N)	43.3	56.8	1.43

[a]Peptides identified using Scaffold; termini are indicated in parenthesis

[b]Mascot Ion scores >52 indicate identity or extensive homology ($p<0.05$)

[c]Protein scores >65 are significant ($p<0.05$)

[d]Scores are reflected –log (e) value

[e]Similar to: PotD [*Pasteurella multocida* subsp. multocida str. Pm70], gi|12720490

[f]Similar to: periplasmic iron-binding protein [*Haemophilus parasuis* SH0165], gi|219691519

Table 6.7. Proteins differentially expressed 1.5-fold or greater for HP iTRAQ-1

Protein	Peptides[a]	Mascot Ion[b]	Mascot ID[c]	HP3	HP2170B	HP409	HP5
FbpA[d]	ADVAPSDLVK	62.1	56.2	Ref	1.5	-1.5	5.0
	AFLEGLK	37.5	56.2	Ref	0.43	-0.19	-0.078
	EGELSPADVLLTVDISR	61.1	56.0	Ref	0.41	-0.85	-0.36
	LNHEYPVK	45.8	56.0	Ref	0.82	-0.85	0.37
	NAYNVSLFAAMIEHYGEEK	77.2	55.8	Ref	0.53	-0.61	-0.32
	VGALPAGFDYLDLAKPEYK	34.6	55.9	Ref	2.7	-0.44	0.91
	VIYTSK	23.9	54.3	Ref	0.79	-0.15	0.24
	VNVIFADK	42.1	56.2	Ref	0.5	0.23	-0.079
ABC transporter	AAALLK	30.4	56.6	Ref	-0.86	0.4	0.1
	AINIIAEEAALYPIIHR	54.4	55.9	Ref	-0.25	0.48	0.37
	ALIEAQGQSVFDANPVGTGPYK	62.2	56.0	Ref	-1.1	0.98	-0.13
	LLDAAVAAK	45.1	56.2	Ref	-1.1	0.42	-0.071
	LTIIK	25.3	57.1	Ref	-1.0	0.56	-0.084
	LVDVVFLGNAK	N/A	N/A	Ref	-0.86	0.45	0.14
	MTWFLLSDDAAR	43.6	55.6	Ref	0.13	1.2	1.7
	QPYLALAAK	50.0	56.4	Ref	-0.9	0.35	-0.52
	VAAQESGR	34.6	57.0	Ref	-0.49	0.74	0.55
	WSNTPEYAEVQK	29.2	55.8	Ref	-1.1	0.89	0.3
	WVVDSVQMILEDWNK	42.6	56.0	Ref	-0.48	0.92	0.24
HPS_06844	ELIDYLNVVALK	70.3	56.1	Ref	-1.4	-1.2	-0.51
	FAVIGLTTEDTAK	79.3	55.8	Ref	-1.2	-1.1	-0.36
	FPFISANVINK	60.7	55.9	Ref	-1.0	-1.1	-0.44
	FTVLHVNDTHGHFWK	40.8	55.8	Ref	-0.84	-0.81	-0.56
	LGNPDVTENVVFNDPIK	35.1	56.0	Ref	-1.0	-0.54	N/A
	NDKGEYGFAAQK	N/A	N/A	Ref	-0.03	-0.44	0.36
	VSVPDYCAAGGDGYPILK	64.3	56.0	Ref	-1.4	-1.3	-0.67
	YELIPVNLK	33.7	56.3	Ref	-1.4	-1.3	-0.9
MglB	AKPEGIPVVFFNK	25.0	56.0	Ref	0.077	2.1	-0.1
	KLPIFGVDALPEVLQLIQK	49.9	54.5	Ref	-0.31	1.2	-0.31
	LGIQTEELFVDTGMWDAALAK	81.9	55.9	Ref	1.9	2.8	0.52
50S ribosomal L7/L12	SVSEIVELITAMEEK	73.6	56.0	Ref	0.17	0.8	0.77

Table 6.7. (continued)

Protein	Peptides[a]	Mascot Ion[b]	Mascot ID[c]	HP3	HP2170B	HP409	HP5
Fe^{3+} ABC	SPLQAEVLPQFK	39.9	56.0	Ref	-0.22	-0.73	-0.95
transporter	YNVETQFIHGGTGTILGK	54.9	56.0	Ref	-0.4	-0.59	-0.98
nitrate reductase	GVWANHLIYNIHLLTGK	43.1	55.9	Ref	-0.7	-0.65	-0.76
D-ribose	GLNVMENLLASHGSAK	41.6	56.3	Ref	-0.33	-1.0	-0.79
transporter	IGELGVEAADKV			Ref	0.52	0.15	-0.45
SOD (Cu-Zn)	DVGTVTITESPYGLVFTPNLK	38.0	56.2	Ref	1.9	-0.18	N/A
chelated iron ABC	AVVESITKPGAEIHDYQPTPQDIVK	40.2	56.0	Ref	0.96	-0.27	0.55
transporter	ELYLWAINQDEQGTPK	39.0	56.4	Ref	0.87	0.08	0.52
TRAP transporter	ATMNVILAAK	73.3	56.4	Ref	-0.48	-0.58	-0.65
iron binding	ADVAPSDLVK	62.1	56.2	Ref	1.5	-1.5	0.33
protein	EGELSPADVLLTVDISR	61.1	56.0	Ref	0.38	-0.88	-0.53
	GWGTYSTDALK	31.8	55.9	Ref	0.87	-0.53	-0.44
	NAYNVSLFAAMIEHYGEEK	77.2	55.8	Ref	0.5	-0.63	-0.49
HPS_10240[e]	DGGYDVIAPSNYFVSK	39.6	56.1	Ref	-0.51	0.076	N/A
	EVFNIALLK	38.8	56.3	Ref	-0.25	0.24	-0.77
	LINYLLSAPVAEK	77.1	56.1	Ref	-0.86	-0.79	-1.2
	LTLEIGYPTSNVK	58.7	56.0	Ref	-0.19	0.18	-0.68
HPS_07840	AVDAQEHPIGIFWSAK	43.9	56.0	Ref	0.34	0.6	0.25

[a]Peptides identified using Scaffold Q+

[b]Mascot Ion scores >52 indicate identity or extensive homology ($p<0.05$)

[c]Protein scores >65 are significant ($p<0.05$)

[d]Similar to: periplasmic iron-binding protein [*Haemophilus parasuis* SH0165], gi|219691519

[e]Similar to: PotD [*Pasteurella multocida* subsp. multocida str. Pm70], gi|12720490

Table 6.8. Proteins differentially expressed 1.5-fold or greater for HP iTRAQ-2

Protein	Peptides[a]	Mascot Ion[b]	Mascot ID[c]	HP3	HP2170B	HP409	HP5
chelated	IVALDQPLR	24.99	55.6	Ref	0.83	0.07	0.56
iron ABC	NALIYIENIR	29.95	56.4	Ref	1.6	0.24	0.28
transporter	VPTYIDLLNVTVSTIVAGFEK	57.25	56.0	Ref	0.57	0.13	0.4
	VVTTFTVIQDIAQNVAGDK	42.45	56.0	Ref	0.54	0.16	-0.19
	WLVTSEGAFSYLAR	24.9	56.0	Ref	1.0	0.11	0.66
	YGGVLYVDSLSTK	19.68	56.2	Ref	0.79	0.053	-0.0021
FbpA[d]	AFLEGLK	40.57	56.2	Ref	0.0092	0.29	-0.17
	EGELSPADVLLTVDISR	67.22	56.0	Ref	0.79	0.47	0.0021
	FDDFGAK	32.26	56.0	Ref	0.52	0.61	-0.95
	LPAGFDYLDLAkPEYK	N/A	N/A	Ref	-2.5	0.67	-1.8
	QPYLIEPMLK	46.49	56.3	Ref	0.4	-1.7	-0.25
	VGALPAGFDYLDLAkPEYK	40.98	56.0	Ref	2.1	0.0022	0.083
	VIYTSK	30.84	54.4	Ref	0.69	0.48	-0.55
	VNVIFADK	41.64	56.3	Ref	0.62	0.46	-0.26
50S ribosomal	FGVSAAAAAVAVAAGPAEAAEK	77.63	56.0	Ref	-0.55	-0.093	N/A
L7/L12	SVSEIVELITAMEEK	56.92	56.1	Ref	-1.1	-0.3	-1.0
	SVSEIVELITAMEEK	59.94	55.9	Ref	-0.45	-0.45	0.3
HPS_06844	EVDMGAYPQFAGVSMVVDR	27.66	56.0	Ref	0.13	0.81	0.65
	FAVIGLTTEDTAK	45.91	55.9	Ref	-1.1	-0.57	-0.49
	GAFDLIIGGHTHDTVCVDEK	49.83	56.0	Ref	-1.3	-1.5	-0.033
	YELIPVNLK	38.35	56.4	Ref	-1.6	-1.1	-0.36
DNA	AALEATLNAISESLK	85.31	56.0	Ref	0.36	-1.3	-0.79
binding	TELVDAIAAGADLSK	67.74	56.2	Ref	0.93	-0.2	-0.18
protein HU	TNEAIEIPAANVPAFVAGK	47.6	56.0	Ref	0.31	-0.35	-0.5
HPS_10240[e]	EGPVLWVDTLAIPSNAK	70.92	55.9	Ref	-0.09	0.32	N/A
	EVFNIALLK	40.27	56.4	Ref	-1.1	-0.25	-0.31
	LTLEIGYPTSNVK	72.72	56.0	Ref	-1.1	-0.5	-1.1
acyl carrier protein	IIVDQLGAK	62.51	55.9	Ref	-0.8	-0.74	-0.98
elongation	SVNTSVANFVR	43.65	56.0	Ref	-1.1	-0.28	0.074
factor Ts	VAAEGVILAR	36.32	55.2	Ref	-1.5	-0.45	-0.2

Table 6.8. (continued)

Protein	Peptides[a]	Mascot Ion[b]	Mascot ID[c]	HP3	HP2170B	HP409	HP5
glucose-specific PTS enzyme IIA	FDLELLQSK	58.09	56.0	Ref	-0.74	-0.36	-0.82
	SVLTPVVISNMDEVTNLQK	59.74	56.0	Ref	-0.99	-0.42	-1.1
gamma-glutamyl phosphate reductase	ALEVIANAK	36.58	55.9	Ref	-1.2	0.014	0.069
plp0007	ILAQEETK	38.4	56.6	Ref	-1.5	-0.85	-0.19
50S ribosomal L10	GALSAVVADSR	48.95	56.6	Ref	-1.1	-0.47	0.31
acetaldehyde dehydrogenase	AIEVIGGAAK	43.47	55.8	Ref	-0.77	-0.24	0.6
ABC transporter	FVSAVK	35.91	56.0	Ref	0.6	0.5	0.093
M. haemolytica acyl carrier protein	IIVDQLGAK	62.52	56.3	Ref	-0.56	-0.56	-0.57
	KIIVDQLGAK	26.61	56.5	Ref	-0.65	-0.31	0.067

[a]Peptides identified using Scaffold Q+

[b]Mascot Ion scores >52 indicate identity or extensive homology ($p<0.05$)

[c]Protein scores >65 are significant ($p<0.05$)

[d]Similar to: periplasmic iron-binding protein [*Haemophilus parasuis* SH0165], gi|219691519

[e]Similar to: PotD [*Pasteurella multocida* subsp. multocida str. Pm70], gi|12720490

Table 6.9. Proteins differentially expressed 1.5-fold or greater for HP iTRAQ-3 HP409 aerobic vs. HP409 7.5% CO_2

Protein	Peptides[a]	Mascot ion[b]	Mascot ID[c]	HP409	HP409 7.5% CO_2
FbpA[d]	ADVAPSDLVK	61.08	55.3	Ref	0.34
	AFLEGLK	43.45	55.9	Ref	0.22
	DSNGEWFGLTK	28.31	55.7	Ref	0.83
	EGELSPADVLLTVDISR	72.8	53.8	Ref	1.0
	FDDFGAK	48.08	55.9	Ref	1.1
	GWGTYSTDALK	53.46	54.8	Ref	0.67
	LIEYLSGNQAQALYAK	38.8	53.6	Ref	0.39
	LNHEYPVK	35.28	56.1	Ref	-2.4
	LPAGFDYLDLAKPEYK	49.78	55.9	Ref	1.5
	NAYNVSLFAAMIEHYGEEK	81.14	52.9	Ref	0.65
	QPYLIEPMLK	46.24	56.3	Ref	N/A
	VGALPAGFDYLDLAKPEYK	31.21	52.6	Ref	0.18
	VIYTSK	29.46	54.4	Ref	1.5
	VNVIFADK	43.32	55.6	Ref	1.1
HPS_07840	FDSFSPELQQAILDAAK	47.8	56.0	Ref	-0.81
heme-binding protein A	LIFEIVPDATAR	55.11	56.1	Ref	0.61
	LQAGACDLIDFPNAADLEK	39.99	56.0	Ref	N/A
	NAIIDAVYR	26.45	56.5	Ref	-0.47
50S ribosomal L7/L12	SLTNEQIIEAIASK	23.43	54.3	Ref	0.71
	SVSEIVELITAMEEK	57.54	53.8	Ref	0.84
	TEFDVILADAGANK	70.42	54.3	Ref	-0.14
OMP P2	LVTDITK	46.9	56.2	Ref	1.1
PEP protein phosphotransferase	LQTLGLAQGTIITLSAEGEDEQK	96.14	54.5	Ref	2.2
tRNA pseudouridine synthetase C[e]	FDNTDPIGDYTLDLQINDTIFPTQK	56.12	55.4	Ref	-1.0
Fe^{3+} binding protein	LPAGFDYLDLAKPEYK	49.78	55.9	Ref	1.6

[a]Peptides identified using Scaffold Q+

[b]Mascot Ion scores >52 indicate identity or extensive homology ($p<0.05$)

[c]Protein scores >65 are significant ($p<0.05$)

[d]Similar to: periplasmic iron-binding protein [*Haemophilus parasuis* SH0165], gi|219691519

[e]Similar to: hypothetical protein HAPS_0711 [*Haemophilus parasuis* SH0165], gi|219691134

Table 6.10. Proteins differentially expressed 1.5-fold or greater for HP iTRAQ-3 HP2170B aerobic vs. HP2170B 7.5% CO_2

Protein	Peptides[a]	Mascot ion[b]	Mascot ID[c]	HP21	HP21 7.5% CO_2
ABC	AINIIAEEAALYPIIHR	62.63	53.6	Ref	0.26
transporter	ALDGFKPLSTTGMSFIGVSR	32.66	56.0	Ref	1.5
	ALIEAQGQSVFDANPVGTGPYK	42.81	52.6	Ref	0.56
	EAGVDKLEFTTR	22.09	54.4	Ref	1.1
	LKYPFALFK	25.01	55.7	Ref	1.8
	LLDAAVAAK	62.65	55.5	Ref	1.2
	LVDVVFLGNAK			Ref	1.1
	MTWFLLSDDAAR	32.72	54.5	Ref	1
	QPYLALAAK	59.15	55.6	Ref	0.79
	SLFAQFIPFIK	46.57	54.4	Ref	2.2
	VQAIENVPYLDADR	41.47	56.3	Ref	1.2
	WSNTPEYAEVQK	41.82	54.3	Ref	1.6
	WVVDSVQMILEDWNK	58.78	53.5	Ref	1.4
	WVVDSVQMILEDWNKIPGVK	35.95	54.7	Ref	3.1
HPS_06844	ELIDYLNVVALK	67.44	54.5	Ref	-1.8
	FAVIGLTTEDTAK	57.55	54.4	Ref	-0.55
	FTVLHVNDTHGHFWK	32.69	53.1	Ref	-0.58
	YELIPVNLK	35.28	56.3	Ref	-0.67
HPS_07840	FDSFSPELQQAILDAAK	47.8	56.0	Ref	-0.63
HPS_10240	AAYEELLK	37.75	55.2	Ref	-0.63
	EGPVLWVDTLAIPSNAK	55.79	55.6	Ref	-0.21
	EVFNIALLK	60.04	55.3	Ref	-0.66
	GDNFTAWGDLWKPEFK	31.92	56.0	Ref	-1.3
	LINYLLSAPVAEK	79.77	55.9	Ref	-0.72
	LTLEIGYPTSNVK	65.28	56	Ref	-0.65
	VQLLDDAR	38.27	56.1	Ref	-0.82
alanine aminotransferase	DGNAADITEEILVAMGGK	50.41	56.1	Ref	1.4
hypothetical protein GCW	ALNIPSLR	33.71	54.8	Ref	1.4

Table 6.10. (continued)

Protein	Peptides[a]	Mascot ion[b]	Mascot ID[c]	HP21	HP21 7.5% CO_2
heme-binding	LIFEIVPDATAR	55.11	56.1	Ref	0.96
protein A	LQAGACDLIDFPNAADLEK	39.99	56.0	Ref	0.99
	NAIIDAVYR	26.45	56.5	Ref	0.32
DNA binding	AALEATLNAISESLK	100.13	53.8	Ref	1.3
protein HU	TELVDAIAAGADLSK	82.78	54.3	Ref	0.97
Fe^{3+} ABC transporter	DNPQADIWYGGTIEPHFQAGQMGLLEAYR	38.52	55.1	Ref	-1.1
OMP P2	LVTDITK	46.9	56.2	Ref	1.1
PEP protein phosphotransferase	LQTLGLAQGTIITLSAEGEDEQK	96.14	54.5	Ref	0.83
SOD (Cu-Zn)	DVGTVTITESPYGLVFTPNLK	45.57	52.7	Ref	-0.55
	GLSHGLHGFHIHEKPSCEPK	34.01	52.3	Ref	-0.8
	LVAGLGAGGHWDPK	53.24	54.5	Ref	-0.51
	SLMIHAGGDNHSDHPAPLGGGGAR	45.44	52.8	Ref	-0.57
transaldolase B	LTIAPALLK	52.69	55.5	Ref	-0.76
tRNA pseudouridine synthetase C[d]	FDNTDPIGDYTLDLQINDTIFPTQK	56.12	55.4	Ref	0.68

[a]Peptides identified using Scaffold Q+

[b]Mascot Ion scores >52 indicate identity or extensive homology ($p<0.05$)

[c]Protein scores >65 are significant ($p<0.05$)

[d]Similar to: hypothetical protein HAPS_0711 [*Haemophilus parasuis* SH0165], gi|219691134

Table 6.11. Proteins differentially expressed 1.5-fold or greater for HP iTRAQ-4 HP3 aerobic vs. HP3 7.5% CO_2

Protein	Peptides[a]	Mascot ion[b]	Mascot ID[c]	HP3	HP3 7.5% CO_2
chelated	FFAQVK	28.4	54.7	Ref	-2.2
iron	IVALDQPLR	34.28	55.3	Ref	-1.5
transporter	NALIYIENIR	28.04	56.4	Ref	-0.39
	VPTYIDLLNVTVSTIVAGFEK	57.79	55.3	Ref	-1.4
	VVTTFTVIQDIAQNVAGDK	65.36	55.9	Ref	0.071
	WLVTSEGAFSYLAR	27.22	56.0	Ref	-0.72
	YGGVLYVDSLSTK	19.98	56.3	Ref	-1.7
acyl carrier protein	IIVDQLGAK	65.25	55.9	Ref	1.4
OMP P2	LVTDITK	43.31	56.8	Ref	1.9
glucose-specific PTS enzyme IIA	SVLTPVVISNMDEVTNLQK	39.35	56.0	Ref	0.6
DNA binding protein HU	AALEATLNAISESLK	91.16	55.4	Ref	1.6
50S ribosomal L7/L12	SVSEIVELITAMEEK	66.68	56.1	Ref	1.8
UDP-sugar diphosphatase	ADIGIMNSGGIR	44.53	56.8	Ref	-0.65

[a]Peptides identified using Scaffold Q+

[b]Mascot Ion scores >52 indicate identity or extensive homology ($p<0.05$)

[c]Protein scores >65 are significant ($p<0.05$)

Table 6.12. Proteins differentially expressed 1.5-fold or greater for HP iTRAQ-4 HP5 aerobic vs. HP5 7.5% CO_2

Protein	Peptides[a]	Mascot ion[b]	Mascot ID[c]	HP5	HP5 7.5% CO_2
D-ribose transporter	VIQLEGIAGTSAAR	50.03	56.0	Ref	0.92
SOD	LVAGLGAGGHWDPK	44.53	62.3	Ref	0.43
(Cu-Zn)	SLMIHAGGDNHSDHPAPLGGGGAR	37.07	56.0	Ref	1.2
UDP-sugar diphosphatase	ADIGIMNSGGIR	45.51	56.5	Ref	0.98
PEP protein phosphotransferase	LQTLGLAQGTIITLSAEGEDEQK	56.65	54.7	Ref	-0.61
OMP P2	LVTDITK	43.31	56.8	Ref	1.1
GGDEF family protein	MVSAVK	41.38	55.6	Ref	-0.74
50S ribosomal L7/L12	SVSEIVELITAMEEK	66.68	56.1	Ref	1.2

[a]Peptides identified using Scaffold Q+

[b]Mascot Ion scores >52 indicate identity or extensive homology ($p<0.05$)

[c]Protein scores >65 are significant ($p<0.05$)

Supplemental Figures

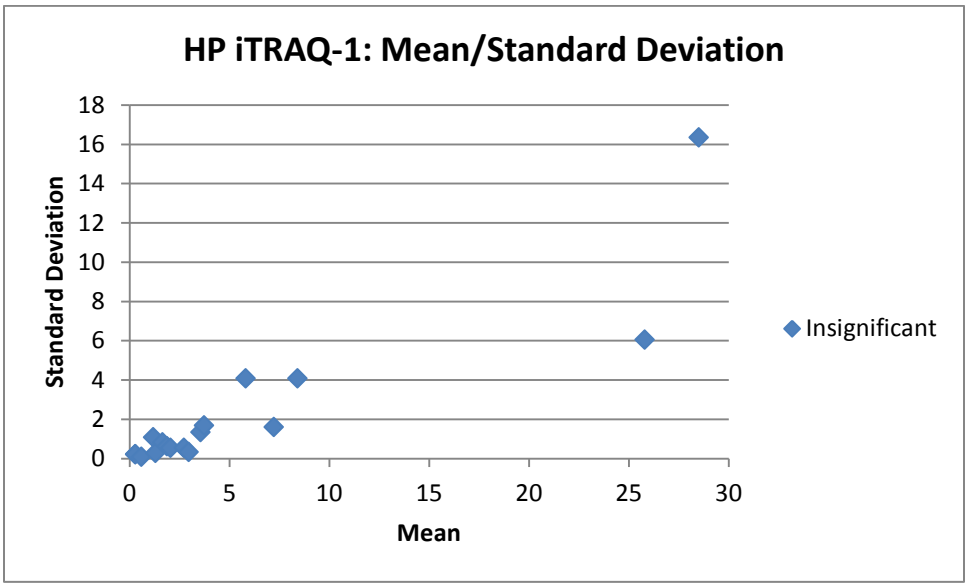

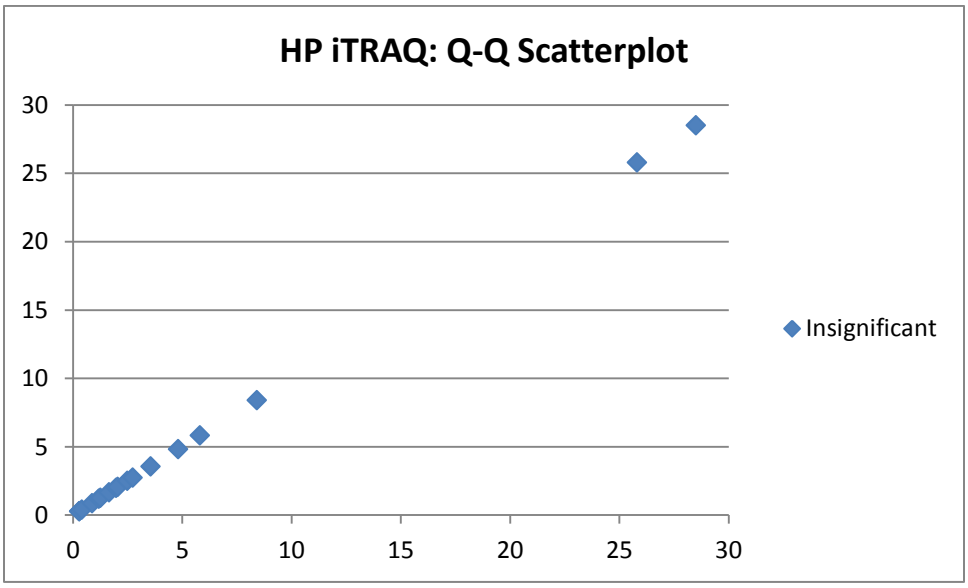

Supplemental Figure S6.1. Quantitative Scatterplots for HP iTRAQ-1. The proteins of significant difference between categories, as determined by coefficient of variation quantitative analysis test, are plotted as red points. All other proteins plot as blue points. The Mean / Deviation Scatterplot shows how the standard deviation for the Q-Q plot is calculated. The forward, reverse and subset iTRAQ samples were compared to one another.

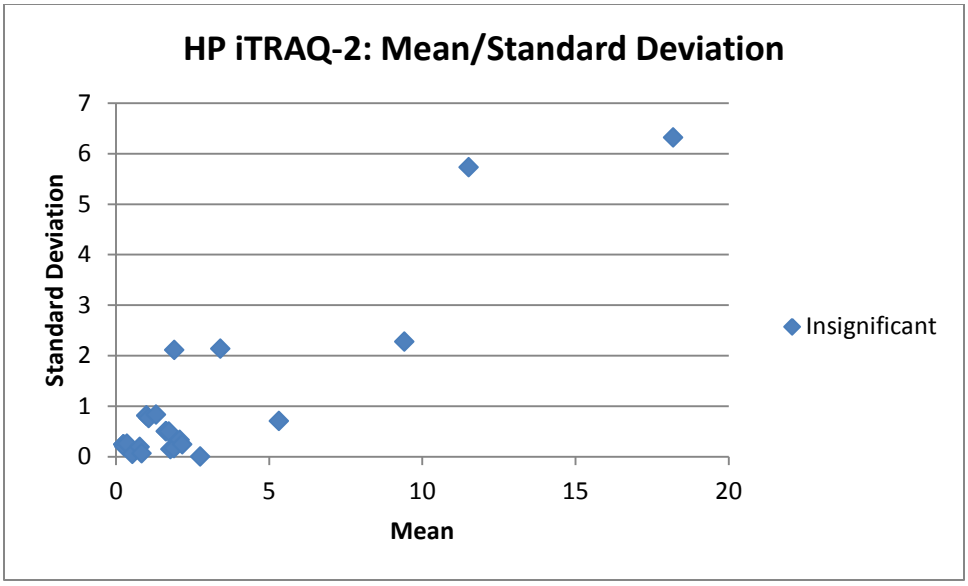

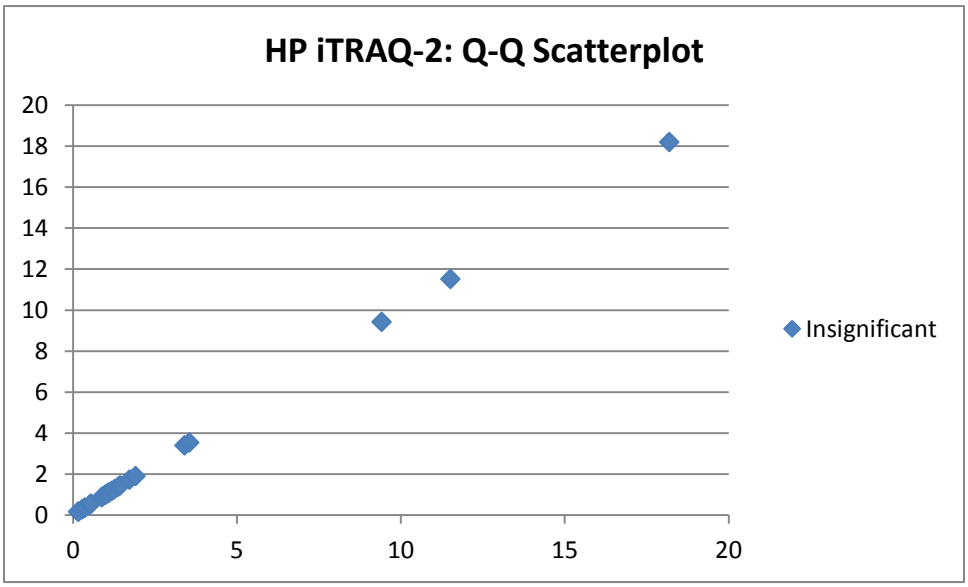

Supplemental Figure S6.2. Quantitative Scatterplots for HP iTRAQ-2. The proteins of significant difference between categories, as determined by coefficient of variation quantitative analysis test, are plotted as red points. All other proteins plot as blue points. The Mean / Deviation Scatterplot shows how the standard deviation for the Q-Q plot is calculated. The forward, reverse and subset iTRAQ samples were compared to one another.

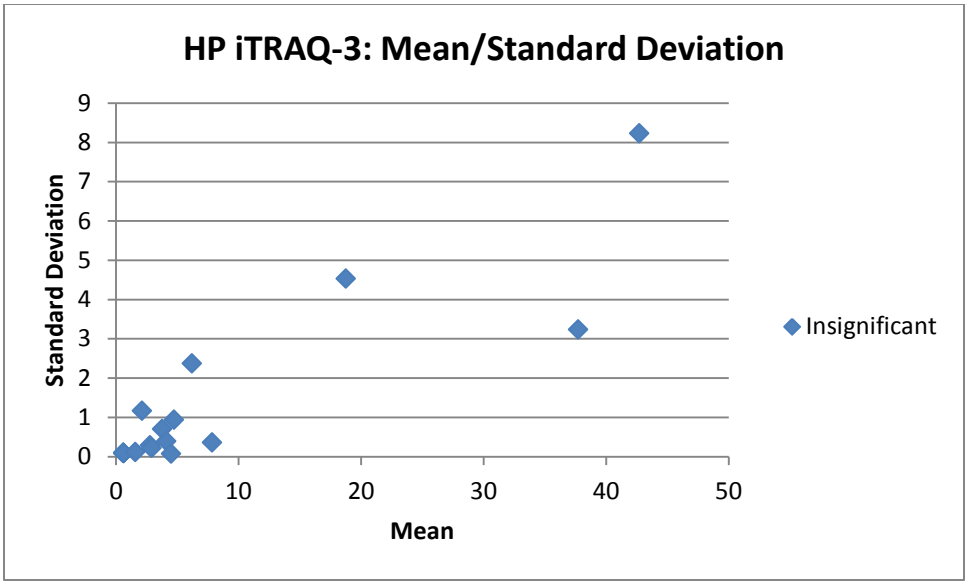

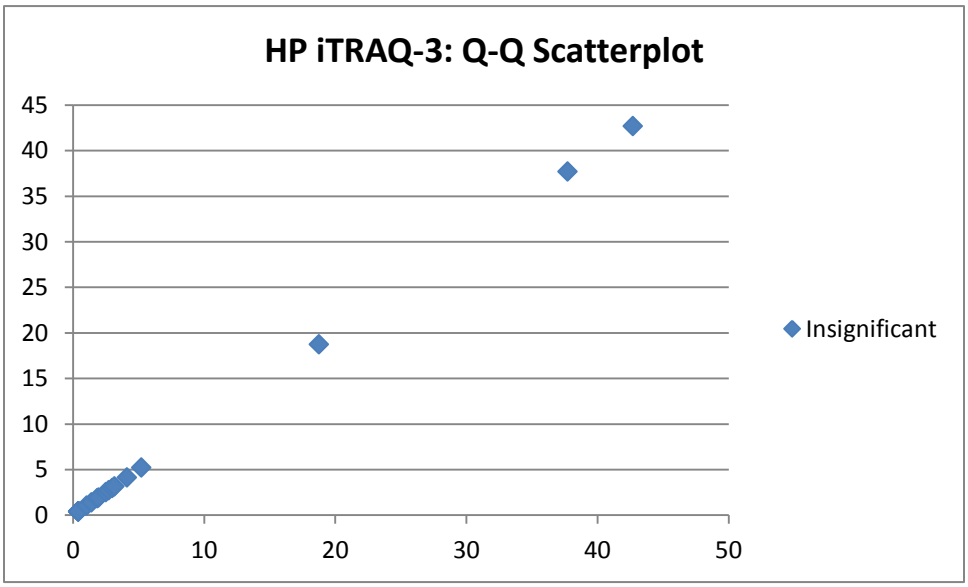

Supplemental Figure S6.3. Quantitative Scatterplots for HP iTRAQ-3. The proteins of significant difference between categories, as determined by coefficient of variation quantitative analysis test, are plotted as red points. All other proteins plot as blue points. The Mean / Deviation Scatterplot shows how the standard deviation for the Q-Q plot is calculated. The forward, reverse and subset iTRAQ samples were compared to one another.

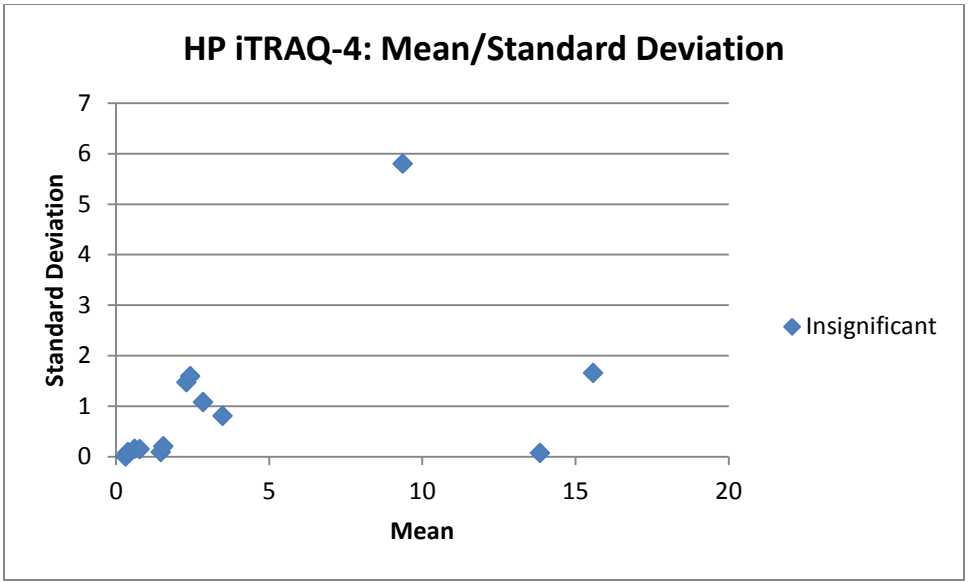

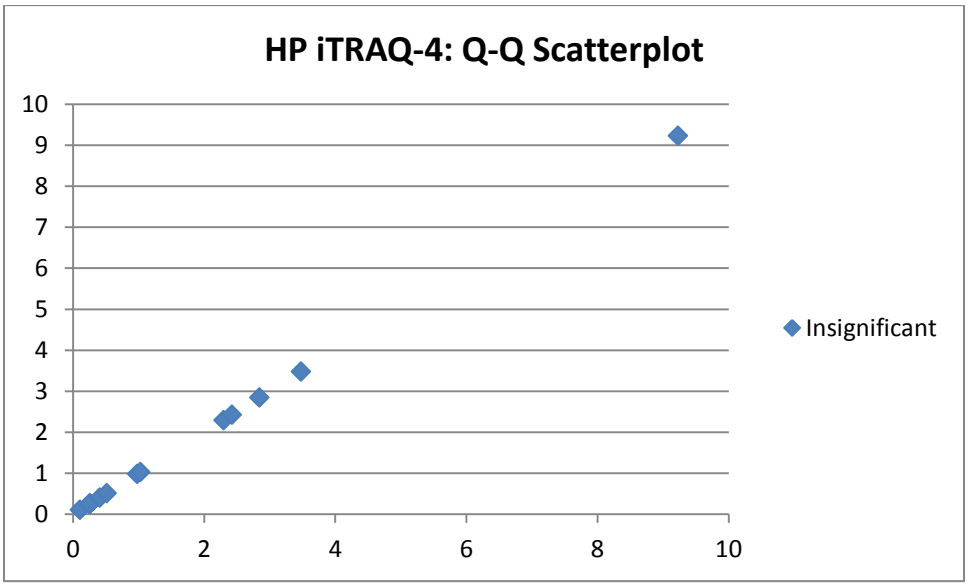

Supplemental Figure S6.4. Quantitative Scatterplots for HP iTRAQ-4. The proteins of significant difference between categories, as determined by coefficient of variation quantitative analysis test, are plotted as red points. All other proteins plot as blue points. The Mean / Deviation Scatterplot shows how the standard deviation for the Q-Q plot is calculated. The forward, reverse and subset iTRAQ samples were compared to one another.

a)

gi|167855400 (100%) 37,666.3 Da
FbpA [Haemophilus parasuis 29755], gi|167853466|gb|EDS24714.1| FbpA [Haemophilus parasuis 29755]

MKKSLSVLAL ALSSVISTSA LAANEVNVYS YRQPYLIEPM LKDFEKQTGI KVNVIFADKG
LVERVQKEGE LSPADVLLTV DISRVMQIVK AGLAQKVDSK TLEKNIPAQF RDSNGEWFGL
TKRARVIYTS KDRVGALPAG FDYLDLAKPE YKGKVCVRSG KNAYNVSLFA AMIEHYGEEK
TKAFLEGLKA NLAQKPQGGD RDQVKAIKEG ICDYALGNSY YYGKMLDDEK QRSWAESANI
NFPNGQYGTH VNISGVALAK HSPNKANAIK LIEYLSGNQA QALYAKLNHE YPVKADVAPS
DLVKGWGTYS TDALKLEDIA KNYEKALKLV DEVKFDDFGA K

b)

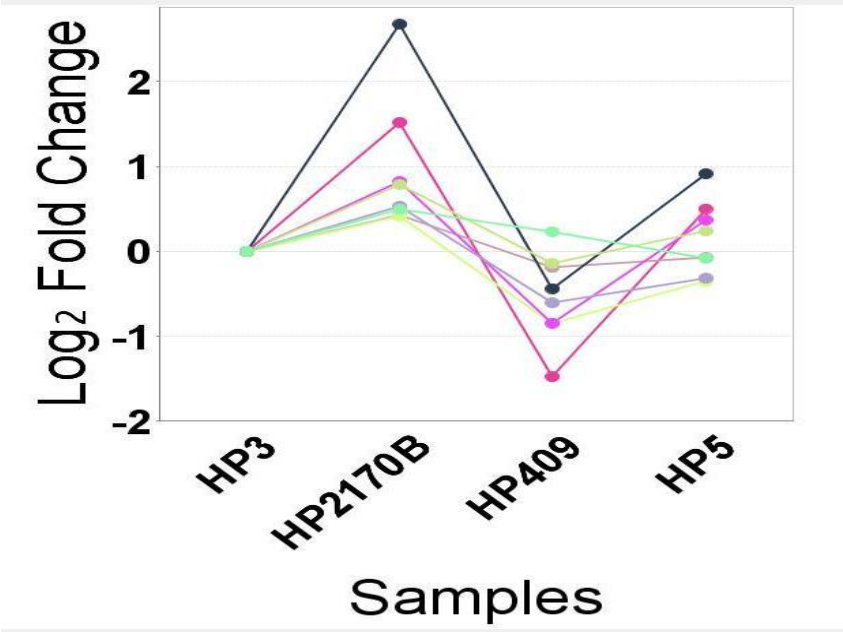

Supplemental Figure S6.5. Protein sequence coverage map (a) and protein expression profile (b) for HP iTRAQ-1 FbpA. Each line in (b) represents a peptide shown in (a).

a)

gi|167855391 (100%) 57,888.3 Da
ABC transporter, periplasmic binding protein [Haemophilus parasuis 29755], gi|167853457|gb|EDS24705.1| ABC transporter, periplasmic binding protein [Haemophilus p

M T K H F E H N E S R R G F M K L V A G V G A G L A F S G S I G T F A S Q A Y A A P A K G S T I E A G I A Y P I S T G F
D P M S S T G A S S M A A N I H I F E G L V D L H P A T R Q P Y L A L A A K E P E K V D D V T Y R I T L R D G A V F H N
G S A V T S A D V V F S F E R V L D P N T K S L F A Q F I P F I K S V T A V D Q K T V E F K L K Y P F A L F K E R L T I
I K I V P K A L I E A Q G Q S V F D A N P V G T G P Y K F V S A V K D D R I V F E A N P A Y T G P Y P A T V E K M T W F
L L S D D A A R V A A Q E S G R V Q A I E N V P Y L D A D R L K R K A A V E S V Q S F G L I F L M F N C E K A P F N N K
K V R Q A L Q Y A I D T Q K L V D V V F L G N A K P A T S Y V Q D S H P D Y V K A S T V Y D F D P K K A A A L L K E A G
V D K L E F T T R S T A H K W V V D S V Q M I L E D W N K I P G V K V T N I A S Q S P Y N D G V D A G N F E V L I A P G
D P S V F G N D L D L L L S W W Y R G D V W P K K R F R W S N T P E Y A E V Q K L L D A A V A A K T P A E A R E I W G K
A I N I I A E E A A L Y P I I H R K L P T A W S N K A L D G F K P L S T T G M S F I G V S R K

b)

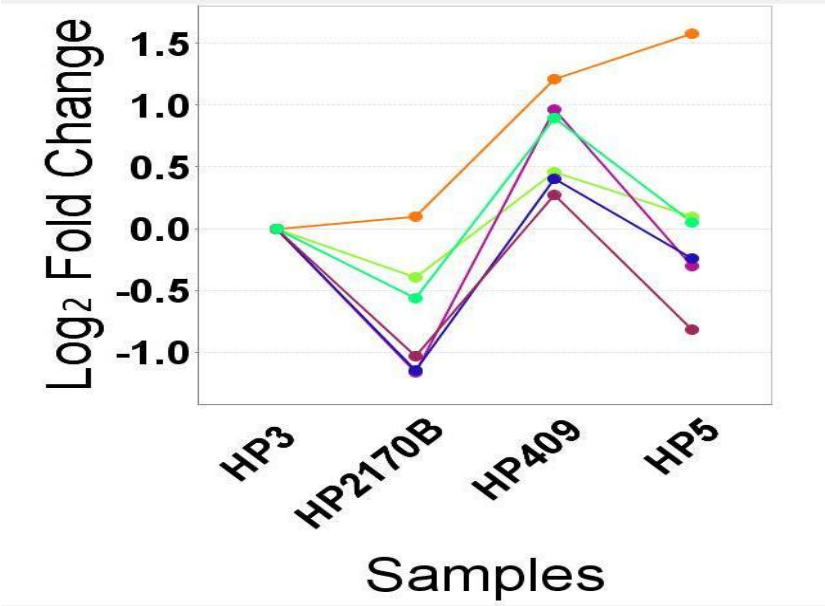

Supplemental Figure S6.6. Protein sequence coverage map (a) and protein expression profile (b) for HP iTRAQ-1 ABC Transporter. Each line in (b) represents a peptide shown in (a).

a)

gi|167855124 (100%) 60,868.0 Da
hypothetical protein HPS_06844 [Haemophilus parasuis 29755], gi|167853759|gb|EDS25001.1| hypothetical protein HPS_06844 [Haemophilus parasuis 29755]

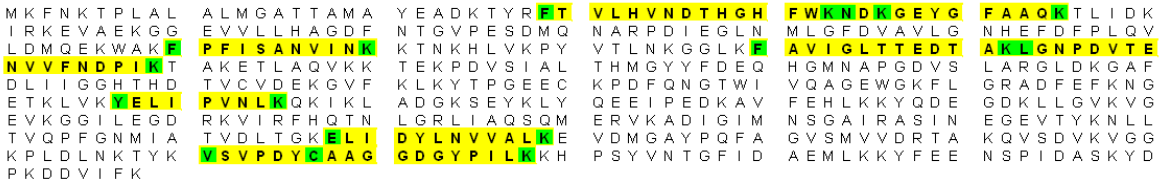

b)

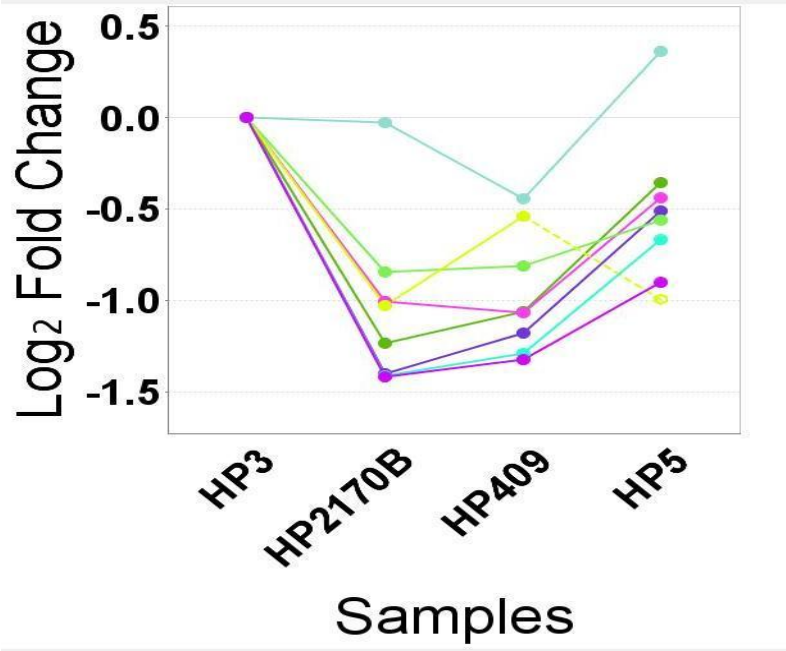

Supplemental Figure S6.7. Protein sequence coverage map (a) and protein expression profile (b) for HP iTRAQ-1 HPS_06844. Each line in (b) represents a peptide shown in (a).

a)

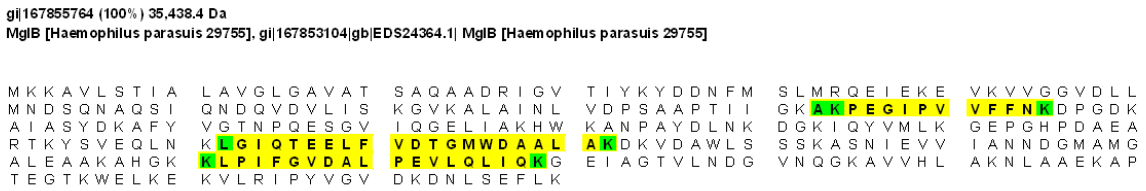

b)

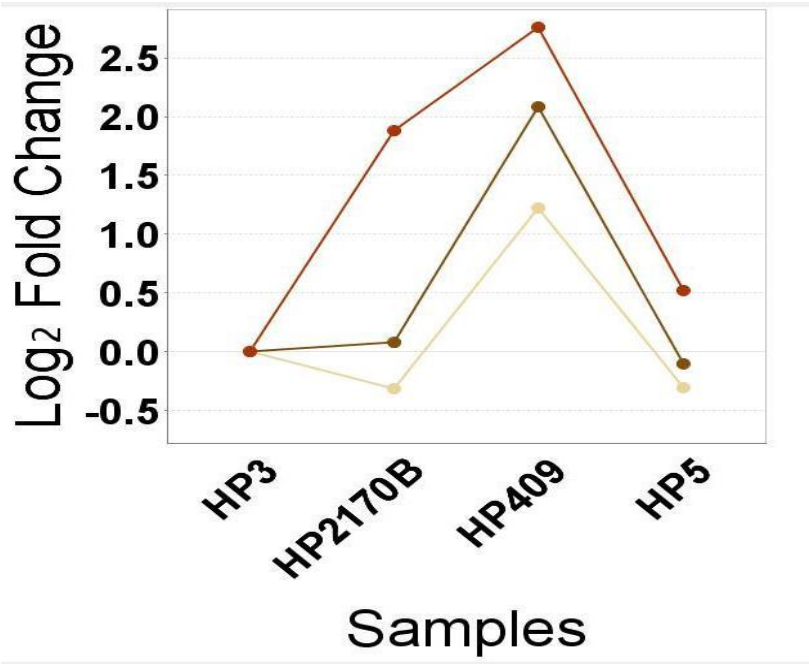

Supplemental Figure S6.8. Protein sequence coverage map (a) and protein expression profile (b) for HP iTRAQ-1 MglB. Each line in (b) represents a peptide shown in (a).

a)

gi|167856581 (85%) 12,391.4 Da
50S ribosomal protein L7/L12 [Haemophilus parasuis 29755], gi|219871555|ref|YP_002475930.1| 50S ribosomal protein L7/L12 [Haemophilus parasuis SH0165], gi|25480637

MSLTNEQIIE AIASKSVSEI VELITAMEEK FGVSAAAAAV AVAAGPAEAA EEKTEFDVIL
ADAGANKVAV IKAVRGATGL GLKEAKDLVE SAPAALKEGI SKGEAEALKK ELEEAGAKVE
IK

b)

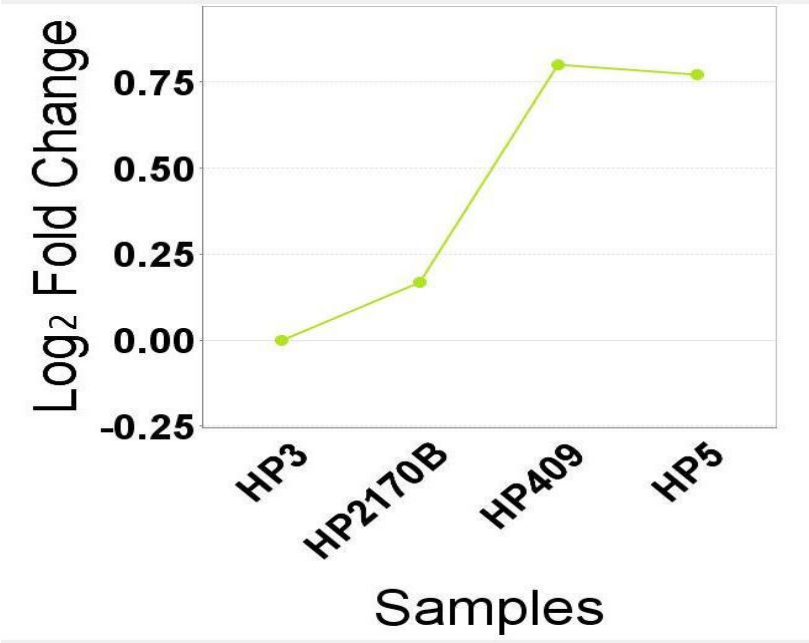

Supplemental Figure S6.9. Protein sequence coverage map (a) and protein expression profile (b) for HP iTRAQ-1 50S ribosomal protein L7/L12. Each line in (b) represents a peptide shown in (a).

a)

gi|167854980 (100%) 38,330.2 Da
50S ribosomal protein L13 [Haemophilus parasuis 29755]. gi|167853937|gb|EDS25176.1| 50S ribosomal protein L13 [Haemophilus parasuis 29755]

MKKLQLKKWF SSLFLLSPLV FAASNAQAEG KLTVYCGVQN KVCEDLTKRF SQKYNVETQF
IHGGTGTILG KLKAEKDNPQ ADIWYGGTIE PHFQAGQMGL LEAYRSPLQA EVLPQFKALQ
ESEAGKYTSI AYLMVLGFGI NTEKLKQLGV DAPKKWADLL DPRLKGEVQL ADPRTSGTMY
TTMITLIQLM GEEKAFEYLK KLDGNISQYV KSTLVTSNLS RGESAVTVGF AHGYASEKEK
GAPVDYVLPK DGVGYALGAA SIIKGARNLD NAKLFMDWVL SKEVQEIPWR DHGLYQTPTN
VKAEVAPQSP KIDGVKLVDV DYARFGSSEE GKRLVDKWLF NIKLSN

b)

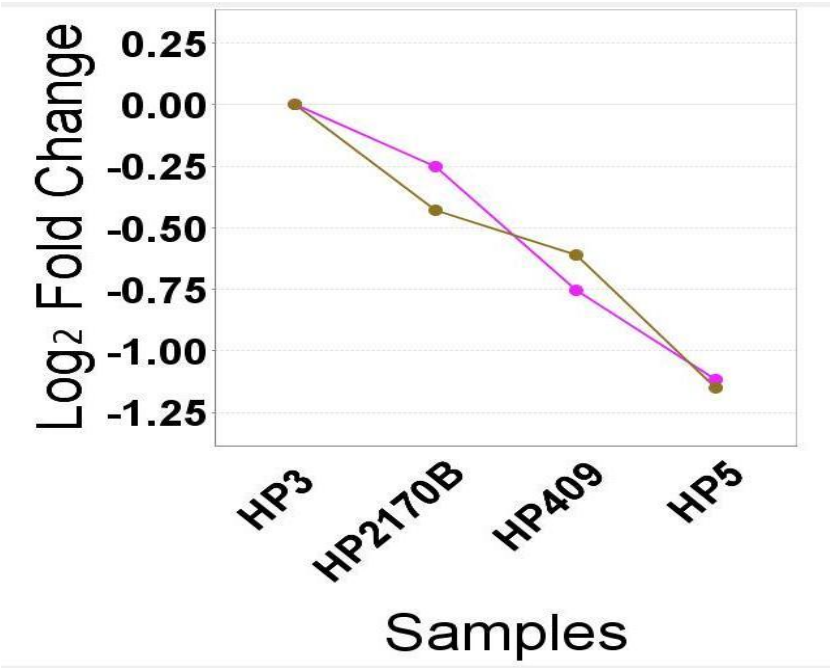

Supplemental Figure 6.S10. Protein sequence coverage map (a) and protein expression profile (b) for HP iTRAQ-1 Fe^{3+} ABC transporter. Each line in (b) represents a peptide shown in (a).

a)

gi|113461649 (85%) 93,018.9 Da
nitrate reductase catalytic subunit [Haemophilus somnus 129PT], gi|123132281|sp|Q0I5G9.1|NAPA_HAES1 RecName: Full=Periplasmic nitrate reductase; Flags: Precurs

M	N	L	S	R	R	D	F	M	K	A	N	A	A	L	A	A	A	S	V	A	G	L	I	I	P	V	K	N	V	N	A
R	V	V	A	S	Q	G	D	P	D	A	E	V	N	R	G	L	N	C	I	K	G	Y	F	L	P	K	I	M	Y	G	K
A	F	K	T	M	A	E	K	F	K	S	A	L	K	A	K	G	P	N	G	V	G	M	F	T	S	G	Q	S	T	I	F
A	A	V	A	F	V	R	T	F	G	I	D	E	P	M	G	C	Y	D	D	I	E	H	A	D	A	F	V	L	W	G	S
L	S	T	F	E	H	R	S	F	E	L	A	D	L	G	I	L	L	K	P	Q	S	D	L	A	I	L	N	Y	I	A	N
G	L	R	P	Q	D	P	R	E	Q	I	A	K	N	V	K	T	A	G	K	M	Y	D	S	S	F	E	E	F	K	K	L
D	P	N	K	K	V	V	S	Y	W	T	M	G	I	N	Q	H	T	R	G	V	W	A	N	H	L	I	Y	N	I	H	L
G	T	F	I	H	R	L	P	A	D	L	V	V	T	K	P	E	H	R	K	I	A	E	K	I	W	K	L	P	E	G	L
N	N	N	M	Q	A	G	P	N	I	N	E	E	T	Y	P	G	W	R	N	P	D	N	F	I	V	V	S	D	P	Y	P
R	T	Q	F	W	R	Q	Q	V	K	A	P	G	E	A	K	S	D	L	W	Q	L	V	E	F	S	K	Y	F	T	T	D
V	N	Q	Y	S	N	D	E	L	K	G	R	L	N	D	E	A	Y	H	F	G	F	Y	I	Q	K	G	L	F	E	E	Y
D	G	K	E	T	L	W	R	Y	R	E	G	Y	D	P	Y	V	K	A	G	E	G	V	S	F	Y	G	Q	A	D	K	R
L	E	H	W	H	T	G	S	M	T	R	R	V	P	E	L	H	R	S	F	P	N	N	L	V	W	M	N	P	N	D	A
R	N	K	C	P	E	G	L	I	Y	T	T	F	F	D	A	G	Q	L	A	N	K	L	I	L	D	A	T	D	P	I	S

K	E	T	D	F	K	K	C	A	V	K	V	V	K	A																	

b)

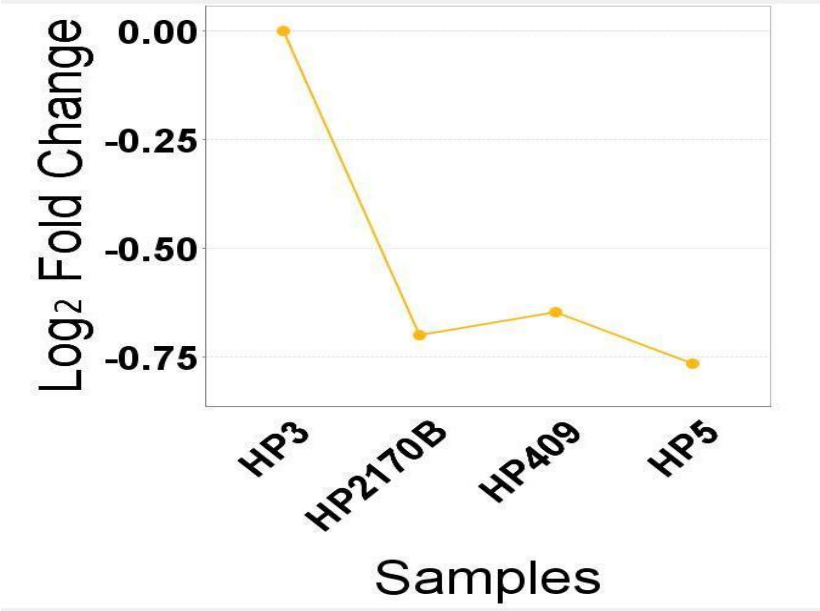

Supplemental Figure S6.11. Protein sequence coverage map (a) and protein expression profile (b) for HP iTRAQ-1 nitrate reductase. Each line in (b) represents a peptide shown in (a).

a)

gi|167856115 (100%) 30,128.9 Da
D-ribose transporter subunit RbsB [Haemophilus parasuis 29755]. gi|167852756|gb|EDS24029.1| D-ribose transporter subunit RbsB [Haemophilus parasuis 29755]

MKKLTSLAIA LGLAFSTSAM AKETIALAIS TLDNPFFVTL KEGAEKKAKE LGYNLVVLDS
QNDPAKELSN VEDVTVRGAT VLLINPTDSE AVGTAVAVAN KKNIPVITLD RGANKGNVVS
HIASDNVAGG KMAGDFIAEK VGKNAKVIQL EGIAGTSAAR ERGEGFKQAI EANQFELLAS
QPADFDRTKG LNVMENLLAS HGSAKAVFAQ NDEMALGALR AIRASGKNIL VVGFDGTDDA
VKAVNGGQLA ATIAQQPDKI GELGVEAADK VLKGEKVDAQ IPVPLKVVTK

b)

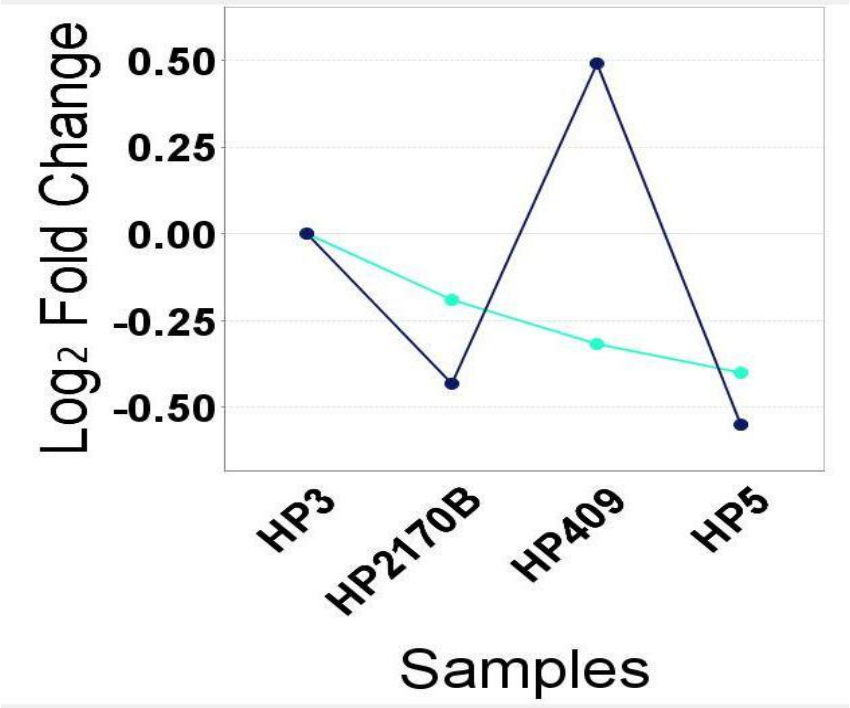

Supplemental Figure S6.12. Protein sequence coverage map (a) and protein expression profile (b) for HP iTRAQ-1 D-ribose transporter RbsB. Each line in (b) represents a peptide shown in (a).

a)

gi|167854701 (93%) 19,003.7 Da
superoxide dismutase (Cu-Zn) [Haemophilus parasuis 29755], gi|219870973|ref|YP_002475348.1| superoxide dismutase [Haemophilus parasuis SH0165], gi|167854238|

MKKTVLTLAL TALFGFSTSA IANSATQIEV KVQQLDLQNG NKDVGTVTIT ESPYGLVFTP
NLKGLSHGLH GFHIHEKPSC EPKEKDGKLV AGLGAGGHWD PKETKKHGYP WSDEAHLGDL
PALAVDHEGN ATNPVLAPRL KKLEEVKGRS LMIHAGGDNH SDHPAPLGGG GARMACGVIN

b)

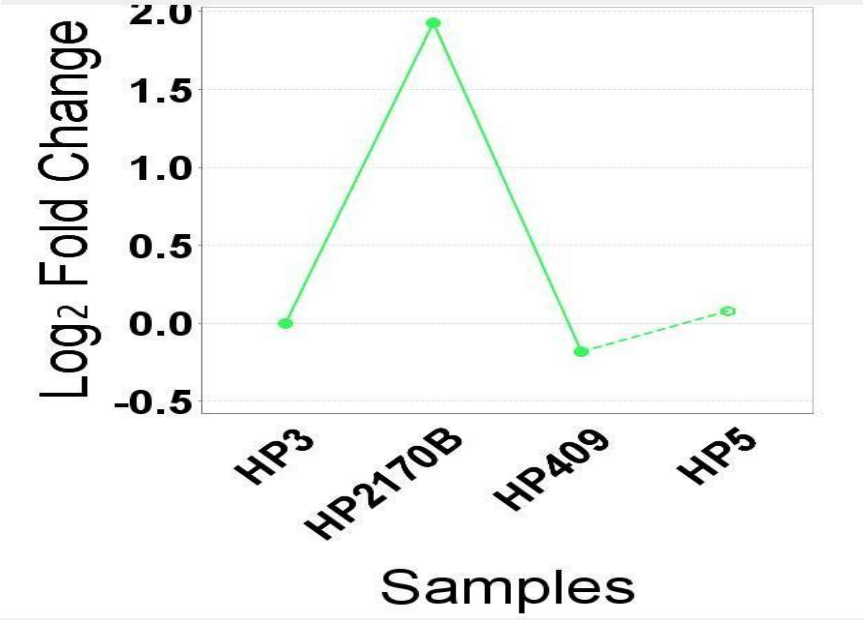

Supplemental Figure S6.13. Protein sequence coverage map (a) and protein expression profile (b) for HP iTRAQ-1 SOD (Cu-Zn). Each line in (b) represents a peptide shown in (a).

a)

gi|219871287 (100%) 32,652.9 Da
chelated iron ABC transporter periplasmic-binding protein [Haemophilus parasuis SH0165]. gi|219691491|gb|ACL32714.1| chelated iron ABC transporter, periplasmic-bindi

MKKLAALLSM LFLVSNPLAA QQFKVVTTFT VIQDIAQNVA GDKAVVESIT KPGAEIHDYQ
PTPQDIVKAQ SADLVLWNGM NLESWFERFF AQVKDKPAVV VTEGIEPISI YEGPYKDKPN
PHAWMSTKNA LIYIENIRQA LVKYDPANAE AYNANAKAYA DKIVALDQPL RERLAKVPEA
QRWLVTSEGA FSYLARDYGF KELYLWAINQ DEQGTPKQIR KVIDQVRKHQ IPVVFSESTI
SDKPAKQVAK ESKARYGGVL YVDSLSTKDG KVPTYIDLLN VTVSTIVAGF EK

b)

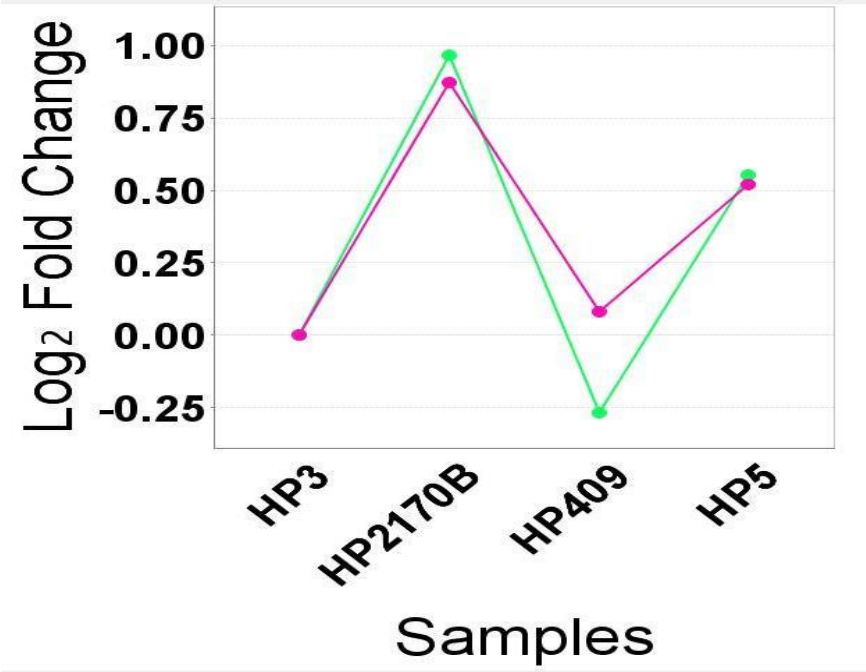

Supplemental Figure S6.14. Protein sequence coverage map (a) and protein expression profile (b) for HP iTRAQ-1 chelated iron ABC transporter. Each line in (b) represents a peptide shown in (a).

a)

gi|152979644 (85%) 34,615.4 Da
TRAP transporter solute receptor TAXI family protein [Actinobacillus succinogenes 130Z], gi|150841367|gb|ABR75338.1| TRAP transporter solute receptor, TAXI family [Act

MKKLFKLSLV AGIALASLNA HAEEKFITIG TGGQTGVYYV VGQSICQLVN RDTAKTGVKC
NAPSTGASVA NLNAIADHQM DMGIAQSDWQ YHAYNGSSSF EGKRNEKLRA VFSLHPEPFT
LMVRDDSGIQ SFDDLKGKRV NVGDPGSGTR ATMNVILAAK GWTNKNFKVA SELKPAEMAS
VMCDNNLDAI TYNVGHPNGA LKEAAASCDS HLVPVTGDAI DKLVADHSYY AKAVIPGGLY
KGTDNPVDTF GVYATLVTSE DVEADKVYAV VKAVFDNFDR FKRLHPAFAN LKQEEMITNA
LSAPLHEGAV RYYKERGWIK

b)

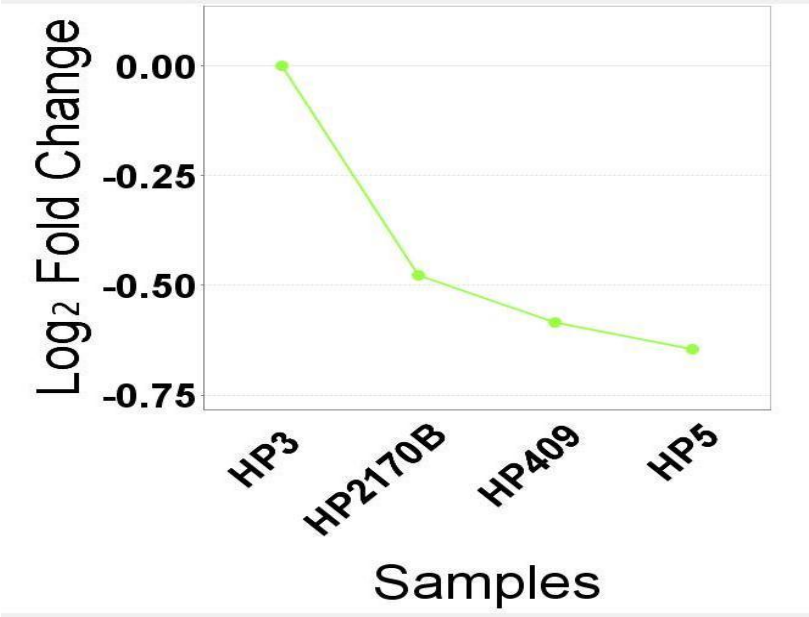

Supplemental Figure S6.15. Protein sequence coverage map (a) and protein expression profile (b) for HP iTRAQ-1 TRAP transporter. Each line in (b) represents a peptide shown in (a).

a)

gi|219871315 (100%) 37,665.4 Da
periplasmic iron-binding protein [Haemophilus parasuis SH0165]. gi|219691519|gb|ACL32742.1| periplasmic iron-binding protein [Haemophilus parasuis SH0165]

MKKSLSVLAL ALSSVISTSA LAANEVNVYS YRQPYLIEPM LKDFEKQTGI KVNVIFADKG
LVERVQKEGE LSPADVLLTV DISRVMQIVK AGLAQKVDSK TLEKNIPAQF RDSNGEWFGL
TKRARVIYTS KDRVGALPAG FDYLDLAKPE YKGKVCVRSG KNAYNVSLFA AMIEHYGEEK
TKAFLEGLKA NLAQKPQGGD RDQVKAIKEG ICDYALGNSY YYGKMLDDEK QRSWAESAII
NFPNGQYGTH VNISGVALAK HSPNKANAIK LIEYLSGNQA QALYAKLNHE YPVKADVAPS
DLVKGWGTYS TDALKLEDIA KNYEKALKLV DEVKFDDFGA K

b)

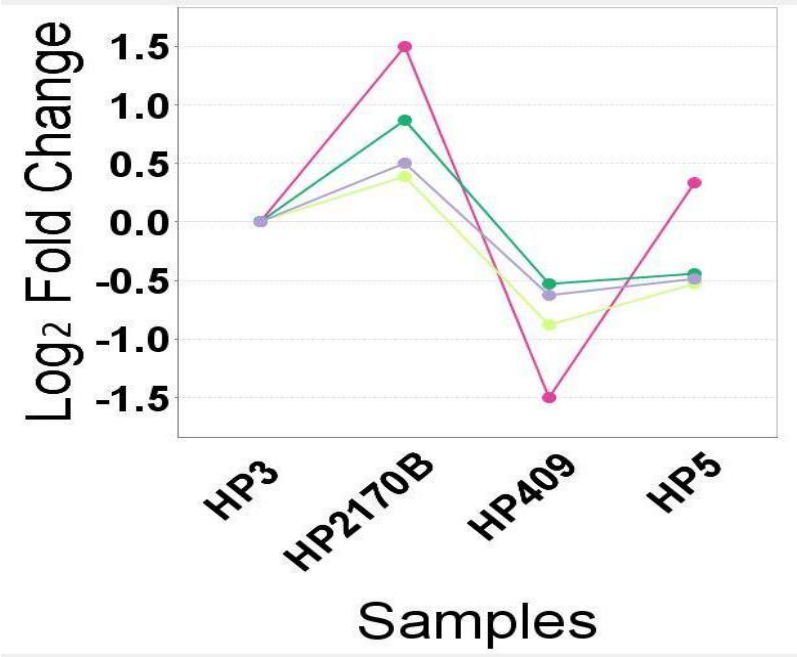

Supplemental Figure S6.16. Protein sequence coverage map (a) and protein expression profile (b) for HP iTRAQ-1 iron-binding protein. Each line in (b) represents a peptide shown in (a).

a)

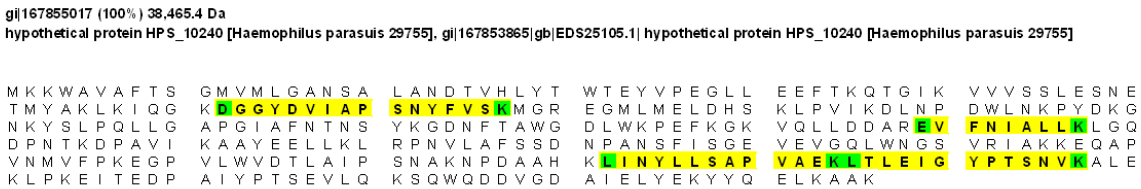

b)

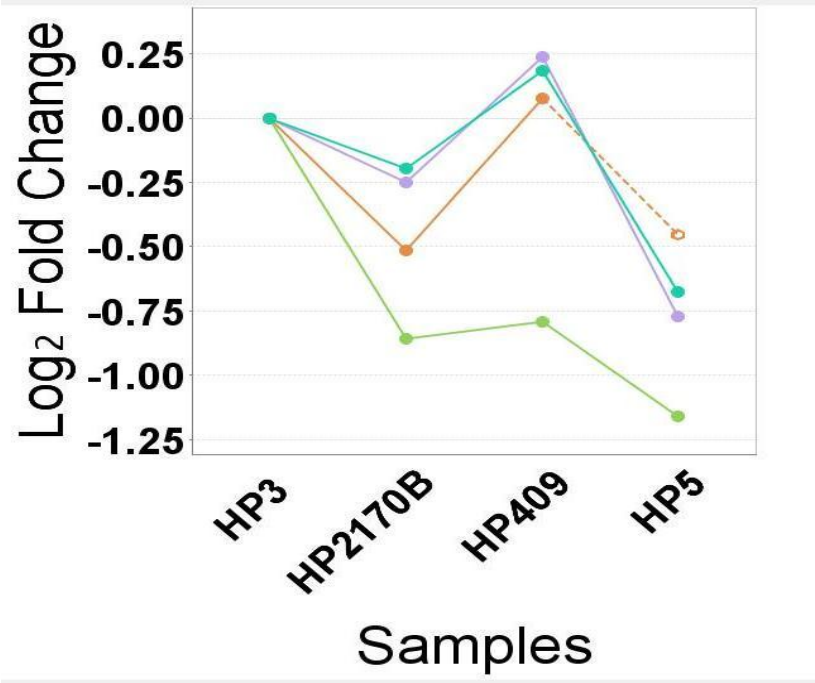

Supplemental Figure S6.17. Protein sequence coverage map (a) and protein expression profile (b) for HP iTRAQ-1 HPS_10240. Each line in (b) represents a peptide shown in (a).

a)

gi|167855966 (81%) 17,140.5 Da
hypothetical protein HPS_07840 [Haemophilus parasuis 29755], gi|167852903|gb|EDS24170.1| hypothetical protein HPS_07840 [Haemophilus parasuis 29755]

MYIQAFSLLG ANPVPMPLSE LYTALETRAV DAQEHPIGIF WSAKLYEVQK HLSLTNHGYT
PLIVVMNKAK FDSFSPELQQ AILDAAKEAG NYQRQLNLEN EKEIIAKLQK AGIQVIEEVD
NKPFKAIIEA DVRKAFIEKN GSELVEKIDG LAK

b)

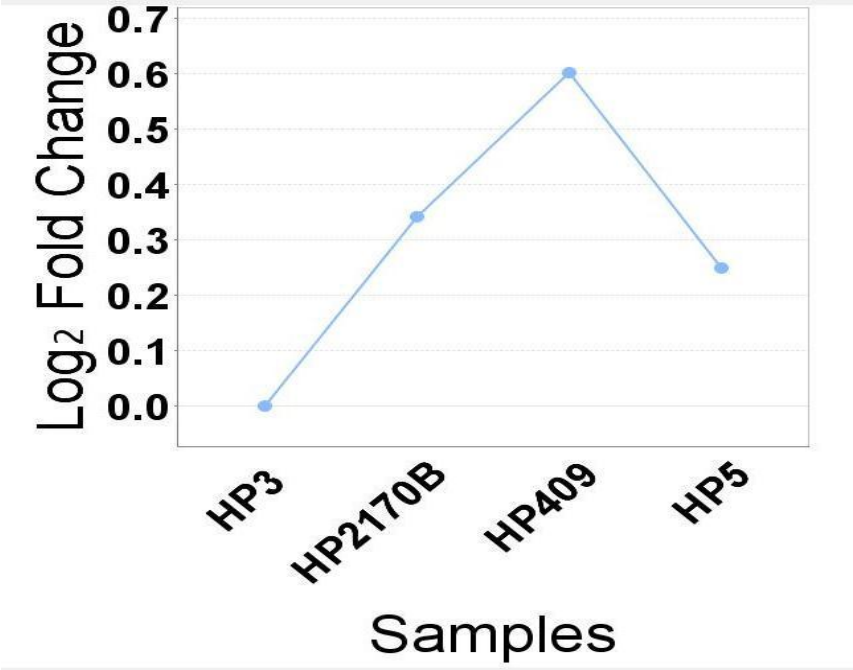

Supplemental Figure S6.18. Protein sequence coverage map (a) and protein expression profile (b) for HP iTRAQ-1 HPS_7840. Each line in (b) represents a peptide shown in (a).

a)

gi|219871287 (100%) 32,652.9 Da
chelated iron ABC transporter periplasmic-binding protein [Haemophilus parasuis SH0165]. gi|219691491|gb|ACL32714.1| chelated iron ABC transporter, periplasmic-bindi

MKKLAALLSM LFLVSNPLAA QQFKVVTTFT VIQDIAQNVA GDKAVVESIT KPGAEIHDYQ
PTPQDIVKAQ SADLVLWNGM NLESWFERFF AQVKDKPAVV VTEGIEPISI YEGPYKDKPN
PHAWMSTKNA LIYIENIRQA LVKYDPANAE AYNANAKAYA DKIVALDQPL RERLAKVPEA
QRWLVTSEGA FSYLARDYGF KELYLWAINQ DEQGTPKQIR KVIDQVRKHQ IPVVFSESTI
SDKPAKQVAK ESKARYGGVL YVDSLSTKDG KVPTYIDLLN VTVSTIVAGF EK

b)

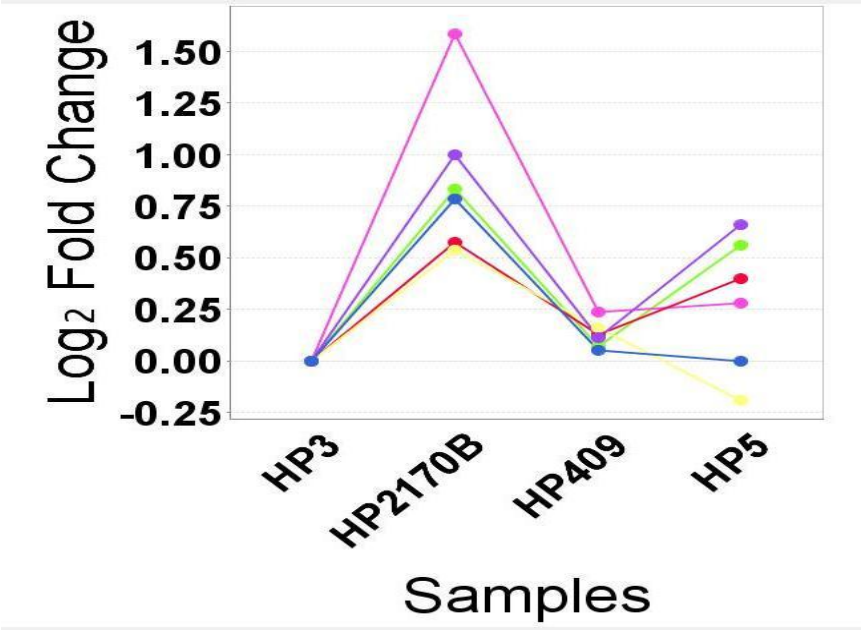

Supplemental Figure S6.19. Protein sequence coverage map (a) and protein expression profile (b) for HP iTRAQ-2 chelated iron ABC transporter. Each line in (b) represents a peptide shown in (a).

a)

gi|167855400 (100%) 37,666.3 Da
FbpA [Haemophilus parasuis 29755], gi|167853466|gb|EDS24714.1| FbpA [Haemophilus parasuis 29755]

MKKSLSVLAL ALSSVISTSA LAANEVNVYS YRQPYLIEPM LKDFEKQTGI KVNVIFADKG
LVERVQKEGE LSPADVLLTV DISRVMQIVK AGLAQKVDSK TLEKNIPAQF RDSNGEWFGL
TKRARVIYTS KDRVGALPAG FDYLDLAKPE YKGKVCVRSG KNAYNVSLFA AMIEHYGEEK
TKAFLEGLKA NLAQKPQGGD RDQVKAIKEG ICDYALGNSY YYGKMLDDEK QRSWAESANI
NFPNGQYGTH VNISGVALAK HSPNKANAIK LIEYLSGNQA QALYAKLNHE YPVKADVAPS
DLVKGWGTYS TDALKLEDIA KNYEKALKLV DEVKFDDFGA K

b)

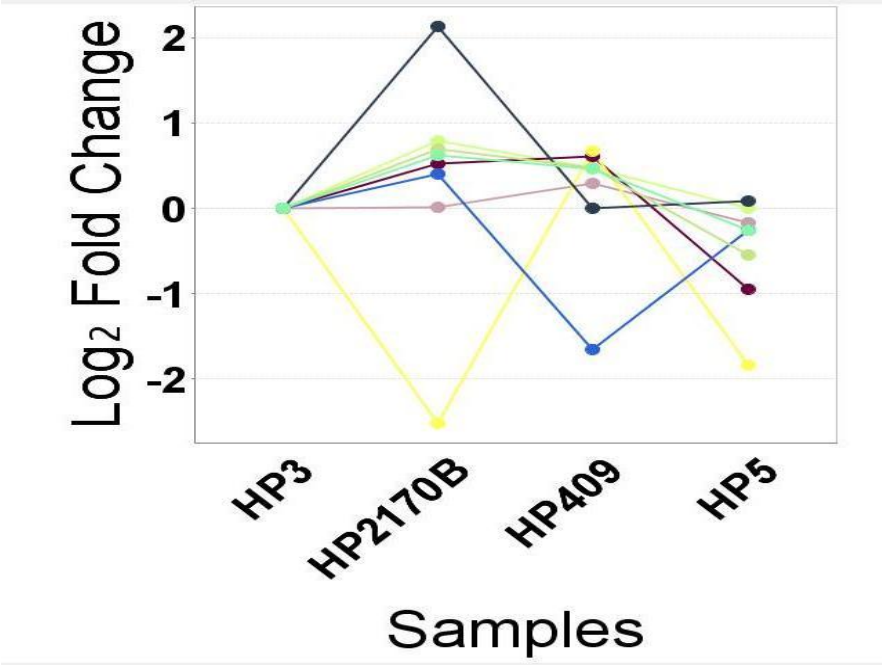

Supplemental Figure S6.20. Protein sequence coverage map (a) and protein expression profile (b) for HP iTRAQ-2 FbpA. Each line in (b) represents a peptide shown in (a).

a)

gi|167856581 (100%) 12,391.4 Da
50S ribosomal protein L7/L12 [Haemophilus parasuis 29755], gi|219871555|ref|YP_002475930.1| 50S ribosomal protein L7/L12 [Haemophilus parasuis SH0165], gi|2548063

MSLTNEQIIE AIASKSVSEI VELITAMEEK FGVSAAAAAV AVAAGPAEAA EEKTEFDVIL
ADAGANKVAV IKAVRGATGL GLKEAKDLVE SAPAALKEGI SKGEAEALKK ELEEAGAKVE
IK

b)

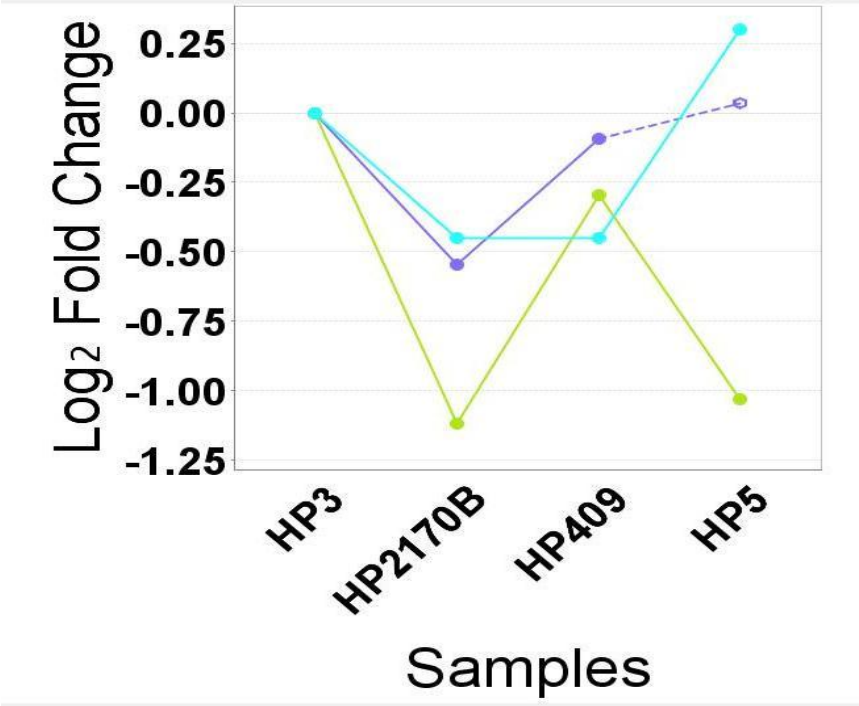

Supplemental Figure S6.21. Protein sequence coverage map (a) and protein expression profile (b) for HP iTRAQ-2 50S ribosomal L7/L12. Each line in (b) represents a peptide shown in (a).

a)

gi|167855124 (100%) 60,868.0 Da
hypothetical protein HPS_06844 [Haemophilus parasuis 29755], gi|167853759|gb|EDS25001.1| hypothetical protein HPS_06844 [Haemophilus parasuis 29755]

```
MKFNKTPLAL  ALMGATTAMA  YEADKTYRFT  VLHVNDTHGH  FWKNDKGEYG  FAAQKTLIDK
IRKEVAEKGG  EVVLLHAGDF  NTGVPESDMQ  NARPDIEGLN  MLGFDVAVLG  NHEFDFPLQV
LDMQEKWAKF  PFISANVINK  KTNKHLVKPY  VTLNKGGLKF  AVIGLTTEDT  AKLGNPDVTE
NVVFNDPIKT  AKETLAQVKK  TEKPDVSIAL  THMGYYFDEQ  HGMNAPGDVS  LARGLDKGAF
DLIIGGHTHD  TVCVDEKGVF  KLKYTPGEEC  KPDFQNGTWI  VQAGEWGKFL  GRADFEFKNG
ETKLVKYELI  PVNLKQKIKL  ADGKSEYKLY  QEEIPEDKAV  FEHLKKYQDE  GDKLLGVKVG
EVKGGILEGD  RKVIRFHQTN  LGRLIAQSQM  ERVKADIGIM  NSGAIRASIN  EGEVTYKNLL
TVQPFGNMIA  TVDLTGKELI  DYLNVVALKE  VDMGAYPQFA  GVSMVVDRTA  KQVSDVKVGG
KPLDLNKTYK  VSVPDYCAAG  GDGYPILKKH  PSYVNTGFID  AEMLKKYFEE  NSPIDASKYD
PKDDVIFK
```

b)

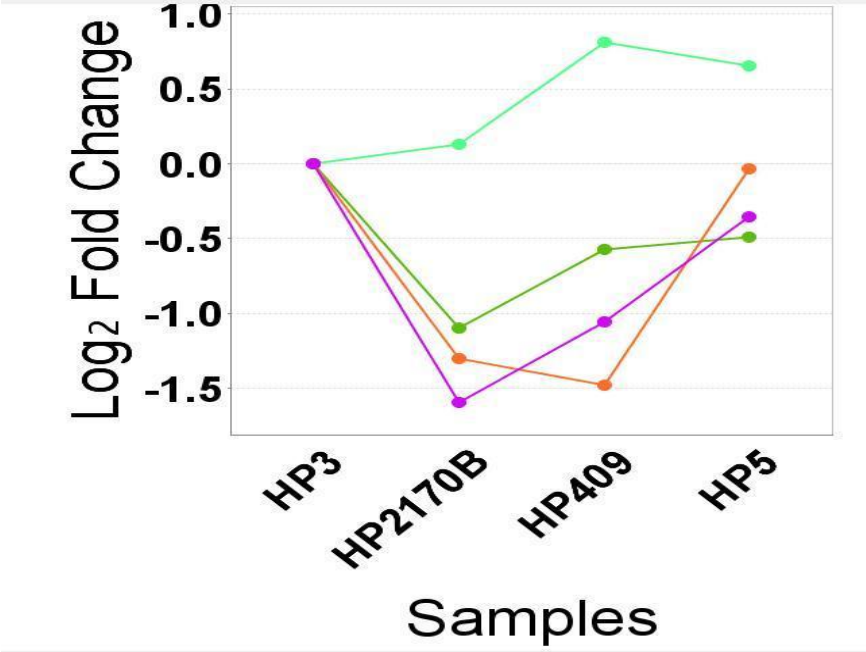

Supplemental Figure S6.22. Protein sequence coverage map (a) and protein expression profile (b) for HP iTRAQ-2 HPS_06844. Each line in (b) represents a peptide shown in (a).

a)

gi|167855819 (100%) 9,459.4 Da
DNA-binding protein HU [Haemophilus parasuis 29755], gi|219871002|ref|YP_002475377.1| DNA-binding protein HU/transcriptional regulator [Haemophilus parasuis SH0165

MNKTELVDAI AAGADLSKKD AKAALEATLN AISESLKKGD SVQLIGFGTF KVNHRKARTG
RNPKTNEAIE IPAANVPAFV AGKALKDLVK

b)

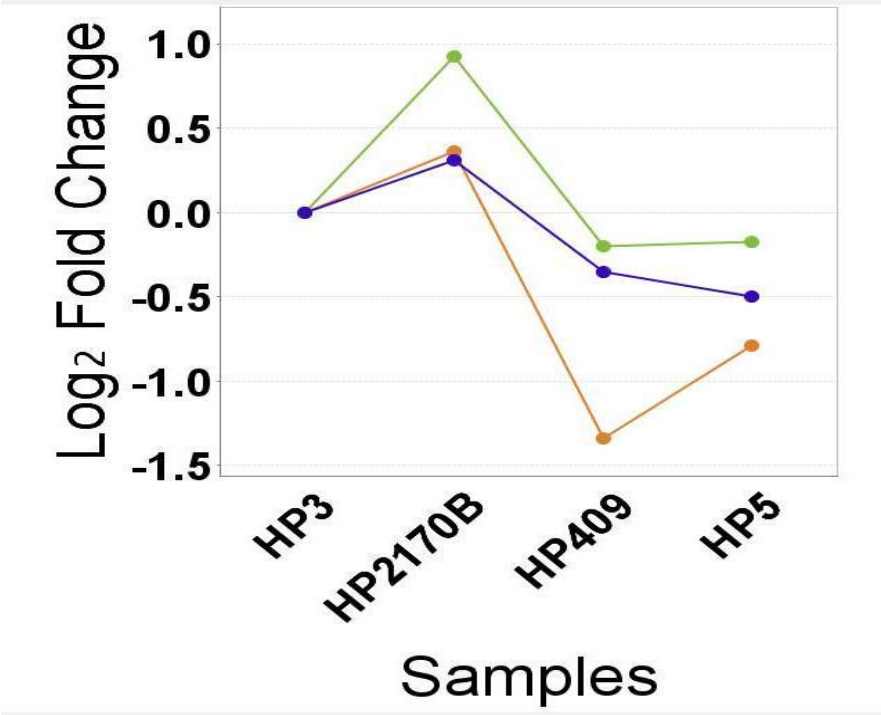

Supplemental Figure S6.23. Protein sequence coverage map (a) and protein expression profile (b) for HP iTRAQ-2 DNA binding protein HU. Each line in (b) represents a peptide shown in (a).

a)

gi|167855017 (100%) 38,465.4 Da
hypothetical protein HPS_10240 [Haemophilus parasuis 29755]. gi|167853865|gb|EDS25105.1| hypothetical protein HPS_10240 [Haemophilus parasuis 29755]

MKKWAVAFTS GMVMLGANSA LANDTVHLYT WTEYVPEGLL EEFTKQTGIK VVVSSLESNE
TMYAKLKIQG KDGGYDVIAP SNYFVSKMGR EGMLMELDHS KLPVIKDLNP DWLNKPYDKG
NKYSLPQLLG APGIAFNTNS YKGDNFTAWG DLWKPEFKGK VQLLDDAREV FNIALLKLGQ
DPNTKDPAVI KAAYEELLKL RPNVLAFSSD NPANSFISGE VEVGQLWNGS VRIAKKEQAP
VNMVFPKEGP VLWVDTLAIP SNAKNPDAAH KLINYLLSAP VAEKLTLEIG YPTSNVKALE
KLPKEITEDP AIYPTSEVLQ KSQWQDDVGD AIELYEKYYQ ELKAAK

b)

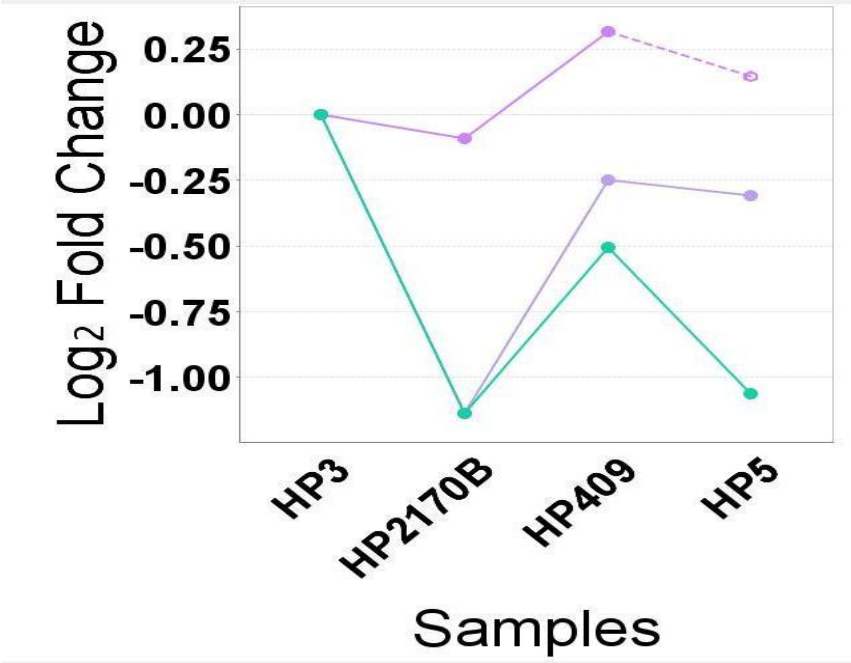

Supplemental Figure S6.24. Protein sequence coverage map (a) and protein expression profile (b) for HP iTRAQ-2 HPS_10240. Each line in (b) represents a peptide shown in (a).

a)

gi|167856064 (89%) 8,497.5 Da
acyl carrier protein [Haemophilus parasuis 29755], gi|219871798|ref|YP_002476173.1| acyl carrier protein [Haemophilus parasuis SH0165], gi|254802114|sp|B8F7C3.1|ACP

M S I E E R V K K I I V D Q L G A K A E D V K P E T S F I E D L G A D S L D T V E L V M A L E E E F D I E I P D E E A E K I A T V Q S A I D Y V Q N N Q

b)

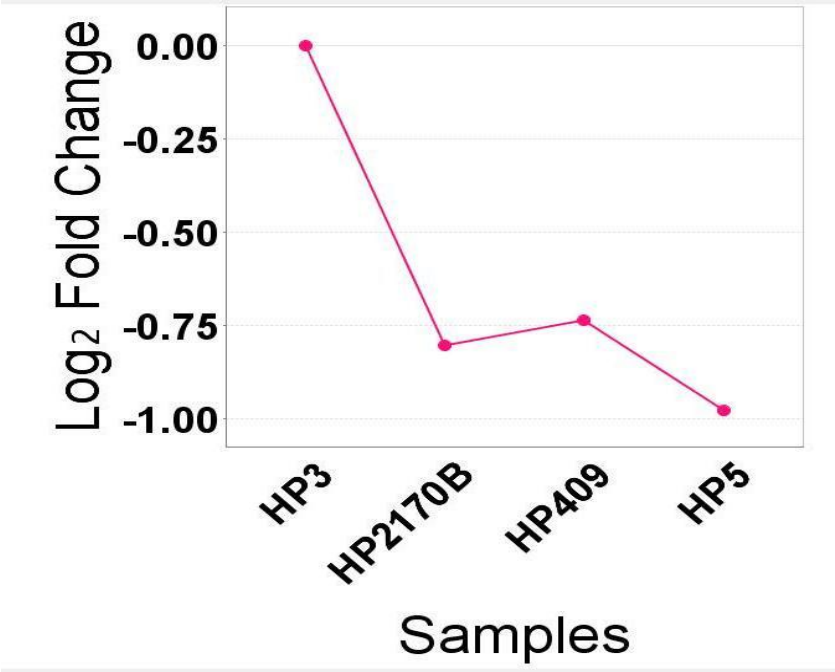

Supplemental Figure S6.25. Protein sequence coverage map (a) and protein expression profile (b) for HP iTRAQ-2 acyl carrier protein. Each line in (b) represents a peptide shown in (a).

a)

gi|167855469 (100%) 30,145.2 Da
elongation factor Ts [Haemophilus parasuis 29755], gi|167853398|gb|EDS24648.1| elongation factor Ts [Haemophilus parasuis 29755]

MAEITAALVK ELRERTGAGM MECKKALVEA NGDIELAIDN MRKSGQAKAA KKAGRVAAEG
VILARIGAGF GVLVEMNCET DFVAKDAGFV GLANEVADYA LANKDTSIEA LQAQFEEKRA
ALVAKIGENM NIRRVQYLEG QVIAQYLHGA KIGVLVAGQG AEEELKKVAM HVAASKPDFV
NPEDVSAEVV AKEREIQIEI AMNSGKPKEI AEKMVEGRMA KFTGEVSLTG QPFVMDPSQT
VGAYLKSVNT SVANFVRLEV GEGIEKVEED FAAEVAKITG GNA

b)

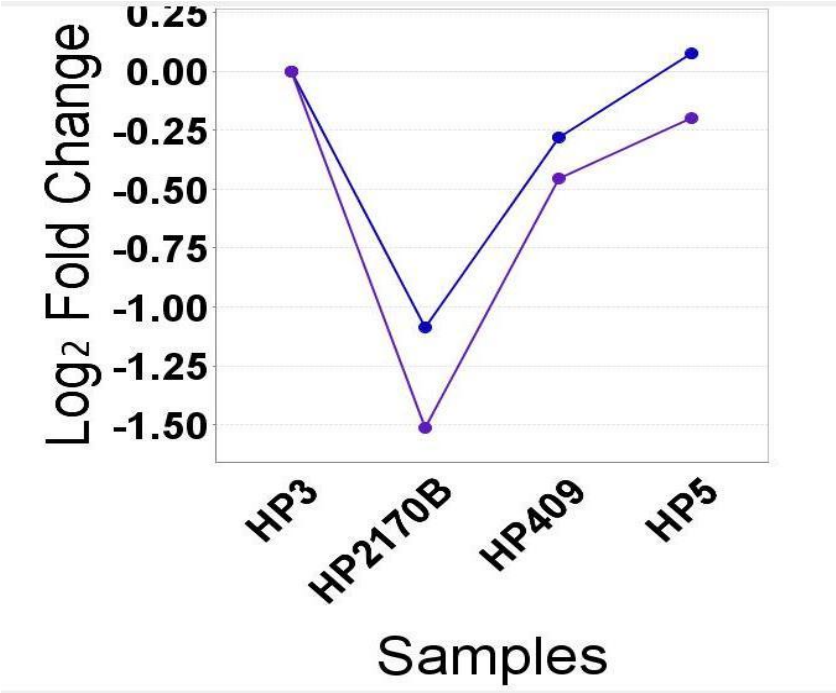

Supplemental Figure S6.26. Protein sequence coverage map (a) and protein expression profile (b) for HP iTRAQ-2 elongation factor Ts. Each line in (b) represents a peptide shown in (a).

a)

gi|167856489 (100%) 18,036.7 Da
glucose-specific PTS system enzyme IIA component [Haemophilus parasuis 29755], gi|219871157|ref|YP_002475532.1| PTS system glucose-specific transporter subunit

MGFFDKLFGG KKEAVAKEVK IYAPLSGEIV NIEDVPDVVF SEKIVGDGIA IRPTGDMIVA
PVNGTIGKIF ETNHAFSIES EDGVELFVHF GIDTVELKGE GFTRLAEENQ EVKVGDPIIK
FDLELLQSKA KSVLTPVVIS NMDEVTNLQK LSGEVVAGES TVLVLTK

b)

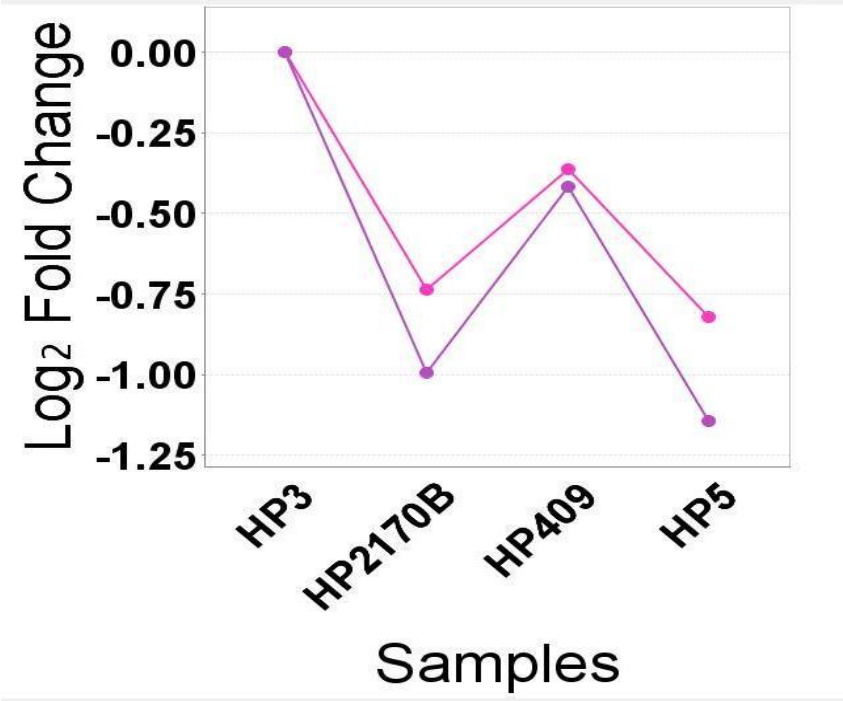

Supplemental Figure S6.27. Protein sequence coverage map (a) and protein expression profile (b) for HP iTRAQ-2 glucose-specific PTS enzyme IIA. Each line in (b) represents a peptide shown in (a).

a)

gi|113969297 (89%) 45,503.7 Da
gamma-glutamyl phosphate reductase [Shewanella sp. MR-4]. gi|113883981|gb|ABI38033.1| glutamate-5-semialdehyde dehydrogenase [Shewanella sp. MR-4]

MSQTNQAQYL QQLGSQAKQA SYALANLSAA QKADLLEAIA EALTQNTQAI LAANAKDVAA
AKAEGLNDAM IDRLLLNESR LAGIIGDIGD VVRLADPVGE EFGSRVLDNG LRLTRRRVPL
GVIGVIYEAR PNVTVDIAVL ALKTGNAVIL RGGKETLESN KLISEVIRGA IASQGLPVDA
VQLIDSPDRA LVTGLLKLDQ YVDMIVPRGG QALQRLCAEQ ATIPVILGGI GICHLYVDKH
ADLERALEVI ANAKVQRPTV CNALDTLLVD NAVAERFVPQ IAEYLHRLGV RFSVCEQSYA
LLDGLGFDIS PATEQSFATE WLSLALGIKV VNDIDTAIAH IRTYSSGHSE AILTDDIHTA
THFMNEVNSA AVYVNASTRF TDGGQFGLGA EVAVSTQKLH ARGPMGLEAL TTYKWLAWGD
YTSRA

b)

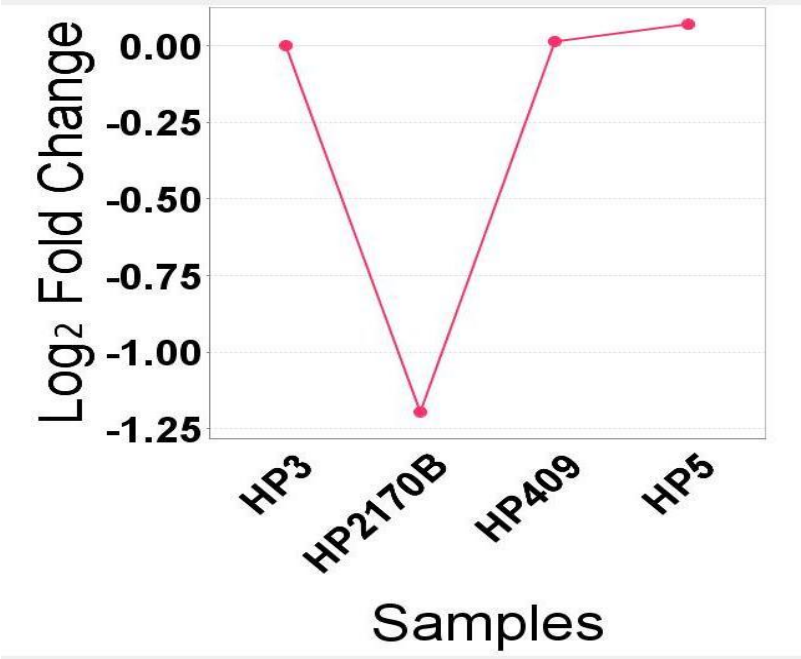

Supplemental Figure S6.28. Protein sequence coverage map (a) and protein expression profile (b) for HP iTRAQ-2 gamma-glutamyl phosphate reductase. Each line in (b) represents a peptide shown in (a).

a)

gi|54295850 (89%) 39,762.5 Da
hypothetical protein plpp0007 [Legionella pneumophila str. Paris]. gi|53755682|emb|CAH17184.1| hypothetical protein plpp0007 [Legionella pneumophila str. Paris]

MNNSIYYLGF NKLLSLTKCS KEALLLDKII FHHQGTLLKR DNRLWFTRKI PDLAAELGFS
ESRIYIYLKS LEEEGLIIRK RFKYYGVPRS FIAITETLQN KLQLIYKEPE TIIEIKEKEI
TPEPDINERM DYLVSTDTIN KEKNRVINNI TFPNSDNKLP FTELNIVKGM LLNVQKQHGV
KLSSPQKVFD EVVFSLNNQE QFQKIGTFQH KINIISQLLR TNRWRTPKGF NKYSPEGKHY
QEKQDQEKAA RLQLKKEECT YSGLDEIATN NRLCNGYELA HHPSTNKELQ KSLQIQQSLI
NGIKKDIKTI KNRNILDNFL K[I]LAQEETK[L] SKLQAELSLQ

b)

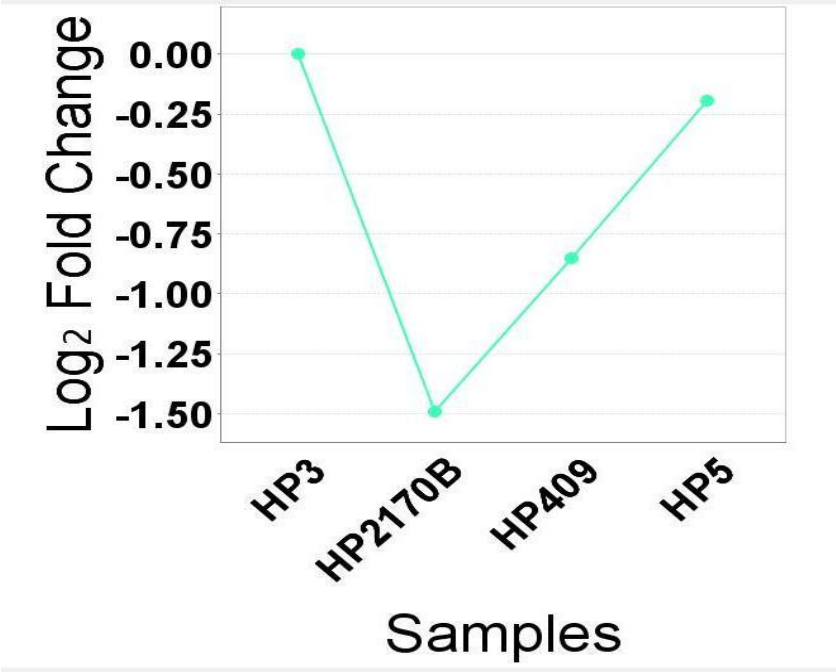

Supplemental Figure S6.29. Protein sequence coverage map (a) and protein expression profile (b) for HP iTRAQ-2 hypothetical protein plp0007. Each line in (b) represents a peptide shown in (a).

a)

gi|91791530 (89%) 17,672.8 Da
50S ribosomal protein L10 [Shewanella denitrificans OS217], gi|122969082|sp|Q12SW8.1|RL10_SHEDO RecName: Full=50S ribosomal protein L10, gi|91713532|gb|ABE53458.1|

MALRLEDKKA IVAEVNEAAK GALSAVVADS RGVTVGAMTV LRKAARANGV YVRVVRNTLA
KRAVEGTAFE CLAETFTGPT LIAFSNEHPG AAARLLKDFA KGNAKFEVKG AAFEGMFIPA
VDIDRLAKLP TYDEALAQLM MTMKEASAGK FVRTLAALRD QKQEAA

b)

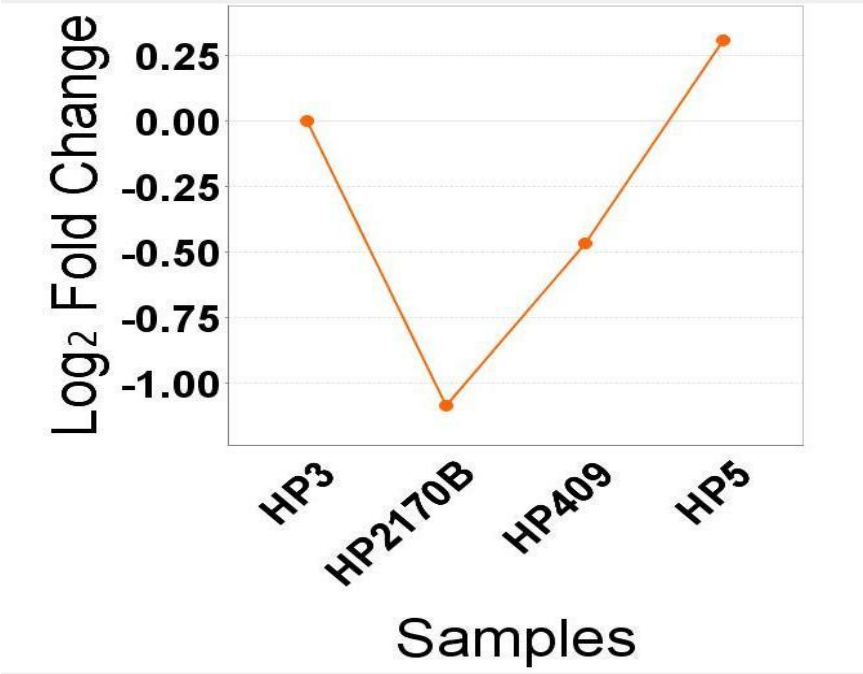

Supplemental Figure S6.30. Protein sequence coverage map (a) and protein expression profile (b) for HP iTRAQ-2 50S ribosomal protein L10. Each line in (b) represents a peptide shown in (a).

a)

gi|111116467 (89%) 32,857.6 Da
acetaldehyde dehydrogenase [Pseudomonas putida], gi|296100271|ref|YP_003617188.1| acetaldehyde dehydrogenase [Pseudomonas putida], gi|19033981|gb|AAL83664.1|

MSKKLKVAII GPGNIGTDLM IKVMRNAEHL EMGAMVGIDP ASDGLARAQR MGVATTHEGV
EGLINLPEFA DIDFVFDATS ASAHVRNDAL LRRAKPGIRL IDLTPAAIGP YCVPVVNLEE
HLAKLNVNMV TCGGQATIPM VAAVSRVAKV HYAEIVASIA SKSAGPGTRA NIDEFTETTS
KAIEVIGGAA KGKAIIIMNP AEPPLIMRDT VFVLSEAVDQ AQVEASIEEM ASAVQAYVPG
YRLKQKVQFD MIPASAPLHI PGLGTFSGLK TSIYLEVEGA AHYLPAYAGN LDIMTSAALA
TAERMAQSLL NA

b)

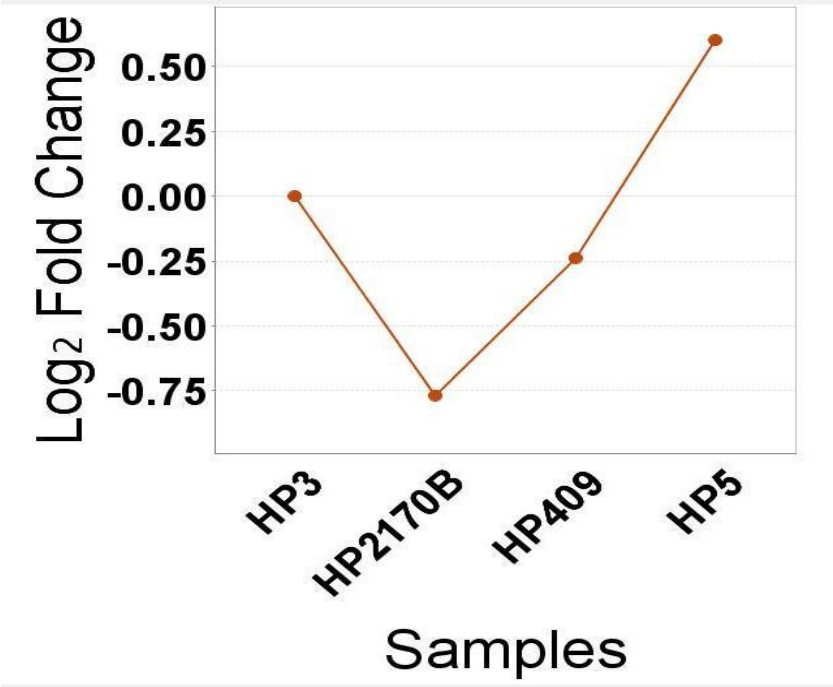

Supplemental Figure S6.31. Protein sequence coverage map (a) and protein expression profile (b) for HP iTRAQ-2 acetaldehyde dehydrogenase. Each line in (b) represents a peptide shown in (a).

a)

gi|167855391 (98%) 57,888.3 Da
ABC transporter, periplasmic binding protein [Haemophilus parasuis 29755], gi|167853457|gb|EDS24705.1| ABC transporter, periplasmic binding protein [Haemophilus p

MTKHFEHNES RRGFMKLVAG VGAGLAFSGS IGTFASQAYA APAKGSTIEA GIAYPISTGF
DPMSSTGASS MAANIHIFEG LVDLHPATRQ PYLALAAKEP EKVDDVTYRI TLRDGAVFHN
GSAVTSADVV FSFERVLDPN TKSLFAQFIP FIKSVTAVDQ KTVEFKLKYP FALFKERLTI
IKIVPKALIE AQGQSVFDAN PVGTGPYKFV SAVKDDRIVF EANPAYTGPY PATVEKMTWF
LLSDDAARVA AQESGRVQAI ENVPYLDADR LKRKAAVESV QSFGLIFLMF NCEKAPFNNK
KVRQALQYAI DTQKLVDVVF LGNAKPATSY VQDSHPDYVK ASTVYDFDPK KAAALLKEAG
VDKLEFTTRS TAHKWVVDSV QMILEDWNKI PGVKVTNIAS QSPYNDGVDA GNFEVLIAPG
DPSVFGNDLD LLLSWWYRGD VWPKKRFRWS NTPEYAEVQK LLDAAVAAKT PAEAREIWGK
AINIIAEEAA LYPIIHRKLP TAWSNKALDG FKPLSTTGMS FIGVSRK

b)

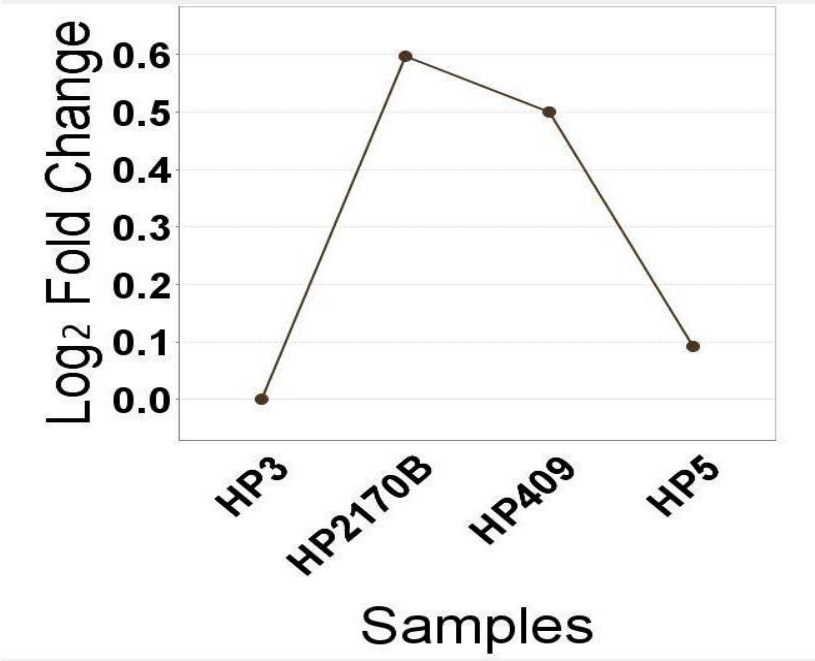

Supplemental Figure S6.32. Protein sequence coverage map (a) and protein expression profile (b) for HP iTRAQ-2 ABC transporter. Each line in (b) represents a peptide shown in (a).

a)

gi|254362200 (100%) 8,497.5 Da
acyl carrier protein [Mannheimia haemolytica PHL213], gi|261493133|ref|ZP_05989668.1| acyl carrier protein [Mannheimia haemolytica serotype A2 str. BOVINE], gi|2614957

MSIEERVKKI IVDQLGAKAE DVKPEASFIE DLGADSLDTV ELVMALEEEF DIEIPDEEAE
KITTVQSAID YVQNNQ

b)

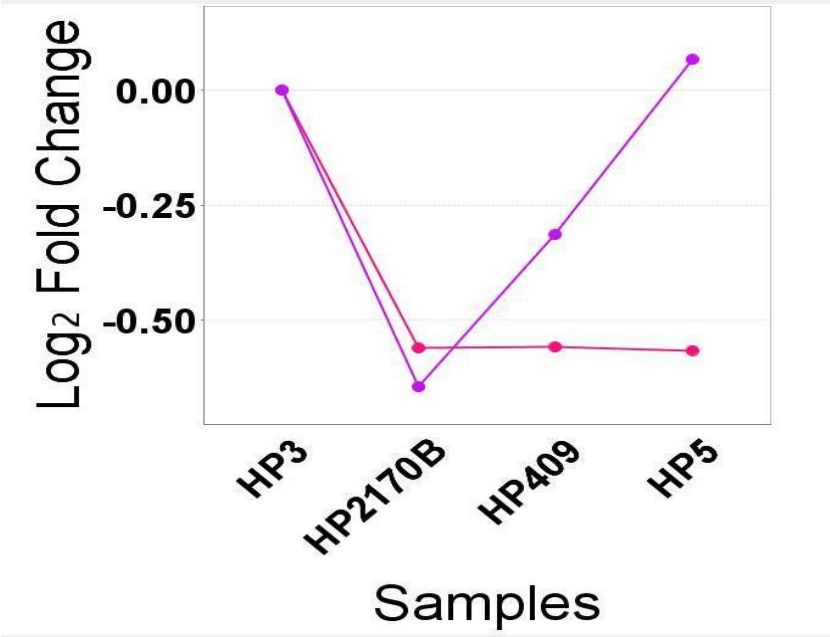

Supplemental Figure S6.33. Protein sequence coverage map (a) and protein expression profile (b) for HP iTRAQ-2 *M. haemolytica* acyl carrier protein. Each line in (b) represents a peptide shown in (a).

a)

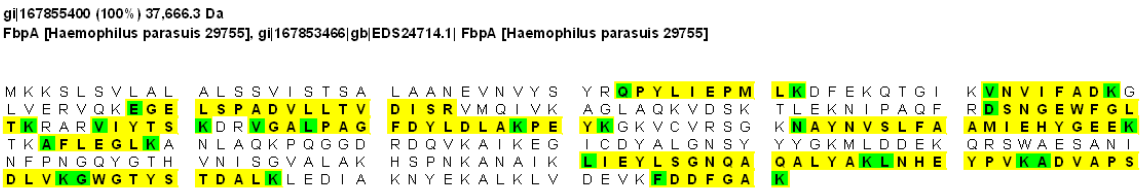

b)

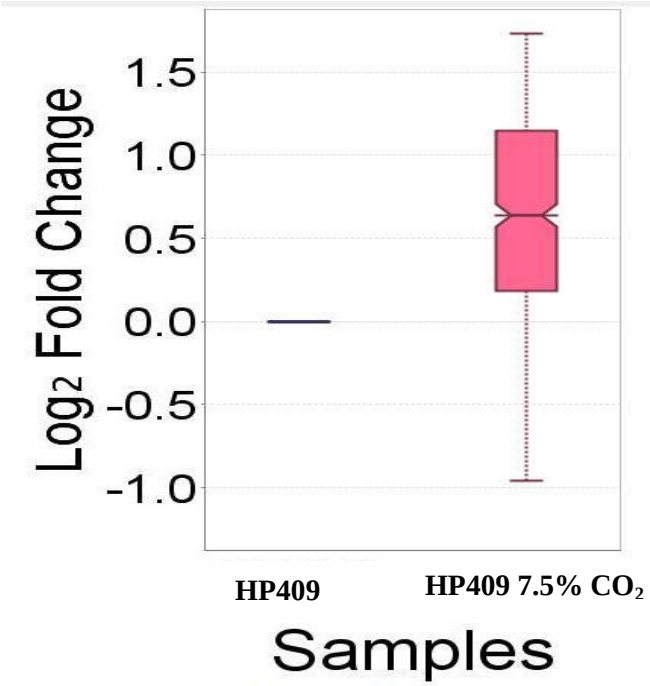

Supplemental Figure S6.34. Protein sequence coverage map (a) and protein expression profile (b) for HP iTRAQ-3 FbpA. The median protein expression and standard deviation, calculated as the interquartile range, are presented for each sample in (b).

a)

gi|167855966 (77%) 17,140.5 Da
hypothetical protein HPS_07840 [Haemophilus parasuis 29755], gi|167852903|gb|EDS24170.1| hypothetical protein HPS_07840 [Haemophilus parasuis 29755]

MYIQAFSLLG ANPVPMPLSE LYTALETRAV DAQEHPIGIF WSAKLYEVQK HLSLTNHGYT
PLIVVMNKAK FDSFSPELQQ AILDAAKEAG NYQRQLNLEN EKEIIAKLQK AGIQVIEEVD
NKPFKAIIEA DVRKAFIEKN GSELVEKIDG LAK

b)

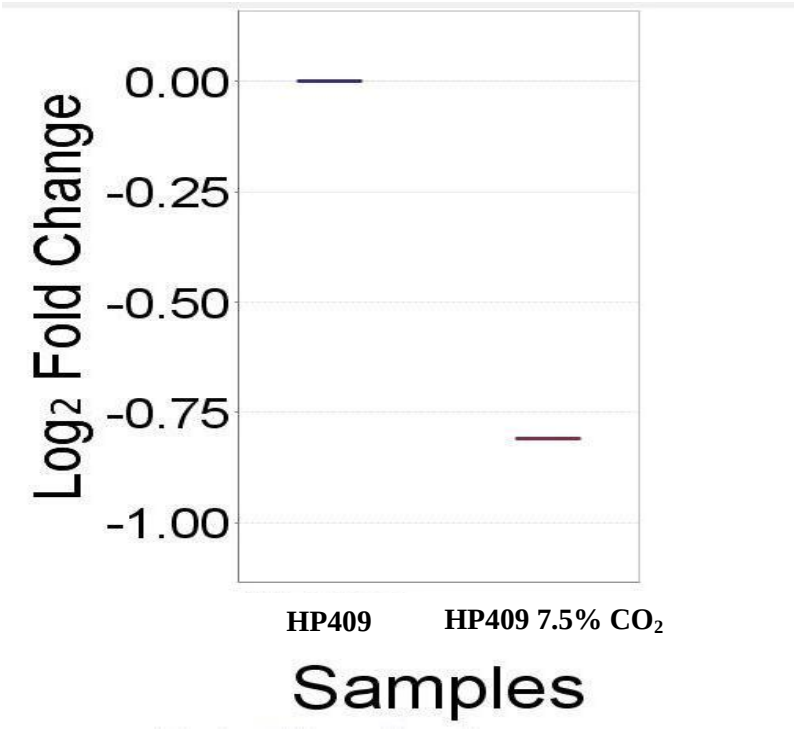

Supplemental Figure 6.35. Protein sequence coverage map (a) and protein expression profile (b) for HP iTRAQ-3 HPS_07840. The median protein expression and standard deviation, calculated as the interquartile range, are presented for each sample in (b).

a)

gi|167855432 (100%) 59,356.0 Da
Heme-binding protein A [Haemophilus parasuis 29755], gi|167853426|gb|EDS24675.1| Heme-binding protein A [Haemophilus parasuis 29755]

```
MKLNTKFSLL  ATTLLVSTVA  QAADKTFINC  VSRSPTGFSP  ALVMDGISYN  ASSQQVYNRL
VEFKRGSTDI  EPALAESWTV  SDDGLTYTFN  LRKGVKFHSN  KEFTPSRDFN  ADDVVFSFQR
QLDPNHPYHN  VSKATYPYFK  AMKFPTLLKS  VEKVDDHTVK  ITLNRQDATF  LASLGMDFIS
IYSAEYADKM  LAAGKPETID  TTPIGTGPFV  FAGYQVDQKS  RYLAHKEYWK  GKADIDRLIF
EIVPDATARY  AKLQAGACDL  IDFPNAADLE  KMKTDPKVNL  LSQEGLNIAY  IAFNTEKAPF
DNVKVRQALN  YAVDKNAIID  AVYRGAGVAA  KNPLPPTIWG  YNNEITGYEY  NPKKAKQLLK
EAGFENGFET  DIWVQPVVRA  SNPNPRRMAE  LVQSDWEKVG  VKSKLVSYEW  GDYIKRTKAG
ELTAGTYGWS  GDNGDPDNFL  SPLFGSENVG  NSNYARFKNP  ELDALLHKAV  GLSDKAERAK
IYEQAQVLLK  EQAPWINVAH  SINFAPTSKR  VQDYKQSPFG  YTYLYGTKLA  D
```

b)

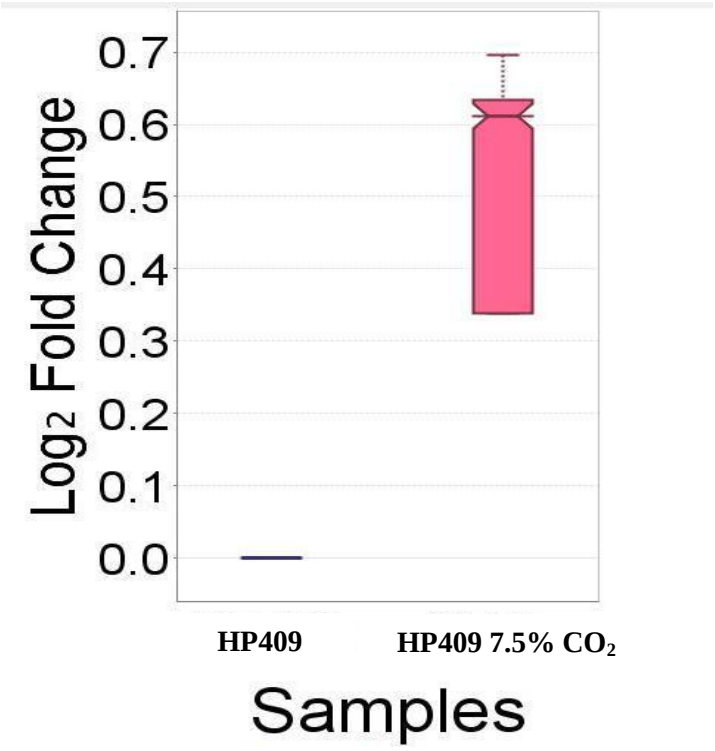

Supplemental Figure 6.36. Protein sequence coverage map (a) and protein expression profile (b) for HP iTRAQ-3 heme-binding protein A. The median protein expression and standard deviation, calculated as the interquartile range, are presented for each sample in (b).

a)

gi|167856581 (100%) 12,391.4 Da
50S ribosomal protein L7/L12 [Haemophilus parasuis 29755], gi|219871555|ref|YP_002475930.1| 50S ribosomal protein L7/L12 [Haemophilus parasuis SH0165], gi|25480637

MSLTNEQIIE AIASKSVSEI VELITAMEEK FGVSAAAAAV AVAAGPAEAA EEKTEFDVIL
ADAGANKVAV IKAVRGATGL GLKEAKDLVE SAPAALKEGI SKGEAEALKK ELEEAGAKVE
IK

b)

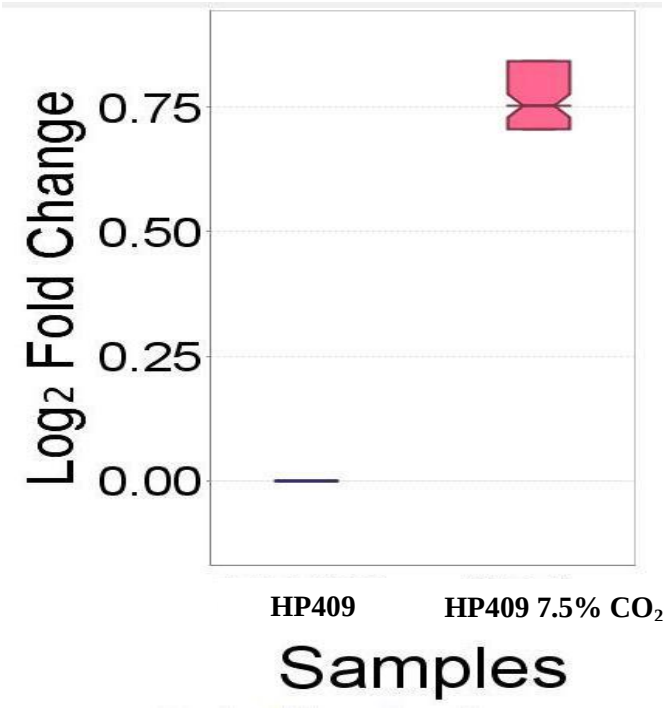

Supplemental Figure S6.37. Protein sequence coverage map (a) and protein expression profile (b) for HP iTRAQ-3 50S ribosomal protein L7/L12. The median protein expression and standard deviation, calculated as the interquartile range, are presented for each sample in (b).

a)

gi|145639805 (67%) 40,783.7 Da
Outer membrane protein P2 precursor [Haemophilus influenzae PittII]. gi|145271173|gb|EDK11088.1| Outer membrane protein P2 precursor [Haemophilus influenzae PittII]

MKKTLAALIV GAFAASAANA AVVYNNEGSK VELGGRLSVI AEQSNTTVDD QKQQHGALRN
QGSRFHIKAT HNFGDGFYAQ GYLETRLVTD ITKNHSDHFG DITTKYAYVT LGNKAFGEVK
LGRAKTIADG ITSAEDKEYG VLDNSKYVRT NGNTVGYTFK GIDGLVLGAN YLLAQERNPT
DFTDPAGEVT PQAISNGVQV GAKYDANNIV AAIAFGRTNY RENSRVTLQS PGKKQQVEGV
LSTLGYRFSD LGLLVSLDSG YAKTKNHTTT TTTSGRSTTP AHYEKRYFVS PGFQYELMED
TNVYGNFKYE RNSVDQGKKT HEQAVLFGVD HKLHKQVLTY IEGAYARTKT NDKGKTEKTG
KEKSVGVGLR VYF

b)

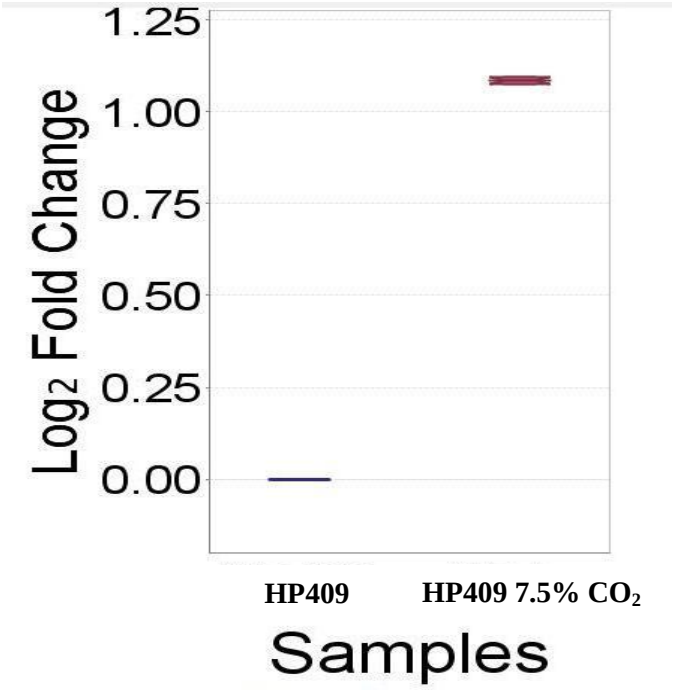

Supplemental Figure S6.38. Protein sequence coverage map (a) and protein expression profile (b) for HP iTRAQ-3 OMP P2. The median protein expression and standard deviation, calculated as the interquartile range, are presented for each sample in (b).

a)

gi|167856491 (77%) 8,972.6 Da
phosphoenolpyruvate-protein phosphotransferase [Haemophilus parasuis 29755], gi|219871159|ref|YP_002475534.1| phosphotransferase system, phosphocarrier protein

MYSKDVTITC PNGLHTRPAA EFVKAAKGFA SDITVTSNGK SASAKSLFKL QTLGLAQGTI
ITLSAEGEDE QKAVDFLVDL IPTLE

b)

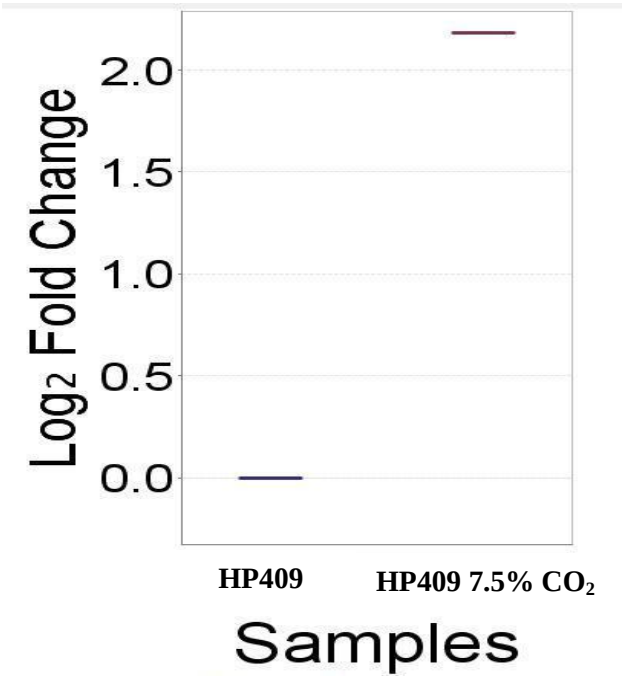

Supplemental Figure S6.39. Protein sequence coverage map (a) and protein expression profile (b) for HP iTRAQ-3 phosphoenolpyruvate phosphotransferase. The median protein expression and standard deviation, calculated as the interquartile range, are presented for each sample in (b).

a)

gi|167854655 (77%) 17,265.7 Da
tRNA pseudouridine synthase C [Haemophilus parasuis 29755], gi|167854192|gb|EDS25426.1| tRNA pseudouridine synthase C [Haemophilus parasuis 29755]

MKKYLITITS LLLPSTMGFA ATADITPEPP MMVLTTIDFS GEVPKSLNST TYSISNKKIQ
LCWEVINVPF TAQNKTTEIF NSPAKSTMRG GQGDNVVSTK DGKMHTITSQ MKSVNNEFIR
RCWKFDNTDP IGDYTLDLQI NDTIFPTQKF KIVK

b)

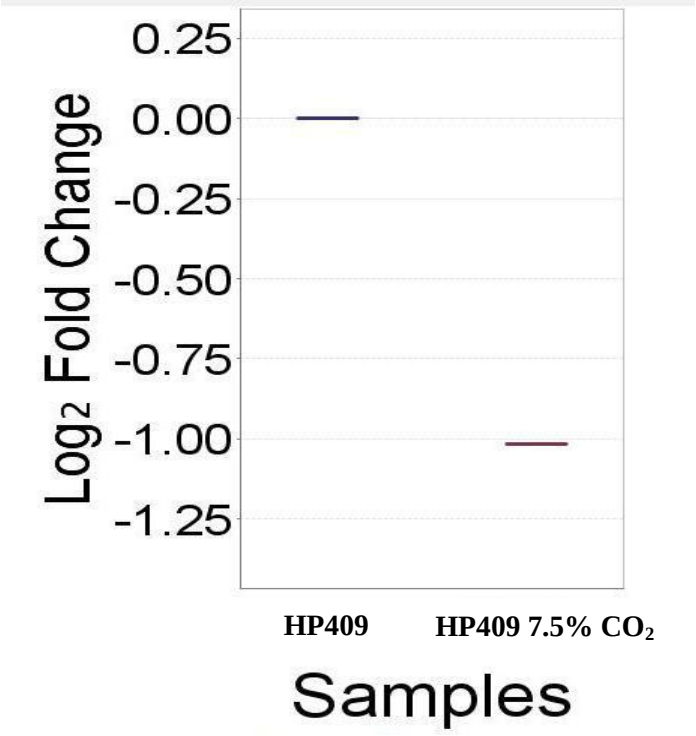

Supplemental Figure S6.40. Protein sequence coverage map (a) and protein expression profile (b) for HP iTRAQ-3 tRNA pseudouridine synthetase C. The median protein expression and standard deviation, calculated as the interquartile range, are presented for each sample in (b).

a)

gi|254360752 (81%) 35,659.0 Da
iron (Fe3+) ABC superfamily ATP binding cassette transporter, binding protein [Mannheimia haemolytica PHL213], gi|153091322|gb|EDN73296.1| iron (Fe3+) ABC superfam

EVNVYSYRQP YLIEPMLKNF EKDTGIKVNI IFADKGLVDR VKQEGELSPA DVLLTVDISR
VMEIVNADLA QKIDSKVLEK NIPAQFRDSN DQWFGLTTRA RVIYTSKDRV GKLPAGFDYL
DLAKPEYKGK VCVRSGKNSY NVSLFAAMIE HYGIEKTKAF LEGLKANLAR KPQGGDRDQV
KAIKEGICDY SIGNSYYYGK MLDDEKQKSW AEAAIINFPS GEHGTHKNIS GVVIAKHSPN
KANAVKLIEY LSGEKAQGLY AELNHEYPVK EGIEPSAIVK GWGTFKSDTI KLEDIAKNYE
AALKLVDEVK FDDFSEKK

b)

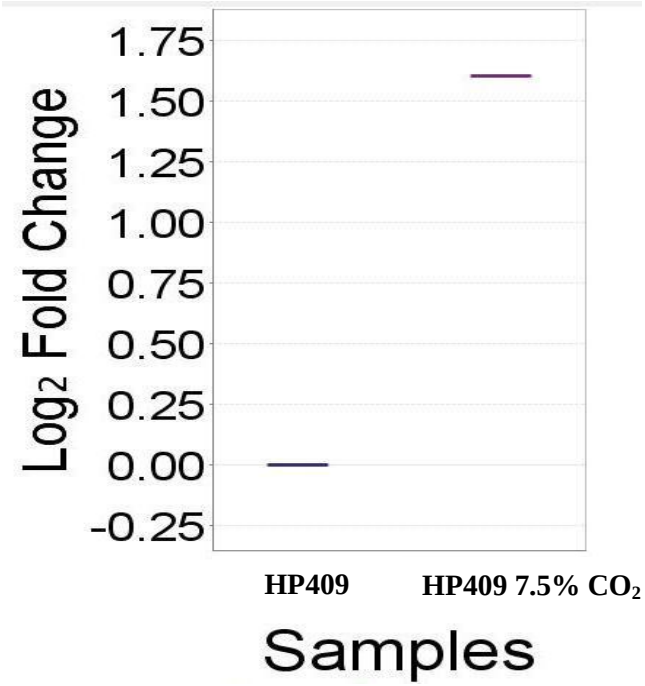

Supplemental Figure S6.41. Protein sequence coverage map (a) and protein expression profile (b) for HP iTRAQ-3 Fe^{3+} binding protein. The median protein expression and standard deviation, calculated as the interquartile range, are presented for each sample in (b).

a)

gi|167855391 (100%) 57,888.3 Da
ABC transporter, periplasmic binding protein [Haemophilus parasuis 29755], gi|167853457|gb|EDS24705.1| ABC transporter, periplasmic binding protein [Haemophilus p

MTKHFEHNES RRGFMKLVAG VGAGLAFSGS IGTFASQAYA APAKGSTIEA GIAYPISTGF
DPMSSTGASS MAANIHIFEG LVDLHPATRQ PYLALAAKEP EKVDDVTYRI TLRDGAVFHN
GSAVTSADVV FSFERVLDPN TKSLFAQFIP FIKSVTAVDQ KTVEFKLKYP FALFKERLTI
IKIVPKALIE AQGQSVFDAN PVGTGPYKFV SAVKDDRIVF EANPAYTGPY PATVEKMTWF
LLSDDAARVA AQESGRVQAI ENVPYLDADR LKRKAAVESV QSFGLIFLMF NCEKAPFNNK
KVRQALQYAI DTQKLVDVVF LGNAKPATSY VQDSHPDYVK ASTVYDFDPK KAAALLKEAG
VDKLEFTTRS TAHKWVVDSV QMILEDWNKI PGVKVTNIAS QSPYNDGVDA GNFEVLIAPG
DPSVFGNDLD LLLSWWYRGD VWPKKRFRWS NTPEYAEVQK LLDAAVAAKT PAEAREIWGK
AINIIAEEAA LYPIIHRKLP TAWSNKALDG FKPLSTTGMS FIGVSRK

b)

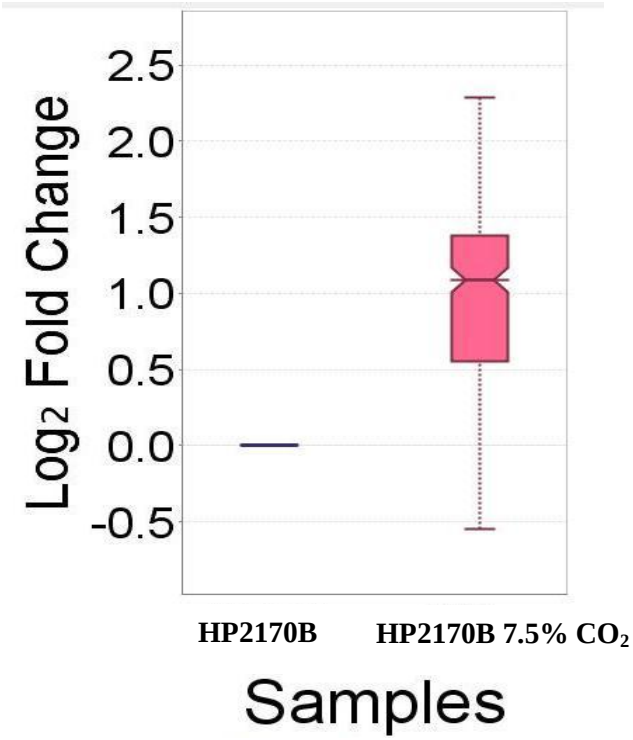

Supplemental Figure S6.42. Protein sequence coverage map (a) and protein expression profile (b) for HP iTRAQ-3 ABC transporter. The median protein expression and standard deviation, calculated as the interquartile range, are presented for each sample in (b).

a)

gi|167855124 (100%) 60,868.0 Da
hypothetical protein HPS_06844 [Haemophilus parasuis 29755], gi|167853759|gb|EDS25001.1| hypothetical protein HPS_06844 [Haemophilus parasuis 29755]

```
MKFNKTPLAL  ALMGATTAMA  YEADKTYRFT  VLHVNDTHGH  FWKNDKGEYG  FAAQKTLIDK
IRKEVAEKGG  EVVLLHAGDF  NTGVPESDMQ  NARPDIEGLN  MLGFDVAVLG  NHEFDFPLQV
LDMQEKWAKF  PFISANVINK  KTNKHLVKPY  VTLNKGGLKF  AVIGLTTEDT  AKLGNPDVTE
NVVFNDPIKT  AKETLAQVKK  TEKPDVSIAL  THMGYYFDEQ  HGMNAPGDVS  LARGLDKGAF
DLIIGGHTHD  TVCVDEKGVF  KLKYTPGEEC  KPDFQNGTWI  VQAGEWGKFL  GRADFEFKNG
ETKLVKYELI  PVNLKQKIKL  ADGKSEYKLY  QEEIPEDKAV  FEHLKKYQDE  GDKLLGVKVG
EVKGGILEGD  RKVIRFHQTN  LGRLIAQSQM  ERVKADIGIM  NSGAIRASIN  EGEVTYKNLL
TVQPFGNMIA  TVDLTGKELI  DYLNVVALKE  VDMGAYPQFA  GVSMVVDRTA  KQVSDVKVGG
KPLDLNKTYK  VSVPDYCAAG  GDGYPILKKH  PSYVNTGFID  AEMLKKYFEE  NSPIDASKYD
PKDDVIFK
```

b)

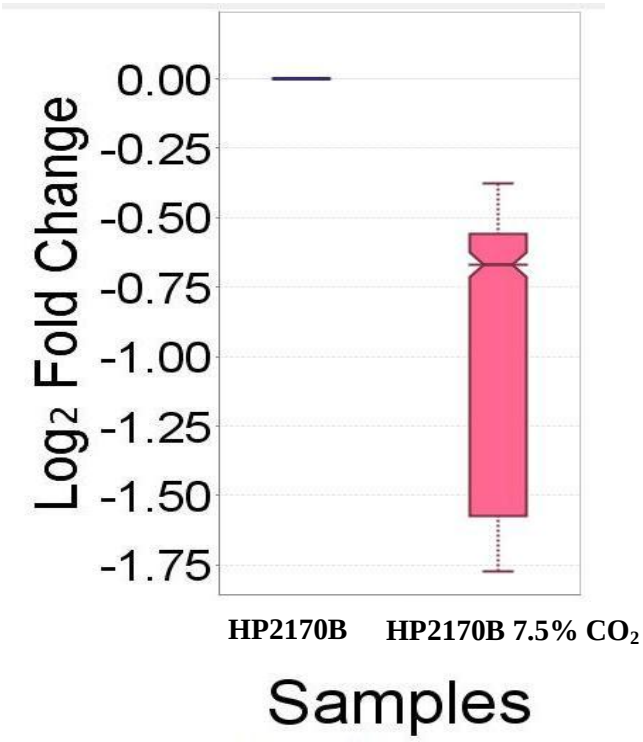

Supplemental Figure S6.43. Protein sequence coverage map (a) and protein expression profile (b) for HP iTRAQ-3 HPS_06844. The median protein expression and standard deviation, calculated as the interquartile range, are presented for each sample in (b).

a)

gi|167855966 (77%) 17,140.5 Da
hypothetical protein HPS_07840 [Haemophilus parasuis 29755]. gi|167852903|gb|EDS24170.1| hypothetical protein HPS_07840 [Haemophilus parasuis 29755]

MYIQAFSLLG ANPVPMPLSE LYTALETRAV DAQEHPIGIF WSAKLYEVQK HLSLTNHGYT
PLIVVMNKAK FDSFSPELQQ AILDAAKEAG NYQRQLNLEN EKEIIAKLQK AGIQVIEEVD
NKPFKAIIEA DVRKAFIEKN GSELVEKIDG LAK

b)

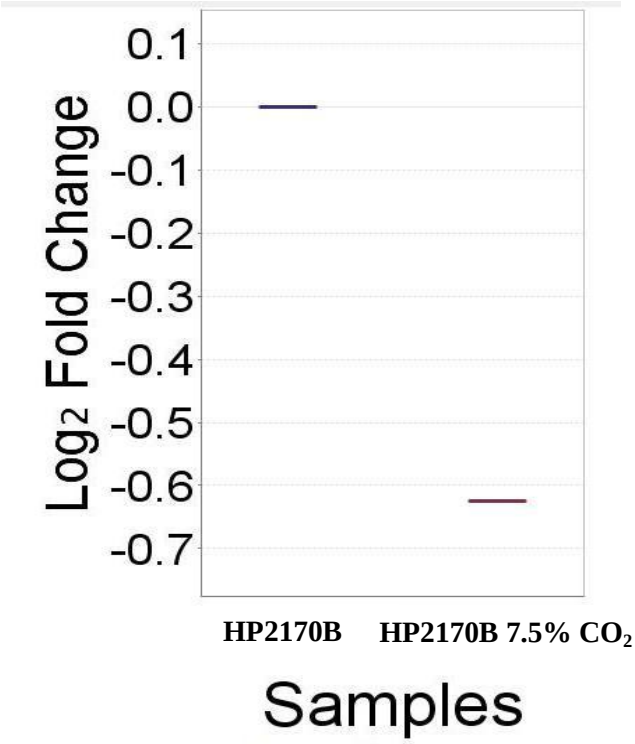

Supplemental Figure S6.44. Protein sequence coverage map (a) and protein expression profile (b) for HP iTRAQ-3 HPS_07840. The median protein expression and standard deviation, calculated as the interquartile range, are presented for each sample in (b).

a)

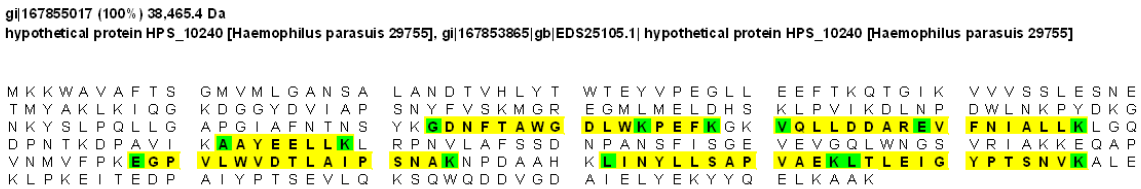

b)

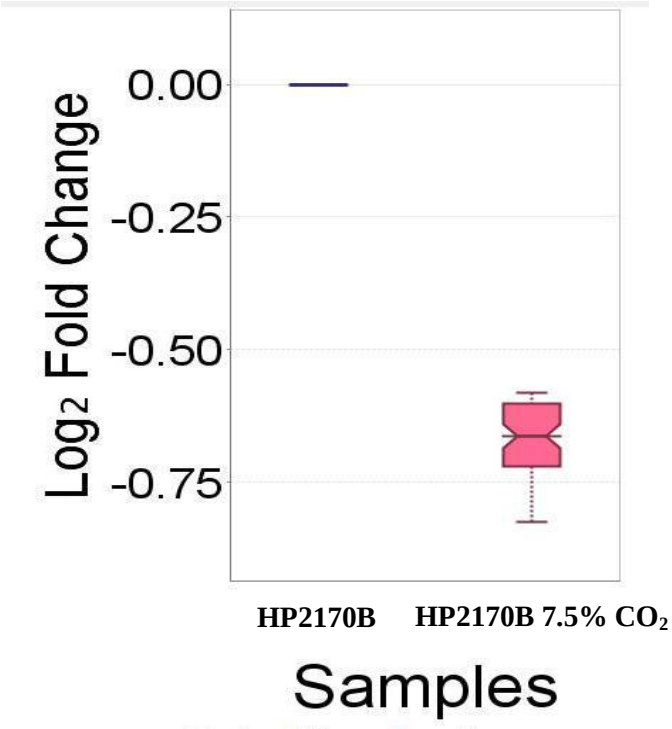

Supplemental Figure S6.45. Protein sequence coverage map (a) and protein expression profile (b) for HP iTRAQ-3 HPS_10240. The median protein expression and standard deviation, calculated as the interquartile range, are presented for each sample in (b).

a)

gi|167854835 (77%) 29,764.5 Da
alanine aminotransferase [Haemophilus parasuis 29755]. gi|219871433|ref|YP_002475808.1| outer membrane protein 26 [Haemophilus parasuis SH0165]. gi|167854014|gb|E

MKNLFKLAAV ASALAFSANT VNANEKIGFV DPNFLIQNHP LTIEANDKFT KFMKDTESKF
APREKQLAAE NKALSDEEKA LLDERKKIEE DAQKLQKEQV TLEAAMKKKV AQLEKDAPRL
KAKEIQARQD KINAEAKPFQ NKVSALQQRE VEFGKKAEEF QKRADEFQKK VAAFQEEIAK
VQKESGVITP EQVQQKVVED INAKIKQVAE SKGYTLVLPP SVALYAKDGN AADITEEILV
AMGGKMPEAP KTEVPAAEVT KPEEVKK

b)

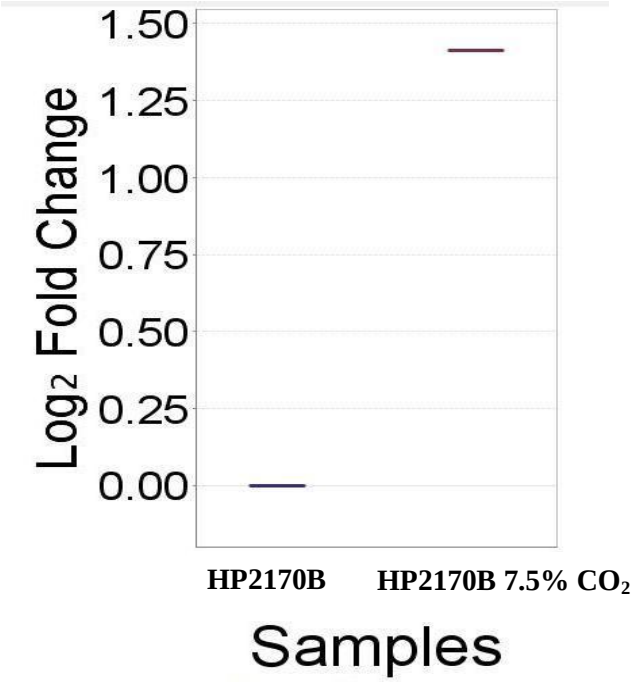

Supplemental Figure S6.46. Protein sequence coverage map (a) and protein expression profile (b) for HP iTRAQ-3 alanine aminotransferase. The median protein expression and standard deviation, calculated as the interquartile range, are presented for each sample in (b).

a)

gi|238022303 (66%) 64,969.4 Da
hypothetical protein GCWU000324_02210 [Kingella oralis ATCC 51147], gi|237866917|gb|EEP67959.1| hypothetical protein GCWU000324_02210 [Kingella oralis ATCC 511

MLIHNEFKPY MAKKEETKRQ VVEGNKRLSW LMLAIGGAFC VLVGHSFRVQ AQHHSELSKF
SENRVVRSIK SPALRGTITD RNGAILAVSR YLKVATFNPK AIYAPKRQGD EINWNAISNE
QFAKLAAILR LPENEVRRKL QERSSQYVQF KTELSLEEAD ALKALNIPSL RFEERTERAY
PTGNLFSHIV GFANDKGEGL EGLERVANQR LTGEDGRQVV LRDRHNNIVE LIDSPENAAA
KSGETLVLSV DQDLQQLAHD QLAATLKNFN AKAGGVVVLD AQTGEILAMT SLPDYDANYY
QEYPATSLRN FAVSETMEPG SVMKPFIIAK ALDDGKIGRN STFNTRPYAI GDKTIRDTHD
YPSLTTQGIL QKSSNVGTSH IAALYDNQSL YQHFSDVGFG RKTGSGVSGE QNKAIKPADK
WSKLDRAVMS YGYAITANLL QMAQGYTIFT AGGKLMPATI YKQTQTPKGT QVIKPETAKQ
MREMMVSITR KGGTGQDGAV PGYDVAAKTG TARKASAGGY ADKYRASFVG FAPAQNPRLI
VAVSIDEPRG KGYYGGTVAG PAFREIMAGG LKKLGVKPTY VNTEPAANVA KKR

b)

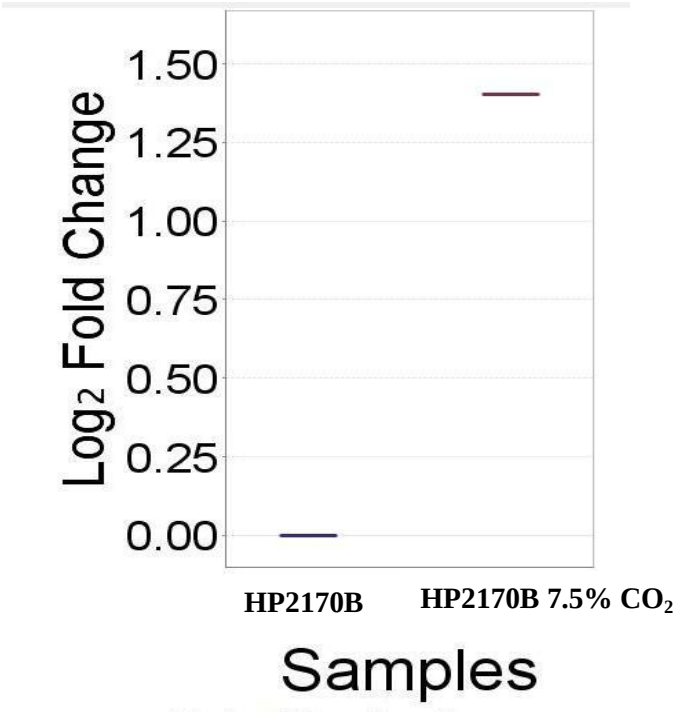

Supplemental Figure S6.47. Protein sequence coverage map (a) and protein expression profile (b) for HP iTRAQ-3 hypothetical protein GCW000324. The median protein expression and standard deviation, calculated as the interquartile range, are presented for each sample in (b).

a)

gi|167855432 (100%) 59,356.0 Da
Heme-binding protein A [Haemophilus parasuis 29755], gi|167853426|gb|EDS24675.1| Heme-binding protein A [Haemophilus parasuis 29755]

MKLNTKFSLL ATTLLVSTVA QAADKTFINC VSRSPTGFSP ALVMDGISYN ASSQQVYNRL
VEFKRGSTDI EPALAESWTV SDDGLTYTFN LRKGVKFHSN KEFTPSRDFN ADDVVFSFQR
QLDPNHPYHN VSKATYPYFK AMKFPTLLKS VEKVDDHTVK ITLNRQDATF LASLGMDFIS
IYSAEYADKM LAAGKPETID TTPIGTGPFV FAGYQVDQKS RYLAHKEYWK GKADIDRLIF
EIVPDATARY AKLQAGACDL IDFPNAADLE KMKTDPKVNL LSQEGLNIAY IAFNTEKAPF
DNVKVRQALN YAVDKNAIID AVYRGAGVAA KNPLPPTIWG YNNEITGYEY NPKKAKQLLK
EAGFENGFET DIWVQPVVRA SNPNPRRMAE LVQSDWEKVG VKSKLVSYEW GDYIKRTKAG
ELTAGTYGWS GDNGDPDNFL SPLFGSENVG NSNYARFKNP ELDALLHKAV GLSDKAERAK
IYEQAQVLLK EQAPWINVAH SINFAPTSKR VQDYKQSPFG YTYLYGTKLA D

b)

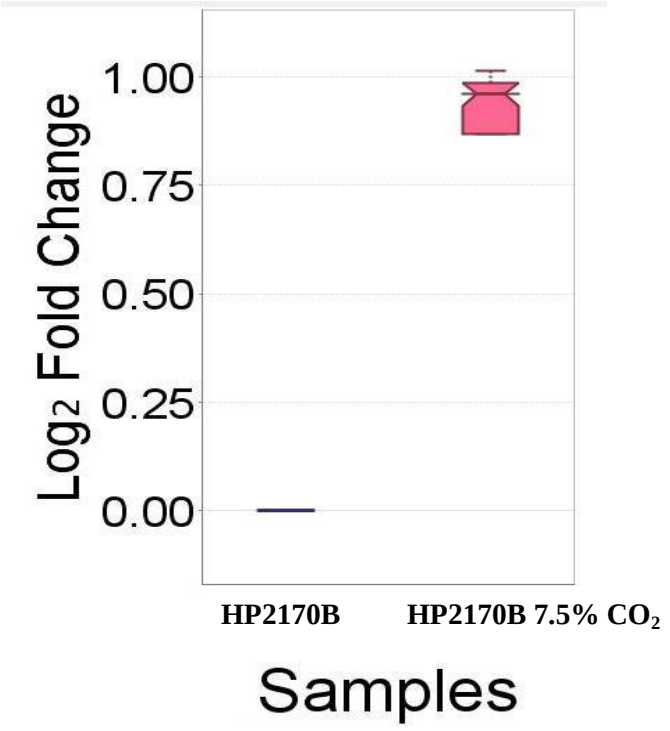

Supplemental Figure S6.48. Protein sequence coverage map (a) and protein expression profile (b) for HP iTRAQ-3 heme-binding protein A. The median protein expression and standard deviation, calculated as the interquartile range, are presented for each sample in (b).

a)

gi|167855819 (100%) 9,459.4 Da
DNA-binding protein HU [Haemophilus parasuis 29755], gi|219871002|ref|YP_002475377.1| DNA-binding protein HU/transcriptional regulator [Haemophilus parasuis SH0165

MNKTELVDAI AAGADLSKKD AKAALEATLN AISESLKKGD SVQLIGFGTF KVNHRKARTG
RNPKTNEAIE IPAANVPAFV AGKALKDLVK

b)

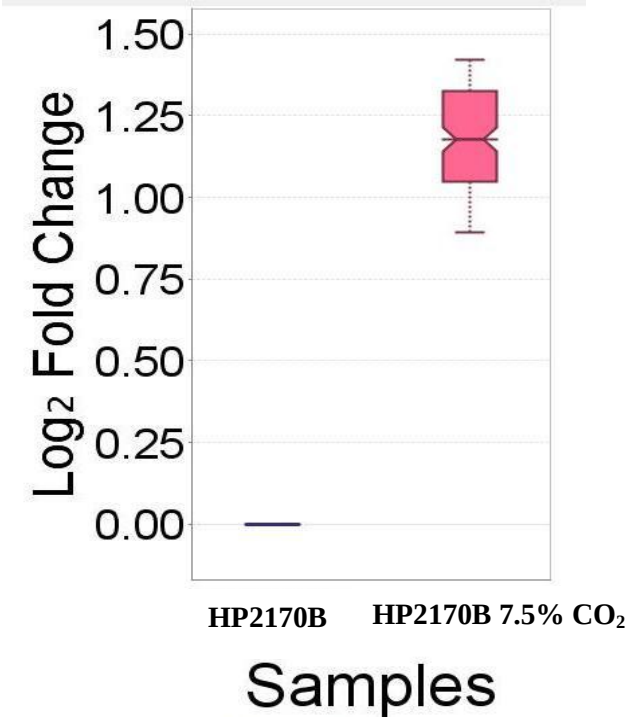

Supplemental Figure S6.49. Protein sequence coverage map (a) and protein expression profile (b) for HP iTRAQ-3 DNA binding protein HU. The median protein expression and standard deviation, calculated as the interquartile range, are presented for each sample in (b).

a)

gi|167854980 (77%) 38,330.2 Da
50S ribosomal protein L13 [Haemophilus parasuis 29755]. gi|167853937|gb|EDS25176.1| 50S ribosomal protein L13 [Haemophilus parasuis 29755]

MKKLQLKKWF SSLFLLSPLV FAASNAQAEG KLTVYCGVQN KVCEDLTKRF SQKYNVETQF
IHGGTGTILG KLKAEKDNPQ ADIWYGGTIE PHFQAGQMGL LEAYRSPLQA EVLPQFKALQ
ESEAGKYTSI AYLMVLGFGI NTEKLKQLGV DAPKKWADLL DPRLKGEVQL ADPRTSGTMY
TTMITLIQLM GEEKAFEYLK KLDGNISQYV KSTLVTSNLS RGESAVTVGF AHGYASEKEK
GAPVDYVLPK DGVGYALGAA SIIKGARNLD NAKLFMDWVL SKEVQEIPWR DHGLYQTPTN
VKAEVAPQSP KIDGVKLVDV DYARFGSSEE GKRLVDKWLF NIKLSN

b)

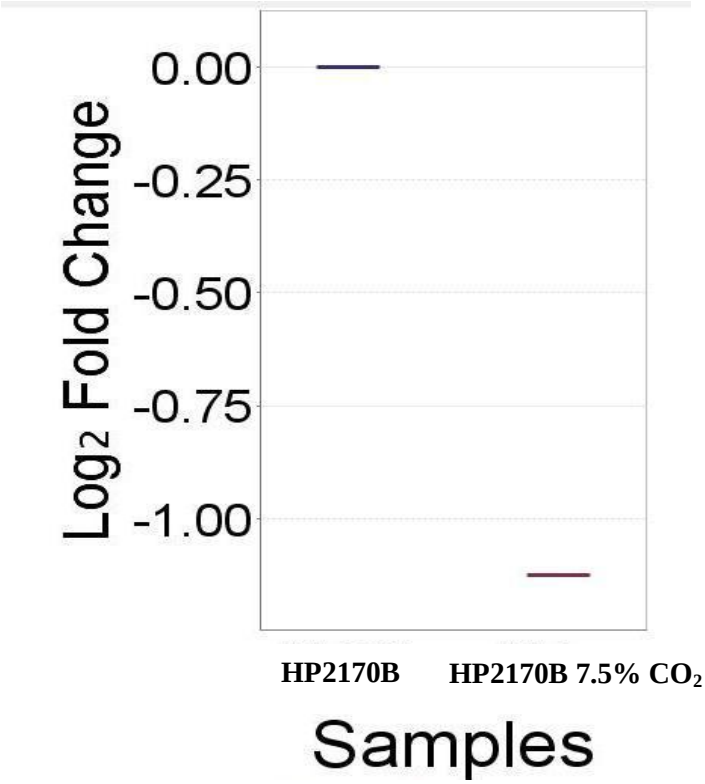

Supplemental Figure S6.50. Protein sequence coverage map (a) and protein expression profile (b) for HP iTRAQ-3 Fe^{3+} ABC transporter (similar to 50S ribosomal protein L13). The median protein expression and standard deviation, calculated as the interquartile range, are presented for each sample in (b).

a)

gi|145639805 (67%) 40,783.7 Da
Outer membrane protein P2 precursor [Haemophilus influenzae PittII]. gi|145271173|gb|EDK11088.1| Outer membrane protein P2 precursor [Haemophilus influenzae PittII]

MKKTLAALIV GAFAASAANA AVVYNNEGSK VELGGRLSVI AEQSNTTVDD QKQQHGALRN
QGSRFHIKAT HNFGDGFYAQ GYLETRLVTD ITKNHSDHFG DITTKYAYVT LGNKAFGEVK
LGRAKTIADG ITSAEDKEYG VLDNSKYVRT NGNTVGYTFK GIDGLVLGAN YLLAQERNPT
DFTDPAGEVT PQAISNGVQV GAKYDANNIV AAIAFGRTNY RENSRVTLQS PGKKQQVEGV
LSTLGYRFSD LGLLVSLDSG YAKTKNHTTT TTTSGRSTTP AHYEKRYFVS PGFQYELMED
TNVYGNFKYE RNSVDQGKKT HEQAVLFGVD HKLHKQVLTY IEGAYARTKT NDKGKTEKTG
KEKSVGVGLR VYF

b)

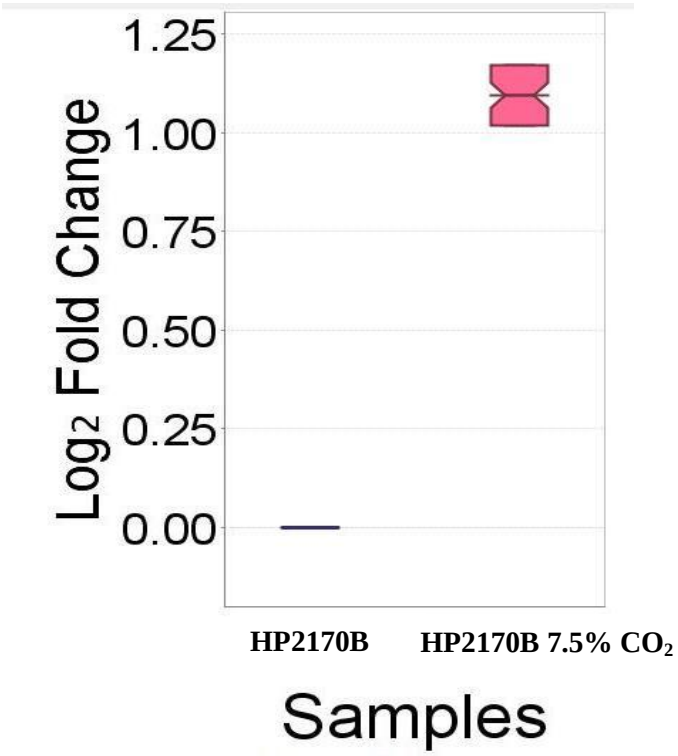

Supplemental Figure S6.51. Protein sequence coverage map (a) and protein expression profile (b) for HP iTRAQ-3 OMP P2. The median protein expression and standard deviation, calculated as the interquartile range, are presented for each sample in (b).

a)

gi|167856491 (77%) 8,972.6 Da
phosphoenolpyruvate-protein phosphotransferase [Haemophilus parasuis 29755], gi|219871159|ref|YP_002475534.1| phosphotransferase system, phosphocarrier protein

MYSKDVTITC PNGLHTRPAA EFVKAAKGFA SDITVTSNGK SASAKSLFKL QTLGLAQGTI
ITLSAEGEDE QKAVDFLVDL IPTLE

b)

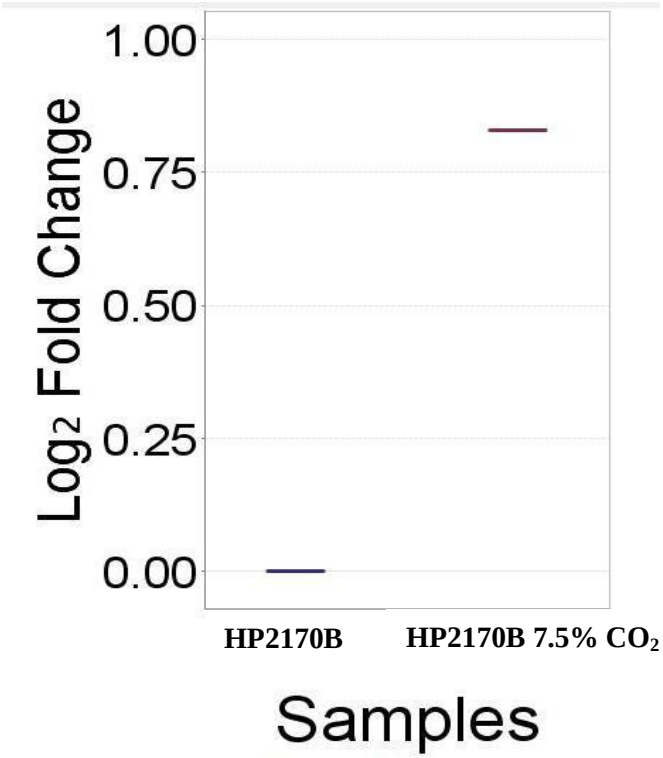

Supplemental Figure S6.52. Protein sequence coverage map (a) and protein expression profile (b) for HP iTRAQ-3 phosphoenolpyruvate phosphotransferase. The median protein expression and standard deviation, calculated as the interquartile range, are presented for each sample in (b).

a)

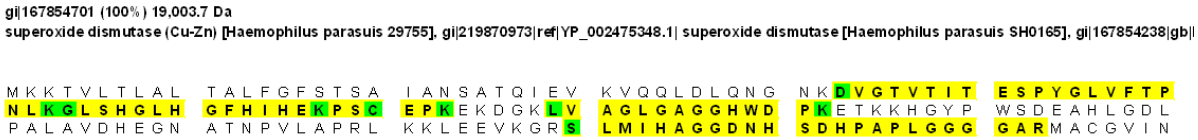

b)

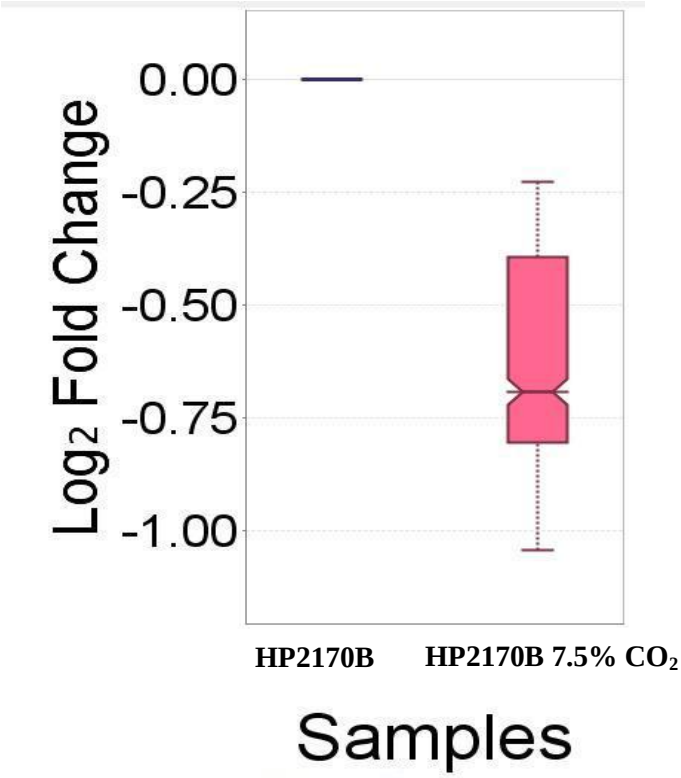

Supplemental Figure S6.53. Protein sequence coverage map (a) and protein expression profile (b) for HP iTRAQ-3 SOD (Cu-Zn). The median protein expression and standard deviation, calculated as the interquartile range, are presented for each sample in (b).

a)

gi|113460350 (89%) 35,163.9 Da
transaldolase B [Haemophilus somnus 129PT], gi|122945177|sp|Q0I1U0.1|TAL_HAES1 RecName: Full=Transaldolase, gi|112822393|gb|ABI24482.1| transaldolase [Haemoph

MTTQLDALRN MTVVVADTGD IDAIKKYQPQ DATTNPSLIL SASSLPQYAP LIDEAIAYAK
AKSADKTQQL IDAEDKLAVN IGLEILKIVP GRISTEVDAR LSYDTQATVE KARKLIALYN
EAGISNDRIL IKIASTWQGI RAAEILEKEG INCNLTLLFS EAQARACAEA GVYLISPFVG
RILDWYKANS DKKEYAPAED PGVISVTKIY NYYKQYGYNT VVMGASFRNV GEITELAGCD
RLTIAPALLK ELQENSTALV RKLEFKGEVQ AKPQPLTESQ FYWQHNSDPM AVEKLADGIR
KFAIDQEKLE KMLLEKF

b)

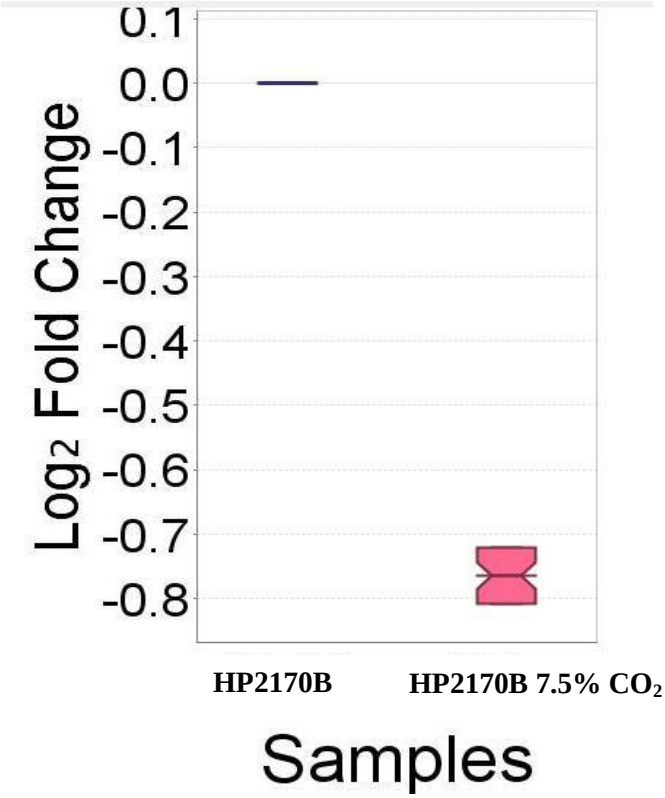

Supplemental Figure S6.54. Protein sequence coverage map (a) and protein expression profile (b) for HP iTRAQ-3 transaldolase B. The median protein expression and standard deviation, calculated as the interquartile range, are presented for each sample in (b).

a)

gi|167854655 (77%) 17,265.7 Da
tRNA pseudouridine synthase C [Haemophilus parasuis 29755], gi|167854192|gb|EDS25426.1| tRNA pseudouridine synthase C [Haemophilus parasuis 29755]

MKKYLITITS LLLPSTMGFA ATADITPEPP MMVLTTIDFS GEVPKSLNST TYSISNKKIQ
LCWEVINVPF TAQNKTTEIF NSPAKSTMRG GQGDNVVSTK DGKMHTITSQ MKSVNNEFIR
RCWKFDNTDP IGDYTLDLQI NDTIFPTQKF KIVK

b)

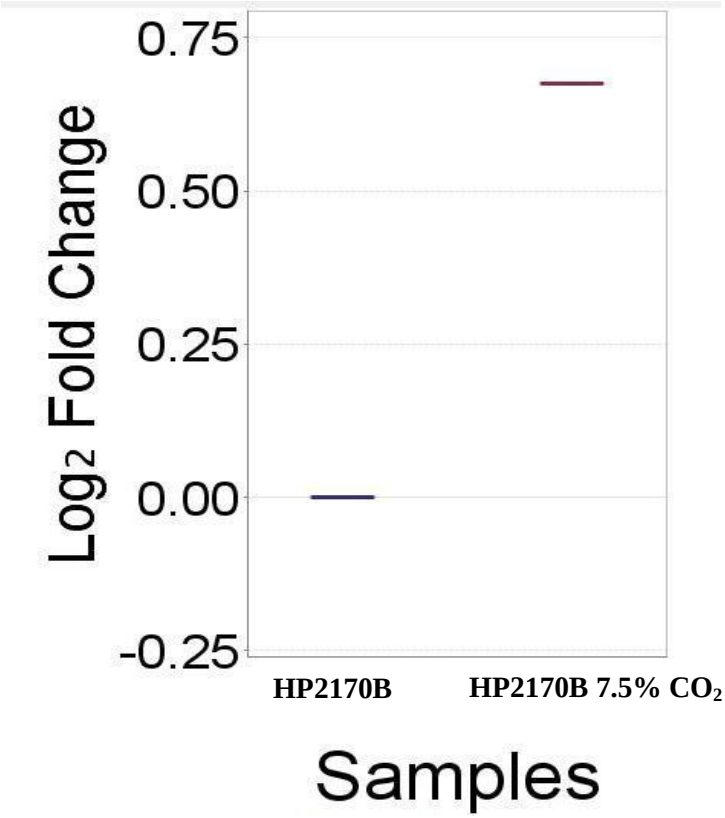

Supplemental Figure S6.55. Protein sequence coverage map (a) and protein expression profile (b) for HP iTRAQ-3 tRNA pseudouridine synthetase C. The median protein expression and standard deviation, calculated as the interquartile range, are presented for each sample in (b).

a)

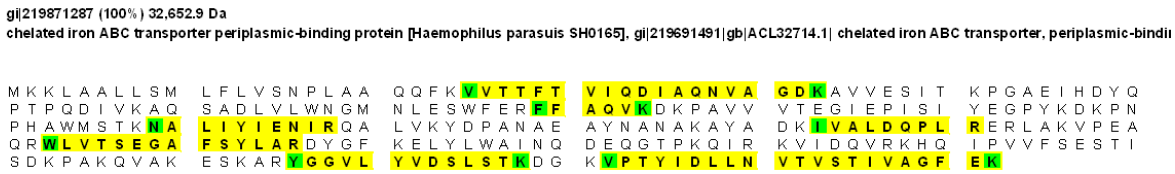

b)

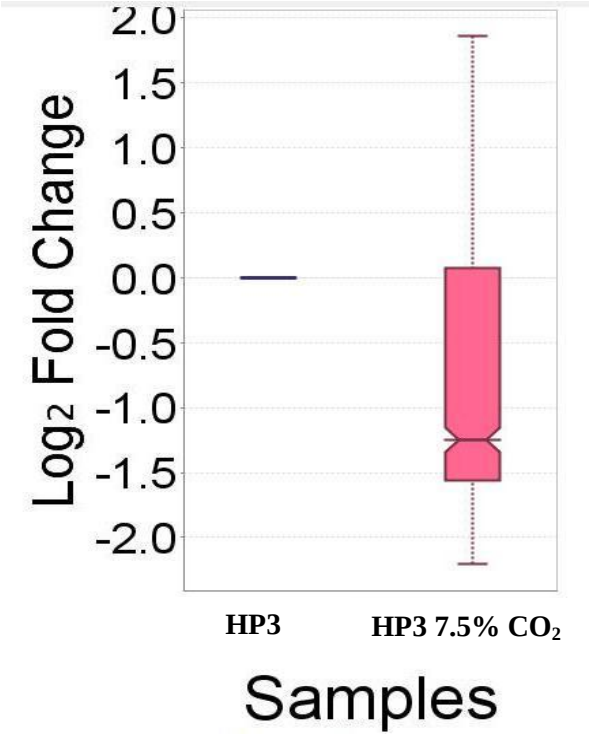

Supplemental Figure S6.56. Protein sequence coverage map (a) and protein expression profile (b) for HP iTRAQ-4 chelated iron transporter. The median protein expression and standard deviation, calculated as the interquartile range, are presented for each sample in (b).

a)

gi|167856064 (89%) 8,497.5 Da
acyl carrier protein [Haemophilus parasuis 29755], gi|219871798|ref|YP_002476173.1| acyl carrier protein [Haemophilus parasuis SH0165], gi|254802114|sp|B8F7C3.1|ACP

M S I E E R V K K I I V D Q L G A K A E D V K P E T S F I E D L G A D S L D T V E L V M A L E E E F D I E I P D E E A E
K I A T V Q S A I D Y V Q N N Q

b)

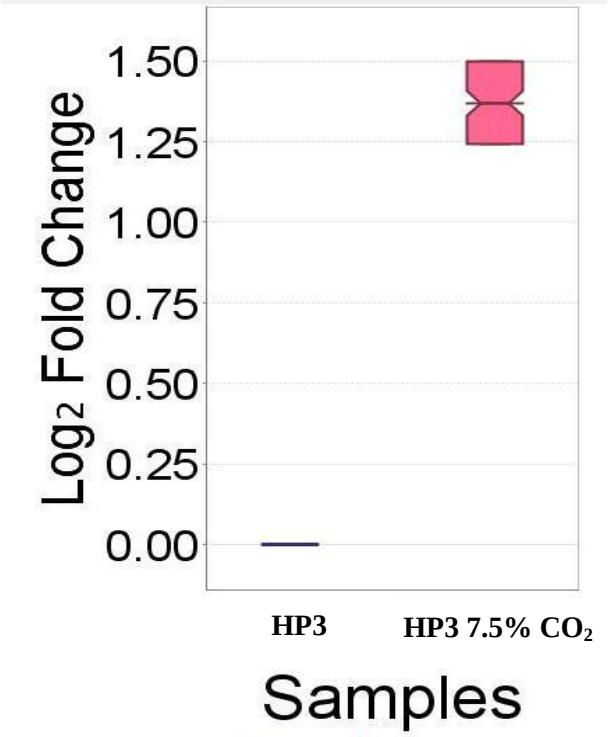

Supplemental Figure S6.57. Protein sequence coverage map (a) and protein expression profile (b) for HP iTRAQ-4 acyl carrier protein. The median protein expression and standard deviation, calculated as the interquartile range, are presented for each sample in (b).

a)

gi|145639805 (89%) 40.783.7 Da
Outer membrane protein P2 precursor [Haemophilus influenzae PittII]. gi|145271173|gb|EDK11088.1| Outer membrane protein P2 precursor [Haemophilus influenzae PittII]

MKKTLAALIV GAFAASAANA AVVYNNEGSK VELGGRLSVI AEQSNTTVDD QKQQHGALRN
QGSRFHIKAT HNFGDGFYAQ GYLETRLVTD ITKNHSDHFG DITTKYAYVT LGNKAFGEVK
LGRAKTIADG ITSAEDKEYG VLDNSKYVRT NGNTVGYTFK GIDGLVLGAN YLLAQERNPT
DFTDPAGEVT PQAISNGVQV GAKYDANNIV AAIAFGRTNY RENSRVTLQS PGKKQQVEGV
LSTLGYRFSD LGLLVSLDSG YAKTKNHTTT TTTSGRSTTP AHYEKRYFVS PGFQYELMED
TNVYGNFKYE RNSVDQGKKT HEQAVLFGVD HKLHKQVLTY IEGAYARTKT NDKGKTEKTG
KEKSVGVGLR VYF

b)

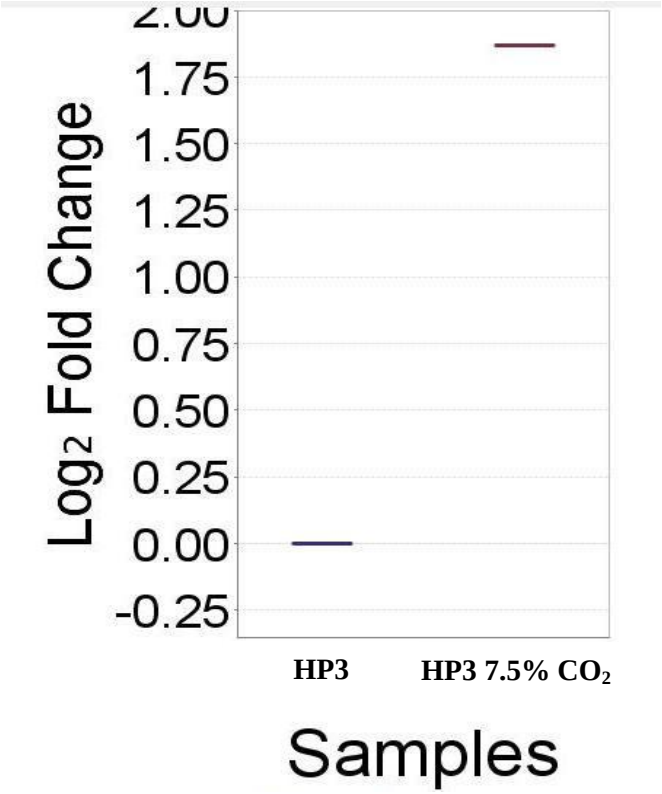

Supplemental Figure S6.58. Protein sequence coverage map (a) and protein expression profile (b) for HP iTRAQ-4 OMP P2. The median protein expression and standard deviation, calculated as the interquartile range, are presented for each sample in (b).

a)

gi|167856489 (89%) 18,036.7 Da
glucose-specific PTS system enzyme IIA component [Haemophilus parasuis 29755], gi|219871157|ref|YP_002475532.1| PTS system glucose-specific transporter subunit

MGFFDKLFGG KKEAVAKEVK IYAPLSGEIV NIEDVPDVVF SEKIVGDGIA IRPTGDMIVA
PVNGTIGKIF ETNHAFSIES EDGVELFVHF GIDTVELKGE GFTRLAEENQ EVKVGDPIIK
FDLELLQSKA KSVLTPVVIS NMDEVTNLQK LSGEVVAGES TVLVLTK

b)

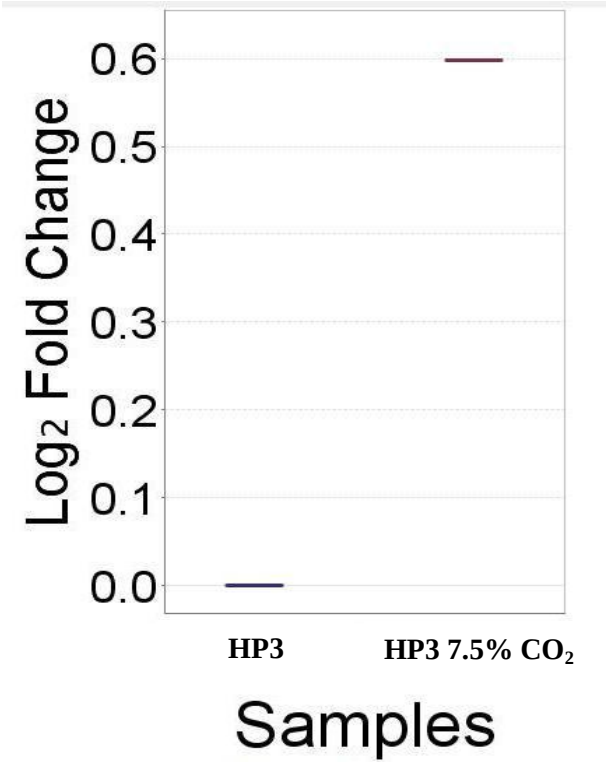

Supplemental Figure S6.59. Protein sequence coverage map (a) and protein expression profile (b) for HP iTRAQ-4 glucose-specific PTS enzyme IIA. The median protein expression and standard deviation, calculated as the interquartile range, are presented for each sample in (b).

a)

gi|167855819 (89%) 9,459.4 Da
DNA-binding protein HU [Haemophilus parasuis 29755], gi|219871002|ref|YP_002475377.1| DNA-binding protein HU/transcriptional regulator [Haemophilus parasuis SH0

MNKTELVDAI AAGADLSKKD AKAALEATLN AISESLKKGD SVQLIGFGTF KVNHRKARTG
RNPKTNEAIE IPAANVPAFV AGKALKDLVK

b)

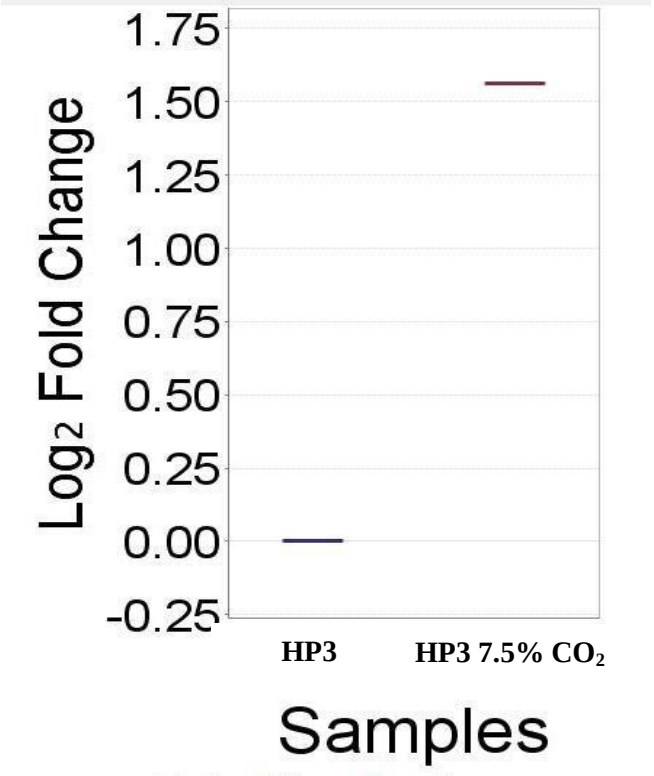

Supplemental Figure S6.60. Protein sequence coverage map (a) and protein expression profile (b) for HP iTRAQ-4 DNA binding protein HU. The median protein expression and standard deviation, calculated as the interquartile range, are presented for each sample in (b).

a)

gi|167856581 (89%) 12,391.4 Da
50S ribosomal protein L7/L12 [Haemophilus parasuis 29755], gi|219871555|ref|YP_002475930.1| 50S ribosomal protein L7/L12 [Haemophilus parasuis SH0165], gi|25480637

MSLTNEQIIE AIASKSVSEI VELITAMEEK FGVSAAAAAV AVAAGPAEAA EEKTEFDVIL
ADAGANKVAV IKAVRGATGL GLKEAKDLVE SAPAALKEGI SKGEAEALKK ELEEAGAKVE
IK

b)

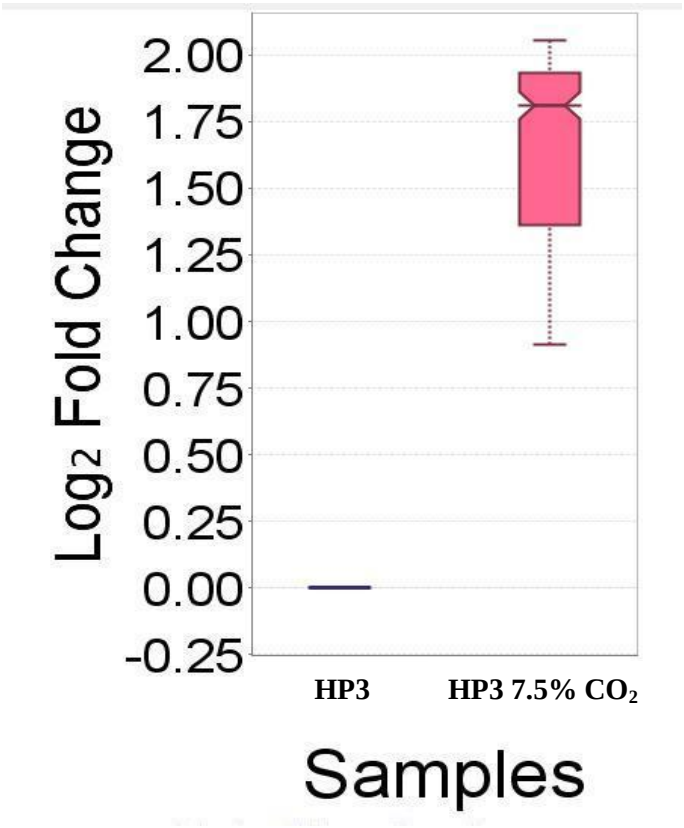

Supplemental Figure S6.61. Protein sequence coverage map (a) and protein expression profile (b) for HP iTRAQ-4 50S ribosomal protein L7/L12. The median protein expression and standard deviation, calculated as the interquartile range, are presented for each sample in (b).

a)

gi|254361285 (95%) 60,979.4 Da
UDP-sugar diphosphatase [Mannheimia haemolytica PHL213], gi|153092781|gb|EDN73824.1| UDP-sugar diphosphatase [Mannheimia haemolytica PHL213]

MRLKKTLLSV ALLSATSAMA YETGKTYRFT VLHTNDIHGH FWQSDKGEYG LAAQKTLVDN
IRKEVAEKGG SVLMLNAGDA NTGVPESDMQ NARPDIEGMN AIGYDAMVLG NHEFDYPLQI
LSMQEKWAKF PFISANVINK KTDKPIVKPY VMLERGGLKI AVIGLTTEDT AKLGNPDVTE
NAFFKNPIET AKNTLAEINQ KEKPDVRIAL THMGYYFDGK HGTNAPGDVT MARTLEKGAF
DLIIGGHTHD TVCIDEKGQF KAKYTPGEEC KPDFQNGTWI VQAGEWGKFV GRADFEFKDG
KATLVKYELI PVNLKKTIKK EDGTKEYRLY QPEIKADEAT YTLLKKYQDE GDKKLNIEVG
RVKGLLDGKR EHIRFQQTNL GRLIAQSQME RVKADIGIMN SGGIRTSLEE GVITYKHILT
VQPFGNMIAT VDLKGQELLD TLTTIALKEV DTGAYPQFAG ISMVVDRTAK TISDVKIGGK
PFDKEKTYKV SLPDYVAAGG DGYPLLKKHP SYVNTGFIDA EMLKKFFEEN KIIEADKYDP
KNQIIFK

b)

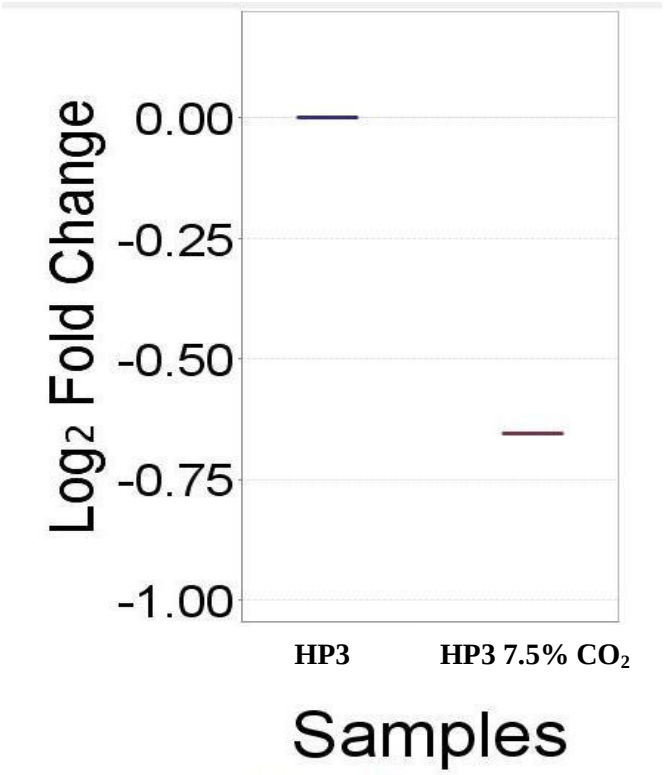

Supplemental Figure S6.62. Protein sequence coverage map (a) and protein expression profile (b) for HP iTRAQ-4 UDP-sugar diphosphatase. The median protein expression and standard deviation, calculated as the interquartile range, are presented for each sample in (b).

a)

gi|117618162 (89%) 29,992.7 Da
D-ribose transporter subunit RbsB [Aeromonas hydrophila subsp. hydrophila ATCC 7966]; gi|117559569|gb|ABK36517.1| ribose ABC transporter, periplasmic ribose-bindin

MKKLNTLLAA AIMSVLGTAQ AADHTLAMVV STLNNPFFVT MKEGAEAKAK ELGYELVVLD
SQNDPAKELS NMEDLTVRKV NAILINPTDS EAVGNAIRLA NKANIPVLTL DRGAAQGDVK
AHIASDNVAG GKLAGDFITQ KLGAGAKVIQ LEGIAGTSAA RDRGEGFALA VAANKLEVLA
SQPADFDRTK GLNVMENLLA AHPSVQAVFA QNDEMALGAI RAVQAAGKEV MIVGFDGTDD
GKAAVAKGKL AATVAQQPAL IGAIGVETAD KVLKGQPVEK SIPVPLQVVS K

b)

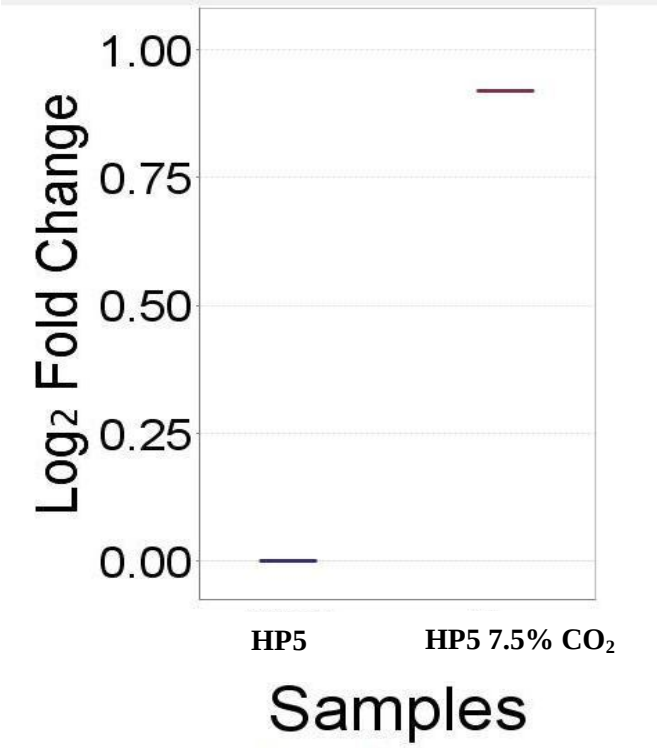

Supplemental Figure S6.63. Protein sequence coverage map (a) and protein expression profile (b) for HP iTRAQ-4 D-ribose transporter. The median protein expression and standard deviation, calculated as the interquartile range, are presented for each sample in (b).

a)

gi|167854701 (89%) 19,003.7 Da
superoxide dismutase (Cu-Zn) [Haemophilus parasuis 29755], gi|219870973|ref|YP_002475348.1| superoxide dismutase [Haemophilus parasuis SH0165], gi|167854238|gb|

MKKTVLTLAL TALFGFSTSA IANSATQIEV KVQQLDLQNG NKDVGTVTIT ESPYGLVFTP
NLKGLSHGLH GFHIHEKPSC EPKEKDGKLV AGLGAGGHWD PKETKKHGYP WSDEAHLGDL
PALAVDHEGN ATNPVLAPRL KKLEEVKGRS LMIHAGGDNH SDHPAPLGGG GARMACGVIN

b)

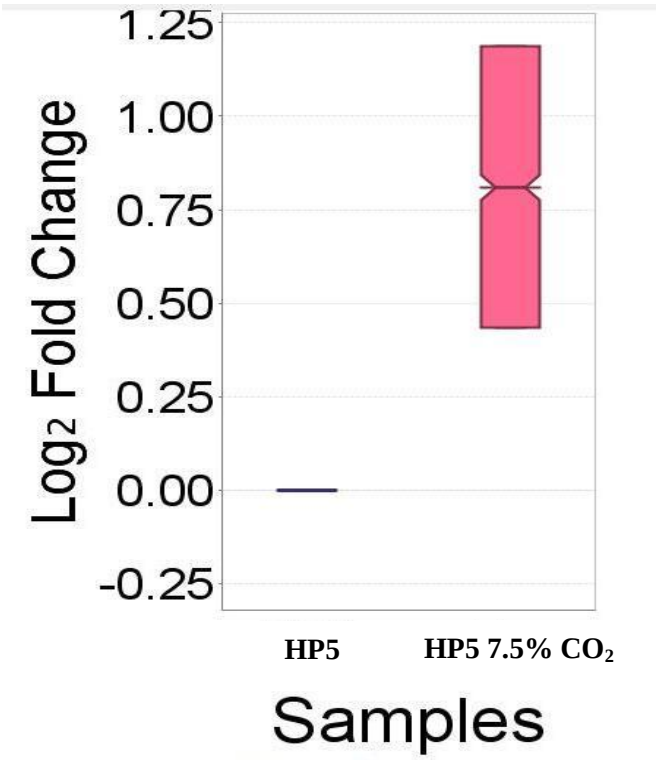

Supplemental Figure S6.64. Protein sequence coverage map (a) and protein expression profile (b) for HP iTRAQ-4 SOD (Cu-Zn). The median protein expression and standard deviation, calculated as the interquartile range, are presented for each sample in (b).

a)

gi|254361285 (89%) 60.979.4 Da
UDP-sugar diphosphatase [Mannheimia haemolytica PHL213], gi|153092781|gb|EDN73824.1| UDP-sugar diphosphatase [Mannheimia haemolytica PHL213]

MRLKKTLLSV ALLSATSAMA YETGKTYRFT VLHTNDIHGH FWQSDKGEYG LAAQKTLVDN
IRKEVAEKGG SVLMLNAGDA NTGVPESDMQ NARPDIEGMN AIGYDAMVLG NHEFDYPLQI
LSMQEKWAKF PFISANVINK KTDKPIVKPY VMLERGGLKI AVIGLTTEDT AKLGNPDVTE
NAFFKNPIET AKNTLAEINQ KEKPDVRIAL THMGYYFDGK HGTNAPGDVT MARTLEKGAF
DLIIGGHTHD TVCIDEKGQF KAKYTPGEEC KPDFQNGTWI VQAGEWGKFV GRADFEFKDG
KATLVKYELI PVNLKKTIKK EDGTKEYRLY QPEIKADEAT YTLLKKYQDE GDKKLNIEVG
RVKGLLDGKR EHIRFQQTNL GRLIAQSQME RVKADIGIMN SGGIRTSLEE GVITYKHILT
VQPFGNMIAT VDLKGQELLD TLTTIALKEV DTGAYPQFAG ISMVVDRTAK TISDVKIGGK
PFDKEKTYKV SLPDYVAAGG DGYPLLKKHP SYVNTGFIDA EMLKKFFEEN KIIEADKYDP
KNQIIFK

b)

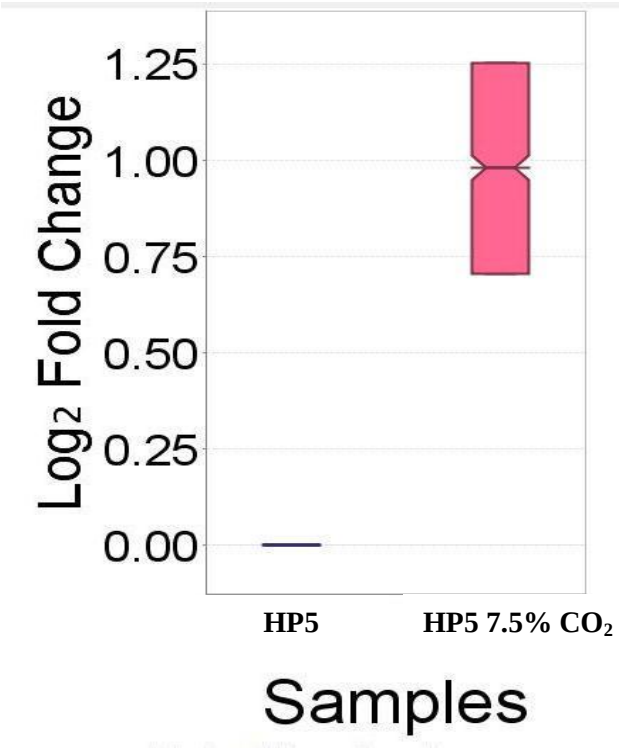

Supplemental Figure S6.65. Protein sequence coverage map (a) and protein expression profile (b) for HP iTRAQ-4 UDP-sugar diphosphatase. The median protein expression and standard deviation, calculated as the interquartile range, are presented for each sample in (b).

a)

gi|167856491 (89%) 8,972.6 Da
phosphoenolpyruvate-protein phosphotransferase [Haemophilus parasuis 29755], gi|219871159|ref|YP_002475534.1| phosphotransferase system, phosphocarrier protein

MYSKDVTITC PNGLHTRPAA EFVKAAKGFA SDITVTSNGK SASAKSLFKL QTLGLAQGTI
ITLSAEGEDE QKAVDFLVDL IPTLE

b)

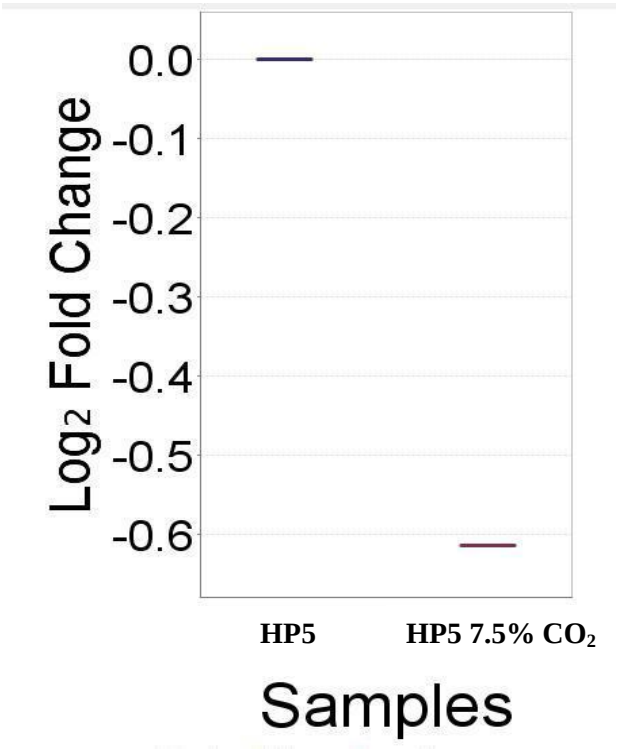

Supplemental Figure S6.66. Protein sequence coverage map (a) and protein expression profile (b) for HP iTRAQ-4 phosphoenolpyruvate phosphotransferase. The median protein expression and standard deviation, calculated as the interquartile range, are presented for each sample in (b).

a)

gi|145639805 (89%) 40,783.7 Da
Outer membrane protein P2 precursor [Haemophilus influenzae PittII]. gi|145271173|gb|EDK11088.1| Outer membrane protein P2 precursor [Haemophilus influenzae PittII]

MKKTLAALIV GAFAASAANA AVVYNNEGSK VELGGRLSVI AEQSNTTVDD QKQQHGALRN
QGSRFHIKAT HNFGDGFYAQ GYLETRLVTD ITKNHSDHFG DITTKYAYVT LGNKAFGEVK
LGRAKTIADG ITSAEDKEYG VLDNSKYVRT NGNTVGYTFK GIDGLVLGAN YLLAQERNPT
DFTDPAGEVT PQAISNGVQV GAKYDANNIV AAIAFGRTNY RENSRVTLQS PGKKQQVEGV
LSTLGYRFSD LGLLVSLDSG YAKTKNHTTT TTTSGRSTTP AHYEKRYFVS PGFQYELMED
TNVYGNFKYE RNSVDQGKKT HEQAVLFGVD HKLHKQVLTY IEGAYARTKT NDKGKTEKTG
KEKSVGVGLR VYF

b)

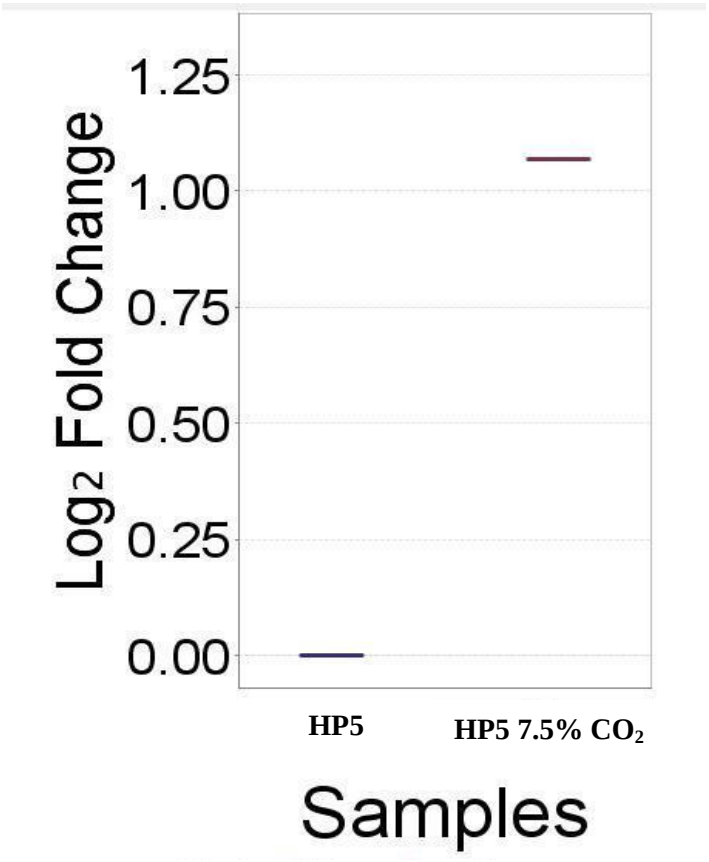

Supplemental Figure S6.67. Protein sequence coverage map (a) and protein expression profile (b) for HP iTRAQ-4 OMP P2. The median protein expression and standard deviation, calculated as the interquartile range, are presented for each sample in (b).

a)

gi|218676105 (79%) 38,938.0 Da
GGDEF family protein [Vibrio splendidus LGP32], gi|218324373|emb|CAV25746.1| GGDEF family protein [Vibrio splendidus LGP32]

MVSAVKIMKK DEFQKSTANL KKAVPLMMKN RVSTTPANYA LWYTYVDNAI PQLTKDMDGI
LEYYGICPPA VGEQLYNNYV ASKSETNIND LRANLELLVS EVSNSMNDTL TDTSAFSEMI
DKSFEDLARV DNESLSIDEV MSLVRQLVSE SRHIRHSTQF LNSQLNSATS EITKLKSQLV
EVQKDALFDS TTTLYNRRSF DRDIETLCEA KQPLCLILLD IDHFKNFNDT YGHLFGDMVL
KGIARKLKQM CREGISAYRF GGEEFAIIVP NKSLRIARQL ADTNRRSLEK LSIKDRRSGQ
QVGSITASFG VAELEPGESA QSLIERADKL LYEAKSLGRN RVMPL

b)

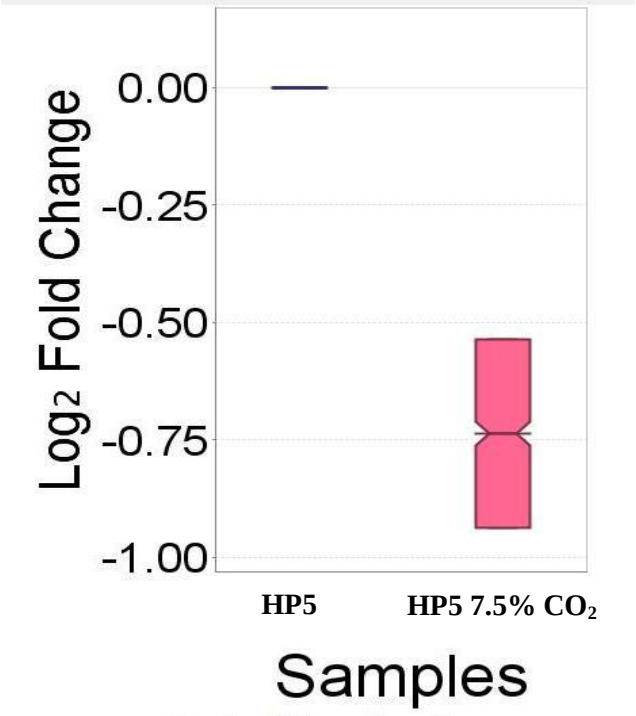

Supplemental Figure S6.68. Protein sequence coverage map (a) and protein expression profile (b) for HP iTRAQ-4 GGDEF family protein. The median protein expression and standard deviation, calculated as the interquartile range, are presented for each sample in (b).

a)

gi|167856581 (89%) 12,391.4 Da
50S ribosomal protein L7/L12 [Haemophilus parasuis 29755], gi|219871555|ref|YP_002475930.1| 50S ribosomal protein L7/L12 [Haemophilus parasuis SH0165], gi|25480637(

MSLTNEQIIE AIASKSVSEI VELITAMEEK FGVSAAAAAV AVAAGPAEAA EEKTEFDVIL
ADAGANKVAV IKAVRGATGL GLKEAKDLVE SAPAALKEGI SKGEAEALKK ELEEAGAKVE
IK

b)

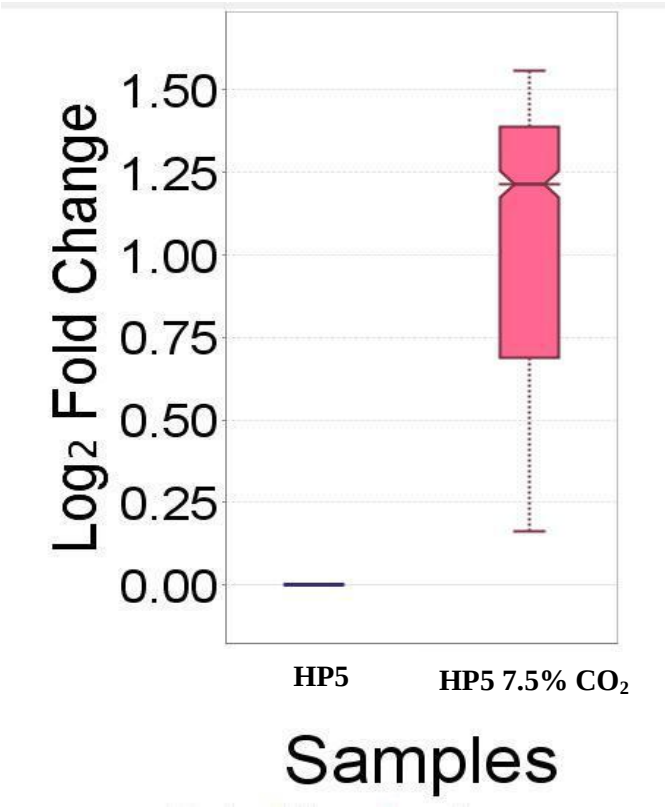

Supplemental Figure S6.69. Protein sequence coverage map (a) and protein expression profile (b) for HP iTRAQ-4 50S ribosomal protein L7/L12. The median protein expression and standard deviation, calculated as the interquartile range, are presented for each sample in (b).

References

1. Glasser, K., . *Quoted in Krankenheinten des Schweines. 5th ed.* **1910,** 1950, (Sharper, Hanover), 106.

2. Kielstein, P.; Methling, W.; Seyfarth, D.; Keller, A., [Importance of Glasser's disease in swine]. *Archiv fur experimentelle Veterinarmedizin* **1986,** 40, (2), 170-82.

3. Harris, D. L., Control of common infectious diseases. In: Multi-site pig production. *Iowa State University Press* **2000**, 98-102.

4. Oliveira, S.; Pijoan, C., *Haemophilus parasuis*: new trends on diagnosis, epidemiology and control. *Veterinary microbiology* **2004,** 99, (1), 1-12.

5. K. Nedbalcova, P. S., Z. Jaglic, R. Ondriasova, Z. Kucerova, *Haemophilus parasuis* and Glässer's disease in pigs: a review. *Veterinarni Medicina* **2006,** 51, (5), 168-179.

6. Kielstein, P.; Rosner, H.; Muller, W., Typing of heat-stable soluble Haemophilus parasuis antigen by means of agargel precipitation and the dot-blot procedure. *Zentralblatt fur Veterinarmedizin. Reihe B. Journal of veterinary medicine. Series B* **1991,** 38, (4), 315-20.

7. Rapp-Garielson, P. K. a. V. J., Designation of 15 serovars of Haemophilus parasuis on the Basis of Immunodiffusion Using Heat-Stable Antigen Extract. *Journal of Clinical Microbiology* **1992,** 30, (4), 862-865.

8. Melnikow, E.; Dornan, S.; Sargent, C.; Duszenko, M.; Evans, G.; Gunkel, N.; Selzer, P. M.; Ullrich, H. J., Microarray analysis of *Haemophilus parasuis* gene expression under in vitro growth conditions mimicking the in vivo environment. *Veterinary microbiology* **2005,** 110, (3-4), 255-63.

9. Jin, H.; Wan, Y.; Zhou, R.; Li, L.; Luo, R.; Zhang, S.; Hu, J.; Langford, P. R.; Chen, H., Identification of genes transcribed by *Haemophilus parasuis* in necrotic porcine lung through the selective capture of transcribed sequences (SCOTS). *Environmental microbiology* **2008,** 10, (12), 3326-36.

10. Xie, Q.; Jin, H.; Luo, R.; Wan, Y.; Chu, J.; Zhou, H.; Shi, B.; Chen, H.; Zhou, R., Transcriptional responses of Haemophilus parasuis to iron-restriction stress in vitro. *Biometals : an international journal on the role of metal ions in biology, biochemistry, and medicine* **2009,** 22, (6), 907-16.

11. Wang, X.; Xu, X.; Zhang, S.; Guo, F.; Cai, X.; Chen, H., Identification and analysis of potential virulence-associated genes in *Haemophilus parasuis* based on genomic subtraction. *Microbial pathogenesis* **2011,** 51, (4), 291-6.

12. Zhou, M.; Zhang, A.; Guo, Y.; Liao, Y.; Chen, H.; Jin, M., A comprehensive proteome map of the *Haemophilus parasuis* serovar 5. *Proteomics* **2009,** 9, (10), 2722-39.

13. Keller, A.; Nesvizhskii, A. I.; Kolker, E.; Aebersold, R., Empirical statistical model to estimate the accuracy of peptide identifications made by MS/MS and database search. *Analytical chemistry* **2002,** 74, (20), 5383-92.

14. Nesvizhskii, A. I.; Keller, A.; Kolker, E.; Aebersold, R., A statistical model for identifying proteins by tandem mass spectrometry. *Analytical chemistry* **2003,** 75, (17), 4646-58.

15. Weller, P. F.; Smith, A. L.; Anderson, P.; Smith, D. H., The role of encapsulation and host age in the clearance of *Haemophilus influenzae* bacteremia. *Journal of Infectious Diseases* **1977,** 135, (1), 34-41.

16. Huber, P. S.; Egwu, I. N., Capsular variation in experimental strains of *Haemophilus influenzae*. *Medical microbiology and immunology* **1985,** 173, (6), 345-53.

17. Carlone, G. M.; Gorelkin, L.; Gheesling, L. L.; Hoiseth, S. K.; Mulks, M. H.; O'Connor, S. P.; Weyant, R. S.; Myrick, J. E.; Mayer, L. W.; Arko, R. J., Potential virulence factors of *Haemophilus influenzae* biogroup aegyptius in Brazilian purpuric fever. The Brazilian Purpuric Fever Study Group. *The Pediatric infectious disease journal* **1989,** 8, (4), 245-7.

18. Wayoff, M.; Jankowski, R., Virulence factors of *Haemophilus influenzae*. *J Chemother* **1989,** 1, (4 Suppl), 26-8.

19. Wispelwey, B.; Hansen, E. J.; Lesse, A.; Scheld, W. M., *Haemophilus influenzae* virulence factors in experimental meningitis. *The Pediatric infectious disease journal* **1989,** 8, (12), 903-4.

20. Bishai, W. R.; Howard, N. S.; Winkelstein, J. A.; Smith, H. O., Characterization and virulence analysis of catalase mutants of *Haemophilus influenzae*. *Infection and immunity* **1994,** 62, (11), 4855-60.

21. Nizet, V.; Colina, K. F.; Almquist, J. R.; Rubens, C. E.; Smith, A. L., A virulent nonencapsulated *Haemophilus influenzae*. *Journal of Infectious Diseases* **1996,** 173, (1), 180-6.

22. Rodriguez, C. A.; Avadhanula, V.; Buscher, A.; Smith, A. L.; St Geme, J. W., 3rd; Adderson, E. E., Prevalence and distribution of adhesins in invasive non-type b encapsulated *Haemophilus influenzae*. *Infection and immunity* **2003,** 71, (4), 1635-42.

23. Hallstrom, T.; Trajkovska, E.; Forsgren, A.; Riesbeck, K., *Haemophilus influenzae* surface fibrils contribute to serum resistance by interacting with vitronectin. *J Immunol* **2006,** 177, (1), 430-6.

24. Forsgren, A.; Riesbeck, K.; Janson, H., Protein D of *Haemophilus influenzae*: a protective nontypeable H. influenzae antigen and a carrier for pneumococcal conjugate vaccines. *Clinical infectious diseases : an official publication of the Infectious Diseases Society of America* **2008,** 46, (5), 726-31.

25. Rosadini, C. V.; Wong, S. M.; Akerley, B. J., The periplasmic disulfide oxidoreductase DsbA contributes to *Haemophilus influenzae* pathogenesis. *Infection and immunity* **2008,** 76, (4), 1498-508.

26. Mason, K. M.; Raffel, F. K.; Ray, W. C.; Bakaletz, L. O., Heme utilization by nontypeable *Haemophilus influenzae* is essential and dependent on Sap transporter function. *Journal of bacteriology* **2011,** 193, (10), 2527-35.

27. Farley, M. M.; Stephens, D. S.; Mulks, M. H.; Cooper, M. D.; Bricker, J. V.; Mirra, S. S.; Wright, A., Pathogenesis of IgA1 protease-producing and -nonproducing *Haemophilus influenzae* in human nasopharyngeal organ cultures. *J Infect Dis* **1986,** 154, (5), 752-9.

28. Fink, D. L.; Buscher, A. Z.; Green, B.; Fernsten, P.; St Geme, J. W., 3rd, The *Haemophilus influenzae* Hap autotransporter mediates microcolony formation and adherence to epithelial cells and extracellular matrix via binding regions in the C-terminal end of the passenger domain. *Cellular microbiology* **2003,** 5, (3), 175-86.

29. Hardy, G. G.; Tudor, S. M.; St Geme, J. W., 3rd, The pathogenesis of disease due to nontypeable *Haemophilus influenzae*. *Methods in molecular medicine* **2003,** 71, 1-28.

30. Mistry, D. V.; Stockley, R. A., The cleavage specificity of an IgA1 protease from *Haemophilus influenzae*. *Virulence* **2011,** 2, (2), 103-10.

31. Cuthbertson, L.; Kimber, M. S.; Whitfield, C., Substrate binding by a bacterial ABC transporter involved in polysaccharide export. *Proceedings of the National Academy of Sciences of the United States of America* **2007,** 104, (49), 19529-34.

32. Wu, Z.; Zhang, W.; Shao, J.; Wang, Y.; Lu, Y.; Lu, C., Immunoproteomic assay of secreted proteins of *Streptococcus suis* serotype 9 with convalescent sera from pigs. *Folia microbiologica* **2011**.

33. Tefon, B. E.; Maass, S.; Ozcengiz, E.; Becher, D.; Hecker, M.; Ozcengiz, G., A comprehensive analysis of *Bordetella pertussis* surface proteome and identification of new immunogenic proteins. *Vaccine* **2011,** 29, (19), 3583-95.

34. Klein, J. S.; Lewinson, O., Bacterial ATP-driven transporters of transition metals: physiological roles, mechanisms of action, and roles in bacterial virulence. *Metallomics : integrated biometal science* **2011**.

35. Zou, L.; Wang, J.; Huang, B.; Xie, M.; Li, A., A solute-binding protein for iron transport in *Streptococcus iniae*. *BMC Microbiol* **2010,** 10, 309.

36. Toyoda, T.; Okano, S.; Shibata, Y.; Abiko, Y., Oxidative stress induces phosphorylation of the ABC transporter, ATP-binding protein, in *Porphyromonas gingivalis*. *Journal of oral science* **2010,** 52, (4), 561-6.

37. Kalscheuer, R.; Weinrick, B.; Veeraraghavan, U.; Besra, G. S.; Jacobs, W. R., Jr., Trehalose-recycling ABC transporter LpqY-SugA-SugB-SugC is essential for virulence of *Mycobacterium tuberculosis*. *Proceedings of the National Academy of Sciences of the United States of America* **2010,** 107, (50), 21761-6.

38. Jonsson, I. M.; Juuti, J. T.; Francois, P.; AlMajidi, R.; Pietiainen, M.; Girard, M.; Lindholm, C.; Saller, M. J.; Driessen, A. J.; Kuusela, P.; Bokarewa, M.; Schrenzel, J.; Kontinen, V. P., Inactivation of the Ecs ABC transporter of *Staphylococcus aureus* attenuates virulence by altering composition and function of bacterial wall. *PloS one* **2010,** 5, (12), e14209.

39. Hiron, A.; Posteraro, B.; Carriere, M.; Remy, L.; Delporte, C.; La Sorda, M.; Sanguinetti, M.; Juillard, V.; Borezee-Durant, E., A nickel ABC-transporter of *Staphylococcus aureus* is involved in urinary tract infection. *Mol Microbiol* **2010,** 77, (5), 1246-60.

40. Stauff, D. L.; Skaar, E. P., The heme sensor system of *Staphylococcus aureus*. *Contributions to microbiology* **2009,** 16, 120-35.

41. Tanabe, M.; Mirza, O.; Bertrand, T.; Atkins, H. S.; Titball, R. W.; Iwata, S.; Brown, K. A.; Byrne, B., Structures of OppA and PstS from *Yersinia pestis* indicate variability of interactions with transmembrane domains. *Acta crystallographica. Section D, Biological crystallography* **2007,** 63, (Pt 11), 1185-93.

42. Whalan, R. H.; Funnell, S. G.; Bowler, L. D.; Hudson, M. J.; Robinson, A.; Dowson, C. G., Distribution and genetic diversity of the ABC transporter lipoproteins PiuA and PiaA within *Streptococcus pneumoniae* and related streptococci. *Journal of bacteriology* **2006,** 188, (3), 1031-8.

43. Speziali, C. D.; Dale, S. E.; Henderson, J. A.; Vines, E. D.; Heinrichs, D. E., Requirement of *Staphylococcus aureus* ATP-binding cassette-ATPase FhuC for iron-restricted growth and evidence that it functions with more than one iron transporter. *Journal of bacteriology* **2006,** 188, (6), 2048-55.

44. Rodriguez, G. M.; Smith, I., Identification of an ABC transporter required for iron acquisition and virulence in *Mycobacterium tuberculosis*. *Journal of bacteriology* **2006,** 188, (2), 424-30.

45. Hanks, T. S.; Liu, M.; McClure, M. J.; Lei, B., ABC transporter FtsABCD of *Streptococcus pyogenes* mediates uptake of ferric ferrichrome. *BMC Microbiol* **2005,** 5, 62.

46. Gat, O.; Mendelson, I.; Chitlaru, T.; Ariel, N.; Altboum, Z.; Levy, H.; Weiss, S.; Grosfeld, H.; Cohen, S.; Shafferman, A., The solute-binding component of a putative Mn(II) ABC transporter (MntA) is a novel *Bacillus anthracis* virulence determinant. *Mol Microbiol* **2005,** 58, (2), 533-51.

47. Anderson, D. S.; Adhikari, P.; Nowalk, A. J.; Chen, C. Y.; Mietzner, T. A., The hFbpABC transporter from *Haemophilus influenzae* functions as a binding-protein-dependent ABC transporter with high specificity and affinity for ferric iron. *Journal of bacteriology* **2004,** 186, (18), 6220-9.

48. Martin, P. R.; Mulks, M. H., Cloning and characterization of a gene encoding an antigenic membrane protein from *Actinobacillus pleuropneumoniae* with homology to ABC transporters. *FEMS immunology and medical microbiology* **1999,** 25, (3), 245-54.

49. Smoot, L. M.; Bell, E. C.; Paz, R. L.; Corbin, K. A.; Hall, D. D.; Steenbergen, J. N.; Harner, A. C.; Actis, L. A., Molecular and genetic analysis of iron uptake proteins in the brazilian purpuric fever clone of *Haemophilus influenzae* biogroup aegyptius. *Frontiers in bioscience : a journal and virtual library* **1998,** 3, D989-96.

50. Shah, P.; Swiatlo, E., Immunization with polyamine transport protein PotD protects mice against systemic infection with Streptococcus pneumoniae. *Infection and immunity* **2006,** 74, (10), 5888-92.

51. Shah, P.; Marquart, M.; Quin, L. R.; Swiatlo, E., Cellular location of polyamine transport protein PotD in Streptococcus pneumoniae. *FEMS microbiology letters* **2006,** 261, (2), 235-7.

52. Ware, D.; Jiang, Y.; Lin, W.; Swiatlo, E., Involvement of potD in Streptococcus pneumoniae polyamine transport and pathogenesis. *Infection and immunity* **2006,** 74, (1), 352-61.

53. Pandher, K.; Murphy, G. L., Genetic and immunological analyses of a 38 kDa surface-exposed lipoprotein of Pasteurella haemolytica A1. *Veterinary microbiology* **1996,** 51, (3-4), 331-41.

54. Pan, Y. H.; Liao, C. C.; Kuo, C. C.; Duan, K. J.; Liang, P. H.; Yuan, H. S.; Hu, S. T.; Chak, K. F., The critical roles of polyamines in regulating ColE7 production and restricting ColE7 uptake of the colicin-producing Escherichia coli. *The Journal of biological chemistry* **2006,** 281, (19), 13083-91.

55. Igarashi, K.; Ito, K.; Kashiwagi, K., Polyamine uptake systems in Escherichia coli. *Research in microbiology* **2001,** 152, (3-4), 271-8.

56. Kashiwagi, K.; Pistocchi, R.; Shibuya, S.; Sugiyama, S.; Morikawa, K.; Igarashi, K., Spermidine-preferential uptake system in Escherichia coli. Identification of amino acids involved in polyamine binding in PotD protein. *The Journal of biological chemistry* **1996,** 271, (21), 12205-8.

57. Kashiwagi, K.; Miyamoto, S.; Nukui, E.; Kobayashi, H.; Igarashi, K., Functions of potA and potD proteins in spermidine-preferential uptake system in Escherichia coli. *The Journal of biological chemistry* **1993,** 268, (26), 19358-63.

58. Houot, L.; Chang, S.; Pickering, B. S.; Absalon, C.; Watnick, P. I., The phosphoenolpyruvate phosphotransferase system regulates *Vibrio cholerae* biofilm formation through multiple independent pathways. *Journal of bacteriology* **2010,** 192, (12), 3055-67.

59. Hansen, E. J.; Pelzel, S. E.; Orth, K.; Moomaw, C. R.; Radolf, J. D.; Slaughter, C. A., Structural and antigenic conservation of the P2 porin protein among strains of *Haemophilus influenzae* type b. *Infection and immunity* **1989,** 57, (11), 3270-5.

60. Munson, R., Jr.; Bailey, C.; Grass, S., Diversity of the outer membrane protein P2 gene from major clones of *Haemophilus influenzae* type b. *Mol Microbiol* **1989,** 3, (12), 1797-803.

61. Cope, L. D.; Pelzel, S. E.; Latimer, J. L.; Hansen, E. J., Characterization of a mutant of *Haemophilus influenzae* type b lacking the P2 major outer membrane protein. *Infection and immunity* **1990,** 58, (10), 3312-8.

62. van Alphen, L.; Eijk, P.; Geelen-van den Broek, L.; Dankert, J., Immunochemical characterization of variable epitopes of outer membrane protein P2 of nontypeable *Haemophilus influenzae*. *Infection and immunity* **1991,** 59, (1), 247-52.

63. Sikkema, D. J.; Murphy, T. F., Molecular analysis of the P2 porin protein of nontypeable *Haemophilus influenzae*. *Infection and immunity* **1992,** 60, (12), 5204-11.

64. Duim, B.; Dankert, J.; Jansen, H. M.; van Alphen, L., Genetic analysis of the diversity in outer membrane protein P2 of non-encapsulated *Haemophilus influenzae*. *Microbial pathogenesis* **1993,** 14, (6), 451-62.

65. Yi, K.; Murphy, T. F., Importance of an immunodominant surface-exposed loop on outer membrane protein P2 of nontypeable *Haemophilus influenzae*. *Infection and immunity* **1997,** 65, (1), 150-5.

66. Neary, J. M.; Yi, K.; Karalus, R. J.; Murphy, T. F., Antibodies to loop 6 of the P2 porin protein of nontypeable *Haemophilus influenzae* are bactericidal against multiple strains. *Infection and immunity* **2001,** 69, (2), 773-8.

67. Galdiero, S.; Capasso, D.; Vitiello, M.; D'Isanto, M.; Pedone, C.; Galdiero, M., Role of surface-exposed loops of *Haemophilus influenzae* protein P2 in the mitogen-activated protein kinase cascade. *Infection and immunity* **2003,** 71, (5), 2798-809.

68. Vitiello, M.; Finamore, E.; Cantisani, M.; Bevilacqua, P.; Incoronato, N.; Falanga, A.; Galdiero, E.; Galdiero, M., P2 porin and loop L7 from *Haemophilus influenzae* modulate expression of IL-6 and adhesion molecules in astrocytes. *Microbiology and immunology* **2011,** 55, (5), 347-56.

69. Mullins, M. A.; Register, K. B.; Bayles, D. O.; Loving, C. L.; Nicholson, T. L.; Brockmeier, S. L.; Dyer, D. W.; Phillips, G. J., Characterization and comparative analysis of the genes encoding *Haemophilus parasuis* outer membrane proteins P2 and P5. *Journal of bacteriology* **2009,** 191, (19), 5988-6002.

70. Li, P.; Bai, J.; Li, J. X.; Zhang, G. L.; Song, Y. H.; Li, Y. F.; Wang, X. W.; Jiang, P., Molecular cloning, sequencing, and expression of the outer membrane protein P2 gene of Haemophilus parasuis. *Research in veterinary science* **2011**.

71. del Rio, M. L.; Gutierrez-Martin, C. B.; Rodriguez-Barbosa, J. I.; Navas, J.; Rodriguez-Ferri, E. F., Identification and characterization of the TonB region and its role in transferrin-mediated iron acquisition in *Haemophilus parasuis*. *FEMS immunology and medical microbiology* **2005,** 45, (1), 75-86.

72. Ekins, A.; Bahrami, F.; Sijercic, A.; Maret, D.; Niven, D. F., *Haemophilus somnus* possesses two systems for acquisition of transferrin-bound iron. *Journal of bacteriology* **2004,** 186, (13), 4407-11.

73. Whitby, P. W.; Sim, K. E.; Morton, D. J.; Patel, J. A.; Stull, T. L., Transcription of genes encoding iron and heme acquisition proteins of *Haemophilus influenzae* during acute otitis media. *Infection and immunity* **1997,** 65, (11), 4696-700.

74. Schryvers, A. B.; Gray-Owen, S., Iron acquisition in *Haemophilus influenzae*: receptors for human transferrin. *J Infect Dis* **1992,** 165 Suppl 1, S103-4.

75. Morton, D. J.; Williams, P., Siderophore-independent acquisition of transferrin-bound iron by *Haemophilus influenzae* type b. *Journal of general microbiology* **1990,** 136, (5), 927-33.

76. Pidcock, K. A.; Wooten, J. A.; Daley, B. A.; Stull, T. L., Iron acquisition by *Haemophilus influenzae*. *Infection and immunity* **1988,** 56, (4), 721-5.

77. San Mateo, L. R.; Toffer, K. L.; Kawula, T. H., The sodA gene of *Haemophilus ducreyi* encodes a hydrogen peroxide-inhibitable superoxide dismutase. *Gene* **1998,** 207, (2), 251-7.

78. D'Mello, R. A.; Langford, P. R.; Kroll, J. S., Role of bacterial Mn-cofactored superoxide dismutase in oxidative stress responses, nasopharyngeal colonization, and sustained bacteremia caused by *Haemophilus influenzae* type b. *Infection and immunity* **1997,** 65, (7), 2700-6.

79. Kroll, J. S.; Langford, P. R.; Saah, J. R.; Loynds, B. M., Molecular and genetic characterization of superoxide dismutase in *Haemophilus influenzae* type b. *Mol Microbiol* **1993,** 10, (4), 839-48.

80. Korshunov, S. S.; Imlay, J. A., A potential role for periplasmic superoxide dismutase in blocking the penetration of external superoxide into the cytosol of Gram-negative bacteria. *Mol Microbiol* **2002,** 43, (1), 95-106.

CHAPTER 7. GENERAL CONCLUSIONS

General Discussion

Overall, the goal of this study was to identify putative virulence factors at the protein level for *Haemophilus parasuis* and rationally design a method in which a subunit vaccine and corresponding diagnostic for Glässer's disease could be created based on the identification and characterization of outer membrane proteins. This was achieved using bottom-up and iTRAQ proteomic techniques, N-terminal sequencing, molecular modeling analysis, and antigenic characterization methods. Identification and profiling of differential expression of the virulence factors of *H. parasuis* has been based primarily on genetic data, with few proteomic profiling studies [1-7]. In order to understand the mechanism of infection of *H. parasuis*, it is imperative to not only identify proteins traditionally associated with virulence but to also recognize differences that exist for those proteins at a molecular and/or expression level.

Previous work on the characterization of *H. parasuis* OMP P5 indicated a pI of approximately 5.5 and an apparent molecular weight of 32 kDa [8]. The P2 protein was predicted to have a molecular weight of 48-55kDa [9]. Given this information, gel plugs with these characteristics were analyzed by tandem mass spectrometry following 2-D SDS-PAGE immunoblots. The genome for *H. parasuis* was not available until 2008, which proved problematic for absolute identification based on mass spectrometric analysis. However, following the availability of the *H. parasuis* proteome, most of the immunoreactive proteins were identified. Proteins identified include: OMP P2, TRAP solute transporter, glucose-specific PTS system enzyme IIA, acetyl-CoA carboxylase biotin carboxylase subunit, purine nucleoside phosphorylase, chelated iron ABC transporter, probable sugar isomerase,

Mn-dependent superoxide dismutase, putative iron ABC transporter, D-ribose transporter, alanine aminotransferase, phosphoribosylglycinamide formyltransferase, FbpA, and hypothetical proteins HPS 06844 and HPS 10240. When compared to the proteomic studies available, few proteins deviate from the calculated pI and molecular weight [3]. An exception includes the P2 protein, which has a higher apparent molecular weight than calculated. This was also observed for 1-D SDS-PAGE analysis in which the P2 protein was identified by immunoblot and N-terminal sequencing [9]. This could be due to nature of extraction of the protein which varied from the previous proteomic profiling study, or the protein may be modified by glycosylation or lipidation as the method used to extract the outer membrane proteins has been shown to maintain glycosylation of proteins [10].

The OMP P2 and P5 proteins were characterized by molecular modeling and antigenic analysis methods, given their importance as virulence factors for *H. influenzae*. Two genes were sequenced for both the P5 and P2 proteins based on the primers used in this study. Both OMPA and OMP P5 have been identified in *H. parasuis* along with OMP P2 [11, 12]. Two genes for P2 were sequenced. When compared to protein immunoblot and N-terminal sequencing data, one form of the P2 protein is expressed [9]. Molecular modeling analysis indicated that regardless of virulence, the P5 protein shared a structure comprising four surface exposed loops, which is similar to the model for P5 of *H. influenzae* and that seen for OMPA of *H. parasuis* [11, 13]. Comparison of antigenic propensity for the surface exposed loops found the antigenic profiles to be comparable regardless of virulence, with the loop 3 and loop 4 comprising a continuous B-cell epitope. OMP P2 presented in two forms which differed by approximately 3-5kDa. A higher apparent molecular weight was observed for avirulent serovars, which links the non-extended form of P2 to virulence of *H. parasuis*.

This shift in apparent molecular weight was observed in 2-D SDS-PAGE analysis but also in previous studies [9]. Differences in antigenic propensity were also noted for OMP P2, with loop 1, loop 4, and loop 8 comprising the highest predicted score of antigenic propensity for the highly virulent serovars. Loops 1, 3, 4, 5, 6, and 8 comprise linear B-cell epitopes for OMP P2 for virulent serovars. The exact role of the extension of loops 3 and 5 of OMP P2 are unknown. The highest scoring antigenic region for loop 3 is an epitope shared between the two forms of OMP P2. There also exists a high scoring B-cell epitope on loop 3 of OMP P2 that is shared regardless of virulence. This study not only characterized the P2 and P5 proteins in accordance to virulence using molecular modeling and antigenic characterization, but also identified probable epitopes for a subunit vaccine against Glässer's disease. The strategy presented here provides a general method that can be applied toward the design of subunit vaccine candidates for extracellular pathogens.

Based on molecular modeling and antigenic characterization of OMP P5, the use of loop 3 and loop 4 as a probable peptide vaccine was taken to an animal model. Results supported the methodology of designing a vaccine based on molecular modeling and antigenic characterization techniques. Preliminary ELISA studies indicated that animals infected with *H. parasuis* had antibody titers to the loop 3, loop 4, and loop 3-4 epitopes of OMP P5. The loop 3 peptide provided protection against heterologous challenge while the loop 4 epitope provided no protection. Therefore, the loop 4 epitope is essentially acting as a decoy which is a trend observed for *H. influenzae* OMP P5 [14]. Superior protection, at 90–100%, was observed in animals with a higher dose of loop 3 peptide combined with bacterin. This likely occurred due to an anamnestic response.

Aside from the P2 and P5 colonization factors, proteins that are not traditionally associated with adherence to the host's epithelial cells could be considered colonization factors as epitopes of the surface localized protein facilitate adherence. The traditional idea of a "colonization factor" is giving way to highly conserved proteins such as glyceraldehyde-3-phosphate dehydrogenase (GAPDH). The first identification and antigenic characterization of a surface-localized GAPDH of *H. parasuis* was presented here. Studies in other bacterial pathogens have found GAPDH to be of importance in colonization and to also serve as a viable vaccine candidate against colonization [15-22].

Given that few proteomic profiling studies have been performed on *H. parasuis*, the iTRAQ method was utilized to not only identify proteins, but to also quantify differential protein expression and evaluate how this differential expression may play a role in virulence of the organism. The results of this study provides researchers the identification of putative virulence factors that can be further examined, including proteins involved with iron acquisition and colonization. Results of the OMP P2 protein expression indicated a 1.5 to 2-fold increase in the presence of 7.5% CO_2 when compared to protein expression in the aerobic environment. Additional differentially expressed proteins for the overall analysis include: MglB, hypothetical protein HPS_06844, Fe^{3+} ABC transporter, TRAP solute transporter, D-ribose transporter subunit RbsB, FbpA, ABC transporters, Cu-Zn SOD, iron binding proteins, chelated iron ABC transporter, hypothetical protein HPS_10240, acyl carrier protein, glucose-specific PTS enzyme IIA, heme-binding protein A, phosphoenolpyruvate-protein phosphotransferase, alanine aminotransferase, hypothetical protein HPS_07840, plp0007 from *Legionella pneumophila*, hypothetical protein GCWU000324_02210 from *Kingella oralis,* transaldolase B, UDP-sugar diphosphatase from

M. haemolytica, tRNA pseudouridine synthetase C, gamma-glutamyl phosphate reductase and nitrate reductase

The idea of reverse vaccinology has been discussed since 2000 [23-27]. This is the process of taking genomic data and analyzing proteins using bioinformatics for the design of vaccine candidates. When reverse vaccinology is combined with protein and/or proteomic profiling data, the design of a subunit vaccine is superior as genetic data does not provide important information related to protein expression including whether or not a protein is excreted, the location of the expressed protein, the presence of post-translational modifications, and differential expression of proteins. Examples presented here include the presence of two OMP P2 genes, with the expression of only one form of P2 at a protein level. Additionally, the surface localized GAPDH would never have been recognized using strictly genomic data as prediction methods place this protein in the cytosol.

General Conclusions

Given the results presented in this dissertation, the following can be concluded:

1. The monoclonal antibody (4BF8) to OMP P5 of *H. influenzae* reacts with multiple epitopes of outer membrane proteins of *H. parasuis* under denaturing conditions.
2. Immunoreactive proteins to the anti-P5 antibody, including OMP P2, were successfully identified by 2-D SDS-PAGE immunoblot analysis followed by tandem mass spectrometry.
3. Molecular modeling analysis indicates that OMP P5 is a β-barrel that comprises four surface exposed loops, an N-terminal domain that is homologous to OMPA

of *E. coli* and a C-terminal domain that is homologous to both PalA of *E. coli* and OMP P6 of H. *influenzae*. This model does not vary in accordance to virulence. Antigenic propensity scores for the surface exposed loops were comparable regardless of virulence of the organism. Continuous B-cell epitope prediction noted a high scoring epitope at the apex of loop 3 and loop 4 for *H. parasuis* OMP P5.

4. Molecular modeling analysis of OMP P2 revealed two forms of the protein which corresponded with virulence of the organism. OMP P2 is homologous to OMP II of *N. meningitidis* and a β-barrel with eight surface exposed loops. An extension exists for the loop 3 and loop 5 regions of OMP P2, and this extension corresponds with a 3-5kDa shift observed by SDS-PAGE analysis of P2 protein. A higher apparent molecular weight is associated with avirulent strains while a lower molecular weight, without the loop 3 and loop 5 extensions, corresponds to virulent strains. The highest antigenic propensity scores were given for loops 1, 4 and 8 for virulent strains. The highest scoring antigenic region for loop 3 was the same regardless of virulence and extension of the loop. This region also comprised a high scoring linear B-cell epitope. Additional high scoring linear B-cell epitopes were predicted for loops 1, 4, 6 and 8.
5. Synthetic peptides to loop 3, loop 4, and a combinatorial loop 3-4 peptide of OMP P5 were designed, and preliminary ELISA results indicated that animals infected with *H. parasuis* had statistically significant ($p<0.05$) antibody titers to these epitopes when compared to control animals.

6. In a heterologous challenge study, the synthetic loop 3 provided a 25% increase in protection when animals were dosed twice with 1ml of peptide in Ribi adjuvant. A 2ml dose of peptide with 2ml dose of bacterin provided 90-100% protection upon heterologous challenge. A challenge study using recombinant loop 4 peptide as a vaccine did not provide any protection, and decreased protection below that of the placebo group was observed when loop 4 was combined with the P5 protein for vaccination dose. The loop 3 epitope of P5 protein appears to be protective while the loop 4 peptide provides no protection and may act as a decoy.
7. The general methodology for vaccine design presented here was validated in preliminary studies as well as an animal challenge study, and this method could be applied to the outer membrane proteins of extracellular pathogens.
8. A putative surface localized glyceraldehyde-3-phosphate dehydrogenase was identified following immunoblot with anti-P5 antibody and N-terminal sequencing. This protein was identified in an avirulent serovar, HP3, and a moderately virulent serovar, HP2. In accordance with observations in other bacterial pathogens, this protein may play a role in colonization of *H. parasuis*.
9. iTRAQ analysis of outer membrane proteins in both aerobic and anaerobic conditions identified proteins and putative virulence factors that can be further characterized as well as used in the design of a subunit vaccine for Glässer's disease. The OMP P2 protein is over-expressed 1.5 to 2-fold in anaerobic (7.5% CO_2) conditions.

Recommendations for Future Research

Given the results presented in this dissertation, subsequent research includes:

1. The application of the reverse vaccinology approach to putative virulence factors identified by bottom-up and iTRAQ proteomic methodologies.
2. Validate the results of the reverse vaccinology strategy for the putative virulence factors, including the verification of surface exposed epitopes and screening sera from infected animals for antibody titers to predicted antigenic epitopes.
3. Screen the sera of animals infected with *H. parasuis* to identify additional surface exposed loop epitopes of the OMP P2 and OMP P5 which may serve as protective in the design of a subunit vaccine.
4. Additional animal challenge experiments using loop 3 peptide of OMP P5 to verify dose dependence.
5. Animal challenge studies using subunit vaccines designed from OMP P2 and other virulence factors that have been validated in a laboratory setting to be antigenic.
6. The design of a complimentary subunit diagnostic for Glässer's disease.
7. Protein-peptide interaction studies between CEACAM-1 and the outer membrane loops of OMP P2 and OMP P5. Previous studies indicate that *H. parasuis* P2 binds human CEACAM-1 [9]. Protein-protein and/or protein-peptide interaction studies with swine CEACAM-1 would be of great importance in elucidating the role of these proteins in possible evasion of the host's immune response.

8. Determine if the *H. parasuis* surface localized glyceraldehyde-3-phostphate dehydrogenase is indeed surface exposed, involved with colonization, and has enzymatic activity.
9. Epitope mapping of the monoclonal antibody 4BF8 and/or obtain a true monoclonal antibody to the OMP P2 and OMP P5 proteins of *H. parasuis* to identify additional P2 or P5 proteins and further characterize the proteins.
10. Perform native immunoblot using monoclonal antibody 4BF8 or antibodies to *H. parasuis* OMP P2 and OMP P5.
11. Determine if OMP P2 is modified by glycosylation or lipidation as the apparent molecular weight by SDS-PAGE analysis is approximately 12kDa higher than expected molecular weight following outer membrane protein extraction method presented here.

References

1. Wang, X., et al., *Identification and analysis of potential virulence-associated genes in Haemophilus parasuis based on genomic subtraction.* Microb Pathog, 2011. **51**(4): p. 291-6.
2. Zhou, H., et al., *Identification of putative virulence-associated genes of Haemophilus parasuis through suppression subtractive hybridization.* Vet Microbiol, 2010. **144**(3-4): p. 377-83.
3. Zhou, M., et al., *A comprehensive proteome map of the Haemophilus parasuis serovar 5.* Proteomics, 2009. **9**(10): p. 2722-39.
4. Xie, Q., et al., *Transcriptional responses of Haemophilus parasuis to iron-restriction stress in vitro.* Biometals, 2009. **22**(6): p. 907-16.
5. Jin, H., et al., *Identification of genes transcribed by Haemophilus parasuis in necrotic porcine lung through the selective capture of transcribed sequences (SCOTS).* Environ Microbiol, 2008. **10**(12): p. 3326-36.
6. Metcalf, D.S. and J.I. MacInnes, *Differential expression of Haemophilus parasuis genes in response to iron restriction and cerebrospinal fluid.* Can J Vet Res, 2007. **71**(3): p. 181-8.
7. Melnikow, E., et al., *Microarray analysis of Haemophilus parasuis gene expression under in vitro growth conditions mimicking the in vivo environment.* Vet Microbiol, 2005. **110**(3-4): p. 255-63.
8. McVicker, J.K. and L.B. Tabatabai, *Isolation and characterization of the P5 adhesin protein of Haemophilus parasuis serotype 5.* Prep Biochem Biotechnol, 2006. **36**(4): p. 363-74.

9. McVicker, J.K., *The identification and characterization of P5 and P2 colonization proteins of Haemophilus parasuis and the targeted binding of Carcinoembryonic Antigen (CEA)*, in *PhD Dissertation*2004, Iowa State University: Ames, IA.

10. Syuto, B.a.M., M., *Purification of a Protective Antigen form a Saline Extract of Pasteurella multocida.* Infection and Immunity, 1981. **37**(3): p. 1218-1226.

11. Tang, C., et al., *Characteristics of the molecular diversity of the outer membrane protein A gene of Haemophilus parasuis.* Can J Vet Res, 2010. **74**(3): p. 233-6.

12. Mullins, M.A., et al., *Characterization and comparative analysis of the genes encoding Haemophilus parasuis outer membrane proteins P2 and P5.* J Bacteriol, 2009. **191**(19): p. 5988-6002.

13. Webb, D.C. and A.W. Cripps, *Secondary structure and molecular analysis of interstrain variability in the P5 outer-membrane protein of non-typable Haemophilus influenzae isolated from diverse anatomical sites.* J Med Microbiol, 1998. **47**(12): p. 1059-67.

14. Novotny, L.A. and L.O. Bakaletz, *The fourth surface-exposed region of the outer membrane protein P5-homologous adhesin of nontypable Haemophilus influenzae is an immunodominant but nonprotective decoying epitope.* J Immunol, 2003. **171**(4): p. 1978-83.

15. Jin, H., S. Agarwal, and V. Pancholi, *Surface export of GAPDH/SDH, a glycolytic enzyme, is essential for Streptococcus pyogenes virulence.* MBio, 2011. **2**(3): p. e00068-11.

16. Dumke, R., M. Hausner, and E. Jacobs, *Role of Mycoplasma pneumoniae glyceraldehyde-3-phosphate dehydrogenase (GAPDH) in mediating interactions with the human extracellular matrix.* Microbiology, 2011. **157**(Pt 8): p. 2328-38.

17. Tunio, S.A., et al., *The role of glyceraldehyde 3-phosphate dehydrogenase (GapA-1) in Neisseria meningitidis adherence to human cells.* BMC Microbiol, 2010. **10**: p. 280.

18. Purves, J., et al., *Comparison of the regulation, metabolic functions, and roles in virulence of the glyceraldehyde-3-phosphate dehydrogenase homologues gapA and gapB in Staphylococcus aureus.* Infect Immun, 2010. **78**(12): p. 5223-32.

19. Perez-Casal, J. and T. Prysliak, *Detection of antibodies against the Mycoplasma bovis glyceraldehyde-3-phosphate dehydrogenase protein in beef cattle.* Microb Pathog, 2007. **43**(5-6): p. 189-97.

20. Fourrat, L., et al., *Cloning, gene expression and characterization of a novel bacterial NAD-dependent non-phosphorylating glyceraldehyde-3-phosphate dehydrogenase from Neisseria meningitidis strain Z2491.* Mol Cell Biochem, 2007. **305**(1-2): p. 209-19.

21. Brassard, J., M. Gottschalk, and S. Quessy, *Cloning and purification of the Streptococcus suis serotype 2 glyceraldehyde-3-phosphate dehydrogenase and its involvement as an adhesin.* Vet Microbiol, 2004. **102**(1-2): p. 87-94.

22. Alvarez, R.A., M.W. Blaylock, and J.B. Baseman, *Surface localized glyceraldehyde-3-phosphate dehydrogenase of Mycoplasma genitalium binds mucin.* Mol Microbiol, 2003. **48**(5): p. 1417-25.

23. Palumbo, E., et al., *Antigen Identification Starting from the Genome: A "Reverse Vaccinology" Approach Applied to MenB.* Methods Mol Biol, 2012. **799**: p. 361-403.

24. Bowman, B.N., et al., *Improving reverse vaccinology with a machine learning approach.* Vaccine, 2011. **29**(45): p. 8156-64.

25. Sette, A. and R. Rappuoli, *Reverse vaccinology: developing vaccines in the era of genomics.* Immunity, 2010. **33**(4): p. 530-41.

26. He, Y., Z. Xiang, and H.L. Mobley, *Vaxign: the first web-based vaccine design program for reverse vaccinology and applications for vaccine development.* J Biomed Biotechnol, 2010. **2010**: p. 297505.

27. Rappuoli, R., *Reverse vaccinology, a genome-based approach to vaccine development.* Vaccine, 2001. **19**(17-19): p. 2688-91.